

Akademiya Nauk SSSR

I.I. Kornilov, Editor

TITANIUM AND ITS ALLOYS

Publication No.10

Investigation of Titanium Alloys

TRANSLATED FROM RUSSIAN

**Published for the National Aeronautics and Space Administration, U.S.A.
and the National Science Foundation, Washington, D.C.
by the Israel Program for Scientific Translations**

AKADEMIYA NAUK SSSR
GOSUDARSTVENNYI KOMITET PO CHERNOI I TsVETNOI
METALLURGII PRI GOSPLANE SSSR
INSTITUT METALLURGII imeni A. A. BAIKOVA

Academy of Sciences of the USSR
State Committee for Ferrous and Nonferrous Metallurgy
of the State Planning Committee of the USSR
Institute of Metallurgy im. A. A. Baikov

I. I. Kornilov, Editor

TITANIUM AND ITS ALLOYS

Publication No. 10

Investigation of Titanium Alloys

(Titan i ego splavy.
Issledovaniya titanovykh splavov)

Izdatel'stvo Akademii Nauk SSSR
Moskva 1963

Translated from Russian

Israel Program for Scientific Translations
Jerusalem 1966

NASA TT F-362
TT 65-50139

Published Pursuant to an Agreement with
THE NATIONAL AERONAUTICS AND SPACE ADMINISTRATION, U.S.A.
and
THE NATIONAL SCIENCE FOUNDATION, WASHINGTON, D.C.

Copyright © 1966
Israel Program for Scientific Translations Ltd.
IPST Cat. No. 1454

Translated by Ch. Nisenbaum, Chem. Eng.
Edited by B. Mandelson, B.Sc.

Printed in Jerusalem by S. Monson
Binding: Wiener Bindery, Jerusalem

Price: \$7.00

Available from the
U.S. DEPARTMENT OF COMMERCE
Clearinghouse for Federal Scientific and Technical Information
Springfield, Va. 22151

TABLE OF CONTENTS

FOREWORD	v
EXPLANATORY LIST OF ABBREVIATIONS	vi
I. REACTION OF TITANIUM WITH OTHER METALS AND THE STRUCTURE OF TITANIUM ALLOYS	1
I. I. Kornilov. Chemical Investigation of Titanium	1
Ge Dzhzhi-Min and E. N. Pylaeva. Investigation of the Phase Equilibrium of the Ti—Al—Mo System in the Titanium-Rich Alloy Field	11
Ge Dzhzhi-Min and E. N. Pylaeva. Investigation of the Phase Transformations in the Ti—Al—Mo System	19
O. K. Belousov, I. I. Kornilov, and V. S. Mikheev. Phase Diagram of the Ti—V—Nb—Mo System	24
K. I. Shakhova and P. B. Budberg. Investigation of Alloys of the Ternary Ti—Nb—Cr System	34
V. S. Mikheev, K. P. Markovich, and L. F. Tabadze. Investigation of the Partial Phase Diagram of the Ti—Al—Cr—Fe—Si—B System (Section with 3% of Al)	40
V. S. Mikheev, T. S. Chernova, and N. M. Dzhibuti. Investigation of the Partial Phase Diagram of the Ti—Al—Cr—Fe—Si—B System for Alloys Containing 6% of Al	47
V. A. Livanov and B. A. Kolachev. Classification of Titanium Alloys According to their Structure	56
N. M. Pul'tsin and V. B. Pokrovskaya. Some Results of the Metallographic and X-ray Investigations of AT Titanium Alloys	65
E. I. Gladyshevskii, V. Ya. Markiv, Yu. B. Kuz'ma, and E. E. Cherkashin. Crystal Structure of Some Ternary Intermetallic Titanium Compounds	73
I. I. Kornilov, E. N. Pylaeva, and M. A. Volkova. A Review of Investigations on the Phase Diagram of the Binary Ti—Al System	76
N. G. Boriskina and I. I. Kornilov. Investigation of the Phase Composition of Alloys of the Ti—Al—Cr—Fe—Si System with Constant Contents of Aluminum (6%) and Silicon (0.3%)	89
R. S. Mints, A. E. Shelest, and Yu. S. Malkov. Dilatometric Investigation of Titanium	99
II. INTERACTION OF TITANIUM WITH GASES AND CORROSION PROPERTIES OF TITANIUM ALLOYS	104
S. A. Gorbunov and I. S. Anitov. Kinetics of Oxidation of Technically Pure Titanium in the Air at High Temperatures	104
S. A. Gorbunov, G. P. Nadutenko, and V. P. Teodorovich. Investigation of the Oxidation of VT-14, VT-8, VT-3—1 Alloys and of No. 1 Experimental Alloy in Air at 800 to 1200°C	113
L. A. Glikman, V. I. Deryabina, N. N. Kolgatin, I. A. Bytenskii, V. P. Teodorovich, and N. S. Teplov. The Influence of Gas-Saturated Layers on the Strength and Plastic Properties of Titanium Alloys	122
S. S. Mozhaev and L. F. Sokiryanskii. Calculation of the Kinetics of the Dissolution of Oxygen in Titanium	137
A. S. Mikhailov and B. S. Krylov. The Influence of Hydrogen on the Tendency of Titanium Alloys to Delayed Cracking	151
F. N. Tabadze, S. N. Mandzhgaladze, I. N. Lordkipanidze, and T. S. Dashniani. The Corrosion Resistance of Titanium Alloys to Various Media in the Chemical and Pharmaceutical Industries	158
F. N. Tabadze and T. A. Lashkhi. Corrosion Resistance of AT Titanium Alloys to Media in the Food Industry	162
B. S. Krylov. The Kinetics of Evolution of Hydrogen in Vacuo from Titanium and its Alloys	167

L. M. Yakimenko, G. N. Kozhanov, I. E. Veselovskaya, and R. V. Dzhagatspanyan. Investigation of the Electrochemical Behavior of Titanium and its Alloys during the Electrolysis of Chloride Solutions	177
F. N. Tabadze, S. N. Mandzhgaladze, T. S. Dashniani, I. N. Lordkipanidze, and L. F. Tavazde. Electrochemical and Corrosion Investigations of Ti-Al Alloys	186
F. A. Orlova, and T. A. Tumanova. Corrosion Resistance and Electrochemical Behavior of Titanium and Its Alloys in Solutions of Inorganic Acids Containing Oxidation Agents	189

III. MECHANICAL AND TECHNOLOGICAL PROPERTIES OF TITANIUM ALLOYS 199

S. G. Fedotov. Dependence of the Elastic Properties of Titanium Alloys on Their Composition and Structure	199
I. I. Kornilov and T. T. Nartova. Investigation of the Heat Resistance of Alloys of the Ti-Al-Sn System by the Bending Method	216
B. K. Vul'f and S. A. Yudina. Mechanical Properties of AT-3, AT-4, AT-6, and AT-8 Heat Treated Titanium Alloys	221
V. S. Mikheev, K. P. Markovich, and Z. G. Friedman. Heat Resistance, Creep, and Thermal Stability of the AT-3 Alloy	229
V. A. Livanov, N. M. Keleshyan, S. M. Fainbron, and R. M. Ryabova. The Composition and Properties of Industrial Melts of the AT-3 Titanium Alloy	233
L. P. Nikitina. The Dependence of the Mechanical Properties and Heat Resistance of AT-Titanium Alloys on the Temperature	239
I. I. Kornilov, V. S. Mikheev, O. N. Andreev, and P. S. Maiboroda. A Comparison of the Heat Resistance of Some Titanium Alloys at 450-700°C	250
A. E. Shelest, Z. S. Falaleeva, and I. M. Pavlov. Alterations in the Mechanical Properties of the AT-3 Alloy After Cold Working and Annealing	262
I. I. Kornilov, A. Ya. Shinyaev, and O. N. Andreev. The Activation Energy of Creep and the Mechanism of Plastic Deformation of Titanium Alloys	268
V. Ya. Ostrenko, N. V. Bogoyavlenskaya, L. D. Bobrikov, E. P. Akimova, V. K. Usov, L. N. Okhramovich, and L. A. Il'vovskaya. Tube Production from the AT-3 Titanium Alloy	271
A. P. Gulyaev, A. E. Shelest, V. I. Mishin, N. N. Kossakovskaya, and I. M. Pavlov. The Influence of Heating in Different Gases on the Toughness [Impact Strength] of Commercial Titanium	279
V. I. Shilov, V. P. Korzh, and L. P. Odinkova. The Investigation of Cold Rolling of a Titanium Alloy Strip	283
M. Kh. Shorshorov and G. V. Nazarov. Phase Transformations in the Heat-Affected Zone of α - and $\alpha + \beta$ -Titanium Alloys and the Criteria for Choosing the Welding Processes	297
M. Kh. Shorshorov, G. V. Nazarov, and V. V. Belov. The Mechanism of Delayed Failure and the Formation of Cold Cracks During Welding of Titanium Alloys and of Steels	303
E. A. Vinogradova, N. F. Lashko, and V. N. Moiseev. Metastable Structural Transformations and their Influence on the Properties of $\alpha + \beta$ -Titanium Alloys	312
N. G. Boriskina and I. I. Kornilov. Mechanical Properties of Ti-Cr-Fe, Titanium-Rich Alloys (Phase Diagram Sections with 0.5 and 1.5% Fe)	320
V. A. Livanov, A. A. Bukhanova, B. A. Kolachev, and N. Ya. Gusel'nikov. Hydrogen Embrittlement of Titanium Alloys	328
A. Ya. Shinyaev and V. V. Bondarev. Soldering and Brazing of AT-3 Titanium Alloys Coated with Different Electrodeposits	336
N. I. Belan, M. S. Borisova, B. M. Idel'chik, and A. A. Chikurova. AT-3, AT-4, AT-6, and VT-3-1 Titanium Alloys Used in the Production of Compressor Rotors (Impellers) Operating in Different Corrosive Media	344
D. V. Budrin, E. L. Sukhanov, and V. I. Shilov. Heating and Cooling of Specimens of Titanium and Its Alloys	354
D. V. Ignatov. Oxidation of Titanium and Its Protection Against Gas Corrosion	361
V. A. Livanov, V. S. Mikheev, S. M. Fainbron, A. A. Kutsenko, and S. E. Ivanova. Short- and Long-Term [Creep] Strength of Six-Component Titanium Alloys AT-3, AT-4, AT-6, and AT-8 (According to Data Obtained with Industrial Melts)	361
V. Ya. Ostrenko, E. P. Akimova, and L. A. Il'vovskaya. The Investigation of the Properties of AT-4 Titanium Alloys and Their Use in the Manufacture of Tubes	381
Decisions of the Second Seminar on the Theoretical and Experimental Investigations of Titanium Alloys	381

FOREWORD

The Second Conference on the Theoretical and Experimental Investigation of Titanium Alloys took place at the Metallurgical Institute imeni A. A. Baikov in March 1962.

The second conference had a considerably wider scope than the first, the proceedings of which were published as Titanium and Its Alloys [Titan i ego splavy], No. 7 (Izdatel'stvo AN SSSR, 1962), and the lectures covered a large number of problems concerning the chemistry of titanium, its metallurgy, its reaction with gases, and the relationship of technological and anticorrosion properties of titanium alloys to their composition and structure.

Participation in the second conference on titanium and its alloys was not limited to scientists of the Metallurgical Institute and papers were also read by workers from other institutes and plants which cooperate with the Metallurgical Institute in this field.

Papers on the reaction of titanium with other elements and on the various properties of titanium alloys were read by members of the Institute of Metallurgy of the Georgian SSR, the Moscow Aviation Technological Institute, the L'vov State University, and other establishments.

A number of papers dealt with the investigation of the technological and mechanical properties of titanium alloys developed by the Metallurgical Institute imeni A. A. Baikov (TsKTI imeni I. I. Polzunov, UKRNITI, the Nevskii Machine-Building Plant imeni V. I. Lenin, and others).

Publication of the proceedings of the second conference on titanium alloys should stimulate further investigation of these alloys and their application in various branches of industry.

I. I. Kornilov, Conference organizer

EXPLANATORY LIST OF ABBREVIATED NAMES OF USSR INSTITUTIONS
AND PERIODICALS APPEARING IN THE TEXT

Abbreviation	Full name (transliteration)	Translation
AN SSSR	Akademiya Nauk SSSR	Academy of Sciences of the USSR
AN UKrSSR	Akademiya Nauk Ukrainskoi SSR	Academy of Sciences of the Ukrainian SSR
GOST	Gosudarstvennyi Obshchesoyuznyi Standart	State All-Union Standard
GSSR	Gruzinskaya SSR	Georgian SSR
Izv. SFKhA	Izvestiya Sektora Fiziko-khimi- cheskogo Analiza	Bulletin of the Section of Physicochemical Analysis
NTI	Nauchno-Tekhnicheskaya Informatsiya	Scientific and Technical Information
OKB	Osoboe Konstruktorskoe Byuro	Special Design Office
OKhN	Otdelenie Khimicheskikh Nauk	Section of Chemical Sciences
OTN	Ordlenie Tekhnicheskikh Nauk	Section of Engineering Sciences
SM SSSR	Soviet Ministrov SSSR	Council of Ministers of the USSR
TsBTI	Tsentral'noe Byuro Tekhnicheskoi Informatsii	Central Office for Technical Information
TsKTI	Tsentral'nyi Nauchno-issledo- vatel'skii Kotlo-turbinnii Institut imeni I. I. Polzunova	Central Scientific Research Institute for Turbines and Boilers imeni I. I. Polzunov
TsITEIN	Tsentral'nyi Institut Tekhniko- Ekonomicheskoi Informatsii	Central Institute for Technical and Economic Information
UFAN	Ural'skii Filial Akademii Nauk SSSR	The Ural Branch of the Academy of Sciences of the USSR
UKrNITI	Ukrainskii Institut Nauchno- Tekhnicheskoi Informatsii	Ukrainian Institute of Scientific and Technical Information
UPI	Ural'skii Politekhnikeskii Institut imeni S. M. Kirova	Ural Polytechnic Institute imeni S. M. Kirov
VINITI	Vsesoyuznyi Institut Nauchnoi i Tekhnicheskoi Informatsii	All-Union Institute of Scientific and Technical Information
VSNKh RSFSR	Sovet Narodnogo Khozyaistva RSFSR	Council of National Economy of the RSFSR
VVIA	Air Force Engineering Academy	Voennno-vozdushnaya Inzhenernaya Akademiya
ZhNKh	Journal of Inorganic Chemistry	Zhurnal Neorganicheskoi Khimii
ZhPKh	Journal of Applied Chemistry	Zhurnal Prikladnoi Khimii

1. REACTION OF TITANIUM WITH OTHER METALS AND THE STRUCTURE OF TITANIUM ALLOYS

CHEMICAL INVESTIGATION OF TITANIUM

I. I. Kornilov

N67 1176

Previous investigations by the author on the chemistry of titanium /1-4/ have dealt with the general problem of the relationship between the formation of solid solutions containing titanium and its compounds and the position of the various alloying elements in the periodic classification system. It was concluded from these investigations that the formation of continuous and limited solid solutions and of titanium compounds with metallic and ionic bonds, depends on the similarity of the atomic radii and of the electron structure of the alloying elements.

The physicochemical properties of titanium alloys were determined and the chief types of equilibrium diagrams of binary and ternary titanium systems were drawn on the basis of the chemical reactions of titanium with other elements.

The discussion of these investigations included a review of the principles according to which the maximum concentrations of α - and β -solid solutions of titanium are determined, while note was taken of the dependence of the peritectic, peritectoid, eutectic, and eutectoid reactions of titanium systems on the electron structure of atoms and on the position of the reacting elements in the periodic system of elements.

It should be pointed out that the laws governing the formation of titanium alloys and the equilibrium diagrams of titanium systems have been examined by other investigators /5-7/, and a discussion of the crystallochemistry of titanium and its compounds has been published /8/. Nevertheless, the most recent data on the chemistry of titanium have not yet been summarized and no comparison has been made between the properties of the metal thus shown and those of elements belonging to different groups and periods of the periodic system.

In the discussion of this problem, it should be borne in mind that titanium belongs to the metals of the IVth group and has four external electrons, two of which are in the incomplete d-shell and the other two in the external s-shell. Titanium has also two crystallographic modifications (β and α) with body-centered cubic and face-centered cubic lattices, and a high chemical activity.

A consideration of the equilibrium diagrams of titanium alloys published by the present author and others /3-7, 9/, should take account of the fact that these alloys were prepared from titanium containing widely varying percentages of oxygen, nitrogen, hydrogen, and other impurities. The equilibrium diagrams of the binary titanium systems may thus be called binary only with some reservations and must be evaluated critically with this limitation in view.

As has been mentioned elsewhere by the author [1-4], metals forming alloys with titanium include those very similar in properties (zirconium and hafnium), whose structure is isomorphic to α - and β -titanium and, in addition, metals of the Vth group (vanadium, niobium, and tantalum) and of the VIth group (chromium, molybdenum, tungsten, and uranium), which also have an incomplete d-shell and are isomorphic to β -titanium. The number of external electrons in the atoms of these metals is:*

Ti	Zr	Hf	V	Nb	Ta	Cr	Mo	W	U
$3d^2 4s^2$	$4d^2 5s^2$	$5d^2 6s^2$	$3d^3 4s^2$	$4d^4 5s^1$	$5d^3 6s^2$	$3d^5 4s^1$	$4d^5 4s^1$	$5d^4 6s^2$	$6d^3 7s^2$

As a result of the relationship between the external electrons in the d- and s-shells of these elements and due to the similarity of their atomic radii and electrochemical properties as well as because of their isomorphic structure, the other metals of the groups mentioned easily replace the atoms in the crystal lattice of titanium, the external electrons being rapidly and uniformly distributed over the interionic space.

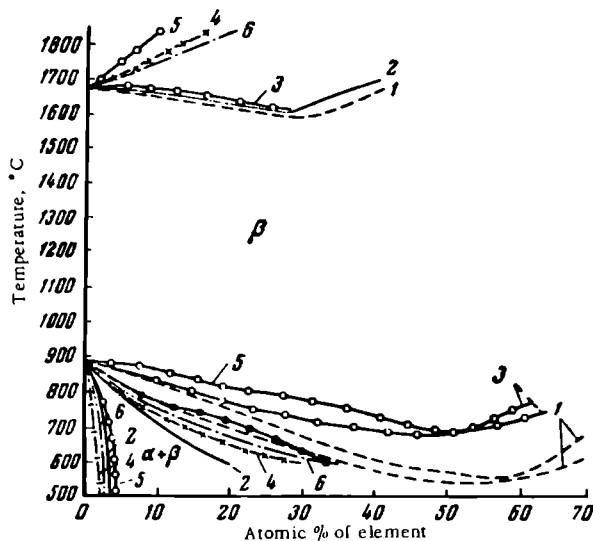


FIGURE 1. Titanium alloys with continuous solid solutions with α - and β -Ti (Ti-Zr, Ti-Hf) and with β -Ti (Ti-V, Ti-Nb, Ti-Ta, Ti-Mo)

1-Ti-Zr; 2-Ti-V; 3-Ti-Hf; 4-Ti-Nb; 5-Ti-Ta; 6-Ti-Mo.

Free equilibrium diagrams of these systems together with liquidus and solidus curves and the $\beta \rightarrow \alpha$ transformations are given in Figure 1. These equilibrium diagrams are characterized by a group of almost identical curves representing the beginning and end of the crystallization and also the α and β transformations.

Because of the complete analogy between titanium, zirconium, and hafnium, the equilibrium diagrams of systems comprising these metals are

* [According to Sneed, Maynard, and Brasted (Comprehensive Inorganic Chemistry, Vol. 1:12-14, Van Nostrand, 1956) the electron configurations for Mo, U, and Ni are as follows:

Mo	U	Ni
$4d^5 5s^1$	$6d^{(1)} 7s^{(2)}$	$3d^8 4s^2$

(numbers in parentheses uncertain).]

almost identical and represent continuous α - and β - solid solutions. The exclusion of thorium from this group of elements is due to the considerable difference between the atomic radii of thorium and titanium. The latter two elements form only limited solid solutions /9/.

The Ti-V, Ti-Nb, Ti-Ta, and Ti-Mo alloys contain continuous solid solutions of β -titanium and a limited range of β -solid solutions. The other two metals of the VIth group—chromium and uranium—are not shown in Figure 1. These, however, form continuous solid solutions with β -titanium, which undergo eutectoid transformations in the solid state. It may be assumed that tungsten, which has similar properties to chromium, molybdenum, and uranium, would also form continuous solid solutions with β -titanium. However, further, investigation is required to confirm the existence of such solutions.

In systems consisting of continuous solid solutions (Figure 1) the author could find no compounds, even of the Kurnakov type, with an ordered structure, which indicates that these solid solutions have no additional chemical bonds between the electrons.

The small degree of deformation of the crystal lattice and the almost uniform electron density of the atoms in the region of uniform solid solutions of titanium with the above elements results in a high degree of plasticity being preserved in α and β solutions of solid titanium alloys with a high content of the alloying metal, despite a considerable increase in strength. These properties are a feature of recently developed alloys of titanium with the above metals, which show high ductility even at temperatures of -196°C and lower /10, 11/.

Metals with different number of external electrons and with different atomic radii react differently with titanium and form alloys which do not contain real solutions but limited α - and β -Ti solid solutions and also intermetallic compounds.

This is convincingly demonstrated by a comparison of the equilibrium diagrams of titanium alloys containing metals of groups V-VIII of the fourth period (to the right of titanium).

The atoms of these metals have the following number of external electrons:

V	Cr	Mn	Fe	Co	Ni	Cu
$3d^3 4s^2$	$3d^5 4s^1$	$3d^5 4s^2$	$3d^6 4s^2$	$3d^7 4s^2$	$3d^8 4s^1$	$3d^{10} 4s^1$

These elements, except copper, belong to the transition metals and are characterized by a gradually increasing number of electrons in the d-shell from three for vanadium to eight for nickel and ten for copper. The atomic radii and the ionization potentials also increase from titanium through vanadium to nickel.

In these systems, titanium, which has a considerable number of electrons (up to six) that do not fill the d-shell and are close to the nucleus, can be, as was pointed out by G. V. Samsonov /7/, an acceptor of electrons introduced by other elements. This propensity of titanium will increase with the increasing number of electrons in the d-shell and with the decrease in the potential of the alloying elements. The acceptor properties of titanium become apparent through the change in the density of electrons and through the formation of additional phases which take place as the maximum concentration of solid solutions of titanium decreases. The solubility decreases as the d-shell of the alloying metal becomes filled. The greater

the difference between the electron structure of the atoms of the alloying metal and that of titanium, the deeper becomes the gradual depression of the solidus curves of the corresponding system and the greater the gradual decrease of the maximum solubility of the alloying metal in β -titanium at the eutectic temperature (Figure 2). The same sequence of variations in the fusibility diagram and of the maximum solubility of alloying metals in β -titanium may also be assumed for the elements belonging to periods 5 and 6. A comparison of the curves showing the beginning of the temperature drop and the $\beta \rightarrow \alpha$ transformation with those of the eutectic temperatures (see Figure 2), shows that the above sequence is reversed (except for chromium). The depression on the curves representing the beginning of the $\beta \rightarrow \alpha$ transformations of the various metals is deepest for manganese and decreases in depth in the order $\text{Mn} \rightarrow \text{Fe} \rightarrow \text{Co} \rightarrow \text{Ni}$. The temperature of the eutectoid transformation increases in the same order. In alloys containing the following elements of the same period the temperatures of the eutectoid transformation increase in the order $\text{Cu} \rightarrow \text{Zn} (?) \rightarrow \text{Ga} \rightarrow \text{Ge}$ and there is a gradual transition to peritectoid transformations (from copper to gallium). The nature of the equilibrium diagrams shown in Figure 2 indicates the possibility of obtaining many alloys with intermediate properties and structures as result of hardening from the β -region.

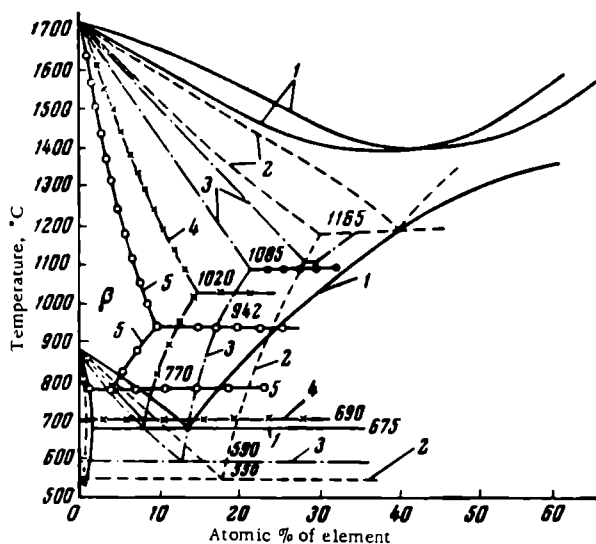


FIGURE 2. Titanium systems with limited α - and β -solid solutions and eutectoid transformations

1 — Ti — Cr; 2 — Ti — Mn; 3 — Ti — Fe; 4 — Ti — Co; 5 — Ti — Ni.

Intermetallic compounds of titanium with the metals given below are formed beyond the solubility limits in β - and α -titanium [9]:

	V	Cr	Mn	Fe	Co	Ni	Cu
Composition of compound . . .	None	TiCr ₃	TiMn	TiFe Ti ₃ Fe (?)	Ti ₃ Co	Ti ₃ Ni	Ti ₃ Cu
Melting point, °C	—	1350	1200	1500 (TiFe)	1055	1015	990

These data and the stoichiometric compositions of the compounds show that the greater the differences between the properties of the constituent elements, the larger the number of titanium atoms in the compound formed (in the order TiCr₃ → TiMn → Ti₃Ni). There is also a gradual decrease in the temperatures of formation of these compounds. An exception to this rule is the Ti—Fe system in which the melting point of Ti₃Fe lies between those of TiMn and Ti₃Co. The intermetallic compounds formed in these systems and their different solubilities in β- and α-titanium greatly influence the solution and the precipitation heat treatment of titanium alloys.

When the differences between the chemical properties of titanium and the alloying elements become even greater, a regularly increasing redistribution of electrons takes place in the different titanium-base phases together with a decrease in the solubility of these phases in β-titanium. There is also a gradual transition from eutectic to peritectic reactions. This is most apparent in the alloys formed by titanium with elements of the second period (Li—Be—B—C—N—O), which are characterized by the following distribution of the external electrons:

Li	Be	B	C	N	O
2s ¹	2s ²	2s ² 2p ¹	2s ² 2p ²	2s ² 2p ³	2s ² 2p ⁴

The wide difference between the atomic radii of lithium and titanium prevents entirely the formation of solutions and intermetallic titanium-lithium compounds. Nevertheless, despite the even less favorable relationship between the atomic radii of titanium and beryllium and despite their greatly differing electrochemical properties, beryllium forms β-solid solutions (with a low beryllium content) with β-titanium and many stable intermetallic compounds exist as follows: TiBe, TiBe₂, TiBe₄, TiBe₁₀, and TiBe₁₂.

The transition in this group from B to O (B → C → N → O) is accompanied by the appearance of external electrons in the p-shell which impart metalloid properties to the elements. In addition, the atomic radii of these elements are quite small and decrease successively from boron to oxygen. The reaction of these elements with titanium is of a quite different nature to those described above. With the passage from boron to carbon, nitrogen, and oxygen, interstitial solid solutions replace substitutional solid solutions; the intermetallic compounds formed by these elements with titanium are also to be found in the interstitial phases and have a high melting point.

An investigation of the general equilibrium diagrams of these systems shows certain peculiarities. The fields of the diagrams of the Ti—B, Ti—C, Ti—N, and Ti—O systems adjacent to the β- and α- solid solutions are indicated in Figure 3. As is seen, the Ti—B system is of a transitional nature. In the case of boron there is a region of small area indicating the formation with β-titanium of a solid solution with a melting point a little lower than that of the eutectic. The other elements — carbon, nitrogen, and

oxygen — react peritectically with titanium, and their solubility in β -titanium at the temperature of the peritectic increases in the following order: $B \rightarrow C \rightarrow N \rightarrow O$. This can be explained by the decreasing atomic radii from boron to oxygen and consequently by the possibility of a full penetration of the atoms of these elements into the lattice of β -titanium.

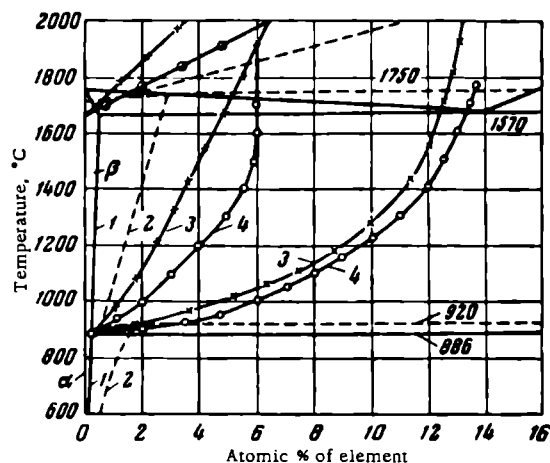


FIGURE 3. Titanium systems with eutectic and peritectic transformations

1 — Ti — B; 2 — Ti — C; 3 — Ti — N; 4 — Ti — O.

The solubility of the above elements in α -titanium greatly differs from that in β -titanium. Boron and carbon have a very low solubility and react peritectically; nitrogen and oxygen considerably widen the field of α -Ti solid solutions.

The wide field of α -solid solutions formed by titanium with nitrogen and with oxygen and the gradual transition toward formation of compounds in these systems is shown in Figure 4 [9]. The field of α -solid solutions is wider in the Ti—O than in the Ti—N system which can be explained by the smaller atomic radius of oxygen.

All these elements, which have small atomic radii, and electron structures quite different from those of titanium, form with the latter rather stable compounds with metallic bonds, giving a stoichiometric ratio between the atoms of titanium and of the alloying compound of at least 1 : 1. The formation of these compounds is due to the additional chemical bond between the external electrons.

The compounds found in these systems have the following compositions:



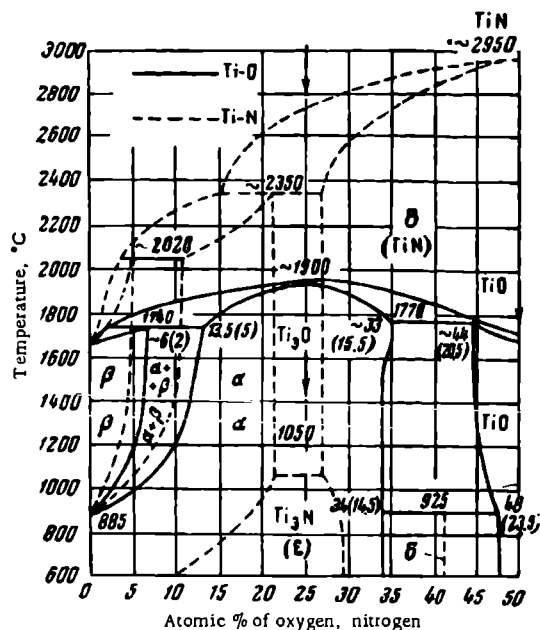


FIGURE 4. Binary Ti—N and Ti—O systems with the possible formation of Ti_3N and Ti_3O compounds

Considerable interest attaches to the formation of compounds of titanium with carbon, nitrogen, or oxygen, in which the number of titanium atoms is larger than that of the other element (suboxides, subnitrides, etc.). The Ti—N system contains a Ti_3N compound (ϵ phase) which is formed in the heterogeneous field of the solid /9/.

Analysis of the published data on the reaction between titanium and oxygen led the author, in 1959, to the conclusion that the compounds Ti_3O and Ti_2O can be formed. The conclusion as to the existence of the compound Ti_3O is based on the fact that the melting curve of the Ti—O system (see Figure 4) has a sloping maximum at a composition corresponding to this compound. The compound has probably an ordered structure.

The existence of Ti_2O has likewise been assumed by other workers /13/.

The investigation of the Ti—O system and of the properties of titanium-oxygen alloys should contribute much to the metallurgy of titanium and elucidate the role of oxygen in the formation of intermediate phases in oxygen-rich titanium alloys.

The existence of Ti_3O and Ti_2O leads to the assumption that the compounds Ti_3C (or Ti_2C) are also to be found. This problem, however, has not yet been investigated in detail /3, 9/.

The transition from metalloids, which have a low solubility in β -Ti, to metals is accompanied by an increase in the solvent power of β -titanium which is apparent from the reaction of titanium with the elements of the IVth group (subgroup B). The external electrons of the elements of this

subgroup are distributed in the following way:

C	Si	Ge	Sn	Pb
$2s^2 2p^2$	$3s^2 3p^2$	$4s^2 4p^2$	$5s^2 5p^2$	$6s^2 6p^2$

The metalloids (carbon and silicon) are followed by germanium, tin, and lead. Despite the same position of the external electrons in the s - and p -shells, these metals give up electrons easier than they attract them and their metallic properties increase in the order $\text{Ge} \rightarrow \text{Sn} \rightarrow \text{Pb}$.

This behavior is facilitated by the increasing distance of the external electrons from the atomic nuclei — in the order $\text{Ge} \rightarrow \text{Sn} \rightarrow \text{Pb}$. This order of variation in the chemical properties of the elements is reflected in their solubility in β -titanium. Figure 5 shows that the solubility in β -titanium is lowest for carbon and increases through silicon, germanium, and tin, to reach a maximum magnitude for lead. The solubility increases in the order $\text{Ge} \rightarrow \text{Sn} \rightarrow \text{Pb}$ despite the increasing differences between the atomic radii of these elements and that of titanium. The varying number of compounds formed in these systems is in full agreement with the differing negative potentials of the alloying elements.

The following compounds are formed in these systems:

Ti — C	Ti — Si	Ti — Ge	Ti — Sn	Ti — Pb
$\text{Ti}_3\text{C} (?)$ $\text{Ti}_6\text{C} (?)$	$\text{Ti}_3\text{Si}_2, \text{TiSi}, \text{TiSi}_2$	$\text{Ti}_3\text{Ge}_2 (?)$	$\text{Ti}_3\text{Sn}, \text{Ti}_2\text{Sn}_3,$ Ti_4Sn_5	$\text{Ti}_4\text{Pb} (?)$

The composition of some titanium compounds containing carbon, germanium, or lead has not yet been exactly determined. Nevertheless, it is obvious that irrespective of whether the elements are metalloids (carbon and silicon) or metals (germanium, tin, lead) their more negative potential results in their formation with titanium of various high-melting compounds whose properties, including their various solubilities in β - and α -Ti should be very important in connection with the solution and precipitation heat treatment of titanium alloys (according to the physico-chemical theory of heat-resisting alloys /14/). The high-melting compounds of titanium (carbides, silicides) are themselves of great importance as the basis for hard, heat-resistant, and other alloys.

The phase diagrams on Figure 5 show no direct relationship between the solubility of alloying elements in α -Ti and the temperature of the $\beta \rightleftharpoons \alpha$ transformations in these systems on the one hand, and the electron structure of the alloying elements on the other. In some systems (Ti—Si, Ti—Pb) the transformations are eutectoid, while in others (Ti—C, Ti—Ge, and Ti—Sn) they are peritectoid. This problem must be investigated further with purer charging materials.

On the basis of a comparison of the reactions of titanium with the elements of the IIIrd group (subgroup B) — aluminum, gallium, indium, thallium — important conclusions have been reached as to the solubility of alloying elements during peritectoid reactions.

The systems Ti—Al, Ti—Ga, and Ti—In have so far been investigated /3, 9/. All these systems have a wide field of β - and α - solid solutions of

titanium and are characterized by peritectoid reactions. Having a negative potential, these alloying elements form a number of intermetallic compounds with titanium, both during crystallization and as a result of the transformations in the solid state. A good example of the chemical transformations taking place in solid titanium solutions is afforded by the Ti—Al system. In this system the compounds Ti_5Al and Ti_3Al are formed in the solid solution /15/.

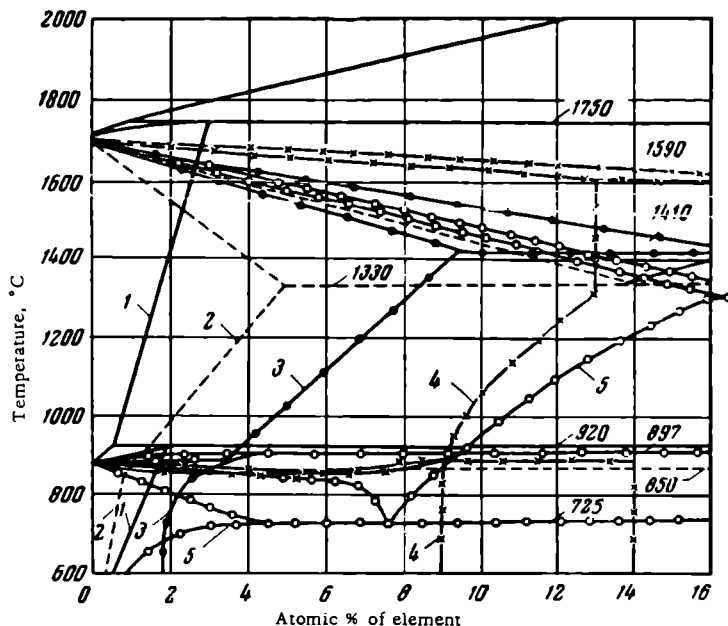


FIGURE 5. Systems of titanium with elements of the IVth group (subgroup B)

1 — Ti—C; 2 — Ti—Si; 3 — Ti—Ge; 4 — Ti—Sn; 5 — Ti—Pb.

In Ti—Ga and Ti—In systems, Ti_3Ga and Ti_3In compounds with an isomorphic structure are also formed. These compounds may serve as a basis for a new group of high-strength titanium alloys. This has been indicated elsewhere by the author /14/ and /16/. The latter investigation deals in particular with the development of a new heat-resisting titanium alloy based on the compound Ti_3Al .

The principles underlying the formation of solid solutions and of titanium compounds as described above and also the comparison of equilibrium diagrams of titanium with elements belonging to different periods and groups of the periodic system are extremely important for the study of the chemistry of titanium, for the elucidation of those equilibrium diagrams of binary titanium systems which have so far received little or no attention, and for theoretical and experimental investigations of the reactions of titanium in ternary, quaternary, and more complex systems.

Bibliography

1. Kornilov, I. I. — *Izvestiya AN SSSR, OKhN*, No. 3:392. 1954.
2. Kornilov, I. I. — *ZhNKh*, 3(2):320. 1958.
3. Kornilov, I. I. and P. B. Budberg. *Diagrammy sostoyaniya dvoynykh i troynykh sistem titana (Phase Diagrams of Binary and Ternary Titanium Systems)*. — Izdatel'stvo VINITI AN SSSR. 1961.
4. Kornilov, I. I. — *Sbornik "Titan i ego splavy"*, No. 7:5, Izdatel'stvo AN SSSR. 1962.
5. Glazunov, S. G. and S. G. Molchanova. *Diagrammy sostoyaniya splavov titana (Phase Diagrams of Titanium Alloys)*. — Oborongiz. 1954.
6. Pherson D. and M. Hansen. — *Zs. Metallk.*, Vol. 45:76. 1945.
7. Samsonov, G. V., V. S. Neshpor, and L. V. Lange. *Metallovedenie i obrabotka metallov (Metallurgy and Machining of Metals)*, No. 1:35. 1956.
8. Ageev, N. V. *Khimiya, metallovedenie i obrabotka titana (Chemistry, Metallurgy and Treatment of Titanium)*. — *Itogi Nauki, Tekhnicheskies Nauki*, Vol. 2:5, Izdatel'stvo AN SSSR. 1959.
9. Hansen, M. and K. Anderko. *Constitution of Binary Alloys*, Vol. 1. — McGraw-Hill Co. 1958. [Russian translation. 1962].
10. Kornilov, I. I., O. K. Belousov, and V. S. Mikheev. — *Doklady AN SSSR*, 145 (5):1102. 1962.
11. Kornilov, I. I., O. K. Belousov, and V. S. Mikheev. — *Sbornik "Titan i ego splavy"*, No. 7:120, Izdatel'stvo AN SSSR. 1962.
12. Kornilov, I. I. — *Trudy analiticheskoi konferentsii geokhimi-cheskogo instituta AN SSSR*, Vol. 10:17, Izdatel'stvo AN SSSR. 1960.
13. Nowotny, H. and E. Dimakopoulou. — *Monatschr. f. Chemie*, 90(5):620. 1959.
14. Kornilov, I. I. *Fiziko-khimicheskie osnovy zharoprochnosti splavov (Physicochemical Principles of Heat Resistant Alloys)*. — Izdatel'stvo AN SSSR. 1961.
15. Kornilov, I. I., N. V. Grum-Grzhimailo, E. N. Pylaeva, and M. A. Volkova. — *Doklady AN SSSR*, 137(3):599. 1961.
16. Kornilov, I. I. and T. T. Nartova. — *Sbornik "Titan i ego splavy"*, No. 7:95, Izdatel'stvo AN SSSR. 1962.

INVESTIGATION OF THE PHASE EQUILIBRIUM OF THE Ti—Al—Mo SYSTEM IN THE TITANIUM-RICH ALLOY FIELD

Ge Dzhzhi-Min and E. N. Pylaeva

A systematic study of the phase diagrams of titanium systems is being carried out at the Institute of Metallurgy imeni A. A. Baikov, as part of an investigation of the quarternary Ti—Al—Mo—V system.

The binary Ti—Al and Ti—Mo systems constitute the side fields of the ternary Ti—Al—Mo system.

The phase diagram of the Ti—Al system has been widely investigated /1-9/. Early investigations /1-3/ assumed the existence of quite a wide field of solubility of aluminum in α -Ti. According to early data /2/, up to 24.5 % of aluminum dissolves in α -Ti at 900°C and up to 34.5 % of aluminum dissolves in β -Ti at 1460°C. The homogeneous field of the γ phase based on the TiAl intermetallic compound, which is formed at 1460°C as a result of a peritectic reaction, extends from 37 to 60 % of aluminum for high temperatures, and from 35.5 to 44.5 % of aluminum for temperatures below 1000°C. In some more recently published works /4-7/ conflicting data are to be found on the existence of new phases in titanium-rich Ti—Al alloys. An indication is given in the work of Sagel et al. /5/ of the existence of a homogeneous α phase containing from 12 to 16 % of Al and of an ϵ -phase with a face-centered tetragonal lattice, containing about 18.5 % of Al. According to the data given in the same work /5/, the solubility of aluminum in α -Ti at room temperature is about 6 %.

Sato, Khuan Yan'-tsin, and Kondo /6/ investigated this system at high temperatures by measuring the electrical resistance. They demonstrated the formation of a solid solution in the field between 26 and 34 % of Al based on Ti_3Al_2 , which undergoes a eutectoid decomposition at 1050°C, and found an α_2 -solid solution on the basis of Ti_2Al containing from 19 to 25 % of aluminum. Later X-ray investigations by Ence and Margolin /7/ did not confirm the existence of a solid solution on the basis of Ti_3Al_2 but the latter authors assumed the existence of a wide field of solid solution on the basis of Ti_2Al and of a solid solution on the basis of Ti_3Al , which is unstable at low temperatures.

By determining the relationship between the Hall constants and the composition of alloys in the Ti—Al system, Grum-Grzhimailo and co-workers /8/ found two intermetallic compounds: Ti_6Al and Ti_3Al . The existence of Ti_3Al was also assumed by other investigators /9, 10/.

Molybdenum forms a continuous series of solid solutions with β -Ti. According to the data of Hansen and others /11/, the solubility of molybdenum in α -Ti at 600°C does not exceed 0.8 % while the field of the $\alpha + \beta$ transformation at this temperature lies up to 28 % of Mo.

In the Al—Mo system, a number of intermetallic compounds are to be found and the solubility of aluminum in molybdenum and vice versa is quite limited /12/.

Little work has been published on the Ti—Al—Mo ternary system. Kessler /13/ determined the boundary of the $\beta/(\alpha + \beta)$ field at contents of aluminum plus molybdenum up to 6%. Margolin and co-workers /14/ investigated this ternary system up to 30% of Mo and 35 % of Al. These workers constructed a thermal section for 1000°C which is in agreement with data published later /15/ by Böhm and Löhberg who showed by means of X-ray investigation that the alloys in the β -solid solution field adjacent to the TiAl—TiMo section will enter an ordered state if kept at 800 to 1000°C; on X-ray photographs this ordering is expressed by superlattice lines. It was assumed /15/ that these lines correspond to the Ti_2AlMo compound which has a crystal lattice of the CsCl type.

The purpose of the present investigation was to determine the phase equilibrium of the Ti—Al—Mo system for the part of the phase diagram representing titanium-rich compositions.

The authors used methods of microstructural and X-ray analysis and measured the hardness of the alloys.

Method of preparation of alloys and their heat treatment

The alloys chosen for the investigation of the ternary Ti—Al—Mo system are represented by sections parallel to the Ti—Mo side of the diagram with a constant aluminum content (0, 5, 10, 15, 20, 25, 30, 35, and 40 weight %) at a total content of aluminum plus molybdenum of 50 weight %. The sections and the compositions of the alloys investigated are shown in the concentration triangle of the Ti—Al—Mo system (Figure 1).

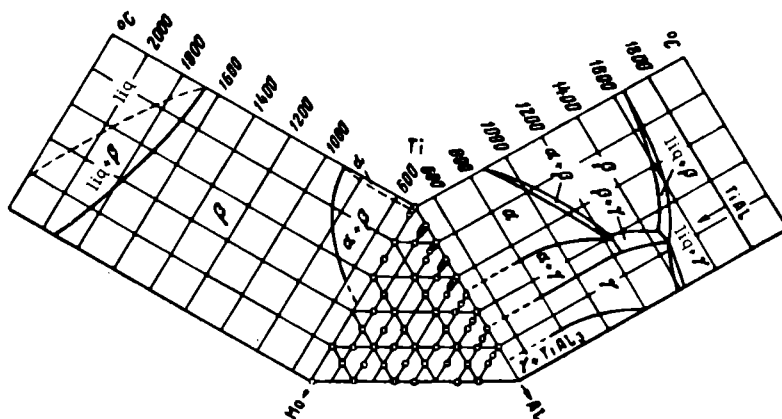


FIGURE 1. Sections and compositions of alloys of the ternary Ti—Al—Mo system and phase diagrams of binary Ti—Al and Ti—Mo systems (from the titanium side)

The experimental material was titanium iodide (99.82 %), pure aluminum (99.99 %), and pure molybdenum (99.9 %)

The specimens for this investigation were prepared by arc melting between neutral tungsten electrodes in an atmosphere of argon and also by induction melting of the material forming a suspension in purified helium [16, 17]. The composition of the specimens was controlled by exact chemical analysis and by weighing before and after smelting. An alloy was considered satisfactory if its weight differed from that of the components by not more than 0.2 %.

The specimens were given a homogenizing annealing at 1200°C for 5 hours followed by 100 hours at 1100°C, and were then quenched in water. After the microstructure and the hardness investigations, the specimens were further annealed at 900°C for 100 hours and at 800°C for 400 hours to be again quenched in water. The specimens were prepared for the construction of the 600°C isothermal section after hardening from 1100°C, by annealing at 900°C for 100 hours, at 800°C for 200 hours, at 700°C for 300 hours, and at 600°C for 600 hours before quenching in water.

Investigation of the microstructure of alloys

The microstructure of cast alloys was investigated after hardening from 1100, 800, and 600°C. The etchant consisted of equal volumes of hydrofluoric and nitric acids with the addition of glycerine and alcohol.

The microstructures of alloys of the Ti—Al—Mo system with various compositions and hardened from 1100, 800, and 600°C are indicated in the table.

Consideration will now be given to the microstructure of some of the alloys of the above ternary system (Figure 2).

The alloys represented by areas adjacent to the Ti—Al side of the diagram, containing approximately up to 24 % Al and up to 0.8 - 1.0 % Mo have at 600°C a single-phase polyhedral α -structure (Figure 2a).

The ternary alloy containing 5 % Al and 5 % Mo has a double-phase ($\alpha + \beta$) structure and the β phase network is visible only on the grain boundaries of the α phase (Figure 2b); as the content of molybdenum in the alloy increases, the thickness of the β phase network increases. A similar characteristic variation of the microstructure is shown by alloys with 5 and with 10 % aluminum.

Figure 2c shows the microstructure of an alloy with 30% Al, which is typical of binary alloys of the $\alpha + \gamma$ field. The light polyhedrons are the α phase, and the dark strips are the γ phase.

The typical microstructure of $\alpha + \beta + \gamma$ -ternary alloys is shown by an alloy with 25 % of Al and 15 % of Mo after hardening from 800°C (Figure 2d). The coarse light grains of the α phase and the thin lamella of the γ phase are visible on the background of the β phase.

A ternary γ -solid solution on the basis of TiAl containing 35 % of Al and 5 % of Mo is shown in Figure 2e. The alloy with 35 % Al and 10 % Mo which has a single-phase structure at 1100 and 800°C, similar to that shown on Figure 2e is transformed into a binary ($\beta + \gamma$) alloy at 600°C (Figure 2f).

The data obtained by X-ray investigation of the alloys confirm the results of the microstructural analysis.

The phase diagram of the investigated part of the ternary system

A systematic investigation of alloys of the ternary Ti—Al—Mo system enabled an equilibrium diagram to be constructed for the part of the system investigated.

Consideration will now be given to the isothermal sections of the system at 1100, 800, and 600°C.

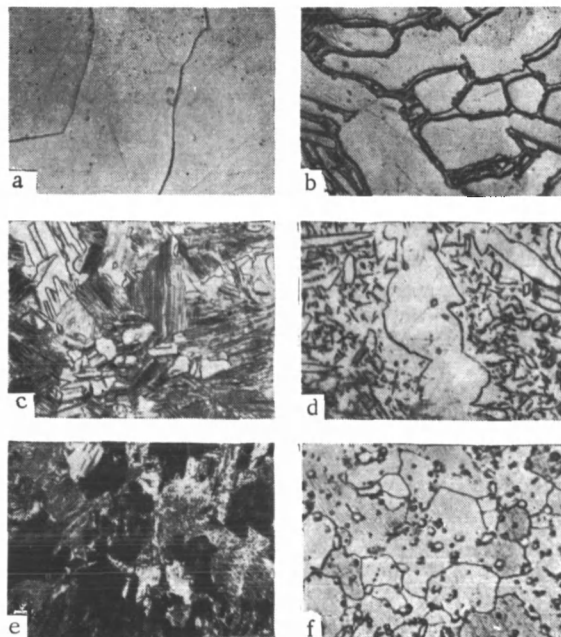


FIGURE 2. Microstructures of alloys of the Ti—Al—Mo system

- a — 5% Al and 0.5% Mo, quenching from 600°C, $\times 260$, α phase;
- b — 5% Al and 5% Mo, quenching from 600°C, $\times 440$, $\alpha + \beta$ phase;
- c — 30% Al, quenching from 600°C, $\times 400$, $\alpha + \gamma$ phase; d — 25% Al and 15% Mo, quenching from 800°C, $\times 660$, $\alpha + \beta + \gamma$ phase;
- e — 35% Al and 5% Mo, quenching from 1100°C, $\times 200$, γ phase;
- f — 35% Al and 10% Mo, quenching from 600°C, $\times 440$, $\beta + \gamma$ phase.

At 1100°C the β phase, which may include from 10 to 20 % of Al, occupies the largest area of the isothermal section. The narrow field of the α phase borders on the Ti—Al side and includes from 10 to about 25 % of Al. The ternary solid solution on the basis of TiAl, designated as the γ phase, takes up only a small field in the ternary system. The maximum solubility of molybdenum in TiAl at 1100°C is about 11 to 12 %. Titanium alloys with a total content of aluminum and molybdenum of less than 12 % have, after hardening from 1100°C, a martensitic structure designated on the diagram as α' (Figure 3a).

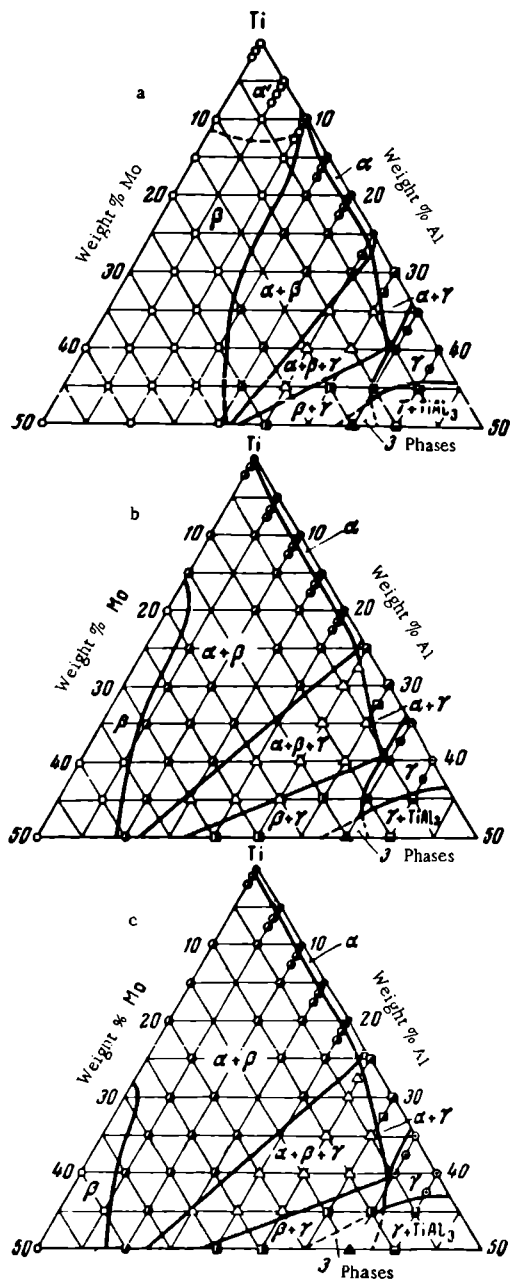


FIGURE 3. Isothermal sections of part of the ternary Ti—Al—Mo system at 1100 (a), 800 (b), and 600°C (c)

Microstructures of Ti—Al—Mo alloys hardened from 1100, 800, and 600°C

Chemical composition, weight %			Hardened from temperature, °C		
Ti	Al	Mo	1100	800	600
100	—	—	α'	α	α
99	—	1.0	α'	$\alpha + \beta$	$\alpha + \beta$
98	—	2.0	α'	$\alpha + \beta$	$\alpha + \beta$
90	—	10.0	α'	$\alpha + \beta$	$\alpha + \beta$
85	—	15.0	β	$\alpha + \beta$	$\alpha + \beta$
80	—	20.0	β	β	$\alpha + \beta$
60	—	40.0	β	β	β
50	—	50.0	β	β	β
95.0	5	—	α'	α	α
94.5	5	0.5	α'	α	α
93.5	5	1.5	α'	$\alpha + \beta$	$\alpha + \beta$
92.5	5	2.5	α'	$\alpha + \beta$	$\alpha + \beta$
90.0	5	5.0	α'	$\alpha + \beta$	$\alpha + \beta$
75.0	5	20.0	β	$\alpha + \beta$	$\alpha + \beta$
70.0	5	25.0	β	$\alpha + \beta$	$\alpha + \beta$
65.0	5	30.0	β	$\alpha + \beta$	$\alpha + \beta$
60.0	5	35.0	β	β	$\alpha + \beta$
55.0	5	40.0	β	β	β
90.0	10	—	$\alpha + \beta$	α	α
89.5	10	0.5	$\alpha + \beta$	α	α
88.5	10	1.5	α'	$\alpha + \beta$	$\alpha + \beta$
87.5	10	2.5	β	$\alpha + \beta$	$\alpha + \beta$
85.0	10	5.0	β	$\alpha + \beta$	$\alpha + \beta$
80.0	10	10.0	β	$\alpha + \beta$	$\alpha + \beta$
70.0	10	20.0	β	$\alpha + \beta$	$\alpha + \beta$
65.0	10	25.0	β	$\alpha + \beta$	$\alpha + \beta$
60.0	10	30.0	β	$\alpha + \beta$	$\alpha + \beta$
55.0	10	35.0	β	$\alpha + \beta$	$\alpha + \beta$
50.0	10	40.0	β	$\alpha + \beta$	$\alpha + \beta$
85.0	15	—	α	α	α
84.5	15	0.5	α	α	α
83.5	15	1.5	$\alpha + \beta$	$\alpha + \beta$	$\alpha + \beta$
82.5	15	2.5	$\alpha + \beta$	$\alpha + \beta$	$\alpha + \beta$
80.0	15	5.0	$\alpha + \beta$	$\alpha + \beta$	$\alpha + \beta$
75.0	15	10.0	$\alpha + \beta$	$\alpha + \beta$	$\alpha + \beta$
65.0	15	20.0	$\alpha + \beta$	$\alpha + \beta$	$\alpha + \beta$
60.0	15	25.0	β	$\alpha + \beta$	$\alpha + \beta$
55.0	15	30.0	β	$\alpha + \beta + \gamma$	$\alpha + \beta + \gamma$
80.0	20	—	α	α	α
75.5	20	0.5	α	α	α
78.5	20	1.5	$\alpha + \beta$	$\alpha + \beta$	$\alpha + \beta$
77.5	20	2.5	$\alpha + \beta$	$\alpha + \beta$	$\alpha + \beta$
75.0	20	5.0	$\alpha + \beta$	$\alpha + \beta$	$\alpha + \beta$
70.0	20	10.0	$\alpha + \beta$	$\alpha + \beta$	$\alpha + \beta$
60.0	20	20.0	$\alpha + \beta$	$\alpha + \beta + \gamma$	$\alpha + \beta + \gamma$
55.0	20	25.0	$\alpha + \beta$	$\alpha + \beta + \gamma$	$\alpha + \beta + \gamma$
50.0	20	30.0	β	$\beta + \gamma$	$\beta + \gamma$
75.0	25	2.5	α	$\alpha + \gamma$	$\alpha + \gamma$
72.5	25	5.0	$\alpha + \beta$	$\alpha + \beta + \gamma$	$\alpha + \beta + \gamma$
70.0	25	10.0	$\alpha + \beta$	$\alpha + \beta + \gamma$	$\alpha + \beta + \gamma$
65.0	25	15.0	$\alpha + \beta + \gamma$	$\alpha + \beta + \gamma$	$\alpha + \beta + \gamma$
60.0	25	20.0	$\alpha + \beta + \gamma$	$\alpha + \beta + \gamma$	$\alpha + \beta + \gamma$
55.0	25	25.0	$\alpha + \beta + \gamma$	$\alpha + \beta + \gamma$	$\alpha + \beta + \gamma$
50.0	25	—	$\beta + \gamma$	$\beta + \gamma$	$\beta + \gamma$
70.0	30	2.5	$\alpha + \gamma$	$\alpha + \gamma$	$\alpha + \gamma$
67.5	30	5.0	$\alpha + \gamma$	$\alpha + \gamma$	$\alpha + \gamma$
65.0	30	10.0	$\alpha + \beta + \gamma$	$\alpha + \beta + \gamma$	$\alpha + \beta + \gamma$
60.0	30	15.0	$\alpha + \beta + \gamma$	$\alpha + \beta + \gamma$	$\alpha + \beta + \gamma$
55.0	30	—	$\beta + \gamma$	$\beta + \gamma$	$\beta + \gamma$
85.0	35	2.5	γ	γ	γ
82.5	35	5.0	γ	γ	γ
80.0	35	10.0	γ	γ	γ
55.0	35	15.0	γ	γ	$\beta + \gamma$
50.0	35	—	3 phases	3 phases	3 phases
60.0	40	2.5	γ	γ	γ
57.5	40	5.0	γ	γ	γ
55.0	40	10.0	$\gamma + \text{TiAl}_3$	$\gamma + \text{TiAl}_3$	$\gamma + \text{TiAl}_3$
50.0	40	—	$\gamma + \text{TiAl}_3$	$\gamma + \text{TiAl}_3$	$\gamma + \text{TiAl}_3$

A comparison of the isothermal section for 1100°C with those for 800 and 600°C indicates that the $\alpha+\beta$ and the $\alpha+\beta+\gamma$ fields widen as the temperature decreases (the latter to a lesser extent); the fields of the β - and γ -solid solutions narrow. The maximum content of molybdenum in the γ -solid solution is 8 % at 600°C and 11 to 12 % at 1100°C (Figures 3a and c).

Figure 3 shows that the part of the ternary system investigated has three single-phase fields: the α -solid solution on the basis of α -titanium with a hexagonal close-packed crystal lattice; the β -solid solution with a body-centered cubic lattice; and the γ -solid solution on the basis of TiAl with an ordered phase centered tetragonal lattice; four two-phase fields $\alpha+\beta$, $\alpha+\gamma$, $\beta+\gamma$, and $\gamma+\text{TiAl}_3$; and two three-phase fields, one of which is the $\alpha+\beta+\gamma$ field.

Hardness

The hardness of quenched specimens after microstructural investigation was determined with a Vickers hardness tester (load 10 kg).

The dependence of the hardness on the composition and on the microstructure of the alloys (Figure 4) shows that irrespective of the quenching temperature, the hardest ($H_v = 400$ to 500 kg/mm^2) are those ternary alloys which have a high content of aluminum and molybdenum and a three-phase ($\alpha+\beta+\gamma$) or two-phase ($\beta+\gamma$) structure. The ternary γ -solid solution on the basis of TiAl has a low hardness ($H_v < 300 \text{ kg/mm}^2$).

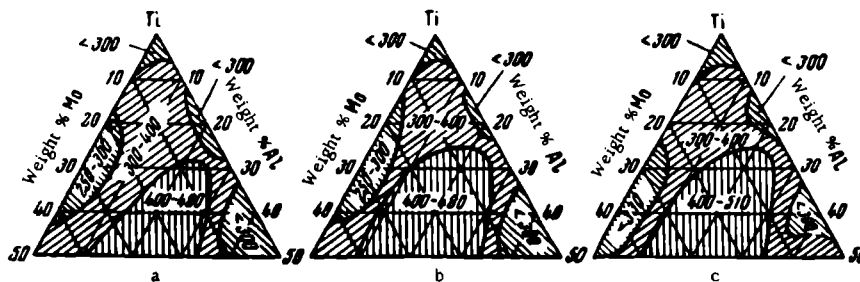


FIGURE 4. Composition-hardness (H_v) diagram of alloys of the ternary Ti-Al-Mo system hardened from 1100°C (a), 800°C (b), and 600°C (c)

Alloys containing ternary α -solid solutions have a hardness H_v of about 250 kg/mm^2 , with a minimum corresponding to about 15% of Al, which coincides with the low hardness of these alloys in the binary TiAl system and is connected with the presence of the Ti_3Al intermetallic compound [8].

Conclusions

1. The titanium corner of the ternary Ti—Al—Mo system has a small field representing a limited α -solid solution on the basis of α -Ti. The maximum solubility of molybdenum in the ternary α -solid solution at 600°C is 0.8 to 1.0%.

The field of the α -solid solution narrows with the increase in temperature from 800 to 1100°C.

2. Alloys of the three-phase ($\alpha + \beta + \gamma$) and of the two-phase ($\beta + \gamma$) fields have the highest hardness. The hardness of the γ -solid solution on the basis of TiAl compounds is relatively low. The ternary α -solid solution has a variable hardness with a minimum at about 15 % of Al.

Bibliography

1. Ogden, H. R., D. J. Maykuth, W. L. Finlay, and R. I. Jaffee. — J. Metals, 3(12):1150. 1951.
2. Bumps, E. S., H. D. Kessler, and M. Hansen. — J. Metals, 4(6): 609. 1952.
3. Duwez, P. and J. L. Taylor. — J. Metals, 4(1):70. 1952.
4. Kornilov, I. I., E. N. Pylaeva, and M. A. Volkova. — Izvestiya AN SSSR, OKhN, No. 7:771. 1956.
5. Sagel, K., E. Schulz, and U. Zwicker. — Zs. Metallk., 47(8): 529. 1956.
6. Sato, Khuan Yan'-tsin and Kondo. — Nippon Kinzoku Gakkaishi, 23(8):456. 1959.
7. Ence, E. and H. Margolin. — Trans. Met. Soc. AIME, 221(1): 151. 1961.
8. Grum-Grzhimailo, N. V., I. I. Kornilov, E. N. Pylaeva, and M. A. Volkova. — Doklady AN SSSR, 137(3):599. 1961.
9. Goldak, H. J. and J. Gordon Pair. — Trans. Met. Soc. AIME, 221(3):639. 1961.
10. Kornilov, I. I. and T. T. Nartova. — Doklady AN SSSR, 140(4): 829. 1961.
11. Hansen, M., E. L. Kamen, H. D. Kessler, and D. J. McPherson. — J. Metals, 3(10):881. 1951.
12. Sperner, F. — Zs. Metallk., 50(10):588. 1959.
13. Kessler, H. D. — Am. res. foundation, report on contract, No. 11-022—ORD to Watertown arsenal. 1951.
14. Margolin, H., T. P. Nielsen, and H. K. Work. — New York Univ. eng. res. div., Final report to Watertown arsenal laboratory on contract, No. AD-030-069-ORD-208. 1954.
15. Böhm, H. and K. Löhberg. — Zs. Metallk., 49(4):173. 1958.
16. Fogel', A. A. — Izvestiya AN SSSR, OTN, No. 2:24. 1959.
17. Fogel', A. A., N. A. Pavlov, I. V. Korkin, and T. A. Sidorova. — Izvestiya AN SSSR, OTN, No. 5:51. 1961.

INVESTIGATION OF THE PHASE TRANSFORMATIONS IN THE Ti-Al-Mo SYSTEM

Ge Dzhi-Min and E. N. Pylaeva

N67 1176

Titanium has two crystal modifications: α and β . The first has a hexagonal and the second a body-centered lattice. At 882°C, titanium undergoes a polymorphic $\alpha \rightleftharpoons \beta$ transformation. The phase diagram of the Ti-Mo system represents continuous solid solutions of molybdenum in β -titanium and a limited solid solution on the basis of α -titanium. Molybdenum greatly decreases the temperature of the $\alpha \rightleftharpoons \beta$ transformation of titanium and increases the stability of the β phase /1/. Unlike molybdenum, aluminum forms limited solid solutions in α - and β -titanium and also intermetallic compounds. It also increases the temperature of $\alpha \rightleftharpoons \beta$ transformation of titanium /2-4/.

The authors present results of the thermal analysis of alloys of the Ti-Al-Mo system with a total content of aluminum and molybdenum of up to 50 %.

The commencement of melting of the alloys was determined by the contact method using an optical pyrometer /5/ calibrated according to the melting points of the pure metals (niobium, titanium, nickel, and copper). The transformation temperatures of solid alloys were determined by the differential method using a N. S. Kurnakov pyrometer /6/.

The specimens for thermal analysis were annealed at 600°C for 600 hours and quenched in water.

The thermal analysis of the alloys included a recording of both the heating (6 to 8°C/min) and cooling curves. Typical thermograms of pure titanium, of a binary titanium alloy with 20 % Al, and of a ternary alloy with 15 % Al and 0.5 % Mo are shown in Figure 1. The thermal effect of the polymorphic $\alpha \rightleftharpoons \beta$ transformation of alloys is more marked during cooling than during heating. The transformation temperatures of the alloys were determined according to the thermal effects taking place during heating, and were checked during cooling.

The measured temperatures corresponding to the beginning of melting of the alloys together with the temperatures of their polymorphic $\alpha \rightleftharpoons \beta$ transformations in the solid state are given in the table.

The solidus isotherms of alloys of the titanium corner of the Ti-Al-Mo diagrams were recorded according to these data. As the content of aluminum increases, the melting point of titanium-aluminum alloys containing up to 5 % molybdenum steadily decreases (Figure 2). The influence of aluminum on the solidus temperature of molybdenum-rich titanium alloys is of a complex nature because of the transition from peritectic reactions to the crystallization of β -solid solutions. The addition of molybdenum to titanium and its alloys with aluminum increases their solidus temperature.

The data furnished by the thermal and microstructural analyses served as the basis for the investigation of twelve polythermal sections of part of the ternary Ti—Al—Mo system.

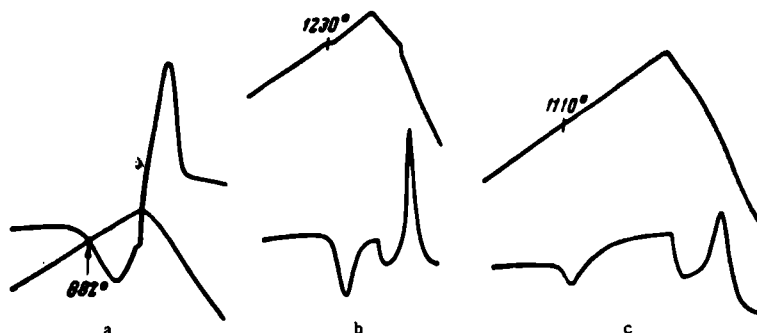


FIGURE 1. Typical thermograms of pure titanium (a), of its alloy with 20% Al (b), and of a ternary alloy containing 15 %Al and 0.5 % Mo (c)

Consideration will now be given to nine polythermal sections parallel to the Ti—Mo side of the diagram, the aluminum content being constant (0.5, 10, 15, 20, 25, 30, 35, and 40%) (Figure 3).

Melting point and $\alpha \rightleftharpoons \beta$ transformations of Ti—Al—Mo alloys

Chemical composition, weight %			Temperature, °C		Chemical composition, weight %			Temperature, °C	
Ti	Al	Mo	melting	$\alpha \rightleftharpoons \beta$ transformation	Ti	Al	Mo	melting	$\alpha \rightleftharpoons \beta$ transformation
100	—	—	1660 *	882 *	80	10	10	1720	~1050
95	5	—	1660	1000—1015	70	10	20	1750	~1050
90	10	—	1630	1100—1130	60	10	30	—	~970
85	15	—	1600	1150—1160	55	10	35	—	~940
80	20	—	1570	1230—1240	84.5	15	0.5	1600	1110—1130
76	24	—	—	~1240	83.5	15	1.5	1610	—
75	25	—	1530	~1240	82.5	15	2.5	1620	—
94.5	5	0.5	—	970—990	80	15	5	1660	~1130
93.5	5	1.5	—	~970	75	15	10	—	~1130
92.5	5	2.5	—	~920	65	15	20	—	~1130
90	5	5	1700	~900	79.5	20	0.5	1570	1220—1230
75	5	20	1780	~860	78.5	20	1.5	1600	—
70	5	25	—	~830	75	20	5	1640	~1160
65	5	30	1800	~820	70	20	10	1700	~1150
60	5	35	—	~720	72.5	25	2.5	1540	—
55	5	40	1850	—	70	25	5	1580	—
89.5	10	0.5	—	1100—1130	65	25	10	1660	—
88.5	10	1.5	—	~1080	55	35	10	—	760 **
85	10	5	1680	~1050					

* Published data.

** Temperature of $\gamma \rightleftharpoons \beta + \gamma$ transformation.

The present investigations of the Ti—Mo binary system confirm the data of Hansen et al./1/ and indicate that molybdenum greatly reduces the temperature of the $\alpha \rightleftharpoons \beta$ transformation of titanium and increases the stability of the β phase. The solubility of molybdenum in the α modification of titanium is low and does not exceed 0.8 % at 600°C (Figure 3a).

The polythermal sections representing alloys with 5 and 10 % of aluminum are similar to the phase diagrams of the Ti—Mo system (Figure 3a and c); both sections pass through the fields of crystallization of β , $\alpha + \beta$, and α phases. It can be seen from these sections that molybdenum increases the temperature of the solidus and decreases [sic] the temperature of $\alpha \rightleftharpoons \beta$ transformation of the alloys. Molybdenum has the same influence on alloys containing 15, 20, and 25 % of Al.

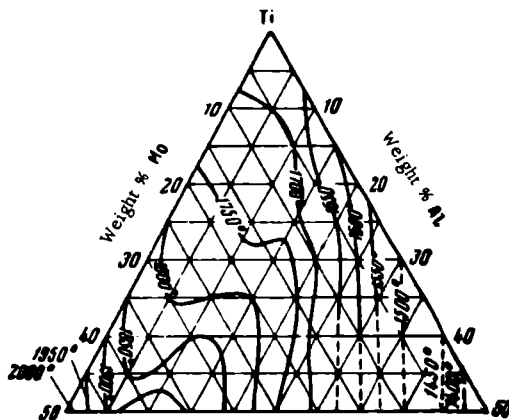


FIGURE 2. Solidus isotherms of alloys of the titanium corner of Ti—Al—Mo system

As the alloy is cooled the β phase is the first to crystallize, and this is further transformed into the α phase from which a ternary γ phase finally separates (Figure 3d, e, f). Passing from the 15 % Al section to the 25 % Al section it can be seen that the $\alpha + \beta + \gamma$ fields become wider and that there is also a new two-phase $\beta + \gamma$ field.

From alloys with 30 % of Al (Figure 3g), a solid β phase precipitates and upon further cooling a γ phase which is finally transformed as a result of a peritectoid reaction into an α phase.

Figure 3h shows that alloys with 35 % Al consist of a mixture of β and γ phases which are crystallized consecutively from the molten alloy. From melts containing 40 % of aluminum, only a single γ phase crystallizes out (Figure 3i).

Figure 4 shows three polythermal sections with a constant content of 0, 0.5, and 5 % of Mo. Thermal analysis of the binary Ti—Al system shows that aluminum decreases the melting point of alloys and increases the temperature of $\alpha \rightleftharpoons \beta$ transformation (Figure 4a).

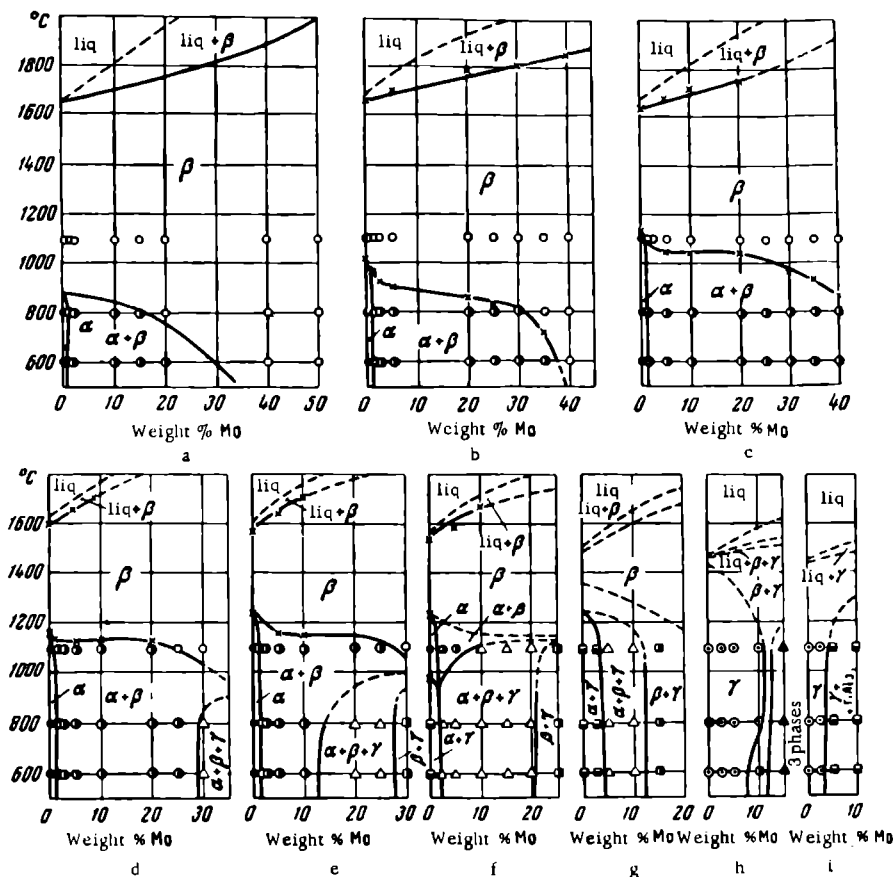


FIGURE 3. Polythermal sections parallel to the Ti-Mo side with a constant content of aluminum

a — without Al; b — with 5% Al; c — with 10% Al; d — with 15% Al; e — with 20% Al; f — with 25% Al; g — with 30% of Al; h — with 35% Al; i — with 40% Al.

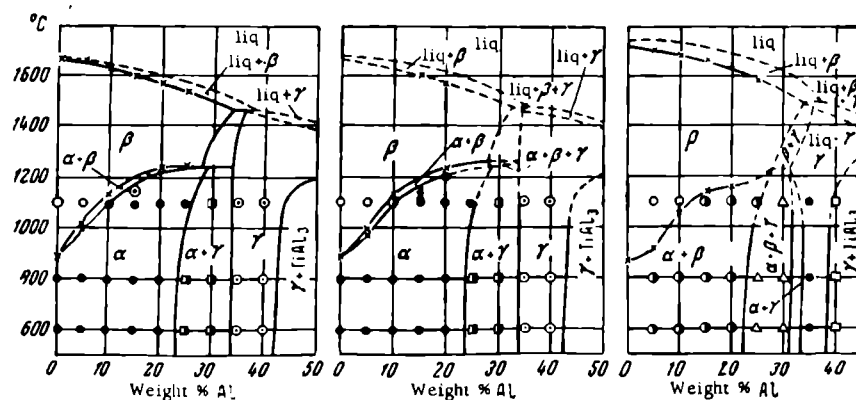


FIGURE 4. Polythermal sections parallel to the Ti-Al side with constant molybdenum content

The figures from left to right: without Mo; with 0,5% Mo; with 5% Mo.

The 0.5 % Mo section (Figure 4b) differs from the phase diagram of the Ti—Al section by the presence of narrow three-phase (liq+ β + γ) and (α + β + γ) fields and by a somewhat lower temperature of the $\alpha \rightleftharpoons \beta$ transformation of the alloys. The low temperatures of transformation of solid titanium alloys containing 15 % of Al or 15 % of Al and 0.5 % Mo (Figure 4a and b) are possibly due to the presence of the Ti₃Al inter-metallic compound [7, 8]. This problem calls for further investigation.

Figure 4c shows that alloys containing as much as 5 % of molybdenum have no α phase but have a wider two-phase α + β field. At the same time the three-phase (α + β + γ) field extends toward low temperatures.

Bibliography

1. Hansen, M., E.L. Kamen, H.D. Kessler, and D.J. McPherson.—J. Metals, 3(10):881. 1951.
2. Ogden, H.R., D.J. Maykuth, W.L. Finlay, and R.I. Jaffee.—J. Metals, 3(12):1150. 1951.
3. Bumps, E.S., H.D. Kessler, and M. Hansen.—J. Metals, 4(6):609. 1952.
4. Kornilov, I.I., E.N. Pylaeva, and M.A. Volkova.—Izvestiya AN SSSR, OKhN, No. 7: 771. 1956.
5. Mikheev, V.S.—Trudy Instituta metallurgii imeni A.A. Baikova, No. 2:154, Izdatel'stvo AN SSSR. 1957.
6. Tsurinov, G.G. Pirometer N.S. Kurnakova (The N.S. Kurnakov Pyrometer).—Izdatel'stvo AN SSSR. 1953.
7. Goldak, H.J. and J. Gordon Pair.—Trans. Met. Soc. AIME, 221(3):639. 1961.
8. Grum-Grzhimailo, N.V., I.I. Kornilov, E.N. Pylaeva, and M.A. Volkova.—Doklady AN SSSR, 137(3):599. 1961.

PHASE DIAGRAM OF THE Ti—V—Nb—Mo SYSTEM

O. K. Belousov, I. I. Kornilov, and V. S. Mikheev

There are no data on the phase diagram of the Ti—V—Nb—Mo system. The binary Ti—V, Ti—Nb, Ti—Mo systems, however, have been investigated /1-3/. These are systems with a continuous solubility of the alloying metal in β -Ti and a limited solubility in α -Ti.

A microstructural analysis of alloys prepared with titanium iodide, has shown the following solubilities of vanadium, niobium, and molybdenum in α -titanium (weight %):

Temperature, °C	V	Nb	Mo
800	0.9—1.0	1.5	0.5
700	1.5	3.0	0.8—0.9
600	2.2—2.3	3.6—3.8	1.2

These data show satisfactory agreement with results of earlier investigators /1-3/. The latter also give solubilities in β -Ti at 600°C of 30% for vanadium, 28 to 30 % for Mo, and 50 % for Nb.

The Ti—V—Nb system belongs to the second type of titanium alloy (the phase diagram shows a continuous solubility in one modification and a limited solubility in the other modification /4/). This system has been investigated by Kornilov and Vlasov /5/. The alloys were prepared by sintering. Alloys containing 1.5 % V and 0.5 % Nb, as well as those containing 1.5 % Nb and 0.5 % V, had a homogeneous α -structure after annealing at 600°C.

The solubility (of alloying metal) in β -titanium for alloys with V : Nb = 1 : 1 is 45 % at 600°C. The method of preparation, however, resulted in a high degree of contamination of the alloys with oxygen which could lead to a widening of the limits of the $\alpha + \beta \rightarrow \beta$ transformation.

The Ti—Nb—Mo system also gives the second type of ternary titanium alloy diagram. This system has been investigated by methods of thermal and microstructural analysis using sintered specimens /6/. For alloys with Nb:Mo = 1:1 the solubility of alloying elements in β -titanium is 48 % at 600°C.

The Ti—V—Mo system is similar to that described above. Taylor /7/ has determined the lattice parameters of alloys of this system and demonstrated the formation above 885°C of a continuous series of solid solutions with a cubic structure. The melting diagram of this system has been investigated and the boundary of the $\alpha + \beta \rightarrow \beta$ transformation determined by Kornilov and Polyakova /8/. For alloys with V:Mo=1:1, the solubility of alloying elements in β -titanium is 26 to 28 % at 600°C. For the investigation of the Ti—V—Nb—Mo systems, the alloys were prepared by the method of direct melting /9/.

The field of the polymorphic transformation of titanium [has now been] investigated [in quaternary] systems with up to a total content of alloying elements equal to 50 %. All alloys with a total content of alloying elements of up to 20 % were homogenized at a temperature of 1400°C for 25 hours; alloys with a higher content of vanadium, niobium, and molybdenum were annealed at 1500°C for 24 hours. The compositions of the alloys represented by the tetrahedron in Figure 1, correspond to four sections beginning at the titanium corner. The relationship between the alloying elements in the alloys represented by each section is $\text{Mo}:\Sigma\text{V}$, $\text{Nb}=2:1$, $\text{V}:\Sigma\text{Nb}$, $\text{Mo}=2:1$, $\text{Nb}:\Sigma\text{V}$, $\text{Mo}=2:1$, and $\text{V:Nb:Mo}=1:1:1$. Thus, these sections are on the three planes of the tetrahedron which has a tangential plane with a relationship of components 1:1, the section I being common to all three planes. This method is convenient, since it permits the indirect determination of the solubility of alloying elements in α - and β -titanium in ternary systems. In addition, the method enables the investigation to be carried out with the use of only a small number of alloys.

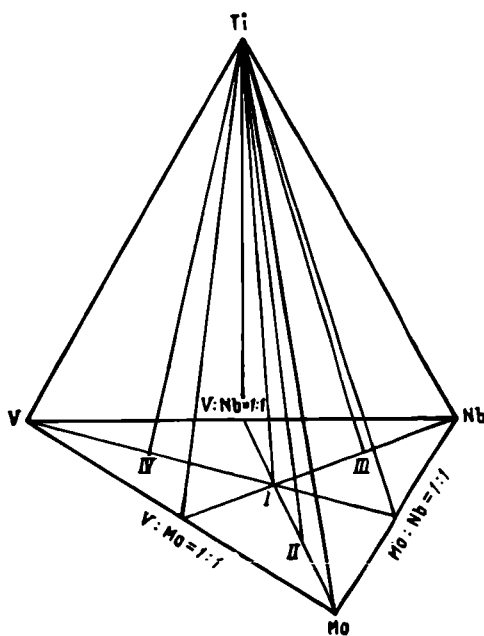


FIGURE 1. Sections of the tetrahedron of the Ti-V-Nb-Mo system

All alloys except those with a high content of molybdenum (ΣV , Nb, Mo = 30 %, section II), were forged at room temperature, and alloys with a total content of alloying elements up to 10 % were cold rolled to a draft of 40 %. The alloys were annealed as follows: 150 hours at 800°C, 350 hours at 700°C, and 880 hours at 600°C. After each heating, the specimens were quenched in water. Those alloys represented by section I with a total content of alloying elements of 30, 33, 40.2, and 50.1 % received an additional annealing at 600°C for 300 hours.

The characteristic structures of alloys are given in Table 1 and in Figure 2.

In alloys with a composition close to the saturation limit ($\alpha \rightarrow \alpha + \beta$ and $\alpha + \beta \rightarrow \beta$) an α or β phase precipitates along the grain boundaries and in the interior of the grains. In this connection, attention should be given to the polythermal sections in the fields of polymorphic transformation (Figure 3), which were constructed on the basis of a microstructural analysis (and, for section I, also on the basis of hardness and electrical resistance measurements). These sections are similar to the phase diagrams of the binary titanium alloys with niobium, vanadium, or molybdenum. The solubilities of the alloying elements in α - and β -Ti for each section are given in Table 2.

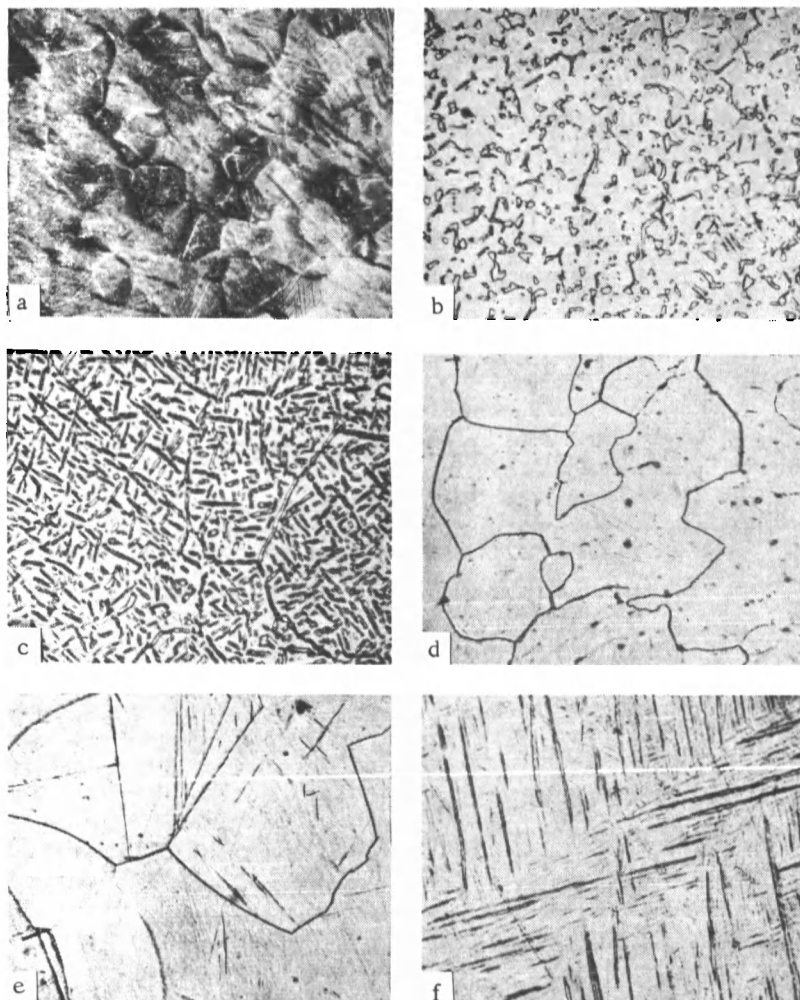


FIGURE 2. Microstructures of alloys of the Ti-V-Nb-Mo systems

a-V:Nb:Mo-1:1:1, Σ - 1.5%, hardening at 600°C, α phase (side illumination); b-V:ΣNb, Mo-2:1, Σ - 3.0%, hardening at 600°C, $\alpha + \beta$ phase; c-V:Nb:Mo-1:1:1, Σ - 15%, hardening at 600°C, $\alpha + \beta$ phase; d-Nb:ΣV, Mo-2:1, Σ - 4.02%, hardening at 700°C, β phase; e-V:Nb:Mo-1:1:1, Σ - 15%, hardening at 900°C, β phase (martensite); f-V:Nb:Mo-1:1:1, Σ - 10.2%, hardening at 900°C, β phase (martensite).

TABLE 1
Structure of alloys of the quaternary Ti—V—Nb—Mo system

Content, weight %				Hardening from a temperature of, °C		
V	Mo	Nb	Σ	800	700	600
Section I (V: Nb: Mo = 1:1:1)						
0.14	0.14	0.14	0.42	α	α	α
0.27	0.27	0.27	0.81	α (traces of β)	α	α
0.5	0.5	0.5	1.5	α + β	α	α
0.7	0.7	0.7	2.1	α + β	α + β	α (traces of β)
0.8	0.8	0.8	2.4	α + β	α + β	α + β
1.0	1.0	1.0	3.0	α + β	α + β	α + β
1.4	1.4	1.4	4.2	α + β	α + β	α + β
2.0	2.0	2.0	6.0	α + β	α + β	α + β
3.4	3.4	3.4	10.2	β (martensite)	α + β	α + β
4.0	4.0	4.0	12.0	β (martensite)	α + β	α + β
5.0	5.0	5.0	15.0	β (martensite)	α + β	α + β
6.0	6.0	6.0	18.0	β (martensite)	α + β	α + β
6.7	6.7	6.7	20.1	β	β (traces of α)	α + β
10.0	10.0	10.0	30.0	β	β	β (traces of α)
11.0	11.0	11.0	33.0	β	β	β
13.4	13.4	13.4	40.2	β	β	β
16.7	16.7	16.7	50.1	β	β	β
Section II (Mo: ΣV, Nb = 2:1)						
0.07	0.07	0.28	0.42	α + β	α	α
0.135	0.135	0.54	0.81	α + β	α (traces of β)	α
0.25	0.25	1.0	1.5	α + β	α + β	α + β
0.35	0.35	1.4	2.1	α + β	α + β	α + β
0.4	0.4	1.6	2.4	α + β	α + β	α + β
0.5	0.5	2.0	3.0	α + β	α + β	α + β
0.7	0.7	2.8	4.2	α + β	α + β	α + β
1.7	1.7	6.8	10.2	β (martensite)	α + β	α + β
2.5	2.5	10.0	15.0	β (martensite)	α + β	α + β
3.35	3.35	13.4	20.1	β	β	α + β
5.0	5.0	20.0	30.0	β	β	β
6.7	6.7	26.8	40.2	β	β	β
8.35	8.35	33.4	50.1	β	β	β
Section III (Nb: ΣV, Mo = 2:1)						
0.07	0.28	0.07	0.42	α	α	α
0.135	0.54	0.135	0.81	α	α	α
0.25	1.0	0.25	1.5	α + β	α	α
0.35	1.4	0.35	2.1	α + β	α + β	α
0.4	1.6	0.4	2.4	α + β	α + β	α
0.5	2.0	0.5	3.0	α + β	α + β	α (traces of β)
0.7	2.8	0.7	4.2	α + β	α + β	α + β
1.7	6.8	1.7	10.2	β (traces of α)	α + β	α + α
2.5	10.0	2.5	15.0	β (martensite)	α + β	α + β
3.35	13.4	3.35	20.1	β (martensite)	α + β	α + β
5.0	20.0	5.0	30.0	β (martensite)	β (martensite)	α + β
6.7	26.8	6.7	40.2	β	β	β (traces of α)
8.35	33.4	8.35	50.1	β	β	β
Section IV (V: Σ Mo, Nb = 2:1)						
0.28	0.07	0.07	0.42	α	α	α
0.54	0.135	0.135	0.81	α + β	α	α
1.0	0.25	0.25	1.5	α + β	α (traces of β)	α
1.4	0.35	0.35	2.1	α + β	α + β	α + β
1.6	0.4	0.4	2.4	α + β	α + β	α + β
2.0	0.5	0.5	3.0	α + β	α + β	α + β
2.8	0.7	0.7	4.2	α + β	α + β	α + β
6.8	1.7	1.7	10.2	β (martensite)	α + β	α + β
10.0	2.5	2.5	15.0	β (martensite)	α + β	α + β
13.4	3.35	3.35	20.1	β (martensite)	β (traces of martensite)	α + β
20.0	5.0	5.0	30.0	β	β	β
26.8	6.7	6.7	40.2	β	β	β
33.4	8.35	8.35	50.1	β	β	β

α -titanium shows the highest dissolving power for niobium-rich alloys represented by section III, and the lowest dissolving power for alloys represented by section II.

The solubility of the alloying elements in α -titanium of alloys represented by section I is 1.9 to 2.0 weight %.

TABLE 2
Solubilities of alloying elements in $\alpha + \beta$ -Ti in the quaternary Ti-V-Nb-Mo system

Temperature, °C	Solubility, weight %		Temperature, °C	Solubility, weight %	
	in α -Ti	in β -Ti		in α -Ti	in β -Ti
Section I (V:Nb:Mo = 1:1:1)			Section III (Nb:ΣV, Mo = 2:1)		
800	—	9.5–10.0	800	—	10.0–11.0
700	—	20.0–21.0	700	—	25.0–26.0
600	1.9–2.0	31.0–32.0	600	2.8–2.9	39.0–40.0
Section II (Mo:ΣV, Nb = 2:1)			Section IV (V:ΣNb, Mo = 2:1)		
800	—	9.0	800	—	7.0–8.0
700	—	18.0–19.0	700	—	16.0–19.0
600	1.0–1.2	26.0–27.0	600	1.9–2.0	29.0–30.0

In order to determine the phase boundary $\alpha + \beta \rightarrow \beta$ of the particularly important section I, the specific electrical resistance of alloys annealed at 600°C was measured by the ammeter-voltmeter method (at a low heating rate — 1 to 2°C/min). For alloys with a total content of alloying elements lower than 15 % these data satisfactorily coincided with the data obtained by microstructural analysis. At higher contents of alloying elements, however, the critical transformation points in the alloys could not be pinpointed for any exact temperature, which indicates a slow diffusion of atoms during the dissolution of the α phase. This effect (for example, in an alloy with a total content of alloying elements equal to 15%, Figure 4), shows that the α phase slowly dissolves during the heating and that the alloy is not always in a condition corresponding to the equilibrium diagram. The higher the temperature of transformation, the sharper the dip at the transformation point. Pure titanium has a zero temperature coefficient of electrical resistance at a temperature corresponding to the $\alpha \rightarrow \beta$ transformation /10/.

The alloys represented by section I, if hardened from the β -field at a temperature of 900°C (heating for 24 hours) have either a martensitic structure or a polyhedral structure without any traces of martensite. Martensite is absent from the alloy only if the total content of alloying elements is about 18 to 20 %. Figure 5 shows the results of the measurements of hardness and of the electrical resistance of alloys hardened from 900°C and annealed at 600°C.

The boundary of the $\alpha + \beta \rightarrow \beta$ transformation in annealed alloys is clearly expressed. The properties of the alloys change additively in the two-phase field. Alloys hardened from the β -field have clearly expressed maxima of

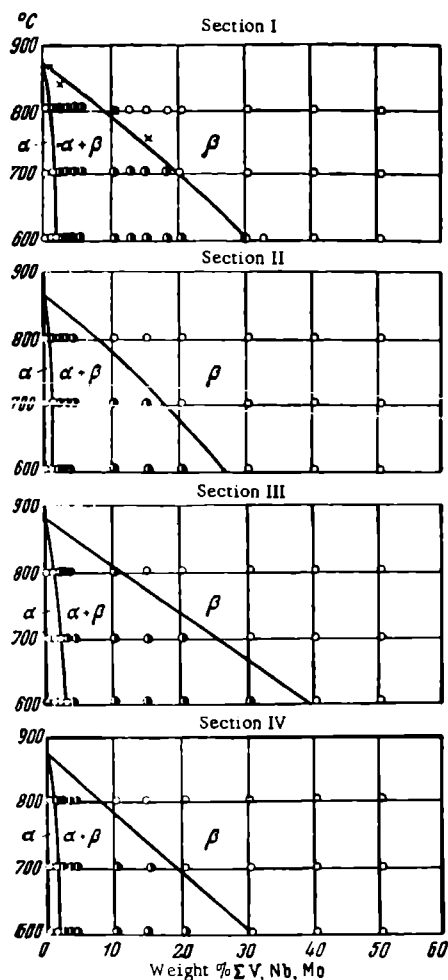


FIGURE 3. Polythermal sections in the field of polymorphic transformations in the Ti-V-Nb-Mo systems

○ — according to the results of microstructural analysis;
 ● — according to the data obtained from electrical resistance measurements.

nature of the variation of the boundary in the polythermal sections and also in the binary systems where, at a temperature of 600 to 650°C, it is less inclined towards its temperature axis; in addition, at 600°C the equilibrium is reached very slowly.

The additional annealing at 600°C for 300 hours, given to alloys represented by section I, yielded no new data as to the position of the boundary of the $\alpha + \beta \rightarrow \beta$ transformation.

hardness and electrical resistance, which correspond to a total content of alloying elements equal to 15 %. Hardened alloys show two hardness maxima. The first (at a total content of alloying elements equal to 1.5 %) can be explained by the supersaturation of α -titanium with alloying elements, while the second maximum, which is due to the separation of an ω phase from the metastable β -solid solution, lies in the region of $\beta + \omega$ phases [11, 12]. The low hardnesses of alloys with a total content of alloying elements from 2.1 to 10.2 % may be due to the friable, fine acicular structure of the α'' phase which is formed as a result of an incomplete $\beta \rightarrow \alpha$ transformation. Figure 2, which shows the characteristic microstructures of alloys with a total content of alloying elements equal to 15 % and hardened from 900°C, indicates that in addition to the grains of the β -solid solution which have no martensite, the alloy has also grains with clear streaks of martensite.

Alloys with a total content of alloying elements equal to 10.2 % have a fine acicular martensitic structure.

From the data obtained for alloys annealed at 600°C and then hardened, isothermal sections were constructed (Figure 6), from which it may be concluded that the solubilities of alloying elements (1:1 ratio) in α titanium for the Ti-V-Mo, Ti-V-Nb, and Ti-Nb-Mo ternary systems are about 1.3, 3.3, and 1.8 weight % respectively. The boundary curve of the $\alpha + \beta \rightarrow \beta$ transformation in these systems, varies somewhat with the temperature (Figure 7). At 600°C it is slightly concave for all the three sections chosen, while at higher temperatures it is slightly convex. This is apparently due to the

The data obtained on the position of the boundary of the $\alpha + \beta \rightarrow \beta$ transformation at 600°C for ternary systems are similar to those obtained in some earlier investigations [6, 8]. There are, however, discrepancies between these results and those obtained in one investigation [5], which gave the solubility for alloys with V : Nb = 1 : 1 as being about 45 % (as against only 33 % found in the present work). The incorrect results obtained in the earlier investigation [5], were due to the contamination of the alloys with oxygen, which resulted in the extension of the boundaries of the $\alpha + \beta \rightarrow \beta$ transformation, as shown by Hansen et al [1].

The phase diagram of the Ti-V-Nb-Mo system for 600°C (Figure 8) is characterized by a small volume of α -solid solutions, by a large volume of β -solid solutions, and by a medium volume of $\alpha + \beta$ phases.

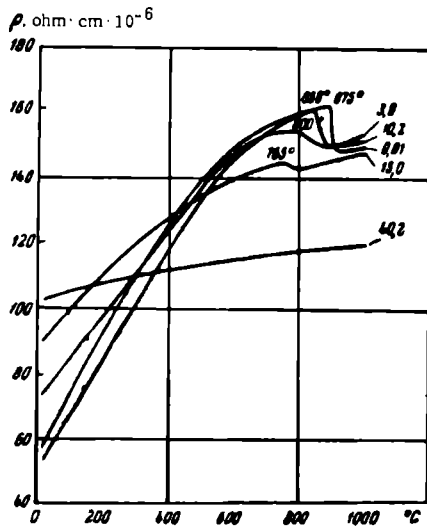


FIGURE 4. Relationship between the electrical resistance and the temperature of alloys characterized by section I

(ΣV, Nb, Mo = 0.81, 3.0, 10.2, 15.0, and 40.2 weight %.)

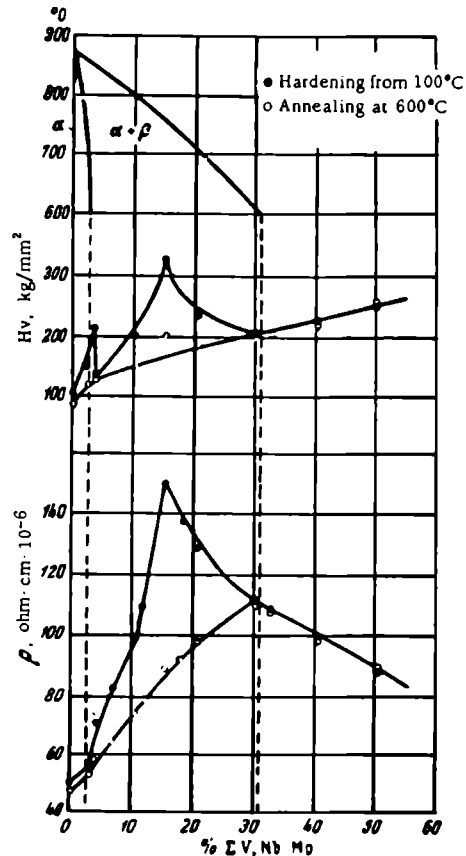


FIGURE 5. Hardness and electrical resistance of alloys of section I hardened from 900°C and annealed at 600°C

According to the classification of quaternary metallic systems [13], the diagram of the Ti-V-Nb-Mo system can be related to the phase diagrams

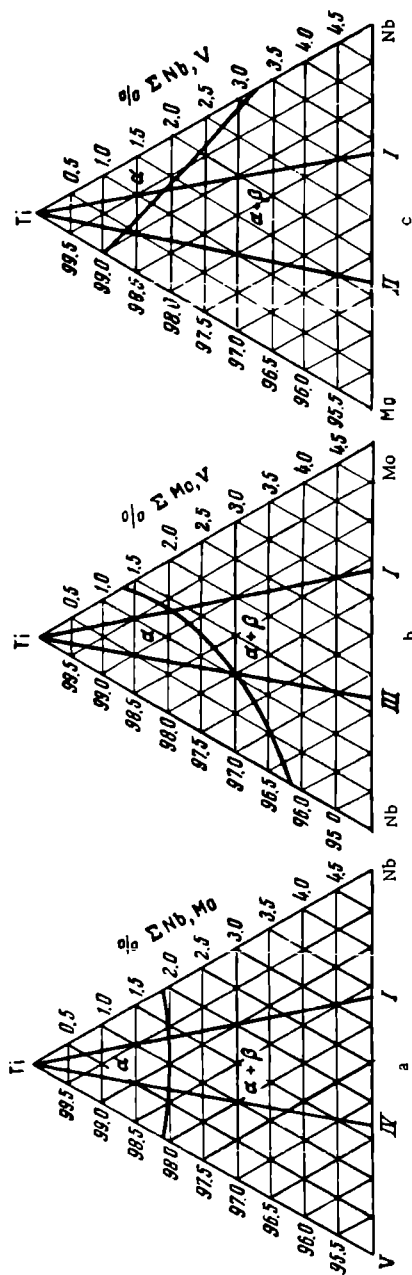


FIGURE 6. Isothermal section for alloys with a total content of alloying elements equal to 5% (Ti-V-Nb-Mo system with Nb: Mo = 1:1 (a), Mo: V = 1:1 (b), and Nb: V = 1:1 (c))

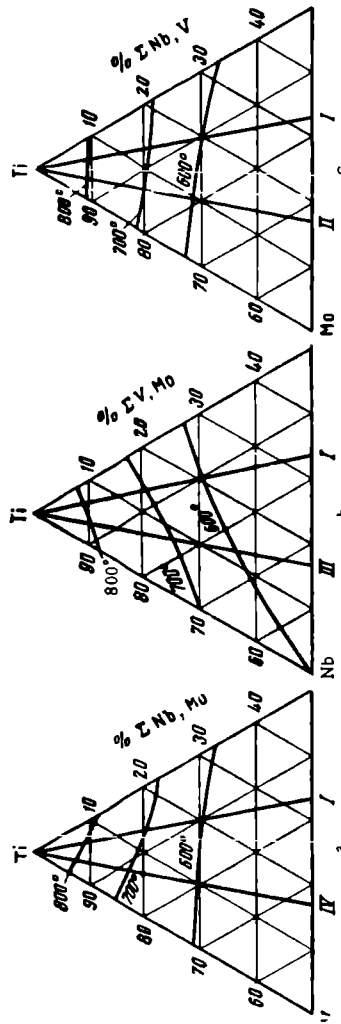


FIGURE 7. Variation of the boundary of the $\beta \rightarrow \alpha + \beta$ transformation for three isothermal sections of the Ti-V-Nb-Mo system (for alloys hardened from 800, 700, and 600°C. Nb: Mo = 1:1 (a), V: Mo = 1:1 (b), and Nb: V = 1:1 (c))

of the second type (systems with continuous solid solutions in one, two, or three ternary systems and with limited solid solutions in the other system).

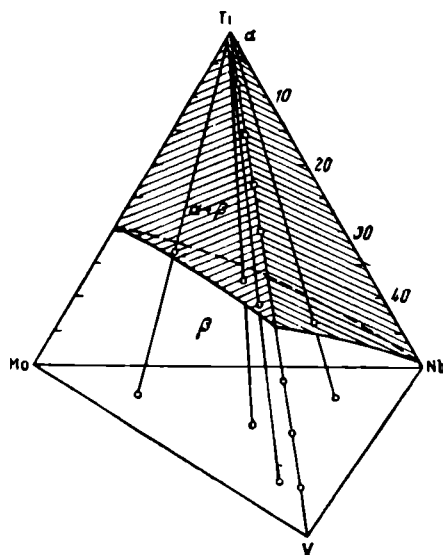


FIGURE 8. Phase diagram of the Ti-V-Nb-Mo system for 600°C and a total content of alloying elements equal to 50 %

This system may provide the basis for the construction of more complex phase diagrams of titanium alloys.

Conclusions

On the basis of a microstructural analysis, and measurements of hardness and electrical resistance, diagrams have been constructed corresponding to a quaternary Ti-V-Nb-Mo system at 800, 700, and 600°C for alloys with a total content of alloying elements equal to 50 %.

The following conclusions are drawn:

1. The solubility of V, Nb, Mo in α - and β -titanium at 600°C is as follows (%):

Section	α -Ti	β -Ti
I	1.9-2.0	31-32
II	1.0-1.2	26-27
III	2.8-2.9	39-40
IV	1.9-2.0	29-30

2. Alloys hardened from the β field have clearly expressed maxima of hardness and electrical resistance which reflect the presence of metastable phases. The fields of the $\beta + \omega$ phase in the binary systems in section I, determine the field of $\beta + \omega$ phases in the quaternary system.

3. The system investigated can provide the basis for the development of complex titanium alloys and also for the construction of more complex phase diagrams of titanium alloys.

Bibliography

1. Hansen, M., H. Kessler, E. Kamen, and D. McPherson. — J. Metals, 3(10):881. 1951.
2. Adenstedt, H.K., I. Peqignot, and I. Raymer. — Trans. Am. Soc. Met., Vol. 44:990. 1952.
3. Pietrokowsky, P. and P. Duwez. — J. Metals, 4(6):627. 1952.
4. Kornilov, I.I. and P.B. Budberg. Diagrammy sostoyaniya dvoynykh i troynykh sistem titana (Phase Diagrams of Binary and Ternary Titanium Systems). — Izdatei'stvo VINITI AN SSSR. 1961.
5. Kornilov, I.I. and V.S. Vlasov. — ZhNKH, 4(7):1630. 1959.
6. Kornilov, I.I. and R.S. Polysakova. — ZhNKH, 3(4):879. 1958.
7. Taylor, J. — J. Metals, Vol. 8, No. 8, sec. 2, p. 959. 1956.
8. Kornilov, I.I. and R.S. Polyakova. — Izvestiya AN SSSR, OTN, No. 1:85. 1960.
9. Fogel', A.A. — Izvestiya AN SSSR, No. 2:24. 1959.
10. Ames, L. and A. McQuillan. — Acta metallurgica, No. 2:831. 1954.
11. Bagaryatskii, Yu. A., G.I. Nosova, and T.V. Tagunova. — Doklady AN SSSR, 122(4):595. 1958.
12. Ageev, N.V. and L.A. Petrova. — Doklady AN SSSR, 138(2):359. 1961.
13. Kornilov, I.I. Fiziko-khimicheskie osnovy zharoprochnosti splavov (Physicochemical Principles of the Heat Resistance of Alloys), p. 324. — Izdatel'stvo AN SSSR. 1961.

INVESTIGATION OF ALLOYS OF THE TERNARY Ti—Nb—Cr SYSTEM

K. I. Shakhova and P. B. Budberg

An investigation has been carried out of a part of the Ti—Nb—Cr diagram representing some very promising heat resisting alloys.

No data have been published on this ternary system, although the component binary systems have been investigated in detail [1, 2].

The alloys were produced in an arc furnace in an atmosphere of argon. Specimens weighing 10 to 20 g were resmelted 6 to 7 times. The alloys were prepared from: niobium 99.27 %, titanium TG-00, titanium iodide, and electrolytic chromium 99.98 %.

All specimens were homogenized by annealing in a TVV-2M* furnace in an atmosphere of argon (1300 to 1500°C). Specimens with a high content of titanium were annealed for 60 to 70 hours and those with a high content of chromium and niobium for 200 to 240 hours.

A selective investigation of the microstructure of specimens has shown that, at the above annealing temperatures, the specimens achieved an equilibrium condition. The specimens were heat-treated in soldered double quartz vacuum ampoules. The heat treatment was carried out as follows: hardening from 1000°C (holding time 100 to 150 hours), hardening from 800°C (holding time 350 to 450 hours); hardening from 600°C (holding time 500 to 550 hours).

In order to reveal the microstructure, the titanium alloys were etched in mixtures of various amounts of nitric and hydrofluoric acids.

The X-ray investigations were carried out on powdered alloys. The effect of work hardening was annulled by heating the alloys at 600°C for 20 to 30 min. The X-ray photographs were taken in a Debye chamber (57.3 mm diameter), by the asymmetric method using unfiltered vanadium radiation.

A discussion will follow on the results of the investigation of that part of the ternary system limited by the Ti—Nb binary system and by the section representing the TiCr_2 and NbCr_2 intermetallic compounds.

The specimens investigated were represented by four radial sections starting from the chromium corner and having titanium-to-niobium ratios of 4:1, 3:2, 2:3, and 1:4, and also by the section between the TiCr_2 and NbCr_2 intermetallic compounds. These compounds are formed in binary alloys of the Ti—Cr and Nb—Cr systems and are in their crystallochemical nature similar to the Laves phases. The TiCr_2 and NbCr_2 intermetallic compounds have two polymorphic modifications. The low-temperature modification of these compounds has a lattice of the MgCu_2 type. In the Ti—Cr system this modification is stable up to a temperature of 1050–1100°C, and in the Nb—Cr system up to 1590°C. The lattice parameters are, for TiCr_2 , 6.943 \AA [3] and for NbCr_2 , 6.95 \AA [2]. The high-temperature

* [TVV—Russian abbreviation for High-frequency Induction Furnace.]

modifications have a lattice of the $MgZn_2$ type, i.e., hexagonal with 12 atoms in the elementary cell. The lattice parameters are, in this case, as follows; for $TiCr_2$: $a = 4.932 \text{ \AA}$, $c = 9.47 \text{ \AA} / 5$; for $NbCr_2$: $a = 4.92 \text{ \AA}$, $c = 8.10 \text{ \AA} / 2$.

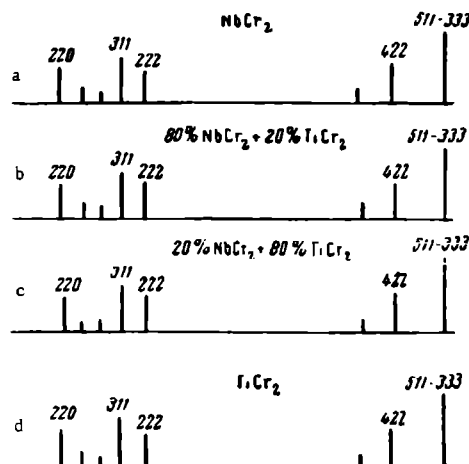


FIGURE 1. Diffraction pattern of alloys of the $TiCr_2$ - $NbCr_2$ sections hardened from $1000^\circ C$

a— $NbCr_2$; b—80% $NbCr_2$ + 20% $TiCr_2$; c—20% $NbCr_2$ + 80% $TiCr_2$; d— $TiCr_2$.

The identical lattice types and similar parameters of the above Ti and Nb compounds with chromium permit the assumption that a continuous series of solid solutions can be formed between the low-temperature and the high-temperature modifications of these compounds.

In order to confirm this assumption, an X-ray investigation was carried out of alloys represented by the $TiCr_2$ - $NbCr_2$ section, after hardening from 1000, 800, and $600^\circ C$. The diffraction pattern of alloys belonging to this section, and hardened from $1000^\circ C$ (Figure 1), show that all alloys belonging to this range of compositions have the same system of links which is characteristic of a phase with a cubic lattice. The same pattern is seen on X-ray photographs of alloys hardened from 800 and $600^\circ C$. It can, therefore, be concluded that at 1000, 800, and $600^\circ C$, $TiCr_2$ and $NbCr_2$ compounds form between them a continuous series of solid solutions and the section is quasi-binary.

Alloys of this system hardened from $1000^\circ C$ have only two types of structure: a single-phase structure which is that of the solid solution on the basis of β -Ti, and a two-phase structure consisting of a mixture of a solid solution of the compound $(TiNb)Cr_2$ (γ phase) (Figures 2 a and b). Alloys of this system, hardened from $800^\circ C$, have either a single-phase structure (β -solid solution) or a two-phase structure ($\alpha + \beta$) and $\beta + (TiNb)Cr_2$, where α is a solid solution on the basis of α -Ti. These types of structure can be easily distinguished under a microscope, since the α phase precipitates as thin lamellae in a matrix of the β -solid solution while the

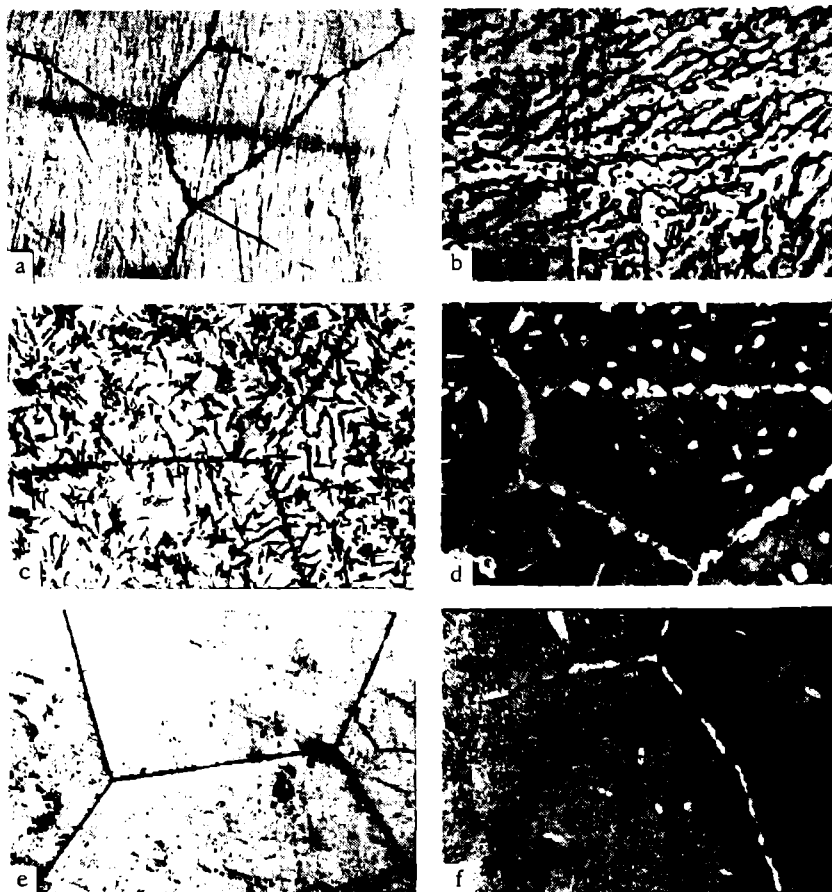


FIGURE 2. Microstructure of alloys of the Ti-Nb-Cr system, $\times 200$

a — 15% Cr, 51% Ti, 34% Nb, hardened from 1000°C; b — 55% Cr, 27% Ti, 18% Nb, hardened from 1000°C; c — 5% Cr, 90% Ti, 5% Nb, hardened from 800°C; d — 25% Cr, 45% Ti, 30% Nb, hardened from 800°C; e — 5% Cr, 38% Ti, 57% Nb, hardened from 600°C; f — 25% Cr, 45% Ti, 30% Nb, hardened from 600°C.

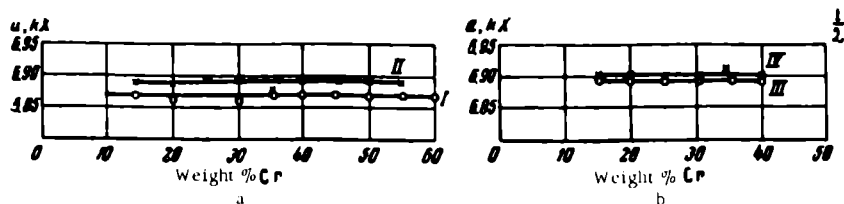


FIGURE 3. Variation of the lattice parameters of β -solid solutions

a — radial sections I and II, b — radial sections III and IV.

(TiNb)Cr₂ compound has a clearly acicular shape (Figure 2c and d). The investigation of alloys hardened from 600°C is of the greatest interest, since in this case, part of them undergoes a eutectoid transformation. The single-phase structure was preserved by the alloys containing 5 and 10 % of Cr and represented by sections III and IV respectively (Figure 2e). A typical three-phase structure following on the eutectoid transformation of the alloy containing 25 % of Cr represented by the radial section III is shown in Figure 2f. At 600°C the phase composition of alloys of this system is considerably more complex than at 1000 or 800°C. Consequently, in this investigation all alloys hardened from 600°C were also investigated by the X-ray method.

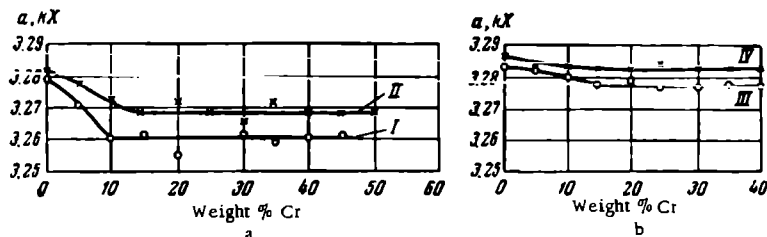


FIGURE 4. Variation of the lattice parameters of the γ phase

a — radial sections I and II; b — radial sections III and IV.

X-ray photographs of α -Ti, TiCr₂, and NbCr₂ were first of all taken; these X-ray photographs were later used as standards.

The X-ray photographs of alloys represented by section I and containing up to 10 % of Cr have only two systems of lines — characteristic α - and β -solid solutions; the latter is more intense. Alloys containing 15 % of Cr have, in addition to the lines of α - and β -solid solutions, others corresponding to a γ phase. The number and the intensity of the latter are rather small. The number and the intensity of the lines representing an intermetallic solid solution increase with the increase in the chromium content. At the same time the intensity of the lines representing the β -solid solution decreases. No lines of the β phase can be found on X-ray photographs of alloys containing more than 35 % of Cr. The intensity of the lines of the α -solid solution increases with the increase in the chromium content. The X-ray photographs of these alloys with up to 10 % of Cr which are represented by section II, have lines of the α - and β -solid solutions but the lines of the α -solid solution are less intense than the lines of alloys with the same chromium content belonging to the radial section I. Lines of the γ phase appear on the X-ray photographs beginning with 15 % of Cr.

The lattice parameters of the β -solid solution of alloys belonging to the radial sections I and II decrease in the two-phase field of the system but remain constant in the three-phase field (Figure 3a).

The X-ray photographs of alloys with 5 % of Cr belonging to radial section III show only lines of the β -solid solution while those of alloys with 10 % of Cr have lines belonging to both the α - and β -solid solutions. X-ray photographs of alloys containing more than 10 % of chromium have three systems of lines, corresponding to α , β , and (TiNb)Cr₂.

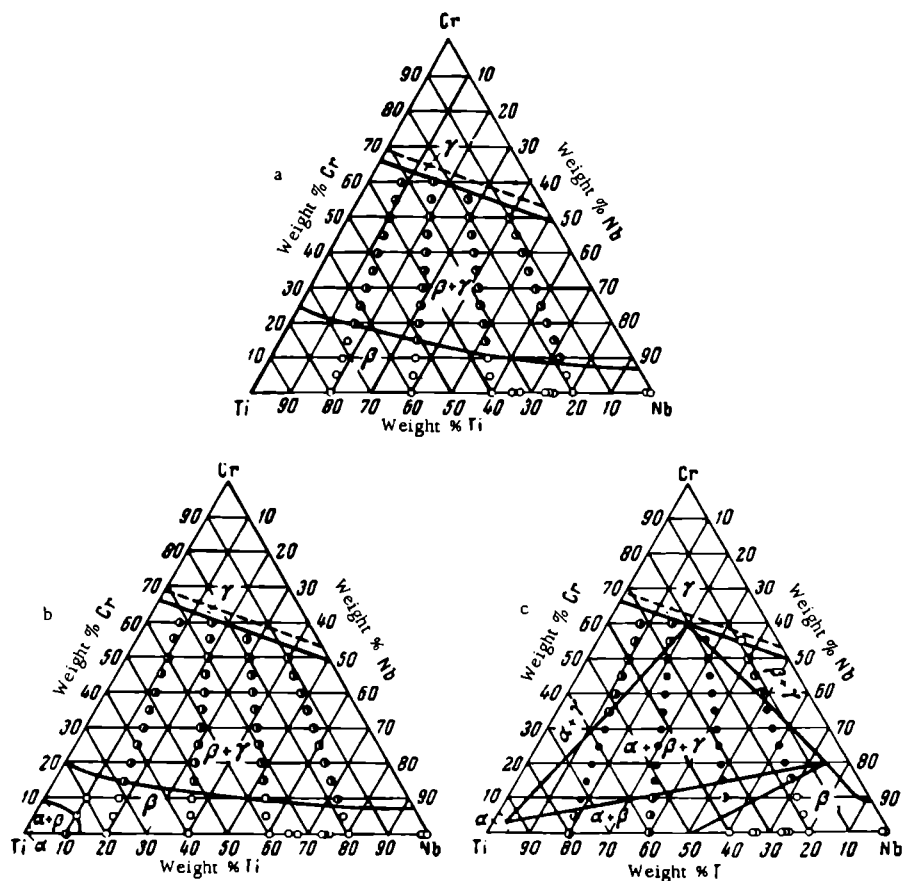


FIGURE 5. Isothermal sections of the system at 1000 (a), 800 (b), and 600°C (c)

○—single-phase alloys; ◐—two-phase alloys; ●—three-phase alloys.

The X-ray photographs of alloys with 10% of chromium belonging to radial section IV show only lines of the β - solid solution. Alloys with up to 35% of chromium have three systems of lines corresponding to α -, β -, and $(\text{TiNb})\text{Cr}_2$ solid solutions. The X-ray photographs of alloys with 40, 45, and 50% of Cr show only lines of the β - and $(\text{TiNb})\text{Cr}_2$ solid solutions. The lattice parameters of β -solid solutions belonging to the radial sections III and IV are given in Figure 3b. The lattice parameter of the $(\text{TiNb})\text{Cr}_2$ intermetallic compound in the three-phase field (Figure 4) remains constant.

Isothermal sections were constructed of the part of the Ti—Nb—Cr phase diagram investigated using the data obtained in microstructural and X-ray phase analysis. The isothermal section for 1000°C is shown in Figure 5a. At this temperature most of the diagram is taken up by the two-phase field of alloys consisting of a mixture of β - and γ - solid solutions. The solid

solution of the $(\text{TiNb})\text{Cr}_2$ intermetallic compound is designated by the letter γ . The region of the β -solid solution gradually narrows as the content of niobium in the alloys increases.

In the isothermal section for 800°C (Figure 5b) the distribution of the phase fields is essentially the same as in the isothermal section for 1000°C , except for the appearance of a narrow two-phase $\alpha + \beta$ field in the titanium corner.

In the isothermal section for 600°C (Figure 5c) a three-phase field $\alpha + \beta + \gamma$ is formed as a result of the eutectoid reaction $\beta \rightarrow \alpha + \text{TiCr}_2$ which takes place in alloys of the binary Ti—Cr system. This three-phase field is adjacent to three two-phase fields $\alpha + \beta$, $\alpha + \gamma$, and $\beta + \gamma$. At this temperature the single-phase β alloys can exist only if the content of niobium exceeds 50 %.

Bibliography

1. Kornilov, I. I. and P. B. Budberg. Diagrammy sostoyaniya dvoynykh i troynykh sistem titana (Phase Diagram of Binary and Ternary Ti Systems). — Izdatel'stvo VINITI AN SSSR. 1961.
2. Pan, V. M. — Fizika metallov i metallovedenie, 12(3):455. 1961.
3. Duwez, P. and J. Taylor — Trans. Am. Soc. Met., Vol. 44:495. 1952.
4. Elyutin, V. P. and V. F. Funke. — Izvestiya AN SSSR, OTN, No. 3: 68. 1956.
5. Levinger, B. W. — Trans. Am. Inst. Met. Eng., Vol. 196:197. 1953.

**INVESTIGATION OF THE PARTIAL PHASE DIAGRAM
OF THE Ti—Al—Cr—Fe—Si—B SYSTEM
(SECTION WITH 3 % OF AL)**

V. S. Mikheev, K. P. Markovich, and L. F. Tabadze

The nature of the reaction between the basic metal and the alloying elements provides the scientific basis for the development and the preparation of new alloys. With this principle in view, and with the object of developing new alloys of titanium a systematic investigation has been carried out to determine the basic conditions for the formation of titanium compounds and solid solutions as well as to classify the metallic and the chemical properties of titanium. The various alloying elements can be divided into four groups, as they form with titanium continuous and limited solid solutions, metallic and ionic compounds, or do not react with titanium at all [1-2]. The elements of the first and the second groups which form solid solutions and compounds with titanium are those mainly employed for the preparation of strong and heat-resisting titanium-base alloys.

On the basis of theoretical considerations and of the experimental data obtained from phase diagrams of binary and ternary titanium systems [3-6], the authors have selected the six-component Ti—Al—Cr—Fe—Si—B system as the subject of investigation in the search for new titanium alloys.

The general method of the investigation was to study the influence of varying content of alloying elements (chromium, iron, and silicon), from 0.45 to 2.5 %, on the properties of a ternary α -solid solution with 3 % of Al and 0.01 % of B, and to determine the field of the γ -solid solution in a particular section of the six-component Ti—Al—Cr—Fe—Si—B system in which the ratio of the alloying components was Cr : Fe : Si = 1 : 1 : 1.

Attention is directed to the phase diagram of this system, constructed as a tetrahedron by the method of three-dimensional representation adopted for partial multicomponent systems with any number of elements in solid solution (Figure 1). The origin of the coordinates was taken as a composition corresponding to the ternary α -solid solution with 3 % Al and 0.01 % B. From this point, the contents of chromium, iron, and silicon were plotted on three axes. Three vertexes of the tetrahedron represent the compositions of the TiCr_2 , TiFe , and Ti_3Si_3 intermetallic compounds. The section investigated, with a component ratio of 1 : 1 : 1 extends from the vertex of the tetrahedron towards its interior (Figure 1).

For the purpose of the investigations alloys were prepared having the calculated compositions shown in Table 1.

The starting materials for the preparation of the alloys were: 1) titanium-sponge TG-00 with an ultimate strength of about 37 kg/mm²; 2) A-000 aluminum, (9.999%); 3) reduced iron containing 0.03 % C, 0.01 % Mn, 0.003 % S, and 0.008 % P; 4) technical silicon; and 5) a chromium-boron alloy with 10 % B.

TABLE 1
Chemical composition of alloys, weight %

No. of alloy	Ti	Al	Cr	Fe	Si	B	Σ Cr, Fe, Si
1	96.5	3.00	0.15	0.15	0.15	0.01	0.45
2	96.24	3.00	0.25	0.25	0.25	0.01	0.75
3	95.94	3.00	0.35	0.35	0.35	0.01	1.05
4	95.69	3.00	0.60	0.50	0.50	0.01	1.60
5	94.49	3.00	1.00	0.75	0.75	0.01	2.50

The alloys were smelted in a vacuum arc furnace with tungsten electrodes in an atmosphere of an inert gas. The weight of each specimen was 40 g.

The accuracy of the chemical analysis was checked by weighing the ingots. Ingots in which the losses were more than 1 % were rejected.

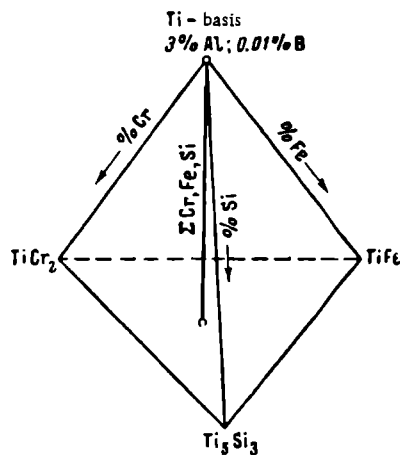


FIGURE 1. A three-dimensional representation of a partial phase diagram of the Ti-Al-Cr-Fe-Si-B system

The cast alloys were forged at 1000°C into 6 mm-diameter rods. The forged rods were annealed in an ordinary electric furnace at 800°C for 30 min and air cooled.

For the construction of the phase diagram section, the following methods of physicochemical analysis were employed: optical method (for the determination of the melting diagram), thermal analysis (for the determination of the phase transformations in the solid alloy), and microstructural analysis.

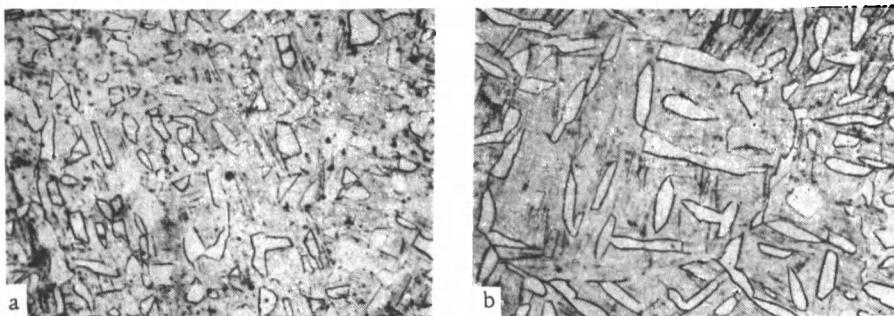


FIGURE 2. Microstructure of alloys of the Ti-Al-Cr-Fe-Si-B system after hardening from 1000°C (holding time—2 hours, quenching in water), $\times 340$

a—0.75% Σ Cr, Fe, Si, $\alpha + \alpha'$ phase; b—1.6% Σ Cr, Fe, Si, $\alpha + \alpha'$ phase.

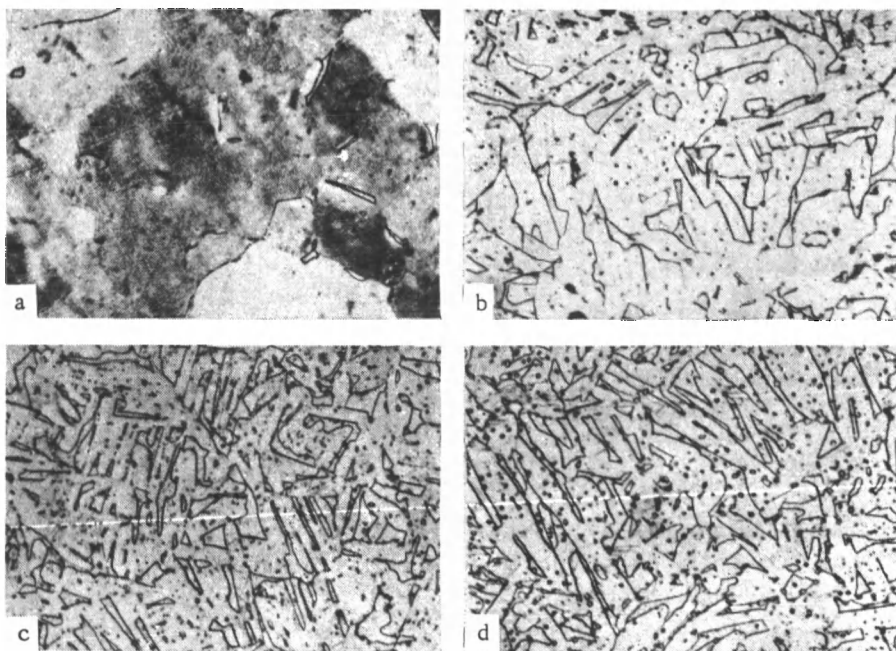


FIGURE 3. Microstructure of alloys of the Ti-Al-Cr-Fe-Si-B system after hardening from 800°C (holding time—300 hours, quenching in water), $\times 340$

a—0.45% Σ Cr, Fe, Si, $\alpha + \beta$ residual; b—0.75% Σ Cr, Fe, Si, $\alpha + \beta$ residual; c—1.6% Σ Cr, Fe, Si, $\alpha + \beta + \gamma$; d—2.5% Σ Cr, Fe, Si, $\alpha + \beta + \gamma$.

Melting diagram

The temperature of the commencement of melting (solidus line) was determined in a short-circuited vacuum furnace. The specimens, fastened in the clamps of the furnace through 2 mm-diameter holes drilled in their centers, were melted by the electric current flowing through them.

The results of melting point determinations of alloys with a constant content of aluminum (3 %) and with varying total contents of chromium, iron, and silicon (0.45 to 2.5%), show that the melting point decreases from 1535° to 1470°C (Table 2) with the increase in the total content of alloying elements.

TABLE 2
Melting point of alloys

No. of alloy	Total content of alloying elements Cr, Fe, Si, weight %	Melting point, °C
1	0.45	1535
2	0.75	1515
3	1.05	1490
4	1.50	1480
5	2.50	1470

Phase transformations in solid alloys

The phase transformations in solid alloys were investigated by methods of thermal and microstructural analysis.

The thermal analysis (recording the differential heating curves by an N. S. Kurnakov pyrometer) was carried out on specimens annealed at 1000°C for 2 hours, at 800°C for 300 hours, and at 600°C for 400 hours, followed by cooling to room temperature without removal from the furnace. The calibration curve of the pyrometer was constructed on the basis of the transformation points of iron, nickel, titanium, and potassium sulfate. Nickel was used as a standard. Heating was carried out in an electric furnace [without any inert gas].

The metallographic analysis was carried out on specimens hardened from 1000, 800, and 600°C (holding time: 2, 300, and 400 hours, respectively). The specimens were quenched from these temperatures in a mixture of water and ice.

The thermograms, obtained by the differential method of recording the heating curves, clearly show the endothermic effects taking place during heating and corresponding to the $\alpha \rightarrow \beta$ transformation (Table 3).

These data show that, while the temperature of the beginning of the $\alpha \rightarrow \beta$ transformation does not change with the increase in the total content of chromium, iron, and silicon from 0.45 to 2.5 %, the end point of the transformation varies from 960 to 1025°.

The microstructural analysis carried out on specimens hardened from 1000°C shows that all alloys have a two-phase structure consisting of α and α' phases (Figure 2).

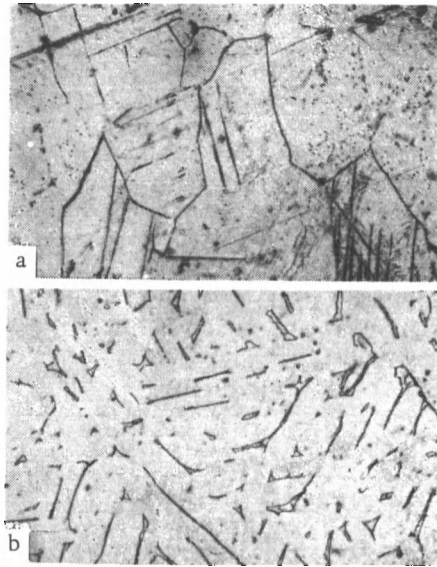


FIGURE 4. Microstructure of alloys of the Ti-Al-Cr-Fe-Si-B system after isothermal annealing (operating conditions: 1000°C (2 hours), 800°C (300 hours), 600°C (400 hours), cooling in water), $\times 340$
a - 0.75% Σ Cr, Fe, Si, α phase; b - 1.6% Σ Cr, Fe, Si, $\alpha + \gamma$ phase.

TABLE 3
Temperature of $\alpha \rightarrow \beta$ transformation

Alloy	Total content of alloying elements Cr, Fe, Si, weight %	Temperature of transformation, °C	
		beginning	end
1	0.45	920	960
2	0.75	930	960
3	1.05	930	1000
4	1.60	935	1010
5	2.50	930	1025

In the case of alloys hardened from 800°C and with a total content of Σ Cr + Fe + Si equal to 0.45 to 1 %, an α -solid solution matrix is observed with a small amount of a residual β phase (Figure 3a and b). The stability of the β phase increases in alloys with a higher content of stabilizing elements (chromium, iron, and silicon) as a result of which the amount of the β phase in such alloys also increases. Thus, the 300-hour long holding time proved to be insufficient for bringing the alloys to an equilibrium condition at this temperature (Figure 3b).

Alloys with a total content of Σ Cr + Fe + Si equal to 1.6% have a three-phase structure at 800°C (Figure 3c). The new γ phase apparently consists of TiCr_2 which precipitates as round inclusions. The composition and nature of this phase are still being investigated.

As the total content of chromium, iron, and silicon is increased to 2.5 % the amount of the γ phase increases and its inclusions become coarser (Figure 3d).

A microstructural analysis of alloys with a total content of Cr, Fe, and Si of 0.45 to 0.75 % hardened from 600°C shows that they belong to the field of γ -solid solutions (Figure 4a).

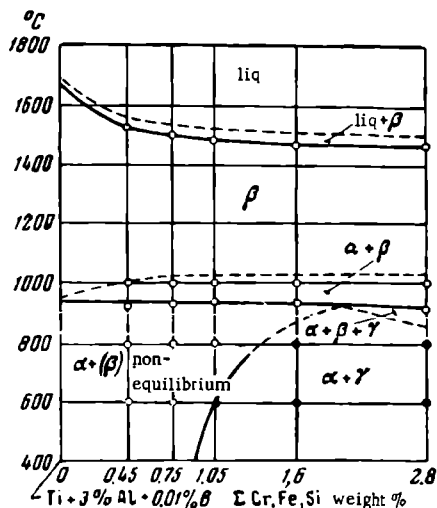


FIGURE 5. Polythermal section of alloys of the Ti-Al-Cr-Fe-Si-B system with 3 % of Al and varying contents of Σ Cr, Fe, Si

If the total content of alloying elements in alloys hardened from 600°C exceeds 1 %, which is their solubility in the ternary α -solid solution at this temperature, then the alloy consists of two phases: an α phase and a γ phase (Figure 4b).

The polythermal section of the six-component Ti-Al-Cr-Fe-Si-B system with 3 % Al and 0.01 % B and a total content of the other alloying elements varying from 0.45 to 2.5 % (Figure 5), was constructed on the basis of the melting point determinations, the investigation of phase transformations in solid alloys, and the microstructural examination of hardened alloys. The phase diagram shows the solidus curves, the single phase fields of α - and β -solid solutions on the basis of titanium, the two-phase fields $\alpha + \beta$ and $\alpha + \gamma$, and the supposedly three-phase field $\alpha + \beta + \gamma$.

At 600°C the α -solid solutions exist up to a total content of chromium, iron, and silicon equal to 1 %. At 800°C α -solid solutions are found when the total content of these elements is as high as 1.5 %.

The field of the β -solid solution lies above 1000°C. The boundary of the two-phase $\alpha + \beta$ field above 800°C is designated by a dotted line, since it is not very exact.

Conclusions

1. The authors have investigated and constructed a polythermal section of the six-component Ti-Al-Cr-Fe-Si-B system with a constant content of 3 % Al and total contents of alloying elements (chromium, iron, silicon),

which varied from 0.45 to 2.5 %. The following phase fields were identified: β , $\alpha + \beta$, α , α + residual phase, and $\alpha + \beta + \gamma$.

2. The melting point of alloys of the six-component Ti—Al—Cr—Fe—Si—B system, with a constant content of 3 % Al, decreases from 1535°C to 1400°C as the total content of alloying elements (chromium, iron, silicon) increases from 0.45 to 2.5 %.

3. It was determined that the total solubility of alloying elements (chromium, iron, silicon) in the α -solid solution of titanium is: 1.0 % at 600°C, and 1.5 % at 800°C.

Bibliography

1. Kornilov, I. I. — Izvestiya AN SSSR, OKhN, No. 3: 392. 1954.
2. Kornilov, I. I. Fiziko-khimicheskie osnovy zharoprochnosti splavov (Physicochemical Principles of Heat-Resistant Alloys). — Izdatel'stvo AN SSSR. 1961.
3. Kornilov, I. I. and P. B. Budberg. Diagrammy sostoyaniya dvoynykh i troynykh sistem titana (Phase Diagrams of Binary and Ternary Titanium Systems). — Izdatel'stvo VINITIAN SSSR. 1961.
4. Kornilov, I. I., V. S. Mikheev, and T. S. Chernova. — ZhNKh, 3 (3): 786. 1958.
5. Kornilov, I. I., E. N. Pylaeva, and M. A. Volkova. — ZhNKh, 3 (6): 1391. 1958.
6. Kornilov, I. I., V. S. Mikheev, and T. S. Chernova. — Izvestiya AN SSSR, OTN, No. 3: 3. 1960.

INVESTIGATION OF THE PARTIAL PHASE DIAGRAM OF THE Ti-Al-Cr-Fe-Si-B SYSTEM FOR ALLOYS CONTAINING 6 % OF AL

V. S. Mikheev, T. S. Chernova, and N. M. Dzhibuti

The physicochemical investigation of heat-resisting alloys [1] has shown that the most heat resisting are those with compositions close to the saturation limit of solid solutions which decompose in the solid state to precipitate finely divided phases. On the basis of theoretical considerations and of data obtained from the phase diagrams of binary [2-5] and ternary [6-8] systems, the authors decided to investigate the six-component Ti-Al-Cr-Fe-Si-B system.

The spatial representation of this system and the polythermal section with a variable content of aluminum (from 0 to 8 %) and a constant total content of alloying elements (chromium, iron, and silicon equal to 1.6 %) have appeared in an earlier publication [9].

The object of the study reported here was to investigate the six-component Ti-Al-Cr-Fe-Si-B system with a 6 % Al content. The phase diagram was drawn by means of a method for the spatial representation of partial multicomponent systems with any number of components in the solid solution of the solvent metal (Figure 1).

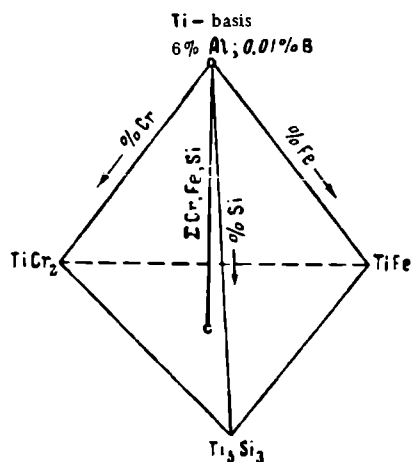


FIGURE 1. A spatial representation of the partial phase diagram of the Ti-Al-Cr-Fe-Si-B system

An alloy with composition corresponding to the ternary solid solution of titanium with 6% of Al and 0.01% of B was taken as the origin of the coordinates of the tetrahedron. From this point, the contents of silicon, chromium, and iron were plotted on the three axes of coordinates. Three vertexes of the tetrahedron represent the $TiCr_2$, $TiFe$, and Ti_3Si_3 intermetallic compounds. After investigations with varying contents of alloying elements a polythermal section was constructed of the six-component Ti-Al-Cr-Fe-Si-B system with a constant content of aluminum (6 %) and boron (0.01 %). The total content of alloying elements varied from 0 to 2.5 % in the ratio Cr : Fe : Si = 1 : 1 : 1, (i.e., a section of the tetrahedron was chosen extending from the vertex towards the interior.

The following methods of physicochemical analysis were utilized to provide data for the construction of this section: the optical method (for the determination of the melting diagrams), thermal analysis (for the determination of phase transformations in solid alloys), microstructural analysis, electrical resistance measurements of alloys from 20 to 1000°C, and also hardness tests. The starting materials for the preparation of the alloys were: titanium sponge TG-00, aluminum A-00, reduced technical iron, silicon KR-0, and electrolytic chromium. Boron was introduced into the alloy as a chromium-boron master alloy containing about 10% of B. The alloys were smelted in a vacuum arc furnace using stable electrodes. The ingots obtained were forged at 1100°C into 6 mm-diameter rods.

Melting diagram

The commencement of melting (solidus line) of the alloys was determined by an OP-48 optical pyrometer. The specimens (rods), with 2 to 2.5 mm-diameter holes drilled in the middle, were fastened between the clamps of a short-circuited vacuum furnace and melted by passage of an electric current.

The data obtained show that the melting temperature of alloys of the Ti-Al-Cr-Fe-Si-B system containing 6% Al gradually decreases with the increase in the total content of alloying elements. Alloys containing no chromium, iron, or silicon have a solidus temperature equal to 1630°C; alloys with a total content of alloying elements (chromium, iron, and silicon) equal to 0.45, 0.75, 1.05, 1.60, and 2.50%, having melting points equal to 1575, 1550, 1540, 1540, and 1480°C, respectively.

Investigation of the phase transformations in solid alloys

The phase transformations in solid alloys were investigated by recording the differential heating curves with a N.S.Kurnakov pyrometer. The transformations were investigated on annealed specimens which consisted of an α -solid solution with small residues of a β phase. An ordinary electric furnace was used. The standard for the recording was pure nickel. The calibration curve was constructed according to the transformation temperatures of K_2SO_4 and Na_2SO_4 . An analysis of the thermograms given by all the alloys indicates that thermal transformations take place during heating. The thermal effects obtained correspond to the $\alpha \rightarrow \beta$ transformation. These thermal effects are small but are of considerable duration.

The transformation temperatures of the alloys as obtained in this investigation are given in Table 1.

Additions of chromium, iron, and silicon decrease transformation temperature of the alloys to some extent. While the commencing temperature of transformation of an alloy with 6% Al is 1030°C, that of an alloy with a total content of chromium, iron, and silicon equal to 1.60% is only 950°C.

TABLE 1

Temperatures of phase transformation taking place in alloys of the
Ti—Al—Cr—Fe—Si—B system as determined by recording
differential heating curves

Total content of chromium, iron, and silicon, weight %	Temperature, °C	
	beginning of transformation	end of transformation
0	1030	1060
0.45	975	1000
0.75	975	1000
1.05	945	1000
1.60	950	1025
2.50	950	1030

The fact that phase transformations also take place in solid alloys became evident as a result of determinations of the electrical resistance of annealed specimens at temperatures from 20 to 1100°C. The electrical resistance of alloys was determined from the potential drop on a given length of the specimen during passage of a direct current. The potential drop on a specimen U_x was automatically recorded by a EPP-09 potentiometer. The results of these determinations on annealed alloys of the six-component Ti—Al—Cr—Fe—Si—B system containing 6 % Al and various amounts of chromium, iron, and silicon are given in Table 2.

TABLE 2

Temperatures of phase transformations in alloys of the Ti—Al—Cr—Fe—Si—B system as determined by measuring the electrical resistance

Total content of Cr, Fe, Si, weight %	Phase transformations	Temperature of phase transformations, °C
0	$\alpha \rightarrow \alpha + \beta$	1020
	$\alpha + \beta \rightarrow \beta$	1050
0.45	$\alpha \rightarrow \alpha + \beta$	960
	$\alpha + \beta \rightarrow \beta$	1000
0.75	$\alpha \rightarrow \alpha + \beta$	925
	$\alpha + \beta \rightarrow \beta$	950
1.05; 1.6; 2.5	Inflections on the curves of electrical resistance related to the variations in the composition of the solid solutions	No exact data are available

The electrical-resistance curve for alloys with a total content of chromium, iron, and silicon of 0.45 to 0.75 % rises in the field of the α -solid solution (Figure 2). As the temperature of the $\alpha \rightarrow \beta$ transformation is approached, this rise slows down to some extent. The transition from

the α to the $\alpha + \beta$ field is characterized by a change in the inclination of the curve. The transformation temperatures of these alloys essentially confirm the transition points determined by thermal analysis.

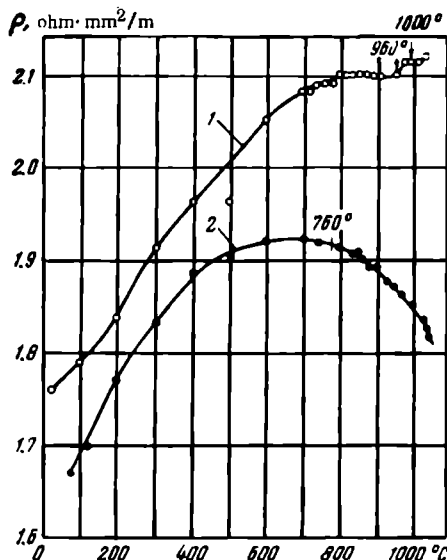


FIGURE 2. Electrical resistance of alloys of the Ti-Al-Cr-Si-B system with 6 % Al

1 — $\Sigma\text{Cr, Fe, Si} = 0.45\%$, 2 — $\Sigma\text{Cr, Fe, Si} = 1.6\%$.

Alloys containing an α -solid solution plus a β phase ($\Sigma\text{Cr, Fe, Si} = 1.05\%$), and those with an $\alpha + \beta$ phase ($\Sigma\text{Cr, Fe, Si} = 1.6$ and 2.5%) show an increase in the electrical resistance over the field of the α -solid solution which slows down as the transformation point is approached. This slowing down is probably due to the rearrangement of atoms in the crystal lattice of the α phase and also to the change in the composition of the α -solid solution according to the phase diagram (see below). There is no sharp change at a point corresponding to the phase transformation of these alloys and, therefore, it is impossible to determine the exact region of phase transformations by means of electrical-resistance measurements.

Microstructure of alloys

The microstructure of alloys belonging to the six-component Ti-Al-Cr-Fe-Si-B system were investigated in the forged condition, after hardening from 1100 and 800°C and in the annealed condition. The specimens were etched in hot sulfuric acid or in a mixture of hydrofluoric and nitric acids.

All forged specimens (Figure 3) and those annealed at 800°C (holding time 30 min) have a structure which is the result of the decomposition of the β -solid solution (α' phase) — coarse-grained with large martensitic needles due to the rapid cooling during forging. The structure of alloys hardened from 1100°C is shown in Figures 4a and b. The specimens were quenched in a mixture of water and ice. At this temperature all alloys investigated consist of a β -solid solution. During hardening the β -solid solution decomposes forming an intermediate α' phase. Because of the high cooling rates it is impossible to obtain a pure β phase at room temperature.

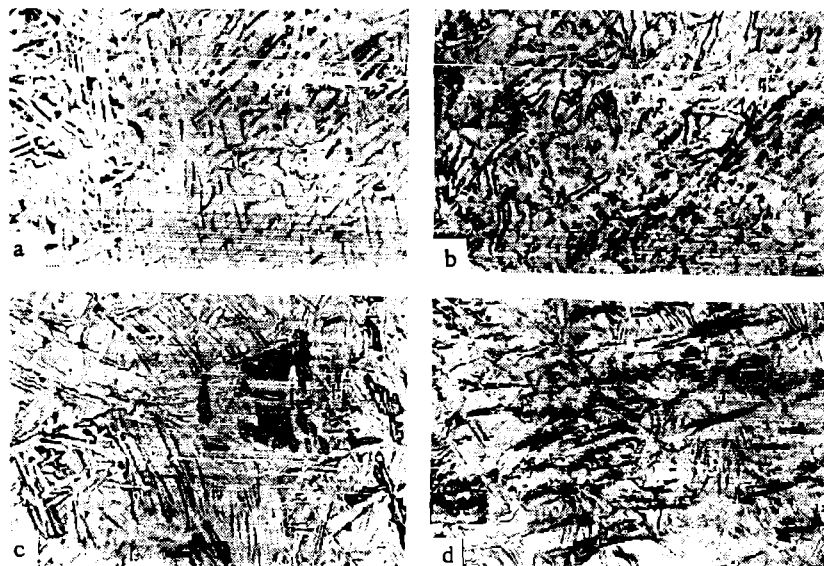


FIGURE 3. Microstructure of alloys of the Ti—Al—Cr—Fe—Si—B system with 6 % Al and Σ Cr, Fe, Si = 0.45 % (a), 0.75 % (b), 1.05 % (c), and 2.5 % (d) after forging

Alloys with a total content of chromium, iron, and silicon from 0.45 to 0.75 (Figure 4c and d)*, hardened from 800°C, consist of an α -solid solution. The polyhedrons of the α crystals are clearly visible on the photomicrographs. Alloys with a total content of chromium, iron, and silicon of 1.05 to 1.6% have a residual β phase since the holding time was too short to permit equilibrium to be reached at this temperature. Chromium, iron, and silicon stabilize the β phase. Therefore, to obtain complete transformation of the β phase, the holding time must be increased if the total content of these alloying elements is high. In these investigations the holding time was 300 hours for all alloys and proved to be insufficient for alloys with a total content of alloying elements equal to 1.05 and 1.6%, so that the alloy

* [See footnote on following page.]

contained a residual β phase. Alloys with a total content of alloying elements equal to 2.5 % consist, at this temperature, of two phases ($\alpha + \gamma$)*. The composition of the γ phase has not been determined, but it may be assumed that it is formed on the basis of the TiCr_2 compound. The microstructure of annealed alloys is shown in Figure 4e and f. After heating, the alloys were cooled in the furnace. Annealed alloys with a total content of alloying elements equal to 0.45, 0.75, and 1.05 % consist of an α -solid solution with small amounts of the β phase which apparently remain as a result of the slow $\alpha \rightarrow \beta$ phase transformation. Annealed alloys with a total content of alloying elements equal to 1.6 and 2.5 % have a small amount of the γ phase.

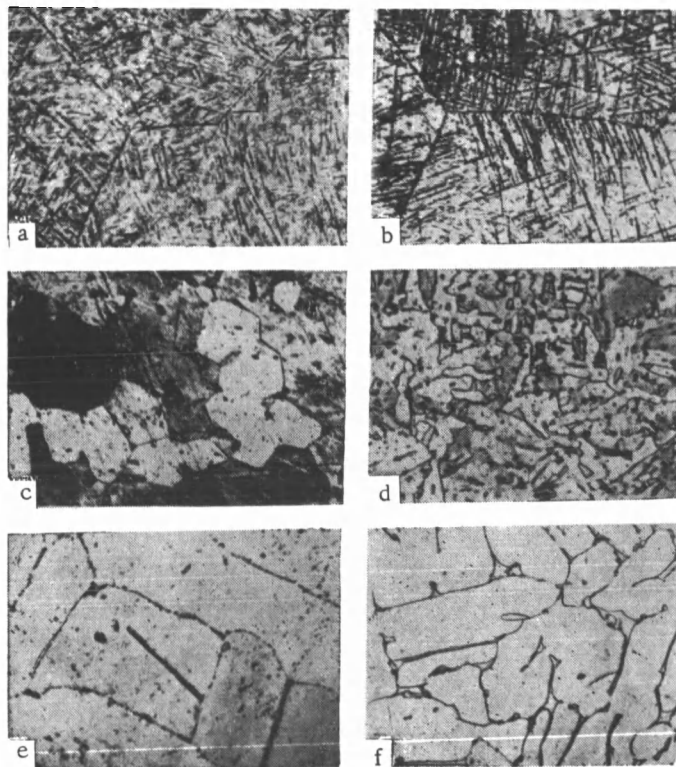


FIGURE 4. Microstructure of alloys of the Ti-Al-Cr-Fe-Si-B system with 6 % Al after various heat treatments

a — hardening from 1000°C, $\Sigma \text{Cr, Fe, Si} = 0.45\%$; b — the same, $\Sigma \text{Cr, Fe, Si} = 1.05\%$; c — hardening from 800°C; $\Sigma \text{Cr, Fe, Si} = 0.45\%$; d — the same, $\Sigma \text{Cr, Fe, Si} = 2.5\%$; e — annealing at a temperature 1100°C (4 hours), 800°C (300 hours), 600°C (500 hours), $\Sigma \text{Cr, Fe, Si} = 0.45\%$; f — the same, $\Sigma \text{Cr, Fe, Si} = 1.6\%$.

- [Photomicrograph 4d is described in the caption as being that of an alloy with 2.5 % alloying elements. It may show $\alpha + \gamma$ phases.]

Hardness of alloys

The hardness of specimens, forged, hardened from 1100 and 800°C, or annealed, was determined on a Vickers hardness tester with a diamond pyramid loaded with 10 kg. The results obtained are shown in Figure 5.

The hardness of forged alloys gradually increases with the increase in the total content of alloying elements. Thus alloys with $\Sigma \text{Cr, Fe, Si} = 0.45\%$ have an $H_v = 342 \text{ kg/mm}^2$, while an alloy with $\Sigma \text{Cr, Fe, Si} = 2.5\%$ has an H_v equal 401 kg/mm^2 . Alloys quenched from 1100°C which consist of an phase are considerably harder than unquenched alloys.

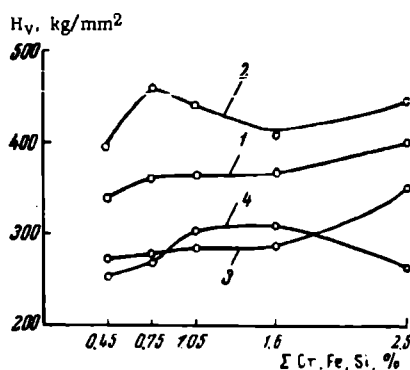


FIGURE 5. Hardness of alloys of the Ti—Al—Cr—Fe—Si—B system with 6% Al after various heat treatment processes

1 — after forging; 2 — hardening from 1100°C; 3 — hardening from 800°C; 4 — annealing at 1100°C (2 hours); 800°C (300 hours), 600°C (500 hours), cooling in the furnace.

Alloys quenched from 800°C are softer than unquenched alloys or alloys hardened from 1100°C. This is due to the fact that these alloys contain an α phase which is considerably softer than the α' phase. The hardness of alloys quenched from 800°C increases with the increase in the total content of alloying elements, as is the case with those hardened from 1100°C. The hardness of alloys, after prolonged annealing, is on the same level as that of alloys quenched from 800°C [up to a certain content of alloying elements].

On the basis of the results of thermal analysis, phase transformation studies in the solid state, microstructural investigations and hardness measurements, after various heat treatment processes, the authors constructed a polythermal section of the Ti—Al—Cr—Fe—Si—B system with constant 6% Al, 0.01% B, and varying contents of alloying elements (Figure 6).

In that part of the polythermal section investigated the following phase fields were identified: 1) single-phase fields of α - and β -solid solutions on the basis of titanium, 2) two-phase fields $\alpha + \beta$ and $\alpha + \gamma$, and 3) a three-phase $\alpha + \beta + \gamma$ field.

The phase boundary of the α -solid solution corresponds [at 600°C] to a total content of alloying elements equal to 1.3 %. At 800°C this boundary corresponds to a total content of alloying elements equal to 1.7 %. In the field of the α -solid solution the residual β phase is given in parentheses. The field of the β -solid solution comprises the largest part of the diagram and lies at temperatures higher than 1000°C.

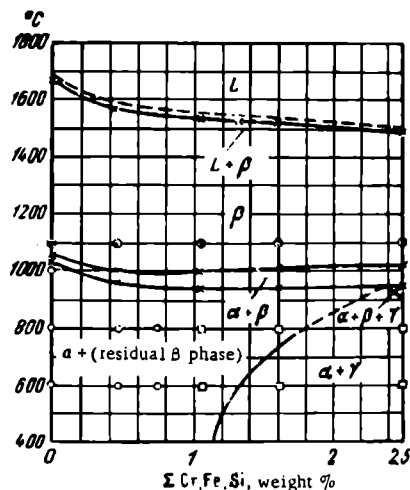


FIGURE 6. Polythermal section of alloys of the Ti-Al-Cr-Fe-Si-B system with 6 % Al and varying total contents of Σ Cr, Fe, Si.

The two-phase $\alpha + \beta$ field is a narrow strip extending from Σ Cr, Fe, Si equal to zero, widening somewhat at a total content of alloying elements equal to 2.5 %. The boundary of the $\alpha + \gamma$ field at temperatures above 800°C has not been exactly determined and is, therefore, shown on the diagram by a dotted line.

Conclusions

On the basis of differential thermal analysis and of investigations of microstructure, hardness, and electrical resistance, the authors have constructed a polythermal section of the six-component Ti-Al-Cr-Fe-Si-B system with constant 6% Al and varying total contents of chromium, iron, and silicon (from 0 to 2.5 %). The following conclusions are drawn from the results:

1. The total solubility of chromium, iron, and silicon in the α -solid solution of titanium is 1.3 % at 600°C and 1.7 % at 800°C.
2. The temperature of the $\alpha \rightarrow \beta$ transformation in the Ti-Al-Cr-Fe-Si-B system is not greatly influenced by the total content of alloying elements.
3. The polythermal section of the six-component Ti-Al-Cr-Fe-Si-B system is of a great practical interest. This section indicates the optimum

compositions of alloys based on the α -solid solutions, which possess high heat resistance and other desirable physicochemical properties.

Bibliography

1. Kornilov, I.I. Fiziko-khimicheskie osnovy zharoprochnosti spлавov (Physicochemical Principles of Heat-Resistant Alloys). — Izdatel'stvo AN SSSR. 1961.
2. Kornilov, I.I. — Doklady AN SSSR, 91(3):549. 1953.
3. Kornilov, I.I., E.N. Pylaeva, and M.A. Volkova. — Izvestiya AN SSSR, OKhN, No. 7:771. 1956.
4. Sagel, K., E. Schulz, and U. Zwicker. — Zs. Metallk., 47(8): 523. 1956.
5. Kornilov, I.I., V.S. Mikheev, and T.S. Chernova. — Trudy Instituta Metallurgii AN SSSR, No. 2:126, Izdatel'stvo AN SSSR. 1957.
6. Kornilov, I.I., V.S. Mikheev, and T.S. Chernova. — ZhNKh, 3(3):786. 1958.
7. Kornilov, I.I., E.N. Pylaeva, and M.A. Volkova. — ZhNKh, 2(6):1391. 1958.
8. Kornilov, I.I. and N.G. Boriskina. — ZhNKh, 5(9):5. 1959.
9. Kornilov, I.I., V.S. Mikheev, and T.S. Chernova. — Izvestiya AN SSSR, OTN, No. 3:70. 1960.

CLASSIFICATION OF TITANIUM ALLOYS ACCORDING TO THEIR STRUCTURE

V. A. Livanov and B. A. Kolachev

The widely-accepted classification of titanium alloys on the basis of their microstructure as α , $\alpha+\beta$, and β alloys requires critical evaluation. In any classification of alloys according to structure, the condition of alloys should be precisely defined. Alloyed steels, for example, are classified according to their microstructure in the annealed or normalized condition. It is not at present usual, when classifying titanium alloys according to their structure, to indicate the condition of the alloys in the above sense. The authors consider this omission to be unjustified.

During the earlier period of their use in industry, titanium alloys were, as a rule, employed in the annealed condition. Alloys of this metal with aluminum and tin were annealed at temperatures corresponding to the α field and air cooled, as a result of which an α structure was established. The conditions for annealing alloys containing β phase stabilizers and also, usually those including aluminum, were specially chosen so as to obtain the most stable mixture of α and β phases. Under these conditions, the classification of all titanium alloys as α , $\alpha+\beta$ and the industrially not yet used β alloys was satisfactorily exact [1, 2].

The range of titanium alloys has now, however, been widened with the development of different processes of heat treatment, while β -titanium alloys have found industrial application. At the present time, therefore, the absence of a generally applicable method of classification of titanium alloys according to their microstructure leads to misunderstandings and controversy.

Thus, the OT-4, OT-4-1, or OT-4-2 alloys are usually classified as $\alpha+\beta$ alloys because they contain aluminum and much manganese and because heating them to relatively low temperatures produces a β phase. In these alloys, however, no stable β phase can be obtained either by hardening or by normalizing. Since hardening produces in these alloys only an α' phase, they are classified as martensitic alloys, belonging to the group of $\alpha+\beta$ alloys. However, some investigators [3, 4] are of the opinion that these alloys belong to the group of α alloys to which, on account of their properties, they have closer affinities than to the group of $\alpha+\beta$ alloys. The OT-4, OT-4-1, and OT-4-2 alloys are thermally stable and have the good weldability characteristic of α alloys.

The alloy S-105VA, developed abroad and containing 2.5 % Al and 16 % V was once classified as an $\alpha+\beta$ alloy, but recently a number of investigators have preferred to include it among the β alloys [5, 6].

Even more controversial is the classification of the VT-14 alloy, which was once considered as a typical β alloy, then as an $\alpha + \beta$ alloy (which is soft in the hardened condition), and has recently even been classified as a martensitic alloy which, as noted above, is close to α alloys [2, 7].

These controversies necessitate the classification of titanium alloys according to their structure under defined conditions. The problem now arises as to what condition should be taken as the basis for this classification. In this connection, it has to be borne in mind that the object of classification is to facilitate the choice of alloys for certain purposes and the development of new alloys with particular properties. Each class of alloys should, therefore, be distinguished by a certain specific range of properties differentiating it from other classes.

First of all, it is obvious that classification according to the structure in the annealed condition is out of the question since the equilibrium structures of titanium alloys containing transition elements establish themselves very slowly. The rate of eutectoid transformations of titanium alloys containing transition elements is so slow that they are never completed under ordinary industrial conditions, and, during cooling, the structure of these alloys changes as though there were no horizontal eutectoid line.

The classification of titanium alloys according to the structure in the normalized or the hardened condition is quite possible, since sufficient information is available on the structure of alloys in these conditions. On the basis of what is known about titanium alloys, the structures of alloys in the normalized or the hardened condition can be related to the isothermal decomposition diagram of the β phase.

The authors have, therefore, attempted to classify titanium alloys according to their structure either in the normalized or in the hardened condition.

The first step in this system of classification is to state the standard dimensions of the specimens, so that the cooling rate will be identical for all alloys. The authors are of the opinion that $14 \times 14 \times 60$ mm specimens are the most suitable. Such specimens are standard for the determination of the mechanical properties of most titanium alloys. For the classification of alloys according to their structure in the normalized or hardened condition, it is also necessary to determine the most suitable temperatures at which to bring the specimens to the stated condition. The temperature most suitable for this purpose is that of the polymorphic transformation of titanium, i.e., 882°C .

It is proposed first of all to consider the classification of titanium alloys according to their structure in the normalized condition. In this case, those normalized titanium alloys which consist of an α phase, or of an α phase with intermetallic compound inclusions, naturally belong to the class of α alloys. Normalized alloys containing α and β phases, with or without other intermediate phases or intermetallic compounds, should be classified as $\alpha + \beta$ alloys. Finally, normalized alloys consisting of either a pure β phase, or of a β phase with intermetallic compound inclusions, belong to the class of β alloys.

The structures of a number of normalized titanium alloys and the classes to which they belong are given in the table.

These data show that although the division of normalized alloys into α , $\alpha + \beta$, and β classes is preserved, the proposed classification has a

strict and logical meaning based not on formal relations derived from the binary phase diagrams but on actual structures reflecting the kinetics of the processes taking place in real alloys.

Classification of titanium alloys according to their structure in the normalized and hardened conditions

Type of alloy	Class of alloy according to the presently accepted classification	Class of alloy according to microstructure in normalized condition	Class of alloy according to the microstructure in hardened condition	Type of alloy	Class of alloy according to the presently accepted classification	Class of alloy according to microstructure in normalized condition	Class of alloy according to microstructure in hardened condition
VT-5 . . .	α	α	α	VT-3-1 . .	$\alpha + \beta$	$\alpha + \beta$	$\alpha + \beta$
VT-5-1 . .	α	α	α	VT-6 . . .	$\alpha + \beta$	$\alpha + \beta$	$\alpha + \beta$
OT-4 . . .	$\alpha + \beta$	α	α	VT-8 . . .	$\alpha + \beta$	$\alpha + \beta$	$\alpha + \beta$
OT-4-1 . .	$\alpha + \beta$	α	α	VT-10 . . .	α	α	α
OT-4-2 . .	$\alpha + \beta$	α	α	VT-14 . . .	$\alpha + \beta$	$\alpha + \beta$	$\alpha + \beta$
VT-3 . . .	$\alpha + \beta$	$\alpha + \beta$	$\alpha + \beta$	VT-15 . . .	β	β	β

The analysis of the properties of alloys within a single class shows that each class has certain characteristic properties which are due to the specific properties of the separate α and β phases.

The characteristic feature of α titanium alloys is their thermal stability and their good weldability by any method. Usually, α alloys cannot be hardened by heat treatment. Exceptions to this are alloys containing intermetallic compounds of varying solubilities in the α phase and those which have the highest hardness after hardening and aging. The heat resistance and the creep resistance of α alloys are higher than those of other alloys with the same amount of alloying elements since α titanium is a better basis than β -titanium for alloys subjected to elevated temperatures. The main alloying element used in the production of these alloys is aluminum. Aluminum increases the strength of titanium by about 6 to 7 kg/mm² for each 1 % of Al added but at the same time it decreases the plasticity of the alloy. The lowest plasticity is shown by titanium alloys containing more than 7.5 % of aluminum, a fact which is connected with the formation of superlattices. It has been noted recently that the addition of small amounts of β -phase stabilizers to Ti-Al alloys does not lead to the fixation of a β phase but impedes the formation of superlattices, thus permitting an increase in the concentration of aluminum in titanium alloys without consequent embrittlement.

Titanium-aluminum alloys containing small amounts of β -phase stabilizers precipitate a β phase when heated to relatively low temperatures, as a result of which the alloys acquire better properties and can be more easily mechanically worked than other α alloys. This is the reason why these alloys are often used for the production of sheets.

Certain neutral strengtheners, such as tin and zirconium, have a beneficial influence on the properties of titanium-aluminum alloys. These

strengtheners increase the strength of Ti—Al alloys without decreasing their plasticity, provided that their concentration does not exceed a certain limit. They also slow down the oxidation of Ti—Al alloys and increase their creep resistance.

During testing procedures α -titanium alloys have a great propensity to hydrogen embrittlement. This takes place at high rates of testing and particularly during impact testing, and is due to the precipitation of a hydride phase. In some cases hydrogen embrittlement also takes place at low tension levels during testing.

At the present time, the best combination of all properties is shown by $\alpha + \beta$ alloys. In order to fix the β phase at room temperature, these alloys must contain transition elements which alone enable the stability of the β phase to be increased sufficiently. The stabilization of the β phase by specific elements is due to a strengthening and, at the same time, solvent action. A β phase stabilized by β -eutectoid elements is stronger but less ductile than a β phase stabilized by β -isomorphic elements. Therefore, $\alpha + \beta$ alloys alloyed only with β eutectoid elements have a high strength in the annealed condition. In order to obtain $\alpha + \beta$ alloys with low strength characteristic in the annealed condition the β phase should be stabilized by β -isomorphic elements.

The solubility of β stabilizing elements in the α phase is low and, therefore, the α phase can be strengthened only by the addition of specific elements which have a high solubility in this phase, as well as being able to strengthen it. The sole α -phase stabilizer which is now added to $\alpha + \beta$ alloys is aluminum. Aluminum not only greatly strengthens the α phase both at room and elevated temperatures but also increases the thermal stability of the β phase. In addition, aluminum reduces the specific gravity of the alloys and thus compensates for the influence of the heavy transition elements.

Alloys belonging to this class have good formability at high temperatures and can be mechanically worked. $\alpha + \beta$ alloys can be strengthened by heat treatment and, if the proper conditions of heat treatment are maintained, their strength after hardening is considerably greater than after annealing. The drawback of $\alpha + \beta$ alloys is their low thermal stability which is due to the low stability of the β phase, and their poor weldability.

Unlike α alloys the $\alpha + \beta$ alloys are liable to hydrogen embrittlement only at low rates of deformation; impact testing causes no hydrogen embrittlement.

The alloys included in the β class have, in the normalized condition, a mechanically stable β phase which does not decompose under the influence of high stresses. Nevertheless, these alloys can be strengthened by heat treatment since the β phase, which is thermally unstable, decomposes upon heating. Alloys with a mechanically stable β phase have a high plasticity when in the hardened condition and a very high strength after aging. When hardened, these alloys have a strength of 130 to 160 kg/mm² (the highest ultimate strength among all Ti alloys). These alloys have also a good weldability. Their chief drawback is poor thermal stability which is due to the low stability of the β phase.

A thermodynamically stable β phase can be obtained in titanium alloys only with such high concentrations of alloying components that the alloys lose their chief advantage — a relatively low specific gravity. The only alloying element with a relatively low specific gravity is vanadium. This metal, however, is very expensive and difficult to obtain. Therefore,

titanium alloys with a stable β phase are not utilized to any great extent in industry and their investigation is still in the laboratory stage.

Alloys with a thermodynamically stable β phase should have good thermal stability and good weldability. They should also be thermally unhardenable, provided that they do not contain elements which form intermetallic compounds with a variable solubility in the β phase.

The classes of α , $\alpha+\beta$, and β alloys are large and they can be subdivided into groups. This subdivision, however, cannot be based on the structure but only on the properties and on the type of the alloying elements.

From the analysis given above it is clear that α alloys can be subdivided into the following groups:

- a) alloys alloyed only with α -phase stabilizers (VT-5);
- b) alloys alloyed with α -phase stabilizers and with neutral strengtheners (VT-5-1);
- c) alloys alloyed with α -phase stabilizers and with small amounts of β stabilizers (OT-4, OT-4-1, OT-4-2);
- d) alloys containing γ and β -phase stabilizers and neutral strengtheners (for example the MST-881 alloy developed abroad containing 8 % Al, 8 % Zr, and 1 % Σ Ta, Nb);

- e) α alloys containing intermetallic compounds.

Alloys of the $\alpha+\beta$ group can be subdivided into the following groups:

- a) alloys alloyed only with transition elements (Ti8Mn: Ti-140A);
- b) alloys alloyed with aluminum and with isomorphous β -phase stabilizers (VT-6, VT-8, VT-14);
- c) alloys alloyed with aluminum and with β -phase eutectoid stabilizers (VT-3);
- d) alloys alloyed with aluminum and with isomorphous and eutectoid β -phase stabilizers (VT-3-1);
- e) $\alpha+\beta$ alloys with intermetallic compounds; such alloys have not yet been developed but they may have a promising future.

Finally, the β alloys can be divided into the following groups:

- a) unstable β alloys;
- b) stable β alloys;
- c) β alloys with intermetallic compounds.

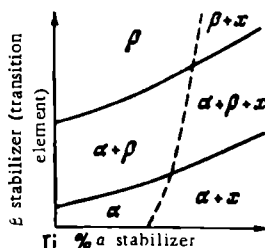


FIGURE 1. Structural diagram of titanium alloys with an α stabilizer and a transition element (β -phase stabilizer). Normalized condition

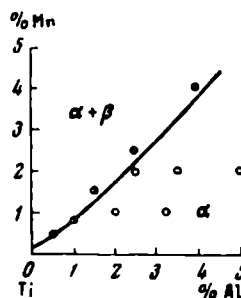


FIGURE 2. Structural diagrams of titanium alloys containing aluminum and manganese. Normalized condition
○ — α alloys; ● — $\alpha+\beta$ alloys.

The structure of titanium alloys containing several alloying elements normalized from 882°C can be represented by diagrams which are similar to those used for the classification of alloyed steel on the basis of structure, either in the annealed or normalized conditions.

Figure 1 shows a schematic structural diagram of titanium alloys alloyed with an α -phase stabilizer together with a β -phase stabilizer (transition elements). The structural diagrams of titanium alloys with other combinations of alloying elements (for instance with two β -phase stabilizers) are of lesser interest.

Unfortunately, the published data on the structure of alloys in various conditions are as yet insufficient to enable structural diagrams to be drawn of actual titanium alloys. An exception here is the Ti—Al—Mn system for which a phase diagram, though partial, of normalized alloys has been constructed on the basis of the data obtained by various authors (Figure 2). On this diagram the field of α alloys is quite clearly separated from the field of $\alpha + \beta$ alloys.

The construction of sufficiently exact structural diagrams of various titanium-base alloys will clearly facilitate the development of alloys with specific properties.

Consideration will now be given to the classification of titanium-base alloys according to their microstructure in the hardened condition. All hardened titanium alloys containing only α -phase stabilizers will have an α structure and, therefore, belong to the class of α alloys. Titanium alloyed with α -phase stabilizers can also precipitate intermetallic compounds if the content of the α stabilizer is sufficiently high. Obviously, the latter group should also be classified along with α alloys since they contain chiefly an α phase.

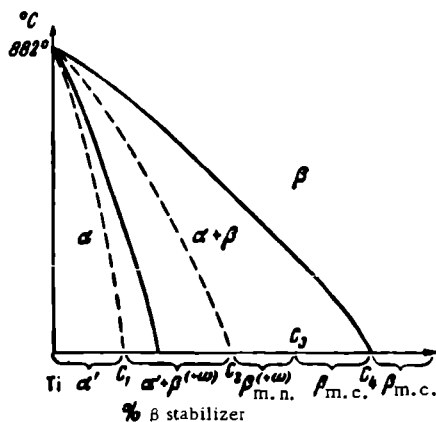


FIGURE 3. Structures formed during hardening of titanium alloys containing a β -phase stabilizer from 882°C

The structures obtained by hardening binary titanium alloys containing transition elements are more numerous and they can be represented by

the diagram given in Figure 3. If the content of the β -phase stabilizer does not exceed C_1 then hardening will produce a martensitic phase of the α' type. If the concentration of the β -phase stabilizer is from C_1 to C_2 a two-phase structure is established (α' and β). If the content of the alloying element exceeds C_2 only the β phase remains.

The stability of the β phase formed during hardening greatly depends on the content of the β -phase stabilizer. If the content of the alloying element does not exceed C_3 then the β phase produced by hardening will decompose when prolonged stresses are applied, so that this phase is considered as mechanically unstable. Decomposition of the β phase can also take place during hardening with the formation of an intermediate ω phase.

If the content of alloying elements exceeds C_3 the β phase produced during hardening does not decompose under the influence of stresses and is considered as mechanically stable. The β phase of these alloys, however, is not thermodynamically stable. When heated, these alloys precipitate dispersed particles of the α phase which permits the strengthening of these alloys by heat treatment. And finally, if the content of alloying elements exceeds C_4 a thermodynamically stable β phase can be produced.

Figure 3 is based on the phase diagram of titanium with a β -phase isomorphous stabilizer. Nevertheless, for titanium alloys with other transition elements the structures given in this diagram will also be correct because of the slow eutectoid transformations.

Hardened alloys with a β phase belong to the class of β alloys. Hardened alloys containing α' and β phases belong to the $\alpha + \beta$ class irrespective of whether or not the β phase decomposes into an ω phase. Hardened alloys with a martensitic structure belong to the α class since their martensitic phase has the same crystal lattice as an α phase. However, it should be pointed out that martensitic alloys are an intermediate formation between typical α alloys and typical $\alpha + \beta$ alloys.

Hardening gives rise to no stable β phase in titanium alloys alloyed with β -phase stabilizers which are not transition elements, and so, when hardened, these alloys contain an α' phase plus some intermetallic compounds if the content of β -phase stabilizers is sufficiently high.

Thus, the division of titanium alloys into α , $\alpha + \beta$, and β classes is also true for the hardened condition. These main classes of titanium alloys can be subdivided according to the structure and properties of the material in the hardened condition:

α -titanium alloys can be divided into the three following groups:

- a) thermally unhardenable alloys;
- b) alloys which can be age hardened;
- c) martensitic alloys.

$\alpha + \beta$ alloys can be divided into two groups: hardenable and unhardenable alloys.

The β -titanium alloys can be divided into three groups:

- a) alloys with a mechanically unstable β phase;
- b) alloys with a mechanically stable β phase;
- c) alloys with a thermodynamically stable β phase.

Some titanium alloys in use at present and their currently accepted classification are given in the table (p.58). This table also shows the structure of these alloys after hardening from 882°C and gives a classification according to the structure of the material in the hardened condition.

The classification of alloys according to their structure in the hardened condition can be corroborated by structural diagrams analogous to those given above for normalized alloys.

There remains the question as to which classification system is best. In the opinion of the authors the classification of alloys according to their structure in the normalized condition is the most suitable at this stage of development of the titanium industry, since most titanium alloys are used in a condition close to normalized. Nevertheless, the classification of alloys according to their structure in the hardened condition is no less logical, and is possibly preferable for the classification of thermally treatable alloys. Practical experience will, however, provide the final answer to this problem.

Conclusions

1. A classification of titanium alloys has been proposed according to their structure in the normalized and hardened conditions, all alloys being divided into α -, $\alpha + \beta$ -, ~~and β -~~, and β -phase classes.

2. The structure of normalized alloys can be subdivided, according to the properties and the types of alloying elements, into the following groups:

a) α alloys: 1) alloys alloyed only with α -phase stabilizers; 2) alloys alloyed with α stabilizers together with neutral strengtheners; 3) alloys alloyed with α - and β -phase stabilizers; 4) alloys alloyed with α - and β -phase stabilizers and with neutral strengtheners; and 5) alloys containing intermetallic compounds;

b) $\alpha + \beta$ alloys: 1) alloys alloyed only with transition elements; 2) alloys containing aluminum and β -isomorphic stabilizers; 3) alloys with aluminum and β -eutectoid stabilizers; 4) alloys alloyed with aluminum and β -isomorphic and eutectoid stabilizers; and 5) alloys containing intermetallic compounds;

c) β alloys: 1) stable alloys; 2) unstable alloys; and 3) alloys containing intermetallic compounds.

3. The main classes of titanium alloys can be subdivided, according to their structure and their properties in the hardened condition, into the following groups:

a) α alloys: 1) unhardenable alloys; 2) alloys which can be age hardened; and 3) martensitic alloys;

b) $\alpha + \beta$ alloys: hardenable and unhardenable alloys;

c) β alloys: 1) alloys with a mechanically unstable β phase; 2) alloys with a mechanically stable β phase; and 3) alloys with a thermodynamically stable β phase.

4. The division of titanium alloys into groups according to their microstructure in the normalized and hardened conditions can be represented by structural diagrams, analogous to those used for the classification of steels according to their microstructure in the normalized and annealed condition.

Bibliography

1. McQuillan, A. D. and M. K. McQuillan. Titanium. — Metallurgy of Rarer Metals, Vol. 2, New York, 1955. [Russian translation, 1958.]
2. Glazunov, S. G. Author's Summary of Thesis. Moskva, 1958.
3. Luzhnikov, L. P. and V. M. Novikova. — Metallovedenie i Termicheskaya Obrabotka Metallov, No. 3:6. 1959.
4. Luzhnikov, L. P. and V. N. Moiseev. — Metallovedenie i Termicheskaya Obrabotka Metallov, No. 7. 1961.
5. Frost, P. D. — Metal Progr., 75(3):95. 1959.
6. Frost, P. D. — Metal Progr., 75(4):91. 1959.
7. Vinogradova, E. A., G. M. Kokhova, and N. F. Lashko. — Sbornik "Titan v promyshlennosti", p. 121, Oborongiz. 1961.
8. Glazunov, S. G. and V. P. Kuraeva. — Sbornik "Titan v promyshlennosti", Oborongiz. 1962.
9. Glazunov, S. T. and V. N. Moiseev. — Sbornik "Titan v promyshlennosti", p. 232, Oborongiz. 1961.

SOME RESULTS OF THE METALLOGRAPHIC AND X-RAY INVESTIGATIONS OF AT TITANIUM ALLOYS*.

N. M. Pul'tsin and V. B. Pokrovskaya

The multicomponent AT titanium alloys constitute a high-strength material with a solid solution structure. The availability of the alloying elements permits the use of these alloys both for special and for general machine building.

Since the content of β -phase stabilizers is within the range of their solubility in the α phase these alloys usually consist of a single phase. Their multicomponent structure results in high strength and high heat resistance [1], while the stable single-phase composition ensures a high, stable heat and corrosion resistance, together with good machining and welding properties.

The single-phase system in these alloys must not be disturbed and the possibility of formation of other phases (metastable β phase, intermetallic compounds, or unstable α' phase), which might result from wrong alloying or faulty heat treatment, should be avoided by careful experimental and theoretical investigations before production in quantity is attempted.

An excessive amount of β -phase stabilizers and a nonuniform chemical composition may produce segregation fields, intermetallic compounds, or other phases with consequent thermal instability, reduction in corrosion resistance, and impairment of the technological properties of the alloys.

In the work reported here, which is based on an analysis of the results obtained by I. I. Kornilov et al and other investigators [1-4] the authors carried out microstructural, X-ray, and hardness studies on AT-3, AT-4, AT-6, AT-8, AT-9, and AT-10 alloys, after different treatments. The various conditions of heating, holding times, and cooling rates were essentially similar to those employed in the heat treatment of these alloys in the machine-building industry.

Experimental material, mode of heat treatment, and methods of investigation

The specimens of all six alloys were prepared from forged square rods (length of the side of a square, 14 to 18 mm). From these rods cylinders 12 mm in diameter and 18 mm long were turned, which were then heat treated.

After heat treatment, each specimen was turned to dimensions of 1.5 to 2 mm diam and 8 mm length, for investigation in the URS-70 apparatus. In

* The authors greatly appreciate the cooperation of I. I. Kornilov and V. S. Mikheev.

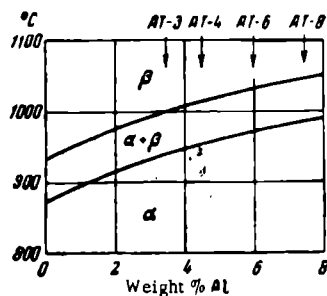


FIGURE 1. Quasibinary section of a phase diagram in the field of allotropic transformations of alloys of the Ti-Al-Cr-Fe-Si-B system with Σ Cr, Fe, Si, B = 1.5 to 1.8%.

order to remove the cold work layer and to obtain a thin "needle" for the X-ray investigations, the specimen was etched to a diameter of 0.3 to 0.4 mm. The "needle" was broken [after X-ray analysis] and a metallographic specimen prepared from the remaining part. This specimen was further used for hardness testing and for the X-ray investigations in the URS-50I apparatus.

The temperatures for the heat treatment were chosen according to the phase diagram of the Ti-Al-Cr-Fe-Si-B system to which the alloys belonged. A schematic section of the quasibinary diagram of these alloys is shown in Figure 1 [2]. This diagram shows that at room temperature

the alloys in question consist of an α -solid solution. Upon heating, these alloys pass into the $\alpha + \beta$ field, the transformation temperature increasing with the content of aluminum. Upon further heating the alloys acquire the structure of a pure β -solid solution. On the basis of this diagram, the temperature ranges of the phase transformations of the alloys were determined and heating temperatures selected for the heat treatment process. The results of the determinations made are given in Table 1.

TABLE 1

Boundaries of the fields of phase transformations and temperatures of heat treatment of the alloys being investigated

Alloy	Boundaries of the two-phase field, °C	Temperature of heat treatment, °C	Alloy	Boundaries of the two-phase field, °C	Temperature of heat treatment, °C
AT-3	940-1000	1020	AT-8	988-1045	1015
AT-4	955-1015	985	AT-9	—	1015
AT-6	970-1030	1000	AT-10	—	1070

It will be noted from the table, that the heat-treatment temperatures for the AT-4, AT-6, AT-8, and AT-9 alloys were chosen in order to give a two-phase structure (though for the AT-4 and AT-9 alloys this was not achieved), while the heating temperature for AT-3 and AT-10 alloys lay in the β -solid solution region.

The holding time for the temperatures selected was 1 hour for all alloys. The alloys were cooled in the air (normalization) and in water at room temperature (quenching).

In addition to heat treatment under the above conditions, cyclic annealing for 36 hours was also carried out on other specimens at temperatures varying from 770 to 830°C each hour. The object of this annealing was to obtain

an α -solid solution with an equiaxial granular structure. However, annealing for 36 hours gave this structure only in the case of the AT-6 alloy. Other alloys had a "woven" structure. Additional annealing caused only some coarsening of the elements of this structure.

The metallographic investigations have been carried out on the turned end of the heat-treated cylinder. Thus, the possible influence on the microstructure of surface saturation during heat treatment was excluded. The cold-worked layer was removed from the end of the specimen by etching in order to obtain a "needle" for the X-ray analysis.

The metallographic specimens were etched at room temperature in a solution containing 1 part by weight of hydrofluoric acid, 3 parts by weight of nitric acid, and 6 parts by weight of water. Parallel microstructural examination was carried out on specimens etched in a 50 % aqueous solution of sulfuric acid at a temperature of 70°C. Similar results were obtained as by the previous method. In addition, an electrochemical etching method described in an earlier publication [5] was also employed.

The hardness was measured by means of a Vickers apparatus with a 30 kg load.

The X-ray photographs were taken in a URS-70 apparatus equipped with a BSV-1-Cu tube (44 kv and 10 ma) i. e., with a copper target. The holding time was 8 to 10 hours. The β line of the spectrum was filtered off by means of a 0.3 mm-thick nickel filter. Secondary radiation was filtered through a single layer of X-ray film placed in front of the X-ray photograph.

The film was inserted asymmetrically into a 57.3 mm-diameter RKD chamber which enabled the X-ray photograph to be used not only for the phase analysis of the alloy but also for an exact determination of the lattice parameters of the various phases present.

The X-ray analysis carried out in a URS-50I ionizing apparatus [spectrometer] showed the reflection [angle] from the needles to be from 19 to 20.5° corresponding to the most intense lines 00.2 and 01.1 for the α -solid solutions and 110 for the β -solid solutions.

Results of investigation of the microstructure and hardness

Structure of initial alloys. Consideration will first be given to the photomicrographs showing the structure of some of the initial alloys (Figure 2), and also to their hardness (Table 2). The AT-3 alloy (Figures 2a and b) has a lamellar structure which is especially clearly seen in Figure 2b. At smaller magnifications (Figure 2a) the lamellae are less clearly visible and the structure has a "woven" or basket-like appearance.

The structure of the AT-4 alloy (Figures 2c and d) is of a similar "woven" type and the lamellae are clearly visible (Figure 2d). The structure of the AT-9 alloy does not differ essentially from that of the above-mentioned alloys, though it is less regular and has no clearly visible lamellae.

It should be pointed out that the higher the number of the alloy, the more disperse is the structure and the higher the hardness of the alloys (Table 2). If we assume that the initial structure of all alloys is the result of about the same treatment, then the finer structure and the higher hardness of the alloys, as designated by a higher number, can be explained by the higher content of alloying elements. The alloying elements apparently inhibit the diffusion and the phase transformations, causing a breaking up of the α phase and the formation of a disperse structure.



FIGURE 2. Microstructure of the investigated alloys after various heat treatment processes
a—AT-3 alloy in initial condition, $\times 450$; b—the same, $\times 1350$; c—AT-4 alloy in initial condition, $\times 340$; d—the same, $\times 1350$; e—AT-4 alloy in normalized condition $\times 340$; f—AT-9 alloy in normalized condition, $\times 1350$; g—AT-8 alloy in normalized condition, $\times 340$; h—AT-4 alloy annealed at 800° , $\times 200$; i—the same, annealed at 1000° .

TABLE 2
Hardness of the alloys in different conditions

Alloy	Temperature of heat treatment, °C	H _v , kg/mm ²		
		initial condition	normalized condition	hardened condition
AT-3	1020	261	248	278
AT-4	985	311	304	356
AT-6	1000	314	308	360
AT-8	1015	368	345	388
AT-9	1015	383	385	462
AT-10	1070	314	362	443

The fact that identical alloys have lamellae with the same shape and dimensions shows that all initial alloys consist essentially of a single-phase solid solution on the basis of α -Ti. This is confirmed by the results of electrochemical etching which show all grains to have the same color over the whole surface of the specimen.

Structure of normalized alloys. All the alloys investigated were normalized, i.e., heated to the temperatures shown in Table 2 and air cooled. The results of the investigation of normalized alloys are shown in Table 2 and in Figures 2e, f, g.

The AT-4 and AT-9 alloys (Figures 2e and f) have an acicular structure. The low alloyed AT-4, which was heated to a temperature apparently lower than the $\alpha + \beta$ field, is characterized by thick and coarse needles. The highly alloyed AT-9 has a fine acicular structure due both to the fact that it has a higher content of alloying elements than the AT-4 alloy and also because it was apparently heated to a temperature above the $\alpha + \beta$ field.

The AT-6 and AT-8 alloys have a somewhat different structure. In addition to the acicular grains these alloys also contain coarse equiaxial grains (Figure 2g).

Structure of hardened alloys. Hardened alloys have the same structure as normalized alloys, except for a somewhat greater degree of disorder in the structural components. In addition, a comparison of the acicular structures of hardened and normalized alloys shows that the hardened alloys have a finer but less stable structure.

An analysis of these structures did not confirm the presence of a β phase.

The influence of the annealing temperature on the structure of alloys. Specimens of the AT-4 alloy were annealed for 1 hour at 800, 850, 900, 950, 1000, 1050, 1100, 1150, and 1200°C. The structures obtained during this operation can be subdivided into two groups:

a) "woven" structure (obtained at temperatures up to 950°C); an example of such structures is shown in Figure 2h;

b) acicular structure (obtained at annealing temperatures from 1000-1200°C) shown in Figure 2i.

The temperature boundary which divides these two types of structure is 950 to 1000°C and corresponds apparently to a two-phase $\alpha + \beta$ field. Annealing temperatures below [the temperature boundary of] this field cause no phase transformation but only a certain coarsening of the elements of the "woven" structure of the α -solid solution. Heating to temperatures above the $\alpha + \beta$ field, which is associated with phase transformations and with the

formation of a β -solid solution, causes a strong grain coarsening during the soaking time and the formation of a fine acicular structure of an α -solid solution during cooling. The nature of the acicular structure is not affected to any extent by the annealing temperature.

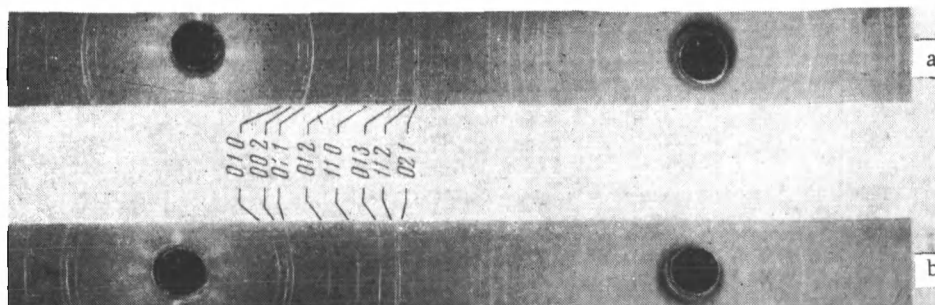


FIGURE 3. X-ray photograph of normalized (a) and hardened (b) AT-6 alloys

Results of X-ray analysis

The metallographic investigations of titanium alloys showed that all alloys, whether in the initial, normalized, or hardened condition, consist chiefly of an α -Ti solid solution.

Nevertheless, the inadequate accuracy of the metallographic analysis, the specific features of the chemical composition of the alloys being investigated, and the nature of the heat treatment permit the assumption that these alloys contain a certain amount of β -Ti solid solution.

In order to verify this assumption an X-ray investigation was carried out with a URS-70 apparatus (the methods of investigation and preparation of the specimens have been described above). X-ray photographs were taken of all six alloys in each of the three conditions: initial, normalized, and hardened. Some of these X-ray photographs are given in Figure 3.

An interpretation of these X-ray photographs and a comparison of the results with the preliminary calculations showed that the only lines on these photographs are those representing a hexagonal lattice. No lines of a cubic lattice were found. This is true for all three conditions of the alloy — initial, normalized, and hardened.

Nevertheless, later investigations with a URS-50I apparatus showed that these alloys contain a certain amount of the β -Ti solid solution.

In the investigation of AT alloys with the URS-50I apparatus, a copper target was used to produce the radiation*. For the analysis metallographic specimens were taken from which the deformed layer had been removed by an additional etching in concentrated hydrofluoric acid. The recording was in the form of a continuous curve with projections corresponding to the particular spectral lines.

* The authors wish to express their gratitude to V. V. Obukhovskii who cooperated in the photographic work with the URS-50I apparatus.

The sections obtained by recording the curve corresponding to the lines 011 of the α phase and 110 of the β phase of the AT-8 alloy (initial, normalized, and hardened conditions) are given in Figure 4.

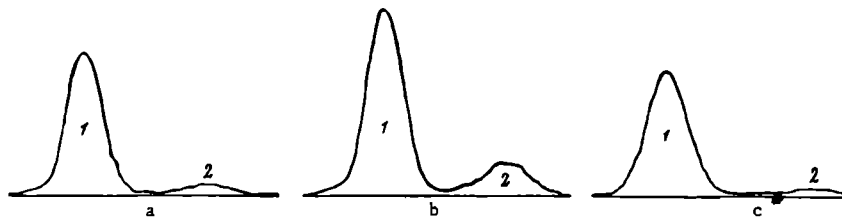


FIGURE 4. Interferential curves of an AT-8 alloy recorded by a URS-501 apparatus using a copper target for the radiation

a — initial condition; b — normalized condition; c — hardened condition; 1 — line 011 of the α phase ($20^{\circ}10'$); 2 — line 110 of the β phase ($19^{\circ}42'$).

The projections which correspond to the line 110 of the β phase were obtained for all alloys in all three conditions except for the hardened AT-9 alloy which showed no β phase.

The amount of the β phase in alloys was determined according to the formula given by A. S. Shigarev [7] and which the present authors have corrected by introducing a structural factor:

$$\% \beta = \frac{M_{\beta}}{M_{\beta} + M_{\alpha}},$$

where

$$M_{\beta} = \frac{I_{\beta}}{p_{\beta} c_{\beta}}; \quad M_{\alpha} = \frac{I_{\alpha}}{p_{\alpha} c_{\alpha}}.$$

The intensities of the lines I_{β} (110 β phase) and I_{α} (011 α phase) were taken as the integrated area under the curves. The reproducibility factors p_{β} (110 β phase) and p_{α} (011 α phase) and the structural factors c_{β} and c_{α} were taken from published data.

The content of the β phase (%) in the three alloys investigated is given, for different conditions, in Table 3.

TABLE 3
Amount of the β phase in titanium alloys

Alloy	Condition	Amount of β phase, %	Alloy	Condition	Amount of β phase, %
AT-4	Initial	10	AT-8	Hardened	2
AT-4	Normalized	9	AT-9	Initial	1
AT-4	Hardened	9	AT-9	Normalized	8
AT-8	Initial	4	AT-9	Hardened	0
AT-8	Normalized	10			

The fact that AT-4 alloys contain more of the β phase than AT-8 and AT-9 alloys is apparently due to the somewhat higher content of β -phase stabilizers — chromium, iron, silicon, and boron — and to the lower content of aluminum in AT-4 alloys.

Conclusions

1. Metallographic investigations using an ordinary white-black etch and a color etch, showed that all alloys, irrespective of the type, content of alloying elements, and nature of heat treatment, contain an α -solid solution with either a "woven" or an acicular structure. The structure is determined by the content of alloying elements, by the heating temperature, and by the cooling rate during the heat treatment.
2. An ordinary X-ray analysis with a URS-70 apparatus confirmed the results of the metallographic analysis and showed that all alloys investigated consist basically of an α -solid solution.
3. An X-ray analysis with a URS-501 apparatus showed that the alloys contain very small amounts of the β phase.
4. A hardness test showed that the properties of the α -solid solution are not identical in all alloys investigated. This may be due to the different degrees of grain refinement of the α -solid solution and to the distortion of the crystal lattice.
5. The problem of whether the lattice parameters of the α -solid solution change as a result of alloying and heat treatment, must be further examined.
6. AT titanium alloys consist, even under the most favorable conditions of heat treatment, of almost a pure α -solid solution, the content of the β phase being small.

Bibliography

1. Kornilov, I.I. Fiziko-khimicheskie osnovy zharoprochnosti splavov (Physico-Chemical Theory of Heat Resistant Alloys).—Izdatel'stvo AN SSSR. 1961.
2. Kornilov, I.I., B.K. Vulf', V.S. Mikheev, and S.A. Yudina.—Sbornik "Metallicheskie splavy dlya aviatsionnoi tekhniki", No. 883:30, Izdatel'stvo VVAA imeni Prof. Zhukovskogo. 1961.
3. Kornilov, I.I. and A.M. Yakimova.—Fizika Metallov i Metallovedenie, 12(4):550. 1961.
4. Kornilov, I.I. and P.B. Budberg. Diagrammy sostoyaniya dvoinykh i troinykh sistem titana (Phase Diagrams of Binary and Ternary Titanium Systems).—Izdatel'stvo VINITI AN SSSR. 1961.
5. Pul'tsin, N.M. and V.V. Pokrovskaya.—Zavodskaya Laboratoriya, No. 4:424. 1961.
6. Pul'tsin, N.M. Titanovye splavy i ikh primeneniye v mashinostroenii (Titanium Alloys and Their Application in Machine Building).—Mashgiz. 1962.
7. Shigarev, A.S. Metallovedenie i termicheskaya obrabotka metallov (Physical Metallurgy and Heat Treatment of Metals), No. 1:42. 1962.

CRYSTAL STRUCTURE OF SOME TERNARY INTER-METALLIC TITANIUM COMPOUNDS

E. I. Gladyshevskii, V. Ya. Markiv, Yu. B. Kuz'ma,
and E. E. Cherkashin

A number of systems $A-B-C$, where $A = \text{Mg, Sc, Ti, V, Cr, Mn, Zr, Nb, Hf, Ta}$; $B = \text{Cu, Fe, Co, Ni}$; $C = \text{Al, Si, Ga, Ge, In, Sn, Sb, Bi}$ (with a composition of ABC , AB_2C , and $A_5B_{16}C_7$) contain ternary intermetallic compounds of the following types:

MgCuSb in the Mg-Ni-Sb(Bi) , Mg-Cu-Sn(Sb, Bi) , and Mn-Cu-Sb systems /1/;

MnCu_2Al in the Mn-Co-Ge(Sn) , Mg-Ni-Sn(Sb) , Mn-Ni-Ge(Sn, Sb) , Ti-Ni-Al , and Mn-Cu-Al(In, Sn) systems /2/;

$\text{Mg}_6\text{Cu}_{16}\text{Si}_7$ in the $\text{Sc(Ti, Mn, Zr, Nb, Hf, Ta)-Ni-Si(Ge)}$, V(Cr, Mn)-Ni-Si , $\text{Zr(Nb, Hf, Ta)-Co-Si(Ge)}$, and Ti-Co-Si systems /3/.

The purpose of the present investigation of ternary titanium systems was to find intermetallic compounds of the above-mentioned structural types. The authors investigated ABC , AB_2C , and $A_5B_{16}C_7$ alloys of the following ternary systems: Ti-Co-Al , $\text{Ti-Fe(Co, Ni, Cu)-Ga}$, $\text{Ti-Fe(Co, Ni, Cu)-In}$, Ti-Co(Ni)-Si , Ti-Fe(Co, Ni)-Ge , $\text{Ti-Fe(Co, Ni, Cu)-Sn}$, and $\text{Ti-Fe(Co, Ni, Cu)-Sb}$.

The alloys were prepared by smelting the metals (not less than 99.9 % pure) in an electric resistance furnace in an atmosphere of an inert gas.

Since stratification was observed in the AB_2C alloys of the Ti-Fe(Co)-In system these alloys were not investigated further. The other alloys were annealed at 600°C for two weeks.

As a result of X-ray and microstructural investigations, the existence of $\text{Mg}_6\text{Cu}_{16}\text{Si}_7$ type ternary intermetallic compounds was determined among alloys of the Ti-Ni-Si(Ge) and Ti-Co-Si systems.

The structure of $\text{Mg}_6\text{Cu}_{16}\text{Si}_7$ (cubic syngony, space group $Fm\bar{3}m - O_h^8$) belongs to the type with a high coordination number /4, 5/ and a close-packed lattice of various dimensions /6/. The largest atoms (Mg) take up a position with a coordination number 17; the medium atoms (Si) take up a position with coordination numbers 14 and 12; the smallest atoms (Cu) take up a position with coordination numbers 13 and 12. In the ternary intermetallic compounds found, titanium ($r_{\text{Ti}} = 1.46 \text{ \AA}$) is the largest atom (coordination number 17). Atoms of silicon and germanium ($r_{\text{Si}} = 1.34 \text{ \AA}$, $r_{\text{Ge}} = 1.39 \text{ \AA}$) have coordination numbers 14 and 12 respectively, while atoms of cobalt and nickel ($r_{\text{Co}} = 1.25 \text{ \AA}$, $r_{\text{Ni}} = 1.24 \text{ \AA}$) have coordination numbers 13 and 12.

X-ray photographs of AB_2C alloys of the Ti-Co-Al , Ti-Fe(Co, Ni)-Ga , Ti-Ni(Cu)-In , Ti-Co-Ge , Ti-Fe(Co, Ni)-Sn systems show a cubic face-centered lattice (the lattice parameters are given in the table below). The distribution of the lines on the X-ray photographs, the relation of intensities between them, and the lattice parameters indicate that the

crystal structures of these alloys may belong to the BiF_3 or MnCu_2Al type. Since the corresponding binary systems have no compounds with a BiF_3 structure, the phases found cannot be solid solutions on the basis of some binary compounds but must be ternary intermetallic compounds.

The BiF_3 structure (space group $Fm\bar{3}m - O_h^h$) is characterized by a face-centered cubic lattice. The ternary AB_2C intermetallic compounds of this structure have a statistic distribution of smaller atoms A and B. For instance, in the ternary intermetallic compound $\beta\text{-(Ni, Cu)}_3\text{Sb}$ /7/ the atoms are distributed in the following way: 4Sb in the position 4(a) and 12 (Ni, Cu) in the position 4(b) and 8(c).

The MnCu_2Al structure (space group $Fm\bar{3}m - O_h^h$) differs from the BiF_3 structure in the ordered distribution of the smaller atoms. For instance, in the ternary TiNi_2Al compounds /8/ the atoms are distributed in the following way: 4 Al in the positions 4(a), 4Ti in the positions 4(b), and 8Ni in the positions 8(c).

In order to determine the structure of these compounds, a calculation was made of the intensity [of the diffraction] representing the distribution of the atoms in the structures of the BiF_3 and MnCu_2Al types. The calculations have shown that all intermetallic compounds found to exist in alloys with the composition TiB_2C have a crystal lattice of the MnCu_2Al type (see table).

Lattice parameters of some ternary intermetallic titanium compounds*

Composition	Structure	Lattice parameter, Å	Composition	Structure	Lattice parameter, Å
$\text{Ti}_6\text{Co}_{16}\text{Si}_7$	$\text{Mg}_6\text{Cu}_{16}\text{Si}_7$	11.232	TiCu_3In	MnCu_3Al	6.222
$\text{Ti}_6\text{Ni}_{16}\text{Si}_7$ **	$\text{Mg}_6\text{Cu}_{16}\text{Si}_7$	11.22	TiCo_3Ge	MnCu_3Al	5.823
$\text{Ti}_6\text{Ni}_{16}\text{Ge}_7$	$\text{Mg}_6\text{Cu}_{16}\text{Si}_7$	11.470	TiFe_3Sn	MnCu_3Al	6.074
TiCo_3Al	MnCu_3Al	5.847	TiCo_3Sn	MnCu_3Al	6.059
TiFe_3Ga	MnCu_3Al	5.854	TiNi_3Sn	MnCu_3Al	6.097
TiCo_3Ga	MnCu_2Al	5.848	TiFeSb	MgCuSb	5.957
TiNi_3Ga	MnCu_3Al	5.880	TiCoSb	MgCuSb	5.884
TiNi_2In	MnCu_3Al	6.099	TiNiSb	MgCuSb	5.872

* The parameters were determined with an accuracy of ± 0.004 Å in a camera for negative photography.

** This compound was investigated before in the work /3/.

The AB_2C alloys of the $\text{Ti}-\text{Fe}(\text{Co, Ni})-\text{Sb}$ system are heterogeneous. ABC alloys, the X-ray photographs of which show a face-centered cubic lattice, are homogeneous. The position of the lines on these X-ray photographs is identical with that of lines on the X-ray photographs of compounds of the MnCu_2Al or BiF_3 type, but the intensity of these lines is somewhat different (the lines with $h^2 + k^2 + l^2 = 8n + 3$ are more intense). As an analogy with the $\text{Mg}-\text{Ni}(\text{Cu})-\text{Sb}$ and $\text{Mn}-\text{Cu}-\text{Sb}$ systems it may be assumed that the ternary TiFeSb , TiCoSb , and TiNiSb compounds belong to the MgCuSb structural type (space group $F\bar{4}3m - T_d^2/9, 10/$).

The calculation of the intensity of the X-ray lines of ternary compounds TiFeSb , TiCoSb , and TiNiSb for the following distribution of atoms: 4Sb in position (c), 4Ti in position (d), and 4Fe (Co, Ni) in position 4(a)

confirms that these compounds belong to the MgCuSb structural type.

The data given in the table show that the compounds of the $\text{Mg}_6\text{Cu}_{18}\text{Si}_7$ structural type are formed in titanium alloys containing elements of the IVb subgroup (silicon or germanium); the compounds of the MnCu_2Al structural types are formed in titanium alloys containing elements of the IIIb and IVb subgroups while compounds of the MgCuSb structural types are formed in Ti alloys containing elements of the Vb subgroup of the periodical system.

No compounds of the $\text{Mg}_6\text{Cu}_{18}\text{Si}_7$, MnCu_2Al , or MgCuSb structural types have been found in the Ti—Cu—Ga, Ti—Fe—Ge, Ti—Cu—In, and Ti—Cu—Sb systems.

The authors wish to express gratitude to P.I. Kripyakevich for discussions in the course of this research.

Bibliography

1. Bokii, G. B., B. K. Vul'f, and N. L. Smirnova.—Zhurnal Strukturnoi Khimii, 2(1):98. 1961.
2. Bokii, G. B., K. K. Vul'f, and N. L. Smirnova.—Zhurnal Strukturnoi Khimii, 2(1):81. 1961.
3. Gladyshevskii, E. I., P. I. Kripyakevich, Yu. B. Kuz'ma, and M. Yu. Teslyuk.—Kristallografiya, 6(5):769. 1961.
4. Nagorsen, I. and N. Witte.—Z. anorg. u. allgem. Chem., 271 (3/4):44. 1953.
5. Bergman, G. and J. L. Waugh.—Acta crystallogr., 9(3):214. 1956.
6. Kripyakevich, P. I.—Kristallografiya, 5(1):79. 1960.
7. Rahlfs, P.—Metallwirt., No. 16:64. 1937.
8. Taylor, A. and R. Floyd.—J. Inst. met., Vol. 81:25. 1952.
9. Nowotny, H. and W. Sibert.—Z. Metallk, No. 33:391. 1941.
10. Gladyshevskii, E. I. and P. I. Kripyakevich.—Doklady AN SSSR, 102(4):743. 1955.

A REVIEW OF INVESTIGATIONS ON THE PHASE DIAGRAM OF THE BINARY Ti—Al SYSTEM

I. I. Kornilov, E. N. Pylaeva, and M. A. Volkova

The most important phase diagram of titanium alloys is that of the Ti—Al system, and it is the basis for the development of many important titanium alloys.

The Ti—Al system is comparable in importance to that of the Fe—C system for carbon and alloyed steels. The two elements in the Ti—Al system differ greatly in chemical properties and electron structures.

Great attention is paid in the literature to the reaction between titanium and aluminum. A detailed review of the phase diagram of this system is given in the references /1-4/. A full description of the system was published for the first time in 1951.

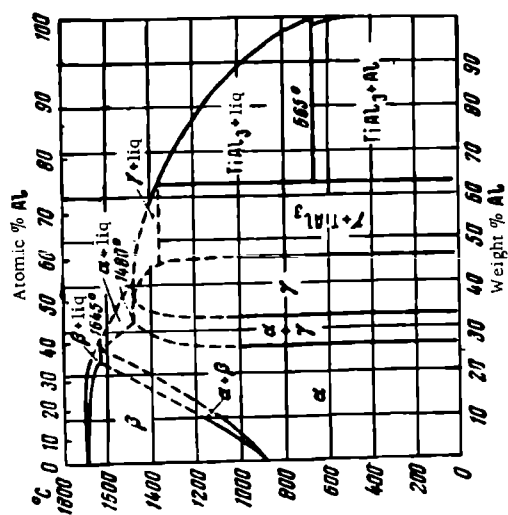
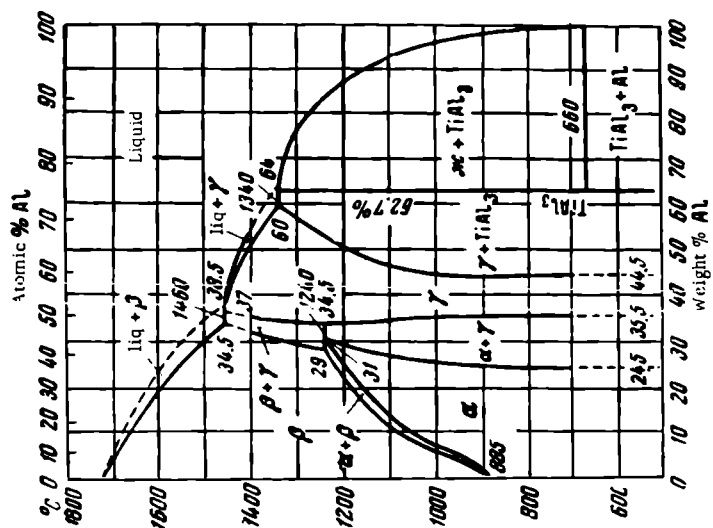
According to Ogden /5/, the maximum solubility of titanium in aluminum (Figure 1) at 510°C is about 0.24 weight %*.

It has been determined that a molten alloy containing 0.15 % of Ti reacts peritectically with the $TiAl_3$ compound. Titanium-base alloys form limited α - and β -solid solutions with hexagonal and cubic body-centered lattices of titanium. The solubility of aluminum in titanium is equal to 26 % at temperatures from 0 to 1050°C. If the system contains 34 to 46 % of Al in solution, a γ phase is formed on the basis of TiAl (the structure of this phase is described by Duwez and Taylor /6/). Ogden et al /5/ determined the temperature of the $\alpha \rightarrow \beta$ transformation and the lattice parameters of the α phase. The lattice parameters of the α phase are also given by Rostoker /7/. A summary of data obtained by different investigators starting with various materials, on the nature of the phases found and on the lattice parameters of these phases, is given in Table 1.

The phase diagram of the Ti—Al system was again investigated by Bumps et al /8/ in 1952. The phases found by these authors (Figure 2) are the same as those which had been found by Ogden et al /5/. The difference between the two diagrams is only that the α phase found by Bumps is formed not as a result of the peritectic liquid + $\beta \rightarrow \alpha$ reaction, but as a result of the peritectoid reaction $\beta + \gamma \rightarrow \alpha$ which takes place at 1240°C; in addition, the γ phase is formed as a result of the $\beta + \text{liquid} \rightarrow \gamma$ reaction.

The present authors published the phase diagram of the Ti—Al system in 1956 /15/. They also verified the phase diagram of this system published in an earlier work /1/. The differences in the position of the phase boundaries can be explained by the different purity of the initial materials. It was also shown by the authors that the heat resistance of the alloys is particularly high at aluminum contents of 7.5 % and more. It is possible that this high heat resistance is due to the presence of phases containing intermetallic compounds.

* All compositions in this paper are given in weight %.



The electrical and magnetic properties of alloys belonging to the α -phase field of the Ti—Al system have been published by Münster et al /11/. The authors of this investigation have shown that the curves of the electrical resistance and of the magnetic susceptibility are different from those characteristic for a homogeneous solid solution. This confirms the assumption that in the Ti—Al system the single-phase field on the basis of α -Ti extends up to 25 % Al.

In 1956, Sagel et al /9/ published a phase diagram of this system (Figure 3a).

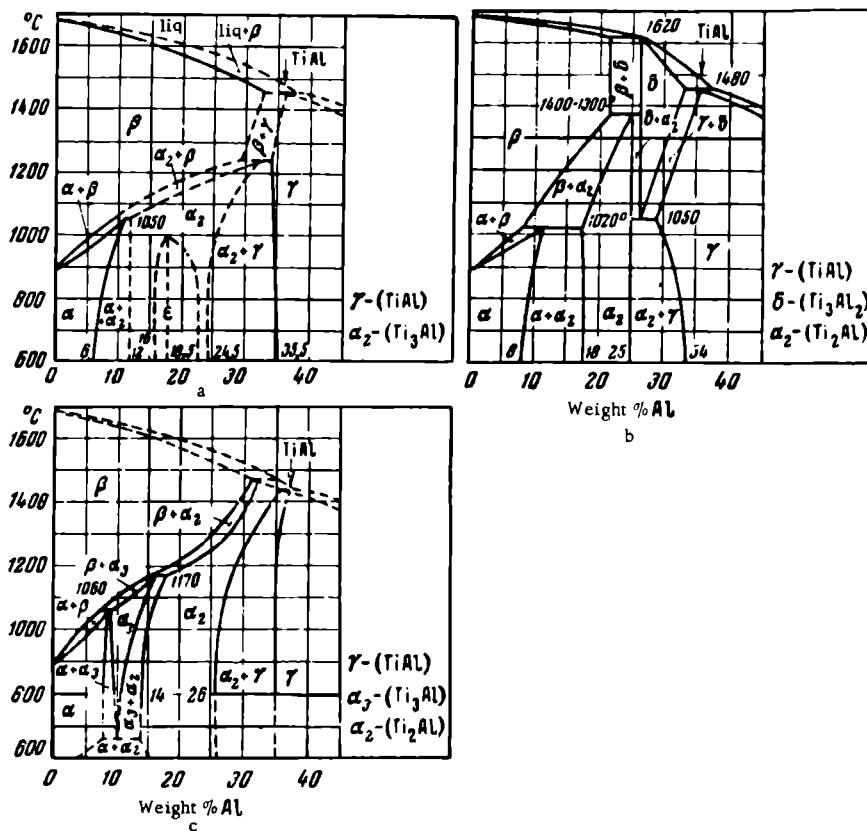


FIGURE 3. Phase diagram of the Ti—Al system

a — according to /9/; b — according to /12/; c — according to /13/.

TABLE 1

Summary of investigations of the Ti-Al system by various authors

Authors	Initial materials	Mechanical treatment of alloys	Heat treatment of alloys	Phases found in the system and their lattice parameters
Ogden et al /5/	Titanium iodide* 99.84 %; aluminum 93.99 %	Alloys with up to 16 % Al were hot-worked at 850°C; alloys with more than 16 % Al were investigated in the as cast condition	Alloys with up to 16 % Al were annealed at 850°C for 3.5 hours; cast alloy: were annealed at 1100 to 1000°C for 48 to 24 hours.	For α phases on the basis of titanium: at 0 % Al $a = 2.951\text{\AA}$; $c = 4.693\text{\AA}$; $c/a = 1.591$; at 25 % Al $a = 2.983\text{\AA}$; $c = 4.623\text{\AA}$; $c/a = 1.604$
Bumps et al /8/	Titanium iodide 99.9 % ($H_B = 100$ to 120 kg/mm ²); aluminum 93.99 %	Alloys with up to 14 % Al were cold-worked	Annealing at 1400°C for 10 min, at 1300°C for 10 min, at 1250°C for 2 hours, at 1000°C for 48 hours, at 700°C for 330 hours	For α phases on the basis of titanium: at 0 % Al $a = 2.943\text{\AA}$; $c = 4.679\text{\AA}$; $c/a = 1.591$; at 29 % Al $a = 2.878\text{\AA}$; $c = 4.617\text{\AA}$; $c/a = 1.604$
Sagel, Schulz, and Zwicker /9/	Titanium iodide ($H_B = 90$ kg/mm ²); technical titanium ($H_B = 130$ kg/mm ²)	Alloys with up to 15 % Al were forged to an area reduction of 40 to 80%; alloys with a higher content of aluminum were forged to a low area reduction	The alloys were homogenized at 1300°C for 3 hours and then annealed in the following way: alloys with 5 to 12 % Al— at 1080°C for 3 hours, at 100°C for 3 hours, at 900°C for 2 hours, at 750°C for 48 hours, and at 550°C for 75 hours; alloys with 18 to 25 % of Al— at 1050°C for 8 hours, at 1000°C for 7 hours, at 900°C for 7 hours, and at 800°C for 135 hours	No lattice parameters have been determined for the α_2 phase; for the ϵ phase, $a = 3.76\text{\AA}$, $c/a = 1.26$

* [The authors apparently mean metallic titanium obtained through titanium iodide.]

TABLE 1 (continued)

Authors	Initial materials	Mechanical treatment of alloys	Heat treatment of alloys	Phases found in the system and their lattice parameters
Anderko et al /10/	Technically pure titanium; purest aluminum	Alloys with 0 to 15% Al were mechanically worked	Homogenization at 900°C for 2.5 hours; annealing of the powders at 400°C for 100 hours	Ti ₃ Al compound (of the Ti ₃ Sn, Ni ₃ Sn, and Ni ₃ In type) length of the grains 2a and c; a ₂ phase in investigation /11/ on the basis of this compound
Sato et al /12/	Titanium sponge 99.7% (H _g = 112 to 116 kg/mm ²); aluminum 99.99%			a ₂ phase on the basis of Ti ₂ Al; δ phase on the basis of Ti ₃ Al ₂
E. Ence and H. Margolin /13/	Titanium iodide, electrolytic titanium; aluminum 99.99%	Alloys with up to 15.5% Al were forged at 1200 to 1300°C	Annealing at 1450°C for 1 hour, at 800°C for 2 months	a ₃ phase on the basis of Ti ₃ Al; a = 11.52Å; c = 4.65Å; c/a = 0.404; a ₂ phase on the basis of Ti ₂ Al(Ti ₃ Sn type): a = 5.775Å; c = 4.638Å; c/a = 0.803
Goldak and Gordon Parr /14/	Titanium iodide		Quenching in liquid air; annealing of powder at 1000°C for 2 hours	Ti ₃ Al compound (of the Ni ₃ Sn, Ti ₃ Sn type): a = 5.77Å; c = 4.62Å; Ti ₆ Al and Ti ₃ Al compounds
Our investigations	Titanium iodide 99.8% (H _g = 110 to 120 kg/mm ²); aluminum 99.99%	The alloys were mechanically worked	Annealing: at 1200°C for 2 hours, at 1100°C for 100 hours, at 1000°C for 200 hours, at 300°C for 250 hours, at 700°C for 300 hours, at 600°C for 500 hours, and at 550°C for 500 hours — quenching in water	

They studied titanium-rich alloys, the remainder of the phase diagram being prepared on the basis of an earlier investigation /1/. Using a metallographic method, Sagel et al found two new phases: α_2 and ϵ . An X-ray investigation of alloys with 0 to 18 % Al revealed the existence of a single hexagonal phase at temperatures below the polymorphic (allotropic) transformation. No precipitated phase was determined by X-ray analysis of alloys with 6 to 12% Al. The phase diagram in Figure 3a shows that at 600°C the phase boundaries $\alpha/\alpha + \alpha_2$ and $\alpha + \alpha_2/\alpha_2$ are at 6 and 12% Al [respectively]. At higher temperatures the two-phase field is shifted toward aluminum-rich alloys and is limited by a peritectoid equilibrium at 1050°C.

The latter authors found that in addition to the α_2 phase alloys with 18 % Al contain an ϵ phase, the structure of which was undetermined. According to preliminary data this phase has a tetragonal face-centered lattice; $a = 3.76 \text{ \AA}$ and $c/a = 1.26$. Thus in the Ti-Al systems metallographic investigations have shown the existence of two new phases: α_2 and ϵ , homogeneous at 12 to 16 % and 18.5 % Al respectively. However, the existence of these phases was not confirmed by X-ray analysis. A schematic phase diagram was, therefore, drawn for this part of the system.

Clark and Terry /16/ have published provisional data on the lattice parameters of alloys of the Ti-Al system, containing up to 20 % Al. They found superlattice lines indicating the existence of an ordered Ti_3Al phase analogous to the ordered Ti_3Sn phase. The present authors obtained composition versus lattice parameter curves for 850°C and 650°C. Parameter (a) indicates clearly a discontinuity between the ordered and disordered alloys.

In investigation of the Ti-Al-O system /17/, Ence and Margolin determined that the superlattice lines are due to the existence of an intermetallic compound in the Ti-Al system. The investigation of alloys with 20 to 30 % Al showed that this intermetallic compound has a field of solubility in the vicinity of Ti_2Al and a hexagonal lattice with the following parameters: $a = 5.775 \text{ \AA}$, $c = 4.638 \text{ \AA}$, $c/a = 0.803$; the structure of Ti_2Al is isomorphic to that of Ti_3Sn . The latter authors indicate that this field may contain another intermetallic compound in addition to Ti_2Al .

An investigation of alloys with 6.8 and 10 % Al was carried out by Crossley and Carew /18/ in order to determine the cause of embrittlement of alloys of the Ti-Al system. Specimens annealed and hardened from different temperatures were tensile-tested at room temperature. It was determined that alloys aged at 550°C have both a lower plasticity and lower yield point. The microstructure of aged specimens indicates the presence of a second phase. The data of X-ray analysis showed that this phase is based on the compound Ti_2Al , i.e., the results of Ence and Margolin were confirmed /17/.

Anderko et al /10/ studied alloys of titanium with 6 to 15 % Al and α -solid solutions in the Ti-In and Ti-Al-In systems. Titanium alloys with 39 % In showed diffractions which can be interpreted as being due to superlattice lines of a hexagonal unit cell with a length of the edges equal to $2a$ and c . The [present] authors assume that this alloy contains a hexagonal ordered Ti_3In phase with the same type of structure as exists in Ni_3In , Ni_3Sn , and Ti_3Sn alloys. The intensity of the lines of the Ti_3In compound was calculated for the binary alloy with 39 % In and satisfactory agreement was obtained between the calculated values and experimental data.

For alloys of the $\text{Ti}_3\text{In}-\text{Ti}_3\text{Al}$ system, the present authors have measured the intensity of the superlattice line 010 and have found that this intensity decreases from Ti_3In to Ti_3Al . In the opinion of the authors, the superlattice lines found coincide with those observed by Clark and Terry /16/ in their investigation of $\text{Ti}-\text{Al}$ alloys.

Thus, the X-ray investigation of $\text{Ti}-\text{In}$, $\text{Ti}-\text{Al}$, and $\text{Ti}-\text{In}-\text{Al}$ alloys have shown that the $\text{Ti}-\text{Al}$ and $\text{Ti}-\text{In}$ systems contain ordered hexagonal Ti_3Al and Ti_3In phases which are mutually isomorphic and form a continuous series of solid solutions /10/.

Tagunova /19/ investigated titanium alloys containing 2 to 18 % Al, after hardening them from temperatures of 1000, 850, 750, and 600°C. No reliable data on the existence of α_2 and ϵ phases /9/ could be obtained.

Saulnier and Croutzelles /20/ carried out an investigation of thin specimens of alloys containing 15 % Al using microscopic and electronographic methods and found phases with a close-packed hexagonal lattice and with the following parameters: $a = 5.77 \text{ \AA}$, $c = 4.65 \text{ \AA}$. This phase is a superlattice of a solid solution of the Mg_3Cd type.

Sato et al /12/ constructed a phase diagram of the $\text{Ti}-\text{Al}$ system based on the electrical resistance of the alloys at elevated temperatures (Figure 3b). The data obtained were confirmed by X-ray and microstructural analyses.

The electrical resistance of the specimens was measured in vacuo at 800 to 1000°C and in an atmosphere of argon at higher temperatures (up to 1450°C). The microstructure of the alloys was investigated in the hardened and in the annealed conditions.

According to the electrical-resistance measurements, an increase in the aluminum content from 0 to 6 % increases the temperature of the polymorphic $\alpha \rightarrow \beta$ transformation. An increase in the aluminum content from 7 to 10 % also increases the temperature of the $\alpha \rightarrow \beta$ transformation. The curves obtained for these alloys show inflections in the region from 400 to 800°C which can be due only to the presence of inclusions of an α_2 phase. The specific resistance curves of alloys with 12 to 18 % Al have inflections at 1020°C (at this temperature the authors have drawn the line of the peritectic equilibrium). Alloys with 22 to 25 % Al have a negative temperature coefficient of electrical resistance and [their specific resistance curves] have no inflection up to 1400°C. Alloys with more than 26 % Al have a positive temperature coefficient of electrical resistance; the [specific resistance] curves of alloys with 26 to 29% Al have an inflection at 1050°C.

Microscopic investigation has revealed a peritectoid structure in alloys with 15 to 18 % Al, a single-phase structure in alloys with 19 to 25 % Al, a single-phase structure (δ phase) in alloys with 27 % Al hardened from 1250°C, and a eutectoid $\alpha_2 + \gamma$ structure if this alloy is annealed at below 1050°C. An X-ray analysis has confirmed the existence of α , α_2 , and γ phases in accordance with published data. No boundaries for the α and α_2 phases could be determined.

According to published data the following peritectic reactions take place in this system: liquid + $\beta\text{-Ti} \rightarrow \delta$ (at 1620°C; 72.5 % Ti, 27.5 % Al) /4/; liquid + $\delta \rightarrow \gamma$ (at 1460°C; 61.5% Ti + 38.5% Al) /8/. It was determined that solid solutions are formed in the system at 19-25 % Al. These are in a state of equilibrium with the $\alpha\text{-Ti}$ phase and correspond to the α_2 phase found by other workers /9/. Sato et al /12/ are of the opinion that the α_2 phase is based on the Ti_2Al compound (21.9 % Al) and not on the Ti_3Al compound (15.9 % Al).

Solid solutions were also found to exist at high temperatures in alloys with 26 to 34 % Al (δ phase). The authors point out that the δ phase exists in the field of Ti_3Al_2 . The following transformations take place in this system:

peritectoid $\beta-Ti + \delta \rightarrow \alpha_2$ (at 1300—1400°C; 78 % Ti+22 % Al);

peritectoid $\beta-Ti + \alpha_2 \rightarrow \alpha - Ti$ (at 1020°C; 92 % Ti+8 % Al);

eutectoid $\delta \rightarrow \gamma + \alpha_2$ (at 1050°C; 73,5 % Ti+26,5 % Al).

The solubility of aluminum in α -Ti at 400°C is 7 %.

The heats of formation of titanium, vanadium, chromium, and manganese aluminides have been determined /21/. The authors of this investigation point out that the alloy with 25 atomic % of Al contains not an α phase but a Ti_3Al compound with a structure of the Mg_3Cd type, which is in agreement with the work mentioned above /20/.

Figure 3c shows a phase diagram of the Ti—Al system constructed according to the data of Ence and Margolin/13/. Microstructural, X-ray analyses and determinations of hardness and of microhardness were used. The system contains α , β , α_3 (Ti_3Al), α_2 (Ti_2Al), and γ ($TiAl$) phases. The α_3 phase on the basis of Ti_3Al is formed during the peritectoid reaction: $\beta + \alpha_2 \rightarrow \alpha_3$ at 1170°C; this phase can be transformed by hardening into a structure similar to titanium martensite. The α_3 phase has a hexagonal lattice with the following parameters: $a = 11.52 \text{ \AA}$, $c = 4.65 \text{ \AA}$, and $c/a = 0.404$. The α phase forms at 1060°C according to the reaction $\beta + \alpha_3 \rightarrow \alpha$ (9% Al), while the α_2 phase forms according to the peritectoid reaction $\beta + \text{liquid} \rightarrow \alpha_2$ (the α_2 phase is based on Ti_2Al and has a hexagonal lattice with the following parameters: $a = 5.775 \text{ \AA}$, $c = 4.638 \text{ \AA}$, and $c/a = 0.803$; during hardening the α_2 phase transforms in the same way as the α_3 phase).

An investigation was carried out by Goldak and Parr /14/ to determine definitely the structure of Ti_3Al , necessary in view of the contradictory published data. X-ray photographs were obtained up to a temperature of 900°C in a vacuum of 10^{-6} mm Hg. The results of this investigation show the existence of a hexagonal structure. No superlattice lines were obtained at temperatures above 600°C. The magnitudes of $\sin^2 \theta$ and the relative diffraction intensity of the Ti_3Al compound were calculated for alloys with 25 at % Al.

The latter authors obtained good agreement between the calculated and measured intensities which in their opinion confirms the existence of the DO_{19} structure. The following lattice parameters were calculated: $a = 5.77 \text{ \AA}$ and $c = 4.62 \text{ \AA}$. The authors are also of the opinion that this phase is most probably based on Ti_3Al (Ni_3Sn type) and not on Ti_2Al as was indicated in the earlier investigation /17/.

In 1961 the present authors published a report /22/ on the phases present in titanium base α -solid solutions, as indicated by the relationship between the Hall constants and the compositions. Previous investigation of the galvanomagnetic effects showed that the composition versus property curves have inflections which correspond to the stoichiometrical composition of the chemical compounds.

The first inflection in the Hall constant versus composition curve of the Ti—Al system corresponds to 14.3 at.% (9 weight %) Al, which is equivalent to the Ti_6Al intermetallic compound. The most notable point is that representing a composition of 25 at. % (16 weight %) of Al which corresponds to the Ti_3Al compound. The third inflection represents $TiAl$ with 50 at. % (36.02 weight %) Al. This compound has been earlier determined by methods of physicochemical analysis.

Since the study of the phase diagram of the Ti—Al system gives conflicting results, the present authors carried out an additional investigation of this system (from 0 to 26 % Al) by thermal and X-ray analyses, by determining the microstructure, and also by measuring the specific electric resistance, hardness, and the Hall effect.

Titanium iodide, Ti(99.8 %), and Al (99.99 %) were the initial materials. The alloys were smelted in an arc furnace in an atmosphere of argon, mechanically worked at 850 to 1000°C, and heated at 1200°C for 2 hours, at 1100°C for 100 hours, at 1000°C for 200 hours, at 800°C for 250 hours, at 700°C for 300 hours, at 600°C for 500 hours, and at 550°C for 500 hours. After each heating the specimens were quenched in water. In this investigation titanium iodide replaced the calcium hydride used in the earlier investigation /15/. In this investigation the specimens were smelted in an arc furnace (in a previous research the specimens were sintered and fused in an induction furnace).

After the prolonged step-by-step annealing (see above) a differential recording of the heating curves up to 1200°C was taken with a N. S. Kurnakov pyrometer. The microstructure of the alloys was investigated using specimens which had been hardened from the above-mentioned temperatures. The hardness was measured on a Vickers tester using a 10 kg load. The electrical resistance of specimens annealed at temperatures from 1100 to 600°C was measured by the compensation method with a potentiometric device.

The temperatures of the $\alpha \rightarrow \beta$ transformations obtained by the method of differential recording of the heating curves, are given in Figure 4. These curves have no maxima. As is evident from this figure the temperature of the $\alpha \rightarrow \beta$ transformation increases smoothly from 960°C for an alloy with 4 % Al to 1230°C for an alloy with 22 % Al.

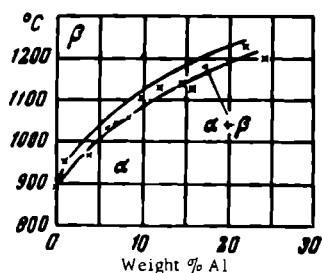


FIGURE 4. Temperature of $\alpha \rightarrow \beta$ transformations in alloys of the Ti—Al system

Alloys containing from 0 to 18 and from 0 to 10 % Al (Figure 5a) have a β -phase structure if hardened from 1200 and 1100°C respectively, while alloys with 20 % Al and 12 % Al hardened from those temperatures have a two-phase $\alpha + \beta$ structure (Figure 5b). Alloys with 16 % Al hardened from 1100°C have a single-phase α_2 structure (Figure 5c). Alloys with 11 to 13 % Al hardened from 1050 or 1000°C have a two-phase $\alpha + \alpha_2$ structure (Figure 5d), which differs from the structure of the $\alpha + \beta$ field. Alloys with more than 13 % Al have a polyhedral structure of a solid solution (α_2 phase). Alloys with up to 7 % Al hardened from 900, 800, 700, and 600°C have a single-phase uniform structure of an α -solid solution (Figure 5e). Alloys with 8 to 14 % Al have a two-phase structure: $\alpha + \text{Ti}_6\text{Al}$ (alloys with 8 % Al, Figure 5f) and $\text{Ti}_6\text{Al} + \alpha_2$ (alloys with 12 % Al, Figure 5g). Alloys with more than 14 % Al have a single phase structure of a α_2 -solid solution (Figure 5h).

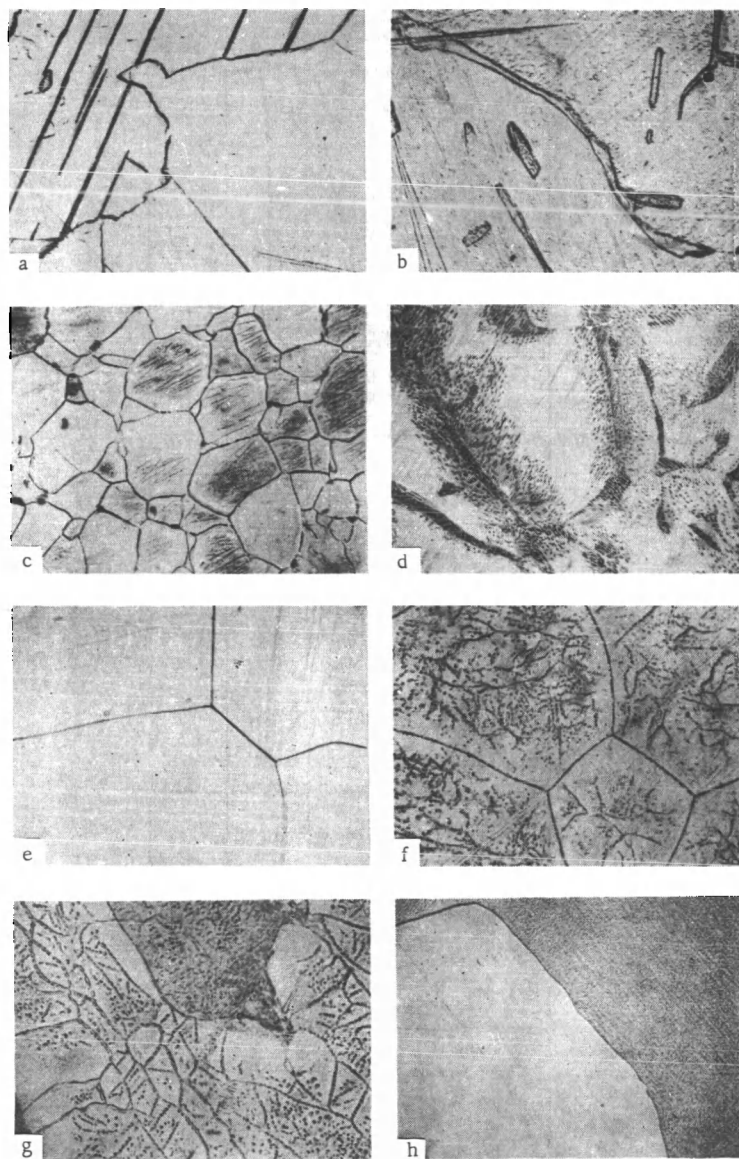


FIGURE 5. Microstructures of alloys of the Ti-Al system

a — 7% hardened from 1200°C, transformed β phase, $\times 200$; b — 12 % Al, hardened from 1100°C, α + transformed β phase, $\times 200$; c — 16 % Al, hardened from 800°C, α_2 phase, $\times 200$; d — 12% Al, hardened from 1050°C, α + α_2 phase, $\times 200$; e — 4% Al, hardened from 800°C, α phase $\times 200$; f — 8 % Al, hardened from 600°C, α + Ti_6Al , $\times 340$; g — 12% Al, hardened at 800°C, Ti_6Al + α_2 , $\times 340$; h — 21 % Al, hardened at 900°C, α_2 phase, $\times 200$.

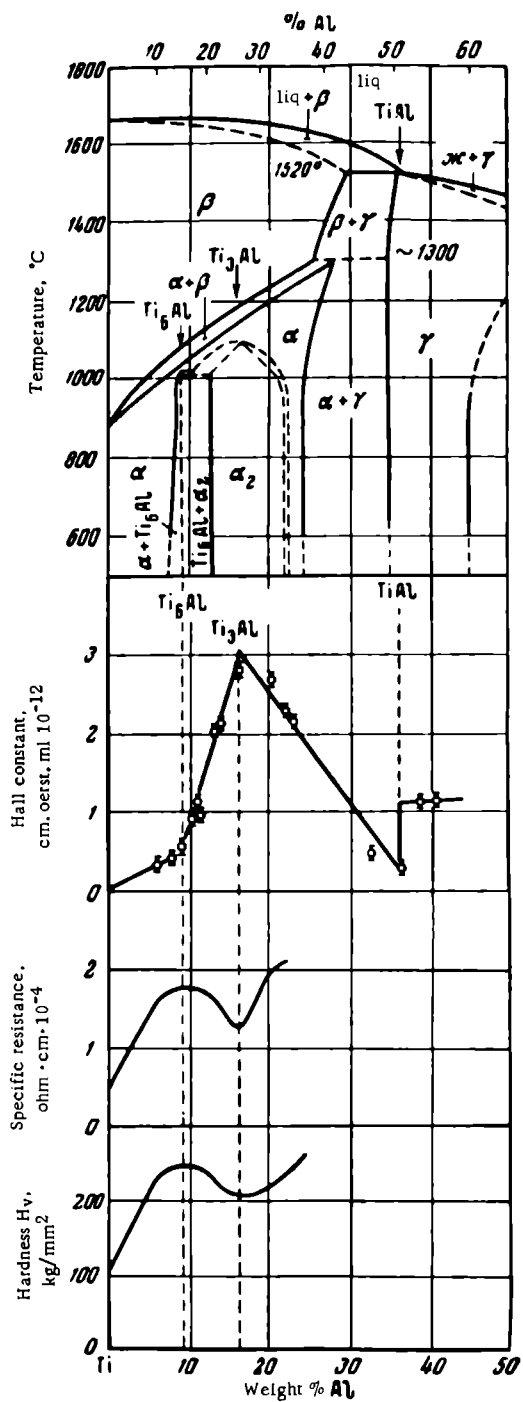


FIGURE 6. Phase diagram and properties of alloys of the Ti—Al system

The lower part of Figure 6 shows the variation of the specific resistance and of the hardness of alloys annealed at 600°C. It is evident that the course of the curves changes at 7 to 8 % and 13 to 14 % Al, which corresponds to the phase boundaries given in the diagram. The minima of the specific resistance and hardness correspond to about 16 % Al (Ti_3Al —15.9 % Al). Figure 6 (composition versus Hall effect curve) shows that the inflections at 9, 16, and 36 % of Al correspond to the stoichiometrical compositions of the following intermetallic compounds: Ti_6Al (8.6 % Al), Ti_3Al (15.9 % Al), and TiAl (36.02 % Al) /22/. On the basis of data obtained (mainly from the minima on the curves of specific resistance and hardness, from the inflections of the Hall effect curves, and from the microstructures of alloys hardened from various temperatures), it may be assumed that the [Ti—Al] system contains Ti_6Al and Ti_3Al intermetallic compounds.

Figure 6 shows a hypothetical phase diagram which takes into account the existence of Ti_6Al (found by the Hall effect method) and Ti_3Al compounds which are formed upon ordering of the α -solid solution.

As a result of these investigations it may be assumed that the Ti—Al system contains:

1) An α -solid solution on the basis of titanium with 0 to 7.5 % and 22.5 to 24.5 % (at 600°C); 2) a two-phase field $\alpha + \text{Ti}_6\text{Al}$ with 7.5 to 9.0 % Al and a two-phase field $\text{Ti}_6\text{Al} + \alpha_2$ with 9 to 14 % Al; 3) two intermetallic compounds Ti_6Al with 9 weight % (14.3 at. %) Al with a small field of homogeneity and a Ti_3Al compound with 15.8 weight % (25 at. %) Al with a large field of homogeneity.

The assumed presence of Ti_6Al and Ti_3Al compounds is confirmed by the data on the elasticity coefficient of the alloys of this system*.

It is expected that the existence of the compounds Ti_6Al and Ti_3Al , found by the authors as described above, will be confirmed by a structural analysis; investigations are being conducted in this direction.

Bibliography

1. Hansen, M. Constitution of Binary Alloys, 2nd edition.— McGraw-Hill Co. 1958.
2. Vol, A. E. Stroenie i svoistva dvoynykh metallicheskich sistem (Structure and Properties of Binary Metallic Systems), Vol. 1: 471.— Fizmatgiz. 1959.
3. Eremenko, V. E. Titan i ego splavy (Titanium and Its Alloys), No. 2.— Izdatel'stvo AN USSR. 1960.
4. McQuillan, A. D. and M. K. McQuillan. Titanium.— Metallurgy of Rarer Metals, Vol. 2, New York. 1955. [Russian translation. 1958.]
5. Ogden, H. R., D. J. Maykuth, W. L. Finlay, and R. I. Jaffee.— J. Metals, 3(12): 1150. 1951.
6. Duwez, P. and J. Taylor.— J. Metals, 4(1): 70. 1952.
7. Rostoker, W.— J. Metals 4(2): 212. 1952.
8. Bumps, E. S., H. D. Kessler, and M. Hansen.— J. Metals, 4(6): 609. 1952.
9. Sagel, K., E. Schulz, and U. Zwicker.— Zs. Metallk., 47(8): 529. 1956.

* See the article by S. G. Fedotov, p. 199.

10. Anderko, K., K. Sagel, and U. Zwicker. — *Zs. Metallk.*, 48(2): 57. 1957.
11. Münster, A., K. Sagel, and U. Zwicker. — *Acta metallurgica*, 4(5): 558. 1956.
12. Sato, Khuan, Yan'-tsin, Kondo. — *J. Japan Inst. Met.*, 23(8): 456. 1956.
13. Ence, E. and H. Margolin. — *Trans. Am. Ins. Met. Eng.*, Vol. 221: 151. 1961.
14. Goldak, A. G. and J. Gordon Parr. — *Trans. Am. Inst. Met. Eng.*, Vol. 221: 639. 1961.
15. Kornilov, I. I., E. N. Pylaeva, and M. A. Volkova. — *Izvestiya AN SSSR, OKhN*, No. 7: 771. 1956.
16. Clark, D. and J. C. Terry. — *Bull. Inst. Met.*, 3(13): 116. 1956.
17. Ence, E. and H. Margolin. — *Trans. Am. Inst. Met. Eng.*, Vol. 209: 484. 1957.
18. Crossley, F. A. and W. F. Carew. — *J. Metals*, 9(1): 43. 1957.
19. Tagunova, T. V. — *ZhNKh*, 3(3): 815. 1958.
20. Saulnier, A. and M. Croutzelles. — *C. r. d. sci.*, Vol. 246: 3622. 1958.
21. Kubaschewski, O. and G. Heymer. — *Trans. Faraday soc.*, 56(4): 473. 1956.
22. Grum-Grzhimailo, N. V., I. I. Kornilov, E. N. Pylaeva, and M. A. Volkova. — *Doklady AN SSSR*, 137(3): 599. 1961.

INVESTIGATION OF THE PHASE COMPOSITION OF ALLOYS
OF THE Ti—Al—Cr—Fe—Si SYSTEM WITH CONSTANT
CONTENTS OF ALUMINUM (6 %) AND SILICON (0.3 %)

N. G. Boriskina and I. I. Kornilov

In the course of the investigation of the structure of titanium base alloys, the authors studied titanium rich alloys of the five-component Ti—Al—Cr—Fe—Si system. Aluminum, chromium, iron, and silicon are the chief alloying components of a number of alloys of the AT series which are, at present, in the stage of industrial testing /1/.

The polythermal section of this system for alloys containing up to 7.5 % Al and also 0.5 % Cr, 0.5 % Fe, and 0.5 % Si was investigated by Kornilov et al /2/.

As the subject of the present investigation, the authors have chosen alloys represented by the section of the Ti—Al—Cr—Fe tetrahedron containing 6 % Al. Silicon was added to all alloys in amounts corresponding to its solubility in solid α -titanium (0.3 %).

At a constant content of components comprising the solid solution of titanium /3/, the section of the tetrahedron can be represented as a ternary system in which one of the vertexes represents a solid solution of titanium with 0.3 % Si and 6 % Al.

The nature of the chemical reactions between titanium and aluminum, titanium and iron, titanium and chromium, titanium and silicon, and also the structures of the Ti—Cr—Al, Ti—Al—Fe, Ti—Cr—Fe systems, have been investigated in detail by Soviet and foreign authors /4-6/.

Without dwelling too long on the phase diagrams concerned, the authors would only like to point out that chromium, iron, and silicon are β -phase stabilizers of titanium, with which they give phase diagrams of the eutectoid type. The Ti—Fe system is characterized by the presence of two compounds: TiFe and TiFe₂. The reaction between titanium and chromium results in the crystallization of TiCr₂ from the β -solid solution. This compound has a lattice of the MgZn₂ type at 1100°C to 1350°C and a lattice of the MgCu₂ type at temperatures below 1100°C. The most titanium-rich compound of the Ti—Si system is Ti₅Si₃. Aluminum increases the temperature of the polymorphic $\beta \rightleftharpoons \alpha$ -Ti transformation and is, therefore, an α -phase stabilizer of titanium. The wide fields of α -solid solutions of titanium with aluminum have recently been found to contain Ti₄Al and Ti₃Al intermetallic compounds /7/; the existence of a Ti₂Al compound has also been assumed in /8/. In addition, titanium forms with aluminum TiAl and TiAl₃ intermetallic compounds.

The structure of alloys of this section of the tetrahedron is to a considerable degree dependent on the structure of the alloys of the Ti—Cr—Fe system. This system is characterized by the presence of a wide field of

solid solutions on the basis of TiFe_2 and TiCr_2 compounds with a hexagonal modification /9/. A solid solution on the basis of the compound $\text{Ti}(\text{CrFe})_2$ crystallizes from the liquid alloys at widely varying contents of iron and chromium. At certain temperatures this solid solution is in a two- and three-phase equilibrium with α - and β -Ti, with TiFe and TiCr_2 compounds, with α -Fe, and also with $\text{Ti}_5\text{Cr}_7\text{Fe}_{17}$ /10/, which exists in iron-rich alloys.

Methods of preparation and heat treatment of alloys

For the investigations alloys with compositions corresponding to 3 radial sections [of the tetrahedron] and with constant iron to chromium ratios of 3:1, 1:1, 1:3 (up to 30 % Fe + Cr) were prepared. These sections will be designated by numbers I, II, and III, respectively. The compositions of the investigated alloys are given in the table below. The initial materials were TG-00 titanium, electrolytic chromium, KR-1 silicon, A00 aluminum, and iron containing 0.03 % C; 0.01 % Mg; 0.003 % S; and 0.008 % P. The alloys were prepared by smelting in an arc furnace with tungsten electrodes and in an atmosphere of argon.

Chemical composition of alloys investigated, %

Ti	Al	Si	Fe			Cr		
			section I	section II	section III	section I	section II	section III
93.5	6.0	0.3	0.15	0.1	0.05	0.05	0.1	0.15
93.2	6.0	0.3	0.375	0.25	0.125	0.125	0.25	0.375
92.7	6.0	0.3	0.75	0.5	0.25	0.25	0.5	0.75
91.2	6.0	0.3	0.875	1.25	0.625	0.625	1.25	1.875
88.7	6.0	0.3	3.75	2.5	1.25	1.25	2.5	3.75
86.2	6.0	0.3	5.625	3.75	1.875	1.875	3.75	5.625
83.7	6.0	0.3	7.50	5.0	2.5	2.50	5.0	7.5
78.7	6.0	0.3	11.25	7.5	3.75	3.75	7.5	11.25
73.7	6.0	0.3	15.0	10.0	5.0	5.0	10.0	15.0
63.7	6.0	0.3	22.5	15.0	7.5	7.5	15.0	22.5

Alloys of sections I and II with up to 15 % Fe + Cr and of section III with up to 20 % Fe + Cr were forged at 1000 to 1200°C into rods of 8 to 9 mm diameter. All alloys were homogenized by annealing at 1000°C for 15 hours in vacuum quartz ampoules. Some of these specimens were hardened from this temperature, and some were cooled together with the furnace to 800°C (cooling time 300 hours) and quenched in water. The remaining specimens were cooled in the furnace to 500°C, kept at this temperature for 750 hours, and further cooled in the furnace at room temperature. The specimens which were hardened from 1000°C were further heated to 1100°C and, after keeping at this temperature for 5 hours, were quenched in water.

The investigation was carried out mainly by means of microstructural and X-ray analyses. Both the specific resistance and the hardness of the alloys were measured after each heat treatment operation. For the approximate identification of the phase components of the alloys, the microhardness testing method was used.

Results

A microstructural investigation of alloys belonging to sections I, II, and III, has shown that the first to crystallize from cast alloys with up to 30 % Fe+Cr is the β -solid solution of titanium. In alloys with 30 % Fe+Cr, belonging to section I the grains of the β -solid solution are surrounded by a two-phase mixture which is probably a β +TiFe eutectic. The grain boundaries of alloys with 30 % Fe+Cr, belonging to section II, contain small amounts of the second phase. In alloys of the radial sections containing up to 2.5 % Fe+Cr, hardened from 1100°C, the β -solid solution undergoes an intensive martensitic decomposition. Alloys of sections I and III with 5 to 25 % Fe+Cr and alloys of section II with 5 to 30 % Fe+Cr contain two phases (Figures 1a and b). According to the data of X-ray analysis, the alloys of section I consist of β -Ti and TiFe while alloys of section III contain TiCr_2 of the hexagonal modification or, in analogy with the Ti-Cr-Fe system, a $\text{Ti}(\text{Cr}, \text{Fe})_2$ phase (arbitrarily a γ phase).

The alloys of the radial sections with up to 1 % Fe+Cr which have been hardened from 1000°C contain, in addition to the transformed β phase, a considerable amount of equilibrium α grains, the amount of which decreases with the increase in the total content of iron and chromium.

Alloys with 2.5 % of Fe+Cr have no grains of the equilibrium α phase but contain an α' phase which is present in a state of equilibrium with the β -solid solution of titanium. At 1000°C alloys with 5 to 25 % Fe+Cr, belonging to the radial sections, contain a β -solid solution of titanium. Annealing at 1000°C of alloys belonging to sections I and III and containing 30 % Fe+Cr increases the amount of the secondarily precipitated phases TiFe and $\text{Ti}(\text{CrFe})_2$ respectively. The β -solid solution of alloys of section II with 30 % Fe+Cr also transforms [on annealing] to give a γ phase.

Alloys of all three radial sections with 0.2 % Fe+Cr, hardened from 800°C, consist of solid solutions on the basis of α -Ti. The structure of these alloys is similar to that shown in Figure 1c.

Alloys with a higher content of alloying elements contain grains of the β -solid solution (Figure 1e). Its content increases with the increase in the total amount of iron and chromium. Alloys of sections I and III, with 10 % Fe+Cr and of section II with 15 % Fe+Cr, retain the β -solid solution of titanium. The β -solid solution of alloys with a higher content of iron and chromium decomposes precipitating the corresponding intermetallic compound.

The microhardness of the second phase of alloys belonging to section I and containing 15 % Fe+Cr is 375 units (β -Ti = 286 units). According to the data of an X-ray analysis, this phase consists of the TiFe intermetallic compound. The decomposition of the β -solid solution of alloys of sections I and II, with 20 % Fe+Cr, entails the formation of two phases which precipitate within the β grains and along the grain boundaries. The microstructure of these alloys is similar to that shown in Figure 1e. According to the data of X-ray analysis the phase components of these alloys are β -Ti, TiFe, and the γ phase.

Alloys of section I containing 30 % Fe+Cr have, in addition to the TiFe grains, many grains of the $\text{Ti}(\text{CrFe})_2$ phase. The microhardness of the phase components of this alloy are: β -Ti = 473 units, TiFe = 600 units, $\text{Ti}(\text{CrFe})_2$ = 673 units. Alloys of section II with 30 % Fe+Cr have more and larger grains of $\text{Ti}(\text{CrFe})_2$. In addition, these alloys contain small amounts of minute TiFe crystals precipitated along the grain boundaries of

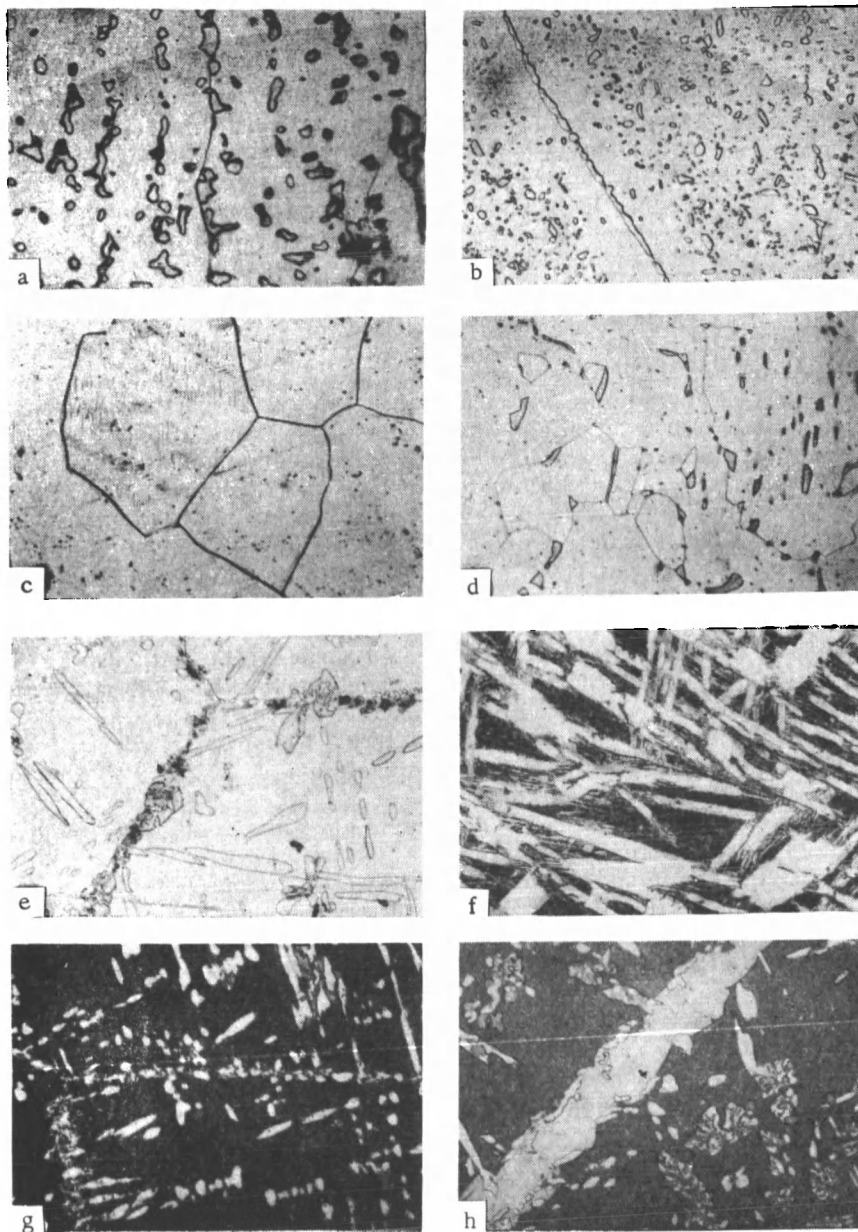


FIGURE 1. Microstructures of investigated alloys after various heat treatment processes; $\times 310$
a — section I, 30% (Fe+Cr), hardened from 1100°C; b — the same, section III; c — section I, 0.2% (Fe+Cr), hardened from 800°C; d — the same, 0.5% (Fe+Cr); e — section II, 20% (Fe+Cr), hardened from 800°C; f — section I, 7.5% (Fe+Cr), hardened from 500°C; g — the same, 20% (Fe+Cr); h — section II, 20% (Fe+Cr), annealed at 500°C.

Ti(CrFe)₂ grains. At 800°C, the decomposition of the β -solid solution of alloys belonging to section III and containing 20 % Fe + Cr is accompanied by a precipitation of two phases. Alloys of this section, containing 30 % Fe + Cr and annealed at 800°C, may also have a three-phase structure. The X-ray photographs of these alloys show, in addition to the diffraction lines corresponding to β -Ti and to the γ phase, also faint lines of the α -solid solution of titanium.

After prolonged annealing at 500°C the alloys, represented by the radial sections and containing 0.2 % Fe + Cr, consist of a titanium α -solid solution. In alloys with a higher content of iron and chromium, the titanium β -solid solution undergoes a eutectoid decomposition, which is indicated by the intensive coloring of the grains during etching and by the increased microhardness of the grains.

The microhardness tests also show that at this temperature alloys of sections I, II, and III containing up to 10 % Fe + Cr have also an α -solid solution of titanium. The microstructure of these alloys is similar to that shown in Figure 1f. The amount of the α phase increases with the increase in the content of iron and chromium in the alloys. An annealing at 500°C increases the amount of the precipitated intermetallic phases in alloys containing more than 10 % Fe + Cr.

The use of the Ence and Margolin [11] etchant, enabled these phases to be differentiated more clearly. The two-phase mixture TiFe + Ti(CrFe)₂ (Figure 1g) precipitates along the grain boundaries and within the grains of the eutectoid of alloys belonging to section I and containing 20 and 30 % of Fe + Cr. Alloys of section II with 20 and 30 % Fe + Cr have three precipitated phases. The grain boundaries of the eutectoid contain numerous phases, the composition of which has not yet been determined. The grain boundaries and the microscopic field show the presence of light grains of the Ti(CrFe)₂ phase, which decompose to form the TiFe compound (which takes up a brown color) (Figure 1h). The X-ray photographs of these alloys clearly show lines of the Ti(CrFe)₂ and TiFe phases and of the α -solid solution of titanium. Alloys of section III with 20 and 30 % Fe + Cr also contain two auxiliary phases. The X-ray photographs of these alloys show diffraction lines of the Ti(CrFe)₂ and of α -Ti. The X-ray photographs of alloys annealed at 500°C have a very thin and diffuse line of the titanium β -solid solution which indicates an incomplete eutectoid decomposition.

On the basis of the data of microstructural and X-ray analyses the authors have constructed approximate phase diagrams of that section of the tetrahedron which represents alloys with 6 % Al for temperatures of 1100, 1000, 800, and 500°C (Figure 2). Alloys in which the β -solid solution decomposes during hardening forming an α' phase are marked with a cross.

On the isothermal section corresponding to 1100°C, the field of titanium β -solid solutions covers almost all compositions of the investigated alloys, and borders on the corresponding fields of the β -solid solutions of the Ti-Al-Fe and Ti-Al-Cr systems. On the isothermal section for 1000°C the field of β -solid solutions is narrower chiefly because of the polymorphic $\beta \rightarrow \alpha$ transformation which takes place in alloys with up to 1.0 % Fe + Cr. On the sides representing the Ti-Al-Fe and Ti-Al-Cr systems, the investigated section for 1000°C shows two-phase $\alpha + \beta$ alloys. Therefore, in the phase diagram for 1000°C, the field of β -solid solutions is limited above and at two sides by fields of $\alpha + \beta$ -solid solutions of titanium. In alloys with higher

contents of iron and chromium the β -solid solution is in a state of equilibrium with the TiFe compound and with the γ phase. On the basis of the data of microstructural analysis, the authors have marked out the fields of homogeneous five-component solid solutions on the basis of α - and β -Ti at 800°C. At this temperature these solid solutions are in a two- and three-phase equilibrium with each other and with the corresponding intermetallic compounds. The field of β -solid solutions is in this case considerably narrower, both as a result of the polymorphic $\beta \rightarrow \alpha$ transformation which takes place in alloys containing about up to 8 % Fe+Cr and as a result of the decomposition of the β -solid solution entailing the formation of TiFe and $\text{Ti}(\text{CrFe})_2$ intermetallic compounds. Microstructural investigations show that the β -solid solution of alloys which have been annealed for a long time at 500°C, undergoes a eutectoid decomposition. The composition of the eutectoid, however, has not been definitely determined. The structure of alloys of sections II and III, containing 20 % Fe+Cr and more, indicates that there are phases the nature of which remains unclear. Since the X-ray photographs of alloys annealed at 500°C show only diffraction lines of the titanium α -solid solution, of the TiFe compound, and of the γ phase, the isothermal section for 500°C may be represented by Figure 2d. It is, however, possible that the section of the tetrahedron investigated intersects the tie tetrahedron of the four-phase equilibrium $\alpha + \text{TiFe} + \text{Ti}(\text{CrFe})_2 + \text{titanium-aluminum compounds}$. The latter may be a solid solution on the basis of Ti_3Al with an α -Ti lattice.

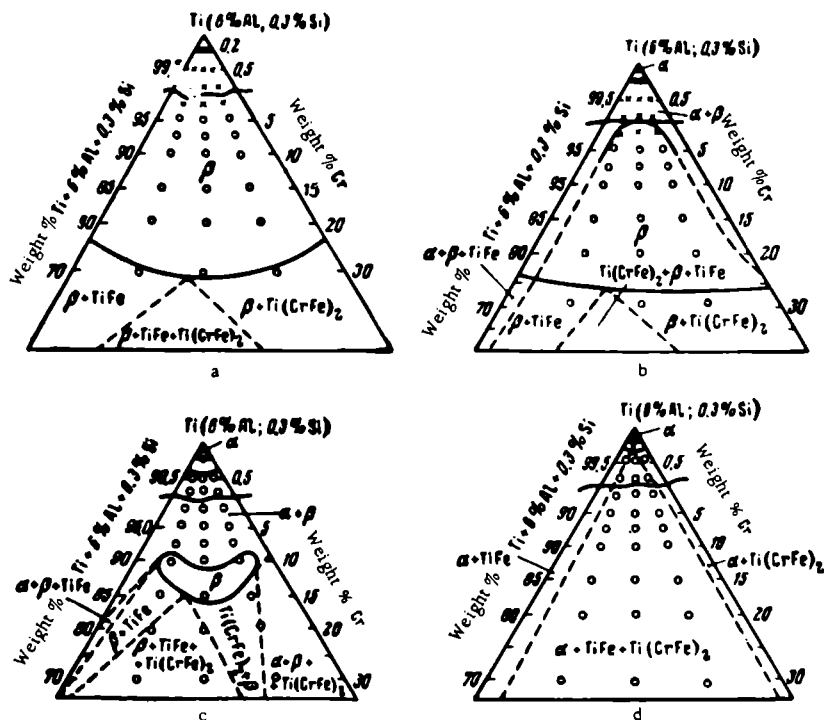


FIGURE 2. Isothermal sections of the tetrahedron Ti (0.3% Si) - Al - Cr - Fe with 6 % Al for 1100°C (a), 1000°C (b), 800°C (c), and 500°C (d)

It should be pointed out that the placing of the $\text{Ti}(\text{CrFe})_2$ phase in the isothermal sections of alloys which are close to the $\text{Ti}-\text{Al}-\text{Cr}$ system is arbitrary and based on the assumption that the $\text{Ti}-\text{Al}-\text{Cr}$ system contains a stable hexagonal TiCr_2 modification (as far as is known this has not yet been investigated).

The analysis of the phase diagrams of the section of the tetrahedron, representing alloys with 6 % Al and 0.3 % Si, shows that they have the greatest resemblance to the phase diagrams of the $\text{Ti}-\text{Cr}-\text{Fe}$ system.

An increase in temperature of the polymorphic transformation of alloys with 6 % Al results in the formation of $\alpha+\beta$ -solid solutions at as low a temperature as 1000°C . Since aluminum is an α -phase stabilizer of titanium its presence accelerates the rate of the eutectoid decomposition of the β -solid solution. Heating at 550 and 450°C for a total of 2000 hours causes no full eutectoid decomposition of the β -solid solution in alloys of the ternary $\text{Ti}-\text{Cr}-\text{Fe}$ system. The β -solid solution of titanium, in alloys containing aluminum, decomposes as in alloys of the $\text{Ti}-\text{Cr}-\text{Fe}$ system with the formation of TiFe and of the γ phase. The nature of this decomposition, however, differs somewhat from the decomposition of alloys of the $\text{Ti}-\text{Cr}-\text{Fe}$ system. Additional investigations are required to elucidate the kinetics of the decomposition of the titanium β -solid solution.

Hardness

The hardness of alloys was investigated by a Vickers hardness tester with a diamond pyramid loaded with 10 kg. The results of the hardness measurements were used for the construction of composition versus hardness diagrams (Figure 3) which show that the hardness variations are the same for all alloys of the radial sections annealed at identical temperatures.

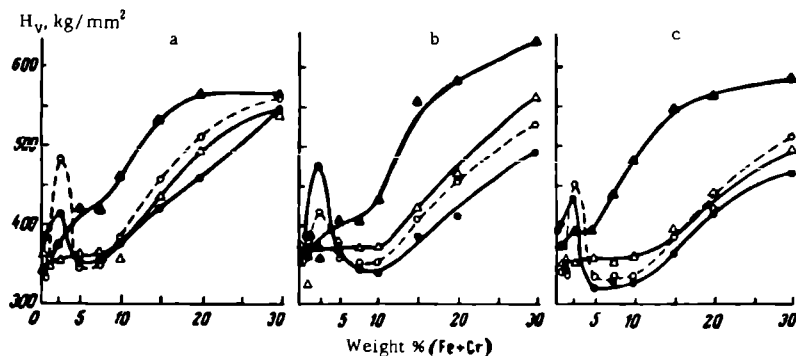


FIGURE 3 Dependence of the hardness of alloys on their composition and on the temperature of heat treatment

a — section I; $\text{Fe}:\text{Cr}=3:1$; b — section II; $\text{Fe}:\text{Cr}=1:1$; c — section III; $\text{Fe}:\text{Cr}=1:3$;
 ● — hardened from 1100°C ; ○ — the same, 1000°C ; △ — the same, 800°C ; ▲ — annealed at 500°C .

The hardness versus composition curves of alloys hardened from 1100 and 1000°C have maxima corresponding to a composition with 2.5 % $\text{Fe}+\text{Cr}$.

This alloy has the highest content of iron and chromium at which a martensitic $\beta \rightarrow \alpha'$ transformation is possible. With the formation of a β -solid solution in alloys with 5 % Fe+Cr there is a considerable decrease in hardness which then changes little over the range from 5 to 10 % Fe+Cr. A further increase in the content of iron and chromium raises the hardness, which reaches a maximum value in alloys with 30 % Fe+Cr.

The hardness of alloys with 0.2 to 2.5 % Fe+Cr hardened from 800°C is considerably lower as a result of the formation of equilibrium grains of the α phase. The hardness curve of alloys with a higher content of iron and chromium is similar to that of alloys hardened from 1100 and 1000°C. In general, it can be said that the hardness of alloys hardened from 800°C differs little from that of alloys hardened from 1100 and 1000°C.

The hardness of alloys annealed at 500°C and containing 0.2 to 2.5% Fe+Cr is almost the same as that of alloys hardened from 800°C, but it considerably increases over the range of 5 to 30 % Fe+Cr. The hardness of alloys with 5 to 30 % Fe+Cr, annealed at 500°C, is considerably higher than that of [identical] alloys hardened from 1100, 1000, and 800°C, because of the eutectoid decomposition of the β solution. The hardness increase is most notable in chromium rich alloys (sections II, III), and less so in alloys of section I. This is probably due (as in the alloys of the Ti—Cr—Fe system) to the formation in the alloys of section I of a large amount of TiFe grains, the hardness of which is lower than that of $\text{Ti}(\text{CrFe})_2$ grains which are formed chiefly in alloys of section III. These curves reflect the variation of the phase composition of alloys.

Electrical resistance

The electrical resistance of alloys increases continuously with the increase in the total content of iron and chromium (Figure 4). Alloys hardened from 1000°C have the highest electrical resistance, except in the case of alloys of section III containing 15 and 20 % Fe+Cr. The very high electrical resistance of alloys belonging to section II (15 % Fe+Cr), which have been hardened from 1000°C, and of alloys belonging to section III (20 % and 30 % Fe+Cr), hardened from 800°C, has found no satisfactory explanation. For alloys of section III this phenomenon may confirm the formation of the Ti_3Al compound or of any other phase. The electrical resistances of all the alloys with up to about 10 % Fe+Cr hardened from 1000° and 800°C are about the same and are almost independent of the iron to chromium ratio. The intensive decomposition of the phase components of alloys during annealing at 500°C leads to a considerable decrease in their electrical resistance. Comparing these graphs with similar graphs for ternary Ti—Cr—Fe alloys, it may be noted that alloys containing aluminum have a considerably higher electrical resistance: the maximum values for the specific resistance of ternary alloys ($1.63 \text{ ohm} \cdot \text{m/mm}^2$) corresponds to the minimum values of five-component alloys. These graphs also lack the maxima, characteristic of alloys of the Ti—Cr—Fe system. These maxima are a feature of alloys with an ω phase, the formation of which is apparently suppressed by aluminum.

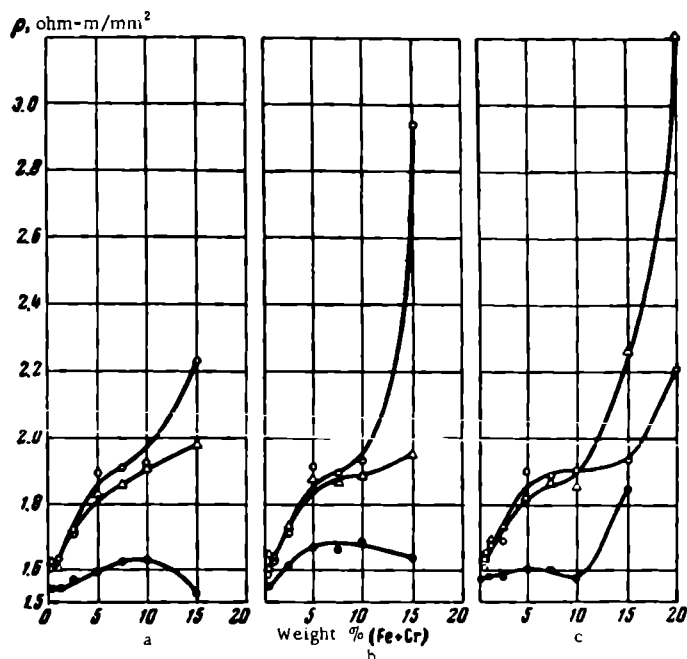


FIGURE 4. Dependence of the electrical resistance of alloys on their composition and on the temperature of heat treatment

a — section I; Fe:Cr=3:1; b — section II; Fe:Cr=1:1; c — section III, Fe:Cr=1:3; ○—hardened from 1000°C; △—the same, 800°C; ●—annealed at 500°C.

Conclusions

1. Determinations have been made of the solubility of iron and chromium in the five-component α - and β - solid solutions of titanium at 1100, 1000, 800, and 500°C. Between 500 and 800°C, the α -solid solution of titanium with 6 % Al and 0.3 % Si can dissolve no more than 0.4 % Fe+Cr.
2. The phase transformations taking place in five-component alloys at different temperatures of heat treatment are reflected by the changes in their hardness and electrical resistance.

Bibliography

1. Kornilov, I. I., V. S. Mikheev, T. S. Chernova, and K. P. Markovich. —Sbornik "Titan i ego splavy", No. 7:140, Izdatel'stvo AN SSSR, 1962.

2. Kornilov, I. I., V. S. Mikheev, and T. S. Chernova. — Izvestiya AN SSSR, OTN, No. 3:70. 1960.
3. Kornilov, I. I. — Doklady AN SSSR, 81(2):191. 1951.
4. Eremenko, V. N. Titan i ego splavy (Titanium and its Alloys). — Izdatel'stvo AN USSR. 1960.
5. McQuillan, A. D. and M. K. McQuillan. Titanium. — Metallurgy of Rarer Metals, Vol. 2, New York. 1955. [Russian translation. 1958.]
6. Kornilov, I. I. and P. B. Budberg. Diagrammy sostoyaniya dvoynykh i troynykh sistem titana (Phase Diagrams of Binary and Ternary Titanium Systems). — Izdatel'stvo VINITI AN SSSR. 1961.
7. Grum-Grzhimailo, N. V., I. I. Kornilov, E. N. Pylaeva, and M. A. Volkova. — Doklady AN SSSR, 136(3):599. 1961.
8. Ence, E. and H. Margolin. — J. Metals, 9(1/2):484. 1957.
9. Van-Thyne, R. J., H. D. Kessler, and M. Hansen. — Trans. Am. Inst. Min. Met. Eng., Vol. 197:1209. 1953.
10. Boriskina, N. G. and I. I. Kornilov. — Izvestiya AN SSSR, OTN, No. 1:50. 1960.
11. Ence, E. and H. Margolin. — J. Metals, 6(1):346. 1954.

DILATOMETRIC INVESTIGATION OF TITANIUM

R. S. Mints, A. E. Shelest, and Yu. S. Malkov

This investigation of the coefficient of linear expansion of metallic titanium and the investigation of the kinetics of sintering of compressed titanium powder was carried out with a universal high-temperature vacuum dilatometer DTs-4 (Figure 1). This apparatus was developed in the alloy chemistry laboratory of the Institute of Metallurgy im. A. A. Baikov and is applicable to the investigation of the kinetics of cyclic sintering of metallic powders, as well as of the thermal expansion and the coefficient of thermal expansion of heat-resisting and easily oxidizing metals [1].

The specific feature of the DTs-4 dilatometer is the possibility of obtaining high temperatures (up to 2000-2200°C) and high heating rates (more than 500 degrees/min). The linear changes of the specimens during heating and cooling are directly read on a pointer dial with a scale of 1 μ per division.

The apparatus (Figure 1) is fastened on a shelf fixed to the wall and fitted with shock absorbers.

The massive copper plate (1), is cooled with running water and supports a vacuum glass bell (2). A pointer dial (3) is located beneath the bell. A cylindrical heater (4), 120 mm high and 20 mm in diameter, made of heat resisting sheet (molybdenum and tungsten) 0.2 to 0.4 mm thick, is inserted into a conical opening in the center of the plate. In the heating space a quartz or ceramic tube (5), which is fixed on the plate, rests with its bottom against the specimen (6). The specimen may be shaped as a cylinder 4 to 5 mm in diameter and 20 to 50 mm long or as a parallelepiped. The dimensional changes of the specimen during heating and cooling are transmitted to the pointer by a pusher (7), made of the same material as the specimen. A water-cooled cylinder (8) with the heater in its middle is fastened to the bottom of the plate through insulators.

Current is fed to the apparatus through conductors (14) from a TNN-40 autotransformer and from an OSU-20 transformer. The voltage is 4 to 10 v and the current 300 to 400 amp. The rates of cooling and heating are automatically regulated by a Warren motor with a two-side conical transmission which operates the transformer control. A vacuum of 1.10^{-4} mm Hg is produced by an RVN-461 vacuum backing pump and a TsVL-100 diffusion pump.

A specimen of technically pure titanium VT-1 was turned out of a rod of the metal worked at 900 to 1100°C and cooled in the air. Etching of the specimen in its initial condition by a mixture of equal parts of hydrofluoric acid, glycerine, and alcohol revealed an α' phase (Figure 2). The photomicrograph shows the characteristic α' -Ti needles, at an angle of 60° (martensitic structure).

The specimen was shaped as a cylinder 4 mm in diameter and 20 mm long, and was heated and cooled at a rate of 30°C/min.

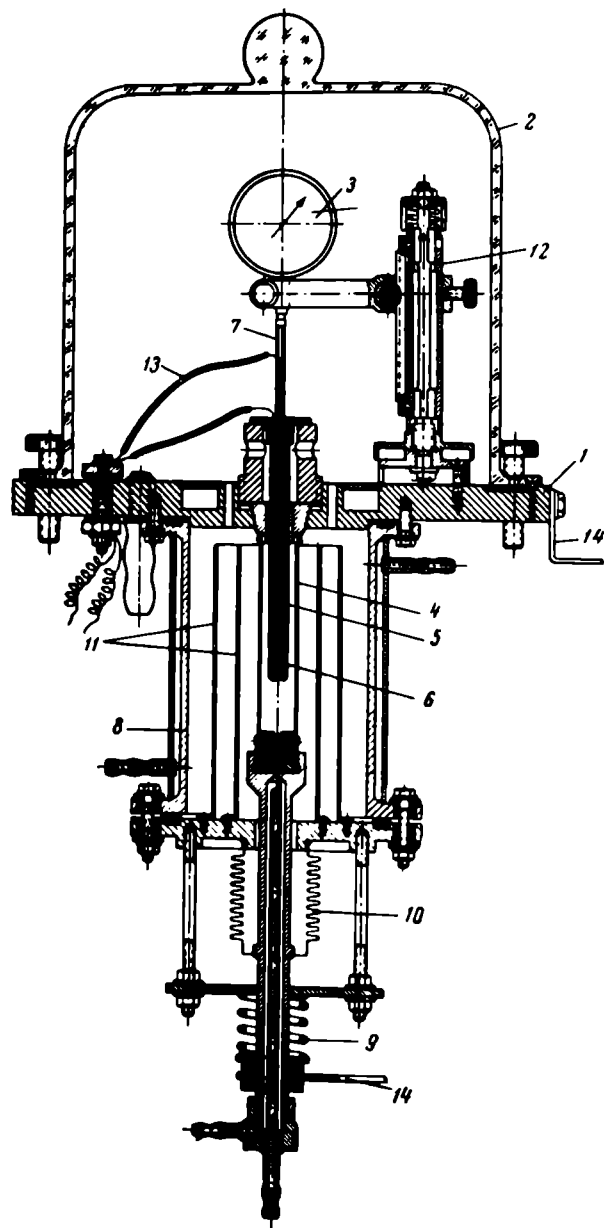


FIGURE 1. Diagram of the DTs-4 dilatometer

1—plate; 2—glass bell; 3—dial indicator; 4—molybdenum heater; 5—tube containing the specimen; 6—specimen; 7—pusher; 8—water-cooled cylinder; 9—spring; 10—siphon; 11—molybdenum screen; 12—support for indicator; 13—thermocouple; 14—current conductor.

The dilatometric curve for compact titanium (Figure 3) shows that the allotropic α '- β transformation of titanium takes place at 890°C which is in agreement with published data [2, 3], according to which the temperatures of the polymorphic transformation of titanium are 882.5, 885, and 880°C.

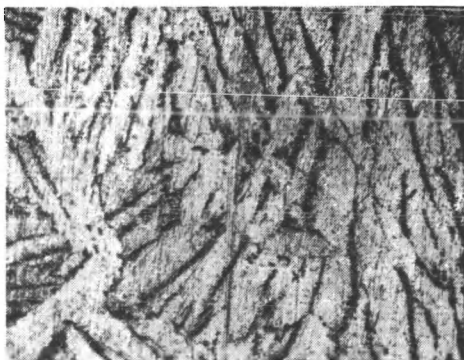


FIGURE 2. The microstructure of a titanium specimen (initial condition) $\times 200$

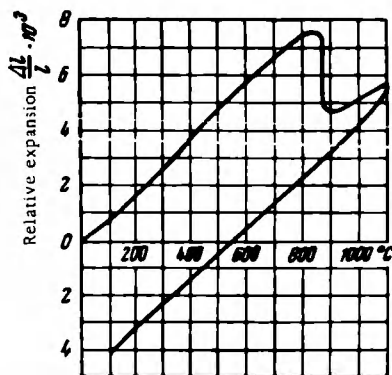


FIGURE 3. Dilatometric curve of (compact) titanium

The dilatometric investigation showed that the $\alpha \rightarrow \beta$ transformation of titanium is accompanied by a sharp volume decrease, a considerable consumption of heat, and the evolution of gaseous impurities. The latter is evident from the vacuum drop in the dilatometer from $2 \cdot 10^{-3}$ to $8 \cdot 10^{-3}$ mm Hg which takes place at temperatures from 850 to 900°C. It should be pointed out that if the dilatometric investigation of titanium is carried out in vacuo, the temperature range of the allotropic transformation is considerably narrower: instead of a sharp drop, the heating curve has only a small inflection. After recording the dilatometric curve, i.e., after heating to 1100°C at a rate of 30°C/min and cooling at the same rate to 100°C, the titanium specimen consists of an α phase (Figure 4). The magnitudes of the relative expansions $\Delta L/L$ and of the coefficient of linear expansion of titanium forged at 400 to 1100°C are given in the table.

The investigation of the kinetics of sintering of powder-titanium specimens has been carried out with a DTs-4 dilatometer as described by Mints [4]. The titanium powder is encased in a elastic rubber bag compressed from all sides in a liquid (pressure 800 kg/mm²). The specimens for the dilatometric investigation (diam = 7 mm and l = 15 mm) were turned out of a bar of extruded metal. Prior to the experiments, a vacuum of $1 \cdot 10^{-3}$ mm Hg was created in the dilatometer. The specimen was frequently cooled and heated in the apparatus at a rate of 50°C/min. The curve of the cyclic sintering of titanium (Figure 5) shows (by repeated heating to 1100°C and cooling to about 300°C) that with each subsequent heating cycle the degree

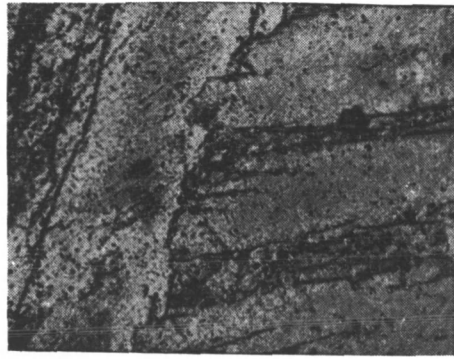


FIGURE 4. Microstructure of a titanium specimen after recording the dilatometric curve, $\times 200$

Coefficient of linear expansion of titanium

Temperature, °C	Relative expansion, $\Delta l/l \cdot 10^3$	Coefficient of linear expansion $\alpha \cdot 10^{-6}$	Temperature, °C	Relative expansion, $\Delta l/l \cdot 10^3$	Coefficient of linear expansion $\alpha \cdot 10^{-6}$
400	3.62	9.10	800	7.43	9.34
500	4.82	10.05	900	4.66	5.30
600	5.77	9.95	1000	5.10	5.20
700	6.62	9.75	1100	5.45	5.20

of sintering of the specimen increases and the shrinkage decreases. After nine cycles of heating to 1100°C the pressed titanium specimen was a compact metal with a specific gravity of 4.25 and a hardness $H_v = 250 \text{ kg/mm}^2$. The microstructure of titanium after repeated sintering is that of a compact metal with a small number of minute pores (Figure 6). Such titanium can be forged.

The investigation of the kinetics of sintering of pressed titanium powder in a DTs-4 dilatometer shows that the process may be carried out by repeated heating and cooling cycles which may, consequently, replace the isothermal process of sintering.

The requirements of thermal process of cyclic sintering may be determined from the dilatometric curve obtained by the DTs-4 dilatometer. In addition, the influence of various rates of heating and cooling on the process of sintering may be investigated.

The repeated heating of a sintered specimen in a dilatometer may be used for checking the degree of sintering, any shrinkage during heating and cooling being an indication that the process has not been completed.

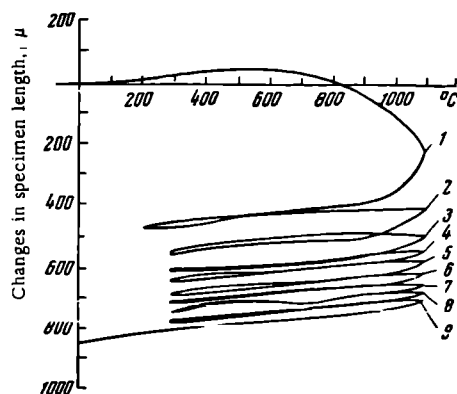


FIGURE 5. Curve of cyclic sintering of titanium powder (the figures designate the number of the cycle)

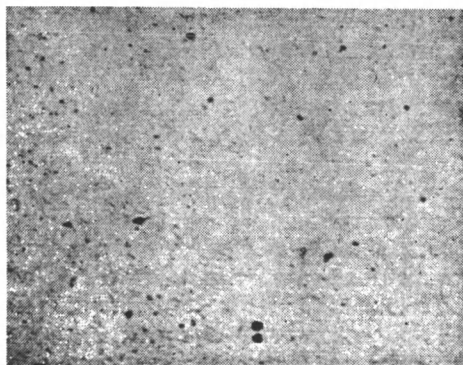


FIGURE 6. Microstructure of titanium powder sintered by the cyclic process, $\times 200$

Bibliography

1. Mints, R. S., Yu. S. Malkov, and E. I. Turtikov. — Tsentral'nyi Institut Tekhniko-Ekonomicheskoi Informatsii, P-62-35/5. 1962.
2. Jaffe, R. I., H. R. Ogden, and D. J. Maykuth. — J. Metals, 2 (10): 1261. 1950.
3. McQuillan, A. D. and M. K. McQuillan. Titanium. — Metallurgy of Rarer Metals, Vol. 2, New York. 1955 [Russian translation. 1958.]
4. Mints, R. S. — Doklady AN SSSR, 118(3):543. 1958; ZhNKh, 5(4): 908. 1960.

II. INTERACTION OF TITANIUM WITH GASES AND CORROSION PROPERTIES OF TITANIUM ALLOYS

17 11775

KINETICS OF OXIDATION OF TECHNICALLY PURE TITANIUM IN THE AIR AT HIGH TEMPERATURES*

S. A. Gorbunov and I. S. Anitov

The oxidation of titanium and of its alloys, unlike that of iron and some other metals, results not only in the formation of scale but also of gas-saturated layers which are solid solutions of oxygen in titanium [1]. An investigation of the relationship between the kinetics of oxidation of titanium and of the growth of gas-saturated layers to the temperature and the duration of heating of the metal is urgently required. Studies so far carried out in this direction [2-7] give no idea as to the nature of the oxidation process taking place in titanium metal at 800 to 1200°C. Methods of protection of semifinished and finished titanium products against oxidation cannot be developed in the absence of a true picture of this process.

The purpose of the investigation reported here was to obtain data on the degree to which oxidation can take place and the depth of the gas-saturated layers formed when technically pure titanium is heated in the air to 800-1200°C, as well as to elucidate the mechanism of the process.

Materials and methods

The investigations were carried out on specimens cut out from 8 kg ingots of VT-1 titanium produced by double smelting of TGO titanium-sponge electrodes in a vacuum arc furnace.

Impurities present were: ~ 0.20% Fe; ~ 0.08% Si; ~ 0.05% C; ~ 0.06% Cl₂; ~ 0.08% N₂; ~ 0.15% O₂; ~ 0.012% H₂.

The ingots were forged into 16 mm-diameter rods or into 30×30 and 40×40 mm square rods. Cylindrical (10 mm diameter, l = 15 mm) and cubic (20 × 20 × 20 and 30 × 30 × 30 mm) specimens were prepared from these. During the preparation of the specimens the gas-saturated layer formed during forging was completely removed. The velocity of oxidation of titanium in undried laboratory air at 800, 900, 1000, 1100, and 1200°C was investigated by periodically weighing the specimens. The duration of the tests was 32 hours at 800 to 900°C, 16 hours at 1000°C, 8 hours at 1100°C, and 4 hours at 1200°C. The method of periodical weighing gives the results of the joint action of two factors which together make up the process of oxidation of titanium. The interpretation of the data is thus rendered somewhat difficult. Nevertheless, this method enables variations in the process of oxidation to be followed qualitatively. The investigation was supplemented by a gravimetric separation of the total oxygen into two component parts:

* This investigation was carried out with the participation of G. P. Nadutenko.

1) the oxygen forming the oxide film and 2) the oxygen expended in the development of the gas-saturated layers.

The depth of the gas-saturated layers [as indicated by their hardness] was measured by a PMT-3 device loaded with 50 g. The thickness of the scale layer was measured by a micrometer and its structure by an X-ray analysis (radiation from a copper target filtered through nickel).

Investigation of the process of scale formation

The X-ray analysis of oxide films formed on titanium at high temperatures showed that they contain only titanium dioxide in the form of rutile. No other intermediate oxides were found in the scale. Nevertheless, although their phase composition remains constant, the external appearance and the properties of the oxide films change with increase in temperature. As the specimens are heated from 800 to 1000°C the color of the external part of the scale gradually changes from white to pale yellow. The internal layer remains white but at 1000°C it becomes covered with fine bluish specks. At 1100 and 1200°C the external scale layers become orange red in color, bright, and dense. At 1200°C the surface of the scale becomes covered with dark smudges and its electrical conductivity at room temperatures is higher than that of the previously formed white and orange-red scale. As the temperature is increased and the duration of the test is prolonged, a white powdery layer is formed beneath the compact scale film. At 1100 to 1200°C the external surfaces of the scale include characteristic bright specks (with a glitter similar to that of emery), which are visible under a binocular microscope as regular, well-formed crystals, the dimensions of which increase with the time of heating. The thickness changes of scale formed on cubic specimens are shown in Table 1.

TABLE 1

Thickness of scale formed during oxidation of technically pure VT-1 titanium, mm

Temperature of test, °C	Duration of test, hours						
	0.5	1	2	4	8	16	32
800	—	—	—	—	0.005	0.017	0.029
900	0.012	0.02	0.03	0.05	0.075	0.100	0.25
1000	0.035	0.060	0.100	0.190	0.25	0.30	—
1100	0.060	0.1	0.15	0.190	0.25	—	—
		(0.22)	(0.23)	(0.26)	(0.30)	—	—
1200	0.14	0.25	0.32	0.360	0.390	—	—

Note. The thickness of the scale where it agglomerates is given in brackets.

The thickness of the scale formed on specimens heated to 1100°C is not uniform. At the places where the orange-red spots appear the scale is thicker (the figures are given in Table 1 in brackets) than in the white areas. The surface of the specimens from which the scale has been removed has a characteristic appearance: pits remain at the spots where the smudges had

been present. The surface of specimens heated to 1200°C do not have this appearance. A gravimetric determination was made of the amount of oxygen used for the formation of the scale and the amount which diffuses into the titanium. The percentage of oxygen in the gas-saturated layer, as related to the total amount of oxygen used up for the whole process of oxidation, is calculated according to the formula:

$$q'_a = \frac{q_a}{q_1 - q_0} \cdot 100\% = \frac{(q_1 - q_0) - 0.4(q_1 - q_a)}{q_1 - q_0} \cdot 100\%,$$

where q_a = weight of oxygen in the gas-saturated layer, g;
 q_0 = weight of the specimen before the experiment, g;
 q_1 = weight of the specimen after the experiment, g;
 q_s = weight of the specimen after the experiment, without the scale, g;
0.4 = the coefficient used for the calculation of the amount of oxygen in the scale the composition of which is assumed to be TiO_2 .

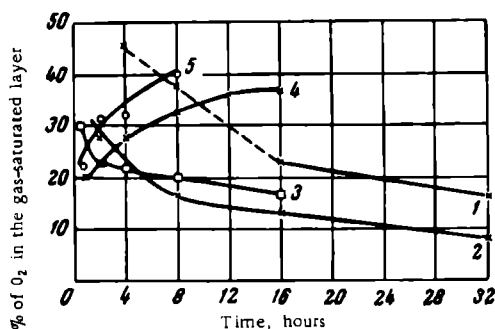


FIGURE 1. Dependence of the content of oxygen in the gas-saturated layer on the duration of heating at 800°C (1), 900°C (2), 1000°C (3), 1100°C (4), and 1200°C (5)

The data on the content of oxygen in the gas-saturated layers, oxidized at different temperatures, are shown in graphical form in Figure 1. It should be pointed out, that the percentage of oxygen given in this figure for the gas-saturated layer, formed during the oxidation at 800°C for 4 and 8 hours, is somewhat higher than in reality, because of the difficulties encountered in removing the scale from the specimens. It was determined that, at 800 to 1000°C, the share of oxygen used up for the formation of the scale increases with the increase of the heating time, while at 1100 to 1200°C the opposite is true [i.e., the proportion of oxygen absorbed by the metal increases]. However, in all investigated processes the [actual] amount of oxygen used up for the formation of scale exceeds that which diffuses into the metal.

In some experiments marking signs were used (thin platinum wire) to indicate the direction of the diffusion processes at different temperatures. It was thus shown that, while at 800 to 1000°C a diffusion of oxygen through the oxide film is prevalent and the scale is formed on the metal-scale

boundary (the marking sign remained on the surface of the scale), at 1100 to 1200°C the diffusion of titanium ions through the scale towards the surface of the specimen takes place to an increasing extent and the new scale is then formed chiefly at the external surface of the existing scale (the marking sign becomes covered by the agglomerated layer).

Investigation of the growth process of gas-saturated layers

The depth and the nature of the diffusion of oxygen into titanium was investigated by measuring the microhardness of oxidized specimens at different distances from the metal-scale boundary, since the hardness of titanium increases regularly with the increase in the amount of oxygen dissolved. On the basis of these results, graphs were constructed representing the relationship between the microhardness and the distance from the metal-scale boundary. The following characteristics were taken into account: H_c — mean magnitude of the microhardness in the center of the section where no oxygen has penetrated, kg/mm^2 ; $H_{10\text{ maximum}}$ — mean value of microhardness at 10μ from the edge of the section, kg/mm^2 ; B — the depth of the whole gas-saturated layer determined from the intersection of the microhardness curve with the H_c point, mm; B' — depth of the hard gas-saturated layer obtained at temperatures of oxidation above the $\alpha \rightarrow \beta$ transformations of Ti; the depth of the latter layer was determined from the intersection of the microhardness curve with the point $H_c + 250 \text{ kg/mm}^2$.

The investigation of the microhardness of specimens oxidized at different temperatures enabled the distribution of oxygen within the specimens to be determined as well as the depth of the gas-saturated layers. The results of investigation of the cubic specimens are given in Table 2.

The curves of microhardness versus depth of the gas-saturated layer of titanium specimens heated at temperatures above the allotropic transformation have two sections (Figure 2). The first section, which represents a layer with a high microhardness, i. e., with a high content of oxygen (B'), characterizes diffusion into α -Ti and a high solubility of oxygen. The second section, which represents a layer with a low content of oxygen ($B-B'$) characterizes the depth of diffusion of oxygen into β -Ti. The white oxidized layer, which is revealed by etching, comprises only three-quarters of the first section of the hard gas-saturated layer. The clear division of the gas-saturated layer into two sections, and particularly the determination of the presence of (and of the causes for) the formation of the second section containing 0.5 to 2 % of dissolved oxygen (judging by its microhardness) are of considerable practical interest. However, this belief has apparently not been held by a number of investigators who, in their studies of nature of the oxidation of titanium by means of microhardness measurements, have abandoned further measurements after obtaining a hardness of 400 to 500 kg/mm^2 . The oxygen-rich layers on the surface of titanium may be the cause of poor mechanical and technological properties.

From the practical point of view it is very interesting to note that as the temperature rises and the duration of the test increases, the first section

* The magnitude of 250 kg/mm^2 was chosen on the assumption that if the solubility of oxygen in titanium at 1000 to 1200°C is about 2 weight % then the hardness of the metal increases by about 250 kg/mm^2 .

of the gas-saturated layer grows considerably more slowly than the second section in which the content of oxygen is low. Thus, for instance, if the specimens are heated for 1 to 4 hours at 1100°C the second section is 15 to 18 times thicker than the first one. It has also been determined that as a result of a temperature increase from 1000 to 1100°C the total thickness of the gas-saturated layer strongly increases while an increase in temperature from 1100 to 1200°C greatly thickens the layer with the high microhardness.

TABLE 2
Results of investigation of gas-saturated layers formed during heating
in the air of cubic specimens of technically pure VT-1 titanium

Temperature of heating, °C	Duration of experiment, hours	$H_{\text{max}}-H_0$, kg/mm ²	B_1 , mm	B_2 , mm	Temperature of heating, °C	Duration of experiment, hours	$H_{\text{max}}-H_0$, kg/mm ²	B_1 , mm	B_2 , mm
800	2	672	—	0.04	1000	4	802	0.06	1.20
800	4	349	—	0.08	1000	8	582	0.07	1.30
800	8	344	—	0.15	1000	16	630	0.08	2.00
800	16	630	—	0.20	1100	1	1455	0.08	1.65
800	32	925	—	0.22	1100	2	1113	0.12	2.15
900	1	449	—	0.10	1100	4	1345	0.20	2.70
900	2	630	—	0.15	1100	8	865	0.22	3.30
900	4	722	—	0.23	1100	16	1215	0.35	4.00
900	8	627	—	0.28	1200	0.25	1113	0.25	1.30
900	16	537	—	0.37	1200	0.5	1435	0.35	1.55
900	32	715	0.065	0.46	1200	1	1320	0.10	1.65
1000	0.5	401	—	0.75	1200	2	745	0.15	2.40
1000	1	930	0.055	0.85	1200	4	1265	0.70	3.70
1000	2	373	0.4	1.05	1200				

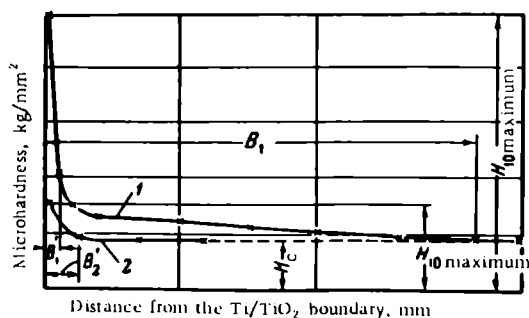


FIGURE 2. Schematic curves representing the microhardness (distribution of the oxygen) inside gas-saturated layers formed at a temperature higher than the temperature of the α -Ti \rightarrow β -Ti transformation (1) and below that temperature (2)

Investigation of the general kinetics of oxidation

Consideration will now be given to the results of the investigation of the kinetics of oxidation of cylindrical and cubic titanium specimens by the method of periodical weighing during heating at temperatures from 800 to 1200°C (Figures 3 and 4). The curves for the oxidation of titanium at 800 to 1000°C can be represented by a parabolic time-dependence curve, though at 900°C this parabola changes into a straight line. In the case of oxidation at temperatures of 1100 to 1200°C (after a certain duration of time) the curves can be represented by an equation with a cubic exponent. The higher the temperature, the sooner the transition from the parabolic equation to the equation with the cubic exponent.

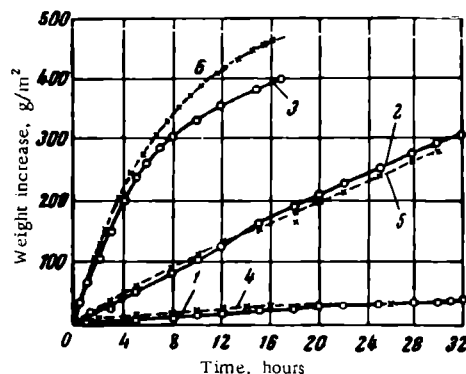


FIGURE 3. Kinetic curves of the oxidation of titanium in undried laboratory air (cylindrical (1, 2, 3) and cubic (4, 5, 6) specimens)

1 and 4 — 800°C; 2 and 5 — 900°C; 3 and 6 — 1000°C.

In order to elucidate the influence of gas-saturated layers on the oxidation of titanium, prolonged heating (up to 100 hours) of 2.3 mm-thick plates was carried out at a temperature of 1000°C. The specimens were periodically weighed. The results of these experiments are represented in Figure 5 in the form of curves drawn to logarithmic coordinates. If it is assumed that the oxidation of titanium is governed by the equation $q^n = k\tau$, then the different inclinations of several straight lines which comprise the general curve of oxidation (Figure 5) indicate that the exponent n in the formula representing the oxidation depends on the rate of the oxidation. The first change is noticed after 8 hours.

During the preliminary experiments it was noted that after exactly 8 hours of heating, two fronts of diffusing oxygen streaming from opposite surfaces meet at the center of the plates, i.e., oxidation of the entire titanium plate takes place. Subsequent oxidation takes place in metal which already has a high content of oxygen. It is probable that after 50 hours, when the inclination of the last straight-line section on Figure 5 is only 7°, oxidation of titanium proceeds in a specimen the center of which contains more oxygen than the maximum solubility of the gas in β -Ti at 1000°C.

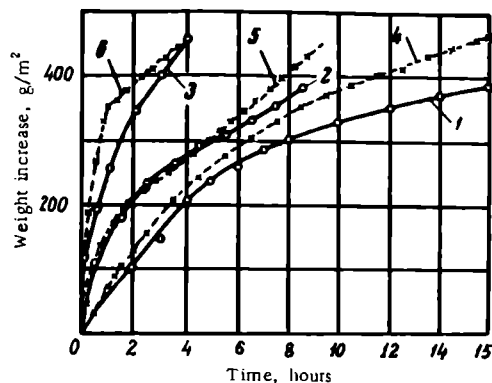


FIGURE 4. Kinetic curves of the oxidation of titanium in undried laboratory air (cylindrical (1, 2, 3) and cubic (4, 5, 6) specimens)

1 and 4 — 1000°C; 2 and 5 — 1100°C, 3 and 6 — 1200°C.

It may, however, be assumed that the rate of oxidation drops because this process is influenced by the growth and the structural changes of the film (although no qualitative changes of the scale were noted during the 100 hours of heating at 1000°C).

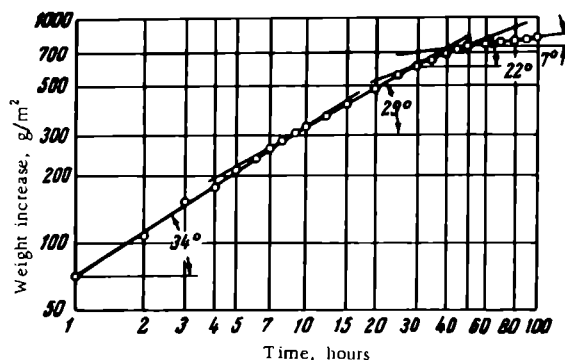


FIGURE 5. Kinetic curves of oxidation of titanium plates in undried laboratory air at 1000°C

In order to check the latter assumption, a special experiment was carried out in which specimens (20×20×20 mm) were heated 6 consecutive times at 1000°C for 8 hours, the scale being removed after each heating and the specimens weighed with the scale and without it. The distribution of oxygen between the scale and the gas-saturated layer was thus determined during the oxidation of specimens, the surfaces of which were coated with oxygen-containing layers of different thicknesses. The results of these experiments are shown in Table 3.

TABLE 3

Oxidation experiments on titanium, with repeated removal of the scale
(temperature of testing 1000°C, duration of each oxidation 8 hours)

Oxidation	Total weight increase, g/m ²	Oxygen weight increase in the scale, g/m ²	Weight increase of the gas-saturated layer, g/m ²	Amount of oxygen in the gas-saturated layer, g/m ²
In the initial condition	386.8	313	73.8	19
After the first scale removal . . .	221.6	213	8.6	3.9
After the second scale removal . .	214.5	208	6.6	3.0
After the third scale removal . . .	169.8	159	10.8	6.3
After the fourth scale removal . .	118.8	111	7.8	8.0
After the fifth scale removal . . .	116.5	110	6.5	5.5
After the sixth scale removal . . .	120	115	5.0	4.2

The data in Table 3 show that the oxidation of a specimen, the surface of which is covered with a layer with a high content of oxygen, proceeds at a considerably lower rate. This is so because the amount of oxygen which enters the scale and, particularly, the gas saturated layer is somewhat lower. The higher the concentration of oxygen in the surface layer of the specimen (after each successive removal of the scale the amount of oxygen in the solid solution of titanium on the surface increases) and the thicker the gas-saturated layer, the lower the oxidation velocity constant of the titanium.

These experiments also indicate that the chief factors resulting in a decrease in the oxidation velocity of titanium with time is the growth and the structural changes of the scale, the presence of an oxygen-saturated layer on the surface of the metal and the increase in thickness of this layer (particularly of its first section). The decrease is due to the difficulties encountered by oxygen in diffusing into the octahedral voids of the hexagonal lattice of α -Ti as these voids are gradually filled with oxygen ions.

Conclusions

In the present investigation, several characteristic features of the oxidation of titanium at high temperatures were determined.

1. At 1100 to 1200°C the following takes place:

- a) the structure of the scale changes as shown particularly by agglomeration of the external layer;
- b) the distribution of oxygen between the scale and the gas-saturated layer is changed;

c) the gas-saturated layers grow thicker, which is due chiefly to the growth of the regions with a low content of oxygen. The growth of regions of low oxygen content can be correlated with the transformation to β -Ti and the solubility of oxygen in this phase;

d) the equation representing the oxidation of titanium changes from parabolic to an equation with a cubic exponent;

e) the velocity of diffusion of titanium ions to the surface of the specimen increases in the general process of oxidation.

2. All these facts indicate that the general nature of the oxidation of titanium at 1100 to 1200°C is somewhat different from that of the process at 800 to 1000°C; the chief causes for these differences are apparently the increased velocity of diffusion of titanium ions to the oxide-air boundary and the agglomeration of the scale.

3. If titanium is oxidized at temperatures above the critical point of the α -Ti \rightarrow β -Ti transformation, the diffusion layer of the solid solution of oxygen in titanium consists of two regions. The first region, which is rather thin, is adjacent to the metal-scale interface. It is very hard (because of the high oxygen content) and reflects the diffusion and the dissolution of oxygen in α -Ti. The second region, the thickness of which (at high temperatures and prolonged heating times) may reach several millimeters, has only a somewhat higher hardness than titanium metal (the oxygen of which is about 0.15 to 2 %) and indicates the diffusion and the dissolution of oxygen in β -Ti.

Bibliography

1. Schofield, T. H. and A. E. Bacon. — J. Inst. met., 84(2):47. 1955-1956.
2. McQuillan, A. D. and M. K. McQuillan. Titanium. — Metallurgy of Rarer Metals, Vol. 2, New York, 1955. [Russian translation. 1958.]
3. Kofstad, P., K. Hauffe, and H. Kjollesdal. — Acta chem. Scand., Vol. 12:239, 1958.
4. Jenkins, A. E. — J. Inst. met., 82(1):213. 1953-1954.
5. Jenkins, A. E. — J. Inst. met., 84(2):1. 1955-1956.
6. Hurlen, T. — J. Inst. met., 89(4):128. 1960.
7. Moiseev, V. N. — Sbornik "Titan i ego splavy", No. 3:17, Izdatel'stvo AN SSSR, 1960.

**INVESTIGATION OF THE OXIDATION OF VT-14, VT-8,
VT-3-1 ALLOYS AND OF No. 1 EXPERIMENTAL
ALLOY IN AIR AT 800 TO 1200°C**

S. A. Gorbunov, G. P. Nadutenko, and V. P. Teodorovich

This work consists of an investigation on the kinetics of the oxidation and of the formation of gas-saturated layers in VT-14, VT-8, VT-3-1 alloys and in the No. 1 experimental alloy, and comparison is made with the data for technically pure titanium*.

The elucidation of the kinetics of formation of gas-saturated layers, which strongly impair the mechanical properties of technical titanium alloys, is of great practical importance.

The chemical compositions of the alloys investigated in this work are given in Table 1.

TABLE 1
Chemical composition of alloys, %

Alloys	Al	V	Mo	Sn	Cr	C	N ₂	Fe	Si	H ₂
VT-14	4.20	1.00	2.92	—	—	0.05	0.04	0.10	0.07	0.008
VT-3-1	4.90	—	1.83	—	1.78	0.05	0.03	0.05	0.07	0.008
VT-8	5.90	—	2.90	—	—	0.05	0.01	0.04	0.04	0.006
No. 1	4.95	2.18	—	3.50	—	0.05	0.03	0.10	0.08	0.007

The alloys were prepared in a vacuum furnace by double smelting of TG-00 titanium-sponge electrodes (VT-14 alloys) and of TG-0 titanium electrodes (for other alloys).

The oxidation of alloys in undried laboratory air at 800 to 1200°C was traced by periodical weighing of specimens (12 mm diameter, l = 15 mm). In order to investigate the formation of gas-saturated layers, the authors prepared microsections from cylindrical specimens in such a way as to exclude the influence of the penetration of oxygen from the butt ends. The hardness of the gas-saturated layer was measured by a PMT-3 device loaded with 50 g and the thickness of the scale was measured by a micro-meter (the scale was taken from the butt-end surfaces). The microstructure of the gas-saturated layers was also investigated.

* See paper by S. A. Gorbunov and I. S. Anitov in this book, p. 104.

Experimental

The results of these investigations of the oxidation of alloys at 800 to 1200°C (at the same time technically pure VT-1 titanium was also oxidized) show that at 800 to 900°C all the alloys examined are oxidized more slowly than technically pure titanium. The results of work by Anitov /1/ show that the velocity constants of oxidation of alloys containing 5 % molybdenum or 5 % of aluminum are lower for this temperature range than that of [pure] titanium, and that the addition of up to 1.5 % V has little influence on the tendency to oxidation of titanium. The investigation of alloys with 5 % Al and 1.5, 5, or 10 % V or Mo, shows that the "catastrophic" oxidation of alloys with 5 or 10 % V or with 5 % Mo does not occur until 1000°C.

It has been experimentally determined by the present authors that the addition of Al (5 %) and molybdenum or vanadium (up to 10 %) decreases the total velocity of oxidation.

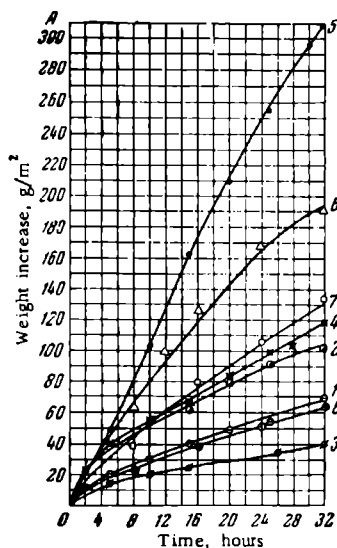


FIGURE 1. Kinetic curves of oxidation of alloys in undried laboratory air at 900°C

1 — VT-14; 2 — VT-3-1; 3 — VT-8; 4 — experimental No. 1; 5 — VT-1; 6 — Ti + 5 % Al; 7 — Ti + 1.5 % Mo; 8 — Ti + 1.5 % Mo + 5 % Al.

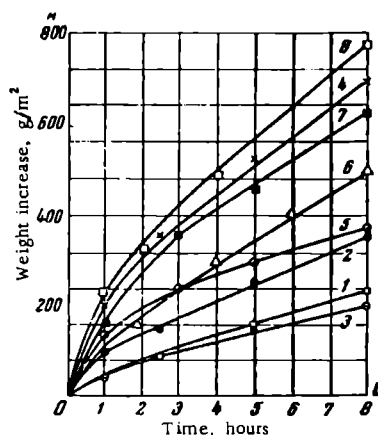


FIGURE 2. Kinetic curves of oxidation of alloys in undried laboratory air at 1100°C

1 — VT-14; 2 — VT-3-1; 3 — VT-8; 4 — experimental No. 1; 5 — VT-1; 6 — Ti + 5 % Al; 7 — Ti + 5 % Sn + 5 % Al; 8 — Ti + 5 % Sn.

The curves in Figure 1 clearly show how molybdenum and aluminum [together] decrease the oxidability of titanium alloys. The VT-14 alloy has almost the same degree of oxidation as the alloy with 1.5 % Mo and 5 % Al, while the oxidability of the VT-8 alloy is somewhat lower because of its higher aluminum content and the absence of vanadium.

Over the whole temperature range investigated (800 to 1200°C), the VT-14, VT-8, and VT-3-1 alloys are oxidized more slowly than VT-1 technically pure titanium. Nevertheless, as the temperature increases to 1200°C the differences in the oxidation rates diminish.

The somewhat more rapid oxidation of the VT-3-1 alloy is due apparently to the presence of chromium which increases the oxidation velocity of titanium over the whole range of temperatures /1/.

The results of the oxidation of alloys at 1100°C are given in Figure 2.

It was experimentally determined that the addition of 5 % Sn to titanium somewhat increases the oxidation velocity at 1000°C /1/; this influence becomes even more apparent at 1100 and 1200°C. The addition of 5 % Al to tin-containing titanium alloys has not the same effect as an identical addition to alloys containing molybdenum or vanadium.

The experimental alloy [No. 1] which contains elements increasing the velocity constants of oxidation was oxidized more slowly than the VT-1 metal up to 1000°C and only after 6 hours of heating at 1000°C and at 1100° to 1200°C did its oxidation velocity considerably exceed that of VT-1 titanium.

The element responsible for this strong oxidation is probably tin which is included in the experimental alloy.

According to published data /2/, the oxidation of titanium at 300 to 650°C can be represented by a time-dependence equation with a cubic exponent. Within this range of temperatures the oxygen diffuses into the metal and forms gas-saturated layers. The thickness of the oxide film remains constant during this process /3/.

An analysis of the laws governing oxidation of alloys has shown that the presence of alloying elements (in particular, aluminum, molybdenum, vanadium, and apparently also chromium) leads to the shifting of the field in which the processes are represented by an equation with a cubic exponent, towards higher temperatures. Thus, for VT-8 and VT-3-1 alloys this equation is true at 800°C. At 900°C the equation can be applied for VT-8 alloys during the first 32 hours and for the VT-3-1 alloy during the first 8 hours. The oxidation processes in VT-8 (beginning at 1000°C), in VT-14 (at 800 to 1200°C), and in the VT-3-1 alloy (800 to 1100°C) are described by a parabola.

The oxidation of the No. 1 alloy is, at 800 to 1100°C, an almost parabolic function while at 1200°C it is a linear function. This linear function, and also the high velocity constants of oxidation of the No. 1 alloy at high temperatures, are apparently due to the formation on the metal-scale boundary of a phase with a low melting point and to the capacity of this phase to react avidly with the oxygen of the protective film.

The liquid phase is formed as a result of the increased concentration of tin in the interior of the metal (this concentration is many times higher than the concentration of tin on the surface). This was noted during the investigation of oxidized titanium-tin alloy specimens /4/. In addition, the scale formed on No. 1 alloy specimens at high temperatures is cracked as a result of the internal stresses raised as a result of the formation of TiO-type scale on the metal surface and of TiO₂ scale in the external layer. During the present investigation an X-ray analysis of the scale of other alloys revealed only titanium dioxide in the form of rutile.

The measurement of scale thickness (Table 2) shows that on all alloys the scale becomes thicker as the temperature of oxidation increases. The scale growth is most intensive during the first hour at temperatures up to

1000°C, and during the first 30 min at 1100 to 1200°C. It is interesting to compare the scale growth on VT-14, VT-8, and VT-3-1 alloys with that on technically pure titanium. In the alloys, the scale growth is retarded after reaching a certain optimum thickness. Thus it has been determined that after four hours at 800°C all alloys have a thicker scale than the VT-1 metal and after 16 hours of heating all alloys have a scale of almost the same thickness as that on technically pure titanium; at 900 to 1000°C all alloys have a thinner scale than VT-1. An exception here (particularly at temperatures above 1000°C) is the [No. 1] experimental alloy, the oxidation of which is represented by a linear function (or a function close to linear). The protective properties of such films are very low [1].

TABLE 3
Thickness of scale formed on some alloys, mm

Temperature of testing, °C	Duration of experiment, hours	VT-14	VT-3-1	VT-8	No. 1	VT-1
800	4	0.01	0.01	0.01	0.01	—
800	16	0.015	0.02	0.02	0.045	0.017
900	1	0.030	0.01	0.03	0.015	0.015
900	4	0.035	0.02	0.035	0.04	0.03
900	16	0.045	0.035	0.055	0.085	0.12
1000	1	0.02	0.01	0.04	0.04	0.09
1000	4	0.040	0.040	0.075	0.09	0.33
1000	16	0.08	0.13	0.13	0.64	0.53
1100	0.5	0.03	0.04	0.06	0.13	0.10
1100	1	0.04	0.08	0.07	0.18	0.15
1100	4	0.12	0.17	0.15	0.50	0.28
1200	0.5	0.055	0.11	0.075	0.14	0.13
1200	1	0.07	0.12	0.09	0.18	0.15
1200	4	0.30	0.31	0.18	0.51	0.32

Analysis of the data on the kinetics of the oxidation of alloys and on the thicknesses of the scale layers leads to the conclusion that the VT-14 and VT-8 alloys are the most resistant.

The oxidation of titanium and of its alloys takes place in two stages: 1) growth of oxide films and 2) formation of gas-saturated layers. The second stage of this process was studied by measuring the depth and investigating the nature of oxygen diffusion by means of microhardness tests of oxidized specimens at different distances from the metal-scale boundary. The dissolution of oxygen in titanium results in the formation of solid solutions, the microhardness of which increases proportionally to the oxygen content. On the basis of these measurements the authors constructed graphs of microhardness versus distance from the metal-scale boundary on which the following characteristics were noted; $H_{10\max}$ = average magnitude of microhardness 10μ from the edge of the microscopic specimen, kg/mm^2 ; H_c = average microhardness at the center of the microscopic specimen (the center is not influenced by the action of oxygen), kg/mm^2 ; B — total thickness of the gas-saturated layer (determined from the intersection of the microhardness curve with the H_c point), mm; B' — thickness (mm) of the gas-saturated layer with a high microhardness (determined

TABLE 3
Thickness of gas-saturated layers on some alloys

Temperature of test, °C	Duration of test, hours	VT-14			VT-3-1			VT-8			Experimenta No. 1		VT-1	
		$H_{10 \max}$, kg/mm ²	B' , mm	B , mm	$H_{10 \max}$, kg/mm ²	B' , mm	B , mm	$H_{10 \max}$, kg/mm ²	B' , mm	B , mm	$H_{10 \max}$, kg/mm ²	B' , mm	$H_{10 \max}$, kg/mm ²	B' , mm
800	1	165	0.030	0.050	168	0.030	0.120	245	0.035	0.060	117	0.015	170	0.025
800	4	95	0.030	0.070	160	0.060	0.160	350	0.045	0.100	308	0.030	—	0.135
800	16	90	0.060	0.100	272	0.080	0.175	165	0.055	0.125	525	0.045	—	0.235
800	32	308	0.100	0.300	288	0.110	0.323	175	0.060	0.200	—	—	430	0.310
900	1	65	0.040	0.060	308	0.050	0.110	225	0.050	0.150	447	0.050	210	0.045
900	4	140	0.060	0.330	260	0.070	0.340	288	0.075	0.180	230	0.060	210	0.030
900	16	323	0.080	0.500	356	0.160	0.560	235	0.100	0.250	411	0.090	565	0.040
900	32	395	0.220	0.840	463	0.320	0.900	205	0.175	0.850	—	—	805	0.075
1000	1	245	0.065	0.330	427	0.080	0.275	185	0.175	0.520	410	0.080	—	0.690
1000	4	125	0.070	0.430	288	0.080	0.575	370	0.320	0.930	374	0.150	360	0.085
1000	16	353	0.460	1.160	430	0.275	1.300	804	1.000	5.800*	330	0.250	730	0.040
1100	0.5	320	0.080	0.800	220	0.090	0.320	625	0.140	0.600	328	0.100	810	0.080
1100	1	250	0.250	1.300	310	0.120	0.750	235	0.190	0.800	230	0.150	630	0.060
1100	2	280	0.350	1.600	570	0.260	2.200	287	0.350	1.050	341	0.170	830	0.080
1100	4	370	0.750	2.000	778	0.920	3.250	300	0.450	2.000	420	0.200	—	1.050
1200	0.5	225	0.150	1.050	696	0.300	1.100	370	0.400	0.980	—	—	—	—
1200	1	595	0.175	1.300	390	0.300	1.350	459	0.540	1.220	190	0.225	580	0.180
1200	4	595	0.350	3.600	—	—	—	875	0.90	4.500	—	1.100	1030	0.110
													1080	0.200
													1080	0.950
													—	4.800

* The gas-saturated layer reached the center of the specimen as a result of which the values of H_c there are somewhat higher.

from the intersection of the microhardness curve with the $H = H_c + 100 \text{ kg/mm}^2$ point for alloys, and with the $H = H_c + 250 \text{ kg/mm}^2$ point for pure titanium; the magnitudes of 100 and 250 kg/mm^2 were chosen empirically on the basis of the analysis of the microhardness curves.

The investigation of the microhardness of specimens oxidized at different temperatures made it possible to show the distribution of oxygen in the specimens and to determine the depth of the gas-saturated layers. The results of these investigations are given in Table 3.

The analysis of the microhardness curves of oxidized alloys indicates the same sequence of changes as those found for pure titanium*.

The microhardness-depth curves of the gas-saturated layers of alloys heated to temperatures above the point of allotropic transformation also consist of two sections. Figure 3 shows microhardness curves of the VT-14 alloy which are characteristic of all alloys. The first section represents the layer with a high microhardness, i. e., with a high oxygen content (B' characterizes the diffusion and the high solubility of oxygen in α -Ti); the second section represents a layer with a lower content of oxygen ($B-B'$ characterizes the depth of diffusion of oxygen into β -Ti).

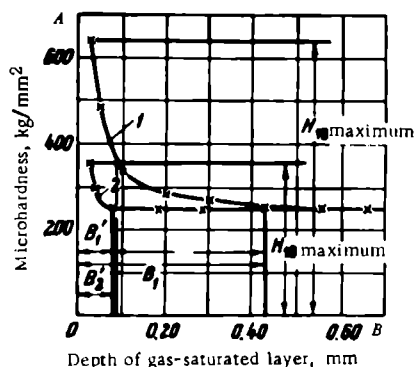
The division of the whole gas-saturated layer into two regions, and particularly the determination of the regions with the low oxygen content, is of interest for the solution of many problems which arise during the fabrication of semifinished products and articles made of titanium alloys.

The layers with the low microhardness are considerably thicker than those which have a high microhardness. Thus, in VT-14 alloys heated to 1000°C (for 4 hours) the layers with the low microhardness are four times

as thick as the layers with the high microhardness. For the VT-3-1 alloy this ratio is 4.5:1, for the VT-8 alloy it is 1.9:1, and for the No. 1 experimental alloy it is 1.7:1.

Although the amount of oxygen in the layers with the low microhardness is lower than that in the layers with the high microhardness it is nevertheless sufficiently high in the former to influence the mechanical properties of titanium since, according to published data, an oxygen content in excess of 2 atomic % leads to a decrease in the plasticity of the metal. The maximum solubility of oxygen in the "tails" is about 5 to 6 at. % as determined by the microhardness measurements.

FIGURE 3. Microhardness curves (distribution of oxygen) of the gas-saturated layers of VT-14 alloys heated to 1100°C (holding time 30 min) (1) and to 800°C (holding time 16 hours) (2).



The regions with a low microhardness appear in the VT-14 alloy at 900°C (1 hours), in the VT-8 alloy at 900°C (32 hours), in the experimental alloy No. 1 at 1000°C (16 hours), in the VT-3-1 alloy at 1200°C (4 hours) and in technically pure titanium the "tails" appear after heating to 900°C for 32 hours.

* See article of S. A. Gorhunova and I. S. Anitov in this book, p. 104.

The microhardness curves show that all alloys investigated have shallower gas-saturated layers than technically pure titanium. The shallowest gas-saturated layers are found in the VT-8 and VT-14 alloys.

The microscopic analysis of etched gas-saturated layers has shown that the alloys investigated all have clearly visible layers consisting of an α phase with a high microhardness. These layers are formed when the temperature of the experiment exceeds the temperature of the allotropic transformation of alloys. At first, the oxygen diffuses into a thin layer normal to the cylindrical surface. Later on, the diffusion of oxygen takes place selectively both along the grain boundaries and through the grains of the metal. As a result, the surface layer has continuous thick peaks and separated regions of the α phase. The most nonuniform α -phase layers, formed as a result of the most selective diffusion of oxygen, can be found in VT-14 and VT-3—alloys which contain more β -phase stabilizers than any other alloy. The No. 1 experimental alloy is less subject to the selective formation of the α -phase layers. The characteristic microstructures of some alloys are given in Figure 4.

The results of this investigation permit an evaluation of the general oxidability of alloys and also of the depth and the nature of formation of gas-saturated layers.

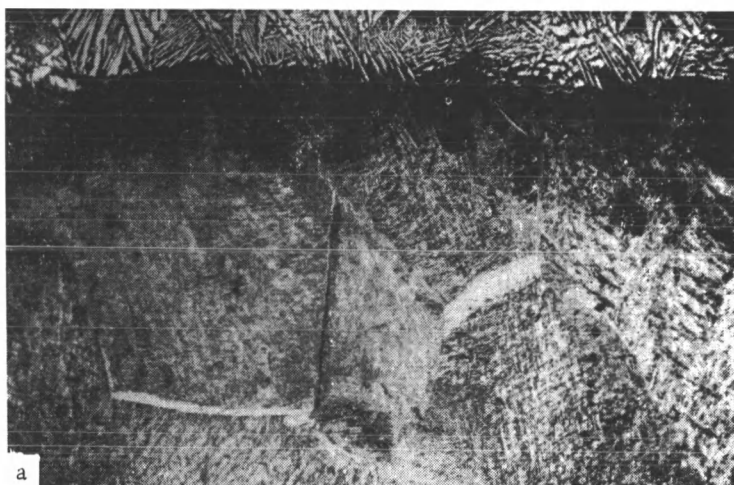


FIGURE 4. Microstructure of alloy surfaces, $\times 70$

a — VT-8 alloy, testing temperature 1100°C , holding time — 1 hour;

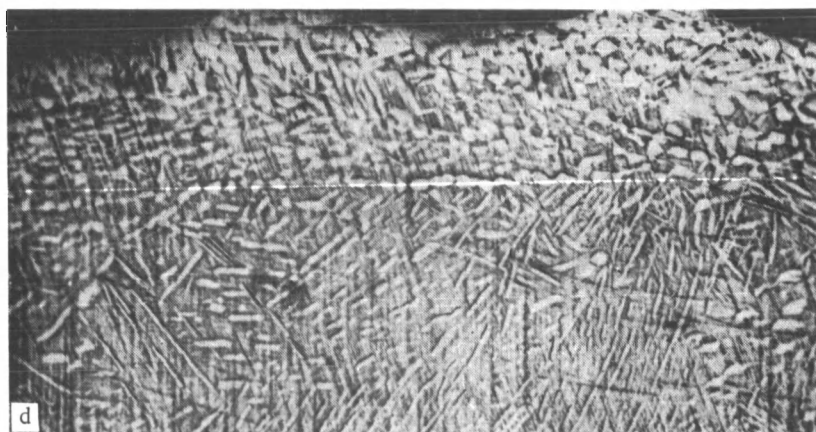
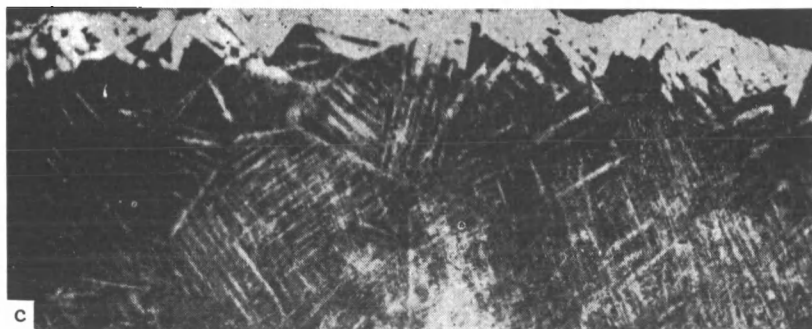
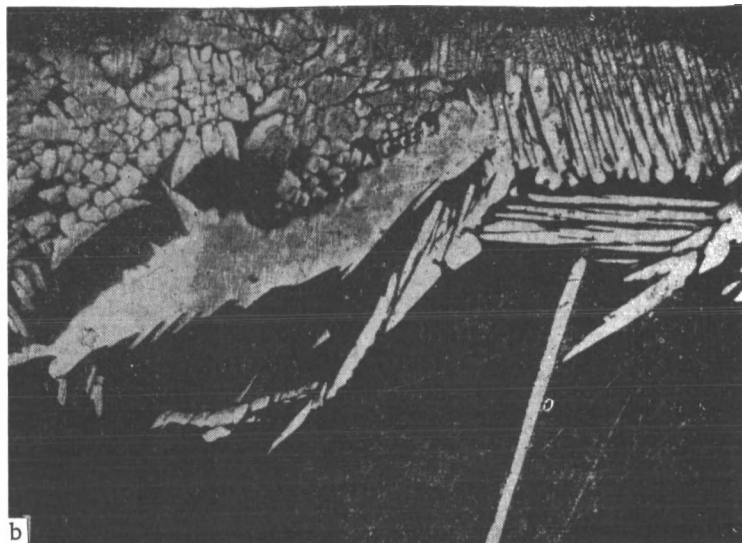


FIGURE 4 (continued)

b — the same, holding time 16 hours; c — experimental alloy, holding time 1 hour;
 d — the same, testing temperature 1000°C, holding time 32 hours.

Bibliography

1. Anitov, I. S. and S. A. Gorbunov. — ZhNKh, 34(4):725. 1960.
2. Kofstad, P., K. Hauffe, and H. Kjollesdal. — Acta chem. Scand., Vol. 12:239. 1958.
3. Tsypin, M. I. Stroenie okaliny na titane (Structure of Titanium Scale). Author's Summary of Thesis. — Gintsvetmetobrabotka. 1961.
4. Anitov, I. S. and S. A. Gorbunov. — Trudy 3-go soveshchaniya "Primenenie titana v promyshlennosti", ONTI. 1961.
5. Eremenko, V. N. Titan i ego splavy (Titanium and Its Alloys). — Izdatel'stvo AN USSR. 1960.

THE INFLUENCE OF GAS-SATURATED LAYERS ON THE STRENGTH AND PLASTIC PROPERTIES OF TITANIUM ALLOYS

L. A. Glikman, V. I. Deryabina, N. N. Kolgatin, I. A. Bytenskii,
V. P. Teodorovich, and N. S. Teplov

Purpose and method of investigation

Semifinished titanium products, heated to high temperatures in the air, become oxidized. In addition, their surface becomes covered (beneath the scale) with a gas-saturated layer which has a high hardness and a low plasticity. This layer greatly influences the strength and plastic properties of titanium parts [1, 2].

The purpose of this investigation was to elucidate the influence of the gas-saturated layer formed during heating of titanium in the air at 800 to 1100°C for 0.5 to 4 hours, on the mechanical properties σ_y , σ_u , δ , ψ , and a_1 of VT-14, VT-3-1, VT-8 alloys and of the No. 1 experimental alloy.

In addition, the influence of the gas-saturated layer on the notch sensitivity of bent and unbent alloy specimens was investigated. The chemical composition of the alloys investigated is given in Table 1.

TABLE 1
Chemical composition of alloys, %

Alloy	Al	Mo	V	Cr	Sn
VT-14	4.20	2.92	1.0	—	—
VT-3-1	4.80	1.83	—	1.78	—
VT-8	5.90	2.90	—	—	—
No. 1 experimental alloy	4.95	—	2.18	—	3.50

The investigated alloys were rolled into small plates and annealed at 800°C. In order to produce a gas-saturated layer these were heated in the air at the above-mentioned temperatures. Some of the specimens were subjected to tension and impact tests.

Other specimens of the alloys were heat treated at temperatures and for durations which, in every case, were the same as those to which the alloys had been subjected to produce the condition of gas saturation. After heating, the specimens were air cooled, given another heat treatment, and shaped as required for tension and impact bending tests. The cross section of the

plates was 25×25 mm so that, before preparing them for mechanical testing, the gas-saturated layers could be fully removed.

Thus, the conditions of heating specimens with and without gas-saturated layers were identical. The specimens were machined in the direction perpendicular to the direction of rolling.

In order to obtain a gas-saturated surface the tension test specimens ($l_0 = 36$ mm, $d_0 = 6$ mm) and the impact bending test specimens (10×10×55 mm) were air heated at 800 and 1000°C for 1, 2, and 4 hours, and at 1100°C for 0.5 and 2 hours. The plates were then air cooled. The same heating and cooling treatments were given to the plates from which the scale and gas-saturated layers were removed.

After removal of the scale* the cooled specimens were subjected to mechanical tests at room temperature**.

In order to determine the response of alloys with gas-saturated layers to stress testing, specimens with adequately sharp notches were prepared (Figure 1).

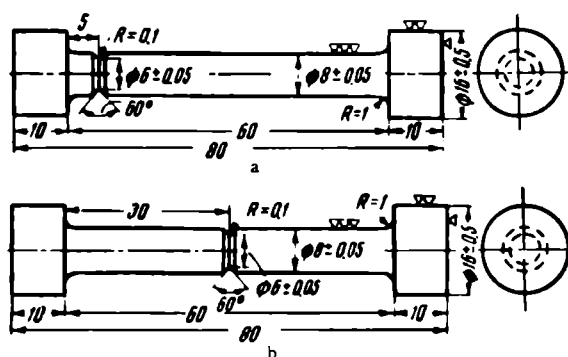


FIGURE 1. Notched and bent specimens for tension tests, angle of bending 8° (a), no bending (b)

Results and discussion

The results of the mechanical tests (σ_y , σ_u , δ , ψ , and a_1) of plain and notched specimens of the initial and gas-saturated alloys are given in Tables 2 and 3 and in Figures 2 to 7. The dependence of the mechanical properties of the alloys on the temperature and on the duration of oxidation is shown in Figures 2 to 7 (magnitude related to the starting values %).

The characteristic features of the data obtained are as follows.

The oxidation considerably decreases the strength, plasticity, and toughness of all investigated alloys. The plastic properties (δ and ψ) and the toughness are more impaired than the strength (σ_y and σ_u). No strength

- * The scale was removed from the heated specimens mechanically.
- ** Heating at 800 to 1100°C for two hours had little influence on the diminution of the dimensions of the specimens. The greatest decrease in the diameter of a specimen for tension testing or in the thickness of a specimen for impact bending was 0.08 to 0.1 mm.

decrease (σ_y and σ_u) was noted on plain specimens of the investigated alloys after oxidation at 800 and 1000°C for four hours.

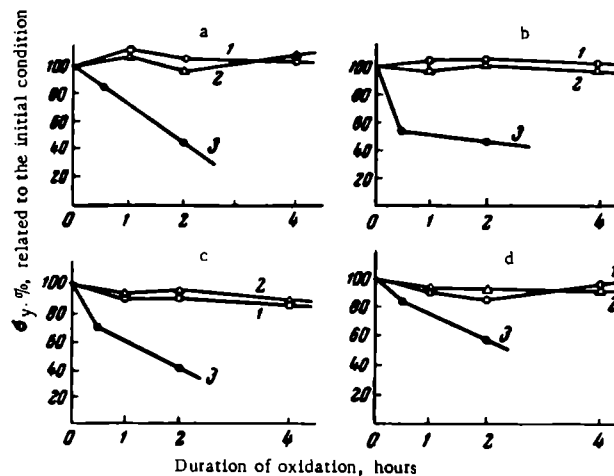


FIGURE 2. Effect of the duration of oxidation [(including gas-saturation)] on the yield point of VT-14 (a), VT-3-1 (b), VT-8 (c), and the No. 1 experimental alloy (d) (temperature of oxidation 800 (1), 1000 (2), and 1100°C (3))

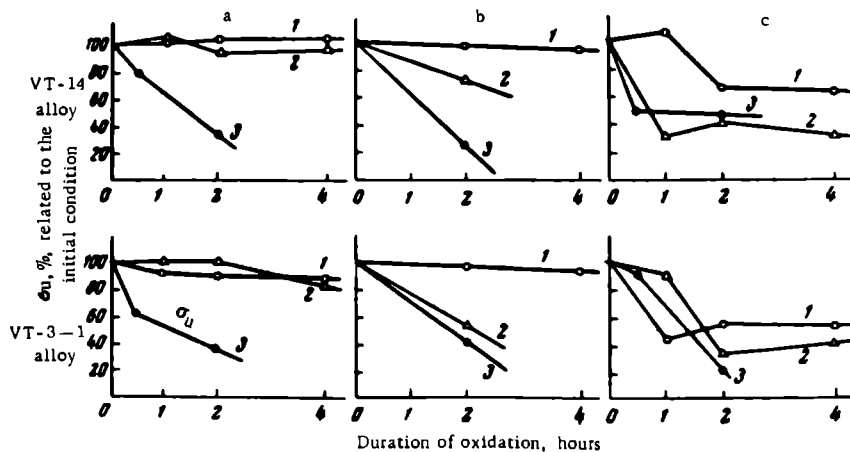


FIGURE 3. Effect of the duration of [oxidation, including] gas-saturation, on the ultimate strength of VT-14 and VT-3-1 alloys during testing of plain (a), notched and unbent (b), and notched and bent (c) specimens (temperatures of oxidation 800 (1), 1000 (2), and 1100°C (3))

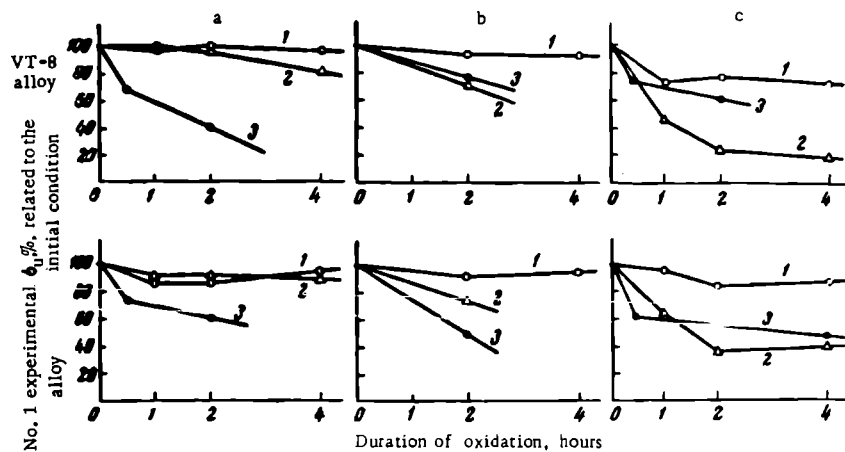


FIGURE 4. Influence of the duration of oxidation [including gas-saturation] on the ultimate strength of VT-8 and the No. 1 experimental alloy during testing of plain (a), notched and unbent (b), and notched and bent (c) specimens at temperatures of oxidation 800(1), 1000(2), and 1100°C (3)

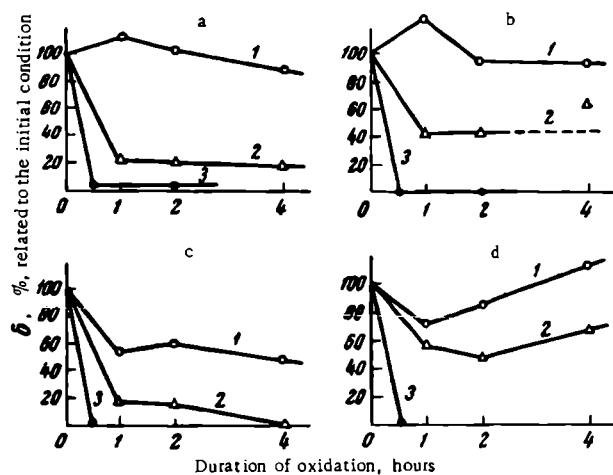


FIGURE 5. The influence of the duration of oxidation [including gas-saturation] on the elongation of VT-14 (a), VT-3-1 (b), VT-8 (c), and the No. 1 experimental (d) alloys, (temperature of oxidation 800(1), 1000(2), and 1100°C (3))

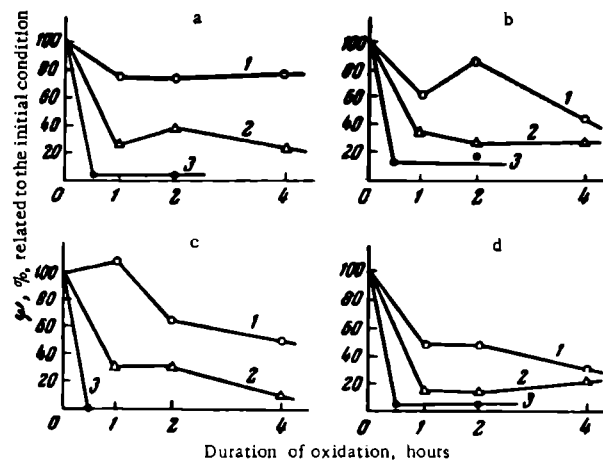


FIGURE 6. The influence of the duration of oxidation [including gas-saturation] on the reduction in area of VT-14(a), VT-3-1(b), VT-8(c), and the No. 1 experimental (d) alloys (temperature of oxidation 800 (1), 1000 (2), and 1100°C (3))

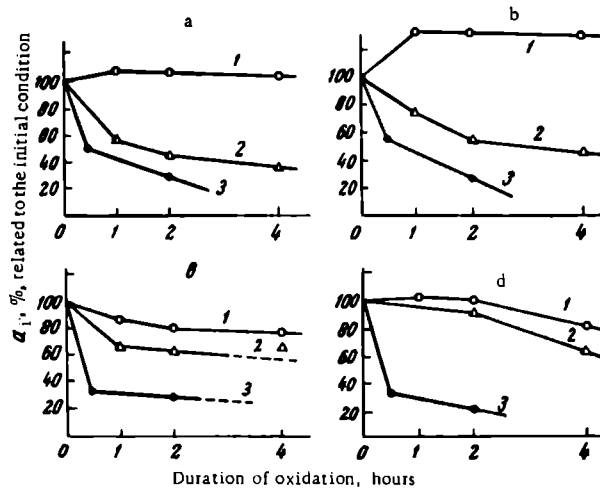


FIGURE 7. The influence of the duration of oxidation [including gas-saturation] on the toughness of VT-14(a), VT-3-1(b), VT-8(c), and the No. 1 experimental (d) alloys (at temperatures of oxidation 800 (1), 1000 (2), and 1100°C (3))

A considerable decrease in the magnitudes of σ_y and σ_u of the alloys is noted after oxidation at 1100°C. In VT-14, VT-3-1, and VT-8 alloys oxidation for 2 hours decreases these coefficients by about 60 % (Figures 2a,

b, c; 3a, and 4a). The No. 1 experimental alloy loses only 40% of these coefficients (Figures 2d and 4a).

The strength of bent and unbent notched specimens made of alloys with a gas-saturated layer also decreases considerably. Bent and notched specimens whose strength was very little affected by notching and were even stronger than plain specimens before oxidation showed increased notch sensitivity after their surfaces were covered with a gas-saturated layer. Unbent specimens oxidized at 800°C tend to lose their ultimate strength (σ_u) and this becomes more noticeable in unbent specimens oxidized at 1000 and 1100°C. Unbent specimens of the VT-14 alloy showed the highest loss of σ_u [at 800°C] (up to 80%). The other three alloys also lost much of their σ_u on oxidation. This loss amounts to 30-60% after oxidation for 2 hours at 1100°C.

The ultimate strength of the notched specimens, whether bent or unbent, considerably decreases after oxidation. The ultimate strength (σ_u) of bent specimens begins to decrease considerably after oxidation at 800°C; for VT-14 and VT-3-1 alloys, oxidation for 2 hours reduces the ultimate strength by 40 to 50% while the ultimate strength drop in VT-8 and in the No. 1 experimental alloys is under these conditions of oxidation, only 20%. The ultimate strength of bent specimens oxidized at 1000 to 1100°C is reduced by 60 to 80%.

When comparing the data for VT-14, VT-8, and the No. 1 experimental alloy it is noteworthy that the ultimate strength of bent specimens oxidized at 1100°C decreases less in the course of the process than the ultimate strength of bent specimens oxidized at 1000°C. This is probably due primarily to the fact that heating at a higher temperature (1100°C) so strongly oxidizes the surface of the notch that it becomes somewhat dull. Further, in all the alloys investigated, the bent specimens have high notch sensitivity before oxidizing and have a low ultimate strength (up to 22.7 to 28.1 kg/mm²) in the initial condition (preliminary heating at 1100°C). Although the absolute magnitude of σ_u decreases after heating [for some time] to 1100°C [Table 2], the relative decrease is smaller than that of specimens heated to 1000°C.

The oxidation influences chiefly the plastic properties (δ and ψ) and the impact toughness of the specimens α_i . While σ_y and σ_u remain more or less stable after oxidizing at 800 and 1000°C, the magnitudes of δ , ψ , and α_i considerably decrease, beginning with 800°C*. The most sensitive indicator of oxidation is the reduction of area which for all four alloys decreases by 30 to 60% upon heating to 800°C. After heating at 1000 and 1100°C the ψ and δ of alloys drop almost to zero while the impact toughness is reduced by 60 to 80%.

* [Figures 5, 6, and 7 show the following: δ (elongation) in the case of VT-8 decreases at all oxidation temperatures; in the case of VT-3-1, δ decreases at 1000° and 1100°C; in the case of experimental alloy No. 1, rapid reduction in δ takes place at 1100°C, while for 800° and 1000°C, an initial reduction is followed by an increase in δ ; ψ (reduction of area) decreases in all alloys with increasing temperature of oxidation; α_i (impact toughness) decreases for all alloys after oxidation at 1000°C, but not so markedly in the case of experimental alloy No. 1 for 1000°C; α_i is not greatly affected by oxidation at 800°C; in the case of experimental alloy No. 1, this factor begins to decline after 2 hours oxidation.]

Microscopic investigation of the failure of alloys with a gas-saturated layer

If the bent specimens for tension and impact tests are heated to 800, 1000, or 1100°C in the air their surface becomes coated with a gas-saturated layer. This saturation is due chiefly to the diffusion of oxygen into the surface layer of the alloys. According to the Ti - O₂ phase diagram a concentration of oxygen higher than 5 weight % in the gas-saturated layer causes the β phase, which exists in a state of equilibrium at temperatures above 900°C, to be transformed into an α phase* (i. e., a layer with an α phase is formed).

With diffusion of oxygen into the metal, its concentration in successive layers will reach the 5 % level and the depth of the α phase will consequently increase. The concentration of oxygen in layers closer to the surface can then be higher than the above value.

Oxygen-saturated specimens cooled from high temperatures show, after etching, an oxygen-saturated surface layer (white streak) and an α phase formed as a result of the thermal $\beta \rightarrow \alpha$ transformation.

The oxygen-saturated surface layer consists of closely packed grains and of deeply penetrating elongated inclusions. In some cases the oxygen-saturated phase is formed on the grain boundaries and penetrates to a considerable depth. The gas-saturated layers are not formed under the same conditions of heating for all alloys. In the VT-14 and VT-3-1 alloys (Table 3) an oxygen-saturated layer is formed after heating at 1000°C for one hour. In the VT-8 and in the No. 1 experimental alloy the formation of the oxygen-saturated layer requires more severe conditions of heating: for alloys VT-8 — heating at 1100°C for 0.5 hours and for No. 1 experimental alloy — heating at 1100°C for 4 hours.

The oxygen-saturated layer and the inclusions of the α phase have a high microhardness, they are brittle, and have a low plasticity (Table 3). Therefore, during tensile tests, this weakened layer and the inclusions of the α phase are the first to fail. The destruction takes place chiefly along the gas-saturated layer and, as has been experimentally shown, specimens with a gas-saturated layer have low strength characteristics (σ_y and σ_u), a low plasticity (δ and ψ), and a low impact toughness a_i .

Notched specimens heated in the air have also a low plasticity, toughness, and strength, although on some of them no oxygen-saturated layer could be found by metallographic examination. The low magnitudes of δ , ψ , and a_i of plain specimens and the low magnitudes of σ_u of notched specimens is apparently due to the presence in the surface layers of oxygen, and perhaps nitrogen, in an amount which does not exceed 5 weight %. Although this layer cannot be determined metallographically its presence is evident from the high microhardness** of oxygen-saturated layers (Table 3). In addition the failed round impact test specimens of all four alloys, on which no oxygen-saturated layer could be determined after heating, show microscopic cracks and crevices on their sides. These cracks are the deeper, the higher the temperature and the longer the holding time of the specimens during heating. The failed round and spare specimens, tested before heating, show no cracks or crevices on their sides.

* According to the Ti - O₂ phase diagram, the formation of the α phase begins at concentrations of oxygen equal to 2-2.5 weight %.

** The high microhardness of these alloys after being saturated with oxygen was also determined by S. A. Gorbunov, G. P. Nadutenko, and V. P. Teodorovich (whose paper appears in this book, page 113).

TABLE 2

The mechanical properties of plain and notched specimens* of the alloys in their initial condition (before oxidation [including gas-saturation])

Alloy	Temperature of oxidation, °C	σ_y , kg/mm ²	σ_u , kg/mm ²			δ , %	ψ , %	σ_L , kg/mm ²
			plain specimen	notched specimen				
				unbent	bent			
VT-14	800	73.2	87.4	122.5	33.0	11.3	26.6	8.0
		75.3	87.0	121.3	35.9	14.1	35.2	7.6
		73.4	87.3	121.5	76.2	8.9	20.4	—
	1000	86.1	94.8	135.3	90.1	6.6	21.3	5.2
		76.7	87.5	136.1	59.1	7.4	19.0	5.7
		83.5	93.0	132.3	106.8	9.2	18.4	7.4
	1100	76.4	88.4	123.8	—	12.4	21.9	4.7
		75.2	88.8	126.9	—	10.2	29.1	4.5
	VT-3-1	800	85.3	95.7	134.5	83.2	11.4	26.8
88.2			98.2	136.2	80.5	8.3	7.8	5.0
84.2			95.5	138.3	40.5	9.5	22.0	5.1
1000		91.1	98.3	131.3	48.2	5.9	16.5	6.1
		91.0	98.1	135.8	84.2	5.6	11.0	6.0
		88.3	96.9	138.3	50.4	6.8	20.2	6.5
1100		86.7	96.2	134.8	30.5	4.6	2.6	5.6
		88.7	95.6	133.7	28.1	3.4	19.2	4.7
VT-8		800	84.1	100.1	137.3	33.5	9.4	14.2
	88.4		100.3	139.9	52.0	10.3	17.7	5.8
	88.9		101.0	137.8	32.6	9.5	18.1	8.3
	1000	90.2	100.1	137.2	69.4	9.6	24.3	6.6
		91.2	100.8	139.9	57.1	10.3	21.9	5.6
		91.5	102.8	137.0	57.7	10.9	26.3	7.6
	1100	85.6	90.9	133.5	27.3	6.5	8.5	5.6
		91.0	100.3	130.9	22.7	5.6	12.9	5.5
	No. 1 experi- mental alloy	800	93.5	103.6	138.1	34.2	10.9	17.4
93.8			101.4	140.0	33.4	9.3	23.4	6.1
90.8			101.0	140.8	32.3	9.4	21.5	6.0
1000		84.7	95.0	139.6	71.4	6.1	12.9	4.1
		87.7	96.2	136.0	38.9	8.8	30.0	3.9
		81.4	97.4	135.9	39.1	8.0	30.5	—
1100		81.5	96.5	127.2	36.6	6.9	20.2	8.0
		83.8	95.8	123.2	27.6	9.6	18.4	4.1

* In the case of notched specimens only the ultimate strength σ_u was determined

Removal of the gas-saturated surface layers from the specimens

The data given above clearly indicate that the gas-saturated surface layer has a considerable influence on the plastic and strength characteristics of alloys. In loaded samples it is this layer which develops the initial cracks leading to the failure of the material.

TABLE 3

Properties of alloy specimens with gas-saturated layers: thickness and micro-hardness of the gas-saturated layers and the presence of cracks (crevices) on the side

Alloy	Conditions of gas saturation		Depth of oxygen-saturated layer, mm		Maximum increase in microhardness of gas-saturated layer, kg/mm ²	Thickness of layer with a high microhardness, mm	Depth of cracks (rupture on the side surface of the specimen), mm
	temperature	time, hours	continuous	with inclusions			
VT-14	800	1	0	0	110	0.05	0.025
		2	0	0	50	0.15	0.025
		4	0	0	200	0.50	0.060
	1000	1	0.06	0.20	540	0.25	0.10
		2	0.15	0.45	740	0.30	0.15
		4	0.17	0.45	650	0.50	0.20
	1100	0.5	0.10	0.10	300	0.25	Few but deep cracks
		2	0.30	0.50	820	0.50	No cracks present
	VT-3-1	800	1	0	0	160	0.25
2			0	0	700	0.12	0.035
4			0	0	820	0.50	0.06
1000		1	0.12	0.40	1100	0.50	0.12
		2	0.15	0.30	1340	0.40	0.20
		4	0.12	0.50	1040	0.40	No cracks present
1100		0.5	0.22	0.22	1640	0.40	Many small but deep cracks
		2	0.20	0.45	810	0.50	No cracks present
VT-8		800	1	0	0	—	—
	2		0	0	840	0.40	0.05
	4		0	0	580	0.45	0.10
	1000	1	0	0	520	0.50	0.12
		2	0	0	580	0.50	0.25
		4	0	0	420	0.50	—
	1100	0.5	0.25	0.30	620	0.40	Few but deep cracks
		2	0.40	0.60	1320	1.00	Deep cracks
	Experimental No. 1	800	1	0	0	100	0.10
2			0	0	400	0.15	0.03
4			0	0	280	0.10	—
1000		1	0	0	360	0.45	0.10
		2	0	0	680	0.50	0.12
		4	0.12	0.12	500	0.40	0.20
1100		0.5	0.15	0.15	520	0.30	Small but deep cracks
		2	0.35	0.35	280	0.50	No cracks present

It was, therefore, of interest to determine whether the removal of the gas-saturated layers from the air heated specimens could restore the mechanical properties of the alloys.

With this end in view, special specimens were prepared, allowance being made for the depth of the scale and of gas-saturated layers which were formed under specific conditions. After oxidation, the scale was removed from the specimens and a surface layer machined down on a lathe. This layer was 0.14 to 1.20 mm thick (i. e., the continuous oxygen-saturated layer plus a layer several times its thickness) (2 to 4, Table 3).

With some exceptions the depth of the layer removed was 0.5 to 3 times the thickness of the oxygen-saturated layer. The data on the removal of the gas-saturated layers and on the mechanical properties of the specimens from which these layers were removed are given in Tables 4 to 7.

These data show that, after the gas-saturated layers are removed, the strength characteristics (σ_y and σ_u) of the alloys investigated are restored and in some cases even augmented.

In order to restore the strength characteristics (σ_y and σ_u) of gas-saturated specimens, the layer removed must not be thinner than 1.5 to 2 times the thickness of the continuous oxygen-saturated layer.

After removal of a layer twice the thickness of the continuous oxygen-saturated layer the plasticity (δ and ψ) of the alloy remains the same as that of the specimens on which the gas-saturated layers are intact.

This low plasticity is apparently due to the fact that although the oxygen-saturated surface layer is removed, the metal still retains an oxygen-saturated layer with a high hardness and a low plasticity (Table 3). Such specimens also retain a layer with α -phase inclusions. The low plasticity of titanium alloys with a gas-saturated layer (up to 4 atomic % O_2) was also observed by Jenkins et al in forgings heated to over 1000°C /3/.

The retention of oxygen by the remaining surface layers is apparently also the cause of the high strength characteristics (σ_y and σ_u) which are sometimes found in specimens from which the oxygen-saturated surface layer has been removed. Similar data are reported in the monograph of V.N. Eremenko /4/, who observed that ultimate strength and hardness of titanium alloys increase with their oxygen content.

The plastic properties of the alloys can be restored by the removal of a deeper layer which includes both the oxygen-saturated surface layer and the layer with the high microhardness. The maximum thickness of the layers removed in the present investigation was 1.2 mm. The removal of such a gas-saturated layer was sufficient to restore the strength characteristics (σ_y and σ_u) of all investigated alloys (VT-14, VT-3-1, VT-8, and No. 1 experimental alloy and the plastic properties (δ and ψ) of the VT-8 and No. 1 experimental alloys. The plastic properties (δ and ψ) of the VT-3-1 alloy were also restored by this removal.

Conclusions

1. VT-14, VT-3-1, VT-8 alloys and the No. 1 experimental alloy form a gas-saturated layer with a high hardness and a low plasticity on their surfaces at 800 to 1100°C.

TABLE 4
Mechanical properties of VT-14 alloy after gas saturation and after the removal of the
gas-saturated layer*

Conditions of gas saturation		Thickness of the layer removed, mm		σ_y , kg/mm ²			σ_u , kg/mm ²			δ , %			ψ , %			
Temperature, °C	Duration of the process, hours			in the initial condition	with the gas-saturated layer	after removing the gas-saturated layer	in the initial condition	with the gas-saturated layer	after removing the gas-saturated layer	in the initial condition	with the gas-saturated layer	after removing the gas-saturated layer	in the initial condition	with the gas-saturated layer	after removing the gas-saturated layer	
800	4	0.14	0.21	73.9	73.8	73.6	87.2	89.6	99.2	11.4	10.1	9.4	27.4	21.2	4.6	
						79.2			95.4			5.4			7.3	
1000	4	0.22	0.24	82.1	86.2	95.2	91.7	91.1	100.5	7.7	1.4	0.8	19.6	5.4	3.4	
						96.1			105.4			0				
1100	0.5	0.18	0.27													
				67.5	67.5	91.1							1.7			
	2	0.24	0.31													
		0.55	0.50													
	1.20	1.20	1.21													

* For comparison, the mechanical properties of the alloy before oxidation are also given.

TABLE 5
Mechanical properties of the VT-3-1 alloy after gas saturation and after the removal of the gas-saturated layer

Conditions of gas saturation		Thickness of the layer removed, mm	σ_y , kg/mm ²			σ_H , kg/mm ²			δ , %		ψ , %		
Temperature, °C	Duration of the process, hours		in the initial condition	with the gas-saturated layer	after removing the gas-saturated layer	in the initial condition	with the gas-saturated layer	after removing the gas-saturated layer	in the initial condition	with the gas-saturated layer	after removing the gas-saturated layer	in the initial condition	with the gas-saturated layer
800	4	0.17	83.6	77.1	91.4	96.5	85.5	105.9	9.7	9.1	7.8	18.9	7.8
		0.16			87.7			104.1			5.5		10.8 8.6
1000	4	0.18	90.2	82.3	80.3	97.7	85.4	80.3	6.1	3.9	0.5	15.9	6.2
		0.17			75.1			75.1			0		1.7 4.9
1100	0.5	0.18		62.3	86.4		68.0	90.8		0	0.1		1.6
		0.27			71.1			71.3			1.2		4.5 2.5
	2	0.32			19.3			19.3			2.8		0
		0.20			9.6			9.6			1.3		0
	2	0.48	87.7	36.9	46.2	95.9	36.9	46.2	4.0	0	0	10.9	2.5
													0
		1.15			83.3			108.2			1.7		10.6
		1.17			98.6			106.0			—		—

TABLE 6
Mechanical properties of the VT-8 alloy after gas saturation and after the removal of the gas-saturated layer

Conditions of gassaturation		Thickness of the layer removed, mm	σ_y , kg/mm ²			σ_u , kg/mm ²			δ , %			ψ , %		
Temperature, °C	Duration of the process, hours		in the initial condition	with the gas-saturated layer	after removing the gas-saturated layer	in the initial condition	with the gas-saturated layer	after removing the gas-saturated layer	in the initial condition	with the gas-saturated layer	after removing the gas-saturated layer	in the initial condition	with the gas-saturated layer	after removing the gas-saturated layer
800	4	0.22 0.22	87.1	89.1	83.1 86.0	100.4	98.2	98.1 100.0	9.7	7.2	8.3 9.7	16.6	9.2	16.4 16.8
1000	4	0.13 0.18	90.9	89.5	88.0 90.2	101.6	84.1	93.8 96.9	10.2	0 0	2.3 1.2	24.1	0 5.7	1.7 5.1
1100	0.5	0.18 0.14	88.3	65.9	91.5 91.9	70.9	95.6	101.7 93.8	6.0	0.15	1.3 1.9	10.6	4.0	0 4.0
	2	0.31 0.30		42.3 22.4	43.6			101.4 65.2			2.8 1.2			6.4 3.0

TABLE 7

Mechanical properties of the No. 1 experimental alloy after gas saturation and after the removal of the gas-saturated layer

Conditions of gas-saturation		Thickness of the layer removed, mm	σ_y , kg/mm ²			σ_u , kg/mm ²			δ , %			ψ , %		
temperature, °C	duration of the process, hours		in the initial condition	with the gas-saturated layer	after removing the gas-saturated layer	in the initial condition	with the gas-saturated layer	after removing the gas-saturated layer	in the initial condition	with the gas-saturated layer	after removing the gas-saturated layer	in the initial condition	with the gas-saturated layer	after removing the gas-saturated layer
800	4	0.17	92.7	88.8	89.8	102.0	99.1	100.5	9.8	10.9	9.5	20.6	6.0	20.1
		0.17			89.7			100.9			8.4			21.7
1000	4	0.24	84.6	77.7	91.0	96.2	90.5	96.0	7.6	4.9	2.7	24.4	5.3	5.5
		0.18			90.5			98.5			3.1			3.8
1100	0.5	0.24		67.6	91.0		71.4	96.0		0.5	2.7		1.3	5.5
		0.23			90.5			98.5			3.1			3.8
		0.20			20.7			20.7			1.9			3.1
		0.37			24.4			24.4			1.9			4.3
		0.55	82.6	60.2	66.3	96.1	60.2	66.3	8.2	0.15	6.0	19.3	7.3	14.4
					83.8			100.8			11.1			21.3
		1.20			88.6			102.2			9.6			14.8

2. The mechanical properties σ_y , σ_u , δ , ψ , and a_i of titanium alloys are considerably impaired by the gas-saturated layer. The oxidation of alloys at 1100°C reduces the strength characteristics (σ_y and σ_u) by 40 to 60 % (as compared with the initial condition), the impact toughness by 70 to 80%, while the plasticity (δ and ψ) drops to zero.

3. The gas-saturated alloys investigated, whether bent or unbent, exhibit high notch sensitivity which, particularly in bent specimens, becomes evident after heating at relatively low temperatures (800°C), i.e., when no oxygen-saturated layer has yet been formed on the surface of the alloys.

4. The mechanical properties (σ_y , σ_u , δ , and ψ) of the gas-saturated alloys can be restored to the initial magnitudes if the oxygen-saturated surface layer is mechanically removed. In order to restore the strength and plastic characteristics of titanium alloys (VT-14, VT-3-1, VT-8, and experimental alloy No. 1), it is necessary to remove a layer 5 to 6 times as thick as the oxygen-saturated surface layer together with the inclusions, i.e., for the conditions of the present investigation (oxidation at 1000°C, for 4 hours, and at 1100°C for 2 hours) this layer should be 2 to 3 mm thick.

Bibliography

1. Sakharov, G. S. and N. G. Evlanov. — Vestnik Mashinostroeniya, No. 12: 41. 1960.
2. Petunina, E. V. — Metallovedenie i Termicheskaya Obrabotka Metallov, No. 6: 50. 1961.
3. Jenkins, A. E., and H. W. Warner. — J. Inst. met., 12(18): 157. 1951.
4. Eremenko, V. N. Titan i ego splavy (Titanium and its Alloys). — Izdatel'stvo AN USSR. 1960.

CALCULATION OF THE KINETICS OF THE DISSOLUTION OF OXYGEN IN TITANIUM

S. S. Mozhaev and L. F. Sokiryanskii

The capacity of titanium to dissolve large amounts of oxygen during plastic deformation leads to embrittlement of the surface layers and to a tendency toward cracking of finished parts. This has impeded the adaptation of titanium in industry and has hampered the production of high-quality constructional materials.

The dissolution of oxygen in titanium begins at about 500°C and greatly increases with the rise in temperature. The laws governing this process, however, are still insufficiently investigated. There are almost no data in the Soviet literature on the kinetics of the saturation of titanium with oxygen and the few data which can be found in foreign publications are conflicting and require verification.

No more reliable quantitative data will apparently be available until a suitable mathematical technique for the processing of investigational results is developed. Such a technique will not only enable quantitative characteristics of the process to be obtained but will also facilitate the verification of certain physical theories, the evaluation of experimental errors, and the specification of the accuracy required in determinations of the necessary physical constants.

The first serious attempt to use mathematical analysis for investigating the diffusion of oxygen into titanium was undertaken by Vasilevskii and Kehl in 1954 [1]. Experimental data published since then have confirmed certain assumptions made by the workers.

Diffusion of oxygen into α -Ti

The distribution of oxygen within the gas-saturated layer at temperatures below the allotropic transformation can be represented by the Fick law of diffusion, which for the diffusion through a flat surface in one direction will be:

$$\frac{\partial C}{\partial \tau} = \frac{\partial}{\partial x} \left[D(C) \frac{\partial C}{\partial x} \right]. \quad (1)$$

When solving this equation, it is usually necessary to make some assumptions, among them that the specimen is a semi-infinite body, since its linear dimensions considerably exceed the expected depth of the diffusion layer, and that the surface plane of the specimen is a mathematical boundary

plane. It is further assumed that the diffusion coefficient does not depend on the concentration [of O_2], that in the initial specimen the oxygen is uniformly distributed through the volume, i. e.,

$$C(x, 0) = C_0, \quad (2)$$

and that a certain concentration, which subsequently remains constant, is instantaneously achieved in the boundary plane at the commencement of the process,

$$C = (0; \tau) C_0. \quad (3)$$

This constant concentration of oxygen is equal to its maximum solubility in the metal.

The Fick equation for boundary conditions is:

$$C = (C_0 - C'_0) \operatorname{erfc} \left(\frac{x}{2\sqrt{D\tau}} \right) + C'_0, \quad (4)$$

where

$$\operatorname{erfc} \left(\frac{x}{2\sqrt{D\tau}} \right) = 1 - \frac{2}{\sqrt{\pi}} \int_0^{\frac{x}{2\sqrt{D\tau}}} e^{-z^2} dz.$$

The amount of gas which diffuses into the metal through a unit of surface during the time τ , is in this case determined by the parabolic time dependence

$$q = 2(C_0 - C'_0) \sqrt{\frac{D\tau}{\pi}}. \quad (5)$$

The assumed condition (3), that a constant concentration of oxygen is maintained in the surface of the metal, is only approximate since it is obvious that the maximum concentration of oxygen on the surface of the metal can be reached only after a certain time, the duration of which depends on the properties of the medium and of the metal under the given conditions as well as on the kinetics of their interaction.

Vasilevskii and Kehl/1/ have therefore proposed another equation for the boundary condition

$$\frac{\partial C(0, \tau)}{\partial x} = h(C_0 - C_{0\tau}), \quad (6)$$

where h = maximum conductivity;

$C_{0\tau}$ = actual magnitude of the surface concentration.

In this case the surface concentration increases with time approximately exponentially, and asymptotically approaches the maximum level C_0 .

At the boundary conditions selected, the absorption of oxygen during short time intervals is approximately proportional to $\tau^{1/2}$. As the time increases the absorption increases almost linearly and as the surface concentration approaches the maximum magnitude C_0 , the relationship between the absorption of oxygen and the time approaches a parabolic function. However, there is still no experimental confirmation that such is the nature of absorption of oxygen by titanium. There are only data indicating that at relatively low

temperatures the absorption of oxygen is indeed governed by a parabolic function, provided that this process lasts for a sufficiently long time.

This is possibly the reason why most investigators assume that the maximum surface concentration is achieved in a negligibly short time. Characteristic from this point of view is the investigation of A.V. Revyakin /2/, who determined the diffusion of oxygen in titanium at 800 to 900°C (holding time 3 hours). The deviation of the oxidation from the parabolic law during the first 10 to 15 min is explained by the author by the fact that a maximum concentration of oxygen has been established at the surface. He assumed, therefore, in his further calculations that the maximum concentration on the surface is reached instantaneously.

However, the results of direct experimental determinations of the surface concentration which have been carried out by a number of investigators show that the maximum solubility on the surface of titanium is not reached even after considerably longer stretches of time.

Thus, Jenkins /3/ has determined that after a heating period lasting 72 hours the surface concentration did not exceed 12 at. % at 650°C, 19 at. % at 800°C, and 25 at. % at 900°C, i.e., in all cases the concentration was considerably lower than the maximum solubility of oxygen in titanium.

Hurlen /4/ has determined that at 500°C the dissolution of oxygen in titanium is very slow and that very small changes on the X-ray photographs can be noted only after the specimens have been heated for 2 days.

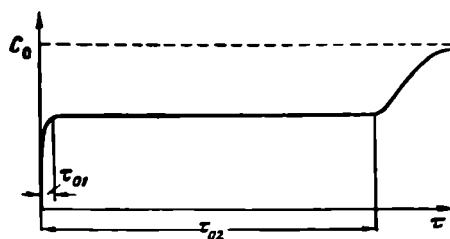


FIGURE 1. Variation of surface concentration at $\sim 700^\circ\text{C}$

Specimens in which a concentration of 14 to 15 at. % was achieved at 650°C showed no further change though they were heated for 2 days.

At 700°C, the oxygen concentration of 13 to 17 at. % remained constant for almost a day before showing a further rise.

The variation of the surface concentration is diagrammatically shown in Figure 1. Thus, the theory of Vasilevskii and Kehl on the continuous variation of the surface concentration from 0 to infinity has not been confirmed by these experimental data.

On the basis of his own observations, Hurlen assumed that at 650 to 700°C, oxygen dissolves more readily in specimens with a surface concentration of 14 to 15 at. % of O_2 than at higher concentrations so that the Ti_6O compound is more stable than other compounds of the Ti—O system.

However, Hurlen, has not explained the additional increase in the concentration which takes place after a certain time.

The comparison of various experimental data permits another interpretation of the variations in surface concentration (which have been observed by Hurlen /4/).

For the boundary conditions (2) and (3), equation (1) determines the absorption capacity of titanium when the gas is supplied to a surface of the metal at a sufficient rate, i.e., when the potential possibilities of titanium to absorb oxygen are fully exploited.

Since the surface of titanium is coated with a thin, highly-protective oxide film firmly adhering to the metal, a lesser amount of gas is supplied to the surface than can be absorbed by the metal. As a result, the gas-saturation of the metal is governed by the supply rate of oxygen to the scale-metal boundary.

If it is assumed that, at 700°C, the absorption of oxygen proceeds for a considerable time in accordance with the parabolic function, then the relationship between the amount of oxygen absorbed to that which could have been theoretically absorbed as determined (for a given surface concentration) by equation (5), should be constant for a given temperature:

$$\frac{q_{\text{real}}}{q_{\text{calculated}}} = \gamma = \text{const}, \quad (7)$$

for $\gamma < 1$.

In this case the amount of oxygen absorbed in accordance with the equations (5) and (7) is determined by the following equation:

$$q_{\text{real}} = 2\gamma (C_0 - C'_0) \sqrt{\frac{D\tau}{\pi}}. \quad (8)$$

If this formula is considered a boundary condition of the second type for the initial differential equation (1), then the following equation is obtained for the variation of the concentration of oxygen in titanium:

$$C = (C_0^* - C'_0) \operatorname{erfc} \left(\frac{x}{2\sqrt{D\tau}} \right) + C'_0, \quad (9)$$

where C_0^* = concentration of oxygen at the surface of the metal, as determined by the equation:

$$C_0^* = \gamma C_0 - C'_0(1 - \gamma) \approx \gamma C_0.$$

Equation (9) shows that under certain conditions it is possible to obtain a certain stable concentration at the surface of titanium which is, however, lower than the maximum solubility of oxygen in the metal. This equation shows the distribution of oxygen at a moment τ (see Figure 1), which is determined by the formula

$$\tau_{01} \leq \tau < \tau_{02}. \quad (10)$$

It has been experimentally determined that the protective properties of the oxide film decrease and the rate of oxidation increases with the increase

in the duration of heating. An attempt was, therefore, made by the authors to connect the increase in the surface concentration after prolonged heating, which was noted by Hurlen, with the transition from the parabolic to the linear law of scale formation.

Thus, according to Jenkins /5/, the transition from the parabolic to the linear law of oxidation takes place after 20 to 30 hours at 700°C, which is the same period after which Hurlen detected a further increase in the surface concentration.

In addition, it was mathematically found /5/ that, at 650°C, the transition from the parabolic to the linear law of oxidation should take place in about 53 hours which contradicts the experiments carried out by Hurlen, who found no further increase in the surface concentration of oxygen after two days of heating.

This comparison permits the assumption that the increase in the surface concentration to a maximum is due to a deterioration in the protective properties of the oxide film during its growth, which leads to an accelerated supply of oxygen to the surface of titanium and, consequently, to an increased absorption of the gas by the metal.

The protective properties of the oxide film rapidly deteriorate with the increase in the temperature, as a result of which the maximum surface concentration is more rapidly attained and the time (10) during which equation (9) may be applied decreases.

In order to determine the diffusion field at a temperature close to the allotropic transformation it is necessary to use the more general equation (1), which is correct for any variation in the surface concentrations with time,

$$C(0, \tau) = f(\tau). \quad (11)$$

In this case the solution of the Fick equation for a semi-infinite body at boundary conditions (2) and (11) is

$$C(x, \tau) = \frac{x}{2\sqrt{\pi D}} \int_0^\tau \frac{f(\tau - \xi)}{\xi^{3/2}} \exp\left(-\frac{x^2}{4D\xi}\right) d\xi. \quad (12)$$

Equation (12) cannot be properly solved because of the lack of the necessary experimental data relating to the dependence of the surface concentration on the temperature and the duration of heating. When such data become available, investigators will be in a position to represent equation (11), with fair accuracy, in the form of some simple function which, after integrating, will enable a formula to be obtained adequate for practical calculations.

From the foregoing it can be seen that the degree of saturation of titanium with oxygen can be better calculated, the more reliable the data relating to the boundary conditions and the diffusion coefficient. Further, the exactness of determination of the diffusion coefficient depends on the correctness of the boundary conditions assumed.

The latter assumption can be shown by the following example.

In a paper published by Revyakin /2/, the diffusion coefficient was calculated from the amount of the oxygen dissolved, using formula (5). It was assumed that the concentration of oxygen at the surface of the metal was in all cases equal to the maximum solubility. If, however, on the

basis of the above-mentioned experimental results obtained by Jenkins /3/, it is assumed that at 800°C the surface concentration does not exceed 10 at. %, then the diffusion coefficients calculated by Revyakin /2/ for this temperature are as much as 3.5 times too low. The diffusion coefficients of oxygen in α -Ti given in the earlier works /6, 7/, should also be accepted with caution as they were calculated on the basis of formula (4) which had also been derived on the assumption of an instantaneous establishment of the maximum concentration at the metal surface.

The evaluation of the depth of penetration of oxygen into titanium is also of great practical interest. The depth of penetration b is determined by the distance at which the excessive concentration of oxygen is equal to zero, i.e.,

$$C(b, \tau) - C'_0 = 0. \quad (13)$$

Since, however, the diffusion field in an infinite space is in the mathematical sense also unlimited, this condition is true only for distances $x = \infty$. Therefore, in order to determine the thickness of the gas-saturated layer, it is necessary to determine the minimum concentration Δ , beyond which the excessive concentration can be neglected.

In the general case the thickness of the gas-saturated layer can be determined by the formula

$$C(b, \tau) = \frac{b}{2\sqrt{\pi D}} \int_0^\tau \frac{f(\tau - \xi)}{\xi^{3/2}} \exp\left(-\frac{b^2}{4D\xi}\right) d\xi = C'_0 + \Delta. \quad (14)$$

In the particular case when the distribution of oxygen is represented by formula (9), the depth of penetration of oxygen into titanium may be calculated by a simpler parabolic function,

$$b = 2\psi(\Delta)\sqrt{D\tau}, \quad (15)$$

where $\psi(\Delta)$, a simple function of Δ , is expressed by the formula

$$\operatorname{erfc}[\psi(\Delta)] = \frac{\Delta}{C^* - C'_0}. \quad (16)$$

It can be proved that an error in the qualitative determination of C'_0 will have little influence on the depth of oxygen penetration. Thus, if Δ and C'_0 are limited to a range within which these magnitudes may vary during the solution of practical problems, i.e.,

$$\left. \begin{aligned} 0.01\% &< \Delta < 0.1 \text{ wt. \%}, \\ 14\% &< C'_0 < 29 \text{ at. \%}, \end{aligned} \right\} \quad (17)$$

then the variation of the Kramp function $\psi(\Delta)$ will be in accordance with (16) within the following range:

$$1.65 < \psi(\Delta) < 2.35. \quad (18)$$

Within this range, the variation of the function $\operatorname{erfc} [\psi (\Delta)]$ can be approximately represented (with an error which does not exceed 2 %) by the following power function:

$$\operatorname{erfc} [\psi (\Delta)] \approx \frac{1.38}{[\psi (\Delta)]^{8.44}}. \quad (19)$$

Taking into account this approximate equation the depth of the penetration of oxygen into α -Ti can be expressed by the formula

$$b \approx 2.8 \left(\frac{C_0^*}{\Delta} \right)^{0.12} \sqrt{D\tau}. \quad (20)$$

This equation indicates that if the surface concentration C_0^* changes within the limits (17) (more than twofold) the depth of penetration will change by not more than 10 %. Thus, the accuracy of determination of the thickness of the gas-saturated layer will depend chiefly on the accuracy of the experimental determination of the diffusion coefficient of oxygen into titanium.

Diffusion of oxygen in β -Ti

The derivation of the mathematical laws governing the diffusion of oxygen into titanium at temperatures above the allotropic transformation is complicated by the fact that the presence of small amounts of oxygen in titanium excludes the presence of a β phase.

Vasilewski and Kehl have suggested the following approximate mechanism of the physical process /1/.

If the external pressure of the gas is higher than the equilibrium pressure then the concentration of oxygen at the surface will be higher than its maximum solubility in the β phase.

On the basis of the investigation of Rhines /8/, the authors are of the opinion that the formation of heterogeneous fields necessary for the continuous variation of the concentration of the dissolved substance is impossible from the thermodynamical point of view. Therefore, as soon as the surface becomes saturated with oxygen, the formation of an α layer begins, provided that the supply of gas is sufficiently high. From this moment, one part of the oxygen which penetrates into the titanium is used up for maintaining the growth of the α layer while another part diffuses into the β core. At the phase boundary the concentration drops suddenly (Figure 2). The boundary concentrations of oxygen at a given temperature are determined by the Ti—O phase diagram.

In their formula, Vasilewski and Kehl /1/ have further schematized the process by assuming that the diffusion coefficient of oxygen into the body-centered lattice of the β phase is several orders higher than the diffusion coefficient of oxygen into the close-packed lattice of the α phase and that the growth of the α -phase layer may, therefore, be disregarded. These workers, therefore, took as the surface of the β phase the initial surface of the specimen and not the mobile boundary plane between the phases,

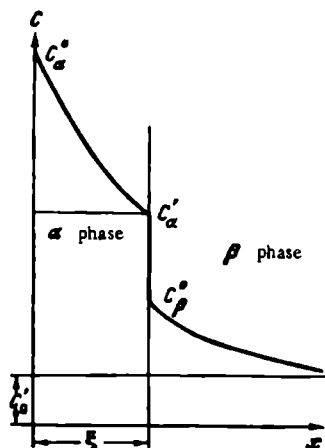


FIGURE 2. Variation of the concentration of oxygen in α - and β -titanium according to /1/

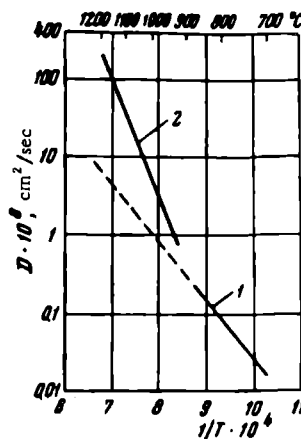


FIGURE 3. Diffusion coefficient of oxygen in α -(1) and β -(2) titanium according to /9/

considerably simplifying the solution of the problem. The experimental determination of the diffusion coefficients of oxygen in α - and β -Ti has not confirmed the assumed discrepancies between their magnitudes, and, moreover, some investigators /7/ have found no differences between the diffusion coefficients of oxygen into the two different titanium phases. Roe et al /9/ have shown that the magnitudes of D_α and D_β at temperatures close to the temperature of allotropic transformations are very similar. The extrapolation of the equation obtained by the latter authors

$$D_\alpha = 5.08 \cdot 10^{-8} \exp(-33500/RT) \quad (21)$$

shows that up to 1100°C (Figure 3) the difference between the magnitudes of the diffusion coefficients do not exceed one order. Some recent hypotheses throw a different light on the mechanism of diffusion of oxygen into titanium /9/, and the assumption that $D_\alpha \ll D_\beta$ seems now to be without sufficient foundation.

Therefore, it would be useful to examine the mathematical description of the initial mechanism /1/, without imposing any limitation on the magnitudes of the diffusion coefficients.

In the general case this problem can be mathematically formulated as a system of differential equations with extreme conditions which follow from

the Vasilewski and Kehl theory (see Figure 2):

$$\begin{aligned}
 \frac{\partial C_\alpha(x, \tau)}{\partial \tau} &= D_\alpha \frac{\partial^2 C_\alpha(x, \tau)}{\partial x^2} \quad (\tau > 0; 0 < x < \xi); \\
 \frac{\partial C_\beta(x, \tau)}{\partial \tau} &= D_\beta \frac{\partial^2 C_\beta(x, \tau)}{\partial x^2} \quad (\tau > 0; \xi < x < \infty); \\
 D_\alpha &= \text{const}; \quad D_\beta = \text{const}; \\
 C(x, 0) &= C(\infty, \tau) = C'_0, \\
 C_\alpha(0, \tau) &= C_\alpha^0, \\
 C_\alpha(\xi, \tau) &= C'_\alpha, \\
 C_\beta(\xi, \tau) &= C_\beta^0, \\
 -D_\alpha \frac{\partial C_\alpha(\xi, \tau)}{\partial x} d\tau &\sim -D_\beta \frac{\partial C_\beta(\xi, \tau)}{\partial x} d\tau + (C'_\alpha - C_\beta^0) d\xi,
 \end{aligned} \tag{22}$$

where C_α^0 and C'_α = the maximum and minimum solubilities of oxygen in α -Ti at a given temperature;

C_β^0 = the maximum solubility of oxygen in β -Ti at a given temperature;

D_α and D_β = diffusion coefficients of oxygen in α - and β -Ti.

At the given boundary conditions the distribution of oxygen in α - and β -titanium is determined by the following formulas:

$$C_\alpha = C_\alpha^0 - (C_\alpha^0 - C'_\alpha) \frac{\text{erf}(x/2 \sqrt{D_\alpha \tau})}{\text{erf}(n_0/2 \sqrt{D_\alpha \tau})} \quad (0 < x < \xi), \tag{23}$$

$$C_\beta = C'_\alpha + (C_\beta^0 - C'_\alpha) \frac{\text{erfc}(x/2 \sqrt{D_\beta \tau})}{\text{erfc}(n_0/2 \sqrt{D_\beta \tau})} \quad (\xi < x < \infty). \tag{24}$$

The boundary between the α - and β -fields shifts according to the parabolic function:

$$\xi = n_0 \sqrt{\tau}. \tag{25}$$

The constant n_0 in this equation depends only on the diffusion constants and is determined by the transcendental equation

$$\begin{aligned}
 \sqrt{D_\alpha} (C_\alpha^0 - C'_\alpha) \frac{\exp(-n^2/4 D_\alpha)}{n \text{erf}(n/2 \sqrt{D_\alpha})} - \\
 - \sqrt{D_\beta} (C_\beta^0 - C'_\alpha) \frac{\exp(-n^2/4 D_\beta)}{n \text{erfc}(n/2 \sqrt{D_\beta})} = \frac{\sqrt{\pi}}{2} (C'_\alpha - C_\beta^0),
 \end{aligned} \tag{26}$$

which can be solved graphically.

The depth of penetration of oxygen into titanium is determined by the formula:

$$b = 2\varphi(\Delta) \sqrt{D_\beta \tau} = k_\beta \sqrt{\tau}. \tag{27}$$

In this case the coefficient $\varphi(\Delta)$ can be found from the equation

$$\operatorname{erfc}[\varphi(\Delta)] = \frac{\Delta}{C_{\beta}^0 - C_0'} \operatorname{erfc}(n_0/\sqrt{4D_{\beta}}). \quad (28)$$

The last two formulas show that the minimum depth of penetration of oxygen (b_{\min}) can be determined by assuming the thickness of the α layer as negligibly small and assuming the existence of a binary diffusion into β -Ti. In this case $\varphi(\Delta)_{\min}$ can be determined from the equation:

$$\operatorname{erfc}[\varphi(\Delta)_{\min}] = \frac{\Delta}{C_{\beta}^0 - C_0'}. \quad (29)$$

The maximum depth of penetration b_{\max} can be determined by applying the principle of superposition to the diffusion field, i.e., by assuming that the diffusion field consists of two regions (α and β) each of which grows independently of the other:

$$b_{\max} = b_{\min} + b', \quad (30)$$

where

$$b' = 2\varphi(\Delta')\sqrt{D_{\alpha}\tau}, \quad (31)$$

$$\operatorname{erfc}[\varphi(\Delta')] = \frac{C_{\alpha}' - C_0'}{C_{\alpha}^0 - C_0'}. \quad (32)$$

Thus, the depth of the penetration of oxygen into titanium can be determined by the simple formula

$$b_{\min} < b < b_{\min} + b'. \quad (33)$$

The calculation of the characteristics of the gas-saturated layer can be greatly simplified by presenting the above relationships as graphs and charts.

In Figures 4 to 7, nomographs* are shown which have been constructed on the basis of the diffusion constants obtained in the works /9-11/. The diffusion coefficient of oxygen in the α layer was determined by extrapolation on the basis of equation (21), and the initial concentration of oxygen in titanium was assumed ($C_0' \approx 0.1\%$) to be equal to that in the specimens used for the determination of the diffusion coefficient by Roe et al /9/.

The use of the nomographs can be explained as follows. It is required, for example, to determine the maximum permissible holding time at 1150°C at which the depth of penetration of oxygen into titanium, at an excess concentration of oxygen $\Delta = 0.05$ weight %, will not exceed 1.2 mm and then calculate what will be the depth of the highly brittle α -phase layer. It is also required to calculate the differences in the concentration of oxygen in the gas-saturated layer after each 100 μ .

* M. A. Gorodskii and L. G. Maksimova have taken part in the construction of the nomographs.

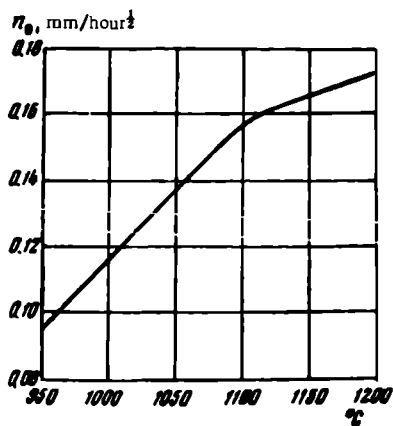


FIGURE 4. Relationship between the coefficient n_0 and the temperature

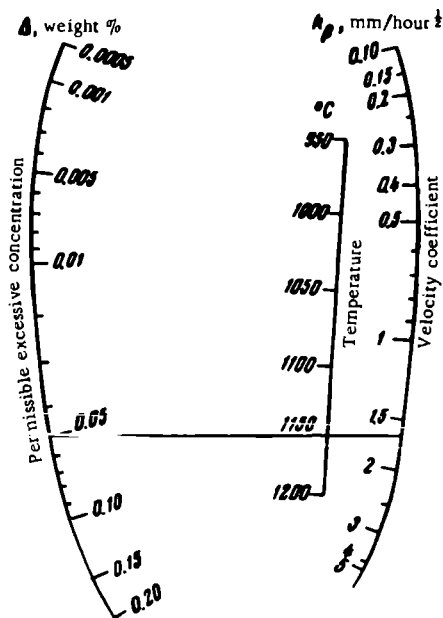


FIGURE 5. Nomograph for the determination of the coefficient k_β

TABLE 1

The concentration of oxygen at various distances from the surface of the specimen

Distance from the surface, x, μ	Concentration of oxygen, C , weight %	Distance from the surface, x, μ	Concentration of oxygen, C , weight %
0	14	700	0.40
100	4.7	800	0.32
200	1.1	900	0.25
300	0.91	1000	0.21
400	0.71	1100	0.17
500	0.58	1200	0.15
600	0.48		

The coefficient n_0 , which determines the velocity of advance of the phase boundary at a given temperature (Figure 4) is

$$n_0 = 0.165 \text{ mm/hour}^{\frac{1}{2}}.$$

The coefficient K_β , which characterizes the depth of penetration of oxygen into titanium is found from the nomograph (Figure 5):

$$K_\beta = 1.65 \text{ mm/hour}^{\frac{1}{2}}.$$

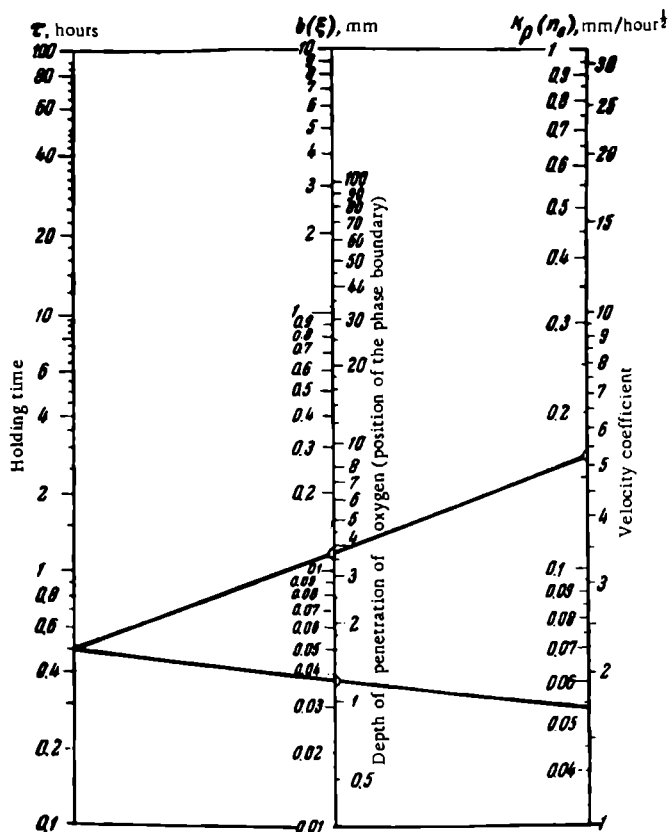


FIGURE 6. Nomograph for the determination of the thickness of the gas-saturated layer and of the position of the α - and β -phase boundary

On the basis of this value of K_p the time can be found on the nomograph in Figure 6 during which a gas-saturated layer $b = 1.2$ mm is formed:

$$\tau = 0.5 \text{ hours.}$$

On this nomograph the phase boundary can also be found:

$$\xi \approx 0.12 \text{ mm.}$$

And finally, the concentration of oxygen at a given point (Table 1) can be found from curve 1 (Figure 7).

It should be pointed out that these nomographs are rather approximate, since the values of the equilibrium concentration which have been used for their construction, and particularly the diffusion coefficient, are not very accurate. This becomes apparent from the comparison (Table 2) of the diffusion coefficients of oxygen in titanium with the activation energies which

are given by various sources. In addition, there are no published data on the diffusion of oxygen into the α -layer at temperatures above the temperature of the $\alpha \rightarrow \beta$ transformation.

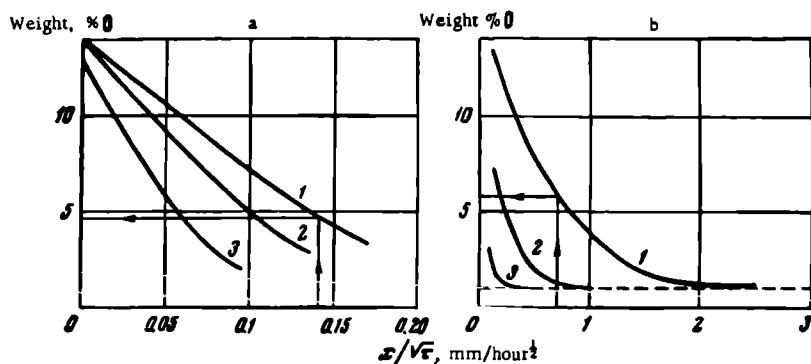


FIGURE 7. Nomograph for the determination of the distribution of oxygen in α -Ti(a) and β -Ti (b) at temperatures 1150 (1), 1050 (2), and 950°C (3)

TABLE 2

Diffusion coefficient D of oxygen in titanium and activation energy Q according to various published data

Temperature, °C	Diffusion coefficient*			$D \times 10^6, \text{ cm}^2/\text{sec}$		
	Reference					
	/1/	/12/	/6/	/7/	/9/	/2/
700	—	—	—	—	0.015	—
750	—	—	—	—	0.035	—
800	—	—	0.0015	—	0.075	0.0087
850	—	—	—	0.044	0.15	0.019
900	—	—	—	0.18	—	0.036
950	0.39	—	—	0.70	1.6	—
1000	0.84	—	—	2.4	5.0	—
1050	1.7	—	—	7.2	14.0	—
1100	3.4	—	—	10.0	36.0	—
1150	6.3	130.0	—	54.0	87.0	—
1200	11.0	190.0	—	—	200.0	—
1250	19.0	280.0	—	—	—	—
1300	32.0	380.0	—	—	—	—

Activation energy Q , cal/mole

Q_α	—	—	—	75 300	33 500	35 900
Q_β	48 200	31 200	—		68 700	—

* The diffusion coefficient has been calculated according to the equations given by these sources for certain temperature ranges.

These data show that the characteristics of the gas-saturated layer depend only on the diffusion coefficient. Since the usual method of the determination of the diffusion coefficient, which is based on the measurement of microhardness of successive layers, is insufficiently accurate, more accurate physical methods of investigation should be used. In this connection, the X-ray method is very promising since the lattice coefficients of titanium are considerably influenced by the content of oxygen ($4.68 \text{ \AA} < C < 4.81 \text{ \AA}$), and they can be determined with a fair degree of accuracy [11].

It can be concluded that, in the calculation of the kinetics of oxygen dissolution in titanium, all physical assumptions must be verified in order to render the mathematical treatments more precise, and attention must also be given to the development of experimental methods which will ensure a reliable determination of the diffusion constants.

Bibliography

1. Vasilewski, R. and G. Kehl. — J. Inst. met., 83(3):94. 1954.
2. Revyakin, A. V. — Izvestiya AN SSSR, OTN, No. 5:113. 1961.
3. Jenkins, A. — J. Inst. met., 82(5):213. 1954.
4. Hurlen, T. — J. Inst. met., 89(4):128. 1960.
5. Jenkins, A. — J. Inst. met., 84(1):1. 1955.
6. Koncz and Koncz-Deri. — Titanium abstract bulletin, Vol. 2, No. 3. 1957; Vol. 4, No. 1. 1958.
7. Reynolds, J. E., H. R. Ogden, and R. I. Jaffee. — Trans. Am. soc. met., Vol. 49:280. 1957.
8. Rhines, F. Surface Treatment of Metals. — Am. soc. met. 1941.
9. Roc, W., H. Palmer, and W. Opie. — Trans. Am. soc. met., Vol. 52:191. 1960.
10. Schofield, T. and A. Bacon. — J. Inst. met., 84(2):47. 1956.
11. Makarov, E. S. and L. M. Kuznetsov. — Zhurnal Strukturnoi Khimii, 1(2):170. 1960.
12. Claisse, F. and H. P. Koenig. — Acta metallurgica, 4(6):650. 1956.

THE INFLUENCE OF HYDROGEN ON THE TENDENCY OF TITANIUM ALLOYS TO DELAYED CRACKING

A. S. Mikhailov and B. S. Krylov

Titanium alloys are being rather reluctantly introduced into modern engineering. This reluctance is to a certain degree due to instances of failure of some welded titanium structures. It was earlier assumed that cracking was due to the embrittlement of the alloys caused by the high content of nitrogen and oxygen in the basis metal or to the absorption of these gases from the air during welding. Later, however, it was found that cracks also arise in structures made of titanium with a low content of nitrogen and oxygen and welded under conditions which practically exclude the possibility of absorption of these gases. A more probable cause for the delayed cracking of titanium alloys is hydrogen embrittlement [1-3].

A thorough analysis of a number of cases of delayed cracking of structures made of titanium alloys has shown that this phenomenon occurs when the alloy is not properly chosen or when the technology of the assembly process is faulty. Unequivocal data are as yet unavailable on the tendency of various titanium alloys to the formation of cold cracks and on the mechanism of delayed cracking. This has made the choice of titanium alloys for constructional work rather difficult.

The present investigation of the tendency of titanium alloys to delayed cracking has been carried out using the method of prolonged bending [3]. This method is based on the accelerated formation of cracks resulting from the prolonged action of additional stresses, which act on the specimen both directly and indirectly by accelerating the decomposition of nonequilibrium phases or intensifying diffusion processes. The test was carried out by prolonged bending of specimens freely resting on two supports and having the load applied to their center (Figure 1).

During the first stage of the investigation each alloy was tested in three different ways. The first test consisted of giving the specimen such a deflection that stresses equal to 0.8 of the yield point in bending of the given alloy would arise in the external elongated fibers, the specimens being then maintained in this condition. In the other two (accelerated) tests an initial deflection corresponding to a stress equal to 0.5 of the yield point in bending was imparted and then increased—in the first case by 0.1 mm after every 5 days and in the second case by 0.2 mm per day. In the last test the deflection was increased every day for 40 days (if the specimens did not fail earlier) after which it was kept constant. All specimens were inspected daily through a binocular microscope, by means of which a fairly exact determination could be made of the moment when the cracks appeared on the surface of the specimen.

The initial deflection was determined from the formula

$$f_0 = \frac{k\sigma_{y(bend)} l^3}{aEh},$$

where k = coefficient equal to 0.8 for the first and 0.5 for the second and third testing methods;

$\sigma_{y(bend)}$ = bend yield point in bending;

E = calculated length of the specimen;

h = thickness of the specimen.

Preliminary investigations showed that the second and the third testing methods are more sensitive. On the other hand, the first method permits more rapid testing and was, therefore, adopted for the present investigation. The tests were carried out on welded specimens with a longitudinal joint.

In order to determine the dependence of the resistance of titanium alloys to delayed-action cracking on the content of hydrogen, a number of speci-

mens of various alloys were taken with different contents of hydrogen. After vacuum annealing their contents were $H_2 \leq 0.002\%$, and after saturating with hydrogen their hydrogen contents were 0.005, 0.010, 0.015, 0.020, and 0.030%. The vacuum annealing and the saturation with hydrogen of the (plate) specimens were carried out before welding.

The specimens were saturated with hydrogen at 700°C by the thermal diffusion method.

The nitrogen and oxygen contents were in all cases about the same.

The chemical compositions of the investigated alloys are given in Table 1 and their mechanical properties in Table 2. The content of alloying elements was for all alloys, except OT-4-2 and VT-14, which contained a high content of aluminum, within the limits of the technical specifications.

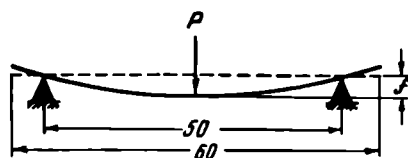


FIGURE 1. Diagram of prolonged bend testing

TABLE 1

Chemical composition of investigated alloys

Alloy	Content of alloying elements, %						
	Al	Sn	Cu	Mn	Mo	V	Si + Cr + Fe
VT-5-1	4.43	2.66	—	—	—	—	—
TiAl4Sn6Cu2 . . .	4.05	5.72	1.62	—	—	—	—
OT-4	2.51	—	—	1.32	—	—	—
VT-4	4.48	—	—	1.38	—	—	—
OT-4-2	8.03	—	—	1.74	—	—	—
T-4	4.77	—	—	—	—	—	1.70
VT-6	5.61	—	—	—	—	4.39	—
VT-14	5.08	—	—	—	2.95	1.27	—

TABLE 2
Mechanical properties of investigated alloys

Alloy	Last treatment before testing	Thickness of material, mm	Ultimate tensile strength, kg/mm ²	Angle of short time bending, degrees
VT-5-1	Vacuum annealing	1.2	92.1	85
TiAl4Sn6Cu2 . . .	The same	1.1	99.3	72
OT-4	"	1.1	74.0	113
VT-4	"	1.1	84.9	89
OT-4-2	"	1.5	107.0	52
T-4	"	1.1	86.4	88
VT-6	"	1.5	98.0	61
VT-14	Hardening	1.6	102.0	74
VT-14	Hardening + aging	1.6	116.0	32

The VT-14 specimens were heat treated (hardened and aged). Hardening consisted of heating the specimens in an electric furnace to 850°C, holding for 20 to 25 min at this temperature, and cooling in a 5 % aqueous solution of NaCl. The aging was also carried out in an electric furnace at 520°C (holding time — 12 hours) after which the specimens were air-cooled.

The results of the prolonged bending tests of titanium alloys are given in Table 3.

These data show that welded joints of all investigated alloys (except VT-14) with 0.002 and 0.005 % H₂ are resistant to delayed cracking. In VT-5-1, TiAl4Sn6Cu2, and OT-4 alloys the tendency to cracking becomes apparent at a hydrogen content equal to 0.010 % and increases further with the increase in the hydrogen content. Cracks were also found in welded joints of VT-4 with 0.020 % H₂ and more, and in the joints of T-4 alloy with 0.030 % H₂.

VT-14 alloys showed cracks after hardening and aging in the air irrespective of their hydrogen content. Alloys with H₂ = 0.010 % or less, all have practically the same resistance to the formation of delayed cracks. If, however, the content of hydrogen increases, the tendency to delayed cracking considerably increases*.

Metallographic investigations showed the presence of a hydride phase in VT-5-1 and OT-4 alloys with 0.030 % of hydrogen. In other alloys no hydride phase was found either in the base metal or in the welded joint.

Analysis of the results confirms that the high content of hydrogen** may be the cause for the delayed cracking. It should be noted that titanium alloys containing either an α phase or an $\alpha + \beta$ phase and hydrogen in amounts above a certain "critical" level are subject to delayed cracking, irrespective of whether they also contain a hydride phase or not. With passage of time, the diffusion processes taking place in the crystal structure of alloys with a high content of hydrogen decrease the resistance of the metal to delayed cracking. The stresses and deformations produced during welding and those which are additionally imparted during the prolonged bending tests considerably accelerate these processes. In welded joints, these structural changes are most intensive in the metal of the joint and in the heat-

* For most investigated alloys the resistance of the base metal to delayed cracking is somewhat higher than that of the welded joints, but for VT-4 and T-4 alloys the opposite is true.

** The OT-4-2 and VT-6 alloys are the least sensitive to delayed cracking caused by a high hydrogen content. No cracks were found in these alloys in the course of the investigation.

TABLE 3

Results of bend tests of titanium alloys*

Hydrogen content, %	Base metal and initial deflection, mm								Welded joint and initial deflection, mm									
	VT-5-1; 1.85	TiAl4Sn6Cu2 1.71	OT-4; 1.81	VT-4; 1.99	OT-4-2; 1.87	T-4; 1.74	VT-6; 1.90	VT-14 (after harden- ing); 1.38	VT-14 (after harden- ing and aging); 2.00	VT-5-1; 1.85	TiAl4Sn6Cu2 1.71	OT-4; 1.83	VT-4; 1.99	OT-4-2; 1.87	T-4; 1.74	VT-6; 1.90	VT-14 (after harden- ing); 1.38	VT-14 (after harden- ing and aging); 2.00
0.002	400** 9.85	400** 9.71	400** 9.83	400** 9.99	300** 9.87	400** 9.74	300** 9.90	90 9.38	53 10.0	400** 9.85	400** 9.71	400** 9.83	400** 9.99	300** 9.87	400** 9.74	300** 9.90	80 9.38	19 5.6
0.005	400** 9.85	400** 9.71	400** 9.83	400** 9.99	300** 9.87	400** 9.74	300** 9.90	100 9.38	65 10.0	400** 9.85	400** 9.71	400** 9.83	400** 9.99	300** 9.87	400** 9.74	300** 9.90	83 9.38	18 5.4
0.010	328 9.85	400** 9.71	90 9.83	400** 9.99	300** 9.87	400** 9.74	300** 9.90	92 9.38	66 10.0	37 9.05	47 9.71	71 9.83	400** 9.99	300** 9.87	400** 9.74	300** 9.90	81 9.38	15 4.8
0.015	31 7.85	33 8.11	24 6.43	250 9.99	300** 9.87	400** 9.74	300** 9.90	64 9.38	46 10.0	18 5.25	41 9.71	28 7.23	400** 9.99	300** 9.87	400** 9.74	300** 9.90	39 8.98	10 3.8
0.020	15 4.65	28 7.11	23 6.23	28 7.39	300** 9.87	45 9.74	300** 9.90	40 9.18	22 6.2	17 5.05	32 7.91	15 4.63	32 8.19	300** 9.87	400** 9.74	300** 9.90	34 7.98	5 2.8
0.030	15 4.65	20 5.51	19 5.43	10 3.79	300** 9.87	24 6.34	300** 9.90	29 6.98	3 2.4	17 5.05	16 4.71	8 3.23	16 4.99	300** 9.87	38 9.14	300** 9.90	13 3.78	2 2.2

* The upper figure designates the number of days which passed until cracks appeared, and the lower figure indicates the deflection, mm.

** No cracks were found; the investigations continue.

affected zone, since it is in these regions that the metal structures formed are least stable as a consequence of the rapid cooling after welding.

It is interesting to note that the cracks are first formed in the heat-affected zone (Figure 2).



FIGURE 2. Cracks formed during prolonged bend tests of welded specimens

At one time it was assumed that the delayed cracking of single-phase (α) alloys with a high content of hydrogen, is the result of the precipitation of a hydride phase. The results of recent investigations show that the relatively rapid formation of cracks in α -phase alloys can also take place when no hydride phase is present. This leads to the conclusion that in addition to the embrittlement caused by the hydride phase, there must also be some other hydrogen embrittlement which is due only to the diffusion processes and which leads to a microsegregation of hydrogen in certain spots of the crystal lattice. In the opinion of some investigators /4, 5/, hydrogen forms in such cases so-called Cottrell clouds around dislocations, their mobility thus being hampered, which leads to an embrittlement of the metal. It is also possible that the reduced resistance to delayed cracking is also due to the surface-adsorption of hydrogen at defective spots of the crystal lattice. The layer of adsorbed hydrogen atoms reduces the surface energy and promotes the development and growth of cracks.

The tendency of titanium alloys to the delayed cracking is greatly influenced by the plastic properties of the metal. Alloys with a high content of nitrogen and oxygen have low plastic properties as a result of which cracks are formed in welded structures. In specimens welded without the sufficient protection against air, cracks appear much more rapidly.

The relatively low resistance of the VT-14 alloys to delayed cracking during the tests reported here can also be accounted for by low plasticity resulting from the formation of an α phase during heat treatment.

The investigation of the resistance of titanium alloys to delayed cracking showed that the VT-5-1, TiAl4Sn6Cu2, OT-4, and VT-14 alloys, which are of importance in the production of structures subjected to prolonged loading, should have their upper hydrogen limit (0.015 % according to present technical specifications) reduced. For other alloys investigated this limit can probably be maintained.

However, as regards T-4 alloys, the final conclusion as to their resistance to delayed cracking must await the results of testing melts with higher strength characteristics, since the strength of the melt investigated in this study was below the specified norm.

Structures not subjected to prolonged loading can obviously be made from VT-5-1, TiAl4Sn6Cu2, and OT-4 alloys, with a hydrogen content corresponding to the upper limit given by existing specifications, since in these structures there is no danger of delayed cracking. Nevertheless, in order to avoid the formation of delayed-action cracks, welded constructions made of titanium alloys should be heat treated to relieve the internal stresses. Heat treatment decreases the total internal stresses and reduces the danger of the formation of delayed cracks. The more resistant the alloy to delayed cracking, the longer may be the break between the welding and heat treatment.

The VT-14 alloy should obviously be additionally tested for its tendency to delayed-action cracking under conditions which will exclude the influence of thick oxygen-saturated layers, formed during hardening from 850°C.

Conclusions

1. The investigation of the influence of hydrogen (up to 0.030 %) on the tendency of VT-5-1, TiAl4Sn6Cu2, OT-4, VT-4, OT-4-2, T-4, VT-6, and VT-14 alloys to delayed-action cracking has shown that a high hydrogen content may be the cause of the formation of delayed cracks.
2. The resistance of welded joints of most titanium alloys to delayed cracking is somewhat lower than that of the base metal. Nevertheless, for some alloys (VT-4 and T-4) the opposite is true.
3. All investigated alloys, with α or $\alpha + \beta$ phases and hydrogen contents above the critical limit, developed cracks during prolonged bend tests irrespective of whether or not they contained a titanium hydride phase.
4. Structures subjected to prolonged loading should be made of VT-5-1, TiAl4Sn6Cu2, OT-4, or VT-14 alloys with hydrogen contents lower than 0.015 % which is the [present] maximum permissible limit.

Bibliography

1. Guseva, E. A. — Svarochnoe Proizvodstvo, No. 2:10. 1958.
2. Daniels, K. D., E.J. Quigg, and A. D. Troiano. — Trans. Am. Soc. Met., Vol. 51:843. 1959.
3. Krylov, B. S. and A. S. Mikhailov. Novyi metod ispytaniya titanovykh splavov na treshchinoobrazovanie (A New Method of Testing the Resistance of Titanium Alloys to Crack Formation). — TsITEIN, No. 20, M-60-82/20. 1960.
4. McQuillan, A. D. Hydrogen in Titanium and Its Alloys. — The University of Birmingham. Lecture II. 1956.
5. Haynes, R. — J. Inst. met., 88(12):509. 1960.

THE CORROSION RESISTANCE OF TITANIUM ALLOYS TO VARIOUS MEDIA IN THE CHEMICAL AND PHARMACEUTICAL INDUSTRIES

F. N. Tabadze, S. N. Mandzhgaladze, I. N. Lordkipanidze,
and T. S. Dashniani

The slightest corrosion of chemical equipment is highly detrimental to pharmaceutical preparations. In addition, frequent replacement of corroded apparatus and the losses resulting from failures and idling cause heavy financial losses. For instance, in the Tbilisi chemical-pharmaceutical plant which uses chiefly tinned equipment, replacements of tinned apparatus must be made about once in three months.

Sometimes technological advances in pharmaceuticals manufacture is hampered by the lack of reliable data on the corrosion resistance of materials.

Apparatus in the chemical-pharmaceutical industry is, for the most part, manufactured from 1Kh18H9T stainless steel and from tinned copper. These materials, however, are insufficiently resistant to corrosion. The Tbilisi chemical-pharmaceutical plant of the GSSR Sovnarkhoz has, therefore, organized the corrosion testing of a number of materials, including titanium alloys. The following titanium alloys were investigated: VT-1, OT-4, OT-40, AT-3, AT-4, AT-6, and AT-8.

In the work reported here, a comparison was made of the corrosion resistance of these alloys with that of copper and austenitic chromium-nickel steel.

Various tinctures and extracts of natural origin and also solutions of tannin and gallic acid were used as corrosive media. Synthetic media were not investigated. The experiments were carried out under laboratory and industrial conditions.

Vegetable tinctures containing alkaloids, glycosides, and ethereal oils are obtained by percolation. The corrosion tests were carried out in the following tinctures: iodine, opium, corvalleria majalis, pectoral elixir, ginseng, ammonia anisate drops, shizandria, Valeriana officinalis, and others.

The following extracts were used: *satureia hortensis*, water pepper [*Polygonum hydropiper*], maize crown, and digolen-neo*.

Titanium appeared to be resistant to all these media.

The medium that turned out to be most corrosive was the tincture of iodine which causes a pitting corrosion of stainless steel and of tinned copper. Iodine vapors are also very corrosive. A comparison of the resistance to tincture of iodine of titanium alloys and copper (Figure 1) shows that tinned copper fails about 15 times more rapidly than titanium alloys. In other solutions investigated, the same relationship was found between the corrosion resistance of titanium alloys and copper.

* [Transliteration of the Russian.]

The experiments with the extracts were carried out at high temperatures. Here the tinned copper also appeared to be less corrosion resistant. In extracts of water pepper the OT-4 and VT-1 alloys were attacked more rapidly than the AT-alloys (Figure 2). Chemical analysis showed that these extracts leached out manganese from the solid solution of the OT-4 alloy, with consequent change of their color.

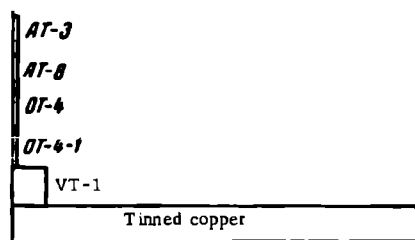


FIGURE 1. A comparison of the corrosion resistance of alloys in an iodine-tincture solution 1:2

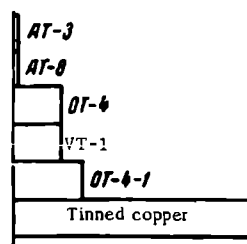


FIGURE 2. A comparison of the corrosion resistance of alloys in an extract of water pepper solution 1:50 at 80°C

In extracts of *satureia hortensis* all titanium alloys are fully resistant and only technical titanium (VT-1 alloy) undergoes a pitting corrosion at a rate of 0.02 mm per year.

In order to obtain a fuller picture of the behavior of alloys the authors investigated the kinetics of the corrosion of alloys under semi-industrial conditions.

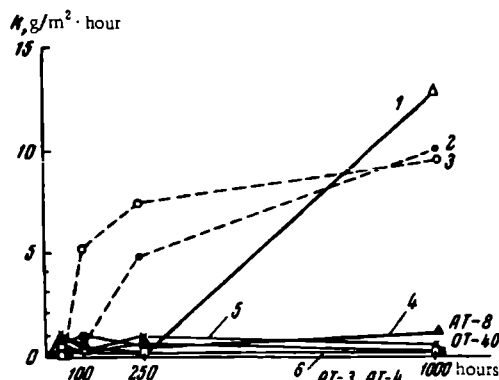


FIGURE 3. Kinetics of corrosion in a *corvallis majalis* tincture

1 — 1Kh18N9T steel; 2 — copper; 3 — tinned copper;
4 — AT-8 alloy; 5 — OT-40 alloy; 6 — AT-3 and
AT-4 alloys.

The corrosion velocity of 1Kh18N9T steel in a tincture of corvaldaria majalis sharply increases with time while that of copper is stabilized after 250 hours (Figure 3). In opium tinctures the increase in the corrosion velocity with time is characteristic of both copper and the OT-4 alloy. The behavior of alloys in other solutions of galenica is the same.

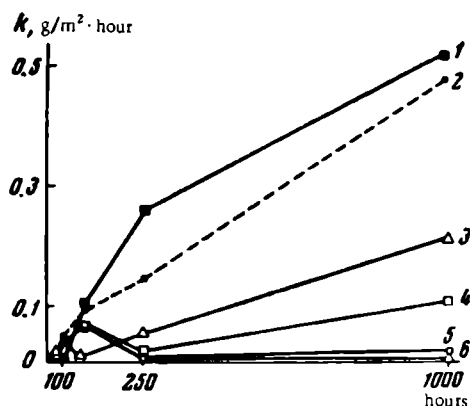


FIGURE 4. Kinetics of corrosion in aqueous solutions of tannin

1 — EI-533 steel; 2 — nickel; 3 — OT-4 alloy; 4 — AT-6 alloy; 5 — AT-3 alloy; 6 — AT-8 alloy.

In aqueous solutions of tannin the experiments were carried out under industrial conditions. Only nickel and the EI-533 steel have a corrosion velocity in any way comparable to that of titanium alloys (Figure 4). Nevertheless, the corrosion velocity of these metals as well as that of the OT-4 alloy increases with time. Solutions which were tested under laboratory conditions in containers with specimens of OT-4 alloys and ferrous alloys, darkened as a result of leaching out of manganese and iron.

In solutions of gallic acid the corrosion velocity of titanium alloys is considerably lower than that of other metals and alloys. Only the corrosion velocity of technical titanium VT-1 is somewhat higher.

Conclusions

The authors have investigated the corrosion resistances of VT-1, AT-3, AT-4, AT-6, AT-8, OT-4, and OT-40 titanium alloys in extracts and tinctures of galenica, and compared them with the corrosion resistances of tinned copper and austenitic chromium nickel stainless steel.

The following conclusions are drawn from the results.

1. Titanium alloys have a good corrosion resistance in solutions encountered in the chemical-pharmaceutical industry.

In tinctures of iodine, ammonium anisate, pectoral elixir, and ginseng, the corrosion resistance of AT alloys is 10 times higher than that of

tinned copper. The corrosion resistance of AT titanium alloys in extracts of digolen-neo, water pepper, and satureia hortensis is 15 times higher than that of tinned copper.

The results of experiments carried out with aqueous solutions of tannin and gallic acid have shown that the corrosion resistance of AT alloys is 90 times higher than that of the VT-1 alloy, 300 times higher than the resistance of tinned copper, and 220 times higher than the resistance of 1 Kh18N9T steel.

2. Solutions of galenica in contact with OT-4 and OT-40 alloys leach out manganese.

3. The first experimental equipment (percolator, reactor, and a worm diffuser) for industrial tests will be made from AT-3 and AT-4 alloys.

CORROSION RESISTANCE OF AT TITANIUM ALLOYS TO MEDIA IN THE FOOD INDUSTRY

F. N. Tabadze and T. A. Lashkhi

The purpose of this investigation is to determine the possibility of using titanium alloys in the food industry for machinery coming into contact with chlorides, chlorine-containing solutions, and with some organic compounds.

This problem has been investigated in a number of countries. The Canadian firm "Hykes" has tested boiling kettles made of titanium for the preparation of pickles, sauces, and ketchups. The solutions used in the manufacture of these products contain sodium chloride and acetic acid (a medium characteristic of the canned food industry). The acidity of the solutions varied from 2 to 5 % calculated as acetic acid; pH = 3 to 4. At the same time tests were carried out with kettles made of nickel and grade 316 stainless steel.

After six weeks the stainless steel and nickel kettles were considerably corroded while those of titanium were in good shape; the presence of fresh onion and garlic considerably accelerates the corrosion of metals.

It is generally believed that organic compounds are not very corrosive to metals. This assumption is not without foundation, although as regards the food industry, the situation in this connection is exceptional. The majority of organic compounds prevalent in food are not only corrosive agents but at certain concentrations of chlorides and acids they also dissolve metals and alloys.

Equipment and apparatus in the food industry must be made of completely corrosion-resistant metal, since the presence in food of metal salts in

TABLE 1

The chemical composition and some physicochemical

Technical solution	Tartaric acid, %	Citric acid, %	Malic acid, %	Salicylic acid, %	Formic acid, %	Acetic acid, %	Ethyl alcohol, %	Methyl alcohol, %	Glucose, %	Oxalic acid, %
V-I	3	1	0.5	0.3	0.5	1.5	12	0.6	1	—
V-II	3	1	0.5	0.3	0.5	1.5	20	0.6	1	—
V-III	3	1	0.5	0.3	0.5	1.5	12	0.6	25	—
K-I	2	2	0.5	—	—	2	—	—	2	3
CH-I	—	—	—	—	—	—	—	—	—	—

Note. The solution V-1 corresponds to a typical dry wine, solution V-II to a typical alcoholic wine, the CH-1 to tea industry.

amounts which exceed even to a slight extent the permissible concentration, can be detrimental to the product or spoil it completely.

The purpose of the present work was to determine the corrosion resistance of AT titanium alloys in the presence of some characteristic foods (wine, canned food, tea, and caffeine). The corrosion tests were carried out both under laboratory and industrial conditions.

AT-3, AT-4, AT-6, and AT-8 alloys were investigated.

The laboratory tests were carried out both at room and at elevated temperatures using pure organic acids and technical solutions with physico-chemical properties identical with those of the commercial products (Table 1).

The AT-3, AT-4, and AT-8 alloys were investigated for 200 hours in boiling acetic and formic acids, and in vapors of these acids. The corrosion of AT alloys tested in acetic acid vapors was somewhat higher than that of the alloys in contact with the liquid. This can obviously be explained by the stronger oxidizing properties of acetic acid solutions in comparison with the vapor as a result of which the oxide films on titanium alloys in the solution are strengthened. No such difference has been noted between the corrosion in formic acid and in its vapors, apparently due to the stronger oxidizing properties of this acid.

There is also no noticeable difference between the corrosion resistance of AT-3, AT-5, and AT-8 alloys which have different aluminum contents.

Consideration will now be given to the results obtained with AT-3 and AT-8 titanium alloys in some characteristic technical media (Table 3).

The corrosion tests were carried out by immersion for 2000 hours in solutions mixed in an apparatus equipped with a spindle mechanism. In addition to the above-mentioned alloys, the 1Kh18N9T chromium nickel austenitic stainless steel was also tested. In media characteristic of the wine and tea industry, no differences were found between the corrosion resistance of stainless steel and titanium alloys. However, in tests of media characteristic of the canned-food industry, which have high contents of table salt and acetic acid, a difference was apparent: though no traces of corrosion could be found on titanium alloys, pitted loci could be found on stainless steel.

factors of technical media used in corrosion tests

Malonic acid, %	Sodium chloride, %	Nitrogen, %	Caffeine, %	Saccharose, %	Starch, %	Dextrin, %	Total acid titrated	Active acidity	Glycerine, ml/l	Tannin, g/l
—	—	—	—	—	—	—	1.22	1.80	18	0.3
—	—	—	—	—	—	—	1.23	2.00	18	0.3
—	—	—	—	—	—	—	1.11	1.85	18	0.3
1	2	—	—	—	—	—	2.71	0.81	—	—
—	—	8.7	0.5	2	1	1	0.18	2.6	—	7

solution V-III to a typical sweet wine, solution K-1 to those used in the canned food industry, and solution

TABLE 2
Results of corrosion tests of AT titanium alloys in boiling acids

Alloy	Testing medium	K , g/m ² · hour	π , mm/year	Degree of resistance
Acetic acid				
AT-3	Acid	0.007	0.0133	4
AT-3	Vapors	0.003	0.0057	3
AT-4	Acid	0.01	0.019	4
AT-4	Vapors	0.003	0.0057	3
AT-8	Acid	0.0007	0.00133	2
AT-8	Vapors	0.004	0.0076	3
Formic acid				
AT-3	Acid	0.0008	0.00152	2
AT-3	Vapors	0.002	0.0038	2
AT-4	Acid	0.002	0.0038	2
AT-4	Vapors	0.005	0.0095	3
AT-8	Acid	0.004	0.0076	3
AT-8	Vapors	0.005	0.0095	3

Note. All specimens were uniformly corroded.

TABLE 3
Corrosion of AT-3 and AT-8 titanium alloys in technical solutions

Technical solution	AT-3 alloy			AT-8 alloy		
	K , g/m ² · hour	π , mm/year	degree of resistance	K , g/m ² · hour	π , mm/year	degree of resistance
First	0.00176	0.00334	2	0.00059	0.00112	2
Second	0.00174	0.00331	2	0	0	1
Third	0.00225	0.00428	2	0.00163	0.00187	2
Fourth	0.00347	0.00660	3	0.00098	0.00370	2
Fifth	0.00315	0.00600	3	0.00404	0.00768	3
Sixth	0.00284	0.00540	3	0.00458	0.00580	3
Seventh	0.00351	0.00667	3	0.00305	0.00580	3

Note. All specimens were uniformly corroded.

The investigation of titanium alloys in the Batumi citrus works also yielded quite satisfactory results (Table 4). None of the metallic specimens showed any traces of corrosion and no changes were found in the food after a year of testing (on completion of the tests the most corrosive media were tasted and subjected to chemical analysis, Table 5).

The corrosion resistance of AT-3 and AT-8 alloys was investigated at all stages of the production of caffeine. The specimens were tested at the actual production plant for one year in the five chief media employed. The results of Table 6 show that the AT-3 and AT-8 titanium alloys are resistant in these media.

TABLE 4
Results of corrosion tests of titanium alloys with the
products of the Batumi citrus works

Medium	$K, \text{ g/m}^2 \cdot \text{hour}$	$\Pi, \text{ mm/year}$	Degree of resistance
Titanium alloy AT-3			
Apple pickle	0.0003	0.00057	1
Stewed plum	0.0002	0.00038	1
Plum pickle	0.0002	0.00038	1
Stewed myrobalan	0.0002	0.00038	1
Lemon juice	0.0002	0.00038	1
Titanium alloy AT-4			
Lemon juice	0.0002	0.00038	1
Pear pickle	0.0002	0.00038	1
Stewed myrobalan	0.0047	—	1
Titanium alloy AT-5			
Mandarin juice	0.0047	—	—
Mandarin stew	0.0001	0.00019	1
Stewed myrobalan	0.0002	0.00228	1
Pear pickle	0.0001	0.00019	1
Plum pickle	0.0002	0.00038	1
Lemon juice	0.0001	0.00038	1
Stewed plum	0.0002	0.00038	1
Titanium alloy AT-6			
Mandarin stew	0.0003	0.00057	1
Lemon juice	0.00011	0.00224	1
Stewed myrobalan	0.0002	0.00038	1
Orange juice	0.0001	0.00019	1
Mandarin juice	0.0001	0.00019	1

TABLE 5
Chemical analysis of some characteristic food products after prolonged
testing in contact with titanium alloys

Medium	Alloy	Content of element, %	
		Al	Fe
Stewed myrobalan	AT-3	0.008	0.0017
Plum pickle	AT-4	0.006	0.002
Mandarin juice	AT-6	0.018	0.005
Lemon juice	AT-8	0.012	0.006

Note. No titanium could be found analytically.

TABLE 6

Results of corrosion tests of titanium alloys in media used in caffeine production

Medium	AT-3			AT-8		
	$K, g/m^2 \cdot \text{hour}$	$\pi, \text{mm/year}$	grade of resistance	$K, g/m^2 \cdot \text{hour}$	$\pi, \text{mm/year}$	grade of resistance
Caffeine juice (up to 0.2% caffeine, pH = 4.5 to 5), temperature 80°C . . .	0.0001	0.00011	1	0.00004	0.000044	1
Initial caffeine juice (0.06% caffeine, 1.5-2% dichloroethane, pH=3.5), temp. 80°C	0.0004	0.00044	1	0.00002	0.000022	1
Dichloroethylene extract (90% dichloroethylene, 10% sulfuric acid)	0.0002	0.00022	1	0.00007	0.000077	1
Diffusion solution of keline* (0.08% to 1% chromines*, various dyestuffs, up to 1% of fats), temperature 80°C . . .	0.0002	0.00022	1	0.00009	0.000099	1
Treated keline* juice (5 to 10% chrom-chromines, 90% dichlorethine) temperature 40 to 50°C	0.00005	0.000055	1	0.00004	0.000044	1

* [Unidentified.]

Tests were carried out on AT-3, AT-4, AT-6, and AT-8 titanium alloys in the production of tartaric vinegar. The specimens were tested both in the solutions and in vinegar vapors. The acidity of the medium was up to 9%, and the temperature was increased to 90°C. The experiments were carried out for one year. The results showed that all titanium alloys are fully resistant in this medium.

Corrosion tests were also carried out in a running 10% cooling brine at 10 to 12°C. The year-long tests showed that all titanium alloys are fully corrosion resistant to this medium. On some specimens a film of rust was found, apparently formed as a result of the corrosion of steel pipes.

In conclusion it can be said that titanium alloys are more corrosion resistant to foods and organic acids than 1Kh18N9T Cr-Ni austenitic steel.

As a result of their specific gravity, high strength, and the good corrosion resistance to many organic acids and to food products the AT titanium alloys show great promise in the manufacture of processing machinery.

Conclusions

1. The AT-3, AT-4, AT-6, and AT-8 titanium alloys have good corrosion resistance to acetic and formic acids, as well as to technical solutions used in the wine, canned food, and tea industries.

2. All AT titanium alloys have good corrosion resistance to juices, pickles, and stewed fruits. These alloys do not affect the chemical or physical properties of foods.

3. The high corrosion resistance of AT-3 and AT-8 alloys was demonstrated in the production of caffeine, tartaric vinegar, as well as in cooling solutions used in breweries.

THE KINETICS OF EVOLUTION OF HYDROGEN IN VACUO FROM TITANIUM AND ITS ALLOYS

B. S. Krylov

Titanium and titanium alloys containing hydrogen in excess of a certain critical value become brittle. The production of titanium parts and semi-finished products does not always take place under conditions which prevent the introduction of hydrogen in amounts exceeding the dangerous level. In such cases, the reliability of titanium alloy parts can be improved by as full as possible a removal of hydrogen from the metal. This can be achieved by vacuum annealing.

The absence of systematic investigations on the kinetics of hydrogen removal from titanium alloys and on the influence of various factors on the process renders it difficult, however, to select the most suitable conditions for vacuum annealing.

In this paper, the results of investigations on the process of hydrogen removal from technically pure titanium VT-1-1 and from the OT-4 alloy in vacuo at various heating temperatures, surface conditions, and hydrogen contents, are presented.

The specimens were prepared as forged cubes ($10 \times 10 \times 10$ mm) and as forged plates (19×10 mm), 1.5 and 3 mm thick, cut out from sheets.

The specimens were given a preliminary vacuum annealing in a MEV3-301 furnace (heating to 700°C , holding for 8 hours, and cooling in vacuo in the furnace).

At the end of the annealing process the pressure within the furnace was 10^{-4} mm Hg and the concentration of hydrogen in the specimens was not higher than 0.002 %. In order to determine the influence of the content of hydrogen on its extraction from the metal, hydrogen was introduced into the specimens up to a content of 0.015, 0.030, 0.050, and 0.100 % by the thermomethod (at 700°C). In order to obtain various surface conditions part of the cubic specimens, with 0.015 % of hydrogen, were coated with a chromium-nickel plate and then heated in the air at 525°C for one hour or at 700°C for 6 hours. Heating to 525°C produced a thin oxide film (violet color) while heating to 700°C produced a continuous scale.

The extraction of hydrogen was carried out at 600, 700, 800, and 900°C and in a number of cases also at 650, 750, and 1000°C and continued until any noticeable evolution of hydrogen had ceased.

For the investigation of the kinetics of hydrogen evolution from titanium alloys the author has designed and built a special apparatus which is a simplified variation of the apparatus used for the determination of the hydrogen content by the method of heating in vacuo. The apparatus (Figure 1) consists of the following main parts: an evacuating device, a heating device, a gas collector, and an analytical section.

The process in the degassing device is as follows. After washing in benzine, drying, and weighing, the specimen is placed in a glass tube (1). From this tube the air is evacuated by the backing and the mercury-diffusion pumps (2) to a pressure of $5-10^{-4}$ mm Hg. The pressure is measured by the thermocouple and manometric electron tubes LT-2 and LM-2 and by a VIT-1 vacuumometer. After that, the backing pump is connected by a three-way valve (3) to an automatic system (4), and to a gas collector (5).

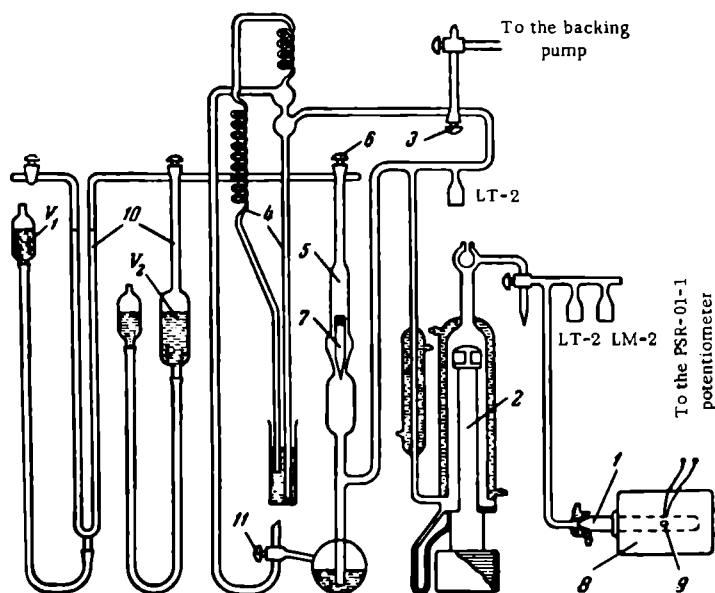


FIGURE 1. Diagram of the degassing device

The automatic system regulates the operation of the gas collector which collects the gas periodically after certain time intervals and stores it in the space between valve (6) and the valve of the gas container (7). The furnace (8), which is preliminarily heated to a given temperature, is then pushed over the quartz tube (1). The tube and the specimen (9) are heated. The hydrogen evolved from the specimen is transferred by the diffusion pump into the gas collector where it is accumulated. The volume of gas is measured after certain time intervals (depending on the amount of hydrogen evolved), mercury being used to push out the hydrogen from the gas collector into the analytical apparatus (10). In order to achieve this, air is passed through the valve (11). If large amounts of hydrogen are evolved their volume is measured in the additional space V_1 . The volume of gas measured is brought to normal pressure and temperature by means of the formula:

$$V_{pr} = \frac{1}{g} \cdot \frac{273}{273 + t} \cdot \frac{P}{760},$$

where V_{pr} = the amount of gas evolved brought to unit weight (1 g), to a normal temperature (0°C), and a normal pressure (760 mm Hg), ml;

g = weight of the specimen, g;

t = temperature of testing, $^{\circ}\text{C}$;

P = pressure during testing, mm Hg.

Consideration will now be given to the curves characterizing the kinetics of evolution of hydrogen (in vacuo) from technically pure titanium with a hydrogen content of 0.015 and 0.030 %, at 600 to 900 $^{\circ}\text{C}$ (Figure 2).

These curves show that the time necessary for expelling hydrogen from a cubic specimen sharply decreases with the increase in temperature. Thus, while after 24 hours at 600 $^{\circ}\text{C}$ there is still an intense evolution of hydrogen from the specimen, this practically ceases after 5 to 6 hours at 700 $^{\circ}\text{C}$, after 3 to 4 hours at 800 $^{\circ}\text{C}$, and after 2 hours at 900 $^{\circ}\text{C}$.

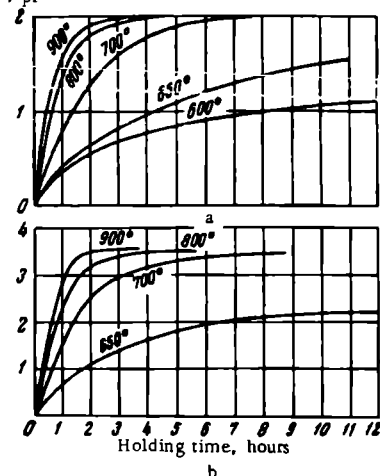


FIGURE 2. Kinetics of evolution of hydrogen from titanium at various temperatures

a — 0.015% H_2 ; b — 0.03% H_2 .

It is interesting to note that the holding time after which the expulsion of hydrogen from the specimen is completed at a given temperature is almost uninfluenced by the hydrogen content provided that this does not exceed 0.100 % (Figures 2 and 3).

The velocity of evolution of hydrogen however, is greatly influenced by its concentration in the metal; the higher the concentration of hydrogen in titanium the higher the velocity of evolution. This is confirmed by the variation in the inclination of the rectilinear line sections of the curves characterizing the velocity of evolution of hydrogen (Figure 4).

The addition of small amounts of alloying elements, for instance of 3 % of Al and 1.5 % of Mn (the OT-4 alloy) has little influence on the process of expulsion of hydrogen from titanium (Figure 5).

Thus, hydrogen is relatively rapidly removed from titanium and its alloys (VT-1 and OT-4) in vacuo at temperatures exceeding 650 $^{\circ}\text{C}$.

A temperature increase greatly accelerates this process. The holding time which is necessary for a practically full removal of hydrogen from titanium considerably decreases with the increase in the temperature within the range of 700 to 900 $^{\circ}\text{C}$ and is little influenced by the hydrogen content.

According to the kinetic curves obtained during the expulsion of hydrogen from specimens of various thicknesses (Figure 6), an increase in thickness from 1.5 to 10 mm has little influence on the time necessary for the removal from the metal.

The surface condition of titanium, however, strongly influences the velocity of evolution of hydrogen.

The degassing of cubic specimens with a chromium-nickel coating (Figure 7) is many times slower than that of uncoated specimens (see Figure 2). The slower degassing process is apparently due to the fact

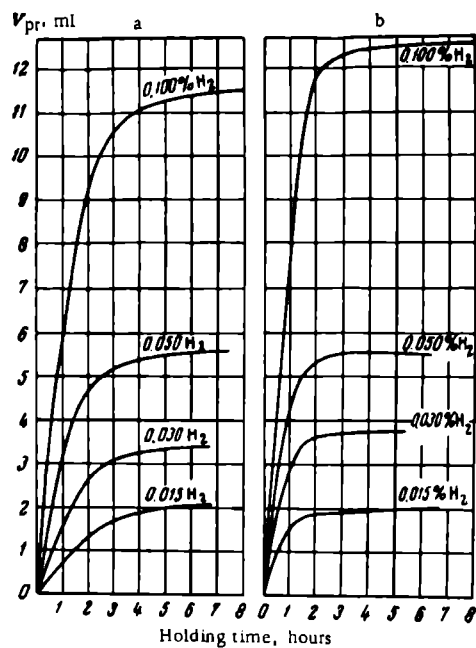


FIGURE 3. Kinetics of evolution of hydrogen from titanium with different hydrogen contents

a — at 700°C ; b — at 900°C .

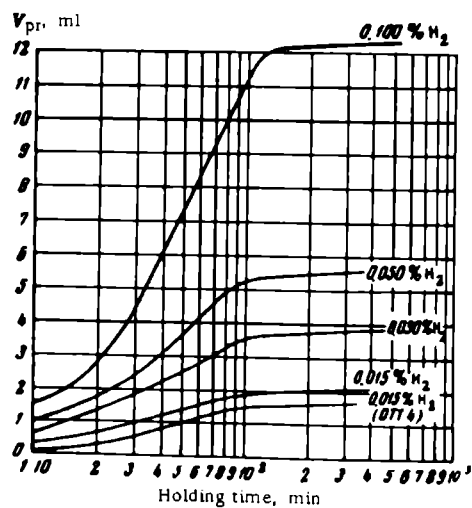


FIGURE 4. Relationship between the velocity of evolution of hydrogen at 900°C and the hydrogen content of titanium

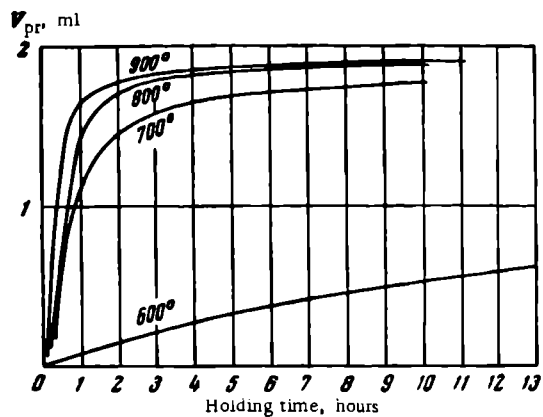


FIGURE 5. Kinetics of the evolution of hydrogen from OT-4 alloys with 0.015% H_2 at various temperatures

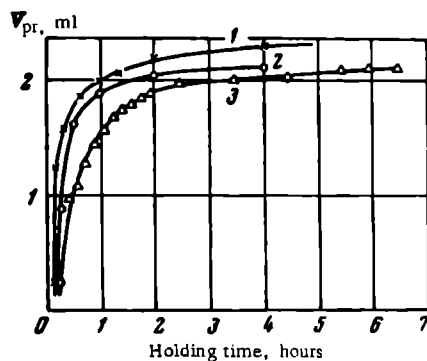


FIGURE 6. Kinetics of evolution of hydrogen from titanium specimens of various thicknesses
1 — 1.5 mm; 2 — 3.0 mm; 3 — 10.0 mm.

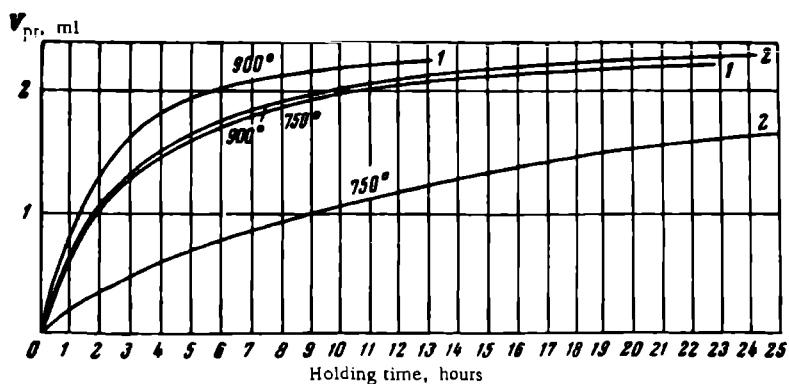


FIGURE 7. Kinetic curves obtained during degassing of titanium ($10 \times 10 \times 10$ mm cubes) coated with chromium-nickel deposits in different solutions [1,2]

that nickel and chromium have a low permeability to hydrogen. The velocity of evolution of hydrogen from specimens with a chromium-nickel coat and from uncoated specimens considerably increases with the increase in the temperature.

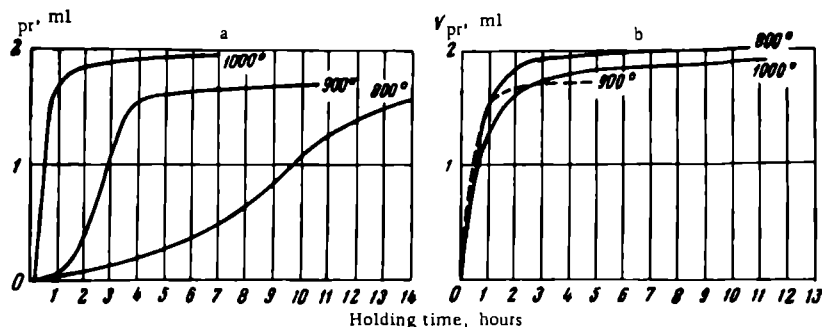


FIGURE 8. Kinetics of evolution of hydrogen from titanium ($10 \times 10 \times 10$ mm cube) with a surface oxidized in the air

a — at 700°C for 6 hours; b — at 525°C for one hour.

The velocity of evolution of hydrogen from specimens coated with chromium-nickel layers in different electrolytes greatly differs (Figure 7). This is apparently due to the different thickness of the nickel-chromium coatings.

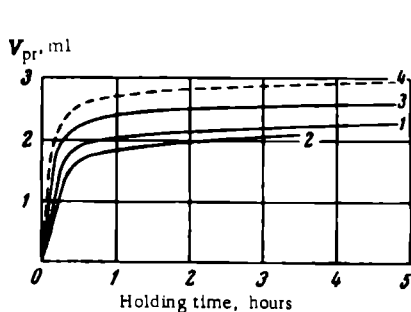


FIGURE 9. Kinetic curves obtained during heating in vacuo (900°C) of titanium specimens in which the hydrogen is differently distributed over the volume of the metal

1 — uniform distribution of hydrogen;
2, 3, 4 — the hydrogen is present mainly in the surface layer.

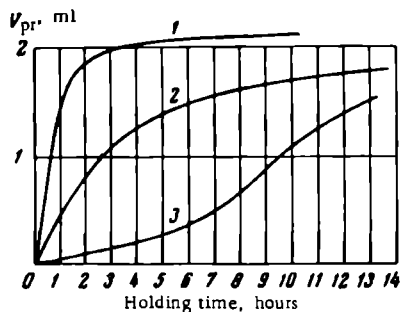


FIGURE 10. The influence of the surface conditions of the specimens on the kinetics of the evolution of hydrogen from titanium (hydrogen content 0.015%, temperature of degassing 800°C)

1 — specimen ($10 \times 10 \times 10$ mm), with a ground surface; 2 — specimen with a chromium-nickel coat; 3 — specimen oxidized at 700°C for 6 hours in air.

The relationship (Figure 8) between the amount of hydrogen evolved and the holding time in vacuo is more complicated for specimens with an oxidized surface (700°C, 6 hours). These curves differ from the previous kinetic curves (Figures 2 to 5), in showing a very slow evolution of hydrogen at the beginning (Figure 8a), after which the intensity increases, to drop later once more. The degassing temperature is in this case of great importance, particularly during the initial period. Thus, while a more or less intense evolution of hydrogen from an oxidized specimen can be noted after 5 to 7 hours at 800°C, it takes place after 1.5 hours at 900°C and only after 10 min at 1000°C.

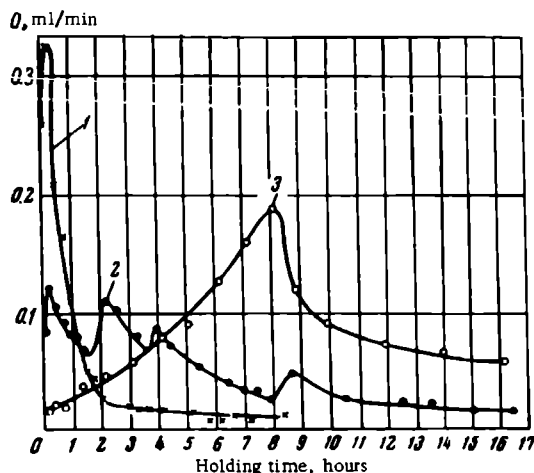


FIGURE 11. The dependence of the velocity of evolution of hydrogen (content 0.015%) from titanium in vacuo on the duration of the process at 800°C and on the surface condition of the specimens (10 × 10 × 10 mm cube)

1 — specimen with a ground surface; 2 — specimen with a chromium-nickel layer; 3 — oxidized specimen (700°C, 6 hours).

The thin oxide film on the surface of titanium obtained at 525°C (holding time — one hour) has little influence on the evolution of hydrogen from the metal (Figure 8b).

No proof was obtained that the nature of the distribution of hydrogen throughout the metal has any considerable influence on the degassing process. This is apparent from the curves (Figure 9) obtained during degassing of titanium plates 1.3 mm thick after hydrogen had been introduced by various methods. Methods of introducing hydrogen into the metal were chosen which ensure either a uniform distribution (curve 1) of the gas throughout the metal (thermodiffusion method) or its concentration chiefly in the surface layer — etching (curve 2), cathodic treatment (curve 3). For comparison, the same figure shows a kinetic curve obtained during degassing an OT-4 alloy specimen which had been subjected to a cathodic treatment (curve 4).

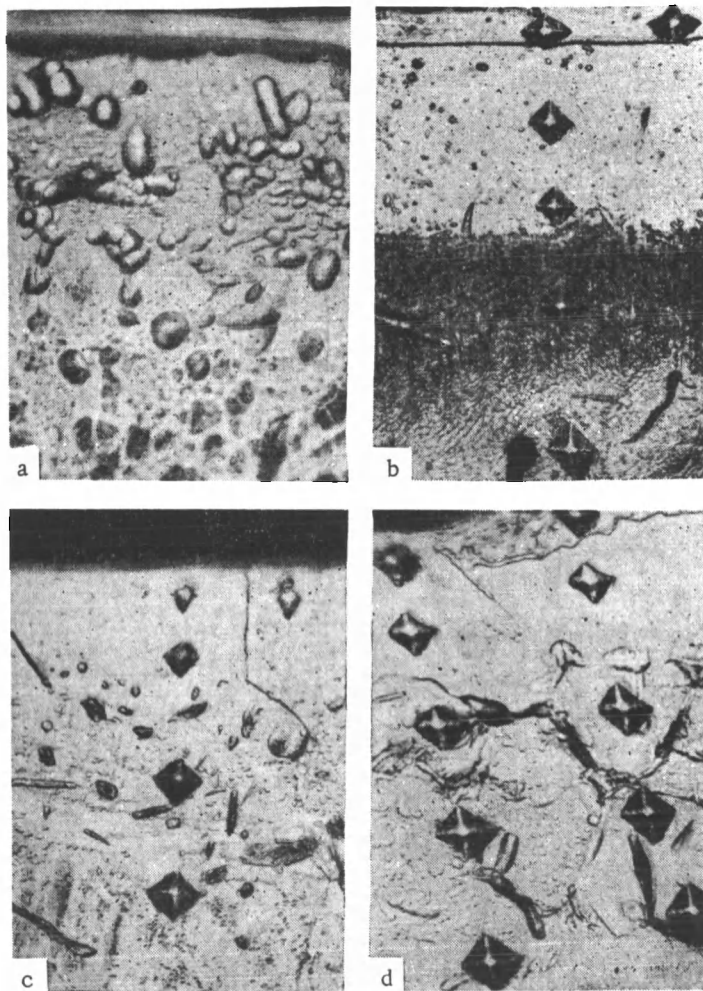


FIGURE 12. Microstructure of titanium with different states of the surface after degassing under different conditions:

- a — a specimen with a chromium-nickel coat degassed at 650°C for 40 hours;
- b — specimen with a chromium-nickel coat degassed at 900°C for 26 hours;
- c — oxidized specimen degassed at 800°C for 25 hours; d — oxidized specimen degassed at 900°C for 10 hours.

These experimental results show that the holding time (at a certain temperature and in vacuo), after which the degassing of titanium is completed, depends little either on the dimensions of the specimens (at a thickness up to 10 mm) or on the content of hydrogen and the nature of its distribution in the metal. At the same time, however, the holding time strongly depends on the surface condition of the specimens (Figure 10).

. It can be assumed from the above data that the intensity of degassing is determined by the velocity of the process taking place at the surface of the metal and is connected with the removal of hydrogen atoms. In this case the diffusion of hydrogen in the metal towards the surface is not an inhibiting factor, since the velocity of this process is high. Therefore, there is no considerable gradient of hydrogen concentration between the interior of the metal and its surface.

If the surface of the specimen is coated with a chromium-nickel layer, the velocity of evolution of hydrogen from titanium greatly decreases (Figure 11). Whereas in specimens with a ground surface the velocity of evolution of hydrogen from the metal smoothly decreases with time and with the concentration decrease of hydrogen, in the case of chromium-nickel-plated specimens, this velocity undergoes sudden changes. The total degassing velocity decreases with the decrease in the hydrogen concentration of the metal. Such a change in the degassing velocity is apparently due to the diffusion processes $\text{Ni} \rightleftharpoons \text{Cr} \rightleftharpoons \text{Ti}$ taking place at higher temperatures and resulting in the formation of layers with different properties and chemical compositions.

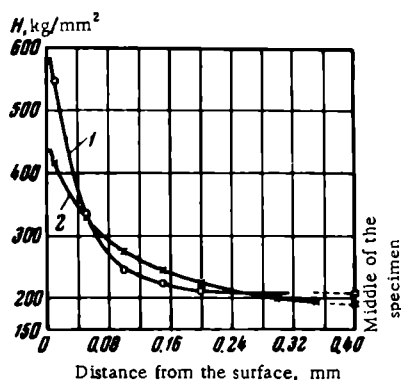


FIGURE 13. The variation of the microhardness of an oxidized surface layer as a result of degassing of the metal in vacuo
1 — at 800°C for 25 hours; 2 — at 900°C for 10 hours.

The changes in the surface layer taking place during the degassing of the metal are apparent from the microstructures shown in Figure 12. These photographs show that specimens with a chromium-nickel coat heated at 900°C have a considerably thicker diffusion layer than those heated at 650°C.

The degassing of hydrogen-containing titanium with an oxidized surface proceeds differently (Figure 11). In this case the velocity of hydrogen evolution shows an initial increase lasting over a considerable period and then begins to decrease. This phenomenon can be explained in the following way. The penetration of hydrogen through the oxidized layer is highly impeded. The velocity of evolution of hydrogen considerably increases as the concentration of oxygen in the surface layer decreases (due to diffusion).

Later the intensity of evolution of hydrogen (as is also the case with specimens with other surface conditions) decreases with the decrease in the content of hydrogen in the metal.

The decrease in the concentration of hydrogen in the surface layers of specimens can be indirectly followed from the changes in their microstructure (Figures 12c and d) and in their microhardness (Figure 13), which are the result of the degassing.

It is interesting to note that, after degassing, the surface of oxidized specimens with a continuous scale was bright and white.

The variations in the velocity of evolution of hydrogen from titanium show that during the initial period of degassing of oxidized specimens the inhibiting factor is apparently the velocity of diffusion of hydrogen through the oxidized layer after which the process taking place at the surface of the metal determines the velocity.

Conclusions

The investigation of the kinetics of evolution of hydrogen from technical titanium with different states of the surfaces and from OT-4 alloys at 600 to 1000°C leads to the following conclusions:

1. A relatively intense removal of hydrogen from the metal takes place at 650°C and higher; the process is considerably accelerated by increase in temperature.
2. The velocity of evolution of hydrogen increases with its content in the alloy.
3. The presence of a chromium-nickel coating or of an oxidized layer on the surface of the metal leads to a considerable inhibition of the degassing process.
4. The duration of degassing, by which hydrogen is more or less fully removed from VT-1 and OT-4 alloys, depends little on either the dimensions of specimens (with a thickness of up to 10 mm) or on the content and the distribution of hydrogen in the metal.

INVESTIGATION OF THE ELECTROCHEMICAL BEHAVIOR OF TITANIUM AND ITS ALLOYS DURING THE ELECTROLYSIS OF CHLORIDE SOLUTIONS

L. M. Yakimenko, G. N. Kozhanov, I. E. Veselovskaya,
and R. V. Dzhagatspanyan

The choice of anode materials is of great importance in the electrochemical industry. From the technical point of view, the possibility of carrying out a given electrochemical operation depends on the nature of the anodes available, which further determines the design of the cells and the economic feasibility of the process as a whole. The choice of insoluble anodes for electrochemical processes is rather limited. The most popular material for [insoluble] anodes is platinum, because of its chemical resistance to various media and because of its electrochemical characteristics. Many anodic processes can take place only on platinum anodes. In this connection it should be noted that the necessity to economize in the use of platinum hampers the development of electrochemical methods for the preparation of dyestuffs and for the synthesis of organic substances.

At the present time the chlorine-producing industry uses graphite anodes. The physicochemical properties of graphite, however, limit the possibilities of intensification of the process which can be accelerated by increasing the current density, by increasing the capacity of the cells, or by automation. Therefore, the replacement of graphite by metallic anodes, for instance of platinum-titanium, presents an urgent problem.

Platinum-titanium anodes (PTA) are produced by coating titanium with a layer of platinum several microns in thickness by electrolysis or by any other method. At the present time, PTA are produced in a number of countries, including the Soviet Union, but the wider introduction of PTA into the industry is limited by the lack of data on their electrochemical characteristics and by the prohibitive prices of platinum.

Another method of introducing insoluble anodes is the development of new alloys and compounds on which a protective surface layer with a high electron conductivity can be produced by anodic polarization. The use of platinum and of some other anodes, for instance nickel anodes in alkalis and lead anodes in sulfuric acid, is based on the formation of conductive oxide films on them.

In their search for anodic materials the present workers have investigated the transition metals (titanium, zirconium, niobium, tantalum, molybdenum, and tungsten) which have a high corrosion resistance to chlorides. Among these titanium has obviously the greatest technical importance.

The electrochemical investigation of these metals and of their alloys was carried out chiefly in order to determine their value either as

corrosion-resistant materials or for the electronics industry. In both cases it is required that the current in the anodic direction shall be as low as possible.

Attention was directed not only to the protective properties of the surface films on the anodes but also to the possibility of evolution of chlorine.

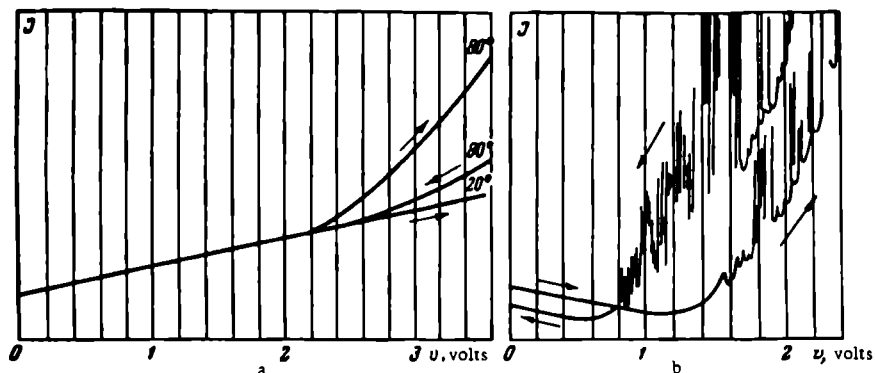


FIGURE 1. Anode polarograms

a — on tantalum in a solution of common salt (300 g/l) at 20 and 80°C; b — on chromium in a solution of common salt (300 g/l) at 80°C.

An approximate comparison of specimens was obtained by means of the "Geologorazvedka" polarograph. The specimens (with a 1.5 mm² surface) were soldered into a glass tube into which mercury was poured (to maintain electrical contact), and the tube was rotated with a velocity of 1000 rpm. The anodic polarization was carried out under conditions similar to those prevailing during the production of chlorine, i. e., in a saturated solution of common salt at high temperatures.

From the current versus anode potential curves obtained in this way*, it is possible to identify the processes taking place on a given anode. For instance, the semiconductive properties of the surface oxide layer are most pronounced in the case of tantalum /1/. The polarogram obtained at 20°C Figure 1a, shows a linear relationship between the current and the potential, which is the same in both directions. At 80°C there is a certain current increase on freshly protected tantalum but the reverse curve approaches a straight line, as at 20°C. These data show that on a tantalum anode there is above all a process of formation of a blocking layer.

The same result is obtained for niobium. The curves are different for chromium, the characteristic feature here being the upsetting of the passivity at high anode potentials /2/. In this case the progressive destruction of the protective oxide film is reflected on the polarogram by the sharp fluctuations and increases of the anode current at potentials higher than 1.2 v. The reverse curve shows that the reproduction of the passive film on chromium is also inhibited and that this is completed only at a lower anode potential than the commencing potential (Figure 1b).

* All potentials are given relative to that of a saturated calomel electrode.

These two examples show that the current versus anode potential curves, obtained by means of a polarograph, reflect accurately the electrochemical behavior of the metals. It was determined by the same method that, under the given conditions of anodic polarization, molybdenum (Figure 2) and zirconium dissolve at potentials lower than the decomposition potential of chlorine. These elements were, therefore, excluded from further consideration. In the case of tungsten, the current increase begins on the polarogram at the decomposition potential of chlorine (Figure 2b).

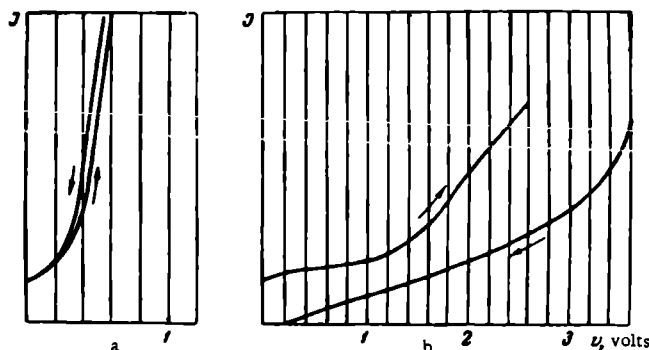


FIGURE 2. Anode polarograms

a — molybdenum in a solution of common salt (300 g/l) at 20 and 60°C or in a solution of sodium chlorate (300 g/l) at 20 and 60°C; b — tungsten in a solution of common salt (300 g/l) with an addition of 0.1N hydrochloric acid at 80°C.

In addition, the formation of a blocking layer is slower on tungsten than on tantalum or niobium. The variations with time of the anode potential of freshly cleaned tungsten, in an acidified solution of common salt at a constant current density, are given in Figure 3a. The above experiments were carried out in unagitated solution with anodes a few square centimeters in surface area [3].

Freshly cleaned tungsten polarized in a solution of common salt at $1.3 \cdot 10^{-4}$ amp/cm² has a plateau at 1.6 v (curve 1), but the potential continuously increases. If the polarization is repeated after an interruption of current, the length of the plateau sharply decreases (curve 2).

In sulfuric acid, tungsten at first dissolves but then becomes passivated until the potential reaches a magnitude of 1.6 v. It is, therefore, clear that the plateau on curve 1 for sodium chloride solutions is due to the process of evolution of chlorine.

An analogous plateau at 1.6 v can also be seen on the polarograms of freshly cleaned titanium recorded at 80°C and at the same current density (Figure 3b, curve 4). The evolution of chlorine on large tungsten or titanium anodes can be detected either directly or by the iodine-starch reaction.

At 80°C and at a current density of $1.3 \cdot 10^{-4}$ amp/cm² no lasting electrolytic evolution of chlorine is possible on tungsten or titanium since under

these conditions an anodic oxidation of metal also takes place at a velocity commensurate with that of gas evolution.

If the current density is increased, the temperature of electrolysis reduced and chloride replaced with chlorate solution, the oxidation of titanium is more rapid and the evolution of chlorine is suppressed (Figure 3b).

Since titanium is used as the basis for platinum-titanium anodes (PTA) and the unprotected electric conductors are also made of titanium [4], it was considered necessary to determine the distribution of current between platinum and titanium under identical conditions of electrolysis. This was carried out by utilizing a PTA model consisting of two anodes (one platinum and the other titanium) connected in parallel in the circuit through two identical resistors*.

In this case, the potential of the titanium anode and the chemical composition of the anolyte and of the gaseous phase are determined by the conditions of polarization of the platinum anode. The electrolysis was carried out at 80 and 90°C in a running electrolyte (270 g/l NaCl) with separated anode and cathode compartments. The current density on the platinum varied from 10^{-3} to $2 \cdot 10^{-1}$ amp/cm² [11].

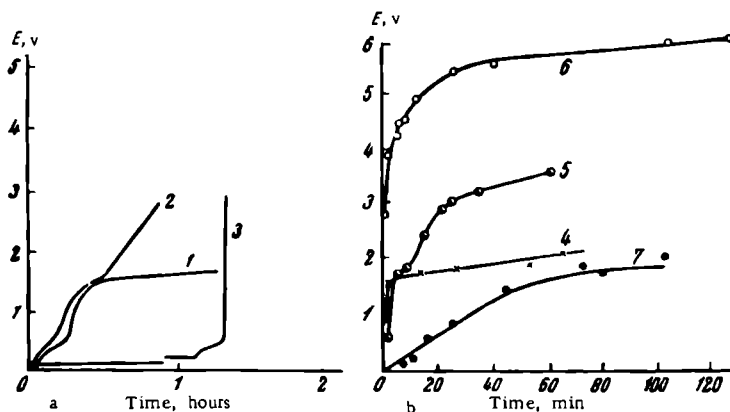


FIGURE 3. Dependence of the potential on the duration of the anodic polarization; tungsten (a) and freshly cleaned titanium (b)

1 — [tungsten] in a solution of common salt (300 g/l) at 80°C and $1.3 \cdot 10^{-4}$ amp/cm² (freshly cleaned anode); 2 — the same, after interruption of current and repeated polarization; 3 — in a solution of 1 N sulfuric acid at 80°C and $1.3 \cdot 10^{-4}$ amp/cm²; 4 — [titanium] in a solution of common salt (300 g/l) at 80°C and $1.3 \cdot 10^{-4}$ amp/cm²; 5 — in a solution of sodium chlorate (300 g/l) at 80°C and $1.3 \cdot 10^{-4}$ amp/cm²; 6 — in a solution of common salt (300 g/l) at 80°C and $1.3 \cdot 10^{-3}$ amp/cm²; 7 — in a solution of common salt (300 g/l) at 20°C and $1.3 \cdot 10^{-5}$ amp/cm².

If only the platinum anode is polarized, the potential of titanium increases up to the equilibrium potential of chlorine. On cessation of the anodic polarization the potential of titanium is reduced to this magnitude. Consequently, titanium absorbs gaseous chlorine and acts as a chlorine electrode of the first order.

* The same method has been used by other investigators for the evaluation of the performance of PTA as a cathodic protection of steel constructions in sea water [5, 6].

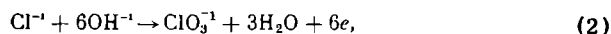
If only the platinum is polarized at a constant current density, the current on the titanium rapidly decreases along an asymptotic curve to a certain constant magnitude termed the "residual current". The relationship between the residual current on titanium, its potential and the overvoltage curve for platinum (recorded simultaneously) is given with semilogarithmic coordinates in Figure 4. Each point was obtained in a separate experiment. Between experiments, the titanium was kept in a 0.1 N solution of hydrochloric acid in order to prevent strong oxidation of the surface.

The increase in the residual current on titanium begins from the equilibrium potential of the evolution of chlorine which confirms the assumption that chlorine may evolve on titanium during this process. The velocity of this process on titanium is, however, tens of thousands of times lower than on platinum under strictly identical conditions.

The varying courses of the polarization curves for platinum and titanium at 1.6 v indicate changes in the anodic process. The left branch represents the discharge of chlorine ions according to the reaction:



The right-hand branch represents the oxidation of the chlorine ion to chlorate according to the reaction:



the velocity of which depends on the pH of the anolyte [the process (1) taking place simultaneously].

The transition between both branches is more clearly defined for titanium than for platinum, and for Ti there is even a hysteresis inflection. A transition from the right-hand branch to the left can be brought about without changing the current density merely by either acidifying the anolyte or else decreasing the thickness of the oxide film on titanium by treatment with dilute hydrochloric acid.

Consequently, the right-hand branch corresponds to the oxidation of the titanium surface. This conclusion is in agreement with the results obtained during the polarization of titanium at a constant current density within the same region of potentials (see Figure 3).

It has already been shown that during the polarization of a platinum-titanium anode in a solution of common salt, several anodic processes take place slowly on the titanium (evolution and oxidation of chlorine and oxidation of titanium). The corrosion velocity of titanium, after a prolonged operation of PTA under industrial conditions, has been evaluated by the authors at about 10^{-7} amp/cm². The residual current on titanium is, under these conditions, equal to $3 \cdot 10^{-6}$ amp/cm² (Figure 4). Consequently, during a stationary electrolysis, the oxidation of titanium takes up less than 10 % of the residual current while the rest of the current is used up for the evolution and oxidation of chlorine. Even at such a low velocity of oxidation, a prolonged electrolysis produces an oxidized layer on titanium a few tenths of a micron thick which becomes apparent from the change in the color of the PTA.

It was further required to know whether it is possible to increase the velocity of evolution of chlorine on titanium and on similar metals by

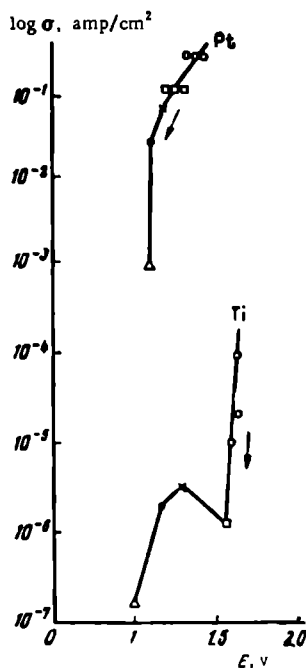


FIGURE 4. Relationship (in semi-logarithmic coordinates) between the residual current on a titanium anode, its potential, and the overvoltage curve for a parallel platinum anode in a solution of common salt (300 g/l) at 95°C

changing the chemical composition of the surface layer. Accordingly, an exploratory investigation was carried out on the metals after various chemical pretreatments and on a number of binary titanium alloys. The following results were obtained.

The addition of small amounts of chlorine ions to the electrolyte leads in all cases to marked interference with the existing blocking layer and to an increase in the residual current, but does not accelerate the discharge of chlorine ions.

Oxides, borides, carbides, silicides, nitrides, and sulfides have an electron conductivity [7].

Surface layers of carbides were produced (by heating the metal under graphite powder at 800 to 1000°C in an atmosphere of nitrogen), of nitrides (by heating in a current of nitrogen at 800°C), and of sulfides (by heating under fused sulfur).

No apparent effects were obtained by nitriding the metals. At 80°C, a potential equal to the decomposition potential of chlorine can be achieved on Ti coated with a surface layer of carbide, at a current density one order of magnitude higher than that at which this decomposition potential is reached on pure titanium. In this case, however, the anode dissolves to some extent. Under the same conditions of polarization, titanium carbide with a content of 15 % C and obtained by sintering at 2200°C, dissolves very rapidly*.

In fused salt media, titanium carbides and titanium nitrides are used as soluble anodes [8].

During the anodic polarization of metals treated in fused sulfur, there is first of all a dissolution of the surface layer after which the potential of the anode rapidly increases with a short break at the potential of chlorine evolution.

A systematic investigation [9] has shown that the corrosion resistance of titanium-base alloys depends on the nature of the alloying element. During the anodic polarization of binary titanium alloys, an intimate relationship was noted between the corrosion resistance of the alloy and the nature and content of the alloying element.

In a solution of common salt (300 g/l) and at 80°C, alloys of titanium with 3 % Mn, 5 % Cr, or 4 % Al form a blocking layer and in their [corrosion] behavior they do not differ from pure titanium. Common salt solution brings about intense dissolution of the aluminum from titanium base alloys containing 30 to 40 % Al, while alloys with 30 % Al are passive in chlorate solutions (300 g/l NaClO₃) up to 2.0 v (Figure 5).

* The specimen was produced in the solid state laboratory of the Physicochemical Institute imeni Karpov.

Anodic dissolution also predominates when titanium alloys with 30 to 45 % V are treated in a solution of common salt (Figure 6). The decomposition potentials of chlorine on alloys with 7.5 or 15 % V and with 4 to 25 % W become established at current densities 3 to 4 times higher than those required for the evolution of chlorine on pure titanium (Figure 7). In the case of tungsten alloys, the decomposition potential does not depend on the content of the alloying metal and there is no visible dissolution of the anodes.

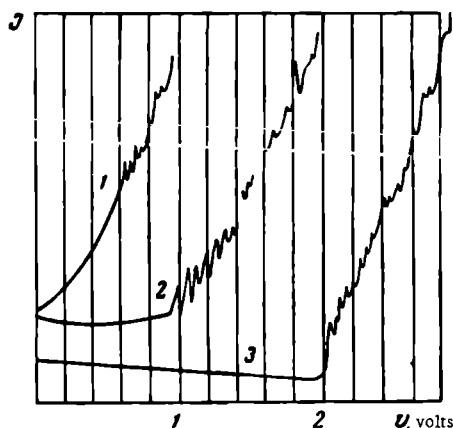


FIGURE 5. Anode polarogram for a Ti+30% Al alloy

1 — in a solution of common salt (300 g/l) at 80°C;
2 — in a solution of common salt (300 g/l) at 20°C;
3 — in a solution of sodium chlorate (300 g/l) at 60°C.

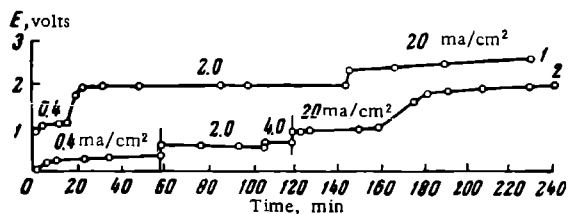


FIGURE 6. Dependence of the [anode] potential on the duration of the anodic polarization of Ti-V alloy in a solution of common salt (300 g/l) at 80°C

1 — alloy Ti+30% V; 2 — alloy Ti+45% V.

If titanium alloys with 15 % V and 4 to 25% W have a surface layer of carbide the evolution of chlorine takes place at 20 to 40 ma/cm², i.e., at current densities close to those maintained in present chlorine-production

technology /3/. Nevertheless, under these conditions the evolution of chlorine is also accompanied by a dissolution of the anode and its service life is therefore limited by the amount of carbide in the surface layer.

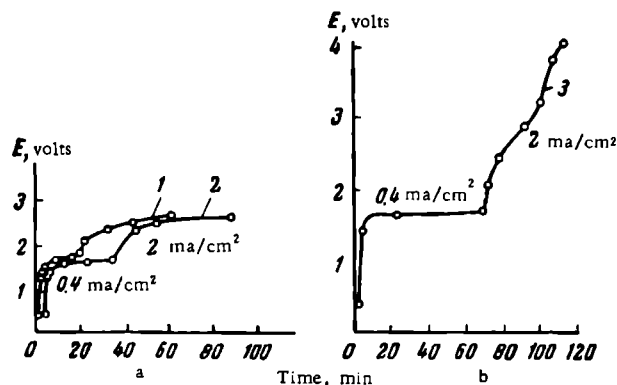


FIGURE 7. Dependence of the [anode] potential on the duration of the anodic polarization of Ti-V and Ti-W alloys in a solution of common salt (300 g/l) at 80°C

1 — alloy Ti + 7.5% V; 2 — alloy Ti + 15% V; 3 — alloy Ti + 15% W.

Below are given the maximum current density values (in m amp/cm²) for various specimens in sodium chloride electrolytes (300 g/l, pH = 7 ± 1) at 80°C and at the decomposition potentials of chlorine (1.6 to 2.0 v):

Titanium VT-1	0.1
Titanium alloys with 7.5 and 15% V	0.4
Titanium alloys with 4.5, 15, and 25% W	0.4
Titanium with surface layer of carbide	1-2
Titanium-tungsten alloy with surface layer [of carbide]	20-40

It has already been mentioned that an oxidation of chlorine to chlorate is possible at these potentials.

It has been determined that an acceleration of the evolution of chlorine is accompanied by some acceleration of the anodic dissolution of the metal.

It should be noted that the most effective alloy is that of titanium with tungsten which is in full accordance with published data on the increasing conductivity of TiO₂ resulting from the introduction of oxides of metals with a higher valency, particularly of WO₃ /10/.

Conclusions

1. In the industrial production of chlorine with titanium anodes the anodic polarization produces a protective oxide film through which a residual current of 10⁻⁵ — 10⁻⁶ amp/cm² passes at a potential of 1.5 v (NCE).*

* [Measured against a normal calomel electrode.]

At this potential, the residual current on titanium is utilized chiefly for the evolution and oxidation of chlorine.

2. An acceleration in the evolution of chlorine, accompanied in most cases by an acceleration in the anodic dissolution of the metal, can be attained by changing the chemical composition of the surface layer of titanium anodes.

3. It was determined that titanium, tantalum, and niobium can be used for the electrolysis of chloride solutions either as unprotected anodes or as a basis for [platinum] electrodeposits.

Bibliography

1. Johansen, H. E., C. B. Adams, and P. Van Rysseberghe. — J. Electroch. Soc., Vol. 104:339. 1957.
2. Kolotyrkin, Ya. M. Problemy fizicheskoi khimii (Problems of Physical Chemistry). — Goskhimizdat. 1958.
3. Yakimenko, L. M., G. N. Kozhanov, I. E. Veselovskaya, and R. V. Dzhagatspanyan. — Khimicheskaya Promyshlennost', No. 1:43. 1962.
4. Dzhagatspanyan, R. V., G. N. Kokhanov, I. E. Veselovskaya, and E. V. Mulin. — Patent No. 124423, Class 12, 18 November 1958; Byulleten' Izobretenii, No. 23. 1959.
5. Bombare, G. and D. Gerardi. — La metallurgia italiana, 51(10):462. 1959.
6. Bibikov, N. N., I. D. Soboleva, and O. Yu. Khenven. — Tekhnologiya Sudostroeniya, 14(6):19. 1960.
7. Kubaschawsky, O. and B. Hopkins. Oxidation of Metals and Alloys. — London, Butterworth Scientific Publications. 1953. [Russian translation. 1955.]
8. Suchkov, A. B., B. A. Borok, M. I. Rodnyi, T. N. Ermakova, E. I. Morozova, and L. D. Boldina. — Tsvetnye Metally, 32(8): 50. 1959.
9. Andreeva, V. V. and V. I. Kazarin. — Doklady AN SSSR, Vol. 128: 748. 1959.
10. Grunewald. — Ann. Phys., Vol. 14:121. 1954.
11. Yakimenko, L. M., I. E. Veselovskaya, R. V. Dzhagatspanyan, and S. D. Khodkevich. — Khimicheskaya Promyshlennost', No. 10. 1962.

ELECTROCHEMICAL AND CORROSION INVESTIGATIONS OF Ti—Al ALLOYS

F. N. Tabadze, S. N. Mandzhgaladze, T. S. Dashniani,
I. N. Lordkipanidze, and L. F. Tavadze

The investigation of Ti—Al alloys is of great practical interest. Aluminum is cheap, readily available, and its addition to titanium decreases the specific gravity and increases the strength of the metal.

The Ti—Al system contains limited solid solutions of α - and β -Ti and is characterized by peritectoid transformations /1/. This system may contain Ti_3Al and Ti_2Al compounds /2/. Several phase diagrams of the Ti—Al system have been constructed and these are reviewed by Sagel et al /3/.

The electrochemical and corrosion properties of titanium and aluminum are to a certain degree similar. Both these elements are thermodynamically rather active. Nevertheless, because of their ability to form protective passive films, they are resistant to many electrolytes. Both titanium and aluminum have a high corrosion resistance when passivated. Thus, in a 0.5N solution of sodium chloride the coefficient of passivity of titanium is 2.44, that of aluminum 0.82, that of chromium 0.74, and that of nickel 0.37. The relatively high corrosion resistance of pure aluminum and of its alloys is due not only to the action of protective films. It is to a certain degree also due to the high hydrogen over-voltage of these metals.

Such data as have been published on the corrosion resistance of certain titanium-aluminum alloys are somewhat conflicting and the authors have found no [comprehensive] data on the resistance of alloys of the Ti—Al system. This lack of adequate information has induced them to carry out this investigation.

A study was made of 19 alloys with a content of 0.5 to 38.5 weight % of Al. The specimens were prepared and heat-treated in the laboratory of alloy chemistry of the Institute of Metallurgy im. A. A. Baikov under the guidance of I. I. Kornilov and V. S. Mikheev. The following heat-treatment process was applied to all alloys: heating to 900°C, holding for 100 hours, cooling in the furnace to 800°C, holding for 200 hours, cooling in the furnace to 700°C, holding for 100 hours, and cooling to room temperature in the furnace.

The corrosive media were inorganic acids (sulfuric, hydrochloric, and nitric) and a 0.5N solution of sodium chloride. The most corrosive concentrations of the acids were determined by preliminary experiments. The acids were analyzed volumetrically and certain alloys underwent a full gravimetric analysis. The electrode potentials of the metals in sodium chloride solutions were also measured.

The experimental results are shown graphically in Figures 1 and 2. The curve representing the relationship between the corrosion velocity in nitric acid and the aluminum content of the alloy, has one clearly expressed maximum at 6 to 8 weight % Al. The corrosion curves for hydrochloric and sulfuric acids have two maxima: the first at 6 to 8 % Al and the second at 25 to 26 % Al. It should be noted that sulfuric and hydrochloric acids are more destructive to the alloys than nitric acid. Among the alloys investigated, the best corrosion resistance was shown by those containing up to 6 % Al, 9 to 12 % Al, and more than 35 % Al. On the basis of these data recommendations can be made for the production of corrosion-resistant alloys.

The curve representing the relationship between the electrode potentials of alloys and their aluminum content (Figure 2) has two minima in the range shown in Figure 1. Alloys with up to 6.5 weight % Al have electronegative potentials. If the content of aluminum is increased to 7.0 - 7.5 % the potential of the alloys sharply increases due to the precipitation of a new phase [3]. Alloys with 8 to 20 % Al are again electronegative while if the concentration of aluminum is further increased their potential rises once more to positive values.

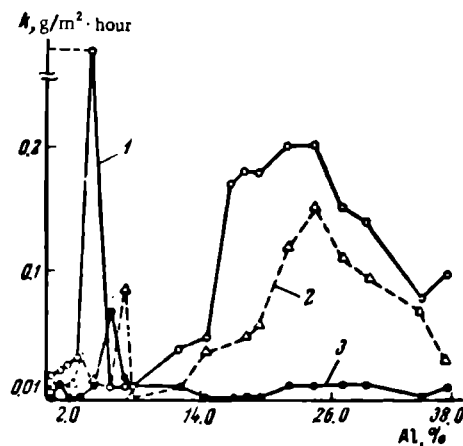


FIGURE 1. Relationship between the corrosion velocity of Ti-Al alloys and their aluminum content

1 — in a 40 % sulfuric acid solution; 2 — in a 60% hydrochloric acid solution; 3 — in a 5% nitric acid solution.

Variations of this nature in the properties of alloys are usually caused by structural transformations.

The polarity of the structural components and the mechanism of their mutual reactions during the corrosion is of great interest. Since the second phase was very finely divided no microelectrode measurements could be carried out. Nevertheless, it is known that if the second phase is more positive than the matrix, the electrochemical heterogeneity cannot last for long and the anodic particles will dissolve, leaving a single-phase surface

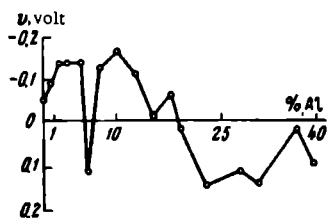


FIGURE 2. Relationship between the electrode potential of Ti-Al alloys and their Al content

layer. If, however, the second phase is more negative than the matrix then the formation of microcathodes usually accelerates the corrosion. The corrosion can in the latter case be inhibited either by the second phase precipitating at the surface of the alloy as a continuous layer, or by the increasing passivation of the microcathodes. The authors have investigated the kinetics of corrosion of alloys and determined that the corrosion velocity of alloys with a heterogeneous structure increases with time and that consequently

the second phase must be a cathode. This assumption is supported by the fact that alloys containing a second phase have a more positive potential [than homogeneous alloys].

A more detailed discussion of this problem can be supported by data on the variation of the electrode potentials with time. The potentials of alloys with a homogeneous structure vary, but they always remains negative (Figure 3a). The potentials of alloys with a heterogeneous structure become more positive with time (Figure 3b).

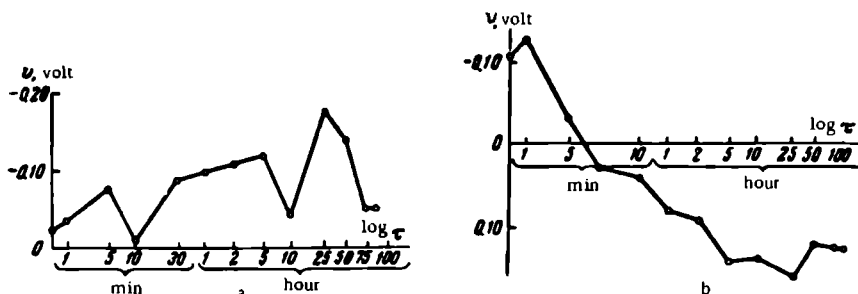


FIGURE 3. Variation of the potentials of titanium alloys
a — with 1% Al; b — with 7% Al.

Conclusions

1. Ti-Al alloys with up to 37.5 weight % Al are resistant to nitric acid except those with 6 to 7 % Al which are uniformly attacked at a rate of 1.42 mm/year.
2. Only alloy groups with up to 6 % Al, with 10 to 12 % or with more than 36 % Al are sufficiently resistant to sulfuric and hydrochloric acids.
3. The considerable changes in the electrochemical and corrosion properties of Ti-Al alloys indicate that the latter contain phases which are more negative than the α -Ti solid solution.

Bibliography

1. Kornilov, I.I. —Doklady AN SSSR, 91 (3): 549. 1953.
2. Sagel, K., E. Schulz, and U. Zwickler—Zs. Metallk., 47(8): 529. 1956.
3. Konstitution des ternären metallischen Systems. — Konpendium, No. 13, Berlin. 1961.

CORROSION RESISTANCE AND ELECTROCHEMICAL BEHAVIOR OF TITANIUM AND ITS ALLOYS IN SOLUTIONS OF INORGANIC ACIDS CONTAINING OXIDATION AGENTS

F. A. Orlova and T. A. Tumanova

Titanium and its alloys are increasingly being used for construction purposes in the chemical industry. A particularly important application of titanium is in the production of equipment for handling highly corrosive media. Titanium has a low resistance to hydrochloric and sulfuric acids, particularly at high concentrations and temperatures. Much work has been published on the passivation of titanium in acid solutions with and without oxidizing properties. Some investigations have also been carried out on the influence of anodic polarization to the resistance of titanium in non-oxidizing acid solutions.

Cotton /1/ has shown that if a sufficiently high anodic current density is applied, the dissolution of titanium in strong inorganic acids, such as concentrated hydrochloric acid, 40 % sulfuric acid, and 35 % phosphoric acid, etc., can be completely suppressed.

Fischer /2, 3/ and Tseitlin /4/ as well as other workers, have investigated the influence of some oxidation agents, particularly of humid chlorine, on the passivation of titanium in solutions of inorganic acids (hydrochloric and sulfuric).

Since several organic compounds are produced by chlorination in solutions of hydrochloric acid or by nitration in sulfuric acid solutions, the determination of the corrosion-resistance of new constructional metals has become an urgent problem.

Experimental methods

In this study, the authors have made use of electrochemical and gravimetric methods. The determination of the electrochemical behavior of titanium and its alloys was carried out in a specially designed electrolytic unit (Figure 1).

The duration of each experiment was 90 to 360 hours. The solution was continuously agitated during the experiment and the potential of titanium was measured against a reference calomel electrode. Determinations were made of the corrosion velocity of titanium, the dependence of the potential on the duration of exposure of the metal, as well as the relationship between the degree of corrosion of titanium and of its alloys and the nature of the oxidation agent. The oxidation agents used were molecular oxygen, chlorine, and nitric acid; the solutions were 5 to 22 % hydrochloric acid and 10 to 30 % sulfuric acid; the experiments were carried out at 20, 60, and 90°C.

TABLE 1
The influence of oxidation agents (chlorine, oxygen, and nitric acid) on the corrosion
resistance of VT-1 titanium in solutions of hydrochloric and sulfuric acids

Medium	Concentration, %	Corrosion velocity, g/m ² ·hour									
		without oxidation agents			with oxidation agents						
					O ₂		Cl ₂		HNO ₃ (1%)		
		Temperature, °C									
		20	50*	20	60	90	20	60	90	90	
HCl	5	0.08	1.08	0.0051	0.63	6.84	—	—	—	—	
	10—12	0.15	8.9—15.3	0.008	8.11	25.7	0.004—0.005	0.009	0.055	—	
	18	0.34	24.3	1.25	7.34	The specimen dissolved	0.0035—0.0050	0.026	0.45—0.55	0.1947	
	20	—	29.90	—	—	—	0.006	0.32	The specimen dissolved	—	
	33	0.86	The specimen dissolved	—	—	—	0.012	The specimen dissolved	—	—	
H ₂ SO ₄	10	—	—	—	—	—	0.0075	0.0106	0.1	0.1198	
	20	2.5**	—	0.023	0.78	—	0.0075	0.033	0.21	0.5426	
	40	5.50**	—	The specimen dissolved	—	—	0.0086	0.058	0.56	0.1626	
	80	22.2**	—		—	—	The specimen dissolved	—	0.1262***		

* According to data of /5/.

** At 30° C., according to data of /6/.

*** 20% HNO₃ has been added to the solution.

Comparative experiments were also carried out in pure acid solutions free of oxidation agents.

The oxidizing influence of nitric acid on titanium was determined in solutions varying in concentration from 0.05 to 20 %.

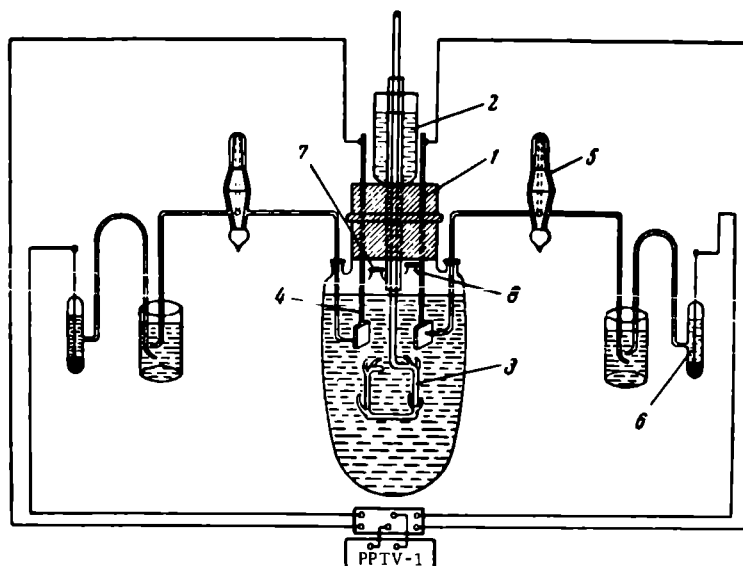


FIGURE 1. Diagram of special electrolytic apparatus

1 — rubber stopper; 2 — hydraulic valve; 3 — mixer; 4 — electrode; 5 — electrolytic valve; 6 — normal calomel electrode; 7 — outlet to the bubbler; 8 — outlet to the cooler.

The unalloyed titanium used was the VT-1 technical grade.

In cooperation with the State Institute for the Scientific Investigation of Rare Metals (Giredmet), the authors investigated the influence of some alloying elements (0.1 to 0.2 % Pd; 20 % Mo; 45 % Nb; 20 % Ta) on the corrosion resistance of titanium in chlorine-containing solutions of hydrochloric acid, to which unalloyed titanium is highly resistant.

Results

The experiments showing the effects of oxidation agents on the corrosion of VT-1 titanium in solutions of hydrochloric and sulfuric acids (Table 1), and the data on the electrochemical measurements of the potentials indicate that oxygen inhibits the corrosion of titanium only in dilute solutions of hydrochloric (5 to 10 %) and sulfuric (10 to 20 %) acids, and at temperatures not exceeding 20°C.

The corrosion velocity of titanium under these conditions is reduced about 7 to 17-fold* and does not exceed 0.05 to 0.023 g/m² · hour**. The increase in temperature leads to a sharp drop in the passivating action of oxygen: at 60°C the corrosion velocity of titanium, in a 5 % solution of

* [As compared with that in solutions containing no oxygen.]

** [This is not indicated in Table 1.]

hydrochloric acid containing oxygen is increased 121-fold* and at 90°C it is increased 1360-fold*, reaching a velocity of $6.84 \text{ g/m}^2 \cdot \text{hour}$.

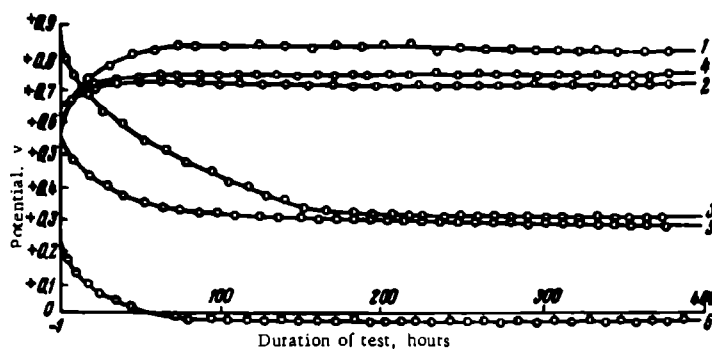


FIGURE 2. The influence of temperature on the electrochemical behavior of titanium in solutions of hydrochloric acid containing chlorine

1 — 12% solution at 20°C; 2 — 12% solution at 60°C; 3 — 12% solution at 90°C;
4 — 18% solution at 20°C; 5 — 18% solution at 60°C; 6 — 18% solution at 90°C.

Molecular chlorine is a considerably stronger oxidation agent [than O_2] and passivates titanium in solutions of hydrochloric and sulfuric acids over a wide range of concentrations and temperatures. Nevertheless, the corrosion resistance and the electrochemical behavior of titanium in the presence of chlorine are also determined by the factors of temperature and acid concentration.

At 20°C titanium is easily passivated in hydrochloric and sulfuric acid solutions of any concentrations containing chlorine except in an 80% solution of sulfuric acid which dehydrates the chlorine.

The corrosion velocity of titanium at 20°C in 10 to 33% hydrochloric acid solutions saturated with chlorine is 0.005 to $0.012 \text{ g/m}^2 \cdot \text{hour}$, i.e., 37 to 71 times lower than in solutions containing no chlorine.

The corrosion velocity of titanium in 10 to 40% solutions of sulfuric acid is very low at 20°C and does not exceed 0.0075 to $0.0085 \text{ g/m}^2 \cdot \text{hour}$. An increase in the concentration of the pure sulfuric acid solution greatly intensifies the dissolution of titanium. Thus, at 30°C the corrosion velocity of titanium in a 40% solution of sulfuric acid is $5.5 \text{ g/m}^2 \cdot \text{hour}$.

The results of the electrochemical measurements show that at 20°C chlorine passivates titanium irrespective of whether the acid is hydrochloric or sulfuric. Under the conditions of the experiment, the potentials of titanium in both acids are very close (from +0.64 to +0.66 v) and the potential-time curves are very similar, i.e., in both cases there is a certain potential increase with time (Figures 2 and 3).

As the temperature increases, the range of concentrations of chlorine-containing solutions of hydrochloric and sulfuric acid, within which titanium is passive, narrows. In a 12% solution of hydrochloric acid saturated with chlorine, the potential of titanium at 20 to 60°C is from +0.78 to +0.65 v. At 90°C the potential decreases with time to +0.37 v (Figure 2, curve 3).

* [As compared with that in solutions containing no oxygen.]

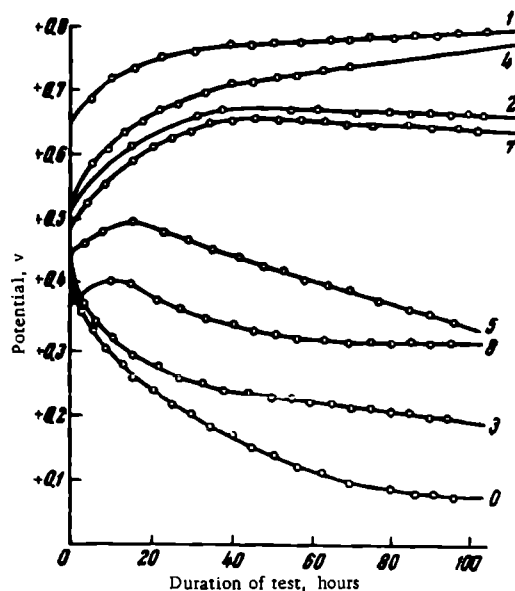


FIGURE 3. The influence of temperature on the electrochemical behavior of titanium in solutions of sulfuric acid containing chlorine

1—10% solution at 20°C; 2—10% solution at 60°C;
3—10% solution at 90°C; 4—20% solution at 20°C;
5—20% solution at 60°C; 6—20% solution at 90°C.
7—40% solution at 20°C; 8—40% solution at 60°C.

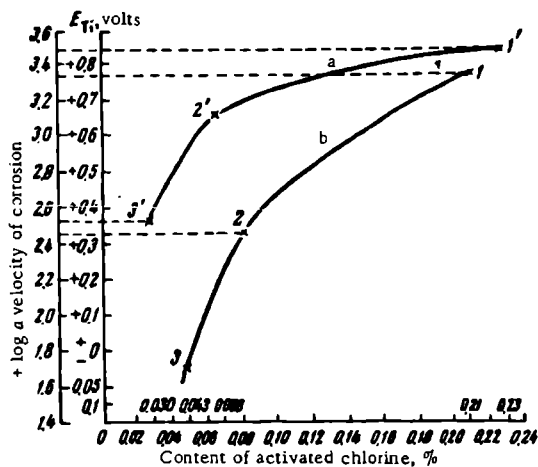


FIGURE 4. Dependence of the potential of VT-1 titanium on the content of activated chlorine in hydrochloric acid

a—12% solution; b—18% solution; 1 and 1'—at 20°C;
2 and 2'—at 60°C; 3 and 3'—at 90°C.

In an 18 % solution of hydrochloric acid the decrease of the potential with time begins at 60°C (the potential is +0.35 v). At 90°C the passivating action of chlorine is insufficient and the potential of titanium acquires a negative value (Figure 2, curve 6).

It was also determined that the amount of active chlorine necessary for the passivation of titanium in hydrochloric acid solution varies with the concentration of hydrochloric acid (Figure 4).

The potential of titanium at 90°C is +0.36 v in a 12 % solution of hydrochloric acid containing 0.03 % of active chlorine, while in an 18 % solution of hydrochloric acid 0.05 % of active chlorine is insufficient for the maintenance of a positive potential, and after 50 minutes of testing it drops to -0.05 v.

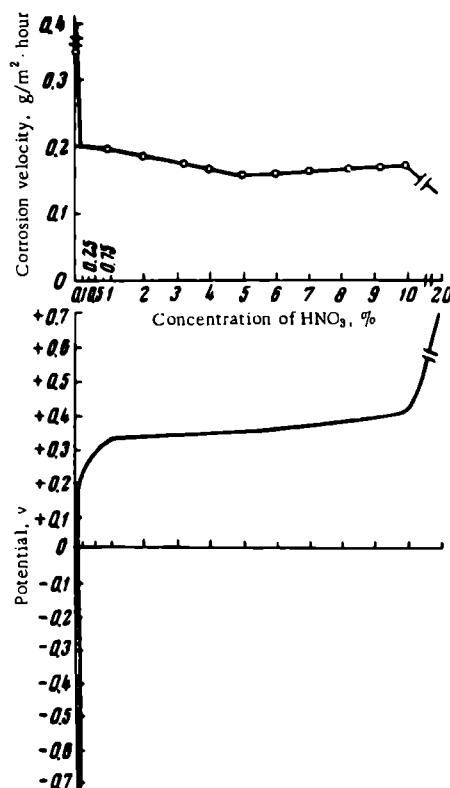


FIGURE 5. Dependence of the corrosion and electrochemical behavior of titanium in an 18 % solution of hydrochloric acid on the content of nitric acid (temperature of test 90°C)

The inhibiting influence of nitric acid on the corrosion of titanium in solutions of inorganic acids also depends both on the concentration of the acid and on the amount of the oxidation agent, i.e., in this case, of nitric acid.

In an 18 % solution of hydrochloric acid titanium is passivated if the solution contains as little as 0.5 % of nitric acid (Figure 5) and the potential of the titanium is then from + 0.18 to + 0.20 v.

An increase in the concentration of nitric acid from 1.0 to 10 % effects little change in the potential of titanium in this medium (from +0.34 to +0.38v), and it may be assumed that a stable passive condition has been reached which can be compared with the condition represented by the vertical sections of the well-known potentiostatic curves for passivated metals when their potentials do not depend on the density of the polarizing current.

If, however, the nitric acid content of the 18 % hydrochloric acid solution approaches 20 %, the potential of the titanium sharply increases and reaches a magnitude of + 0.68 to + 0.72 v.

Figure 6 shows the potential curves of titanium in an 18 % solution of hydrochloric acid containing different oxidation agents (oxygen, chlorine, and 1 % of nitric acid). The data show that if the solution contains 1 % of nitric acid the potential of titanium attains a stable magnitude of + 0.27 to + 0.28 v. As has already been mentioned, the passivating action of chlorine, under the same conditions, is insufficient and the potential of titanium becomes negative (from -0.05 to \approx 0.02 v). [Under these conditions] oxygen promotes no passivation of titanium at all and the potential of the metal immediately becomes negative (-0.68 v).

Thus, at 90°C, the passivating action of oxidation agents on titanium in an 18 % solution of hydrochloric acid decreases as follows: $\text{HNO}_3 \rightarrow \text{Cl}_2 \rightarrow \text{O}_2$.

Corrosion resistance of titanium alloys in an 18 % solution of hydrochloric acid containing chlorine

It has been shown above that an increase in the temperature and concentration of HCl decreases the corrosion resistance of unalloyed VT-1 titanium in solutions of hydrochloric acid containing chlorine.

Considerable data have been published [5,7] indicating that alloying with different elements increases the corrosion resistance of titanium to various media. There are no data, however, on the corrosion resistance of titanium alloys in chlorine-containing solutions of hydrochloric acid. The authors considered it of interest to determine the influence of different alloying elements on the corrosion resistance of titanium alloys under the above-mentioned conditions.

The data obtained on testing titanium alloys containing palladium, tantalum, niobium, or molybdenum are given in Table 2 and in Figure 7.

It will be noted that a titanium alloy with 20 % of Ta has the highest corrosion resistance of all those tested in an 18 % solution of hydrochloric acid saturated with chlorine.

The corrosion velocity of this alloy in an 18 % solution of hydrochloric acid was at 90°C (testing time about 400 hours) not higher than 0.1 mm/year, i. e., 11 times lower than the corrosion velocity of unalloyed titanium (see Table 2). The potential of this alloy under these conditions is from + 0.55 to + 0.45 v (Figure 7) while the potential of unalloyed titanium rapidly decreases [with time] (from -0.05 to 0.1v).

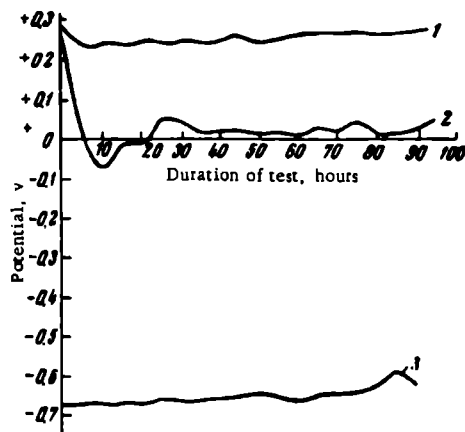


FIGURE 6. Electrochemical behavior of titanium in an 18% solution of hydrochloric acid (temperature of test 90°C) containing oxidation agents

1 — 1% solution of nitric acid; 2 — molecular chlorine; 3 — molecular oxygen.

TABLE 2

The influence of alloying elements on the corrosion resistance of titanium in an 18% solution of hydrochloric acid, containing chlorine, at 90°C (supply of chlorine 40 cm³/min)

Composition of alloy	Duration of test, hours	Corrosion velocity, mm/year		Composition of alloy	Duration of test, hours	Corrosion velocity, mm/year	
		liquid phase	gaseous phase			liquid phase	gaseous phase
Titanium VT-1	83	0.92	0.070	Titanium + 0.2% Pd	377	0.75	0.03
The same	188	0.82	0.054	Titanium + 35% Nb	183	1.52	0.20
" "	282	1.00	0.052	Titanium + 20% Mo	91	1.64	0.50
" "	378	1.14	0.058	Titanium + 20% Ta	95	0.08	0.008
Titanium + 0.01% Pd.	382	0.67	0.02	The same	378	0.09	0.008

Thus, there is good agreement between the data of the electrochemical and the gravimetric investigations in the case of the Ta alloy.

Titanium containing other alloying elements (0.1 to 0.2 Pd; 35% Nb; 20% Mo) showed no satisfactory corrosion resistance under the above conditions. The corrosion velocity of these alloys varies from 0.5 to 1.64 mm/year. The experiments carried out with titanium-molybdenum and titanium-palladium alloys showed no correlation between the potential and the corrosion velocity. Thus, the corrosion velocity of a titanium alloy with 0.1 to 0.2% Pd, in an 18% solution of hydrochloric acid, was

0.75 mm/year (testing time 377 hours), while its potential was from +0.7 to +0.8 v and remained stable during 200 hours. In a number of experiments a sharp potential drop was noted after 200 hours (from +0.05 to 0.15 v).

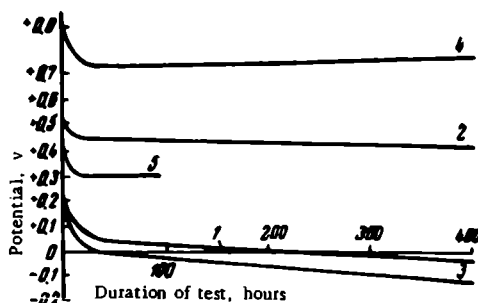


FIGURE 7. Influence of alloying elements on the electrochemical behavior of titanium in an 18 % solution of hydrochloric acid

1 - titanium VT-1; 2 - Ti + 20% Ta; 3 - Ti + 35% Nb; 4 - Ti + 0.1% Pd; 5 - Ti + 20% Mo.

Similar results were given by titanium-molybdenum alloys. The high corrosion velocity (1.64 mm/year) is accompanied by a high positive potential (from +0.30 to +0.46 v).

It may be assumed that the lack of correlation between the potential and the corrosion velocity of the alloy is caused by a nonuniform distribution of alloying elements in the alloy. This assumption, however, requires verification.

For titanium alloys with 35 % Nb there is, as in the case of titanium-tantalum alloys, a full correlation between the corrosion velocity and the potential of the alloy. At a corrosion velocity of 1.52 mm/year the potential of this alloy changes from +0.1 to -0.2 v.

The corrosion resistance of titanium alloys with 35 % of Nb is thus seen to be considerably lower than that of unalloyed titanium.

Welded specimens of a titanium alloy with 20 % Ta were tested under conditions of acid chlorination. No traces of corrosion were found after 1500 hours of testing, either in the basis metal or in the thermal zone of the weld.

It is, therefore, clear that only titanium alloys with 20 % Ta have, at 90°C, a sufficiently high corrosion resistance in 18 % solutions of hydrochloric acid saturated with chlorine.

Conclusions

1. It was determined that only such active oxidation agents as humid chlorine and nitric acid can bring about, under certain conditions, a passivation of titanium in solutions of hydrochloric and sulfuric acids. Oxygen has insufficient oxidizing power and no passivating effect on titanium.

2. Determinations were made of the ranges of concentrations and temperatures at which titanium and its alloys are resistant in solutions of hydrochloric and sulfuric acid containing chlorine.

Titanium preserves a positive potential (from +0.68 to +0.02 v) in the following solutions saturated with chlorine: in 10 to 12 % HCl solutions up to 90°C, in 18 % solutions of HCl at 20 to 60°C, and in 33 % HCl solutions only up to 20°C.

In 10 and 20 % sulfuric acid solutions containing chlorine, the positive potential of titanium is maintained at 20 to 90°C while in a 40 % H₂SO₄ solution the potential only remains positive up to 60°C.

3. It has been shown that titanium is easily passivated in an 18 % solution of hydrochloric acid at 90°C if the medium contains from 0.5 to 1.0 % nitric acid (the potential is from +0.18 to +0.38 v). An increase in the concentration of nitric acid up to 10 % has almost no influence on the potential of Ti but at 20 % HNO₃ the Ti potential has risen markedly.

4. Among the titanium alloys investigated, containing palladium, molybdenum, tantalum, and niobium, only the alloy with 20 % Ta is corrosion resistant at 90°C, in an 18 % solution of hydrochloric acid saturated with chlorine. Under these conditions the potential of this alloy is positive (from +0.35 to +0.45), while the potential of unalloyed titanium is negative (up to -0.10 v). None of the other alloying elements mentioned increases the corrosion resistance of titanium.

Bibliography

1. Cotton, J. B. and H. Bradley. — J. Chem. Ind., 31(3):68. 1958.
2. Fischer, W. R. and O. Ruediger. — Z. Elektrochem., 62(647):803. 1958.
3. Fischer, W. R. — Werkstoffe u. Korrosion, No. 4:243. 1959.
4. Tseitlin, Kh. L. and V. A. Stunkin. — ZhPKh, 33(12):2796. 1960.
5. Andreeva, V. V. and V. I. Kazarin. Nove konstruktivnyye khimicheski stoikiye metallicheskie materialy (New Chemically Resistant Constructional Metals). — Goskhimizdat. 1961.
6. Moroz, L. S., B. B. Chechulin and I. V. Polin. — Sbornik "Titan i ego splavy", Vol. 1:174, Sudpromgiz. 1960.
7. Stern, M. — J. Electrochem. Soc., 106(9):755. 1959.

III. MECHANICAL AND TECHNOLOGICAL PROPERTIES OF TITANIUM ALLOYS

N67 11786

DEPENDENCE OF THE ELASTIC PROPERTIES OF TITANIUM ALLOYS ON THEIR COMPOSITION AND STRUCTURE

S. G. Fedotov

In any investigation of the reactions of titanium with other alloying elements it is important to examine those characteristics which most closely reflect the relationship between the interatomic bonds and the chemical composition of the alloy in the equilibrium and metastable conditions during both heating and cooling. Among these characteristics the most important are the elasticity constants.

The strength of interatomic bonds, the changes taking place in the elementary crystal unit and the changes in the forces of interatomic reaction caused by alloying, heat treatment, and mechanical or thermomechanical treatment influence many physicommechanical properties of alloys. A consideration of these relationships must form the basis for the development of new alloys with improved properties.

The importance of [interatomic] binding forces in the evaluation of the elasticity constants was indicated by the work of Lozinskii and Fedotov /1/, who demonstrated the direct relationship between the indentation hardness and the modulus of normal elasticity in a large group of pure metals over a wide range of temperature.

In addition, consideration should be given to the opinions expressed by N. S. Kurnakov et al /2, 3/ in 1913 and much later also by P. P. Lazarev /4/, to the effect that the indentation hardness and the modulus of elasticity are closely interconnected.

Titanium has relatively low elasticity constants. Thus, for instance, the modulus of normal elasticity of this metal (about 11,500 kg/mm²) is almost half that of iron, nickel, or cobalt (about 22,000 kg/mm²), although titanium has a higher melting point. Therefore the development methods for increasing the modulus of elasticity of titanium presents an urgent problem.

Several works have been devoted to the investigation of the influence of alloying elements on the modulus of normal elasticity of titanium. H. R. Ogden et al /5/ have explored the relationship between the modulus of elasticity of alloys of α -Ti (with 2.5 and 5 weight % Al) and of γ -Ti (37 weight % Al) and their Al contents at both room and at elevated temperatures.

Graft, Levinson, and Rostoker /6/, confirmed the data given in an earlier investigation /5/ showing the beneficial influence of aluminum on the modulus of elasticity of titanium alloys. They also investigated the influence of many other elements on this characteristic. They showed that oxygen (up to 0.6 weight %) and nitrogen (up to 0.73 weight %) increase,

to a small extent, the modulus of elasticity of α -Ti alloys, and that the influence of vanadium, which widens the field of β -solid solutions, on the elastic properties of hardened alloys is rather complex. In order to improve further the modulus of elasticity of titanium alloys, Brooks, Lewis and Forsyth /7/ investigated the elastic properties of Ti-C and Ti-Al-C alloys. The influence of tin (up to 10 weight %) on the Young modulus of α -solid solutions has been investigated by Bungardt and Weigand /8/.

Among the various studies of the elastic properties of titanium alloys those of Knorr and Scholl /9/ are noteworthy. These workers carried out a detailed investigation of the influence of vanadium and molybdenum on the modulus of normal elasticity and on the logarithm of the damping decrement of titanium alloys at room and elevated temperatures after annealing and hardening from the β -field.

However, the available data on this subject are insufficient, since no systematic investigations of the problem have been carried out. The insufficient attention paid by investigators to problems concerning the elastic properties of alloys is apparently due to the old-established and still prevailing opinion that the elastic properties are little influenced by the composition and the structure of the alloys. Even now, some authors are of the opinion that attempts to change the modulus of elasticity of metals by alloying are useless /10/. Morton K. Smith /10/ maintains that the change in the modulus of elasticity caused by heat treatment is so small as to be without technical significance and can be ignored altogether.

It has already been mentioned that some investigations /6, 9/ have shown that considerable changes in the modulus of elasticity of titanium alloys can be achieved by heat treatment. In the work reported in the present paper, it has likewise been found that the elastic properties of titanium alloys (both the Young modulus and the shear modulus) can be almost doubled (by alloying) or decreased (by hardening) as compared with those of the pure metal. Changes of this nature in the elastic properties of alloys are due to alterations in their structure. The investigation of the relationship between the elastic properties of alloys and various other factors, as part of a more comprehensive approach, will therefore provide the possibility of elucidating many phenomena characteristic of the chemical reactions between the elements. A study of the elastic properties of metals and alloys will facilitate, in the opinion of the author, the determination of the conditions and the mechanism of formation of metastable phases, which are a notable feature of titanium alloys.

The present paper will include results of an investigation of the elasticity coefficients of titanium and of binary titanium alloys of the Ti-Mo, Ti-V, Ti-Nb, Ti-Al, and Ti-Sn* systems.

- * The experimental data on the alloys of the Ti-Mo, Ti-V, and Ti-Nb systems have been obtained with the participation of O. K. Belousov; those on the alloys of the Ti-Al and Ti-Sn systems were obtained in cooperation with T. T. Nartova and E. P. Sinodova; the investigation of the properties of titanium was carried out with the participation of E. P. Sinodova.

Preparation of the alloys and methods of investigation

The 30- to 35-g alloy specimens were smelted in an atmosphere of argon in an arc furnace equipped with stable tungsten electrodes. Each alloy was smelted not less than 3 times. The basis metal for the preparation of the alloys was titanium sponge TG00 (99.85 % Ti), with the following impurities: 0.002 % H₂; 0.04 % N₂; and 0.09 % Si.

The molybdenum used contained 99.9 % and the vanadium 99.5 % of the base metal, with the following impurities in the latter case: 0.04 % Fe, 0.005 % Al, 0.02 % Si, 0.1 % C, 0.3 % O₂, and 0.01 % N₂. The niobium contained 99.4 % pure metal (impurities: 0.2 % Ta, 0.06 % Si, and 0.05 % Fe). The AV000 aluminum contained 99.9 % of the pure metal.

The ingots of titanium (obtained by high-temperature magnesium reduction) and of its alloys, with molybdenum, vanadium, or niobium of various compositions, were heated in the air to 900-1100°C and forged into rods from which cylindrical specimens were turned.

Specimens of titanium alloys with aluminum and tin (with 12 weight % Al and 25 weight % of Sn) were prepared from forgings. Alloys with higher contents of aluminum and tin were not forged but cast in an atmosphere of argon. Titanium metal, obtained from the iodide, was mechanically worked after heating the ingots in an arc furnace in argon.

These titanium specimens were annealed at 900°C for 2 hours, at 800°C for 10 hours, and at 600°C for 10 hours. Alloys of titanium with molybdenum, vanadium, or niobium were also annealed at 600°C for 400 hours after quenching in water from 900°C (holding time 24 hours) and measurement of the elasticity coefficients at room temperature.

Titanium alloys with aluminum and tin were given the following heat treatment: heating at 1100°C for 50 hours, at 1000°C for 100 hours, at 800°C for 300 hours, and at 600°C for 500 hours with a final slow cooling to room temperature.

Annealing was carried out under vacuum in quartz ampoules.

The composition of the alloys was checked by comparing the weights of the initial materials with that of the ingot and also by measuring the density of the ingot by the hydrostatic method.

The method of determining the elasticity coefficients involved exciting in the specimen longitudinal, transverse, and torsion vibrations.

The modulus of normal elasticity E and the modulus of shear G were calculated from the following formula

$$E = 1.6379 \frac{P}{l} \cdot \left(\frac{l}{d}\right)^4 \cdot 10^{-8} f^2 \text{ kg/mm}^2,$$

where f = frequency of natural transverse vibrations, hertz, and

$$E \text{ or } G = 5.1916 \frac{P}{l} \cdot \frac{l}{d^2} \cdot 10^{-8} f^2 \text{ kg/mm}^2,$$

where f = frequency of natural transverse vibrations for the calculation of the modulus of elasticity E , and the frequency of natural torsional vibrations for the calculation of the shear modulus G ;

P = weight of specimen, g;

l = length of specimen, cm;

d = diameter of specimen, cm.

The Poisson ratio μ was found from the formula

$$\mu = \frac{1}{2} \cdot \frac{E}{G} - 1 \quad \text{or} \quad \mu = \frac{1}{2} \left(\frac{f_{\text{long}}}{f_{\text{tors}}} \right)^2 - 1.$$

The frequencies of natural transverse, longitudinal, and torsional vibrations were determined by the resonance method using the "Elastomat" apparatus produced by the Förster Company /11, 12/ and an electron computer with an accuracy of one hertz.

The magnitudes of the modulus of elasticity obtained in this investigation are given on the basis of measurements of frequencies of natural transverse vibration.

The total error of the elasticity modulus determinations, including the weighing and measuring of the specimen was not higher than 1.0%.

Elastic properties of titanium

The elastic properties of titanium have been studied by many investigators /13-16/. Some of these data are given by McQuillan and McQuillan /17/. These authors are of the opinion that the modulus of elasticity is most probably $E = (11.2 \pm 0.035) \cdot 10^3 \text{ kg/mm}^2$, while the shear modulus $G = (3.94 \pm 0.1) \cdot 10^3 \text{ kg/mm}^2$. The Poisson ratio $\mu = 0.36$.

The elasticity constants obtained by the present author (Young's modulus, shear modulus, and the Poisson ratio) for titanium (obtained from the iodide) resmelted in an arc furnace and worked in an atmosphere of argon and also those for TG00 titanium sponge smelted either in a laboratory arc furnace with stable tungsten electrodes, or in an ore furnace with consumable electrodes, are given in the table, page 203. Data are given for forged specimens as well as after annealing by the above-mentioned process.

These data show that iodided titanium has a lower Young's modulus ($E \approx 11,200$) and a lower shear modulus ($G \approx 4270$) than annealed titanium obtained by the high-temperature magnesium method ($E \approx 11,700$ and $G \approx 4400$). While the modulus of elasticity of TG00 titanium is identical for both melts [tungsten electrode and consumable electrode] the shear modulus of titanium molten in the arc furnace with a consumable electrode is much higher. In the latter case, the Poisson ratio $\mu \approx 0.30$. Even more notable are the differences between the elasticity constants of forged and annealed titanium. The lower Young's modulus and shear modulus of forged specimens is possibly due to the residual internal stresses and also to the texture formed during forging.

The differences in the elastic properties of iodide titanium and of both melts of TG00 titanium are apparently due to the different amounts of impurities, particularly gaseous, in the metal. Oxygen and nitrogen, which form interstitial [solid] solutions with titanium slightly increase its elasticity constants.

* Elastic properties of alloys of the binary Ti-Mo, Ti-V, and Ti-Nb systems

Reviews of investigations carried out on the chemical reactions between titanium and molybdenum, vanadium or niobium, are given by various authors /17-20/. Mo, V, and Nb have a low solubility in α -titanium but have an unlimited solubility in β -titanium.

Modulus of elasticity and shear modulus of titanium*

Designation or method of preparation of titanium	E , kg/mm ²	G , kg/mm ²	μ
Iodide	<u>11 236</u>	<u>4278</u>	<u>0.313</u>
	11 169	4268	0.308
The same (in the annealed condition) . .	11 153	4237	0.311
TG00 (smelted in a furnace with a tungsten electrode)	<u>11 222</u>	<u>4248</u>	<u>0.321</u>
	11 752	4488	0.309
The same	<u>11 166</u>	<u>4318</u>	<u>0.293</u>
	11 722	4476	0.309
"	<u>11 238</u>	<u>4116</u>	<u>0.365</u>
	11 693	4389	0.332
"	<u>11 122</u>	<u>4271</u>	<u>0.302</u>
	11 686	4410	0.325
"	<u>11 104</u>	—	—
	11 685	4307	0.356
"	<u>11 145</u>	<u>4205</u>	<u>0.325</u>
	11 731	4421	0.327
TG00 (smelted in a furnace with a consumable electrode)	<u>11 863</u>	<u>4505</u>	<u>0.317</u>
	11 768	4538	0.297
The same	<u>11 709</u>	<u>4565</u>	<u>0.290</u>
	11 744	4535	0.295
The same (in the annealed condition) . .	11 760	4493	0.309

* The properties of forged metal are given above the line, those of the annealed metal below the line.

The phase diagrams of the Ti-Mo, Ti-V, and Ti-Nb systems are very similar as far as the reactions between the elements are concerned. The differences exist only as regards the solubilities of molybdenum, vanadium and niobium in α -Ti and the extent of the respective $\alpha + \beta$ fields. At 600°C, the solubility of molybdenum in α -Ti is less than 1 weight %, that of vanadium about 2 to 3 weight %, and that of niobium up to 4 weight %. The phase boundary $\alpha + \beta \rightleftharpoons \beta$ of binary titanium alloys corresponds at 600°C approximately to 30 weight % Mo, to somewhat more of vanadium, and to 45 to 50 weight % Nb.

In all three systems the hardening of alloys from the β -field produces a number of metastable phases with an identical structure. The relationship between the temperatures of the martensitic transformations and the compositions of the alloys was investigated by Duwez /21/.

In view of the foregoing, a comparison of the elasticity constants of Ti-Mo, Ti-V, and Ti-Nb alloys, in the equilibrium condition and in the metastable condition, is of great importance.

Consideration will now be given to the dependence of the elasticity modulus E , of the shear modulus G , and of the density of the alloys at room temperature, both after prolonged annealing and after hardening from 900°C, on their compositions and these data will be compared with the phase diagram (Figure 1).

It is evident from the graphs that, for each condition, the elasticity constants vary qualitatively in the same way in all three systems depending on the composition and structure of the alloys. In the equilibrium condition both the elasticity modulus and the shear modulus continuously decrease with the increase in the content of molybdenum, vanadium, and niobium in the titanium alloy.

The elasticity modulus of binary alloys containing 1 at. % of alloying elements is approximately as follows: 60 kg/mm² for Ti-Mo alloys, 65 kg/mm² for Ti-V alloys, and 100 kg/mm²* for Ti-Nb alloys.

These data indicate that if the alloys contain a β -solid solution, their elasticity constants decrease and that this decrease is approximately proportional to the quantitative relationship between the α and β phases. This also indicates that the β -solid solution which has a cubic body-centered structure has a lower elasticity modulus than the α -solid solution with its close-packed hexagonal lattice.

The slower decrease in the elastic properties of two-phase Ti-Mo alloys with the increase in the molybdenum content indicates that the β -solid solution is strengthened to a greater degree by molybdenum than by vanadium, while the β -solid solution with niobium is the weakest of all three. The different values for the elasticity modulus of homogeneous β -solid solutions corresponding to the amounts of molybdenum, vanadium, or niobium required to bring about the $\alpha + \beta \rightarrow \beta$ transformation supports this conclusion.

If the elasticity modulus-composition curves of annealed alloys are compared with the corresponding phase diagrams a curious similarity is seen in the variation of the $\alpha + \beta \rightleftharpoons \beta$ temperature versus concentration curve and the property versus concentration curves. Both the phase transformation temperature and the elasticity curves decrease continuously with increasing concentration of the alloying element. For alloys of the Ti-Mo system these curves are concave towards the abscissa while for the other two systems the curves are convex towards the abscissa.

The similarities of the curves representing these three systems indicate a correlation between the systems. The properties measured reflect the respective interactions between titanium and molybdenum, vanadium and niobium.

The relationship between the elastic properties of hardened alloys and their composition (see Figure 1) is quite different from that of alloys in an equilibrium condition.

In the hardened condition, all three elements — molybdenum, vanadium, and niobium at first sharply decrease (almost to half) the elasticity constants of the alloys, then with the same suddenness these constants are restored to the initial magnitudes or even higher. There

* [According to Figure 1, $E = 11,500$ to $12,500$ kg/mm².]

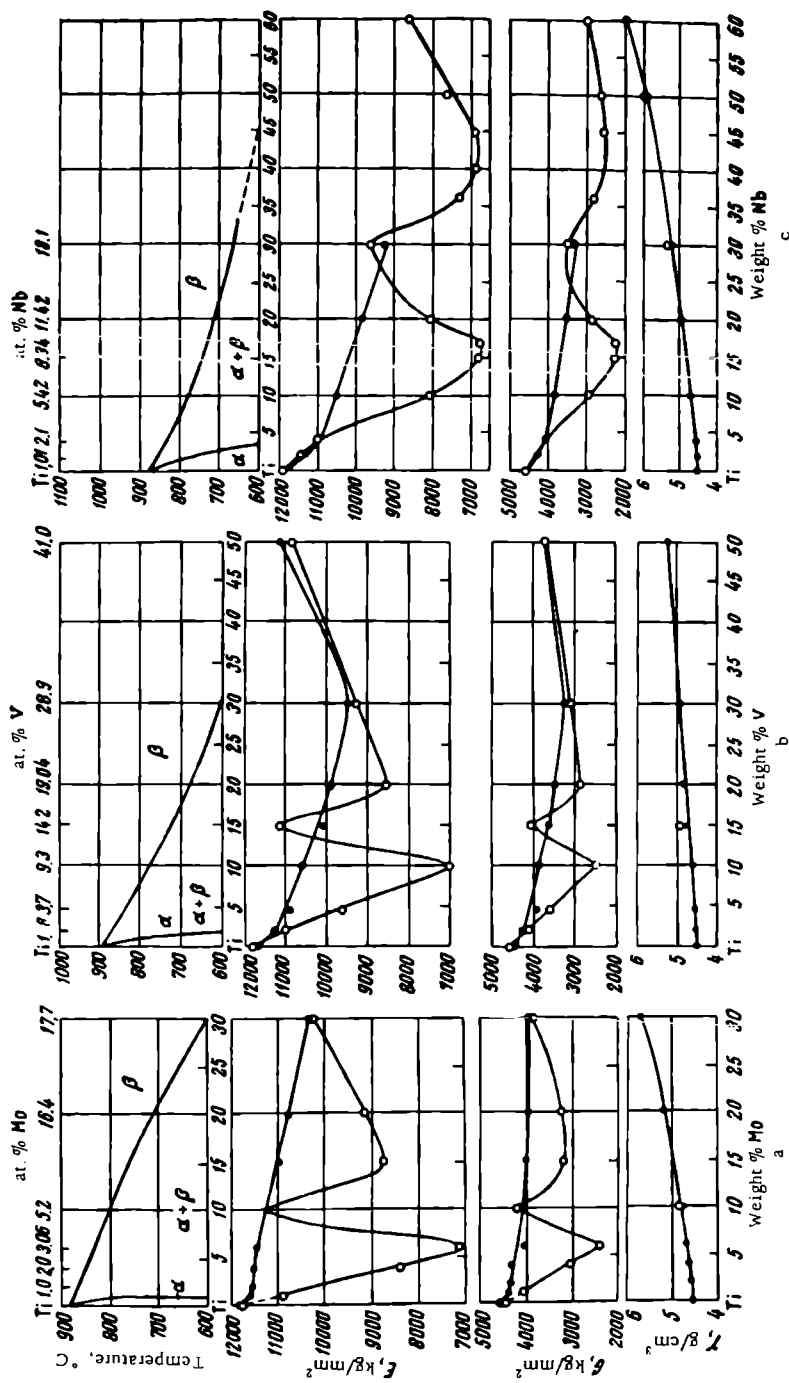


FIGURE 1. Phase diagram and relationship between Young's modulus E , shear modulus G , and density γ of alloys after prolonged annealing, and quenching at 900°C

a—Ti-Mo system; b—Ti-V system; c—Ti-Nb system; ●—annealing at 600°C; ○—annealing at 900°C; — quenching at 900°C.

follows a further decrease and finally there is a continuous increase of elasticity in the β field, apparently up to the level of the elastic constants of the pure metals — molybdenum, vanadium, and niobium.

It should be pointed out that the variation of the elastic properties of hardened alloys is identical for all three systems. The difference is only in the length of certain sections of the concentration-property curves of the Ti-Mo, Ti-V, and Ti-Nb systems.

The rather unusual nature of the variations in the elasticity constants of hardened titanium alloys is a consequence of their structure.

It has already been mentioned that titanium, alloyed with various transition metals, forms a number of metastable phases when the several alloys are hardened from the β field. According to Yu. A. Bagaryatskii, G. I. Nosova, and T. V. Tagunova /22, 23/, the Ti-Mo, Ti-V, and Ti-Nb alloys have the following metastable phases: α' , α'' , ω , and β . They give the following description of these phases /22, 23/.

The α' phase is a supersaturated solid solution of α -Ti with a hexagonal crystal lattice. The presence of the α' phase considerably increases the hardness of the alloys.

The α'' phase differs from the α' phase by the fact that it has a rhombic rather than a hexagonal lattice, as a result of the supersaturation of the α -solid solution with alloying elements. This phase is formed only in titanium alloys containing those transition elements, the atomic radii of which are close to the atomic radius of titanium (V, Nb, Ta, W, Mo, Re). Alloys containing an α'' phase are considerably softer than those with an α' phase.

The presence of the ω phase which has a hexagonal crystal structure, can be determined only by X-ray diffraction analysis. Like the α' phase, it is formed in all titanium alloys containing transition elements, but only at a certain critical concentration; the ω phase strongly increases the hardness of the alloys but makes them more brittle.

All three metastable phases (α' , α'' , and ω) are martensitic. They are formed during hardening from 1000°C and, according to Bagaryatskii et al /22, 23/, at the following concentrations of the alloying element (in atomic %):

	α' phase	ω phase
Mo	2-4	4-5
V	9-10	11-15
Nb	8-15	17-18

It is apparent that at lower contents of molybdenum, vanadium, and niobium, an α' phase is formed and at higher contents of these elements a metastable β phase is formed.

In their studies of the stabilization of the β -solid solution in titanium alloys, N. V. Ageev and L. A. Petrova /24, 25/ give the following minimum concentrations of alloying elements necessary for the production of a single-phase, metastable β -solid solution at room temperature: 5.8 at. % Mo, 18.4 at. % V, and 23 at. % Nb. These data show that a sharp decrease in the elasticity constants of alloys of all three systems is due to the formation of α' and α'' phases. On the other hand, alloys containing the ω phase have the maximum elastic properties. The second minimum (see Figure 1) corresponds to the formation of the metastable β -solid solution.

The sharp decrease in the elastic properties of hardened alloys with high contents of molybdenum, vanadium, and niobium is due to the deformation of the hexagonal crystal lattice as a result of the supersaturation of the α -solid solution. A large supersaturation of the α -solid solution causes a considerable deformation of the lattice and consequently a sharp decrease in the elastic properties. The residual β phase, the amount of which increases with the increase in the content of alloying elements, will also contribute to this decrease. Obviously it may be concluded that the first minimum on the curves of elastic properties will correspond to the maximum value of the permissible deformation of the hexagonal α phase lattice. This maximum deformation can apparently be quantitatively determined by the d/a ratio. A minimum of the elastic properties corresponds to the maximum content of alloying elements above which the hexagonal crystal lattice loses its elastic stability.

Another, very important feature of the curves is that this minimum value of elasticity is practically the same for all three systems. This means that the maximum permissible deformation of the α lattice is identical for all three systems and does not depend on the alloying element.

It may be expected that in this case the d/a ratio will be constant.

Since the elasticity constants of hardened alloys change continuously, the author is of the opinion that the necessary conditions for the precipitation of an α'' phase as an independent metastable phase are lacking. The fact that alloys containing an α'' phase are (according to Yu. A. Bagaryatskii and others), softer than alloys with a lower concentration [of alloying elements] (and containing an α' phase) is due to the low strength of interatomic bonds (low elasticity constants). In fact, there will be nothing extraordinary if in other alloys of titanium containing transition elements and hardened from the β phase there will be no hardness decrease upon transformation from the α' -solid solution to the ω phase. The increase or decrease in hardness will depend on the degree to which the elasticity constants have decreased.

Consideration will now be given to another very important problem connected with the formation of the ω phase.

The high elasticity constants caused by the formation of the ω phase are due to a metastable condition of a different type than that connected with the formation of the α phase.

While the metastable condition related to the α' phase is due to the supersaturation of the α -solid solution of titanium as a result of the completed $\beta \rightarrow \alpha$ martensitic transformation, the metastable ω condition is the result of an incompleting polymorphic $\beta \rightarrow \alpha$ transformation. The dynamic forces of polymorphism have not completed the $\beta \rightarrow \alpha$ transformation and, therefore, hardened alloys with an ω phase have a higher density than alloys in the equilibrium condition and have no acicular structure.

The second minimum on the elasticity constant curves correspond, as already mentioned, to the formation of a single metastable β phase. The stronger binding forces in β -solid solutions with a minimum concentration of molybdenum, vanadium or niobium are sufficient to exceed the forces of the $\beta \rightarrow \alpha$ transformation and to preserve a β phase stable under the given conditions. A further increase in the concentration of the alloying elements (i.e., of pure molybdenum, vanadium, or niobium) naturally leads to an increase in the elasticity constants to magnitudes nearer to those of the pure metals.

Aluminum seems to be the most effective strengthening constituent of titanium alloys and notably increases their heat resistance.

Despite the numerous investigations on the Ti-Al phase diagram the nature of the chemical reaction between these two elements which differ so greatly in physicochemical properties, has not yet been elucidated. There is no unanimous opinion as to either the compositions of the intermetallic compounds or the conditions of their formation. The structure of titanium-rich alloys has also not yet been determined.

Nevertheless, Sagel, Schulz and Zwicker /26/ have shown that there are concentration fields (6 to 12 weight % Al and about 18 weight % Al) over which the [normal] variation of properties is interrupted. Later, N. V. Grum-Grzhimailo, I. I. Kornilov, E. N. Pylaeva, and M. A. Volkova /27/ investigated the Hall constants of Ti-Al alloys and likewise found inflection on the curves corresponding to compositions with 14.3 at. % (9 weight %) Al and with 25 at. % (16 weight %) Al. In their opinion /27/, these compositions correspond to the Ti_3Al and Ti_5Al intermetallic compounds.

The investigations of the relationship between the elastic properties of alloys of this system and their composition (Figure 2) lead to the conclusion that aluminum decreases the specific gravity of the alloys, and increases the Young modulus and the shear modulus. There is also a tendency to decrease the Poisson ratio.

It should be pointed out that the curves representing the relationship between the elasticity constants of alloys and their composition up to 26 weight % Al are not uniformly continuous, but show inflections, a maximum, and other specific features. Curves of this nature, reflecting as they do the complex chemical reactions between titanium and aluminum, obviously indicate a more complex structure of

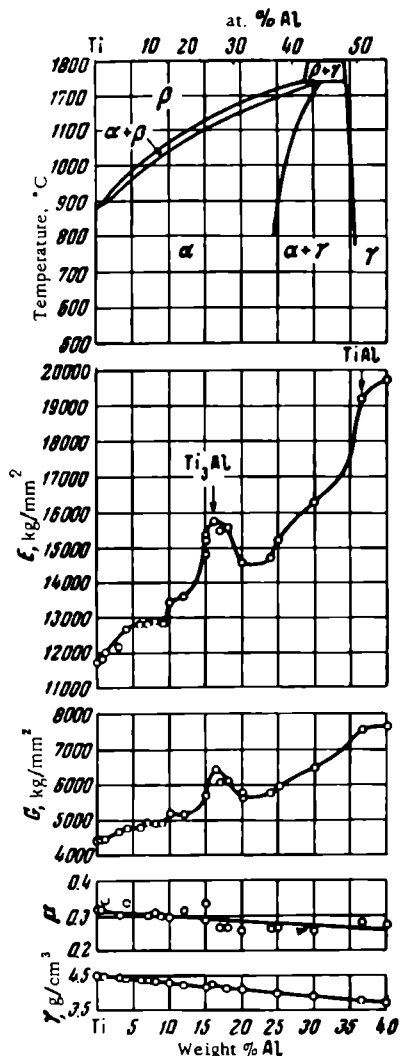


FIGURE 2. Phase diagram and the dependence of the Young modulus, E , shear modulus, G , Poisson ratio, μ , and the density of alloys, γ , on the composition of Ti-Al alloys

Ti-Al alloys. This is contrary to previous opinions (cf. phase diagram in Figure 2 and data in /28/) according to which these alloys consisted of a single-phase α -solid solution.

A closer look at the relationship between the elastic properties of alloys and their composition shows that relatively small additions of aluminum (up to 5 to 6 weight %) greatly increase the elastic properties which then, up to 9 weight % of Al, remain almost unchanged. An increase from 9 to 10 weight % Al causes a sudden increase in the elasticity constants. If the content of aluminum is further increased, the curves representing the dependence of the Young modulus and of the shear modulus on the composition of the alloy pass through a steep maximum at 16 weight % Al, corresponding on the ordinate to the intermetallic compound of composition Ti_3Al .

Alloys with 20 to 25 weight % Al have somewhat lower elastic properties. The transition into the $\alpha+\gamma$ fields entails a rapid increase in the magnitude of the elasticity coefficients. The maximum elasticity modulus (19,000 kg/mm²) in the investigated part of the Ti-Al system corresponds to alloys on the basis of $TiAl$ with an ordered tetragonal structure. Thus, it has been determined that the elasticity modulus of this compound is almost twice as high as that of unalloyed titanium. This indicates a high chemical binding force between the atoms of the $TiAl$ compound.

Since the increase in the aluminum content causes an increase in the elastic properties of the α phase and also a considerable increase in the temperature of the $\alpha \rightarrow \alpha + \beta$ transformation, the author is of the opinion that, as in the case of other systems (Ti-Mo, Ti-V, and Ti-Nb, see Figure 1), there is a correlation between these characteristics reflecting the nature of the reaction between titanium and aluminum. The acceptance of such a relationship between the elastic properties and the compositions of the alloys, implies that a considerable change should be expected in the field of the phase diagram of the Ti-Al system and also in the curve representing the temperatures of $\alpha \rightarrow \alpha + \beta$ transformations.

Elastic properties of Ti-Sn alloys

Tin is often added to titanium alloys as a strengthening constituent, despite its own low melting point and low resistance to plastic deformation. If added in small amounts (about up to 2 to 4 weight %), tin has little influence on the mechanical properties of the alloy. A further increase in the tin content, in α -Ti up to saturation, leads to a considerable strengthening of the alloy, particularly at high temperatures [29, 30].

These data serve to demonstrate (as is also the case with Ti-Al alloys) that changes in the physicomechanical properties of an alloy and particularly in its strength, are due not to the strength characteristics of the alloying element, but to chemical reactions between different atoms.

The relationship between the elasticity constants and the composition of Ti-Sn alloys over a wide range of compositions (including the Ti_3Sn field), both at room and high temperatures, are given in Figure 3. These data (Young's modulus, shear modulus, Poisson's ratio, and the density) can be compared with the phase diagram of the Ti-Sn system.

It can be seen that addition of a small amount of tin to the α -solid solution of titanium causes a small reduction in the elasticity but as the concentration of tin approaches its maximum solubility in solid solutions, a certain increase in the elasticity constants takes place.

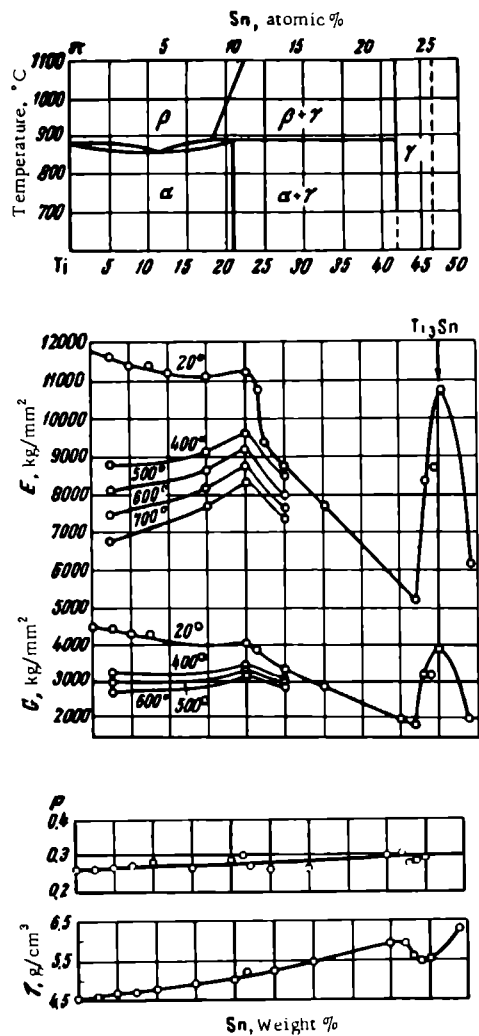


FIGURE 3. Phase diagram and the dependence of the Young modulus E , of the shear modulus G , the Poisson ratio μ , and the specific gravity of Ti-Sn alloys on their composition

The transition to the $\alpha + \gamma$ field entails a sharp decrease in the elasticity coefficients. The intensive, almost linear decrease of the elasticity constant of the two-phase alloys, which is connected with the increase in the amount of the (second) γ phase formed during crystallization continues up to the phase boundary of the homogeneous γ field of solid solutions on the basis of the $Ti_{13}Sn$ intermetallic compound. The stoichiometric composition of $Ti_{13}Sn$ corresponds to a high maximum of elastic properties.

Thus, the investigation of the elasticity constants of alloys of the Ti-Sn system with the above-mentioned compositions has resulted in the identification of three fields comprising different phases and having greatly differing properties.

First of all, the minimum of the elasticity curve of α -phase alloys indicates the existence of at least two conflicting factors. These factors are mainly electrochemical and geometrical. The addition of tin influences the electrochemical properties by increasing the binding forces, but the differences between the atomic dimensions of titanium and tin (spatial factor +7) /17/ lead to a deformation of the crystal lattice and to a decrease of the elastic properties. The total action of these two factors depends also on the amount of alloying atoms dissolved. Consequently, the elasticity modulus curves, which reflect the reaction between titanium and tin over a wide field of α -solid solutions, show a maximum point.

Attention is also drawn to the similarities in the variation of the elasticity modulus curves and of the temperature curve of the $\alpha \rightleftharpoons \alpha + \beta$ transformation which have a minimum at the same composition [for 20°C].

It is also important to determine the causes for the sharp decrease in the elastic properties of certain solid solutions in the γ field although their composition differs little from the stoichiometrical relationship corresponding to the Ti_3Sn compound. The latter has a hexagonal crystal lattice /32/, with the following parameters: $a = 5.916 \text{ \AA}$, $c = 4.76 \text{ \AA}$, and $c/a = 0.805$. The alloys belonging to the γ field have an ordered structure with a close-packed Ti_3Sn lattice /33/.

No special investigation has been carried out by the author to elucidate this problem. By analogy with the known data on the variation of a number of properties (electrical, mechanical, specific gravity, etc.), of solid solutions with a defective structure, based on NiAl in the Ni-Al system /34, 35/ and on NiSb in the Ni-Sb system /36/, it may also be assumed that similar solid solutions exist on the basis of Ti_3Sn . This assumption is confirmed by the variation of the specific gravity of Ti-Sn alloys in the γ field (see Figure 3). Solid solutions with a defective crystal lattice were discovered by Bradley and Taylor /37/, and their formation was theoretically explained by S. T. Konobeevskii /38/.

The variation of the elastic properties of two-phase alloys is determined by the properties shown by each of the phases separately and by their relative amount. In the present case this variation is an approximately additive function. The formation in the alloy of a γ -terminal solid solution (second phase) with low elastic constants, leads to a sharp drop in the elastic properties of the alloys. This decrease is proportional to the amount of the second phase in the alloy.

The curves representing the dependence of the Young modulus, the shear modulus, and the Poisson ratio on the temperature in α -solid solution alloys containing 2.5, 15, or 20 weight % Sn and for two-phase $\alpha + \beta$ alloys with 25 weight % Sn (Figure 4) indicate a varying influence of temperature on the elastic properties of homogeneous solid solutions. The elastic properties of the alloys with 2.5 weight % Sn sharply decrease with the increase in the temperature. An increase in the tin content of the alloy considerably decreases the intensity of this drop. The higher the amount of tin in the alloy, the higher the elastic properties of alloys at high temperatures. This is also shown by the isothermal curves of elastic properties at 400, 500, 600, and 700°C (see Figure 3).

The elasticity of two-phase alloys with 25 weight % Sn, is of low magnitude at room temperature and changes little upon heating.

The Poisson ratio of all those alloys remained almost constant for all testing temperatures. Only alloys with 2.5% Sn show a tendency toward increasing the Poisson ratio upon heating.

The increase in the heat resistance of α -Ti solid solutions, caused by the increase in the tin content up to saturation, has been determined by I. W. Suiter /29/ and I. I. Kornilov and T. T. Nartova /30/. This should be related to the increase in the interatomic binding forces which results in greater stability of these alloys during heating as compared with pure titanium and solid solutions with a low content of alloying elements.

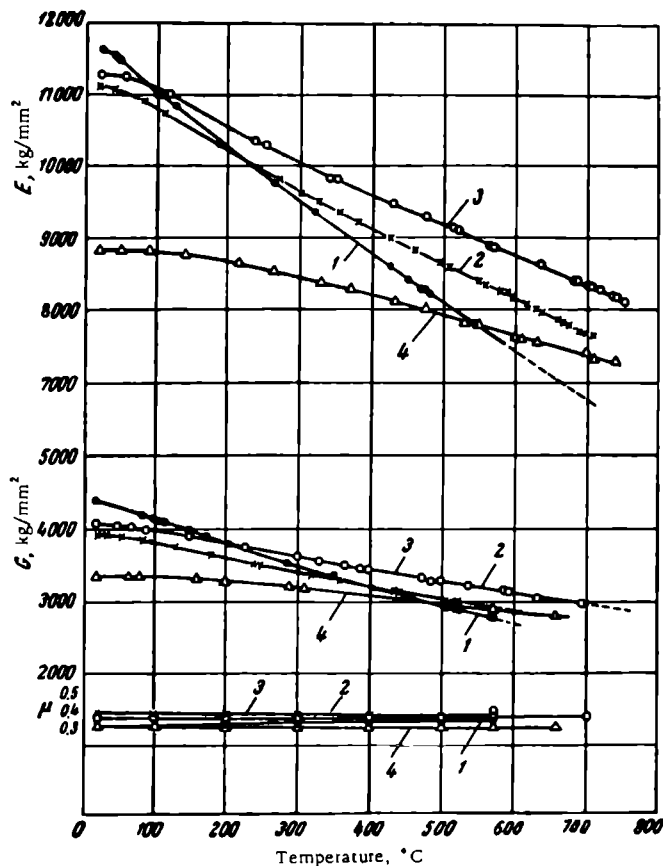


FIGURE 4. The Temperature dependence of the Young modulus E , of the shear modulus, G , and of the Poisson ratio μ of Ti-Sn alloys

1 — 2.5 weight % Sn; 2 — 15 weight % Sn; 3 — 20 weight % Sn; 4 — 25 weight % Sn.

Conclusions

An investigation has been carried out of the dependence of the elasticity constants on composition for alloys of the Ti-Mo, Ti-V, Ti-Nb, Ti-Al, and Ti-Sn systems over a wide range of compositions.

1. It was determined that molybdenum, vanadium, and niobium decrease the elasticity constants of annealed alloys in the field of homogeneous α -solid solutions and of two-phase $\alpha + \beta$ compositions. The Young modulus and the shear modulus are greatly influenced by the structure of alloys hardened from the β field (Ti-Mo, Ti-V, and Ti-Nb systems). The metastable α' and β phases have the lowest elastic properties while the phase is characterized by the highest elasticity constants.

2. Aluminum, unlike molybdenum, vanadium, or niobium, sharply increases the elasticity constants of titanium alloys. The elasticity modulus of certain alloys, with compositions corresponding to those of the TiAl compounds and of the presumed Ti_3Al compound are 19,000 and 15,000 kg/mm² respectively. Thus, it has been experimentally determined that by alloying with aluminum, the elasticity constants of titanium can be almost doubled while their specific gravity is decreased. The elasticity coefficients of titanium-aluminum alloys are comparable with those of certain steels and nickel alloys which are twice as heavy.

3. Tin has little influence on the elasticity constants of α -solid solutions at room temperature. Nevertheless, in α -solid solutions of titanium with greater amounts of tin the elastic properties decrease less upon heating and the Poisson ratio has a more stable value than in titanium alloys with little tin or in pure titanium.

The maximum on the elasticity modulus curves corresponds to the chemical composition of Ti_3Sn . The characteristic feature of solid solutions on the basis of this compound is the considerable decrease in the elastic properties caused by a small deviation from the stoichiometric composition.

4. The relationship between the curves of the $\beta \rightleftharpoons \alpha + \beta$ transformations (for Ti-Mo, Ti-V, and Ti-Nb systems), the curves of the $\alpha \rightleftharpoons \alpha + \beta$ transformation (for Ti-Al and Ti-Sn systems), and the curves representing the dependence of the elasticity constants on the chemical composition, are very closely interrelated for the alloys investigated.

Bibliography

1. Lozinskii, M.G. and S.G. Fedotov. — Izvestiya AN SSSR, OTN, No. 3:59. 1956.
2. Kurnakov, N.S. and S.F. Zhemchuzhnyi. — Izv. SPb. Politehnicheskogo Instituta, Otdel Tekhniki, Estestvoznaniya i Matematiki, Vol. 19, No. 2. 1913.
3. Kurnakov, N.S. and Ya. Rapke. Tverdost' i modul' uprugosti izomorfnykh smesey medi s nikel'm (Hardness and Elasticity Modulus of Isomorphic Mixtures of Copper and Nickel). — Zhurnal Russkogo Fiziko-Khimicheskogo Obshchestva, Chast' Khimicheskaya, Vol. 46, No. 2. 1914.

4. Lazarev, P. P. O sootnoshenii mezhdu tverdost'yu i uprugimi, termicheskimi i opticheskimi konstantami elementov (On the Relationship between the Hardness, the Elastic, Thermal, and Optical Constants of Elements), Collected Works, Vol. 2. — Izdatel'stvo AN SSSR. 1950.
5. Ogden, H. R., D. J. Maykuth, W. L. Finlay, and R. I. Jaffee. — J. Metals, 5(2):267. 1953.
6. Graft, W. H., D. W. Levinson, and W. Rostoker. — Trans. Am. Soc. Met., Vol. 49:263. 1957.
7. Brooks, H., G. I. Lewis, and J. I. M. Forsyth. — Metallurgia, Vol. 56:277. 1957.
8. Bungardt, K. and H. Weigand. — Zs. Metallk., 51 (3) : 181 1960.
9. Knorr, W. and Scholl. — Zs. Metallk., 51(10):605. 1960.
10. Smith, Morton K. Principles of the Physics of Metals. [Russian translation. 1962.]
11. Förster, F. — Zs. Metallk., 4(29):109. 1937.
12. Förster, F. — Industrieanzeiger, Vol. 64:77. 1955.
13. Köster, W. — Zs. Metallk., 39(1):1. 1948.
14. Köster, W. — Zs. Metallk., 39(5):145. 1948.
15. Reynolds, M. B. — Trans. Am. Soc. Met., Vol. 45:839. 1953.
16. Bradford, C. I., J. P. Catlima, and E. L. Wemple. — Met. Progr., No. 3:348. 1949.
17. McQuillan, A. D. and M. K. McQuillan. Titanium. — Metallurgy of Rarer Metals, Vol. 2, New York. 1955. [Russian translation. 1958.]
18. Eremenko, V. N. Titan i ego splavy (Titanium and Its Alloys). — Izdatel'stvo AN USSR. 1960.
19. Kornilov, I. I. and P. B. Budberg. Diagrammy sostoyaniya dvoynykh i troynykh sistem titana (Phase Diagrams of Binary and Ternary Ti Systems). — Izdatel'stvo VINITI AN SSSR. 1961.
20. Jaffee, R. I. Principles of the Metallurgy of Titanium Alloys. [Russian translation. 1961.]
21. Duwez, P. — Trans. Am. Soc. Met., Vol. 45:934. 1953.
22. Bagaryatskii, Yu. A., G. I. Nosova, and T. V. Tagunova. — Doklady AN SSSR, 122(4):593. 1958.
23. Bagaryatskii, Yu. A., T. V. Tagunova, and G. I. Nosova. Problemy metallovedeniya i fiziki metallov (Problems of Metallurgy and Physics of Metals). — Sbornik Trudov TsNIIChermet, No. 5 : 210, Metallurgizdat. 1958.
24. Ageev, N. V. and L. A. Petrova. — Sbornik "Titan i ego splavy", p. 3, Izdatel'stvo AN SSSR. 1958.
25. Ageev, N. V. and L. A. Petrova. — Doklady AN SSSR, 138 (2) : 359. 1961.
26. Sagel, K., E. Schulz, and N. Zwickler. — Zs. Metallk., 47 (8) : 529. 1956.
27. Grum-Grzhimailo, N. V., I. I. Kornilov, E. N. Pylaeva, and M. A. Volkova. — Doklady AN SSSR, 137 (3) : 599. 1961.
28. Hansen, M. and K. Anderko. Constitution of Binary Alloys, Vol. 1. — McGraw Hill Co. 1958. [Russian translation. 1962.]

29. Suiter, I. W. — J. Inst. Met., 83(10):460. 1955
30. Kornilov, I. I. and T. T. Nartova. — Izvestiya AN SSSR, OTN, No. 5:138. 1960.
31. Frantsevich, I. N. — Sbornik "Voprosy poroshkovoï metallurgii i prochnosti materialov," No. 3:15, Izdatel'stvo AN USSR, 1956.
32. Pietrokowsky, P. — J. Metals, 4 (2):211. 1952.
33. Worner, H. W. — Tin, 81(11):521. 1953.
34. Guseva, L. N. and B. I. Ovechkin. — Izvestiya AN SSSR, OTN, No. 3:118. 1958.
35. Guseva, L. N. — Doklady AN SSSR, 127(3):415. 1951.
36. Makarov, E. S. — Izvestiya SFKhA, 16(1):149. 1943.
37. Bradley, A. I. and A. Taylor. — Proc. Roy. Soc., 159(896):56. 1937.
38. Konobeevskii, S. T. — Izvestiya SFKhA, 16(1):19. 1943.

INVESTIGATION OF THE HEAT RESISTANCE OF ALLOYS OF THE Ti-Al-Sn SYSTEM BY THE BENDING METHOD

I. I. Kornilov and T. T. Nartova

The Ti-Al system is the basis for the production of many heat-resisting titanium alloys. It has been definitely determined that this system contains the compounds TiAl and TiAl_3 formed by a peritectic reaction /1/. According to one of the most recent publications /2/, the formation of Ti_5Al and Ti_3Al from solid solutions is also possible.

Since tin dissolves over a wide range of concentrations in α -Ti, its addition to Ti-Al alloys involves the heat resistance of the product to be increased without any reduction in thermal stability.

The investigation of the phase diagram of the Ti-Al-Sn system has shown that it contains fields of α -Ti solid solutions and of intermetallic compounds of titanium with aluminum and tin /3, 4/.

It was therefore of interest to investigate the variation of the heat resistance of these alloys with physico-chemical factors. The basic trends in the variations of the heat resistance of alloys and methods for its augmentation are described by Kornilov /5/.

In order to determine the dependence of the creep resistance on the composition, phase structure, and testing temperature, specimens of Ti-Al-Sn alloys were tested for heat resistance by the centrifugal bending method /6/. Heat resistance was characterized by the time taken by the metal to reach a certain deflection. The specimens were prepared by melting in an arc furnace, and by annealing at 850°C for 0.5 hours.

The heat resistance of alloys of the Ti-Al-Sn system was investigated over a wide range of compositions involving various phase systems at temperatures of 500 - 800°C and at stresses of 15 - 25 kg/mm^2 .

Preliminary investigations of the heat resistance of alloys of the system at 500 - 650°C and a load of 15 kg/mm^2 showed that there are Ti-Al-Sn alloys which cannot be deformed at these temperatures. Such alloys were therefore tested for heat resistance at higher temperatures (700 - 750°C) and at a load of 15 - 25 kg/mm^2 .

Investigations were carried out of the heat resistance of alloys belonging to the radial section [of the phase diagram] with $\text{Al:Sn} = 1:1$, of alloys belonging to the sections passing through the fields of the following compounds: $\text{Ti}_5\text{Al-Ti}_3\text{Sn}$, $\text{Ti}_3\text{Al-Ti}_3\text{Sn}$, $\text{Ti}_2\text{Al-Ti}_3\text{Sn}$, and $\text{TiAl-Ti}_3\text{Sn}$, and others.

The heat resistance tests were carried out in four stages. During the first stage of testing, the specimens were deformed at 700°C and at a stress of 15 kg/mm^2 for a period of 100 hours. During the second stage the tests were carried out for another 100 hours at the same constant temperature but under higher loads (20 kg/mm^2). During the third stage of testing the load was increased to 25 kg/mm^2 and the tests were continued at 700°C for another 100 hours. During the fourth stage of testing, which lasted another 100 hours, the temperature was increased to 750°C while

the load remained at 25 kg/mm². Thus the total time at 700-750°C was 400 hours and the load applied was 15-25 kg/mm².

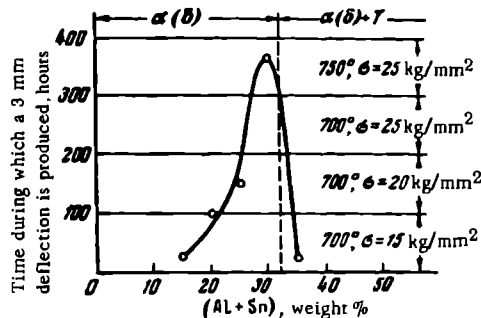


FIGURE 1. Composition versus heat resistance of alloys of the radial section of the Ti-Al-Sn system (Al:Sn = 1:1)

The investigation of alloys of the radial section with Al:Sn = 1:1 showed that pure titanium and alloys with a total content of aluminum and tin (dilute solid solutions) of up to 10 % have a low heat resistance if tested at 700°C with a load of 15 kg/mm² and are deformed almost immediately after application of the stress. As the total concentration of aluminum and tin in the alloys of this section increases, their rate of creep sharply decreases. After 300 hours of testing at 700°C and a load of 15-25 kg/mm² alloys with Al+Sn of up to 10 % show a deflection of 3-9 mm, while the deflection of an alloy with 15 % Al and 15 % Sn under the same conditions is equal to 1 mm. The rate of creep of alloys with 25-30 % Al+Sn increases only a little if the temperature is raised to 750°C (the deflection only increases to 3-5 mm). The alloys represented by these sections are close to the saturation limit of ternary solid solutions. As the aluminum plus tin content increases still further (up to 35 %) the alloys have a much higher rate of creep. According to the phase diagrams, such alloys belong to the two-phase field and contain considerable amounts of a second phase.

The composition versus heat resistance diagram of alloys of the section with Al:Sn = 1:1, in which the heat resistance is characterized by the time during which a 3 mm deflection is produced (Figure 1), shows that the time to reach this deflection increases on the passage from alloys belonging to the field of ternary solid solutions on the basis of α -Ti toward alloys belonging to the field of solid solutions on the basis of Ti₃Al and Ti₆Al and as the limit of maximum solubility is approached. The above curve has a steep maximum in the field close to the transition from solid solutions to heterogeneous alloys (on Figure 1 this boundary is shown by a dotted line). This maximum is due to the additional strengthening of the alloys caused by the crystallochemical reactions taking place in supersaturated solid solutions and to the formation of a finely-dispersed additional phase.

Alloys with a heterogeneous structure belonging to the two-phase field, with considerable amounts of second-phase inclusions (on the basis of TiAl), have a lower heat resistance which is, however, considerably higher than that of low-alloyed heat resisting solid solutions. The composition versus heat resistance diagram belongs to the second type [5].

Considerable interest attaches to the results of heat-resistance tests

of alloys belonging to the Ti_3Al - Ti_3Sn section which represents continuous solid solutions on the basis of Ti_3Al and Ti_3Sn intermetallic compounds.

Investigations of the alloys of these sections at $700^\circ C$ and a load of 15 kg/mm^2 have shown that the alloy corresponding to the stoichiometric composition of Ti_3Sn has the highest rate of creep. After 100 hours, the deflection of this alloy was 13 mm. At this temperature, these specimens failed under a stress of 20 kg/mm^2 .

The Ti_3Al compound is more heat resisting than the Ti_3Sn compound. An alloy with a stoichiometric composition of Ti_3Al was deformed only to a small extent at $700^\circ C$ under a $15\text{--}25\text{ kg/mm}^2$ load applied for 300 hours (deflection 7.5 mm). Only after the temperature was increased to $750^\circ C$ and the load to 25 kg/mm^2 , could an increase in the rate of creep be noted.

The results of the investigation of the phase diagram show that all other alloys of this section with different Ti_3Al to Ti_3Sn ratios are continuous solid solutions on the basis of these intermetallic compounds. These alloys are characterized by a certain proportional relationship between the rate of creep and the composition and concentration of solid solutions.

The most heat resisting of these alloys are those containing 30-50% Ti_3Sn , or 70-50% Ti_3Al . At $700^\circ C$ and under a $15\text{--}25\text{ kg/mm}^2$ load applied for 300 hours,

their deflection was 4-5 mm. At $750^\circ C$, a 100 hour long deformation produced a deflection of only 7 mm.

On the composition-heat resistance curve of alloys belonging to the Ti_3Al - Ti_3Sn section (Figure 2), the heat resistance is characterized by the time needed to produce a deflection of 2, 3, 4, 5, and 7 mm. All these curves are similar and have a steep maximum approximately at a composition with 50% Ti_3Sn + 40% Ti_3Al . At $700^\circ C$ and $750^\circ C$ the specimens loaded with $15\text{--}25\text{ kg/mm}^2$ have a high heat resistance. Thus, for instance, the time required to produce a 7 mm deflection is 400 hours.

Alloys of the Ti_3Al - Ti_3Sn section which are continuous solid solutions of intermetallic compounds, show a linear variation of heat resistance with composition and give the first type of composition versus heat resistance diagram [5]. The characteristic feature of these alloys is that they contain solid solutions of two intermetallic compounds Ti_3Al and Ti_3Sn . This is the only case where the first type of composition versus heat resistance diagram is given by continuous solid solutions of intermetallic compounds.

The present study also included the heat resistance of alloys of the Ti - Al - Sn system belonging to the section passing through the field of the Ti_3Sn compound and of the presumed Ti_2Al compound. It was determined that the alloys of this section have an even higher heat resistance than the alloys of the Ti_3Al - Ti_3Sn section.

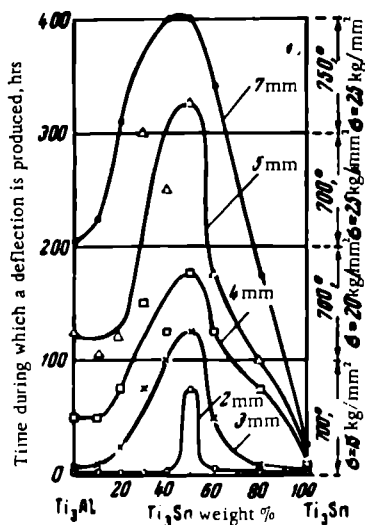


FIGURE 2. Composition versus heat resistance of alloys of Ti_3Al - Ti_3Sn section of the Ti - Al - Sn ternary system

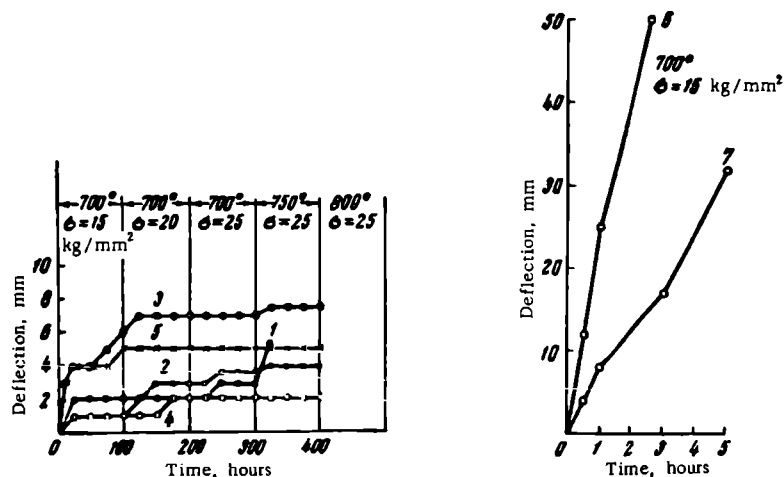


FIGURE 3. Relationship between the deflection and the duration of the deformation of alloys of the TiAl-Ti₃Sn section

1 — 100% TiAl; 2 — 80% TiAl + 20% Ti₃Sn; 3 — 60% TiAl + 40% Ti₃Sn; 4 — 90% TiAl + 10% Ti₃Sn; 5 — 70% TiAl + 30% Ti₃Sn; 6 — 20% TiAl + 80% Ti₃Sn; 7 — 40% TiAl + 60% Ti₃Sn.

Among all alloys of the Ti-Al-Sn system, the most heat resistant are those based on the TiAl compound. Alloys of this group are represented by the section passing through the Ti₃Sn and TiAl regions, both in the field of the ternary γ -solution (on the basis of TiAl), and in the adjacent two-phase field. The results of the investigation of the heat resistance of the alloys belonging to this section are given in Figure 3.

The investigation of the alloys of this section has shown that the TiAl compound (curve 1) and its solid solutions with tin (curves 2-5) have high heat resistances of up to 750°C.

At 700°C, TiAl-base solid solutions deformed but little after a 300 hour long loading with 15-25 kg/mm². The rate of creep of these alloys does not increase even if the temperature is increased to 750°C. TiAl-base alloys tested for 500 hours at 700-750°C show a deflection of only 4-8 mm. Alloys with 20-40% TiAl and 80-60% Ti₃Sn containing coarse inclusions of the second phase have a low heat resistance at 700°C. Under these conditions of testing, the deflection was 30-40 mm after 3-20 hours (curves 6 and 7).

The investigations of the heat resistance of ternary Ti-Al-Sn alloys by the centrifugal bending method have shown the existence in this system of a number of fields of ternary alloys with a high heat resistance at 700-750°C.

The investigation has shown that it is possible to produce highly heat-resisting alloys on the basis of intermetallic compounds and of intermetallic solid solutions, able to preserve a high degree of strength at more elevated temperatures than solid solutions of the metals and certainly of the single components.

Conclusions

1. The results of the investigation of the heat resistance of alloys of the Ti-Al-Sn system by the centrifugal-bending method has shown that alloys containing intermetallic solid solutions and those in the vicinity of the maximum solubility of solid solutions based on α -Ti and on Ti-Al-Sn intermetallic compounds have a very high heat resistance. The composition versus properties diagrams of these alloys belong to those of the second type.

2. Alloys of the Ti_3Al - Ti_3Sn section with continuous solid solutions of these two intermetallic compounds, show a linear relationship between the heat resistance and the composition of the alloys (sloping maximum). The composition-property diagram corresponds to those of the first type.

3. The TiAl-base alloys have the highest heat resistance among all the alloys of the Ti-Al-Sn system investigated.

Bibliography

1. Hansen, M. and K. Anderko. Constitution of Binary Alloys, Vol.1.—McGraw-Hill Co. 1958. [Russian translation. 1952.]
2. Grum-Grzhimailo, N.V., I.I. Kornilov, E.N. Pylaeva, and M.A. Volkova. — Doklady AN SSSR, 137 (3):599. 1961.
3. Kornilov, I.I. and T.T. Nartova. — Doklady AN SSSR, 131 (4):837. 1960.
4. Kornilov, I.I. and T.T. Nartova. — Doklady AN SSSR, 140 (4):829. 1961.
5. Kornilov, I.I. Fiziko-khimicheskie osnovy zharoprochnosti splavov (Physicochemical Principles of Heat Resistance of Alloys). — Izdatel'stvo AN SSSR. 1961.
6. Kornilov, I.I. — Izvestiya Sektora Fiziko-khimicheskogo analiza, Vol.18:72. 1949.

MECHANICAL PROPERTIES OF AT-3, AT-4, AT-6, AND AT-8 HEAT TREATED TITANIUM ALLOYS

B. K. Vul'f and S. A. Yudina

This work is a continuation of the investigation of the heat-treatment of the titanium alloys of the Ti-Al-Cr-Fe-Si-B system, developed under the general guidance of I. I. Kornilov /1/.

The results of the earlier investigations were published in 1959 and 1961 /2, 3/ and the work carried out until then was dealt with during the first seminar on the theoretical and experimental investigations of titanium alloys /4/.

The purpose of the present investigation is to elucidate the effect of heat treatment (temperature of hardening, temperature of aging, and duration of aging) on the changes in phase composition, microstructure, and mechanical properties of the AT-6 alloy. Further, as a result of this study, it was found possible, on the basis of the analysis of the experimental data, to arrive at some general conclusions concerning the entire series of alloys.

The preparation of the AT-6 alloy, and its properties in the initial condition

The AT-6 alloy was produced in an industrial vacuum arc furnace with consumable electrodes by the method of double smelting*. The diameter of the crystallizer used during the second smelting was 350 mm.

The machined ingots (weight about 500 kg) were subjected to a number of mechanical-working operations. After an intermediate drawing of the ingots to ϕ 150 mm, the calibrated slabs were hammer-forged into rods by means of a 3-ton hammer at 1050-1080°C to 870-840°C, the temperature of the hammers being 200-250°C.

The rods (ϕ 14 mm and 25 mm diameter) were sandblasted and were used for the preparation of specimens for the mechanical tests and the microstructure investigations.

The chemical composition of the alloy was as follows: 5.6 % Al, 0.52 % Cr, 0.23 % Fe, 0.3 % Si, 0.01 % B, 0.011 % N₂, and 0.01 % H₂. The mechanical properties of the alloy in the initial condition and also after aging at 400°C for 100 hours are given in Table 1.

In the initial condition the alloy consisted of an α phase, a stressed α' phase, and possibly also of some residual β phase remaining after

* The smelting and forging operations were carried out under the guidance of V. S. Mikhnev.

cooling from the forging temperature. After aging, which caused no noticeable changes in the microstructure, the strength was somewhat reduced and the elongation somewhat increased. However, the mechanical properties underwent little change, which indicates a high thermal stability of the AT-6 alloy in the forged condition.

TABLE 1

Mechanical properties of AT-6 alloy in the initial condition and after aging for 100 hours at 400°C

Conditions of treatment	σ_u , kg/mm ²	δ , %	ψ , %	H_{RC} , kg/mm ²	a_i , kg·m/cm ²
Forging and air cooling	108	12.1	26.5	35	4.04
Forging, air cooling + aging at 400°C for 100 hours	105.5	14.6	25.1	35	3.2

The influence of the hardening temperature on the structure and properties of the AT-6 alloy

The specimens for the testings were machined from 25-mm diameter rods and were 60-70 mm in length. The treatment was carried out in electric muffle furnaces in an air atmosphere; the duration of heating was 1 hour.

The specimens were air-hardened at temperatures ranging from 700 to 1150°C at 50°C intervals.

From these rods specimens were cut for tension tests at the Gagarin testing machine for the determination of σ_u , δ , and ψ and also for shock tests. The shock-test specimens were also used for the determination of the Rockwell hardness.

The results of these tests are graphically shown on the diagram (Figure 1).

These data show that the temperature of hardening (up to 1150°C) has little influence on the ultimate strength, hardness, and toughness of the material.

The reduction in area, ψ , increases steadily up to a hardening temperature of 850-900°C, after which this value begins to decrease. A similar relationship, though somewhat less definite, can be seen in the case of the elongation δ .

The form of the plasticity curves is connected with the relationship between the critical temperatures of phase transformations and the aluminum content (Figure 2) and is the result of structural changes. This is confirmed by microstructural analysis.

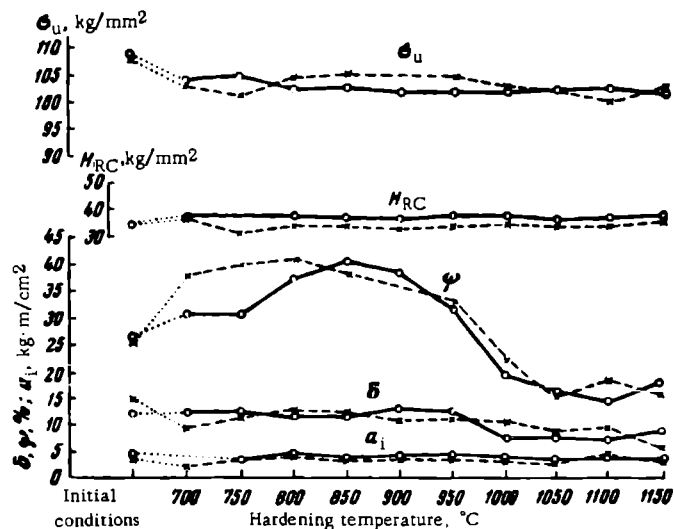


FIGURE 1. Mechanical properties of the AT-6 alloy

○ — after hardening at various temperatures; × — after hardening and aging at 400°C.

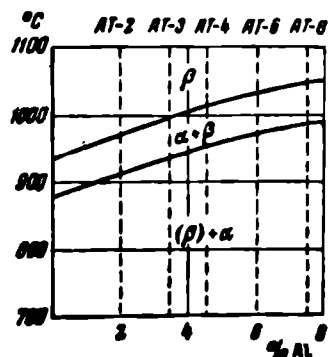


FIGURE 2. Relationship between the phase transformations of titanium alloys of the Ti-Al-Cr-Fe-Si-B system and their aluminum content /5/

After hardening from temperatures below the beginning of the phase transformations, the initial structure is preserved, but the internal stresses in the metal decrease, apparently because of the $\alpha' \rightarrow \alpha$ transformation (Figure 3a). If the hardening temperature is increased to about 950°C there is a tendency toward spheroidizing of the lamellae of the α phase; this process, which is accompanied by a decrease in the internal stresses caused by hardening, leads to an increase in plasticity.

Heating to temperatures above 950-975°C results in the formation of a β phase, which is partially transformed into a martensite-like α' phase upon hardening (Figure 3b). Heating above 975°C accelerates the grain growth (Figure 3c). These structural changes account for the decrease in the plasticity of the alloy.

Thus the hardening temperature at which the optimum combination of strength and plasticity can be obtained is somewhat below the limit of the two-phase field of the phase diagram (850-875°C).

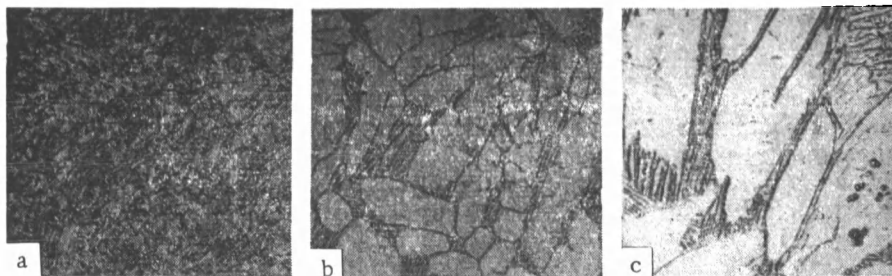


FIGURE 3. Microstructure of AT-6 alloys after hardening from 800 (a), 1050 (b) and 1150°C (c) and cooling in the air, $\times 300$

Aging of AT-6 alloys

Two series of specimens of hardened alloys were aged.

The specimen of the first series, hardened from various temperatures as mentioned above, were aged at 400°C for 100 hours. The results of these investigations are presented in Figure 1.

Specimens of the second series were aged at 450 and 550°C after air hardening from the optimum temperature of 875°C. Changes in the structure and properties of the alloys were observed after aging from 1 to 100 hours.

The data of aging at 400°C show that this process causes only small changes in the mechanical properties of the alloys [after hardening] and that the temperature-property relationships found for hardened alloys in general remain unaltered for aged alloys.

The structures of alloys aged at 400°C remain almost the same as those of the hardened alloys.

This indicates that alloys air-hardened from 700-1150°C have a high thermal stability at 400°C.

The results obtained after aging at 450 and 550°C confirm the stability of the hardened alloys (Table 2).

The investigations showed that aging changes the mechanical properties of hardened alloys by not more than 5-7 %. This is also true for even such a sensitive characteristic as the reduction in area, ψ , which shows little change after aging for 100 hours. The relatively higher increase in the percentage elongation δ which takes place after a few hours of aging at 450°C can be explained as being due to the relief of the internal stresses appearing during hardening.

The metallographic investigations confirmed the stability of the structure during the whole aging period at 450 and 550°C.

TABLE 2

Mechanical properties of AT-6 alloys hardened from 875°C and aged at 450 and 550°C

Aging temperature, °C	Duration of aging, hours	Mechanical properties				
		σ_u , kg/mm ²	δ , %	ψ , %	σ_i , kg·m/cm ²	H_{RC} , kg/mm ²
450	0	97.3	11.7	41.0	3.8	33
	1	104.0	12.15	38.4	3.4	34
	2	97.4	21.1	39.4	3.0	33
	5	98.1	15.4	33.1	3.3	34
	10	103.0	11.0	33.5	3.0	34
	25	100.7	5.5	34.2	3.5	34
	50	103.0	10.7	35.1	3.2	34
	75	103.3	13.12	43.9	2.5	34
	100	99.0	13.2	34.7	3.0	34
550	0	97.3	11.7	41.0	3.8	33
	1	101.1	8.8	35.2	3.2	34
	2	100.9	10.8	36.2	2.8	34
	5	99.4	11.6	36.5	3.3	35
	10	97.7	10.5	42.4	2.7	35
	25	102.5	11.2	29.4	2.0	34
	50	100.5	10.4	30.3	2.4	34
	75	95.5	11.5	33.0	2.5	33
	100	93.6	11.6	40.6	3.0	33

The mechanical properties of heat treated AT-titanium alloys
with various aluminum contents

Consideration will now be given to the comparative diagrams representing the dependence of the mechanical properties of hardened and aged AT-3, AT-4, AT-6, and AT-8 alloys (with different aluminum contents) on the hardening temperature (Figures 4 and 5).

An increase in the aluminum content leads to a higher ultimate strength of both hardened and aged alloys, irrespective of the hardening temperature.

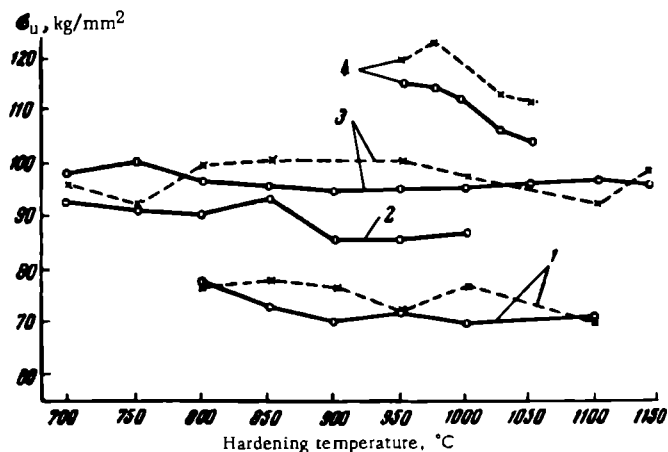


FIGURE 4. Ultimate strength of titanium alloys AT-3 (1), AT-4 (2), AT-6 (3), and AT-8 (4)

O — after hardening from various temperatures; X — after hardening and aging at 400°C (AT-3, AT-4, AT-6 alloys) and 500°C (AT-8 alloy).

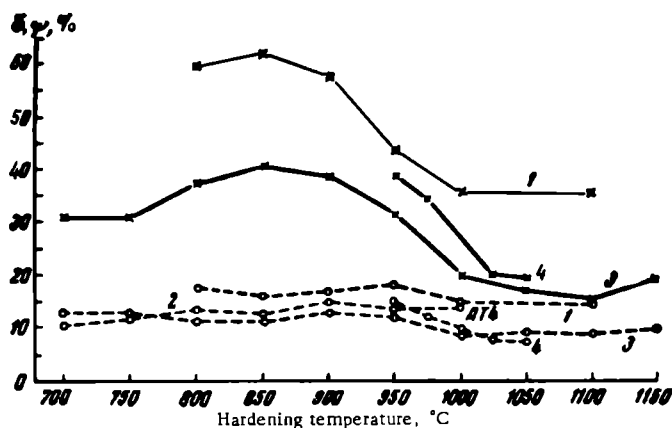


FIGURE 5. Relationship between the plasticity characteristics of AT-3 (1), AT-4 (2), AT-6 (3), and AT-8 (4) alloys and the hardening temperatures

O — percentage elongation; X — reduction of area.

Whereas the ultimate strength of AT-3, AT-4, and AT-6 alloys, which have a relatively low aluminum content, is little influenced by the hardening temperature, the ultimate strength of AT-8 alloys (both hardened and aged) shows a marked decrease [with the decrease in the] hardening temperatures beginning from 950-975°C, a temperature which lies close to the two-phase field boundary. This is apparently due to the fact that at high temperatures solid solutions are weakened to a relatively greater extent as a result of higher stresses caused by a higher aluminum content.

Generally speaking, the absolute magnitudes of the ultimate strength are somewhat increased by aging, particularly in the AT-8 alloys.

The course of the plasticity curves [for aged alloys], particularly of the reduction in area, curves σ_ψ , are very characteristic. Hardened alloys (Figure 6) show a regular increase in ψ up to certain hardening temperatures, after which ψ sharply decreases.

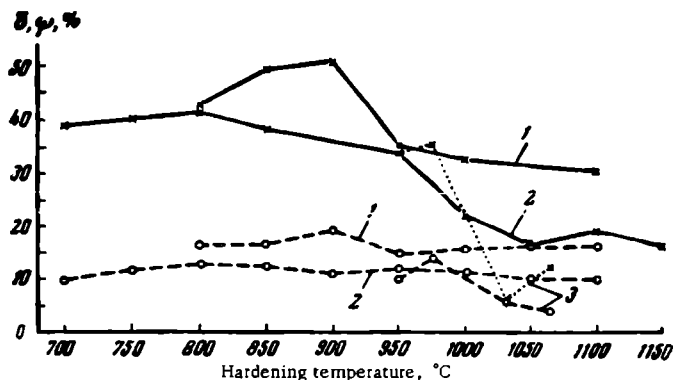


FIGURE 6. Plasticity characteristics of hardened titanium alloys, AT-3 (1), AT-6 (2), and AT-8 (3) after aging for 100 hours at 400°C (alloys AT-3 and AT-6) and at 500°C (AT-8)

○ — elongation; × — reduction of area.

The course of these curves is in accordance with the conclusion arrived at earlier that the highest plasticity, which is quantitatively expressed by the reduction of area ψ , is attained at hardening temperatures close to the boundary of the two-phase field on the phase diagram. These temperatures increase with the aluminum content of the alloys. At these hardening temperatures, most stresses raised during mechanical working are relieved, but no considerable grain growth takes place and no metastable phases with a low plasticity are formed after hardening. For the AT-3 alloy, the hardening temperature which ensures the maximum plasticity is about 850°, for the AT-6 alloy it is about 875°C, and for the AT-8 alloy it is about 925°; these hardening temperatures should be considered as the optimum for attaining the best combination of strength and plasticity in heat-treated alloys.

The various alloys tested give, after aging, the same type of ψ versus hardening temperature curve although the position of the maximum is not determined by the composition in the same way for all the alloys.

The elongation curves (δ) also rise up to a point with the increase in the hardening temperature, after which they decrease (Figure 5).

The plasticity, which is characterized by the elongation, is similar for all investigated hardened alloys. Among the aged alloys the above feature can be found only in the AT-8 alloy (Figure 6).

Conclusions

1. AT-6 alloys hardened in the air from 700-1150°C have almost the same strength, hardness, and impact toughness.
2. The reduction of area ψ for the AT-6 alloy increases up to a hardening temperature of 850-875°C, which is close to the two-phase field boundary of the phase diagram, after which it sharply decreases. To a lesser degree this relationship also holds for the elongation σ .
3. Aging at 400, 450, and 550°C for 100 hours has little influence on the mechanical properties of the AT-6 alloy. The plastic properties of this alloy remain almost at the level of hardened alloys under these conditions, which indicates a high thermal stability.
4. The ultimate strength of hardened AT-alloys increases with the aluminum content, while the plasticity decreases. After aging, the influence of aluminum on the mechanical properties of these alloys changes. Except for the AT-8 alloy (with a high content of oxygen) the alloys of these series are not embrittled by aging.
5. The properties of all investigated heat-treated AT alloys change in the same way as those of the AT-6 alloy: an increase in the hardening temperature has little influence on the ultimate strength of these alloys (except for the AT-8 alloy) while the reduction of the area ψ increases with the increase in the [hardening] temperature up to the two-phase field boundary of the equilibrium phase diagram; it then decreases.
6. In order to obtain the best combination of strength and plasticity in air-hardened alloys, the following hardening temperatures can be recommended: for the AT-3 alloy, 800-850°C, for the AT-4 alloy, 850-870°C, for the AT-6 alloy, 850-875°C, and for the AT-8 alloy, 925-950°C.

Bibliography

1. Kornilov, I.I., V.S. Mikheev, T.S. Chernova, and K. P. Markovich. — Sbornik "Titan i ego splavy", No. 7:140, Izdatel'stvo AN SSSR. 1962.
2. Kornilov, I.I., B.K. Vul'f, V.S. Mikheev, and S. A. Yudina. — Trudy VVIA imeni professora N. E. Zhukovskogo, No. 801, Izdatel'stvo VVIA. 1959.
3. Kornilov, I.I., B.K. Vul'f, V.S. Mikheev, and S. A. Yudina. Metallicheskie splavy dlya aviatsionnoi tekhniki (Alloys for the Aircraft-Building Industry), No. 833:30. — Izdatel'stvo VVIA. 1961.
4. Vul'f, B.K. and S. A. Yudina. — Sbornik "Titan i ego splavy", No. 7:174, Izdatel'stvo AN SSSR. 1962.
5. Kornilov, I.I., V.S. Mikheev, and T.S. Chernova. — Izvestiya AN SSSR, OTN, Metallurgiya i Toplivo, No. 3:70. 1960.

HEAT RESISTANCE, CREEP, AND THERMAL STABILITY OF THE AT-3 ALLOY

V. S. Mikheev, K. P. Markovich, and Z. G. Friedman

The purpose of the present work is to investigate the heat resistance, creep, and the thermal stability of the AT-3 alloy, produced under industrial conditions. Data on the chemical composition and on the chief physical and mechanical properties of this alloy have been published elsewhere [1, 2].

The chemical composition of the alloy investigated was as follows: 2.7 % Al, 0.60 % Cr, 0.30 % Fe, 0.35 % Si, and 0.01 % B (as calculated).

The above-mentioned properties were investigated on specimens annealed at 800°C for 30 min and cooled together with the furnace.

Heat resistance of the AT-3 alloy

The heat resistance of the AT-3 alloy was investigated by determining the long-time strength at 350°C and under different stresses. The results of these investigations are given in Table 1.

TABLE 1
Long-time [creep strength] of the AT-3 alloy at 350°C

σ , kg/mm ²	Duration of test, hours	δ , %	ψ , %
59	108	12.5	68.7
58	1600	13.0	77.6
55	3500	*	*

* Tests continued.

The data in Table 1 show that the AT-3 alloy has a high long-time strength at 350°C. A 3500 hour long testing with a 55 kg/mm² load did not lead to failure. Under higher stresses, the alloy rapidly weakens and under a load of 59 kg/mm² it fails after 108 hours.

Creep of the AT-3 alloy

The creep of this alloy was investigated at 350°C and under different stresses. The data obtained are given in Table 2.

The creep curves of this alloy tested with a load of 30, 37, and 45 kg/mm² show that the residual deformation of the alloy varies little (Figure 1). The elongation is not higher than 0.5%.

TABLE 2
Creep of the AT-3 alloy at 350°C

σ , kg/mm ²	Duration of test, hours	δ , %	σ , kg/mm ²	Duration of test, hours	δ , %
53	—	7.2*	37	5215	1.45**
52	—	6.9*	33	3350	***
45	5940	1.49**	30	6662	0.45*
40	3160	***	15	5454	0.5

* The specimen failed under the load.

** The specimen did not fail.

*** Test continued.

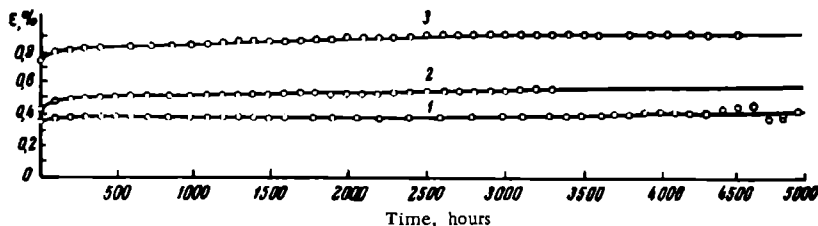


FIGURE 1. Creep curves for the AT-3 alloy at a testing temperature of 350°C and a load = 30 kg/mm² (1), 37 kg/mm² (2), and 45 kg/mm² (3)

Thermal stability of the AT-3 alloy

In order to elucidate the problem of the possible embrittlement of the AT-3 alloy, an investigation was carried out of the aging process at 350 and 400°C in the air (duration up to 5000 hours).

The results of this investigation are given graphically in Figure 2.

These curves show that both the plasticity and the ultimate strength, remain almost unchanged during 5000 hours at 350°C* and during 3000 hours at 400°C. During this time the alloy is not embrittled.

In order to establish the thermal stability of the AT-3 alloy in the range from 300 to 400°C, the mechanical properties of the alloy were determined after a 5000 hours long creep test at 300°C and 30 kg/mm², and after 6600 hours at 350°C and 30 kg/mm².

* [Cf. Footnote on next page.]

The data in Table 3 show that the loaded alloy remains unembrittled after a prolonged test (up to 5000-6600 hours) at 300-350°. The strength remains as in the initial condition, while the plasticity increases to some extent.

TABLE 3
Mechanical properties of AT-3 alloys after creep testing

Mechanical properties of forged alloy				Mechanical properties of the alloy after creep testing, at $\sigma = 30 \text{ kg/mm}^2$ $T = 300^\circ$, $\tau = 5000 \text{ hours}$				Mechanical properties of the alloy after creep testing at $\sigma = 30 \text{ kg/mm}^2$ $T = 350^\circ$, $\tau = 6000 \text{ hours}$			
σ_u , kg/mm ²	σ_y , kg/mm ²	δ , %	ψ , %	σ_u , kg/mm ²	σ_y , kg/mm ²	δ , %	ψ , %	σ_u , kg/mm ²	σ_y , kg/mm ²	δ , %	ψ , %
87.4	84.4	14.0	44.7	83.07	76.90	17.42	48.20	86.09	80.32	13.0	55.31
86.4	85.4	14.0	41.8	83.07	80.00	18.50	52.80	85.07	79.72	16.0	38.51
—	—	—	—	86.84	83.68	18.20	48.40	—	—	—	—
—	—	—	—	80.00	77.69	19.48	51.30	—	—	—	—

The thermal stability of the AT-3 alloy was also tested under conditions of cyclic heating and cooling without applying stress. The tests were carried out on ordinary tensile-test specimens.

The length of the specimen was 65 mm and the diameter of its gage section 5 mm. The conditions of the experiments were as follows: heating up to 350°C, holding for 30 min, and cooling in the air and in water. Altogether the test consisted of 700 cycles. The mechanical properties of the alloys after 700 cycles are given in Table 4.

From this table it is obvious that after such a cyclic thermal testing, the alloy retains satisfactory mechanical properties which do not differ from those in the initial alloy.

The data show that the AT-3 alloy is thermally stable at 300-400°C and is not embrittled**.

TABLE 4
Mechanical properties of the AT-3 alloy after 700 cycles of heating to 350°C and cooling in the air and water

After forging (initial condition)			After cooling					
			in the air			in water		
σ_u , kg/mm ²	δ , %	ψ , %	σ_u , kg/mm ²	δ , %	ψ , %	σ_u , kg/mm ²	δ , %	ψ , %
98.32	13.00	58.72	92.00	12.4	68.13	91.18	15.92	51.40
90.16	14.00	58.08	90.67	14.8	50.00	88.58	14.80	56.90
90.67	14.00	57.51	91.27	12.0	50.10	88.58	12.80	55.40

* [Graph shows only time to 3000 hrs.]

** An identical investigation has been carried out by L.P. Nikitina. The results obtained by her are in full agreement with our data and are described in the article given in this book (see page 239).

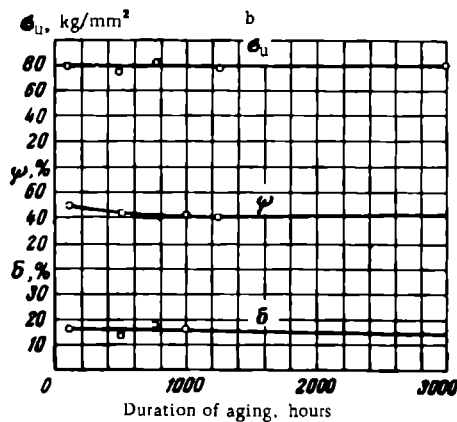
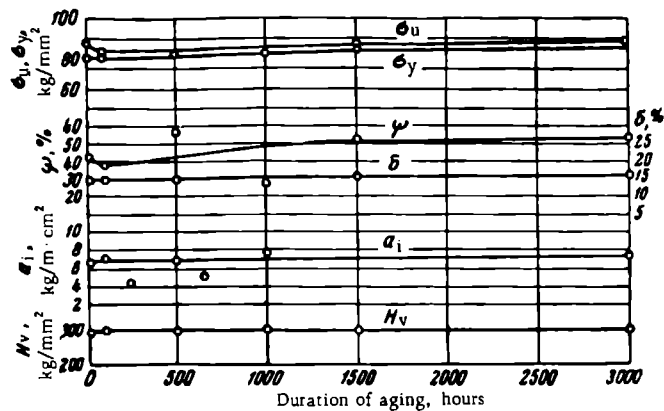


FIGURE 2. Dependence of the mechanical properties of the AT-3 alloy on the duration of aging at 350 (a) and 400°C (b)

Conclusions

1. The creep curves obtained indicate that the relative deformation of the AT-3 alloy under a stress of 15-40 kg/mm² remains almost unchanged. The alloy is not embrittled.

2. The alloy is also not embrittled by a prolonged aging without stress at 400°C for 3000 hours and at 350°C for more than 5000 hours.

Bibliography

1. Kornilov, I.I., V.S. Mikheev, T.S. Chernova, and K.P. Markovich.— Sbornik "Titan i ego splavy", No. 7:140, Izdatel'stvo AN SSSR. 1962.
2. Boriskina, N.G.— Sbornik "Titan i ego splavy". No. 7:150, Izdatel'stvo AN SSSR. 1962.

THE COMPOSITION AND PROPERTIES OF INDUSTRIAL MELTS OF THE AT-3 TITANIUM ALLOY*

V. A. Livanov, N. M. Keleshyan, S.M. Fainbron, and R. M. Ryabova

The AT-3 alloy which has been developed by the Institute of Metallurgy imeni A. A. Baikov is of considerable practical interest since in it titanium is alloyed with cheap and easily available elements: aluminum, chromium, iron, and silicon. This alloy has valuable properties.

With the object of developing a production technology for parts and to check the properties of the alloy, the authors prepared a series of industrial melts. A number of the ingots produced were utilized for the preparation of forgings with a diameter of 90, 100, 120, 130, and 150 mm.

One ingot of the alloy was used for a complete investigation.

The ingots were prepared from TGO sponge with an ultimate strength of 39 kg/mm². The rated chemical composition of the AT-3 alloy was as follows: 3 % Al, 0.6 % Cr, 0.3 % Fe, 0.3 % Si, and 0.01 % B.

The chemical composition of the AT-3 ingot investigated was: 0.02 % C, 2.7-2.8 % Al, 0.25 % Fe, 0.34 % Si, 0.57-0.60 % Cr, 0.03 % N₂, and 0.0099 % H₂.

The mechanical properties of the technological specimen (a forged rod 15 mm in diameter) before heat treatment are as follows: $\sigma_u = 92-95$ kg/mm²; $\sigma_y = 90.7-92.0$ kg/mm²; $\delta = 17.2-18$ %; $a_1 = 5.8-6.2$ kg·m/cm²; $H_B = 277$ kg/mm².

The plan of the investigation was to cut out three 70 mm thick templates from the upper, middle, and bottom part of the ingot respectively. These templates were used for the investigation of the properties of the cast alloy. Part of the ingot between the upper and middle templates was used for the investigation of the properties of pressed alloys. Another part of the ingot, between the middle and the bottom templates was used for the investigation of the properties of pressed alloys.

Investigation of the properties of cast AT-3 alloys

The investigation of the properties of the cast AT-3 alloys consisted of chemical analysis, and a determination of the mechanical properties and of the macrostructure and microstructure of the ingot.

The macrostructure of the ingot was investigated on longitudinal and transversal templates. The middle and bottom templates have a fine-grained equiaxial macrostructure without any especially marked zone of columnar crystals. The upper part of the ingot has a more coarse-grained structure than the middle and lower parts. On the longitudinal sections, a grain growth can be observed from the edges of the ingot toward its center.

* V. S. Mikhnev and S. E. Ivanova participated in this investigation.

The distribution of the chemical elements from the bottom to the top and from the center to the edges of the ingot are shown in the graphs (Figure 1). Almost identical values were obtained for aluminum in the upper, middle, and bottom parts of the ingot (2.6-3.0 %).

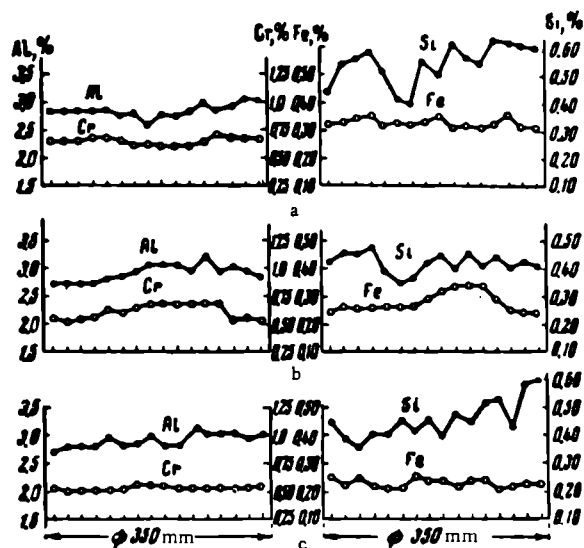


FIGURE 1. Distribution of alloying elements from the bottom to the top and from the center to the edges of the ingots of the AT-3 alloy

a — upper part of the ingot; b — middle part of the ingot; c — bottom part of the ingot.

The upper part of the ingot contains more chromium, iron, and silicon than the middle and bottom parts. The content of aluminum, chromium, and iron increases from the edges toward the center.

The nonuniform distribution of alloying elements in the ingot leads to a different ultimate strength in the various parts.

The upper and middle parts of the ingot have an ultimate strength of 75-95 kg/mm², while the lower part has only 75-85 kg/mm².

The upper, middle, and lower parts of the AT-3 alloy ingot consist of an α -solid solution. The structure does not change from the bottom to the top of the ingot.

Investigation of the properties of forged AT-3 alloys

The AT-3 ingots were forged by a 3-ton hammer according to current technology.

The forging of the ingot into 160 mm diameter rods was carried out

at 1000°C. The rods were forged in the following stages: from 160 mm into 100 mm rods, from 100 mm rods into 65 mm rods, and from 65 mm rods into 15 mm rods. The ingots were forged at 950, 1000, 1050, 1100, 1150, and 1200°C.

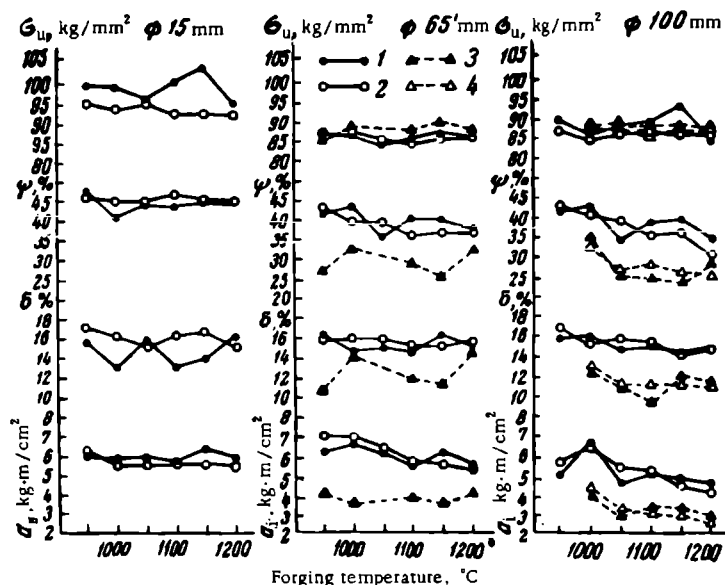


FIGURE 2. Influence of the forging temperature on the mechanical properties of the AT-3 alloy

1 — longitudinal hot forged specimen; 2 — longitudinal heat-treated specimen;
3 — transverse hot forged specimen; 4 — transverse heat-treated specimen.

The degree of deformation* of the forgings was 60, 57, and 94 %.

The initial 160 mm rods had a fine-grained and dense macrostructure. The macrostructure of 100 mm diameter and 65 mm diameter rods forged at different temperatures was investigated in the longitudinal and transverse directions.

These rods had a fine-grained and uniform macrostructure which was not affected to any greater extent by the temperature of forging. Only a forging temperature of 1200°C produces a certain grain growth. The dependence of the mechanical properties of the AT-3 alloys on the forging temperature was investigated on longitudinal and transverse specimens cut out of 100, 65, and 15-mm diameter rods after hot forging and heat treatment under the following conditions: annealing at 900°C, holding for 1 hour, and cooling in the air.

The results of the mechanical tests after heat treatment are given in Figure 2.

A comparison of the properties of longitudinal and transverse specimens of the AT-3 alloy shows a certain anisotropy of the mechanical

* [Reduction in area.]

properties. The mechanical properties of the rods from their periphery toward the center were uniform, apparently because of the uniform macrostructure of the alloy. The influence of the degree of deformation

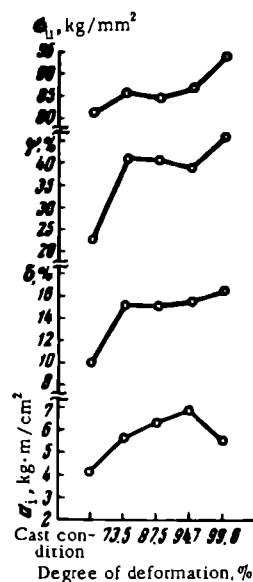


FIGURE 3. Influence of the degree of deformation on the mechanical properties of AT-3 alloys

on the mechanical properties of the AT-3 alloy are shown in Figure 3. Except for toughness, all mechanical properties were improved by an increased degree of deformation.

Forged AT-3 alloys had an α -phase structure irrespective of the forging temperatures. Rods, 15 mm in diameter, forged at 950°C had a relatively fine-grained structure growing coarser as the forging temperature is increased.

Rods, 65 mm in diameter, had a coarser microstructure similar to that of castings. An increase in the forging temperature caused no structural changes. Rods, 100 mm in diameter, had an even coarser structure.

The grains were coarser in the center than at the edges. The forging temperature had little influence on the structure.

The investigation of the properties of mechanically-worked AT-3 alloys

The investigation of the properties of mechanically-worked AT-3 alloys was carried out on forged 120 mm diameter specimens from which profiles were formed at 1000, 1050, 1100, 1150, and 1200°C according to current technology. The macrostructure of the profiled parts was not greatly influenced by the temperature of mechanical working and changed little from the top to the bottom of the pressed part. Only in parts worked at 1100°C did the macrostructure change from the top to the bottom, consisting of fine grains in the middle part of the profile.

The dependence of the mechanical properties of AT-3 alloys on the temperature of mechanical working is shown in the graph (Figure 4). These are properties of specimens cut out from the middle of the profiled parts. The properties changed little from the top to the bottom of the profiled part. Only the toughness of mechanically-worked parts showed an anisotropy. The microstructure was not influenced by the temperature of press forging and was uniform from the top to the bottom of the part. Only at a temperature of press forging equal to 1200°C was there a certain grain growth. Inclusions were found in AT-3 alloys of all conditions (cast, forged, and pressed) (see Figure 5). These inclusions were unetchable and could be seen even on an unetched specimen. The authors are unaware of the nature of these inclusions, which must be the subject of future investigation.

To gain a more complete idea as to the quality of the ingots, the short-time heat resistances and the thermal stability of the ingots were tested. The AT-3 alloy had a high short-time heat resistance (Figure 6).

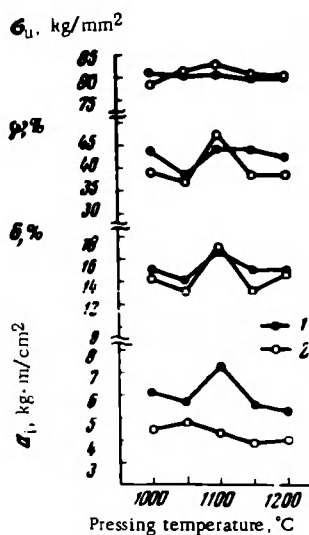


FIGURE 4. The influence of the temperature of press forging on the mechanical properties of AT-3 alloys

1—longitudinal specimens; 2—transverse specimens.

The thermal stability of the alloy was investigated at 400, 450, and 500°C (holding time 100 hours).

At 400 and 450°C the properties of the alloys were stable, but not at 500°C.

The long-time heat resistance of AT-3 alloys was tested at 400°C and under a load of 50 kg/mm², as well as at 500°C and under a load of 25 kg/mm².

In the first case the specimen was tested for 1711 hours. In the second case the following results were obtained: 1 — 994 hours long test, $\delta = 26.8\%$ and $\psi = 77.6\%$; 2 — 191 hours long test, $\delta = 22.0\%$ and $\psi = 77.5\%$.

Conclusions

As a result of the investigation of a single melt of the AT-3 alloy the authors arrived at the following conclusions.

1. The AT-3 alloy has in all conditions (cast, drop, forged, and press forged) a fine-grained uniform macrostructure. An increase in the temperature of drop forging and press forging has little influence on the structure.

2. The AT-3 alloy has uniform and stable mechanical properties. A certain anisotropy of

the mechanical properties can be found in 160, 100, and 65 mm diameter rods.

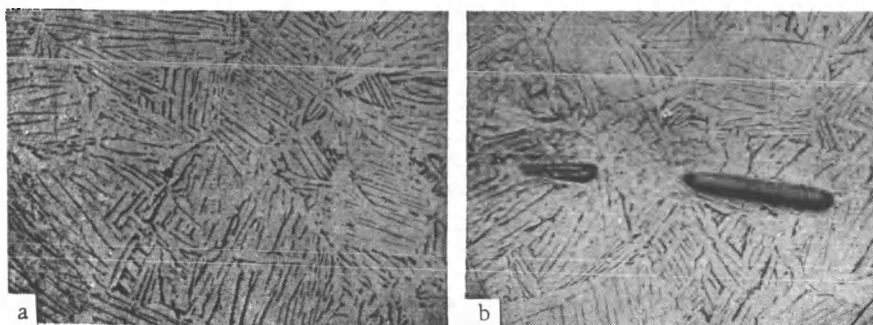


FIGURE 5. Microstructure of AT-3 alloy: normal (a), and with inclusions (b), $\times 300$

The anisotropy of this melt of AT-3 can be apparently explained by the presence of inclusions located in a direction parallel to that of deformation of the metal. In longitudinal specimens, these inclusions have no influence on the mechanical properties of the alloy, but in the transverse specimens, they weaken the metal structure and reduce its mechanical properties.



FIGURE 6. Short-time heat resistance of the AT-3 alloy

3. The AT-3 alloy whether cast, drop forged, or press forged, consists of an α -solid solution irrespective of the temperature of deformation.

4. The AT-3 alloy has a good thermal stability from 400 to 450°C and is not embrittled if heated to this temperature for 100 hours. The alloy has also a good long-time and short-time heat resistance.

THE DEPENDENCE OF THE MECHANICAL PROPERTIES AND HEAT RESISTANCE OF AT-TITANIUM ALLOYS ON THE TEMPERATURE

L. P. Nikitina

The object of this study is to evaluate the mechanical properties and the long-time heat resistance at temperatures from 20 to 400°C of the AT-3 alloy developed in the Institute of Metallurgy imeni A. A. Baikov. Simultaneous investigations were carried out at the Institute of Metallurgy and at the Central Institute of Boilers and Turbines imeni Polzunov. The results of the parallel experiments are reported here.

The AT-3 alloy specimens were prepared from 14 and 20 mm diameter rods.

The rods were heat treated by annealing at 800-900°C for 0.5-1 hours and cooling in the air.

Short-time strength of the alloy

The torsion tests were carried out on an IM-4R machine at a rate of tension of 180 % per hour, using a cylindrical 8 mm diameter specimen with a gage length of 40 mm. The results of the experiments are given in Table 1.

TABLE 1
The results of tension tests of the AT-3 alloy

Temperature of testing, °C	σ_y , kg/mm ²	σ_u , kg/mm ²	δ , %	ψ , %	Variation of the characteristics in % of their value at 20°C			
					σ_y	σ_u	δ	ψ
20	79	84	18	56	—	—	—	—
200	56	61	20	59	-29	-27	+13	+6
300	50	55	16	62	-36	-34	-17	+12
350	47	54	17	64	-39	-36	-6	+14
400	51	55	15	63	-35	-34	-15	+13

TABLE 2

Mechanical properties of semifinished products made of the AT-3 alloy

Semifinished product	σ_y , kg/mm ²	σ_u , kg/mm ²	δ , %	ψ , %	a_i , kg·m/cm ²	H_B , kg/mm ²	Angle of bending, $R_{\text{mandrel}} = b$
Forging, rods, plates	70—85	75—90	12—18	40—60	5—14	250—300	—
Sheet thickness $b=1.5-3.0$ mm.	60—75	70—85	16—24	40—50	—	—	75—90°

The impact tests were carried out on standard Mesnager test specimens at temperatures of from -196 to $+700^\circ\text{C}$. The results of the experiments are given in Figure 1.

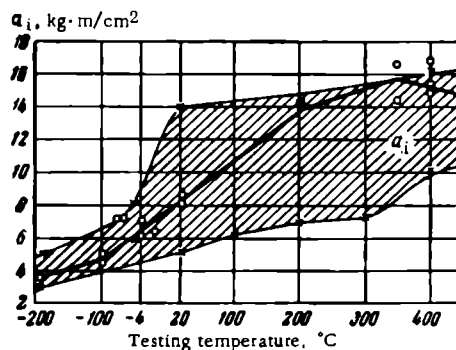


FIGURE 1. The dependence of the impact strength of the AT-3 alloy on temperature

The investigation of the mechanical properties of the AT-3 alloy showed that it has a high strength up to 400°C . The total elongation of the specimen somewhat decreases at test temperatures of $> 300^\circ\text{C}$; at these temperatures the tendency to local plastic deformations, which is reflected by a decrease in the reduction in area of the specimens, is somewhat higher than that at room temperature. Annealed alloys have a rather high impact strength; different melts have different a_i values.

From the determination of the mechanical properties of 30 industrial melts, it was possible to estimate the order of magnitude of the mechanical properties of AT-3 alloys at room temperature, after annealing at $800-850^\circ\text{C}$ and holding at this temperature for 30 min (Table 2).

The evaluation of the deformability of alloys at constant rates of deformation*

The deformability of alloys was determined by the method developed and used by the TsKTI, for materials which undergo a plastic deformation

* This work was carried out by A. A. Chizhik of the TsKTI.

in the zone of the existing stress raisers /1-4/. The tests were carried out at two different rates which differ by almost three orders of magnitude: $v_1 = 180\%$ per hour and $v_2 = 0.8\%$ per hour.

The results of the determination of the elongation and of the reduction in area ψ are given in Figure 2. In addition to the plasticity, the yield point and ultimate strength were also determined. It has been experimentally shown that at the above-mentioned rates of deformation and temperatures the alloys are not embrittled and that the load has little influence on the deformability of the alloy.

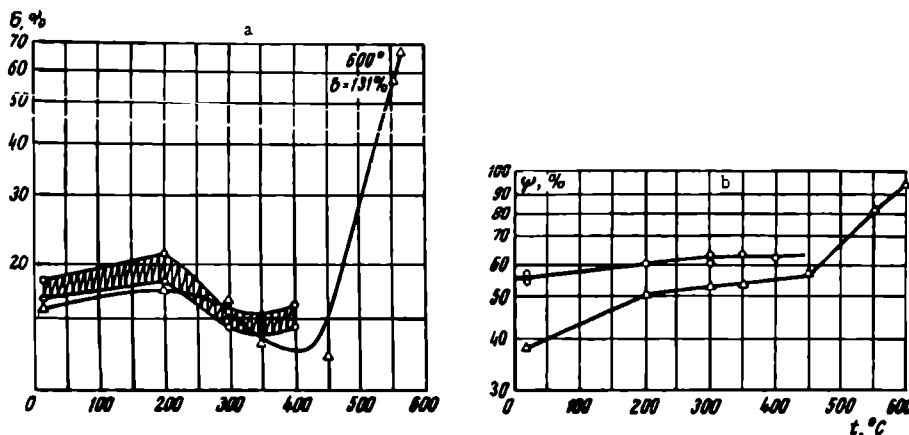


FIGURE 2. The dependence of the elongation (a) and of the reduction in area (b) of the AT-3 alloy on the testing temperature

O — rates of testing 180%/hr; Δ — rates of testing 0.8%/hr.

It should be noted that above 450-500°C the plasticity of the alloy considerably increases while its strength greatly decreases due to the intensive weakening of the material.

Approximate evaluation of the notch sensitivity*

This evaluation was carried out by comparing the results of tension tests at a rate of 0.8 % per hour for specimens of two types: 1) plain specimens 8 mm in diameter and 40 mm long and 2) the same specimens with spiral notches /3/. The dimensions of the notches were as follows: depth 0.75 mm; angle 60°; radius of curvature 0.15 mm, pitch of the notch spiral 12.7 mm. In order to produce a symmetrical deformation in the specimens a double threaded spiral was cut. The specimens with the spiral notches were tested until a crack to be indicated on the stress-strain diagram was formed.

The stress-strain curves (Figure 3) show that at all temperatures the notched specimens failed under lower stresses and deformations than plain specimens. This points to notch sensitivity of the AT-3 alloy.

* This investigation was carried out by A. A. Chizhik.

The sensitivity to spiral notches was evaluated according to two parameters: 1) the coefficient of sensitivity to loads:

$$k_s^a = \frac{\sigma_u^{\text{notched}}}{\sigma_u^{\text{plain}}}$$

and 2) the coefficient of the sensitivity to plastic deformations:

$$k_s^b = \frac{\delta_y^{\text{notched}}}{\delta_y^{\text{plain}}}$$

(δ_y = elongation of the notched specimen at the moment of failure).

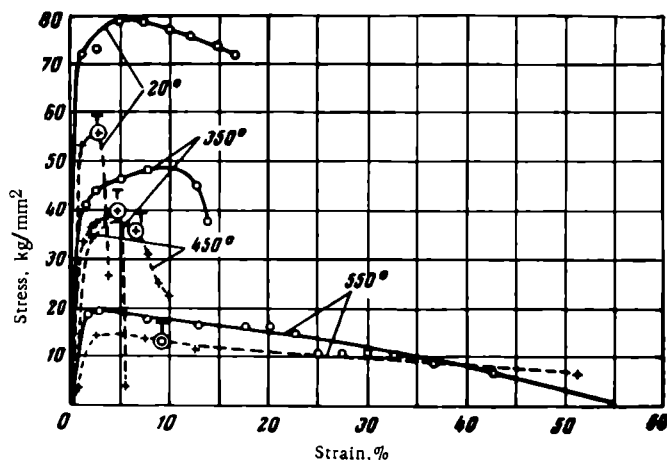


FIGURE 3. Tension testing of plain specimens (continuous lines) and of specimens with spiral notches (dotted line) at a rate of tension equal to 0.8% (the letter T on the curve indicates the appearance of cracks in the specimens)

The dependence of these coefficients on the temperature is shown in Figure 4.

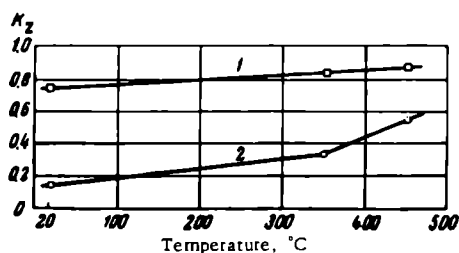


FIGURE 4. The dependence of the coefficients of notch sensitivity to load (1) and to plastic deformation (2) of spiral specimens on the testing temperature

These data indicate that the AT-3 alloy has a notch sensitivity in the temperature range from 20 to 450°C. The stress raisers influence the

plasticity more than the strength of the alloy. If the temperature is raised to 450°C the coefficient k_s^b changes from 0.155 to 0.53, while the $k_s^a \geq 0.75$. The influence of spiral notches on the AT-3 alloy is qualitatively best illustrated by comparing the figures with those of 1Kh18N9T austenitic steel which has at room temperature a $k_s^a = 0.93$ and a $k_s^b = 0.73$.

Creep resistance

The creep tests were carried out by the ordinary method using cylindrical specimens heated to 300, 350, 400, and 500°C. The results of the tests are given in Table 3 and Figure 5.

TABLE 3
Creep resistance of AT-3 alloys

Testing temperature, °C	Stress σ , kg/mm ²	Initial deformation, ϵ_0 , %	Total duration of the test, hours	Minimum rates of creep, %/hrs	Total deformation during, hours			Extrapolation figures for total deformation after 10,000 hours, %
					500	1000	3000	
300	30	~0.3	>1560	0	—	—	—	—
350	15	0.17	1060	0	0.18	0.18	—	0.18
	20	0.19	2000	0	0.20	0.21	0.22	0.22
	25	0.24	2050	$0.1 \cdot 10^{-5}$	0.25	0.26	0.26	0.27
	30	0.29	3200	$0.5 \cdot 10^{-5}$	0.31	0.32	0.33	0.37
	30	0.36	5000	$1.2 \cdot 10^{-5}$	0.39	0.40	0.41	0.51
	37	0.43	3200	$2.0 \cdot 10^{-5}$	0.51	0.52	0.57	0.71
	45	0.75	4500	$2.5 \cdot 10^{-5}$	0.83	0.85	0.91	1.07
400	15	0.16	2600	$1.0 \cdot 10^{-5}$	0.18	0.19	0.20	0.21
	20	0.22	>2000	$2.2 \cdot 10^{-5}$	0.26	0.28	0.30	0.40
	30	0.33	1900	$2.8 \cdot 10^{-5}$	0.41	0.44	0.47	0.69

It has been experimentally shown that at 300°C and under a load of 30 kg/mm² the creep of AT-3 alloys is so slow that it cannot be recorded by the ordinary methods. At 350°C the creep becomes noticeable under a load higher than 25 kg/mm², but even under loads of 25-45 kg/mm² the creep rate is only equal to 10^{-6} - 10^{-5} % per hour. At 400°C the creep is considerably more rapid and becomes noticeable at loads higher than 15 kg/mm². Nevertheless, at this temperature the rates of creep are low and under a load of 30 kg/mm² they reach $3 \cdot 10^{-5}$ % per hour.

At 500°C the creep is rather high; under a load of 5-7 kg/mm² a residual deformation of 0.2% is reached in the AT-3 alloy after 100 hours.

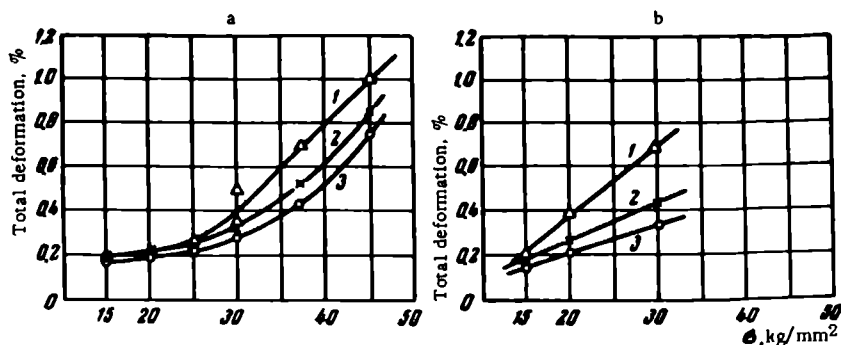


FIGURE 5. Creep resistance of AT-3 alloys at 350 (a) and 400°C (b)

1 - $\tau = 10,000$ hours; 2 - $\tau = 1000$ hours; 3 - $\tau = 0$.

Long-time strength

The long-time strength [better known as creep strength] tests were carried out mainly on cylindrical specimens. The initial creep curves were recorded for some specimens only. The main experiments were carried out at 350 and 400°C, with the aim of determining the maximum long-time strength for a service life of 5000-10,000 hours. In addition, a number of experiments were carried out at higher temperatures. The most characteristic data (Table 4) show that at 350 and 400°C the AT-3 alloy has a high long-time strength. Only stresses of the order of the ultimate strength resulted in failure of the specimens (at the particular temperatures) during periods of time varying from several minutes to 1000-1500 hours. The plasticity of the alloy during long-time strength

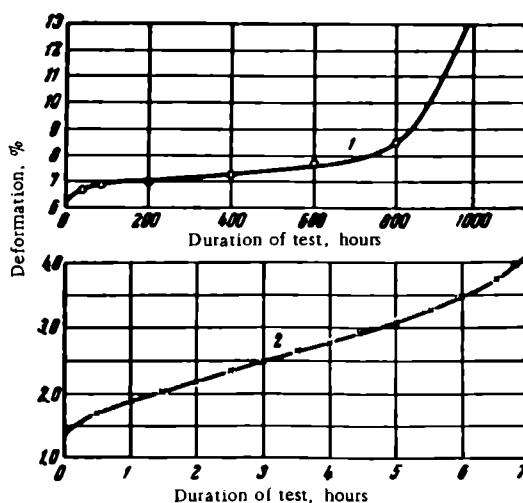


FIGURE 6. Initial curves of long-time strength of the AT-3 alloy at 400°C ($\tau_1 = 967$ hours; $\delta = 13.3\%$)

1 - $\sigma = 55$ kg/mm²; $V_{\min} = 1 \cdot 10^{-3} \%$ /hr; 2 - $\sigma = 54$ kg/mm²; $V_{\min} = 3 \cdot 10^{-4} \%$ /hr.

TABLE 4

Temperature, °C	Stress, σ , kg/mm ²	Initial deformation ϵ_0 , %	Minimum rate of deformation $\dot{\epsilon}$, %/hr	Total duration of test, hours	Deformation of failed specimens		No. of melt	Temperature, °C	Stress, σ , kg/mm ²	Initial deformation ϵ_0 , %	Minimum rate of deformation $\dot{\epsilon}$, %/hr	Total duration of test, hours	Deformation of failed specimens		No. of melt
					ϵ_1 , %	ψ , %							ϵ_1 , %	ψ , %	
350	48	—	—	>1483	—	—	9—659	400	45	0.19	$1.0 \cdot 10^{-4}$	≥ 1000	—	—	1245
	49	—	—	>1484	—	—	9—659	400	50	0.79	$1.9 \cdot 10^{-4}$	>5000	—	—	1245
	50	—	—	>2550	—	—	9—659	400	80	—	—	≥ 800	—	—	9—296
	57	—	—	≥ 1000	—	—	1245	400	50	—	—	≥ 800	—	—	9—297
	54	0.41	$1.2 \cdot 10^{-5}$	>5000	—	—	1245	400	54	1.37	$3.0 \cdot 10^{-4}$	>6500	—	—	1245
	55	0.58	$4.2 \cdot 10^{-5}$	>4000	—	—	1245	400	55	6.2	$1.4 \cdot 10^{-3}$	967	13.3	64.6	1249
	55	—	—	>3300	—	—	9—659	400	56	—	—	0	6.1	80.8	1245
	56	3.2	$1.4 \cdot 10^{-4}$	<2000	—	—	1249	500	30	—	—	≥ 290	31.8	—	—
	57	—	—	>2500	—	—	9—659	500	40	—	—	86	27.5	—	—
	58	—	—	1800	13.0	77.6	9—659	500	50	—	—	3.5	—	—	—
	58	—	—	0.25	6.9	62.7	1245	520	20	—	—	6	—	—	—
	59	—	—	108	12.5	68.7	9—659	600	30	—	—	1	28.5	—	—

TABLE 5
The influence of a 100hour long aging on the mechanical
properties of the AT-3 alloy

Tempera- ture of aging, °C	σ_y , kg/mm ²	σ_u , kg/mm ²	δ , %	ψ , %	σ_i , kg·m/cm ²	Changes in characteristics in % of their initial value				
						σ_y	σ_u	δ	ψ	σ_i
Initial condition*	77,9	83,5	17,7	55,5	8,4	—	—	—	—	—
300	84,8	88,6	17,3	47,2	9,3	+ 8.9	+ 6.1	- 2,3	-15,0	+10,7
350	80,1	83,2	13,9	42,5	9,4	+ 2,8	- 0,4	-21,4	-23,4	+11,9
400	88,9	90,8	15,5	45,9	9,2	+ 14,1	+ 8,8	-12,5	-17,3	+9,5
450	88,2	89,9	13,3	44,5	8,9	+ 13,2	+ 7,7	-24,8	-19,8	+6,0
500	88,5	91,3	9,5	29,3	4,9	+ 13,6	+ 9,4	-46,4	-47,1	-41,6
550	82,7	84,9	14,1	29,5	5,1	+ 6,2	+ 1,7	-20,3	-46,9	-39,2
600	79,8	81,4	13,9	34,1	4,8	+ 2,4	- 2,5	-21,4	-38,6	-40,8

* Annealing at 900°C for 1 hour, and cooling in the air.

TABLE 6
The influence of prolonged heatings at 350 and 400°C on the mechanical
properties of the AT-3 alloy

Duration of aging, hours	Melt 1245 (Σ Cr, Fe, Si = 1,42 %) *					Melt 9-659 (Σ Cr, Fe, Si = 1,26 %) **				
	σ_y	σ_u	δ	ψ	σ_i	σ_y	σ_u	δ	ψ	σ_i
Aging at 350°										
0	77,9	83,5	17,7	55,5	8,4	—	72,7	16,0	62,4	—
100	80,1	83,2	13,9	42,4	9,4	78,2	82,0	17,2	39,8	7,5
500	84,5	86,5	12,7	44,6	8,2	82,4	82,6	16,2	58,5	7,0
1000	91,8	91,5	14,3	46,0	8,0	75,0	80,5	14,0	49,2	7,9
3000	89,9	89,9	13,4	47,8	9,0	81,4	84,8	13,8	51,0	—
4000	81,2	82,4	16,3	41,2	5,2	—	—	—	—	—
Aging at 400°										
100	89,9	90,8	15,5	45,9	9,2	—	78,0	16,5	49,8	—
500	88,9	89,3	13,9	47,4	7,5	—	76,7	15,8	44,3	—
1000	88,4	89,5	12,7	42,5	5,4	—	80,0	16,3	42,4	—
3000	—	—	—	—	—	—	80,5	12,4	43,0	—

* Initial condition — annealing at 900°C for 1 hour.

** Initial condition — annealing at 850°C for 30 minutes.

testing was on the level of the plasticity during short-time strength testing and no considerable embrittlement was noticed. The local deformability, which is characterized by the reduction in area ψ , is 60-80 %. Such a high plasticity is characteristic of alloys with intracrystalline failures; a microstructural analysis of destroyed areas confirmed the intracrystalline type of failure.

Figure 6 shows two initial creep curves recorded for a prolonged period at 400°C. These curves have three well developed sections which indicates that no sudden loss of plasticity can be expected at this temperature.

Since the long-time strength of the AT-3 alloy is very high at 350 and 400°C and of the same order as the ultimate strength, there is no necessity for a further determination of its long-time (5000-10,000 hours) strength at these temperatures.

In future only 1-2 specimens should be tested from each melt in order to determine their long-time plastic properties.

Stressing of the specimens causes a rather high initial plastic deformation together with a work hardening, the effect of which is difficult to annul. No embrittlement of the alloy could be determined during a creep test of up to 6500 hours.

At temperatures of from 500 to 600°C the AT-3 alloy is greatly weakened; no tendency toward embrittlement could be found at high temperatures, but this conclusion must be confirmed by additional and more extended experiments.

Aging of the alloy

The stability of the AT-3 alloy during the prolonged action of high temperatures was evaluated by determining the mechanical properties and the structure of heat-treated specimens.

The chief temperatures of aging were those to which the alloy is subjected during its service life (350 and 400°C).

In addition, the effect of heating to higher temperatures for about 100 hours was checked and also the influence of the annealing temperature on the aging under service conditions (400°C). The specimens for mechanical tests were aged in the air. The aged specimens were usually tested at room temperature except in some cases to be mentioned later.

The results of the mechanical tests of the AT-3 alloy after a 100 hour heating to high temperatures (melt No. 1245) are given in Table 5.

In the evaluation of the experimental results changes of $\pm 10\%$ (related to the initial condition) were ignored, since these are within the limits of the normal scattering of the results. The data in Table 5 show that a 100 hour long aging at 350-600°C decreases both the plasticity and toughness, and somewhat changes the strength characteristics. The latter effect is particularly evident at 500-600°C.

A microstructural analysis has shown that very fine particles of a new as yet undetermined phase are precipitated during aging and that a coagulation of the initial (excess) phase also takes place.

The effect of aging at 350 and 400°C for various periods is shown in Table 6. This table shows that the aging at 350 and 400°C is rather slow

and that after 3000-4000 hours the mechanical properties are not inferior to those required by the existing specifications. The chief property changes take place during the first 100 hours of heating.

TABLE 7
Mechanical properties of AT-3 alloys annealed at different temperatures

Characteristics	Temperature of annealing, °C						
	after forging	800	850	900	950	1000	1100
Ultimate strength σ_u , kg/mm ²	83,7	77,2	78,0	76,5	71,8	77,0	69,4
Elongation δ , % . .	16,5	16,3	16,4	18,9	14,4	15,6	15,8
Reduction in area ψ , %	63,5	42,5	49,5	51,0	34,8	32,5	36,2

The mechanical properties of AT-3 alloys annealed at different temperatures are given in Table 7. The data in this table show that the annealing temperature influences the properties of the alloys. Heating to 950-1100°C after aging at 400°C decreases the plasticity of the alloys. This is due to the preservation of a residual β phase under all conditions of heating. Therefore the optimum heating temperature is 800-900°C.

As a whole, the stability of the AT-3 alloy at 300-400°C is satisfactory. The plasticity and toughness somewhat decrease during the first 100 hours of aging. After that this decrease slows down. Higher aging temperatures (450-600°C) also somewhat decrease the plasticity and the impact strength of the alloy during the first 100 hours. Nevertheless, the impact strength is still sufficiently high (4,8-5 kg·m/cm²). Annealing at temperatures above 900°C leads to a more intensive aging and therefore such high temperatures are harmful.

Conclusions

1. The AT-3 alloy, which contains no expensive alloying elements, is stronger than many α -titanium alloys.
2. Its good [structural] stability and the high heat resistance (up to 400°C), render this alloy fit for service at high temperatures and under stresses for at least 5000-10,000 hours. Higher temperatures lead to a considerable weakening of the alloy and to a decrease of its plastic properties and toughness. Therefore, at temperatures above 400-450°C this alloy has only a short service life.
3. The problem of the industrial applicability of this alloy must be solved by elucidating the influence of the technological factors on the strength characteristics and on the plasticity of finished parts (for instance reduction due to forging, plastic deformation during rolling, and during intermediate heat treatment, etc.).

The plasticity of titanium alloys, particularly of the AT-3 alloy, is of great importance.

This is due to the closeness of the magnitudes of the yield point and ultimate strength, which results in their being very sensitive to stress raisers with consequent danger of cracking in the parts. In the boiler industry, therefore, metals of high plasticity must be used, having considerable differences between the yield point and ultimate strength, both at room and elevated temperatures.

Bibliography

1. Stanyukovich, A.V. and N.D. Zaitsev. — Zavodskaya Laboratoriya, No.9:1101. 1959.
2. Stanyukovich, A.V. — Energomashinostroenie, No.5. 1960.

A COMPARISON OF THE HEAT RESISTANCE OF SOME TITANIUM ALLOYS AT 450-700°C

I. I. Kornilov, V. S. Mikheev, O. N. Andreev, and
P. S. Maiboroda

Various titanium alloys have been developed by the many scientific institutions and plants engaged in this type of work. Some of these alloys have already been adopted by industry, while others are still in the testing stage. In order to elucidate the applicability of these alloys at atmospheric and higher temperatures, the authors undertook comparative tests of the heat resistance of industrial titanium alloys and others still in the developmental stage.

The centrifugal method /1-3/ is one of the simplest for testing the heat resistance and for the comparative evaluation of various alloys.

By this method 24 specimens can be tested simultaneously (on the same machine) by bending at the same temperature and initial stress. A diagram of the centrifugal machine is shown in Figure 1.

With this machine determinations can be carried out of the dependence of the heat resistance of alloys on their composition, structure, temperature, and on other factors. The method gives results identical with those obtainable by ordinary methods and as such, as well as for its simplicity, it has been recommended /4, 5/. It has also been found satisfactory for laboratory investigations of the heat resistance of alloys /6, 7/.

The authors have utilized this method to investigate the heat resistance of several experimental and industrial titanium alloys, the properties of which are given elsewhere /8-10/.

The industrial alloys selected for the investigation were the VT-1 alloy (reference alloy for comparative purposes — with a high creep) and the OT-4, VT-5-1, VT-14 alloys. The experimental alloys were OT-4-2, AT-3, AT-4, AT-6, and AT-8, all developed by the alloy chemistry laboratory of the Institute of Metallurgy imeni A. A. Baikov.

The stress applied was 20 kg/mm² and the specimens were heated as follows: at 450°C for 5000 hours; at 500°C for 250 hours; at 550°C for 100 hours, at 600°C for 50 hours, and at 700°C for 5 hours.

Some alloys were given a creep test at 450 and 500°C by the ordinary tension method. The results of these tests were compared with the data obtained by the centrifugal method.

The specimens of all alloys were prepared from industrial melts.

The chemical composition and the mechanical properties of the tested specimens in the starting condition are given in Tables 1 and 2.

For each test two identical specimens were taken with a diameter 4 (±0.1) mm and a gage length of 60 mm. An exception was made in the case of the 500°C isotherm which was constructed on the basis of a 3-4 identical specimen /11/.

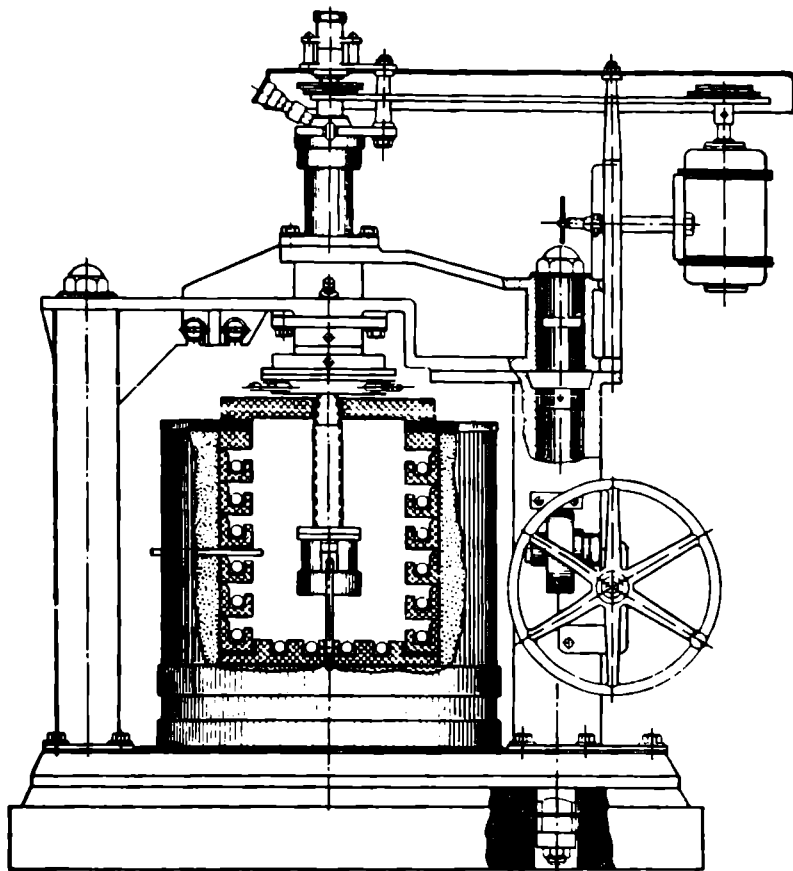


FIGURE 1. Diagram of a centrifugal machine for heat resistance testing by the bending method

The temperature in the furnace was measured and regulated with an accuracy of $\pm 2^\circ$ /12/ by two platinum-platinum-rhodium thermocouples.

The deflection was measured by a special device with an accuracy of up to 0.1 mm after certain time intervals /13/.

Results of the investigation of the heat resistance

The 450°C isotherm. Low-alloyed titanium alloys for the production of sheets were tested at 450°C .

The relationship between the deflection and the duration of the deformation of alloys is shown in the form of creep curves (Figure 2).

These figures show that the VT-1 alloy (technically pure titanium) has, as a result of its low heat resistance, a 40 mm deflection after 30 minutes of testing; at this temperature and under a load of 20 kg/mm^2 the creep of this alloy is highest of all those tested.

TABLE 1
Chemical composition of tested titanium alloys

Alloy	Specimens for testing	Content of alloying elements, weight %							
		Al	Mn	V	Mo	Cr	Fe	Si	B
OT-4	Ø 6 mm wire as supplied	3,5	1,68	—	—	—	0,16	0,14	—
OT-4-2	10 × 10 mm rods, forged	4,95	1,54	—	—	—	—	—	—
VT-6	Ø 6 mm wire, as supplied	5,95	—	3,82	—	—	0,15	0,13	—
VT-14	Ø 8 mm rods, as supplied	4,6	—	1,27	3,2	—	—	—	—
AT without aluminum	20 × 20 mm rods, forged	0	—	—	—	0,8	0,5	0,5	0,01
AT-3	The same	3,2	—	—	—	0,84	0,34	0,4	0,01
AT-4	Ø 6 mm wire, as supplied	4,83	—	—	—	0,86	0,36	0,29	0,01
AT-6	20 × 20 mm rods, forged	5,6	—	—	—	0,52	0,30	0,33	0,01
AT-8	The same	6,81	—	—	—	0,98	0,4	0,59	0,01

TABLE 2
Mechanical properties of tested titanium alloys

Alloy	Mechanical properties			
	σ_u , kg/mm ²	σ_y , kg/mm ²	δ , %	ψ , %
OT-4	82,3	—	14,6	24,3
OT-4-2	102,5	98,3	10,5	39,8
VT-6	95,4	—	13,3	28,8
VT-14*	98,3	—	19,6	69,5
VT-14**	127,5	—	10,9	30,5
AT	75,5	—	16	51
AT-3	89,2	85,0	16,4	48
AT-4	97,5	93	15,3	44
AT-6	106	102	14	36
AT-8	112,3	110	13	33

* As supplied.

** In the hardened and aged condition.

Another alloy with a high rate of creep is the low-alloyed OT-4 titanium alloy. This has an $\alpha + \beta$ -phase structure and a low temperature of eutectoid transformation, which imparts to it a low heat resistance.

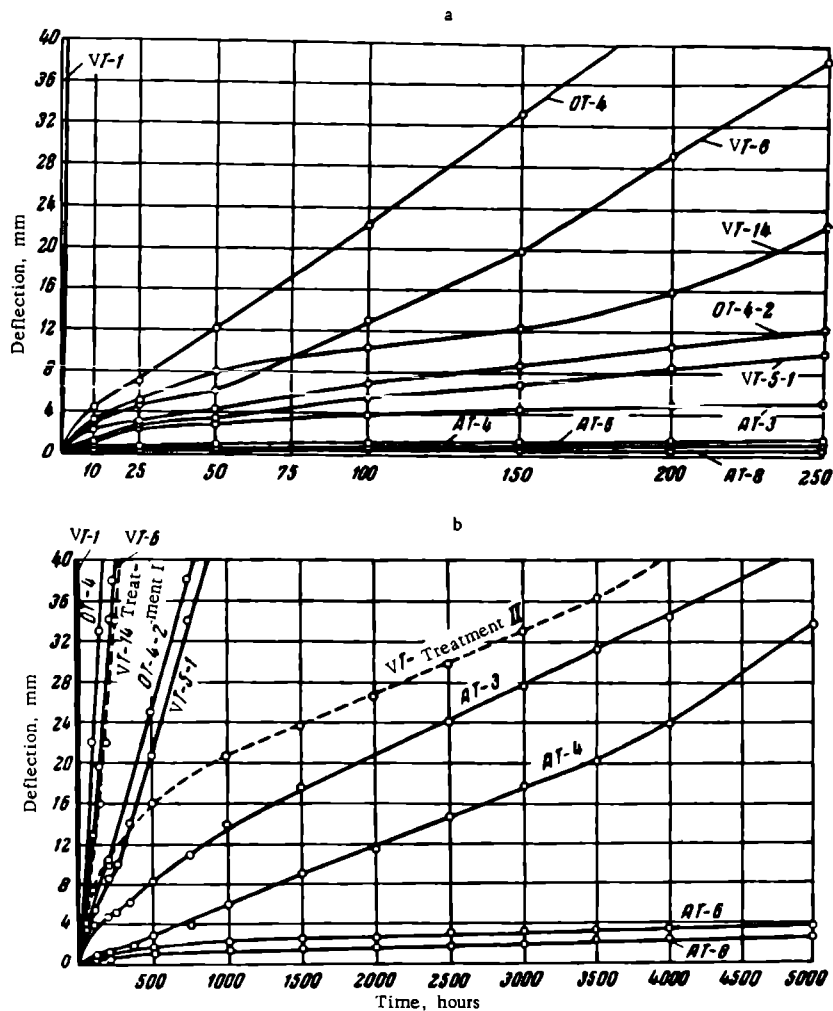


FIGURE 2. Creep of several industrial and experimental titanium alloys at 450°C and a load $\sigma = 20 \text{ kg/mm}^2$; duration of test 250 (a) and 5000 hours (b)

The VT-6 alloy has relatively high rates of creep. At 450°C this alloy also has an $\alpha + \beta$ -phase structure. The VT-14 and OT-4-2 experimental alloys have under these testing conditions a lower creep rate.

The two specimens of the VT-14 alloy yielded different results during testing. After 250 hours the deflection of one specimen was 31 mm while that of the other only 11 mm. The OT-4-2 alloy with 5% Al and 1.5% Mn, and the VT-5-1 alloy with 4-5.5% Al and 2-3% Sn have about the same rates of creep.

The AT-3, AT-4, AT-6, and AT-8 alloys belonging to the 6-component system /10, 14/ with 3, 4.5, 6, and 7.5% Al respectively as well as a total content of Fe + Cr + Si + B equal to 1.2-1.6% have a considerably lower

rate of creep than other investigated industrial and experimental alloys. Figure 2 shows that at 450°C the AT-3, AT-4, AT-6, and AT-8 alloys have a high heat resistance for a period of 250 hours (i. e., during this time they are deformed only to a small extent).

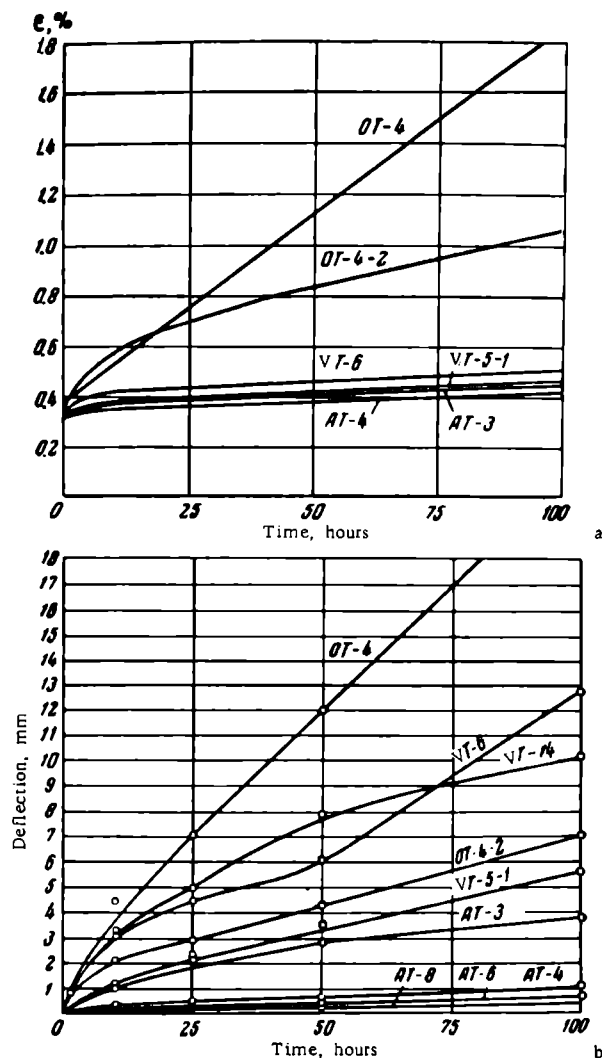


FIGURE 3. Creep of titanium alloys at 450°C and under a load $\sigma = 20 \text{ kg/mm}^2$ for 100 hours (tension tests (a) and bending tests (b))

The AT-alloys have a high $\alpha \rightleftharpoons \beta$ transformation temperature [14] and consist chiefly of a multi-component α -solid solution with small amounts of a residual β phase.

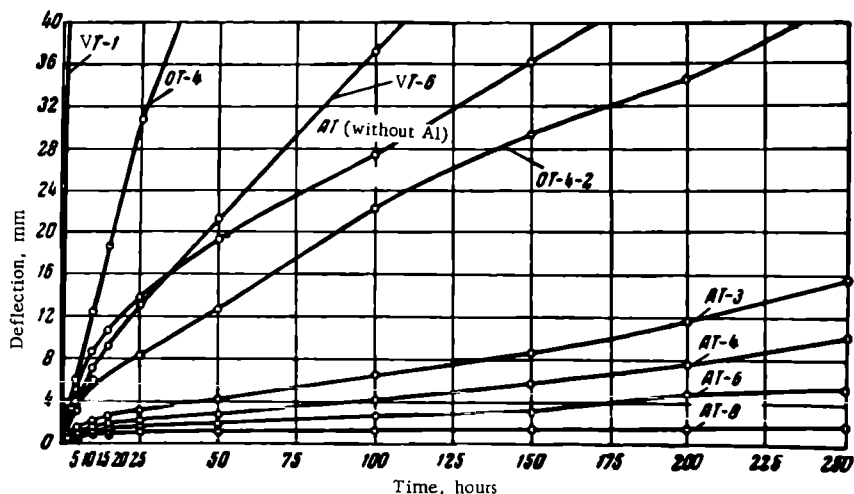


FIGURE 4. Creep of several titanium alloys at 500°C and a load of $\sigma = 20 \text{ kg/mm}^2$ (obtained by the bending method)

An increase in the amount of the chief alloying element (aluminum) increases the heat resistance [15] and decreases the rate of creep of the AT alloys (AT-3 \rightarrow AT-4 \rightarrow AT-6). The AT-8 alloy with 7.5 % Al has the highest heat resistance.

The tension creep tests show the same order of heat resistance of the alloys (except for the VT-6 and OT-4-2 alloys). Figure 3 shows the creep curves (100 hours) obtained by the tension and bending tests. The different positions of the creep curves of the VT-6 and OT-4-2 alloys in Figures 3a and b, can possibly be explained by different initial conditions of the specimens.

The 500°C isotherm. Low-alloyed titanium sheeting was tested at 500°C.

The relationship between the deflection and the duration of the deformation of alloys is shown by the creep curves in Figure 4.

This figure shows that the VT-1 alloy has the highest deformation rate. The OT-4 alloy has a high rate of creep; the VT-6 alloy has a 5-7 mm deflection after 10 hours. The AT alloy, without aluminum, has about the same rate of creep (5-8 mm deflection after 10 hours). The OT-4-2 alloy with a higher degree of alloying has a higher heat resistance than the OT-4 and VT-6 alloys; the deflection of the former is 5-6 mm after 10 hours. Both at 500 and 450°C the AT alloys have the lowest rate of creep. The heat resistance of titanium alloys increases with the aluminum content in the following order: AT-3 \rightarrow AT-4 \rightarrow AT-6 \rightarrow AT-8.

Thus, from the results of creep tests at 500°C, titanium alloys can be arranged in the following order of increasing heat resistance: VT-1 alloy \rightarrow OT-4 \rightarrow VT-6, AT (without aluminum) \rightarrow OT-4-2. The 6-component AT-3, AT-4, AT-6, and AT-8 alloys have a higher heat resistance than the others. The data on the rate of creep (Figure 4) obtained by the bending method are in agreement with the creep curves obtained at the

same temperature by the tension method. The curves in Figure 5 obtained by the latter method are similar to those in Figure 4.

According to the creep curves obtained by tension tests, the OT-4 and VT-5 alloys are less heat resistant than the VT-5-1 and VT-6 alloys. The AT-4 alloy has the highest heat resistance, and the lowest rate of creep.

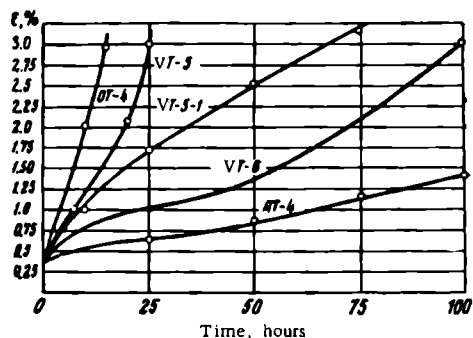


FIGURE 5. Creep of several titanium alloys at a load $\sigma = 20 \text{ kg/mm}^2$ at 500°C (tension method)

The higher heat resistance of AT-3, AT-4, and AT-6 alloys compared with the VT-6, VT-5-1, and VT-3-1 alloys at 500°C is also shown by creep-limit diagrams of the alloys at 500°C (Figure 6).

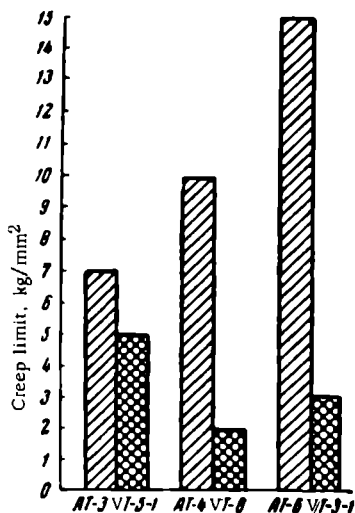


FIGURE 6. Creep limit ($\pm 0.2/100 \text{ kg/mm}^2$) of new titanium alloys AT-3, AT-4, and AT-6 and of the industrial alloys VT-5-1, VT-6, and VT-3-1 at 500°C

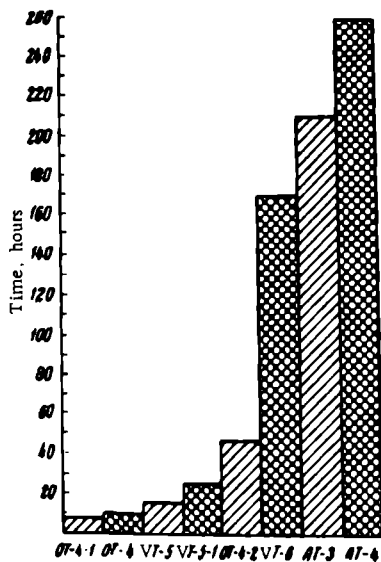


FIGURE 7. Time to failure of titanium alloys at a load of $\sigma = 30 \text{ kg/mm}^2$ at 500°C

Figure 6 shows that the creep limits of AT-3, AT-4, and AT-6 alloys are higher than those of VT-5-1, VT-6, and VT-3-1 alloys. The long-time strength of these alloys can be placed in the same increasing order as the heat-resistance. Figure 7 shows the time to failure of alloys loaded with $\sigma = 30 \text{ kg/mm}^2$ at 500°C .

With the alloys having the higher rate of creep the time to failure is shorter, while for the heat resistant AT-3 and AT-4 alloys time to failure is longest.

The AT-3, AT-4, and AT-6 alloys which have a relatively high heat resistance are also of interest since they do not contain expensive components such as tin (VT-5-1 alloy), vanadium (VT-6 alloy), or molybdenum (VT-3-1 alloy).

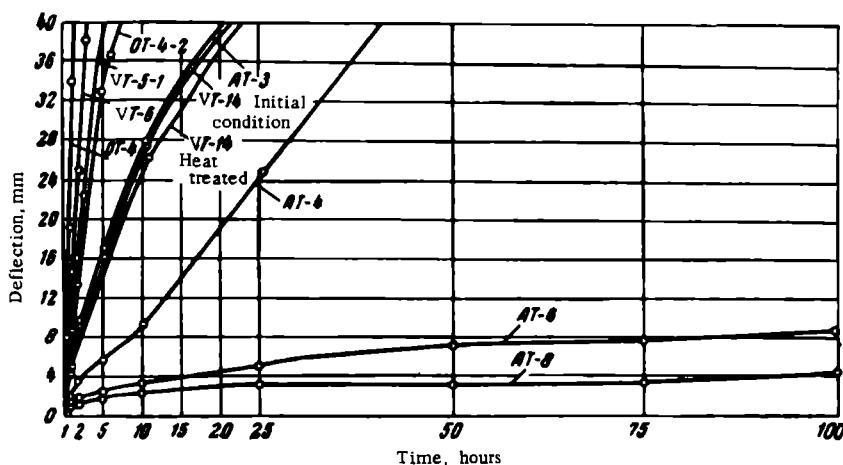


FIGURE 8. Creep of various titanium alloys at a load $\sigma = 20 \text{ kg/mm}^2$ at 550°C

The 550°C isotherm. At 550°C , investigations were carried out on the OT-4, VT-6, VT-5-1, OT-4-2, VT-14 alloys in the initial condition and on the heat treated VT-14, AT-3, AT-4, AT-6, and AT-8 alloys. All these alloys, with the exception of AT-8, are sheet materials.

The dependence of the deflections of these alloys at 550°C on the duration of the deformation is shown in Figure 8.

The OT-4 alloy had a 51.4 mm deflection after 1 hr 30 min. The VT-6 and VT-5-1 alloys also have high rates of creep at this temperature.

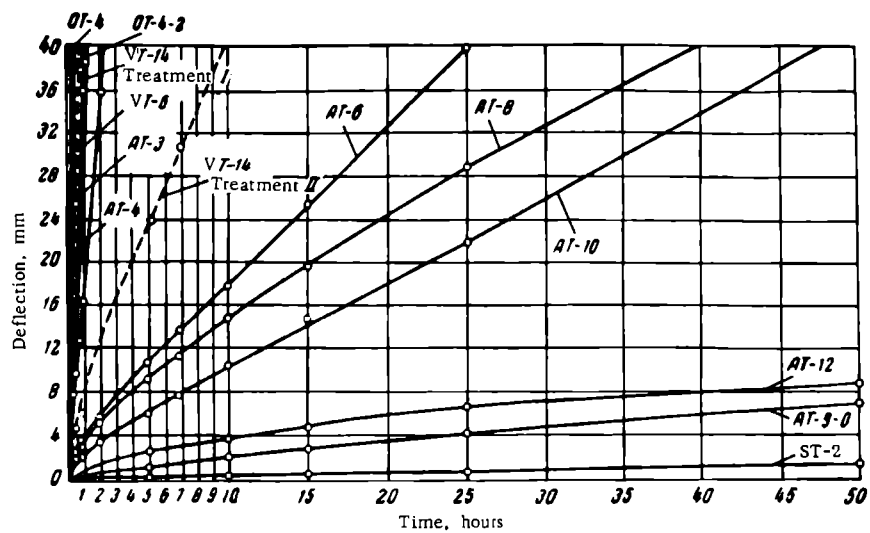


FIGURE 9. Creep of several titanium alloys at a load $\sigma = 20 \text{ kg/mm}^2$ at 600°C

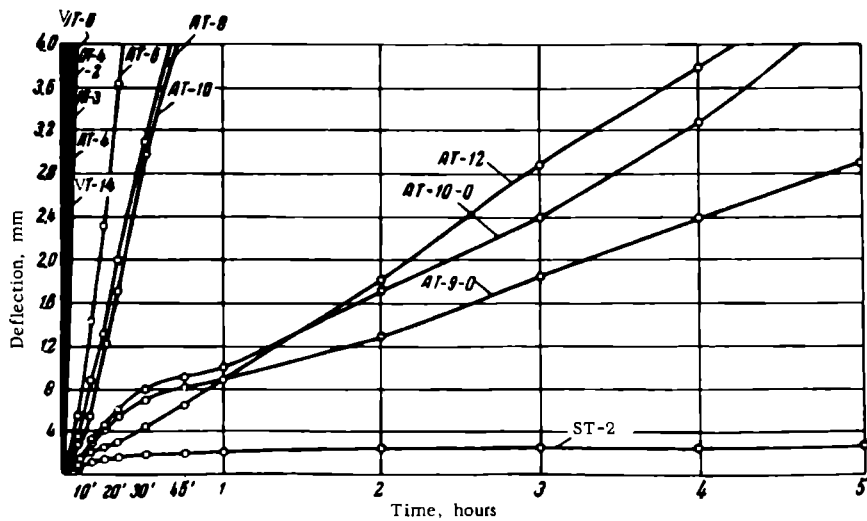


FIGURE 10. Creep of several titanium alloys at a load $\sigma = 20 \text{ kg/mm}^2$ at 700°C

The OT-4-2 alloy has almost the same rate of creep as the VT-6 and VT-5-1 alloys. At this temperature the OT-4-2 alloy shows the greatest differences for two simultaneously tested specimens. The VT-14 and AT-3 alloys have almost identical rates of creep, and the heat resistance of the VT-14 alloy is little influenced by heat treatment.

At 550°C the AT-4, AT-6, and AT-8 alloys have a higher heat resistance than all other titanium alloys examined and the AT-8 alloy has the lowest creep.

From the creep tests at 550°C the investigated alloys can be arranged according to their increasing heat resistance as follows: OT-4 → VT-6 → OT-4-2 → VT-5-1 → VT-14; the VT-14 and AT-3 alloys have similar heat resistances; the AT-4, AT-6, and AT-8 alloys are the most heat resistant of all.

The 600°C isotherm. At 600°C, investigations were carried out of titanium alloy sheets and also of the high strength forged AT-8, AT-10, AT-12, and AT-9-0 alloys, together with the ST-2 experimental alloy on the basis of Ti_3Al , which had been developed at the laboratory [16].

The curves in Figure 9 show that the OT-4, OT-4-2, VT-6, VT-14, and AT-3 alloys have a very high rate of creep, their deflection reaching the permitted maximum in the course of 15-60 min. Next in this series is the AT-4 alloy which at 600°C shows a 36-mm deflection after 2 hours. The AT-6, AT-8, and the 8-component, high-strength AT-10, AT-12, and AT-9-0 alloys have higher heat resistance than all other investigated titanium alloys.

The alloy on the basis of Ti_3Al has the highest heat resistance: after 50 hours at 600°C it showed only a 1-mm deflection.

The creep-tested titanium alloys can be arranged according to their increasing heat resistance at 600°C as follows: OT-4, OT-4-2, VT-5, VT-14, AT-3. The AT-4, AT-6, AT-8, AT-10, AT-12, and AT-9-0 alloys have a higher heat resistance than the other alloys. The most heat-resistant is the alloy on the basis of Ti_3Al .

The 700°C isotherm. The creep-versus-duration of deformation curves for 700°C and $\sigma = 20 \text{ kg/mm}^2$ are given in Figure 10. The VT-6, OT-4-2, AT-3, AT-4, VT-14, AT-6, AT-8, and AT-10 alloys have high rates of creep in this order. They reach the maximum deflection periods of up to 60 minutes.

The AT-12, AT-10-0, AT-9-0 alloys have a much lower rate of creep at 700°C. After 5 hours of testing their deflections are 47, 42, and 29 mm respectively. The experimental alloy on the basis of Ti_3Al has a very low rate of creep. After 5 hours of testing its deflection was only 2.5 mm. After 25 hours of testing no appreciable increase in the deflection could be noted.

Conclusions

After investigation of the heat resistance of several industrial and experimental titanium alloys tested at temperatures from 450 to 700°C, the following conclusions were reached.

1. Technically pure titanium VT-1 has a high creep and cannot be considered heat resistant even at 450°C.

2. The OT-4 and OT-4-2 alloys with an $\alpha + \beta$ structure, which belong to the ternary Ti-Al-Mn system, have a lower heat resistance at 450°C than the AT-3, AT-4, AT-6, and AT-8 alloys of the six-component Ti-Al-Cr-Fe-Si-B system.

Despite their two-phase structure, the ternary alloys containing manganese have a lower temperature of eutectoid transformation and as a result, a lower heat resistance than the VT-5-1 alloy of the Ti-Al-Sn system which consists of a ternary α -solid solution.

3. The VT-6 alloy of the ternary Ti-Al-V system which has an increased content of vanadium is less heat-resistant than the OT-4-2 and VT-5-1 alloy at any temperature. This is due to the fact that the VT-6 alloy has an $\alpha + \beta$ phase structure and that the amount of the poorly heat-resisting β phase increases with temperature, which is confirmed by the polythermal section of ternary-alloy phase diagrams corresponding to the composition of the VT-6 alloy.

4. The hardened and annealed VT-14 alloy has a high strength at room temperature but since it contains an $\alpha + \beta$ phase it turned out to have a low heat resistance at all [elevated] testing temperatures.

5. Among the industrial titanium-alloy sheets, the most heat-resisting is the VT-5-1 alloy of the ternary Ti-Al-Sn system which has a stable α -structure and a high temperature of the $\alpha \rightleftharpoons \beta$ transformation.

6. Multi-component alloying of α -Ti with elements of limited solubility results in an increase of the heat resistance of the alloys. This is confirmed by the fact that the six-component AT-3, AT-4, AT-6, and AT-8 alloys of the Ti-Al-Cr-Fe-Si-B system have a higher heat resistance

At all testing temperatures the heat resistance of the alloys of this series is higher than that of the industrial and experimental titanium alloys OT-4, OT-4-2, VT-6, and VT-5-1 which belong to the Ti-Al-Mn, Ti-Al-V, and Ti-Al-Sn systems.

7. The heat resistance of the 6-component alloys increases with the increase in the aluminum content in the following order: AT-3 \rightarrow AT-4 \rightarrow AT-6 \rightarrow AT-8. This is due to the increasing temperature of the $\alpha \rightleftharpoons \beta$ transformation and to the strengthening of the α -solid solution by the increasing amount of aluminum.

8. The high resistance of AT-3, AT-4, and AT-6 alloys compared with OT-4, OT-4-2, VT-6, and VT-5-1 alloys at 450 and 500°C was confirmed by comparative creep and long-time strength tests carried out by the ordinary tension method.

9. The results of the investigation show that the AT-3 and AT-4 alloys are heat resisting up to 400-500°C, the AT-6 up to 550°C, and the AT-8 alloy up to 550-600°C. Above these temperatures the alloys rapidly weaken and lose their heat resistance.

10. At 600-700°C the most heat resisting alloys are those with an α -phase structure and containing 7-8 alloying elements. To these belong the AT-10 and AT-12 alloys. The experimental alloy on the basis of Ti₃Al has a particularly high heat resistance.

11. It was confirmed that the centrifugal method can be used for the investigation of the relative heat resistance of alloys and for classifying them in the order of their heat resistance. The data obtained by the centrifugal method are in good agreement with the data on the creep and on the long-time strength of the alloys obtained by the ordinary tension method.

Bibliography

1. Kornilov, I.I. — Zavodskaya Laboratoriya, No.1:76. 1949.
2. Kornilov, I.I. — Izvestiya Sektora Fiziko-Khimicheskogo Analiza, AN SSSR, Vol.18:72. 1949.
3. Prokhanov, V.F. — Zavodskaya Laboratoriya, No.8:983. 1957.
4. Oding, I.A., V.S.Ivanova, V.V.Burdugskii, and V.N. Geminov. Teoriya polzuchesti i dlitel'noi prochnosti metallov (Theory of Creep and Creep Strength of Metals). — Metallurgizdat, p.461. 1959.
5. Kuznetsov, V.D. — Sbornik "Issledovaniya po zharoprochnym splavam", Vol.5:361, Izdatel'stvo AN SSSR. 1959.
6. Kornilov, I.I., L.I.Pryakhina, and T.F.Chuiko. — Izvestiya Sektora Fiziko-Khimicheskogo Analiza AN SSSR, Vol.19:437. 1949.
7. Kornilov, I.I. — Izvestiya AN SSSR, OTN, No.4:190. 1959.
8. Glazunov, S.G. and V.N.Sobolev. Titanovye splavy (Titanium Alloys). — Oborongiz. 1958.
9. Mal'tsev, M.V. Metallografiya tsvetnykh metallov i splavov (Metallography of Nonferrous Metals and Alloys). — Metallurgizdat. 1960.
10. Kornilov, I.I. — Khimicheskaya Nauka i Promyshlennost', No.6:6. 1958.
11. Andreev, O.N. — Zavodskaya Laboratoriya, 27(4):471. 1961.
12. Pronin, A.D. and O.N.Andreev. — TsITEIN, No. M-61, No.9:1429. 1961.
13. Andreev, O.N. and A.D. Pronin. — Zavodskaya Laboratoriya, 27(3):356. 1961.
14. Kornilov, I.I., V.S.Mikheev, and T.S.Chernova. — Izvestiya AN SSSR, OTN, No.3:72. 1960.
15. Kornilov, I.I., E.N.Pylaeva, and M.A.Volkova. — Izvestiya AN SSSR, OKhN, No.7:771. 1956.
16. Kornilov, I.I. and T.T.Nartova. — Sbornik "Titan i ego splavy", No.7:95, Izdatel'stvo AN SSSR. 1962.

ALTERATIONS IN THE MECHANICAL PROPERTIES OF THE AT-3 ALLOY AFTER COLD WORKING AND ANNEALING

A. E. Shelest, Z. S. Falaleeva, and I. M. Pavlov

The production of tubes from AT-3 titanium and the manufacture of articles from bent tubing necessitated an investigation of the processes of cold working and heat treatment of this alloy. In normal practice the tubes are etched and thoroughly cleaned after rolling. Bending changes the properties of the tubes, causing work hardening. The degree of work hardening is not the same throughout the entire section of the tube except in the case of the most thin-walled tubes in which it may be approximately assumed as constant.

Optimum strength and plasticity of the alloy can be achieved under certain conditions of deformation and heat treatment, provided that gas saturation of the metal and deterioration of the surface is avoided. This requires limitation of the temperature and of the duration of annealing. In order to determine the [optimum] annealing process for the AT-3 alloy /1/, the authors have constructed work-hardening and softening diagrams for this alloy (composition: 2.8-2.9 Al %; 0.3 Fe %; 0.41 Si %; 0.78-0.80 Cr %; 0.01 B %; balance titanium).

One of the applications of this alloy is the production of 6-76 mm diameter cold-drawn tubes with a wall thickness from 1-6 mm. Since it is difficult to determine the mechanical properties of tubing directly during bending and annealing, the ordinary linear expansion or contraction during bending were taken as being represented by height changes occurring during the rolling of flat 3-mm thick specimens.

Although the various specimens were cut out from the same sheet, their behavior during rolling was not identical. Thus, for instance, specimens cut out from the edges of the sheet were stronger and more difficult to cold roll. Apparently, the thermomechanical process of rolling and annealing of sheets at the plant did not produce a uniform effect over the whole width of the sheet. Saturation of the edges with gases during hot rolling is also possible /2/. In order to find an annealing process which will produce maximum plasticity in the alloy, the authors investigated the mechanical properties and carried out an X-ray analysis of the alloy after various treatments.

The X-ray photographs taken from unannealed rolled sheets (Figure 1a) clearly show that the metal is already work hardened; the maximum values for its mechanical properties under these conditions were: $\sigma_0 = 93.5 \text{ kg/mm}^2$, $\delta = 13.7 \%$; $\psi = 22.6 \%$. Annealing the sheet at 750°C for 1 hour and cooling in the air did not lead to full recrystallization (Figure 1b). The metal was then annealed at 800°C and cooled within the furnace (Figure 1c) and in the

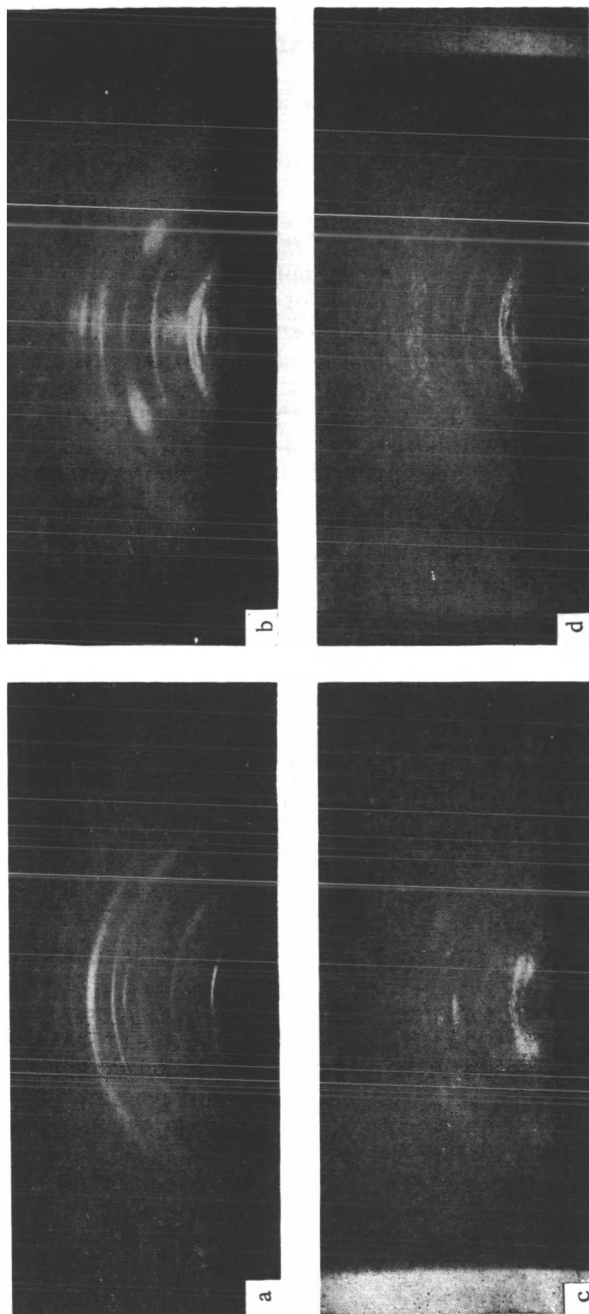


FIGURE 1. X-ray photographs taken from specimens of AT-3 alloys

a—before annealing (after deformation); b—annealing at 750°C for 1 hour, cooling in the air (beginning of recrystallization); c—annealing at 800°C for 1 hour, cooling within the furnace (full recrystallization); d—annealing at 800°C for 1 hour, cooling in the air (full crystallization).

air (Figure 1d). In the first case the plastic properties, as determined by mechanical tests, were very low: $\delta = 8.7\%$; $\psi = 6.1\%$; $\sigma_u = 86.0 \text{ kg/mm}^2$. In the second case the metal had a high plasticity: $\delta = 18.4\%$; $\psi = 29.8\%$; $\sigma_u = 84.5 \text{ kg/mm}^2$. These great differences in the mechanical properties result from the different modes of cooling after annealing, though in both cases the metal was fully recrystallized.

Specimens of alloys in the as-supplied condition and after annealing at 800°C for 1 hour and cooling in the air were cold rolled to a reduction in area of 5, 10, 15, and 20 %. The mechanical properties were investigated in each case on five standard sheet specimens. The dependence of the mechanical properties of the AT-3 alloy on the degree of deformation during cold rolling and on the effect of annealing are given in Figures 2-6. Curve a represents the metal in the as-supplied condition and curve b, the metal after annealing. Articles made of AT-3 alloy are designed for prolonged service life at 350°C . If, however, these articles are cold worked, their properties may be somewhat changed. After annealing at $500\text{--}650^\circ\text{C}$, the strength of the metal decreases. This decrease, together with a corresponding alteration in the reduction in area ψ is particularly apparent in the case of the AT-3 alloy with a degree of deformation equal to 20 %. The authors were unable to determine the temperatures of the beginning and end of recrystallization from the microstructure, the cross-sectional area being too small.

The AT-3 alloy is a 6-component titanium alloy containing aluminum, chromium, iron, silicon, and boron. It has been determined that prolonged homogenizing annealing at $700\text{--}800^\circ\text{C}$ can lead to the formation of an equilibrium α -phase with small inclusions of a TiCr_2 intermetallic compound. In the ordinary condition the AT-3 alloy is an α -Ti-solid solution of alloying elements. Apparently, the α -solid solution of this alloy is supersaturated and its decomposition during an ordinary annealing is very slow. "In deformed alloys a rapid decomposition of the supersaturated solid solution can be achieved at temperatures at which non-wrought alloys either do not decompose at all or begin to decompose only after very prolonged heating" [3/.

Obviously, annealing of deformed specimens at $500\text{--}650^\circ\text{C}$ leads to a decomposition of the solid solution. It will be sufficient to note that these temperatures are close to the temperature of the eutectoid transformation of the Ti-Cr system [4/. A decomposition of the solid solution also takes place during the cooling of the AT-3 alloy within the furnace from a temperature of 800°C . In these cases the lower plasticity can be explained by the TiCr_2 precipitating from the solid solution not only within the grains but also along the grain boundaries.

Passing from deformation by rolling to deformation by bending of tubes, the authors wish to point out the principal difference between the stressed conditions in these cases. Rolling induces a triaxial contraction, while bending induces a linear expansion in the external fibers and a linear contraction in the internal fibers. The triaxial contraction is more favorable for the production of high plastic deformations. In the opinion of the authors, the characteristic determining the selection of the process of deformation (bending) is the residual elongation produced during mechanical tests. In this case we should try to achieve stable values of residual elongation which, however, might differ to a considerable extent from the average magnitudes.

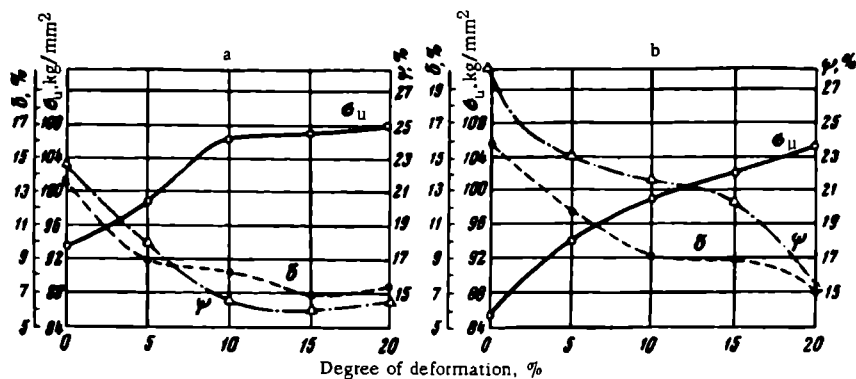


FIGURE 2. Mechanical properties of AT-3 alloys after cold forming

a — in the as-supplied condition; b — annealed at 800°C for 1 hour and cooled in the air.

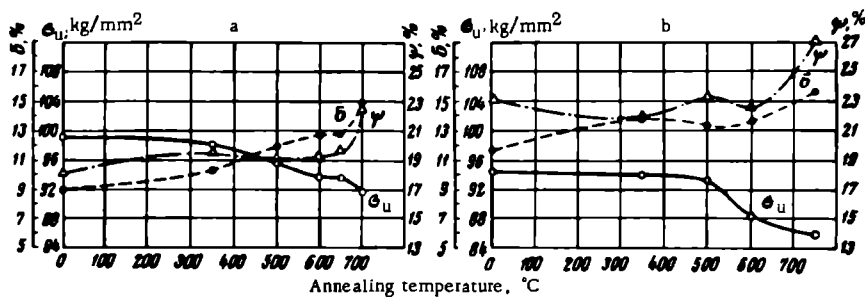


FIGURE 3. Dependence of the mechanical properties of the AT-3 alloy on the annealing temperature after deforming to 5%

a — deformation carried out on specimen in the as-supplied condition; b — specimens annealed at 800°C for 1 hour and cooled in the air before deformation.

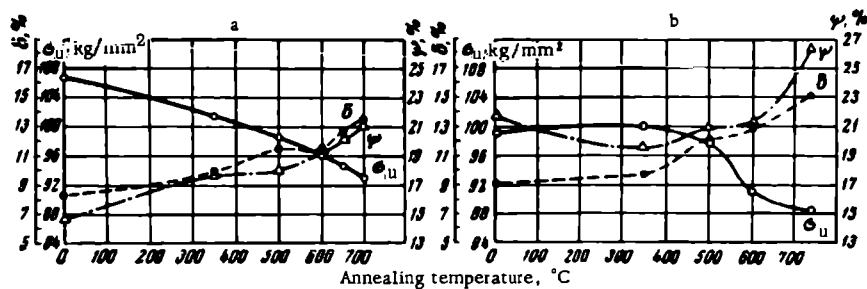


FIGURE 4. Dependence of the mechanical properties of the AT-3 alloy on the annealing temperature after deforming to 10%

a — deformation carried out on specimen in the as-supplied condition; b — specimen annealed at 800°C for 1 hour and cooled in the air.

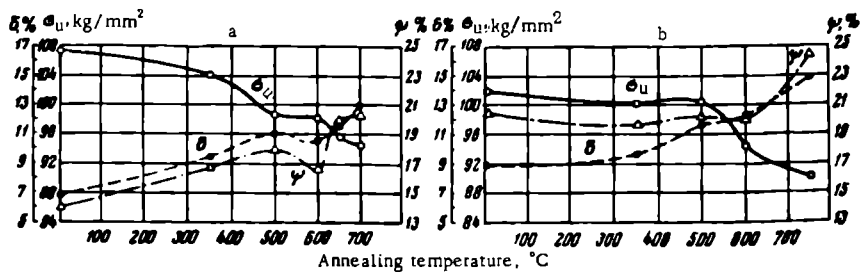


FIGURE 5. Dependence of the mechanical properties of the AT-3 alloy on the annealing temperature after deforming to 15%

a — deformation carried out on specimen in the as-supplied condition; b — specimens annealed at 800°C for 1 hour and cooled in the air before deformation.

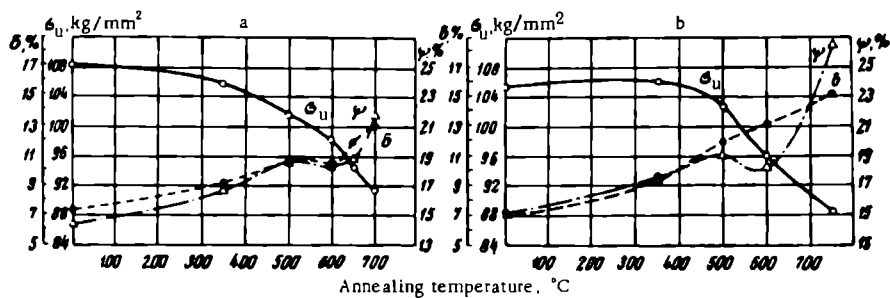


FIGURE 6. Dependence of the mechanical properties of the AT-3 alloy on the annealing temperature after deforming to 20%

a — deformation carried out on specimen in the as-supplied condition; b — specimens annealed at 800°C for 1 hour and cooled in the air before deformation.

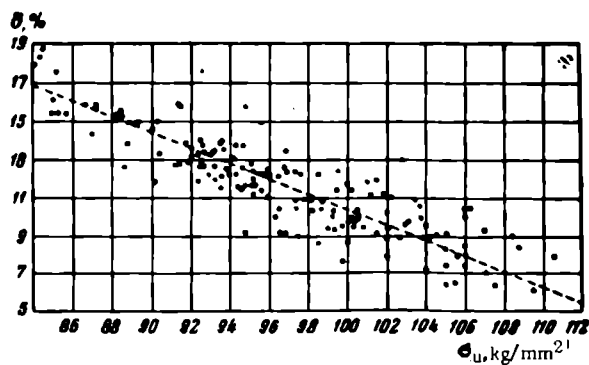


FIGURE 7. Relationship between elongation and ultimate strength of the AT-3 alloy

In this connection, great interest is attached to the relationship between elongation and ultimate strength (Figure 7). In these experiments, the authors obtained a scattering of about $\pm 20\%$ about the average magnitude of elongation. During the mechanical tests, the specimens failed almost without necking down and at a low reduction area ψ .

The data in Figure 2b show that after annealing the tubes can be deformed again by bending to a maximum of 10-12 % ($\delta_{\min} = 15.4\%$). This corresponds to the minimum radius of bending equal to four or five diameters of the tube (of a wall thickness of 3 mm). Tubes with thicker walls can have a smaller radius of bending.

Cold drawn tubes should be annealed before bending, depending on the degree of work hardening and on the thickness of the walls, at 600-700°C for 30 min, and cooled in the air. After bending, the tubes should be annealed again; only in this case will annealing produce a high plasticity and satisfactory strength. These data on the annealing temperatures are of a preliminary nature and should be verified under practical conditions.

Bibliography

1. Kornilov, I.I., V.S. Mikheev, T.C. Chernova, and K.P. Markovich. — Sbornik "Titan i ego splavy", No. 7:140, Izdatel'stvo AN SSSR. 1962.
2. McQuillan, A.D. and M.K. McQuillan. Titanium. — Metallurgy of Rarer Metals, Vol. 2, New York. 1955. [Russian translation, 1958.]
3. Umanskii, Ya.S., B.N. Finkel'shtein, M.E. Blanter, S.T. Kishkin, N.S. Fastov, and S.S. Gorelik. Fizicheskoe metallovedenie (Physical Metallurgy). — Metallurgizdat. 1955.
4. Jaffee, R.I. — Uspekhi fiziki metallov, sbornik IV, Metallurgizdat. 1961. [Russian translation.]

THE ACTIVATION ENERGY OF CREEP AND THE MECHANISM OF PLASTIC DEFORMATION OF TITANIUM ALLOYS

I. I. Kornilov, A. Ya. Shinyaev, and O. N. Andreev

Creep testing of pure titanium by torsion at 13-26.3 kg/cm² over a temperature range of 1000-1450°C has shown that the activation energy of creep $Q_c = 32-33$ kcal/mole irrespective of the stress /1/.

K. A. Osipov and A. A. Sotnichenko /2/ have determined that if the tensile stress is increased from 10 to 20-25 kg/mm² the activation energy of creep of α -Ti decreases by 30 kcal/mole.

These contradictory results led to a series of determinations of Q_c for different titanium alloys.

In the work of Kornilov et al., appearing in this book (see p. 250), data are given on the creep of VT-6, OT-4, AT-3, AT-4, AT-6, AT-8, AT-10, ST-2, and other alloys at 450-700°C and a stress of 20 kg/mm². These alloys consist of an α -solid solution of alloying elements in titanium, and contain only a small percent of β -Ti. On the basis of the data given in the last-mentioned paper, the present authors determined the rate of creep and calculated the activation energy of creep in these alloys. When determining the rate of creep, account was taken only of those curves on which it was possible to identify clearly a straight-line section of steady creep represented by deflections not larger than 4 mm. In such cases the stress changes by not more than 4-5 %, i. e., it can be considered as constant (with an accuracy of 4-5 %). These conditions are satisfactorily met by the AT-3, AT-4, AT-6, AT-8, and ST-2 alloys. The deformation of the VT-1, OT-4, and VT-6 alloys loaded with 20 kg/mm² was so rapid that after 5-10 minutes the deflection exceeded 40 mm and it was therefore impossible to determine the rate of creep in these cases. The rates of creep in AT-3, AT-4, AT-6, AT-8, and ST-2 titanium alloys are given in the table.

On the basis of the data obtained, the authors constructed temperature-versus-rate of creep curves (in semilogarithmic coordinates) for the latter alloys (see figure). As can be seen, all straight lines characterizing the dependence of the rate of creep upon the temperature are parallel. Therefore, the activation energy of creep Q_c calculated from the angle of inclination of these curves is the same for all alloys and is equal to 34 kcal/mole. This magnitude is close to the values of Q_c obtained by Prokoshkin et al. /1/ for β -Ti and differs little from the magnitude of Q_c found for α -Ti under similar loads.

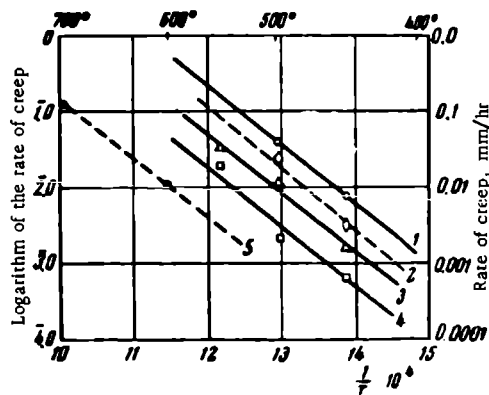
These data lead to the conclusion that an addition of up to 10 % of chromium, aluminum, or other alloying elements to titanium has little influence on the activation energy of creep. Nevertheless, such additions greatly decrease the rate of creep. The decrease in the rate of plastic

deformation is more rapid at higher temperatures (see table), which is in full agreement with the magnitudes of the creep limits of these alloys. Indeed, in passing from the AT-3 to the AT-8 alloy the creep limit increases 2-3 fold.

Rate of creep in titanium alloys loaded with 20 kg/mm², mm/hr

Alloy	Temperature, °C				
	450	500	550	600	700
AT-3 . . .	0.00775	0.040	—	—	—
AT-4 . . .	0.0033	0.029	—	—	—
AT-6 . . .	0.0016	0.012	0.033	—	—
AT-8 . . .	0.00065	0.0022	0.019	—	—
ST-2 . . .	—	—	—	0.043	0.125

These results indicate that the mechanism of plastic deformation of titanium and of its alloys considerably differs from that of the metals belonging to the VIth and VIIIth group of the periodic system. While in the latter alloying leads to a pinning down of part of the slip planes, to the blocking of the dislocations, and consequently to an increase in the activation energy of creep, alloying of titanium apparently only decreases the number of the active centers of plastic deformation and has little influence on the forces of interatomic reaction in the crystal lattice of the alloy. The rate of plastic deformation of Ti alloys is in this case decreased only as a result of the decrease in the number of active centers. Indeed, the AT-8 alloy which has the highest number of alloying elements, has a plastic deformation one-tenth that of the AT-3 alloy.



The dependence of the rate of creep in titanium alloys upon temperature (load $\sigma = 20 \text{ kg/mm}^2$)

1 — AT-3 alloy; 2 — AT-4 alloy; 3 — AT-6 alloy;
4 — AT-8 alloy; 5 — ST-2 alloy.

There is as yet a lack of information as to the physical nature of the active centers. The study of the plastic deformation of α -Ti [4], which is the chief component of the investigated alloys, shows that slip during the plastic deformation of highly pure titanium takes place chiefly along the [1010] and [1120] planes. The alloying of titanium causes an inhibition of the plastic deformation along these planes, as a result of which slip takes place along other planes, [1020] and [0001]. If the alloy is highly stressed and slip develops simultaneously along different planes, a large number of structural defects may arise, causing a transformation from the hexagonal to the body-centered structure, either directly or through an intermediate face-centered modification. From this it may be assumed with a high degree of probability, that the local polymorphic transformations exert an activating effect during the plastic deformation of α -Ti [2].

Bibliography

1. Prokoshkin, D.A., L.I. Ivanov, and V.A. Yanushkevich. — Izvestiya Vysshikh Uchebnykh Zavedenii, Fizika, No.5:65. 1961.
2. Osipova, K.A. and A.A. Sotnichenko. — Doklady AN SSSR, 134(2):333. 1960.
3. Kornilov, I.I., V.S. Mikheev, O.N. Andreev, and P.S. Maiboroda. — This book, page 250.
4. Churchman, A.T. — Proc. Roy. Soc., 226(1165):216. 1954.

TUBE PRODUCTION FROM THE AT-3 TITANIUM ALLOY

V. Ya. Ostrenko, N. V. Bogoyavlenskaya, L. D. Bobrikov,
E. P. Akimova, V. K. Usov, L. N. Okhramovich,
and L. A. Il'vovskaya

In 1961, the Ukrainian Tube Research Institute and the South Nikopol' Tube-Rolling Mill carried out laboratory and plant experiments in order to determine the possibility of production of hot- and cold-drawn tubes from the AT-3 alloy developed by the Institute of Metallurgy imeni A. A. Baikov.

Both the institute and the mill received for their experiments forged and machined billets, 100 mm in diameter and 1000-1300 mm long. Control tests showed these billets to meet with the technical specifications except that some melts had a lower toughness and ultimate strength. In several billets the authors found strings of white and brittle inclusions in the metal. The microhardness of these inclusions was about 1500 units.

The UkrNITI determined the influence of heat treatment on the mechanical properties of AT-3 alloys under laboratory conditions. Figures 1 and 2 show that the mechanical properties and the hardness of the AT-3 alloy undergo considerable change after quenching in water from above 800-900°C but remain almost unchanged after cooling from this temperature in the air or in the furnace. This is due to the precipitation of an $\alpha+\beta$ phase in alloys during quenching in water.

The authors have experimentally determined that alloys quenched in water from the critical temperature of 900°C and aged at 300-500°C have a somewhat higher hardness (from 280 to 310-320 kg/mm² HB). This is apparently due to the transformation of the β phase.

In order to determine the conditions for hot- and cold-rolling of tubes technological tests were carried out in the laboratory of UkrNITI on the piercability, torsion at high temperatures, and the rollability in the cold condition.

Longitudinal sections of shells produced on a laboratory piercing mill at different temperatures (975-1225°C), are shown in Figure 3. As is evident from this figure, the condition of the internal surface of the shells obtained at different temperatures is almost the same in all cases and there are only helical cuts caused by the sticking of the metal to the mandrel. This indicates that the AT-3 alloy has a high plasticity over a wide range of temperatures.

The dependence of the number of twists and of the stress required to destroy the specimens on the heating temperatures is shown in Figure 4. The maximum number of twists corresponds to a temperature of 1100°C.

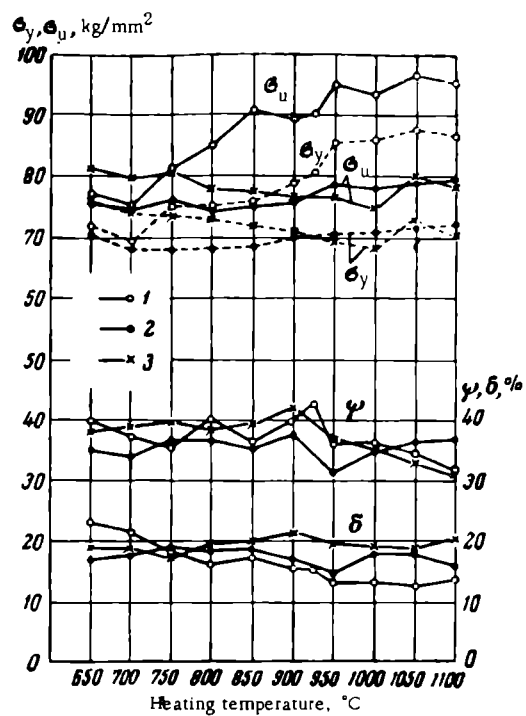


FIGURE 1. Dependence of the mechanical properties of the AT-3 alloy on the conditions of heat treatment

1 — quenching in water; 2 — cooling in the air; 3 — cooling within the furnace.

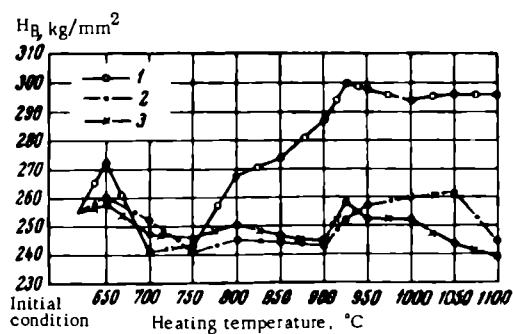


FIGURE 2. Dependence of the hardness of the AT-3 alloys on the conditions of heat treatment

1 — quenching in water; 2 — cooling in the air; 3 — cooling within the furnace.

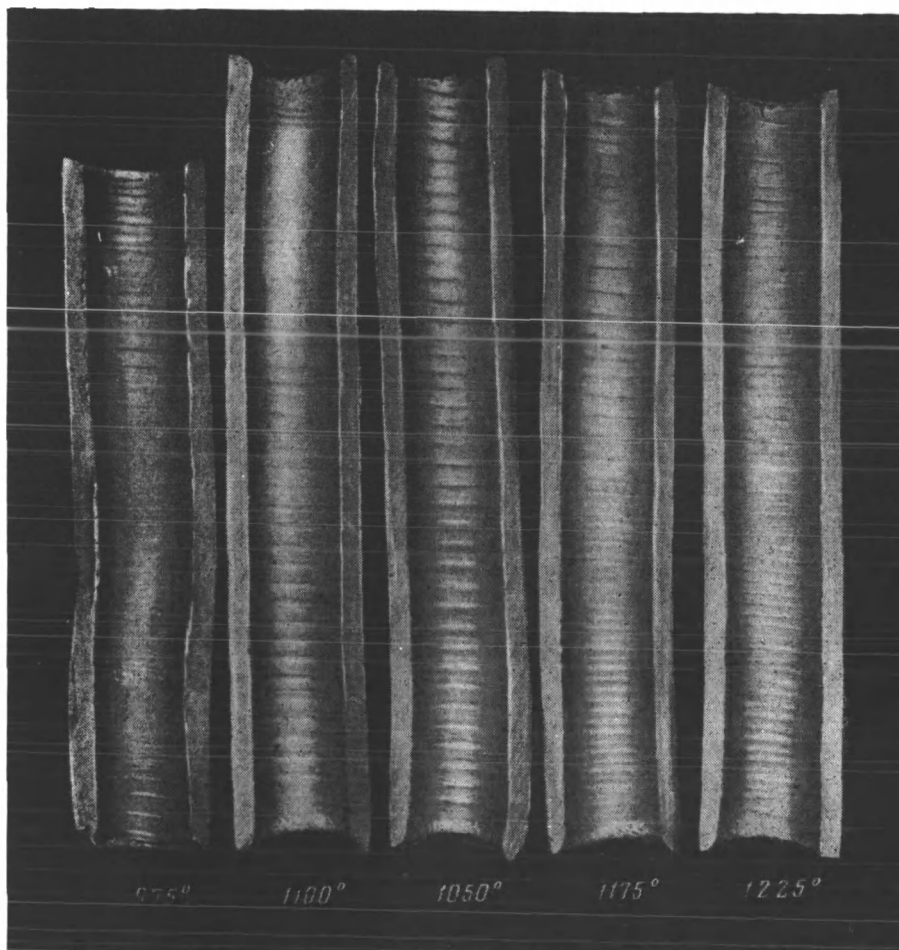


FIGURE 3. Longitudinal sections of pierced billet (shells) of the AT-3 alloy obtained on a laboratory piercing mill at different temperatures

Comparing the results of the piercability and torsion tests and taking into account the high tendency of the metal to stick to the mandrel at temperatures above 1100°C, it has been decided to fix the heating temperature of the AT-3 alloy billets before piercing under industrial conditions at 1080-1125°C.

The rollability of the AT-3 alloy in the cold condition was tested on a laboratory duo-200 rolling mill. The specimens used for this purpose were internally bored out tube-ends 27 × 2.5 mm and 180 mm long.

Before testing, the tube ends were either electrolytically coated with copper or oxidized (oxide-coated) in a fused alkaline salt heated to 410°C. In either case the tubes were lubricated with a mixture of talc and castor oil.

The tests on the rollability in the cold condition yielded the basic parameters for this process under industrial conditions. It was determined inter alia that the degree of deformation during a single pass may be as high as 55 %.

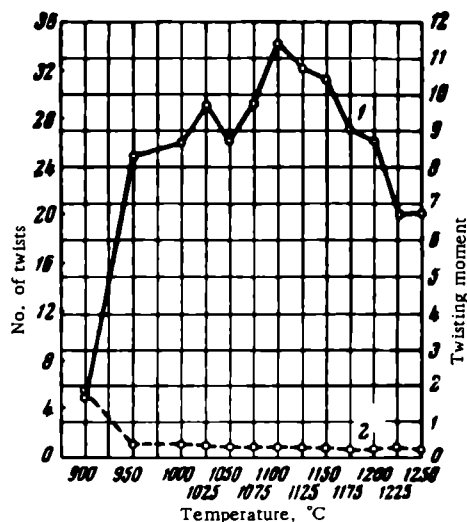


FIGURE 4. Dependence on the number of twists (1) and of the twisting moment (2) on the testing temperature

Hot rolling of tubes from AT-3 alloys was carried on an automatic 140 YuTZ tube rolling mill. Tubes 100 mm in diameter were rolled to 89×7 mm (finished) and to $89 \times 10-13$ mm (for subsequent cold-drawing).

Before rolling, the billets were heated in an ordinary furnace (for heating steel billets) fuelled by natural gas. In order to prevent contact of the billets with the iron scale on the hearth of the furnace the latter was provided with a strip of pure refractory bricks. The temperature of the billets when taken off the furnace was $1080-1120^{\circ}\text{C}$; the duration of heating was 7.5 min per cm of billet diameter.

The rolled tubes were straightened on a straightening roll mill at a temperature of $150-350^{\circ}\text{C}$.

The hot rolling of tubes from the AT-3 alloy proceeded quite regularly (normally) without any difficulties, thus showing that it is possible to produce hot-rolled tubes from this alloy. Nevertheless, because of the sticking of the metal to the rolling tools, cuts were formed on the internal and external surfaces of hot-rolled tubes. In addition, as a result of the high temperatures, the surface of the tubes had a gas-saturated layer. This necessitated mechanical treatment of the hot-rolled tubes and an etching.

Quality inspection of the hot rolled tubes showed that their impact strength, as in the case of billets, is lower than that required by the specification (less than $7 \text{ kg} \cdot \text{m}/\text{cm}^2$).

The microstructure of the metal shows strings of brittle inclusions lying along the direction of rolling.

The hot-rolled tubes in the final stage before cold drawing to 16×2 and 48×4 mm tubing were pierced, machined, and heat treated according to the following process: heating to $820-840^{\circ}\text{C}$, holding for 40 min, and cooling in the air.

After heat treatment, elongation increased from 9-16 to 14-23 % while strength dropped accordingly. Nevertheless, the toughness remained lower than that required by the specifications.

Before cold drawing, the tubes were strongly etched and oxide coated. Because of the high strength of the AT-3 alloy, the cold drawing dies (KhPT) were heated by drawing through them stainless steel tubes.

The AT-3 alloy tubes were drawn on specially designed dies whose dimensions were calculated taking into account the specific deformation of titanium alloys. The tubes were lubricated by a mixture of pharmaceutical talc with castor oil.

The dies were coated by an emulsion applied under low pressure so that it boiled in the zone of deformation.

The cold drawing proceeded in an essentially satisfactory fashion, and no material difference was experienced between drawing the tubes which were heat treated and those which were not.

TABLE 1
Drawing sequence during cold drawing of AT-3 tubing

No. of pass	Dimensions of tube, mm	Deformation, %	Elongation coefficient
0	87×9-10	—	—
1	57×7.5	50	2.0
2	35×5.5	56.5	2.3
3	25×3.2-3.5	53.5	2.15
4	16×2.2	56.5	2.3
0	87×7	—	—
1	63×5.5	43.5	1.77
2	48×4	45.0	1.82

At the same time, tubes cold rolled from billets with a low impact strength (for instance melt No. 1249, $a_1 = 2.4-3.9 \text{ kg} \cdot \text{m}/\text{cm}^2$) cracked. Local cracks and fissures were also formed if the gas-saturated layers or the cuts on the hot rolled tubes were not fully removed.

The data on cold drawn tubes 16 × 2 and 48 × 4 mm are given in Table 1.

After each pass the tubes were degreased, heat treated, etched in an alkaline solution, and brightened in a hydrofluoric-nitric acid solution. The internal surface of the hot rolled tubes had small defects which were difficult to detect by the naked eye. They were removed so as to avoid their further development during the following passes. To do this, the tubes were subjected to a deep or circulation-jet etching during which a 0.1-0.2 mm layer was removed. This left the surface of the tubes completely smooth.

Since after the last pass the tubes were jet etched, they had to have thicker walls.

Since the high tensile strength and yield point and the low toughness rendered it difficult to straighten the tubes, it was necessary to resort to 2-3 operations on a tube straightener (reeler).

The finished tubes were tested according to the specifications by expansion and flattening. Flattening of 16 × 2 mm tubes between two

parallel plates, the distance between which was 5 times the wall thickness of the tubes, caused a widening of the bends.

Satisfactory results were only obtained by flattening specimens between two flat plates the distance between which was seven times the wall thickness of the tube.

TABLE 2
Mechanical properties of hot drawn and heat treated 87×7 mm tubes made of the AT-3 titanium alloy

No. of melt	σ_u , kg/mm ²	σ_y , kg/mm ²	δ , %	ψ , %	a_1 , kg·m/cm ²
1247	80.0	72.6	16.0	—	5.5
	86.0	80.0	17.0	—	5.9
	79.0	70.0	23.0	—	6.0
1251	85.0	78.0	14.5	—	4.0
	89.0	85.0	16.0	—	4.6
	87.0	83.5	18.0	—	4.5
1244	80.0	77.5	15.5	40.5	6.4
	80.0	74.0	19.0	42.0	6.1
	76.5	74.0	17.5	36.0	6.5
1249	74.5	70.0	20.0	37.5	3.5
	90.0	87.5	16.0	37.5	3.9
	91.5	90.0	17.0	34.0	3.4
	94.0	92.5	16.0	34.0	2.4
	98.0	92.5	16.0	37.5	2.45

Flattening of 48×4 mm tubes to a height equal to seven wall thicknesses yielded negative results. Neither did these tubes withstand the expansion tests.

The mechanical properties of hot- and cold-rolled tubes are given in Tables 2 and 3.

It will be noted that most specimens of cold-drawn tubes with an ultimate strength equal to 75-90 kg/mm² have an elongation upon failure equal to 15-20 %.

In addition to the production investigations the chemical treatment of AT-3 titanium tubes was also studied. It was found that the best way to remove scale from the surface of the tubes is by the alkaline-acid method. The hot-rolled, cold-drawn, and heat-treated tubes were etched in an alkaline-nitrate fused salt, consisting of 80 % NaOH + 15 % NaNO₃ + 5 % NaCl, at 430-460°C for 1-1.5 hours. The tubes were then rinsed in cold water, washed under a shower, etched in a hydrofluoric-nitric acid mixture (8 % HNO₃ + 2 % HF) at 40-50°C for 20 seconds and then brightened in a nitric-acid solution and rinsed under a shower (nozzle).

Deep etching of machined tubes before cold drawing in order to expose latent defects, to smooth out the rough peaks and remove the rest of the gas-saturated layer is best of all carried out in a hydrofluoric-nitric acid solution (2 % HF + 8 % HNO₃) at 40-50°C for 4-5 minutes. During such an etching it is necessary to move the tubes continuously along the

bath, in order to create a uniform flow of the solution. Otherwise the etching is nonuniform because of the strong evolution of gases, and so-called hydrogen smudges are formed during a prolonged stationary process (Figure 5). After etching, the tubes were brightened in a 10 % nitric acid solution for 30 seconds.

TABLE 3
Mechanical properties of cold-drawn and heat-treated 16 × 2 and
48 × 4 mm tubes made of the AT-3 alloy

Dimensions of the tubes, mm	$\sigma_{0.2}$, kg/mm ²	$\sigma_{0.5}$, kg/mm ²	δ , %
16×2	98.0	74.5	17.0
	86.5	67.5	20.5
	83.0	66.0	17.5
	100.5	81.5	15.0
	90.0	70.0	16.5
	84.5	71.5	16.0
48×4.0 (melt 1244)	78.5	68.0	18.0
	87.5	77.0	18.0
	99.5	87.5	7.0
	90.5	78.0	11.0
	84.5	75.5	18.5
	77.0	66.0	16.0
48×4.0	91.6	74.3	18.0
	85.5	67.5	18.5
	78.0	68.7	18.7
	79.0	69.4	20.0
	78.6	68.8	12.5
	78.7	65.0	17.7
	78.9	69.8	18.0
	77.9	69.3	15.5

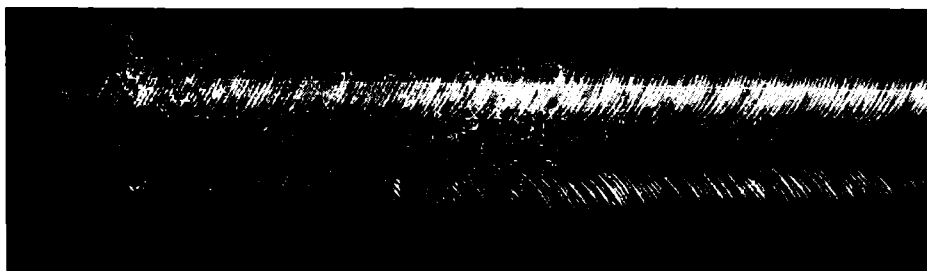


FIGURE 5. Traces of hydrogen smudges on the surface of tubes

After this operation, the surface of the tubes was clean and had a light-gray color.

Lubrication is of great importance in the production of cold-drawn titanium alloy tubes. This is because titanium tends to stick to the dies during drawing, while the lubricant is not adsorbed on the surface of the tube. The surfaces of the tubes must therefore be given some chemical coating to form a basis for the adsorption of the lubricant.

It was experimentally determined that the best chemical coating for this purpose is an oxide film obtained in a fused alkaline salt.

This film is produced by heating the material for 15-20 min at 400-420°C in a fused salt mixture (80 % NaOH + 15 % NaNO₃ + 5 % NaCl). The tubes are then rinsed in cold and in hot water. This treatment together with the lubrication of the surface with a mixture of castor oil (55 %) and talc (45 %) ensures good conditions for drawing. Under industrial conditions the lubricant is removed from the finished tubes in the following way:

- a) processing in an aqueous solution of alkali (40 % NaOH + 10-15 % Na₃PO₄ + 20-30 % water glass) at 80-90°C for 60-90 min;
- b) processing in a fused salt mixture (80 % NaOH + 15 % NaNO₃ + 5 % NaCl) at 380-450°C for 15-20 min;
- c) brightening in a hydrofluoric-nitric acid solution at 45-50°C for 10-15 sec and in a 10 % nitric acid solution for 30 sec.

In order to remove minor defects from the internal surfaces of cold-drawn small tubes the UkrNITI has developed and introduced into the industry a method of jet-circulation etching. A diagram of the device for the jet-circulation etching is given in Figure 6. By this method the etching solution heated to 40-60°C is forced through the tubes by means of a siphon pump. A 0.1 mm thick layer can be removed in the course of 1-2.5 min.

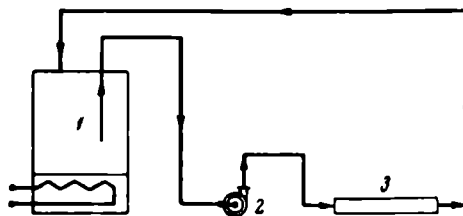


FIGURE 6. Diagram of the device for the jet-circulation etching of tubes

1 — tank with the heated solution (2% HF + 80% HNO₃);
2 — siphon pump; 3 — tube being etched.

Conclusions

The authors have experimentally determined that the AT-3 titanium alloy is suitable for tube production. Nevertheless, because of the tendency of titanium to stick to the dies, the consumption coefficient of metal during drawing of the tubes is rather high.

THE INFLUENCE OF HEATING IN DIFFERENT GASES ON THE TOUGHNESS [IMPACT STRENGTH] OF COMMERCIAL TITANIUM

A. P. Gulyaev, A. E. Shelest, V. I. Mishin, N. N. Kossakovskaya,
and I. M. Pavlov

Heating of titanium and its alloys to high temperatures before hot working or during heat treatment causes an intense formation of scale and a gas saturation. In order to prevent this it is recommended either to accelerate the process of heating (induction heating, electric-resistance heating, etc.) or to decrease the heating temperature as far as the technological requirements of the process permit. It is also possible to heat the articles in special media (protective atmosphere, fused salts, etc.) or to cover them with protective coatings or lubricants. However, very little development work has been carried out in this direction, although the reaction between titanium and various gases has been intensively studied /1/.

Some investigations have recently been carried out /2/ on the behavior of titanium during rolling in vacuo, in the air, and in argon, but these have not dealt with the influence of the heating conditions on the mechanical properties of the metal. In the case of several commercial titanium alloys detailed investigations have been carried out on the dependence of the structure and of the mechanical properties of the metal on their gas content (nitrogen, oxygen, hydrogen) /3-5/. In the present investigation, the authors have elucidated the effect on the toughness of commercial titanium of heating under various conditions (influence of gaseous medium, temperature, duration).

The standard specimens for the determination of impact strength were prepared from heated wrought plates which received no further heat treatment. The impact strength of the specimens at room temperature in the initial condition (as supplied) was 6 kg·m/cm². The specimens were heated, at 100°C intervals, between 700 and 1200°C and held at these temperatures for 10, 60, and 120 min. Heating was carried out in a tubular furnace into which gas was introduced. The specimens were suspended in the middle of the furnace beside the thermocouple. The specimens were weighed before heating and after removal of the scale. From the difference in weight the amount of titanium used up for the formation of the scale was determined. The small weight changes caused by the gas saturation of the metal were disregarded. The toughness was in all cases determined at room temperature.

The specimens were heated in the air, in oxygen, in nitrogen, and in evacuated quartz ampules (vacuum up to $1 \cdot 10^{-2}$ mm Hg). No weight changes were found in specimens heated in vacuo. The weighing changes

after heating in the air and in different gases are plotted in Figure 1. The weight changes are related to a unit of surface and may be used to characterize the development of scale formation. The oxide film formed at 700°C adhered well to the basis metal. No peeling scale was formed during short heating periods even at a temperature of 800°C. Nitrogen had, to a certain degree, a protective influence, little weight change taking place in titanium specimens heated in this gas. Nevertheless, a prolonged heating of Ti in nitrogen at 900°C has the same influence on the toughness of the metal as heating in oxygen (Figure 2). Nitrogen cannot, therefore, be recommended as a protective gas.

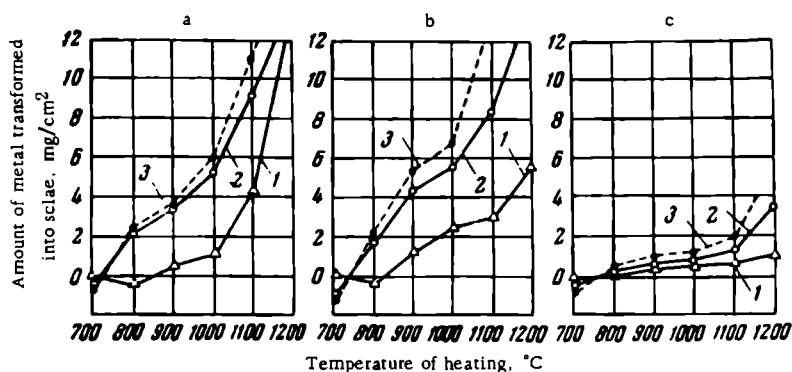


FIGURE 1. The dependence of the amount of metal transformed into scale on the duration of heating and on the environment in specimens of commercially pure titanium;

a — heating in the air; b — heating in oxygen; c — heating in nitrogen 1 — duration of heating, 10 min; 2 — duration of heating, 60 min; 3 — duration of heating, 120 min.

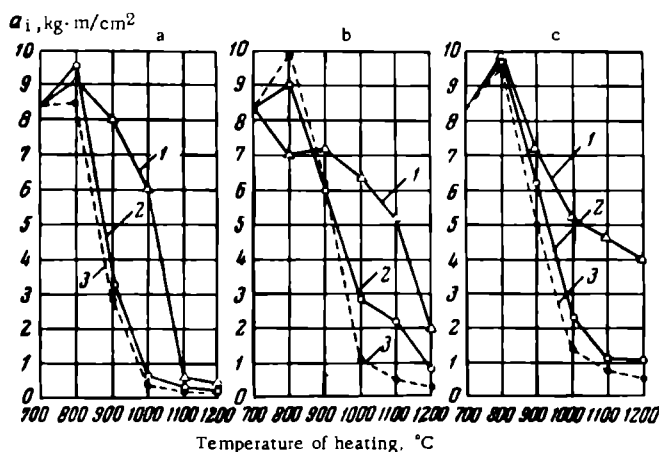


FIGURE 2. The influence of temperature, duration of heating, and environment on the impact strength of commercial titanium

a — heating in the air; b — heating in oxygen; c — heating in nitrogen; 1 — duration of heating, 10 min; 2 — duration of heating, 60 min; 3 — duration of heating, 120 min.

Oxygen and nitrogen form interstitial solid solutions with titanium and thus stabilize the α phase. The surface layer of titanium containing these gases (which may be termed an "alphated" layer*), has a higher strength and a lower plasticity than the basis metal. The authors used a PTM-3 apparatus to measure the microhardness of layer after layer (from the surface toward the center) in specimens subjected to various heating processes. The thickness of the gas-saturated layer (Figure 3) was determined from the microhardness changes. It was found that at a temperature below 900°C the diffusion of nitrogen into α -titanium is less extensive than that of oxygen but that the opposite is true of β -titanium.

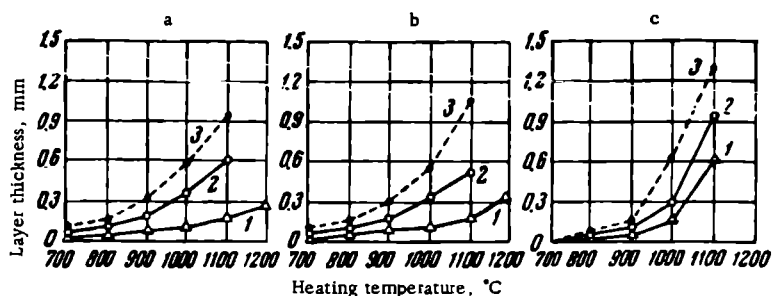


FIGURE 3. The influence of temperature, duration of heating, and environment on the thickness of the gas-saturated layer in commercial titanium

a — heating in the air; b — heating in oxygen; c — heating in nitrogen; 1 — duration of heating, 10 min; 2 — duration of heating, 60 min; 3 — duration of heating, 120 min.

The impact strength of titanium remains high as a result of vacuum heating and is little influenced by the heating time. For instance, after heating at 800°C, the average impact strength was 11.5 kg·m/cm², at 900°C it was 12.0 kg·m/cm², at 1000°C it was 9.2 kg·m/cm², and at 1100°C — 9.0 kg·m/cm².

Heating in the air above 800°C decreases the impact strength of the metal to a greater extent than heating at this temperature in either nitrogen or oxygen. The impact strength increase (as related to the initial material) after heating to 700-800°C is a result of the recrystallization which increases the plastic properties of titanium.

The results of this investigation indicate the importance of analyzing the reaction of the metals concerned with the environment when choosing an atmosphere or coating to protect metals, and particularly titanium, from oxidation and gas-saturation.

Bibliography

1. McQuillan, A. D. and M. K. McQuillan, Titanium. — Metallurgy of Rarer Metals, Vol. 2, New York. 1955. [Russian translation. 1958.]
2. Pavlov, N. M., Yu. M. Sigalov, A. M. Zubko, Ya. B. Gurevich, and A. E. Shelest. — Izvestiya Vysshikh Uchebnykh Zavedenii. Chernaya Metallurgiya, No. 6:106. 1961.

* [A solid solution of gases in α -Ti.]

3. Borisova, E. A. and V. S. Ryzhov. — Sbornik "Titan v promyshlennosti", Oborongiz, p. 160. 1961.
4. Yakimova, A. M. — Sbornik "Titan v promyshlennosti", Oborongiz, p. 203. 1961.
5. Kaganovich, I. N. — Sbornik "Titan v promyshlennosti", Oborongiz, p. 305. 1961.
6. Jaffee, R. I. — Uspekhi Fiziki Metallov, Sbornik 4, Metallurgizdat. 1961.

THE INVESTIGATION OF COLD ROLLING OF A TITANIUM ALLOY STRIP

V. I. Shilov, V. P. Korzh, and L. P. Odínokova

Recently developed high-strength alloys are being increasingly utilized in technology. The production of strips, in particular of thin and very thin grades, from such alloys by cold rolling is a complicated and labor-consuming process which has not yet been sufficiently investigated, although being of great practical and theoretical interest. The authors will present the results of an investigation of the cold rolling of an AT titanium alloy strip and foil /1/*.

This investigation of cold rolling of titanium alloys was carried out with a four high rolling mill $55 \times 260 \times 200$, fitted with devices for measuring the pressure of the metal on the rolls, the tension of the strip, and also the velocities of the rolls and of the coiler drums.

The force interplay during the rolling of titanium alloys: results and discussion

The calculation of the specific pressures must take into account the elastic flattening of the rolls. The length of the zone of deformation, taking into account the elastic flattening of the rolls, is usually calculated according to the formulas derived on the basis of the theory of Hertz and in particular according to the Hitchcock formula /2-4/

$$l' = mrp + \sqrt{m^2 r^2 p^2 + r \Delta h},$$

or according to an equivalent formula

$$l' = \sqrt{r \Delta h + \frac{Pr}{4750b}},$$

where

$$m = \frac{8(1 - \nu^2)}{\pi E};$$

- r = radius of the working roll, mm;
- Δh = area reduction of the strip, mm;
- b = width of the strip, mm;
- ν = Poisson's ratio for the material of the rolls;
- E = modulus of elasticity for the material of the rolls, kg/mm²;
- p = pressure, kg/mm²;
- P = rolling force, kg.

* The specimens of these alloys were supplied by I. I. Kornilov and V. S. Mikheev (Alloy-Chemistry Laboratory of the Institute of Metallurgy imeni A. A. Baikov).

Assuming that for steel rolls $E = 2.2 \cdot 10^4$ kg/mm² and $\nu = 0.3$, then $m = 1.05 \cdot 10^{-4}$ mm²/kg.

The expression for the full pressure is:

$$P = pb(mpr + \sqrt{m^2 r^2 p^2 + r \Delta h}),$$

where

$$p = \frac{P}{\sqrt{br(2Pm + b\Delta h)}}.$$

The specific tension is calculated according to the formulas

$$t_0 = \frac{T_0}{bh_0}$$

and

$$t_1 = \frac{T_1}{bh_1},$$

where T_0 and h_0 , T_1 and h_1 are the respective tension forces and thicknesses of the strip before and after rolling, for a given pass.

The results of the investigation of specific pressure and tension of the strip during cold rolling of titanium alloys are given in Tables 1 and 2. The strip was lubricated by SU machine oil during rolling.

The high rolling pressures (about 450 kg/mm²) obtained can be explained by the high initial resistance to deformation of the alloys being rolled, by their intensive strengthening, and apparently by the high coefficient of friction which is due to the low rate of rolling /5/.

Since cold rolling of titanium alloys produces high pressures, it is necessary to check the [friction] contact strength of the rolls. The specific contact pressures between the working and the back-up rolls are calculated according to the Hertz formula for determining half of the width of the contact surface between two elastic cylinders pressed together /2/. For calculating the full width of contact between rolls with different diameters, the following formula is used:

$$b = 2 \sqrt{mq \frac{rR}{r+R}},$$

where q = pressure on a unit of length of the cylinders, kg/mm;

r and R = radii of the working and back-up rolls respectively, mm;

m = coefficient depending on the material of the rolls, mm²/kg.

When the maximum magnitudes of the force of rolling of the AT-2L alloy strip for the seventh pass is equal to 62.9 tons (see Table 2), the specific contact pressures between the working and the back-up rolls is 185 kg/mm².

Special measurements of the mechanical strength and contact strength of hardened steel /6, 7/, particularly of tool steel, showed the following strength properties of some of these steels.

1) Hardened and annealed 9KhS steel (hardness after hardening and annealing $H_{RC} = 62-64$), the mechanical properties of which are similar to those of the 9Kh steel, has a relative toughness, as determined by compressing grooved specimens, of 436 kg/mm² (the true toughness is only 377 kg/mm²).

2) Hardened and annealed steel balls (steel ShKh15) fail under compressive stresses equal to 780-840 kg/mm², while grooved specimens fail at compressive stresses equal to 350-420 kg/mm².

In the present case, if the roll has an $H_{RC} = 65$ then its Brinell hardness is $H_B \approx 680$ kg/mm² /8/. These data show that during the rolling of thin and very thin titanium alloy strips, the rolls have a certain margin of contact plastic strength $k_{pl} = 680:450 = 1.5$.

TABLE 1

Deformation and force pattern during cold rolling of thin and very thin grade titanium alloy strips. Width of the strip 50 mm; diameter of the rolls 53.9 mm

No. of pass	Thickness of strip, mm		Coefficient of elongation (drawing), λ_i	Force of rolling P_i , tons	Length of the zone of deformation l_i , mm	Specific pressure, P_i , kg/mm ²	Specific tension, kg/mm ²		$2l'_i \left \frac{h_{i-1} + h_i}{h_{i-1} + h_i} \right $
	h_{i-1}	h_i					t_{i-1}	t_i	
AT-3L Alloy									
1	0.205	0.172	1.192	22.0	1.83	236	37.1	32.2	9.71
2	0.172	0.167	1.031	13.5	1.28	207	40.2	19.6	7.55
3	0.167	0.154	1.085	28.1	1.87	294	42.0	36.4	11.6
4	0.154	0.139	1.106	37.4	2.14	345	41.8	22.6	14.6
5	0.139	0.127	1.055	43.2	2.10	400	48.5	39.2	18.1
6	0.127	0.116	1.092	48.4	2.38	396	51.7	24.2	19.6
7	0.116	0.110	1.054	49.7	2.40	406	54.5	42.5	21.2
8	0.110	0.104	1.058	48.5	2.36	404	59.0	26.2	22.0
AT-3M Alloy									
1	0.190	0.172	1.105	18.9	1.64	238	31.4	14.1	9.06
2	0.172	0.154	1.118	25.2	1.85	280	38.2	31.4	11.3
3	0.154	0.142	1.083	39.7	2.23	369	40.0	20.0	15.1
4	0.142	0.133	1.070	45.6	2.36	398	43.8	32.6	17.2
5	0.133	0.126	1.055	50.2	2.46	422	49.5	18.8	19.0
AT-3U Alloy									
1	0.350	0.330	1.061	13.9	1.45	192	17.7	11.1	4.27
2	0.330	0.300	1.100	22.0	1.82	243	18.8	17.5	5.77
3	0.300	0.260	1.153	43.5	2.44	356	22.1	13.2	8.72
4	0.260	0.240	1.082	44.3	2.35	376	22.8	22.0	9.40
5	0.240	0.230	1.043	43.6	2.27	382	27.4	12.9	9.66
AT-4L Alloy									
1	0.340	0.311	1.092	22.1	1.81	245	20.2	17.9	5.56
2	0.311	0.274	1.135	29.5	2.08	284	22.5	11.4	7.12
3	0.274	0.240	1.141	43.5	2.42	362	25.7	22.5	9.43
4	0.240	0.208	1.152	56.2	2.68	419	29.2	14.6	12.0
5	0.208	0.191	1.089	56.5	2.62	431	37.4	30.4	13.1
AT-4M Alloy									
1	0.230	0.216	1.068	18.1	1.55	233	31.0	25.4	6.95
2	0.216	0.197	1.097	26.5	1.87	284	37.1	31.8	9.06
3	0.197	0.178	1.107	43.0	2.33	370	37.4	24.6	12.4
4	0.178	0.169	1.055	46.4	2.35	396	39.8	31.5	13.5
5	0.169	0.158	1.068	50.1	2.45	413	41.4	21.9	15.0
6	0.158	0.149	1.060	55.5	2.56	436	43.2	38.4	17.0
7	0.149	0.143	1.041	60.4	2.64	458	45.4	25.6	18.1

Note. The letters L, M, and U in the designations of the alloys indicate the lower, medium, and upper limits of alloying elements in the alloys, respectively.

The experimental data on the specific pressures (Table 2 and Figure 1) show that for rolling 75 mm wide AT strips at high magnitudes of the shape factor, the curves of the specific pressure have an inflection and pass beyond the field of the approximately stable specific pressure of 380 kg/mm².

TABLE 2

Deformation and force pattern during cold rolling of thin and thinnest grade titanium alloy strips. Width of strip 75 mm, diameter of the rolls 53.6 mm

No. of pass	Thickness of the strip, mm		Coefficient of elongation, λ_i	Force of rolling, P_i , m, tons	Length of zone of deformation l_i , mm	Specific pressure P_i , kg/mm ²	Specific tension, kg/mm ²		$\frac{2l_i}{h_{i-1} + h_i}$
	h_{i-1}	h_i					t_{i-1}	t_i	
AT-2L Alloy									
1	0.220	0.210	1.048	10.0	1.00	131	20.3	12.9	4.67
2	0.210	0.208	1.041	18.1	1.37	203	24.3	11.6	6.56
3	0.208	0.190	1.037	27.8	1.60	230	20.2	11.9	8.03
4	0.190	0.179	1.061	39.3	1.79	289	20.6	13.2	9.75
5	0.179	0.173	1.032	40.9	1.79	302	24.1	10.1	10.3
6	0.173	0.164	1.053	52.3	2.04	340	20.3	12.7	12.1
7	0.164	0.152	1.081	62.9	2.24	371	23.2	25.0	14.2
8	0.152	0.146	1.042	61.9	2.18	375	37.2	13.6	14.6
AT-3M Alloy									
1	0.210	0.208	1.010	6.0	0.70	110	—	—	3.35
2	0.208	0.200	1.040	13.2	1.08	156	—	—	5.29
3	0.200	0.192	1.041	23.9	1.39	220	—	—	7.08
4	0.192	0.181	1.060	34.2	1.66	264	31.2	11.5	8.90
5	0.181	0.168	1.078	49.1	1.97	319	17.4	33.8	11.3
6	0.168	0.161	1.042	51.5	1.98	334	38.2	13.9	12.0
7	0.161	0.160	1.006	53.0	1.97	346	19.6	31.6	12.3
8	0.160	0.155	1.031	64.7	2.19	379	35.2	15.4	13.9
9	0.155	0.145	1.069	65.6	2.24	376	21.3	34.6	14.9
AT-4M Alloy									
1	0.255	0.250	1.020	9.0	0.90	134	16.2	6.93	3.59
2	0.250	0.245	1.020	15.8	1.16	186	22.2	13.6	4.67
3	0.245	0.225	1.089	27.4	1.62	229	17.7	17.7	6.90
4	0.225	0.215	1.046	39.7	1.81	296	20.2	15.3	8.25
5	0.215	0.205	1.048	44.6	1.92	315	18.6	24.3	9.14
6	0.205	0.195	1.051	51.1	2.04	339	19.9	19.6	10.2
7	0.195	0.185	1.053	60.2	2.21	369	20.5	25.8	11.6
8	0.185	0.175	1.057	57.7	2.16	361	23.2	22.4	12.0
9	0.175	0.170	1.029	58.9	2.15	371	27.2	28.0	12.4
10	0.170	0.165	1.030	61.4	2.19	379	24.6	23.0	13.1
11	0.165	0.155	1.064	61.7	2.23	374	27.8	23.8	13.9
AT-6L Alloy									
1	0.360	0.350	1.028	11.3	1.05	141	12.6	11.8	2.97
2	0.350	0.330	1.080	17.0	1.34	167	15.6	18.5	3.94
3	0.330	0.310	1.063	29.0	1.64	233	18.2	17.7	5.13
4	0.310	0.285	1.087	36.5	1.84	261	18.8	20.9	6.18
5	0.285	0.265	1.072	34.6	1.77	260	21.2	18.8	6.42
6	0.265	0.255	1.039	31.8	1.62	258	20.8	21.5	6.23
7	0.255	0.240	1.061	33.8	1.70	261	23.6	20.1	6.88
8	0.240	0.235	1.021	30.9	1.56	261	23.3	23.9	6.57
9	0.235	0.220	1.068	35.4	1.74	268	25.8	20.0	7.65
10	0.220	0.210	1.045	38.1	1.78	285	25.4	28.8	8.20
11	0.210	0.200	1.050	37.4	1.75	282	31.1	21.4	8.52
12	0.200	0.190	1.051	45.8	1.92	315	27.2	27.1	9.84
13	0.190	0.175	1.086	42.8	1.90	290	28.1	27.7	10.4

Note. The letters L, M, and U in the designations of alloys indicate lower, medium, and upper limits of alloying elements in the alloy respectively.

This field characterizes the maximum rollability of the given strip upon rolling under specific conditions and on a specific rolling mill.

It was of interest to determine the minimum thickness for a strip which can be produced under the conditions of maximum rollability. When

determining the conditions of maximum rollability, it is necessary to solve both the equation of Hitchcock for the length of the contact arc and the analytical equation for the determination of the rolling pressures. In both equations the elastic flattening of the rolls must be taken into account. Such solutions are given in the works by M. D. Stone [9], P. P. Lavrov [10], and others.

According to Lavrov, the dependence of the minimum thickness of the rolled strip on the parameters of the rolling mill and of rolling is as follows:

$$h_{\min} = 1.4 \mu d m k,$$

where d = diameter of the rolls;

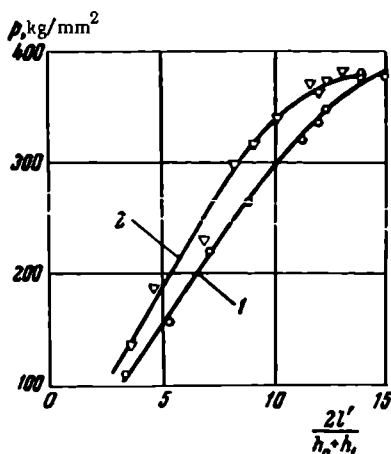
$$m = \frac{8(1-\nu^2)}{\pi E},$$

k = force of resistance to deformation of the strip being rolled;

μ = coefficient of external friction.

FIGURE 1. Dependence of rolling pressures on the shape factor of the zone of deformation during rolling 75 mm wide strips (see Table 2)

1 — AT-3M strip; 2 — AT-4M strip.



For the 11th pass of rolling of AT-4M strips (see Tables 2 and 3) h_{\min} can be found from the conditions of maximum rollability:

$$h_{\min} = \frac{11.2 \cdot 0.115 \cdot 53.6 (1-0.3^2) \cdot 160.2}{3.14 \cdot 22,000} = 0.145 \text{ mm.}$$

The experimentally determined magnitude of h_{\min} (see Table 2) is 0.155 mm.

We will now determine the minimum strip thickness which can be produced on a mill with rolls made of hard alloy (e.g., the VK-10 alloy). We will use the conditions of maximum rollability and a modulus of elasticity $E \approx 5 \cdot 10^4 \text{ kg/mm}^2$ [11]. The magnitudes of ν , k , and μ are assumed equal to those for the other rolls. Then,

$$h_{\min} = \frac{11.2 \cdot 0.115 \cdot 53.6 (1-0.3^2) \cdot 160.2}{3.14 \cdot 50,000} = 0.064 \text{ mm,}$$

i.e., the minimum strip thickness which can be obtained on a mill with rolls made of a hard alloy is 2.3 times lower than that which can be produced on a mill with steel rolls.

In order to increase the contact strength of the rolls and to achieve a maximum rollability during cold rolling of high-strength alloys, the rolls should be made of hard alloys.

Calculation of forces for cold rolling of titanium alloys

In order to calculate the force interplay during rolling the resistance to deformation of the alloy and the coefficient of external friction must be known. There are no experimental data on this coefficient for cold rolling titanium-alloy strips, and its determination from the forward flow is unreliable because of the elastic flattening of the rolls. In a certain sense, it is possible to refer to an average coefficient of external friction for a given pass, which can be analytically determined, for instance, from the data of the experimental pressure /10/.

The influence of the external friction of the tension during cold rolling of metals and alloys can be found from the p/k ratio. There is still no generally accepted method for the determination of the resistance of a metal to deformation and of its work hardening during rolling. It is usually assumed that the strengthening of the metal in the zone of deformation can be represented by a straight-line function /2, 12, 13, and others/, which simplifies the allowance for work hardening in the initial equations. Nevertheless, the graph of strengthening obtained by tension and compression tests for metals and alloys are almost always convex curves. In addition, area reduction along the zone of deformation during cold rolling is very nonuniform. It increases intensively in the first half of the contact arc but its further increase is very small. This also indicates that the law of strengthening of metals in the zone of deformation during cold rolling is represented by a curve. The strengthening of the metal in the zone of deformation during cold rolling should preferably be calculated according to a function represented by a curve /14-17/, particularly by a parabola /18, 19/:

$$\bar{\sigma} = 1.15 \left[\sigma_0 + \frac{2}{3} (\sigma_1 - \sigma_0) \right].$$

It follows that the formula for the determination of the force of resistance to flat deformation with allowance for strengthening and the tension of the metal being rolled is:

$$k = 1.15 \left[\sigma_0 + \frac{2}{3} (\sigma_1 - \sigma_0) \right] - \frac{t_0 + t_1}{2},$$

where $1.15 \sigma_0$ = the resistance to flat deformation at the roll bite;

$1.15 \sigma_1$ = resistance to flat deformation after the strip has left the rolls;

t_0 = specific tension of the strip at the inlet;

t_1 = specific tension of the strip at the discharge point.

As an example, the force of resistance to deformation during cold rolling of AT-4M strip is calculated (see Table 2). The strengthening curve for these alloys, as obtained by the compression method, is shown in Figure 2.

The relationship between the resistance to deformation during rolling and the resistance to deformation during upsetting is represented by the formula

$$\frac{1}{\eta} = \frac{1 + \lambda^2}{2},$$

where $\frac{1}{\eta} = \frac{h_0}{h_1}$ = the coefficient of area reduction (draft) of the metal during a uniform compression;

λ = total coefficient of drawing of the strip during rolling.

When the total coefficients of drawing for each pass are determined and the magnitude $\frac{1}{\eta}$ is found according to the above formula, the resistances

to deformation σ_0 and σ_1 can be obtained from the curve of strengthening. The dependence of $\frac{P}{k}$ on the shape factor of the zone of deformation $\frac{2l'}{h_0 + h_1}$, obtained in rolling the AT-4M strip by the above method according to the data given in Table 3, is shown in Figure 3.

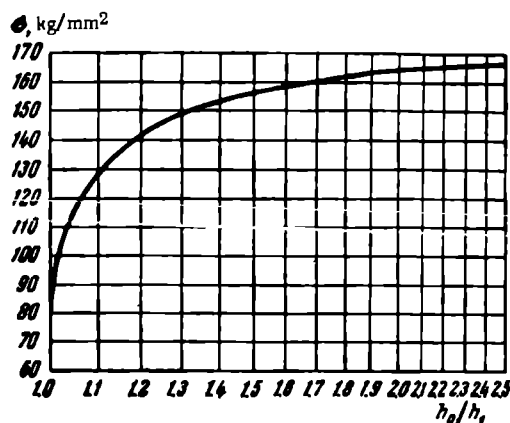


FIGURE 2. Curve of resistance to deformation of the AT-4S alloy, determined by the compression method

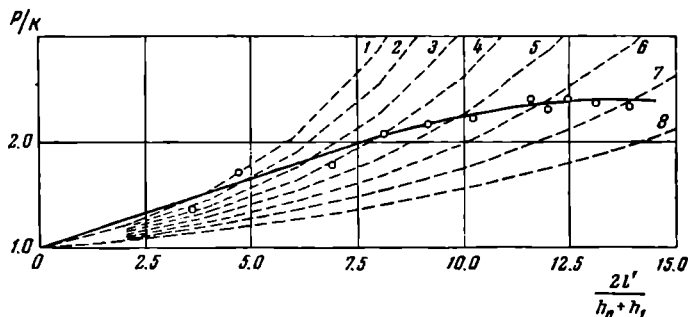


FIGURE 3. Dependence of $\frac{P}{k}$ on the shape factor of the zone of deformation (solid line), obtained experimentally (see Table 3) during cold rolling of AT-4S strip (the shape factor is 0-2.5, the experimental curve is constructed approximately). The dotted lines are constructed on the basis of calculations:

1 — $\mu = 0.24$; 2 — $\mu = 0.22$; 3 — $\mu = 0.20$; 4 — $\mu = 0.18$; 5 — $\mu = 0.16$;
6 — $\mu = 0.14$; 7 — $\mu = 0.12$; 8 — $\mu = 0.10$.

The calculation of rolling pressures was carried out according to the formula of A. I. Tselikov [2]:

$$p = \frac{\xi_1 \cdot 1.15 \sigma_1}{\chi} \left[\left(\frac{\xi_0 \sigma_0}{\xi_1 \sigma_1} \right)^{\frac{h_2}{h_0 + h_1}} \cdot e^{\chi} - \frac{\xi_0 \sigma_0}{\xi_1 \sigma_1} \cdot \frac{h_0}{h_0 + h_1} - \frac{h_1}{h_0 + h_1} \right],$$

TABLE 3

Experimental and calculated data, obtained during cold rolling of AT-4M strip

No. of pass	Experimental data										Calculated data					$\Delta P_i, \%$				
	Thickness of strip, mm		λ_i	P_i, tons	l_i, mm	$P_i, \text{kg/mm}^2$	Specific tension, kg/mm^2		$\frac{1}{\eta_i}$	$\sigma_i - \sigma_{i-1}, \text{kg/mm}^2$	$\sigma_i, \text{kg/mm}^2$	$k_i, \text{kg/mm}^2$	$\frac{P_i}{\sigma_i}$	μ_i	l_i, mm		$P_i, \text{kg/mm}^2$	P_i, tons		
							h_{i-1}	h_i											t_{i-1}	t_i
1	0.255	0.250	1.020	9.00	0.90	134	16.2	6.9	1.020	77.5	105.5	99.1	1.35	0.20	0.88	129	8.39	-6.8		
2	0.250	0.245	1.040	15.8	1.16	185	22.2	13.6	1.040	105.5	113.0	109.2	1.69	0.20	1.12	178	14.8	-6.3		
3	0.245	0.225	1.133	27.4	1.62	229	17.7	17.7	1.142	113.0	135.2	129.3	1.77	0.17	1.65	235	28.7	+4.7		
4	0.225	0.215	1.186	39.7	1.81	296	20.2	15.3	1.203	135.2	142.5	144.0	2.06	0.16	1.80	294	39.2	-1.3		
5	0.215	0.205	1.242	44.6	1.91	315	18.6	24.3	1.272	142.5	147.4	146.3	2.15	0.15	1.89	310	43.4	-2.7		
6	0.205	0.195	1.308	51.1	2.04	339	19.9	19.6	1.356	147.4	151.7	153.3	2.21	0.14	2.03	338	50.7	-0.8		
7	0.195	0.185	1.390	60.2	2.20	369	20.5	25.8	1.452	151.7	155.0	153.9	2.40	0.135	2.20	370	60.3	+0.2		
8	0.185	0.175	1.457	57.7	2.16	361	23.2	22.4	1.562	155.0	157.7	157.5	2.29	0.13	2.25	379	63.1	+0.9		
9	0.175	0.170	1.500	58.9	2.15	371	27.2	28.0	1.625	157.7	159.0	154.8	2.40	0.125	2.16	372	59.4	+0.9		
10	0.170	0.165	1.546	61.4	2.19	379	24.6	23.0	1.696	159.0	160.2	159.8	2.37	0.12	2.24	387	64.2	+4.6		
11	0.165	0.155	1.646	61.7	2.23	374	27.8	23.8	1.855	160.2	162.5	160.2	2.34	0.115	2.33	394	68.0	+9.3		

where

$$\chi = \frac{2\mu l'}{h_0 + h_1}; \quad \xi_0 = 1 - \frac{t_0}{1.15\sigma_0}; \quad \xi_1 = 1 - \frac{t_1}{1.15\sigma_1}.$$

The rolling pressures were calculated in the following order.

1. First, the magnitude of μ is determined, taking into account the velocity of rolling the lubrication, and the condition of the surfaces of the rolls and of the strips.

2. For a given coefficient of drawing the magnitudes of σ_0 and σ_1 were determined from the strengthening curve of the metal.

3. A magnitude of l' was assumed, which was somewhat greater than $l = \sqrt{r\Delta h}$. The magnitude of p was then determined from the formula of A. I. Tselikov, the magnitude of l' was checked according to the Hitchcock formula. If the assumed magnitude of l' coincided with the calculated magnitude, the total pressure P was determined and the calculations terminated.

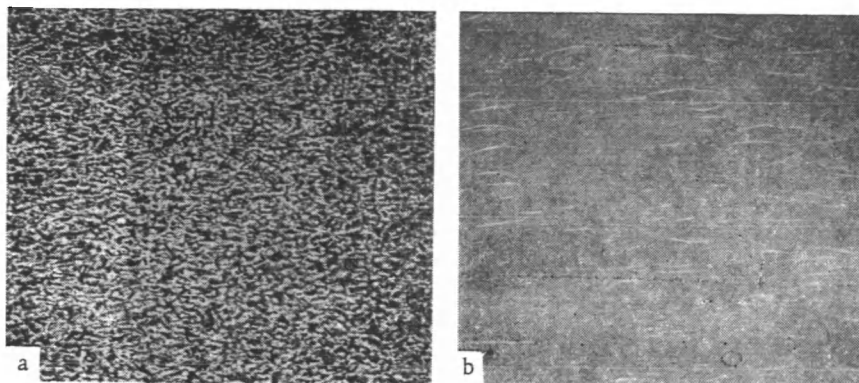


FIGURE 4. Photograph of the surface of AT-4M strip, Kh3

a — before cold rolling; b — after cold rolling.

The results of the calculation of the pressure of the metal on the roll during rolling of a thin AT-4M strip are also shown in Table 3 (on the right-hand side).

Table 3 and Figure 4 show that agreement between the experimental and calculated data can be achieved if it is assumed that the coefficient of the external friction during rolling decreases with each consecutive pass.

This assumption requires direct experimental confirmation, though it appears to be quite probable for two reasons:

Firstly, because of the roughness of the surface of the strip before rolling* (Figure 4) the coefficient of external friction somewhat increases during the first passes/20/.

* The rolls are finished to $\sqrt{V\sqrt{V}}$ 9 according to GOST 2789-51.

Secondly, as area reduction and the strengthening of the metal increase, the specific pressures of rolling also increase, which, according to /21, 22/, should decrease the coefficient of external friction.

Rolling schedule and annealing of cold rolled titanium alloy strip

The data on the process of area reduction during cold rolling of a 75 mm wide strip are given in Table 4.

TABLE 4
Process of deformation during cold rolling of AT titanium foil

No. of pass	78 mm wide AT-3M strip	Total reduction per pass ϵ , %	74 mm wide AT-4L strip	Total reduction per pass ϵ , %	76 mm wide AT-6L strip	Total reduction per pass ϵ , %
1	0.21—0.208— 0.20—0.192— 0.181—0.168— 0.181—0.160— 0.155—0.145	30.9	0.35—0.324— 0.294—0.285— 0.228	34.9	0.36—0.35— 0.33—0.31— 0.285—0.265— 0.255—0.24— 0.235—0.22— 0.21—0.20— 0.19	51.3
2	0.145—0.13— 0.12—0.11— 0.10—0.09	37.9	0.228—0.22— 0.21—0.195— 0.17—0.155— 0.14—0.13	43.0	0.075—0.16— 0.15—0.14— 0.13	25.7
3	0.09—0.08— 0.078	13.3	0.13—0.125— 0.12—0.11— 0.105—0.100— 0.095	26.9	0.13—0.125— 0.12—0.11— 0.105—0.10	23.1
4			0.095—0.085— 0.08—0.078— 0.075—0.07— 0.068	28.4	0.10—0.095— 0.09	10.0
	Total during one cycle	62.8		80.5		75.0

It was of interest to compare the data obtained in this investigation on the deformation of titanium alloys with the data obtained on a mill of the same type during rolling of Kh05 steel strip (130 mm wide) from a thickness of 0.5 mm to a final thickness of 0.025 mm /23/. This size which is achieved after 8 reductions (24 passes) entails a total area reduction of more than $\epsilon = 30\%$.

A comparison of the area reduction achieved in the present investigation with the data obtained in the work mentioned /23/ shows that the reduction per pass of a 75 mm wide titanium alloy strip (usually 0.005-0.025 mm) is lower than that during rolling of a Kh05 strip (0.01-0.05 mm).

The lower area reduction during rolling a titanium alloy strip is due to the fact that titanium alloys have a higher resistance to deformation than

. Kh05 steel and are more intensively strengthened during rolling. Hence, high-strength alloys should be rolled on multi-roll mills with hard rolls.

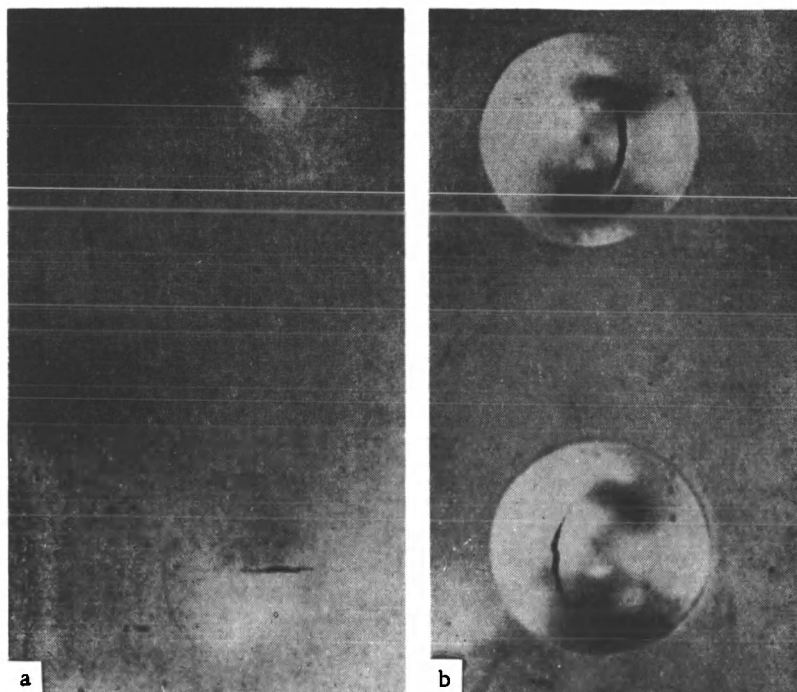


FIGURE 5. Plasticity of 0.13 mm thick cold rolled AT-3M alloy strip before and after annealing
a — strip after cold rolling with an area reduction of more than $\epsilon = 33.7\%$; b — strip after cold rolling and vacuum annealing at 750°C (holding time 30 min).

Data on the annealing of titanium alloys are scarce, both in Soviet and in foreign publications. Since annealing of titanium alloy strips is of great importance both for the production of the strip and articles by stamping and drawing, the authors initiated a number of experiments in this connection.

Coils of titanium alloy strips were annealed in a laboratory vacuum furnace. The following process was initially employed: annealing temperature 750°C , holding time at this temperature 30 min, pressure in the furnace $6 \cdot 10^{-3} - 1.5 \cdot 10^{-2}$ mm Hg. The strip was thoroughly degreased and dried before annealing.

In order to determine the optimum temperature of annealing, the relationship between the plasticity of the alloys and the annealing temperature was investigated. For this purpose strip specimens of a number of titanium alloys were annealed in a vacuum furnace at temperatures from $600-900^\circ\text{C}$ and held at these temperatures for 30 min. Plasticity changes in the strip were evaluated on the PTL (Eriksen) apparatus from the imprint of its indenter.

TABLE 5

Plasticity of cold-rolled titanium strip (AT-4L, AT-6L) and of 35 steel as tested on the PTL device (diameter of indenter 7 mm)

Titanium-alloy or steel grade	Thickness of strip, mm	Temperature of annealing, °C	Depth of indentation, mm	
			in the work-hardened condition	in the annealed condition
AT-4L	0.23	750	1.0	3.8
St 35	0.20	840	2.1	4.2
AT-6L	0.17	700	0.8	3.1
St 35	0.16	840	2.0	4.0

TABLE 6

Tension tests of flat specimens and the plasticity (deformability) of 0.07-0.11 mm strip of annealed titanium alloys

Designation of alloy	Dimensions of the gage length of the specimen, mm			Ultimate strength σ_u , kg/mm ²	Elongation δ , %	Depth of indentation*, mm	Absolute elongation, mm
	thickness	width	calculated length				
AT-2L	0.11	10.01	40.0	77.9	7.5	—	3.0
AT-3M	0.08	10.04	40.0	77.2	5.8	2.1	2.3
AT-4N	0.07	10.04	40.0	73.9	9.8	2.4	3.9
AT-6L	0.10	10.00	40.0	77.7	10.7	2.3	4.3

* Radius of indenter tip 7 mm.

The plasticity of all tested work-hardened titanium alloys is increased by annealing (Figure 5). The depth of indentation during the stamping test is increased 2 to 4-fold, depending on the type of alloy, thickness of the strip, and the annealing temperature.

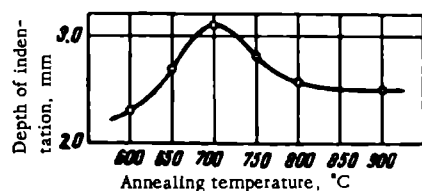


FIGURE 6. The dependence of the plasticity of cold-rolled 0.17 mm AT-6L strip on the annealing temperature (holding time 30 min)

The plasticity of the investigated work-hardened alloys is 2-2.5 times lower than the plasticity of work-hardened medium carbon steel. The differences between the plasticity of annealed titanium alloys and of medium carbon steels is small (Table 5).

The relationship between the depth of the indentation made in a 0.17 mm AT-6L strip and the temperature of the vacuum annealing is given in Figure 6. Alloys annealed at 680-

730°C have the highest plasticity. At higher temperatures titanium alloys and technically pure titanium /24/ undergo an intense grain growth which causes a decrease in their plasticity and even a welding of the strip in the coil.

The results of tension tests of annealed titanium-alloy foil (longitudinal specimens) are given in Table 6. The data obtained by the plasticity tests are also given in the same table.

The lower elongation and deformability (by stamping) of AT-3S foil is due to the grain growth which takes place during the intermediate annealing of this strip.

Conclusions

1. The plastic deformation during cold rolling high-strength titanium alloys takes place at high specific pressures (of the order of $200-450 \text{ kg/mm}^2$) and at specific tension of the strip of $30-60 \text{ kg/mm}^2$ which is not more than 0.3-0.5 of the yield strength of the alloy.

2. In addition to high strength, AT-titanium alloys have satisfactory plastic properties, facilitating the production of foil. By cold rolling of strained AT-3 and AT-4 alloys the authors produced foil of up to 0.07 mm thick and 70-80 mm wide.

3. The work-hardened cold-rolled strip (with an area reduction equal to 40-10 %, depending on the alloy and on the process details) must be given a vacuum annealing at $680-750^\circ\text{C}$.

4. Because of the high specific pressure there is an elastic flattening of the working and back-up rolls during rolling. Therefore, and also because of the necessity to increase the contact hardness of the rolls and to improve the maximum rollability of the strip, titanium alloys should be cold rolled by rolls made of hard alloys.

Bibliography

1. Kornilov, I.I., V.S. Mikheev, T.S. Chernova, and K.P. Markovich. — Sbornik "Titan i ego splavy", Izdatel'stvo AN SSSR, No. 7:140. 1962.
2. Tselikov, A.I. Prokatnye stany (Rolling Mills). — Metallurgizdat. 1946.
3. Hitchcock, I.H. — Am. Soc. Mech., Res. publ. 1930.
4. Suyarov, D.I. and M.A. Benyakovskii. Nastroyka listoprokatnykh stanov (Adjustment of Strip Rolling Mills). — Metallurgizdat. 1960.
5. Sims, R. — J. Inst. Petr., No. 40. 1954.
6. Mekhanicheskie svoystva instrumental'nykh stalei (Mechanical Properties of Tool Steels). — TsBTI, INIMS. 1958.
7. Sakhon'ko, N.M. and I.V. Kolotnikov. Trudy konferentsii "Povyshenie iznosostoikosti i sroka sluzhby mashin", Vol. 1, Izdatel'stvo AN UkrSSR. 1960.
8. Pogodin-Alekseev, G.A., Yu.A. Geller, and A.G. Rakhshadt. Metallovedenie (Process Metallurgy). — Oborongiz. 1950.
9. Stone, M.D. — Iron and Steel Eng., No. 2:61. 1953.
10. Lavrov, P.P. — Sbornik "Prokatnye stany", No. 8, Mashgiz. 1956.
11. Spravochnik metallista (The Metallurgists' Handbook). Vol. 3. — Mashgiz. 1958.

12. Rokotyan, E.S. — [Article in] *Stal'*, No.9:814. 1947.
13. Korolev, A.A. *Mekhanicheskoe oborudovanie prokatnykh tsekhov* (Mechanical Equipment of Rolling Mills). — Metallurgizdat. 1959.
14. Emike, O. and K.Lukas. *Materialy po teorii prokatki* (Contributions to the Theory of Rolling), Part IV. — Metallurgizdat. 1948.
15. Kreindlin, N.N. *Raschet obzhatii pri prokatke listov i lent iz tsvetnykh metallov i splavov* (Calculation of Area Reduction During Rolling of Sheet and Strips of Nonferrous Metals and Alloys). — Metallurgizdat. 1950.
16. Shilov, V.I. *Issledovanie protsessa prokatki-volocheniya v neprivodnykh valkakh* (Investigations on the Rolling-Drawing Processes with Nondriven Rolls). — *Dissertatsiya* (Thesis) Ural'skii politekhnicheskii institut im. S.M.Kirova, Sverdlovsk. 1954.
17. Korolev, A.A. — *Sbornik "Prokatnye stany"*, No.8. Mashgiz. 1956.
18. Tarnovskii, I.Ya. and V.I.Shilov. — *Sbornik "Raschet i konstruirovaniye zavodskogo oborudovaniya"*, No.64. Mashgiz. 1958.
19. Strandell, P.O. — *Jernkont. Annaler*, 143(12):810. 1959.
20. Whitton, P.W. and H.Ford. — *Proc. Inst. Mech. Eng.*, 169(5):123. 1955.
21. Pavlov, I.M. and N.N.Get. — *Metallurg*, No.7. 1936.
22. Kragel'skii, I.V. and I.E.Vinogradova. *Koeffitsienty treniya* (Coefficients of Friction). — Mashgiz. 1955.
23. Tret'yakov, A.V. *Prokatka tonchaishei lenty* (Rolling of Extremely Thin Strips). — Metallurgizdat. 1957.
24. Severdenko, V.P. and V.Z. Shilkin. — *Metallovedenie i termicheskaya obrabotka metallov*, No.10. 1959.

PHASE TRANSFORMATIONS IN THE HEAT-AFFECTED ZONE OF α - AND $\alpha+\beta$ -TITANIUM ALLOYS AND THE CRITERIA FOR CHOOSING THE WELDING PROCESSES

M. Kh. Shorshorov and G. V. Nazarov

In 1961 the New-Metals Welding Laboratory of the Institute of Metallurgy im. A. A. Baikov continued to investigate the kinetics of phase transformations taking place in titanium alloys during welding. With the use of a rapid IMET-DB dilatometer /1/, studies were made of the kinetics of phase transformations in VT-5-1, 48-OT3 and VT-14-1 alloys. The IMET-1 method was employed by the authors /2/ to investigate the influence of the parameters of the thermal cycle of welding on the mechanical properties and the structure of the heat-affected zone in 5 experimental low-alloyed titanium alloys as well as in the VT-14 (two melts), and VT-14-1 alloys.

Characteristics of phase transformations in a number of α - and $\alpha+\beta$ -titanium alloys under conditions of continuous cooling during welding

In a previous investigation /1/, the authors determined that in the commercial VT-1 titanium and in alloys of the martensitic type (OT-4 and AT-3) the relationship between the temperature at the beginning of the $\beta \rightarrow \alpha'$ transformation and the cooling rate is represented by an S-shaped curve. The relationship represented by this curve is also valid for a number of other α and $\alpha+\beta$ alloys discussed in the present work.

The analysis of the diagrams of anisothermal transformation of 48-OT3, VT-5-1, and VT-14-1 alloys during continuous cooling under the conditions prevailing during the thermal cycles of welding shows that in these alloys the temperature of the beginning of the $\beta \rightarrow \alpha'$ transformation also varies with the cooling rate along an S-shaped curve. As distinct from the OT-4 and AT-3 alloys which contain manganese, or chromium, iron, and silicon, the 48-OT3 and VT-5-1 alloys complete almost all $\beta \rightarrow \alpha'$ transformations within an interval of 500-100°C below the temperature of the beginning of the transformation.

In VT-5-1 alloys which contain small amounts of oxygen and nitrogen (0.1 - 0.15 % O₂ and 0.02 % N₂) the temperature of the beginning of the $\beta \rightarrow \alpha'$ transformation decreases from 930-925 to 860-850°C if the cooling rate (within the range of 1000-900°C) is increased from 4.5 to 260°C/sec. The temperature range of transformation is 50-80°C. A VT-5-1 alloy containing more oxygen and nitrogen (the content of these gases in the melt was increased to 0.2-0.25% O₂ and 0.05% N₂) the temperature of the beginning of the $\beta \rightarrow \alpha'$ transformation changes from 955-960°C to 880-895°C if the cooling rate is increased from 4 to 325°C/sec (Figure 1)

The authors determined in an earlier work [1], that in commercial titanium the hydride transformation can be detected by a dilatometric test from an H content as low as 0.008 % H₂. In the VT-5-1 alloy the hydride transformation is considerably less pronounced. For example, the elongation of a specimen containing 0.045-0.068 % H₂, as determined from

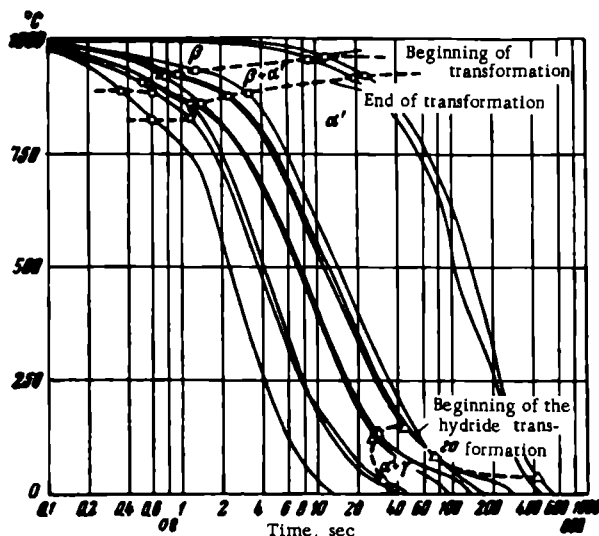


FIGURE 1. Anisothermal transformations in VT-5-1 alloys under conditions of welding. Thermal cycles: heating at a rate of 200°C per sec to 1200°C and cooling at different cooling rates (4.5-260°C per sec) to 1000-900°C. Content of gases in the alloys: 0.3-0.35% O₂, 0.07% N₂, and 0.045-0.068 H₂

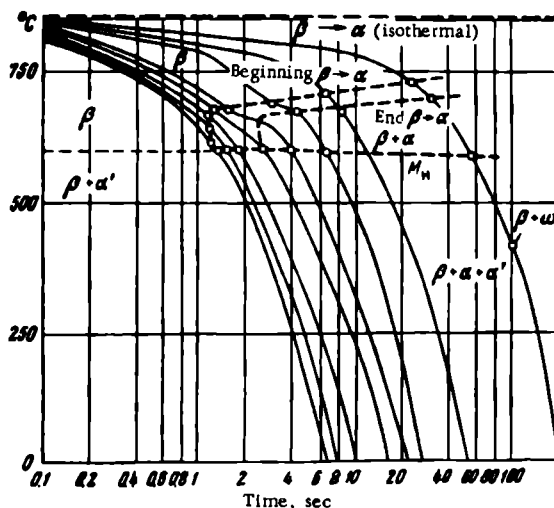


FIGURE 2. Anisothermal transformations in VT-14-1 alloys under conditions of welding. The thermal cycles are the same as in Figure 1. Content of hydrogen 0.015%

the dilatometric curve, is only 0.05-0.07 % while the elongation of a specimen of commercial titanium with 0.25 % H₂ is 0.2-0.25 %. The temperature of the beginning of the hydride transformation changes as the cooling rate alters. For instance, in the VT-5-1 alloy the maximum temperature of the beginning of the transformation is only 100-120°C at a cooling rate (within the range of 250-100°C) of about 5-12°C/sec. As the cooling rate is increased to 50-35°C/sec, the hydride transformation takes place at room temperature. If the cooling rate drops to 1.5°C/sec the temperature of the beginning of the hydride transformation is decreased to 50°C (see Figure 1). In the earlier investigation /1/ the authors have shown that this regular variation of the beginning of the hydrogen transformation in commercial titanium, in α alloys and in the low-alloyed $\alpha + \beta$ alloys, is due to the nature of the distribution of hydrogen in the α' phase, the uniformity of which depends on the velocity of the temperature changes within the range of $\beta \rightarrow \alpha$ transformation temperatures during the subsequent cooling and hydride transformation. In the VT-14-1 alloy (2.6 % Al and 7.5 % Mo) the $\beta \rightarrow \alpha'$ transformation also takes place over a narrow range of temperatures extending over an interval of 30-80°C below the temperature of the beginning of the transformation (Figure 2). On the diagram of the anisothermal transformations of this alloy it can be seen that the temperature of the martensitic transformation decreases by 15°C (from 600 to 585°C), if the cooling rate is decreased from 250 to 5°C/sec. At low cooling rates, a weak transformation was observed accompanied by a decrease in volume. This is apparently the $\beta \rightarrow \omega$ transformation. No hydride transformations were found in this alloy.

The influence of the alloy composition and of the parameters of the thermal cycle of welding on the structure and mechanical properties of the heat-affected zone

In 1961, the authors investigated (by the IMET-1 [welding] method) five experimental alloys of the Ti-Al-Fe, Ti-Al-Cr-Mo, and Ti-Al-V-Fe systems, containing 4.3-5 % Al and 0.7-2.5 % of β -phase stabilizers, and also the VT-14 (two melts) and VT-14-1 alloys. The plastic properties of the metal in the heat-affected zone of Ti-Al-Fe alloys with low content of iron (0.7 % Fe) are not affected to any great extent by the cooling rate.

In alloys containing 2.5 % V+Fe, the elongation and contraction of the metal in the heat-affected zone is smaller than those of the base metal over the whole range of cooling rates. As the cooling rates are decreased to 1.5°C/sec the contraction and the elongation are continuously decreased.

The data obtained with low alloyed experimental alloys fully confirm the conclusions arrived at by the authors elsewhere /3/, on the basis of the results of investigations carried out by the Institute of Metallurgy im. A. A. Baikov on the AT-3 and AT-8 alloys. These martensitic titanium alloys containing up to 5 % Al and a total amount of β -phase stabilizers (iron, chromium, molybdenum, and others) of up to 1.6-1.4 % if not contaminated with gases (σ of sponge less than 45 kg/mm²) have properties in the heat-affected zones which show practically no difference from those of the base metal over a wide range of cooling rates (from 1.5-2 to 150-180°C/sec at a temperature of 950-850°C). It should also

be pointed out that if such alloys contain several β -phase stabilizers, their weldability (at identical strength) is superior to that of alloys containing only one β -phase stabilizers.

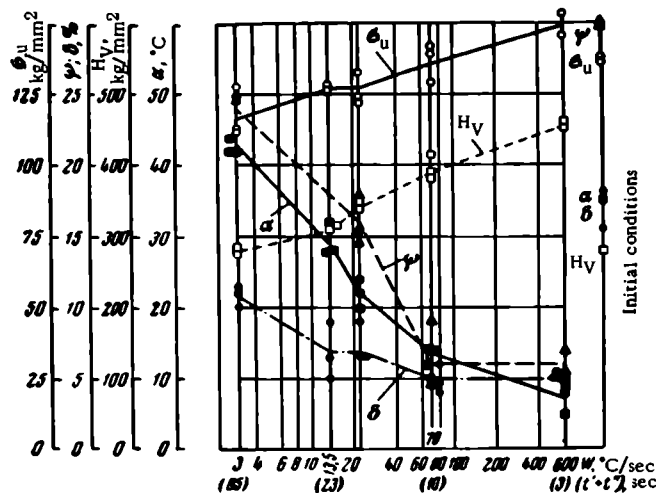


FIGURE 3. The influence of the rate of cooling W from the temperature of the beginning of the $\beta \rightarrow \alpha$ transformation and of the time $t' + t''$ during which the metal is maintained above this temperature, on the mechanical properties of the heat-affected zone of the VT-14 alloy with 3.6% Mo and V

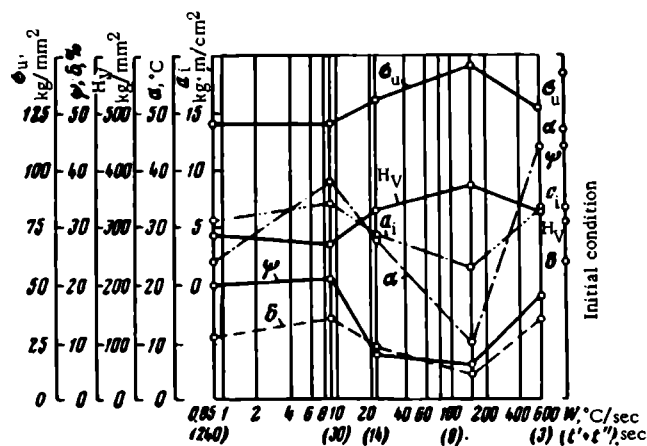


FIGURE 4. The influence of the rate of cooling W from the temperature of the beginning of the $\beta \rightarrow \alpha$ transformation and of the time $t' + t''$ during which the metal is maintained above this temperature, on the mechanical properties of the welding zone of a VT-14 alloy with 4.4% Mo and V

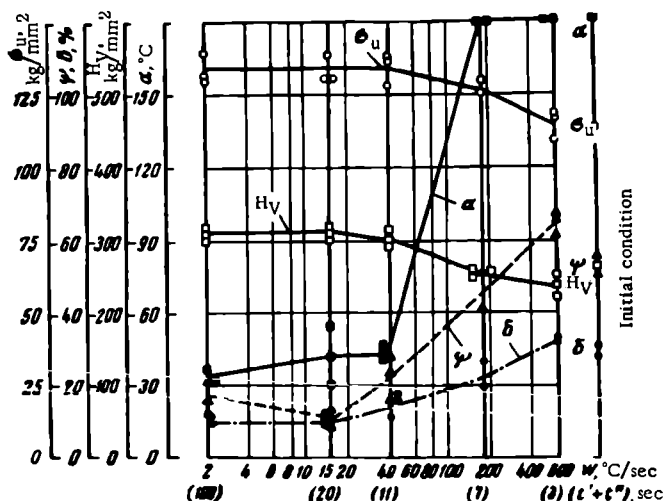


FIGURE 5. The influence of the rate of cooling W from the temperature of the beginning of the $\beta \rightarrow \alpha$ transformation and the time $t' + t''$ during which the metal is maintained above this temperature, on the mechanical properties of the VT-14-1 alloy in the welding zone.

An analysis of the dependence of the mechanical properties of the heat-affected zone on the cooling rates for VT-14 and VT-14-1 alloys shows the following features. In the VT-14 alloy, which has a lower content of β -phase stabilizers (3.6 % Mo and V) the plastic properties of the metal of the heat-affected zone are low if the parts are quenched in water or cooled at a rate of 70°C/sec (Figure 3). A further decrease in the cooling rate from 70 to 3°C/sec improves the plastic properties which do not, however, reach the level of the plastic properties of the base metal in the initial condition. In the more alloyed VT-14 alloy (4.4 % Mo and V) the low plastic properties of the metal of the heat-affected zone are apparent at cooling rates from 150 to 25°C/sec, i. e., at cooling rates characteristic of a single-pass welding of thin or medium-thickness sheets (Figure 4). Quenching in water and cooling at low cooling rates improves the plastic properties of the alloy. Microstructural analysis showed that cooling at medium cooling rates causes a precipitation of a finely dispersed phase (apparently the ω phase).

If VT-14-1 alloys (7.5 % Mo) are cooled in water, the plastic properties of the metal in the heat-affected zone are better than those of the base metal in the annealed condition (Figure 5). The plastic properties remain high if the cooling rate is decreased to 100-180°C/sec. A decrease in the cooling rate to 15°C/sec causes a sharp decline in the plastic properties.

This alloy can be welded by a single-pass bath welding up to a sheet thickness of 2.5-3 mm, which gives joints with high plastic properties. Thicker sheets must be welded by a multipass weld and the cooling rate for each weld must not be lower than 60-100°C/sec.

The difference in the cooling rates between VT-14 and VT-14-1 alloys at which low plastic properties are obtained is due to the influence of the molybdenum content on the structure of the heat-affected zone. The

structure obtained at these cooling rates has an unfavorable ratio of the α' , β , and ω phases in the VT-14 alloy and of the α' and β phases in the VT-14-1 alloy.

The results of the earlier investigations of the authors [1-3] and of the present study show that the dependence of the mechanical properties and of the structure of the heat-affected zone on the cooling rate W and on the time $t' + t''$ during which the metal is maintained above the temperature of the $\beta \rightarrow \alpha$ transformation is different, depending on whether welding is carried out with α -alloys, the low alloyed $\alpha + \beta$ martensitic alloys, or the medium alloyed, aged $\alpha + \beta$ alloys. The alloys of the first and second groups have wide optimum ranges of W and $t' + t''$ over which the plastic properties of the heat-affected zone are good and close to those of the base metal. Usually these ranges correspond to the welding of thin and medium thickness sheets ($W = 10-150^\circ\text{C/sec}$; $t' + t'' = 40-8$ sec). As the gas content and β -phase stabilizing elements in the alloys of the second group increase, these optimum ranges are narrowed and the plastic properties are impaired for high magnitudes of W and small magnitudes of $t' + t''$. This is the result of hardening and, for low magnitudes of W and high magnitudes of $t' + t''$, overheating and grain-growth sensitivity. In the alloys of the third group these optimum ranges can exist for small, medium, or high magnitudes of W depending on the content of β -phase stabilizing elements. This is due to the quantitative relationship between the phases, their types, and the nature of their precipitation (β , α , α' , and ω).

Bibliography

1. Shorshorov, M. Kh. and G. V. Nazarov. — Sbornik "Titan i ego splavy", Izdatel'stvo AN SSSR, No. 7:226. 1962.
2. Shorshorov, M. Kh. and G. V. Nazarov. Svarka titana i ego splavov (Welding of Titanium and Its Alloys). — Mashgiz. 1959.
3. Nazarov, G. V. and M. Kh. Shorshorov. — Sbornik "Titan i ego splavy", Izdatel'stvo AN SSSR, No. 7:234. 1962.

THE MECHANISM OF DELAYED FAILURE AND THE FORMATION OF COLD CRACKS DURING WELDING OF TITANIUM ALLOYS AND OF STEELS

M. Kh. Shorshorov, G. V. Nazarov, and V. V. Belov

The analysis of existing data on the delayed failure of titanium alloys under static loads at temperatures close to room temperature and on the formation of cold cracks in welded joints of these alloys as a result of internal stresses, has made it possible to arrive at certain generalizations regarding the appearance of these phenomena /1, 2/*.

1. Delayed failure and the deformation of cold cracks can be caused by an increase in the temperature, by grain growth, by an increased content of inclusions, in particular of hydrogen, oxygen, and nitrogen, by a decrease in the temperature range of the hydride transformation, by relatively high cooling rates over the ranges of $\beta \rightarrow \alpha$ and of the hydride transformations; or by an increase in the toughness and in the thickness of hardenable parts being welded, etc.

2. The tendency to delayed failure and to the formation of cold cracks decreases with the increase in the temperature of tempering.

3. The tendency of the titanium alloy to delayed failure is greatest if the load is applied during cooling or immediately after its termination. If welded titanium alloys are loaded only after the lapse of a certain period during which no stress is applied, delayed failure does not take place. This phenomenon is called "recovery" and is also observed in weak welded joints in which the residual stresses are insufficient for the formation of cold cracks; by allowing a certain time to elapse before loading of such joints cracking is avoided.

4. Delayed failure takes place mostly when rates of deformation are low (10^{-3} - 10^{-5} mm/sec) or as a result of the prolonged action of stresses below the yield point; the rates of the internal deformation in the heat-affected zone are the same during the last stages of cooling and during subsequent storage at room temperature. As the external or the internal stresses are increased the time to failure decreases. The less intensive the rate of load application, the smaller the destructive external or internal residual stresses. Nevertheless, for each kind of loading there is a certain minimum below which no failure occurs, irrespective of the duration of the stress. The more the stress falls below this minimum, the more complete is the "recovery".

5. Prolonged loading or storage of welded titanium alloys at sufficiently low temperatures (below zero) causes no failure, but if the temperature is afterwards raised to room temperature, destruction is intensified.

* See also the article of M. Kh. Shorshorov and G. V. Nazarov in this book, p. 297.

6. During welding, the tendency of the parts to be joined to delayed failure is higher than that during hardening.

The above-mentioned properties are common to titanium alloys and hardenable steels. Nevertheless, there are some essential differences between the respective behaviors of these materials. This is because of

the great differences between the volumetric changes resulting from the martensitic transformation in steel and those caused by the hydride transformation in titanium alloys, because the moduli of elasticity of the respective crystal lattices of the low-temperature phases of these metals differ and because of a number of other factors. The differences between titanium alloys and hardenable steels in this connection are as follows:

1. More time is usually required for the delayed failure of titanium and of its alloys than for steel (Figure 1). The formation of cold cracks in welded titanium alloys is also slower than in welded steel as for instance in the joints made for the hardness cross test. For titanium alloys with the ordinary content of gases the time to failure may be weeks or months while that for hardenable steels is only hours or days [2].

2. In steels the cold cracks appear only along the grain boundaries, while in titanium alloys these cracks appear both along the grain boundaries and along the cleavage planes [1].

3. Titanium alloys, particularly those with a low content of gases, are frequently destroyed under higher applied or internal stresses than the well-hardenable steels (Figure 1).

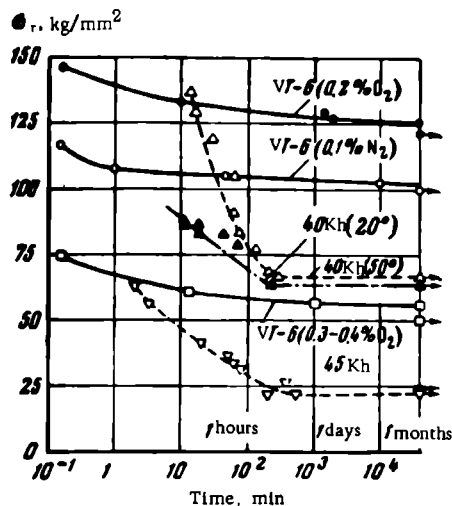


FIGURE 1. The dependence of the true destructive stresses for VT-6 titanium alloys with low and high content of oxygen and nitrogen and for 40 Kh and 45 Kh martensitic steel on the time to failure. Thin flat and notched specimens were tension tested under a constant load on an IMET-4 machine at room temperature and at 50°C (40Kh steel). Prior to this, the specimens were quickly heated to temperatures close to the solidus and rapidly cooled in the air. The content of hydrogen (about 0.01 %) in the VT-6 alloys was identical in all melts, the content of nitrogen in the melts with different contents of oxygen was about 0.03 %, and the content of oxygen in melts with a high content of nitrogen was about 0.2 %. The reduction in area of the failed specimens was nil for 40 Kh steel and 45 Kh steel, 1-5 % for the VT-6 alloy (0.15 % O₂) and nil % for the VT-6 alloy (0.3-0.4 % O₂)

The mechanism of delayed failure and of the formation of cold cracks in steel is at the present time explained by the fact that the slipping takes place along the grain boundaries rather than within the grains and particularly by the tendency of grains to a visco-elastic slipping along the grain boundaries under conditions of slow deformation [1, 3-5]. This property of polycrystalline aggregates is due to the fact that the crystal lattices are not joined at the grain boundaries, as a result of which high concentrations of stresses and lattice defects arise along these boundaries. The least ordered are those grain boundaries with a large angle, these

being characteristic of metals in the recrystallized condition. The liability of grains to a visco-elastic sliding along the grain boundaries at low temperatures is most apparent after hardening from high temperatures, since this process results in the disordered structure being fixed. The more rapid the hardening the less the probability of improving the ordering of the structure at the grain boundaries during cooling. The local deformations at the grain boundaries are of great importance. These take place as a result of phase transformations which are accompanied by a change in volume at relatively low temperatures (for instance, the martensitic transformation in steel and the hydride transformations in titanium alloys). In the latter case, however, the deformations may also arise along the cleavage planes of the grains since the hydrides precipitate in titanium not only along the grain boundaries but also along the prismatic plane (1010).

Because the visco-elastic slipping along the grain boundaries takes place chiefly in the direction of the applied tensile stress σ , the relaxation of the tangential stress τ is accompanied by an accumulation of high,

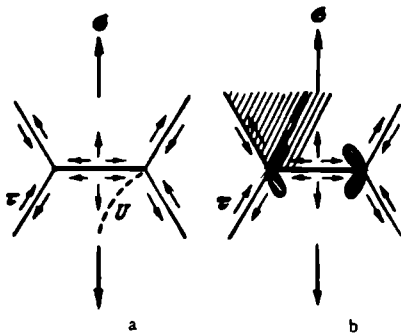


FIGURE 2. Ziener diagram applied to delayed failure. The parts of the grains adjacent to the ends of the slipping grain boundaries in steels (a) are subjected to an elastic deformation while those in titanium alloys (b) are subjected to an elastic-plastic deformation (dashed sections). Therefore, in steels the failure is most probable along the grain boundaries, particularly along the transverse ones (a), while in titanium alloys it is also probable along the cleavage planes in the grain (b)

normal stresses along the transverse grain boundaries (Figure 2). The Ziener theory assumes the development, at certain stages, of elastic-plastic deformations in parts of the grains adjacent to the grain boundaries, as a result of which the concentration of deformations along the grain boundaries gradually decreases and the metal becomes capable of withstanding higher deformations. Nevertheless, as the elastic properties of the grains are augmented, for example, as a result of the phase transformations of the martensitic type or as a result of the temperature decrease, this capacity becomes less and less probable. Therefore, in practice, a delayed failure in steel seems always macroscopically more brittle than in titanium alloys. High stresses of the second type are a particularly aggravating factor in this connection. These arise because of the change of the specific volume and of the coefficient of cubic expansion during

phase transformations, and also because of the anisotropic expansion which is connected with the different orientation of the crystals in relation to their grain boundaries. The lower the transformation temperature, the higher the stresses of the second type and the greater their influence. Because of the development of the stresses of the second type, and also under the influence of the applied or internal stresses of the first type, the tops of the grains which are natural stress raisers and also the transverse grain boundaries of the metal, are subjected to tension in all directions. The relaxation of stresses by plastic deformation is made more difficult

by this tension. Therefore, the most probable places where failure may begin in steel are the transverse grain boundaries and the grain tops.

Nevertheless, the Zener theory does not explain the mechanism of the generation and growth of microcracks to dimensions at which they can develop under the influence of stresses. This may be concluded on the basis of the dislocation theory which enables us to evaluate the minimum stress (by the Stroh method) necessary for a brittle failure under the condition that at the grain tops the deformation is only elastic. Such a calculation shows that at ordinary magnitudes of the free energy of the grain surfaces the formation of cracks requires exceedingly high stress concentrations /6/. Consequently, for the formation of cracks, some process must take place which would lead to a decrease in the free energy of the surface of the grain boundaries or of the cleavage planes to the formation and growth of the nuclei of microplanes and thus to the decrease in the strength of these interfaces. At temperatures close to room temperature this is only possible if the grain boundaries and the cleavage planes are sufficiently saturated with vacancies which, like the atoms of the alloying metals, tend to occupy places at the most deformed points of the crystal lattice and to decrease their free surface energy.

In the case considered here, one of the chief causes for the supersaturation of the metal with vacancies is the hardening from high temperatures. In certain metals the concentration of vacancies at the melting point is 0.1 at. % /7/. Upon hardening from temperatures 100°C lower than the melting point it is possible to preserve up to 0.01 at. % of the vacancies /8/. It has been shown that such a concentration of excessive vacancies is quite sufficient for the formation of concentrations of micropores and planes on the boundaries /9/. Hardening from high temperature produces more paired vacancies while hardening from low temperatures produces more single vacancies. The more rapid the cooling, the more vacancies are preserved. When alloying metals it should be taken into account that the relationship between the atomic diameters of the alloying elements and of the base metal influences the equilibrium concentration of the vacancies at high temperatures. For instance, it is known that an increase in the concentration of chromium in iron from 0 to 5.7 % decreases the excessive concentration of the vacancies from 0.0186 to 0.0056 at. %, i. e., more than threefold /10/.

Another important source of excess vacancies is cold plastic deformation. Whereas the vacancies produced by hardening are uniformly distributed and dispersed over the volume of the metal, the dislocation movements during plastic deformation order them into rows. It is thought that these rows are unstable and can be dispersed into single and paired vacancies. According to the theory which envisages the vacancies as being formed as steps on the dislocations, the concentration of vacancies is proportional to $\epsilon^{3/2}$, where ϵ is the degree of deformation /11/. Therefore, a concentration of vacancies close to that formed during hardening can be obtained only by cold working to high degrees of deformation. During welding and hardening, such concentrations of vacancies can be obtained only during the precipitation of new phases caused by strain hardening. From this point of view, the martensitic transformation in steel should form more vacancies than the hydride transformation in titanium and its alloys.

Nevertheless, because the hydride transformations in titanium take place mainly at low temperatures and have local volume effects which are three times as large as those caused by the martensitic transformation in steel, their considerable influence on the creep strength of titanium becomes evident (despite the small amounts of hydrides formed). The termination of the growth of martensitic needles in steel and the precipitation of hydrides in titanium alloys close to the grain boundaries increase the probability that a certain number of excess vacancies will be introduced into the grain boundaries and planes of cleavage, since, out of the total number of vacancies fixed by hardening, a considerable amount can pass to these planes from adjacent layers about 0.01 mm thick /8/.

The movement of the vacancies is a thermally activated process. There are data on the mobility of single vacancies in copper and silver at a temperature above -30°C , on the mobility of paired vacancies at a temperature above -100°C , and on the complete immobility of vacancies at a temperature of -196°C /8, 11/. The paired vacancies are more mobile than the single ones.

In order to explain the circumstances leading to delayed failure and also to the phenomenon of relaxation, it is essential to discuss the possible outlets of excess vacancies and the influence of the temperature on the stresses and on the effectiveness of these outlets. At certain ranges of negative or low positive temperatures the chief outlets of vacancies may be the grain boundaries, and the steps on the lines of dislocation or the free surfaces (depending on the nature of the metal). At higher temperatures, the thermal activity of atoms becomes increasingly important and therefore a "damping" of the vacancies, i. e., their disappearance through conjunction with the dislocated atoms becomes possible. In addition, at these temperatures the shifting of vacancies and possibly of dislocations from the sources to the outlets and vice versa produces a more complete thermal stability. This leads to an ordering of the structure of the system in general, and particularly of the grain matrix and of both the grain and phase boundaries. Apparently, in steel and in titanium alloys such conditions arise not only during low-temperature annealing or aging, but also directly during slow cooling, as in welding of heated parts. At low temperatures the most effective outlets of vacancies are the grain boundaries, the cleavage planes, and the phase boundaries. Applied or residual stresses can be considered as factors which not only activate and accelerate the movement of the vacancies toward the outlets, but also guide their movement chiefly toward the direction of the action of the tensile components of stress, i. e., toward the transverse grain boundaries. A slipping along the boundaries which are not perpendicular to the tensile stresses, leads to formation of triaxial stresses in the parts of grains adjacent to the transverse grain boundaries (see Figure 2). If a tensile stress is applied, the hydrostatic stress exerts a certain action on the vacancies producing an energy gradient U , which moves the vacancies toward the transverse grain boundaries (see Figure 2a). On the other hand, ordering processes which place the dislocations in a new and more stable position take place at the adjacent continuously slipping boundaries. During the process both the vacancies which are formed in the adjacent grain boundaries during slipping and those which enter these grain boundaries from the grains are usually damped though part of them "jump"

to the transverse boundaries as a result of the high diffusion mobility of atoms at the boundaries or coagulate at the adjacent boundaries.

The generation of microplanes is only possible at high stresses and at a considerable supersaturation of vacancies. High stresses can arise only in places with concentrations of stresses, i.e., at the grain tops or in the projections of the transverse boundaries. It has been calculated that the cavity which is formed can be $1-3 \mu$ long. Since applied or residual stresses direct the flow of vacancies toward the transverse boundaries and cause the grains to slip, they not only promote a formation of cavities but also their growth and development into microcracks. It is not difficult to prove that in each specific case there must be a certain critical stress below which the formation of microcracks is of little probability. Apparently, the chief condition which determines the magnitude of these critical stresses, is the saturation of the transverse grain boundaries with a sufficient number of vacancies, since the stresses required for this saturation should be considerably higher than those which can cause a slip along the adjacent boundaries. At stresses below the critical values, the flow of vacancies toward the boundaries will be limited. The chief outlets of vacancies will then be the dislocations which form block boundaries, the twin grains, and also the slip planes previously generated as a result of the deformation of the grains during cooling from high temperatures or during phase transformations. The visco-elastic slip of grains along adjacent boundaries will under these conditions cause no cracking but on the contrary, will lead to an ordering of the structure of these boundaries. This will cause a greater or smaller recovery, depending on the magnitudes of the stresses.

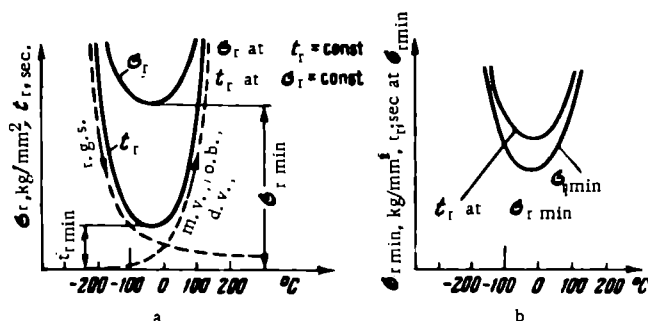


FIGURE 3. Diagram of the influence of the temperature on the destructive stresses σ_r , on the time to failure t_r (a), and on the lowest (critical) stresses $\sigma_r \min$ (b). Two processes with a conflicting influence take place when the temperature is increased: (1) a decrease in the resistance of the grains to slipping (r.g.s.) and a thermal activation of the movement of vacancies (m.v.); (2) an ordering in the structure of the grain boundaries (o.b.) and a damping of the vacancies (d.v.)

If the stresses are increased above the critical limit then the flow of vacancies to the transverse boundaries will be increasingly spontaneous and the rate of slipping along the adjacent boundaries will increase, leading to a decrease in the time necessary for the formation and the growth of microcracks. In steels there will be a growing tendency toward the

formation of cracks along the transverse boundaries, while in titanium alloys cracking will take place along the cleavage planes.

Since the test temperature determines the mobility of the vacancies, the resistance of the boundaries to slipping and also the possible recovery for each alloy, there must be a certain temperature at which delayed failure will be more rapid (Figure 3) for any given alloy. The experiments of the authors have shown that for steels this temperature is close to room temperature (see Figure 1).

In welded steels and in titanium alloys the formation of cold cracks in the welding zone is more intense than in hardened steel, not only because of the higher heating temperature, but also because during the intensive grain growth there is a considerable segregation of harmful impurities along the grain boundaries (oxygen and nitrogen in titanium and in steel and sulfur and phosphorus in steel, etc.). There is sometimes also a fusion of the impurities (overheating), leading to a sharp decrease in the intercrystalline strength. In hardened steels the effect of impurities is less prominent, since holding at high temperatures before quenching is usually sufficient for the establishment of a low equilibrium concentration of these impurities at the grain boundaries.

The difference in the tendencies of titanium alloys and of steels to delayed failure and to the formation of cold cracks is apparently due to the smaller number and lower concentration of stresses of the second kind in titanium alloys, because of the formation of a relatively small number of hydrides and because of the possible relaxation of the stresses. In addition, in the respective welded metals there are apparently differences between the stressed conditions and between the magnitudes of the stresses of the first type. During welding of hardenable steels the heat-affected zone develops a stress pattern which is characterized by considerable longitudinal compression stresses and by smaller transverse tensile stresses (related to the direction of the weld). In addition, on the boundary between the weld and the heat-affected zone there is often a sharp transition from the longitudinal tensile stresses in the weld to the longitudinal compression stresses in the heat-affected zone. Most welded titanium alloys are probably in a condition, both in the weld and in the heat zone, arising from biaxial stresses, since the chief phase transformations ($\beta \rightarrow \alpha$ and $\beta \rightarrow \omega \rightarrow \alpha$) are accompanied by a reduction in volume and not by an increase as it is in steel ($\gamma \rightarrow \alpha$). Nevertheless, the hydride transformation cannot change the sign of the longitudinal residual stresses, because of the small total volume effect. The tensile stresses in the heat-affected zone should be lower in titanium and its alloys than in steel, since titanium has a lower coefficient of thermal expansion and a lower modulus of elasticity. For the development of a visco-elastic slip along the grain boundaries or along the cleavage planes, without which no delayed failure can take place, the biaxial tensile stresses are less favorable than the biaxial tension-compression stresses.

A microscopic analysis of the failure spots shows that in titanium alloys the beginnings of the cracks are not located strictly along the grain boundaries as is the case in steel. Most often the cracks begin at the boundaries between the hydrides and the α phase and also at the cleavage planes in the matrix of the α phase, formed as a result of an intragranular deformation at high temperatures, during cooling, and during the subsequent action of stresses at room temperature. In titanium alloys the

places should serve more effectively as outlets of vacancies and of alien atoms than in steels. This is the case particularly with the cleavage planes, the number of which in titanium alloy grains should be considerably smaller than in grains of steels since α -Ti has a close-packed hexagonal lattice with fewer slip planes than the body-centered cubic lattice of steel. The highly defective nature [defect lattice] of the cleavage planes of titanium and its alloys and also their low modulus of elasticity influence the mechanism of failure since they lead to an increasing role of the grains in the development of deformation processes and to a considerable creep (see Figure 2b). Under these conditions the localization of the deformation along the grain boundaries or along other interfaces which are predisposed toward the visco-elastic slip can be achieved only at very small rates of deformation. This, together with those features of the stressed condition characteristic of the first and second type are the chief causes for the longer time to failure of welded joints in titanium alloys.

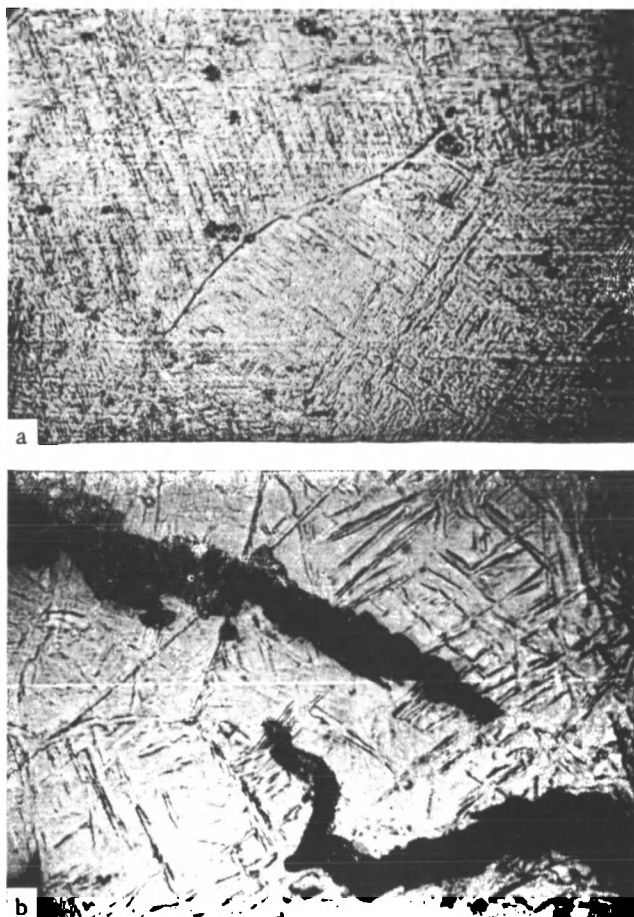


FIGURE 4. Location of cracks in the heat-affected zone of welded titanium alloys

a — along the transverse grain boundary in VT-6 alloys (delayed-failure test carried out on an IMET-4 machine at loads of 128 kg/mm^2 for 5 hours), $\times 340$;
b — partially along the transverse grain boundary and along the grain in the welded joint of an AT-8 alloy, $\times 600$

The example of martensitic steel shows that the tendency of welded metals to develop cold cracks is considerably influenced by the rate of cooling during welding. The most intensive crack formation takes place under average conditions of welding at which there is a negative influence of the grain growth and of the segregation of contaminations at the grain boundaries, though the rate of cooling is sufficiently high to produce an adequate concentration of excess vacancies, and to limit the ordering of the grain boundaries and of the grains during cooling. During welding of pearlitic steels the rate of cooling determines even more the tendency toward cracking, since it permits regulation of the content of martensite in the structure. During welding of titanium alloys the influence of the rate of cooling should also be considerable, since it determines the kinetics of the hydride transformation and the nature of the precipitation of hydrides [2, 3].

The vacancy mechanism advanced to explain formation of microvoids, provides a basis for the existing theories of the influence of hydrogen on the brittleness of metals, since until now it has not been clear how hydrogen can precipitate from a solid solution in the absence of nuclei of voids having a certain critical magnitude.

Bibliography

1. Shorshorov, M. Kh. — Izvestiya AN SSSR, OTN, No. 4:521. 1962.
2. Shorshorov, M. Kh. and G. V. Nazarov. — Sbornik "Titan i ego splavy", Izdatel'stvo AN SSSR, No. 7:226. 1962.
3. Shurakov, S. S. — Sbornik "Metallovedenie", Sudpromgiz, p. 100. 1957.
4. Makara, A. M. — Avtomaticheskaya Svarka, No. 2:9. 1960.
5. Prokhorov, N. N. Tekhnologicheskaya prochnost' metallov pri svarke (Mechanical Strength of Metals during Welding). — Profizdat. 1960.
6. Macklin, D. Granitsy zeren v metallakh (Grain Boundaries in Metals). — Metallurgizdat. 1960.
7. Gertsriken, S. D. and I. Ya. Dekhtyar. Diffuziya v metallakh i splavakh v tverdoi faze (Diffusion in Solid Solutions of Metals and Alloys). — Fizmatgiz. 1960.
8. Cottrell, A. H. Sbornik "Vakansii i tochechnye defekty", Metallurgizdat, p. 7. 1961. [Russian Translation.]
9. Brum, T. and R. K. Kham. — Sbornik "Vakansii i tochechnye defekty", Metallurgizdat, p. 54. 1961.
10. Macklin, D. — Sbornik "Vakansii i tochechnye defekty", Metallurgizdat, p. 197. 1961.
11. Krishtal, M. A. — Fizika metallov i metallovedenie, 9(4):720. 1959.

— METASTABLE STRUCTURAL TRANSFORMATIONS AND THEIR INFLUENCE ON THE PROPERTIES OF $\alpha + \beta$ -TITANIUM ALLOYS

E. A. Vinogradova, N. F. Lashko, and V. N. Moiseev

The specific feature of VT-14 and VT-14-1 alloys is that they may contain relatively large amounts of a stable or metastable β phase. The VT-14 alloy contains a lower amount of β -phase isomorphic elements (Mo and V) than the VT-14-1 alloy, and therefore the latter may contain a larger amount of the β phase than the VT-14 alloy. In VT-14 alloys rapid quenching produces, without diffusion, a martensitic α' phase while in the VT-14-1 alloy it produces, depending on the rate of cooling, an α'' phase (with a rhombic crystal lattice) or α' and β phases.

The X-ray investigations were carried out with metal powders using a CuK_α radiation. The mechanical characteristics of these alloys were tested on specimens cut out from rods. In some cases the authors investigated phases or mixtures of phases which had been electrolytically separated from the alloys.

The cause for the low yield points of hardened titanium alloys

The VT-14 alloy belongs to the group of $\alpha + \beta$ -titanium alloys, the ultimate strength of which continuously increases with the hardening temperature, while the yield point and the σ_y/σ_u ratio decrease at the beginning and after reaching a minimum increase again (Figure 1). No metastable ω phases are usually formed in these alloys (which include some alloys of the Ti-Al-Mn, Ti-Al-V, Ti-Al-Mo-V, and other systems).

In an investigation carried out by Jaffee /1/, the decrease in the yield point was explained by the formation, during hardening, of an unstable β phase, which is transformed into martensite during deformation. According to the data of Khesin /2/, the content of alloying elements in the β phase decreases with the increase in the hardening temperature.

According to the data obtained by the present authors, the composition of the β phase cannot be determined by an X-ray investigation of monolithic specimens, since the parameters of the unit cell of the β phase are in such specimens greatly influenced by the hardening temperature while the parameter of the β phase, separated from the alloy, remains constant irrespective of the hardening temperatures (Figure 2). The influence of hydrogen absorbed during etching has been disregarded.

The lattice of the β phase formed during hardening of monolithic specimens from temperatures above 700°C, is much more elongated than

. the lattice of the separated β phase. The amount of this phase continuously increases with the increase in the hardening temperature, up to 850°C.

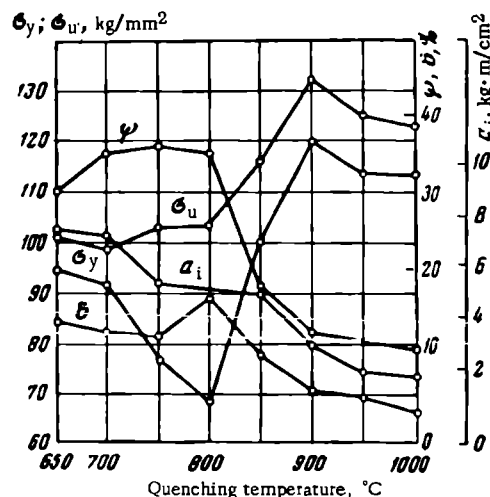


FIGURE 1. Dependence of the mechanical properties of VT-14 alloys quenched in water from different temperatures

The increase in the parameter of the unit cell of the β phase formed during hardening from high temperatures is apparently due to the influence of the surrounding α' phase during cooling. The β phase decreases in

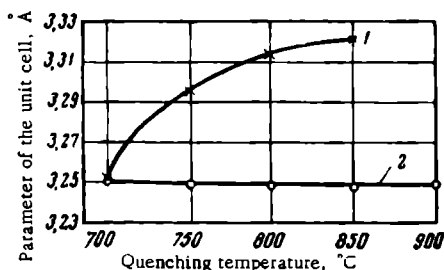


FIGURE 2. The variation of the parameter of the unit cell of the β phase in monolithic specimens (1) and of the β phase separated from the VT-14 alloy (2) after quenching in water from different temperatures

stability as the hardening temperature increases. In alloys hardened from a high temperature this phase is almost completely transformed into martensite. In the VT-14 alloy, an increase in the hardening temperature to 850°C causes an increase in the amount of the β phase to 60 %. After hardening from 900°C the β phase, because of its low stability, remains in the alloy only in small amounts (Table 1). The chemical composition of the β phase should not be greatly influenced by the hardening temperature. The preliminary data on the chemical analysis of anodic deposits confirm this assumption.

The decrease in the yield point of the VT-14 alloy during tension tests is connected with the increasing amount and [lack of] stability of the β phase which decomposes during plastic deformation.

The influence of the decomposition of the metastable β phase and of the α'' phase on the phase composition and on the properties of $\alpha + \beta$ -titanium alloys. Possibility of the $\beta \rightarrow \alpha''$ transformation during aging

The VT-14-1 alloy, which has a higher degree of alloying than the VT-14 alloy also contains a greater variety of phases.

TABLE 1
Phase composition of the VT-14 alloy after quenching in water
from different temperatures

Quenching temperature, °C	Phase composition	Phase ratios, %		Parameter of the unit cell of the β phase
		α	β	
700	$\alpha + \beta$	70	30	3.252
750	$\alpha + \beta$	60	40	3.295
800	$\alpha + \beta$	50	50	3.331
850	$\alpha + \beta$	60	40	3.320
900	$\alpha + \beta$	~100	—	—

Hardened VT-14-1 alloys contain α , α' , α'' , β , and ϵ phases in various ratios, depending on the hardening temperature and on the cooling rate. The X-ray structural analysis has shown no difference between the martensitic α' phase and the α phase. The second martensitic α'' phase is formed during a relatively rapid cooling of the alloy; this phase has a rhombic crystal structure. The ϵ phase has a body-centered crystal structure with a parameter equal to 4.40-4.43 Å.

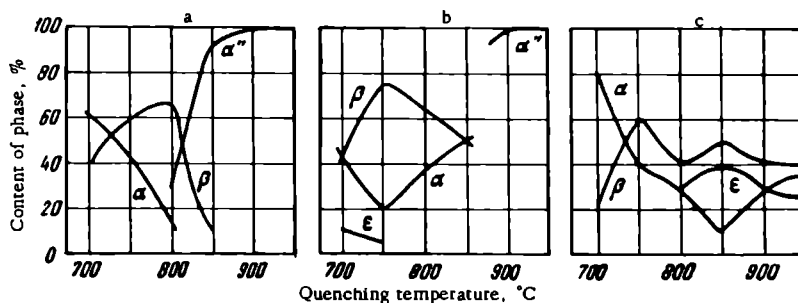


FIGURE 3. The variation of the relative amounts of structural components of the VT-14-1 alloy after heating to different temperatures and cooling in water (a), in the air (b), and within the furnace (c) (monolithic specimens)

The phase composition of the VT-14-1 alloy after quenching and cooling at various rates are given in Table 2 for monolithic specimens and in Table 3 for anodic deposits separated from the alloy.

The dependence of the ratio of these phases in monolithic specimens on the heating temperature and on the rate of cooling is given in Figure 3.

The structural metastability of the alloys increases with temperature of heating and with the cooling rate. For example, in alloys cooled in water the α'' phase is formed only after heating to 800°C while in air

cooled alloys a noticeable amount of the α'' phase can be found only after heating to 900°C. No α'' phase is formed in alloys cooled together with the furnace.

TABLE 2

The results of an X-ray analysis of monolithic VT-14-1 specimens after heating to different temperatures, holding at 1 hour, and cooling

Quenching temperature °C	Phase composition after heating and cooling		
	in water	in the air	within the furnace
700	$\alpha(\alpha') > \beta$	$\beta \approx \alpha(\alpha') > \epsilon$	$\alpha > \beta$
750	$\beta > \alpha(\alpha')$	$\beta > \alpha(\alpha') > \epsilon$	$\beta \approx \alpha > \epsilon$
800	$\beta > \alpha'' \gg \alpha(\alpha')$	$\beta > \alpha(\alpha')$	$\beta > \alpha \approx \epsilon$
850	$\alpha'' \gg \beta$	$\alpha(\alpha') \approx \beta$	$\beta \approx \epsilon > \alpha$
900	α''	α''	$\beta \approx \alpha \approx \epsilon$
950	α''	α''	$\beta \approx \epsilon > \alpha$

TABLE 3

The results of an X-ray structural analysis of anodic deposits separated from a VT-14-1 alloy after quenching in water from different temperatures

Quenching temperature, °C	Phase composition
700	β
750	β
800	$\alpha \approx \beta > \epsilon$
850	$\alpha > \epsilon$
900	$\epsilon > \alpha$
950	$\epsilon \gg \alpha$

The high metastable structure of alloys cooled in water leads to a decrease in their yield point with an increase in the heating temperature to 800-850°C (Figure 4a). The relatively higher stability of the structure after cooling in air results in there being no appreciable decrease in the σ_y/σ_u ratio with the increase in the heating temperature (Figure 4b). Cooling of the alloy within the furnace from different temperatures stabilizes the structure to an even greater extent. In such cases the role of the face-centered ϵ phase becomes more prominent. Figure 4c shows that an increase in the heating temperature causes a gradual decrease in the strength characteristics, and after cooling from 900°C the plasticity also decreases.

Since, after rapid quenching in water, the β phase in the alloy remains metastable, it decomposes after the subsequent aging. This decomposition depends on the initial condition, which is determined by the hardening temperature (Table 4).

After 4-16 hours long aging at 450-550°C of alloys hardened from 750°C the amount of the metastable β phase decreases and becomes roughly equal to the amount of the $\alpha(\alpha')$ phase.

A 4-16 hours long aging at 450°C of an alloy hardened from 800 to 850°C causes a complete decomposition of the metastable β phase which is transformed into an α'' phase and partially into an $\alpha(\alpha')$ phase (if hardened from 800°C).

A 16 hours long aging at 500°C leads to a decomposition of the martensitic α'' phase, which transforms into an $\alpha(\alpha')$ phase; a small amount of the more stable β phase is also formed. Aging at 550°C produces more of the β phase than aging at 500°C.

The changes in the mechanical characteristics of the VT-14-1 alloy after aging at 450-550°C are also connected with the degree of the decomposition of the metastable phases. Isothermal aging at almost all temperatures, causes a decrease in the ultimate strength and an increase in plasticity (Figure 5).

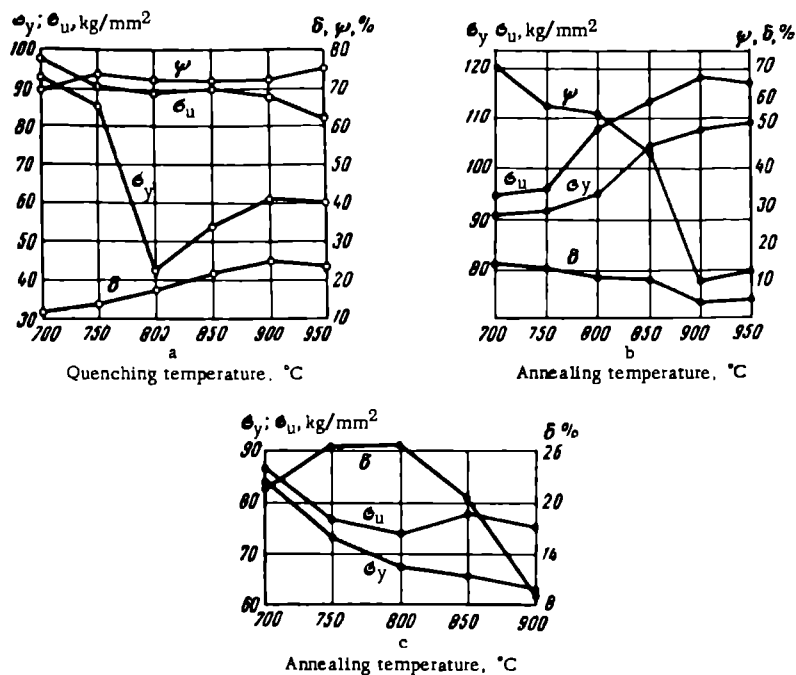


FIGURE 4. Changes in the mechanical properties of the VT-14-1 alloy after heating to different temperatures and cooling in water (a), in the air (b), and within the furnace (c)

TABLE 4

Variation of the phase composition of the VT-14-1 alloy after quenching from different temperatures and aging at 450-550°C for 4 and 16 hours

Heat treatment	Parameter of the unit cell of the β phase, λ	Phase composition
Quenching from 750°+aging 450°, 5 hrs	3.26 ₆	$\alpha \approx \beta$
500°, 4 "	3.24 ₆	$\alpha \approx \beta$
550°, 4 "	3.26 ₆	$\alpha \approx \beta$
450°, 16 "	3.26 ₆	$\alpha \approx \beta$
500°, 16 "	3.24 ₆	$\alpha \approx \beta$
550°, 16 "	3.25 ₇	$\alpha \approx \beta$
Quenching from 800°+aging 450°, 4 "	—	$\alpha' \gg \alpha (\alpha')$
500°, 4 "	3.25 ₃	$\alpha \gg \beta$
550°, 4 "	3.26 ₄	$\alpha > \beta$
450°, 16 "	—	$\alpha \approx \beta$
500°, 16 "	3.25 ₆	$\alpha \gg \beta$
550°, 16 "	3.25 ₆	$\alpha \approx \beta$
Quenching from 850°+aging 450°, 4 "	—	$\alpha \approx \beta$
500°, 4 "	3.25 ₄	$\alpha \gg \beta$
550°, 4 "	3.25 ₃	$\alpha > \beta$
450°, 16 "	—	$\alpha \approx \beta$
500°, 16 "	—	$\alpha \gg \beta$
550°, 16 "	—	$\alpha > \beta$

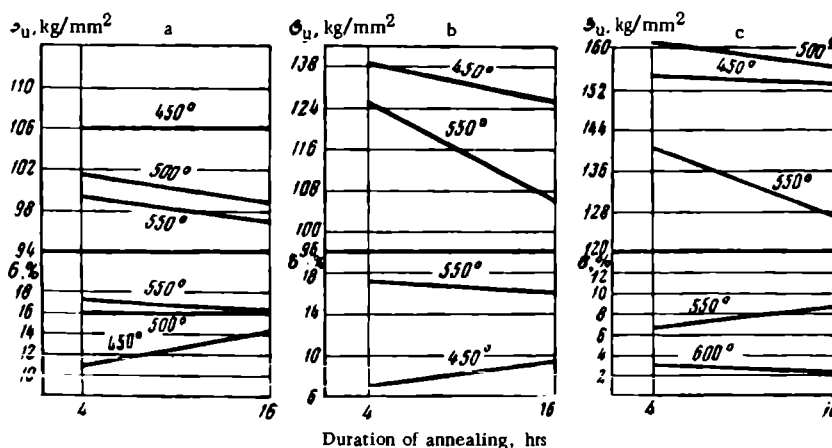


FIGURE 5. The change of the mechanical properties of the VT-14-1 alloy after quenching in water from 750 (a), 800 (b), and 850°C (c) and a subsequent aging at 450-550°C

An increase in the aging temperature of alloys quenched from 750 and 800°C, during which a metastable β phase is formed, leads to a decrease in the ultimate strength, while any noticeable decrease in the ultimate strength of alloys hardened from 850°C when only an α'' phase is formed, is noted only after aging at 550°C.

The first stage of aging (at 450°C) of alloys hardened from 750°C does not change their ultimate strength; only aging [at this temperature] of alloys hardened from 800°C or 850°C results in a decrease in the ultimate strength.

Metastable structural transformations in titanium alloys during plastic deformation. The reversibility of the $\beta \rightleftharpoons \alpha$ transformation

Many titanium alloys form metastable structures during the polymorphic transformation taking place on cooling from temperatures at which a β phase exists. Hardening of titanium alloys (alloyed with increasingly large amounts of transition metals) from the β field, may cause the transformation of three metastable phases: the α' phase (with a hexagonal crystal structure, $c:a \approx 1.6$); α'' phase (with a rhombic crystal structure); ω phase (with a hexagonal crystal structure, $a:c \approx 1.6$).

The reversibility of these transformations and the conditions under which they can take place, have not been investigated to any great extent. It is only known that the $\beta \rightleftharpoons \omega$ transformation is reversible both during cooling and heating.

By analogy with the diffusionless, polymorphic transformation in other alloys, it may be assumed that the transformations $\beta \rightarrow \alpha'$ and $\beta \rightarrow \alpha''$ are also reversible (during cooling and heating).

By analogy with the metastable transformations of ferrous alloys, it may likewise be assumed that in titanium alloys the diffusionless transformation may be caused by plastic deformation. With the object of

studying the possibility of the metastable polymorphic transformations and of determining their reversibility during plastic deformation the authors have carried out investigations on the VT-14-1 alloy.

The plastic deformation was induced by cold rolling. A 6 mm thick sheet was rolled in several passes (without heating) to a degree of deformation equal to 5 and 20 %. From the work-hardened sheets 1 mm diameter specimens were cut out and these were then etched to 0.5 mm diameter in order to remove the work-hardened layer.

The results of the X-ray structural analysis by the powder method using a CuK_α radiation are given in Table 5.

TABLE 5
Phase composition of the VT-14-1 alloy after hardening and different degrees of deformation

Hardening temperature, °C	Degree of plastic deformation, %	Phase composition	Hardening temperature, °C	Degree of plastic deformation, %	Phase composition
750	0	$\beta > \alpha'$	850	0	$\alpha'' \gg \beta$
	5	$\beta \approx \alpha'$		5	$\beta \gg \alpha' (\alpha'')$
	20	α''		20	$\alpha'' > \beta$

Cold pressing of alloys hardened from 750° to a degree of deformation equal to 5 % caused a partial decomposition of the β phase and formation of a martensitic α' phase. Cold pressing to a larger degree of deformation caused a complete decomposition of the β phase, and a formation of a non-equilibrium α'' phase which is characterized by a number of split lines on the Debyegram, corresponding to the α phase.

TABLE 6
Mechanical properties of titanium alloys containing 7.1 % Mo and 2.3% Al after quenching from 750°C in water and cold rolling

Degree of deformation, %	Ultimate strength, kg/mm ²	Elongation, %	Degree of deformation, %	Ultimate strength, kg/mm ²	Elongation, %
0	101.5	6.5	9.0	98.0	10.0
2.5	93.0	10.5	14.0	100.0	9.5
5.0	96.0	11.5	25.0	95.5	15.0

Rolling of alloys, hardened from 850°C, to a degree of deformation of 5 %, caused complete or almost complete decomposition of the α'' phase and formation of a β phase and of a martensitic α' phase. The parameter of the unit cell of the β phase is equal to 3.34\AA , which indicates a lower content of molybdenum (the β phase contains only very small amounts of aluminum) than in alloys hardened from 750°C, and corresponds to the high-temperature β phase of this alloy. The formation of the β phase took place in this case as a result of a reversible diffusionless $\alpha' \rightarrow \beta$ transformation. Consequently the $\beta'' \rightleftharpoons \alpha''$ transformation can be reversible.

A subsequent rolling of the alloys to a total degree of deformation of 20 % promotes the transformation of a considerable part of the metastable β phase into the α'' phase. Part of the β phase, however, remains untransformed. Consequently, the plastic deformation of the investigated alloy causes a polymorphic diffusionless transformation; some of these transformations induced by a low degree of plastic deformation, are reversible.

The changes in the mechanical properties of the VT-14-1 alloy after the plastic deformation are rather unusual, because of the above-mentioned structural transformation. It is known that in relatively stable alloys, including a number of titanium alloys, an increase in the degree of plastic deformation causes a continuous increase in the ultimate strength and a decrease in the plastic characteristics. In the VT-14-1 alloy hardened from 750°C, the plastic deformation to about 25 % decreases the ultimate strength and increases the elongation (Table 6).

Such changes in strength and plasticity are due to the decomposition of the β phase and, apparently, chiefly to the formation of the metastable α'' phase. It has been shown that the α'' phase has a lower hardness than other metastable phases of titanium alloys.

There is no doubt that the plastic deformation of this alloy brings about for the most part diffusionless structural deformations. The diffusion processes, which are associated with a partial transformation of the energy of deformation into thermal energy, are of secondary importance. According to the energy theory of metastable transformation, these diffusion processes form structures which, under identical conditions, are represented by lower magnitudes of the thermodynamic function of state of the system. Unfortunately, a real analysis of the variation of the thermodynamic function of state is difficult to carry out, even approximately.

It would be interesting to determine the change of thermodynamic function of state of the alloy after quenching in water from 750°C and after plastic deformation, a process during which the metastable β phase becomes relatively less stable than the α'' phase, and also to determine why, after hardening from 850°C and a slight deformation, the relative stability of the β phase increases more than that of the α'' phase formed.

Bibliography

1. Jaffe, L. — J. Metals, 7(11):1245. 1955.
2. Khesin, Yu.D. — Sbornik "Metallovedenie", Sudpromgiz, No. 3:298. 1959.

MECHANICAL PROPERTIES OF Ti-Cr-Fe, TITANIUM-RICH ALLOYS (PHASE DIAGRAM SECTIONS WITH 0.5 AND 1.5% Fe)

N. G. Boriskina and I. I. Kornilov

The development of new titanium alloys calls for a thorough and systematic investigation of the properties of titanium alloyed with various elements. The polymorphism of titanium makes it possible to improve the properties of these alloys by choosing the optimum conditions of heat treatment.

The purpose of the present investigation was to determine the effect of iron and chromium and also of the temperature of preliminary annealing on certain mechanical properties of ternary, titanium-rich alloys.

The phase structure of titanium-rich alloys of the Ti-Cr-Fe system has been investigated by Van Thyne et al. /1/, and also by the present authors. Iron and chromium which are β phase stabilizers decrease the temperature of the polymorphic transformation of titanium. No more than 0.5 % Fe /2/ and 0.6 % Cr /3/ can be dissolved in α -Ti at the temperature of the eutectoid transformation. According to our data obtained by the authors, the total solubility of iron and chromium in α -Ti at room temperature is about 0.4 %.

The characteristic feature of alloys of this ternary system is the low rate of the eutectoid decomposition of β -Ti. Van Thyne /1/ found no typical eutectoid structure in ternary titanium alloys. According to the data of the present authors, a very long annealing (total duration of 2000 hours) at 550 and 450°C will induce only a partial eutectoid decomposition of the β -solid solution of these alloys.

The appearance of the Ti-Cr-Fe phase diagram and the martensitic nature of the polymorphic transformation of the alloys it represents are similar to those of an Fe-C diagram of alloys containing elements which widen the field of the γ -solid solutions of iron. Therefore, by analogy it may be expected that heat treatment will induce in titanium-rich alloys a great variety of properties. The available literature contains no systematic investigation of the mechanical properties of the alloys of this system.

In the present study, an investigation was carried out of alloys belonging to the sections containing 0.5 and 1.5 % Fe, together with 0, 0.5, 1.0, 2.0, 3.0, and 5.0 % Cr.

The initial materials were titanium sponge TGOO (99.8 % Ti and 0.06 % O_2), electrolytic iron (99.94 % Fe and 0.028 % C) and chromium (99.9 % Cr and 0.02 % O_2).

Twenty-kilogram ingots obtained by smelting in an arc furnace in an atmosphere of argon, were drawn at 1000-1200°C to 7-8 mm diameter rods. From these rods specimens were prepared for the investigation of the mechanical properties of alloys at room temperature and also specimens for the investigation of the heat resistance and thermal stability.

For the investigation of the mechanical properties of the alloys, the specimens were quenched in water from 1000°C (holding time 5 hours), and from 750°C (holding time 200 hours), and annealed at 400°C (holding time 200 hours).

The ultimate strength and the elongation of the alloys were determined by the micromechanical method on the Chevenard apparatus [4, 5]. The tension specimens were 1.5 mm in diameter and the gage length was 7.5 mm. The heat resistance of alloys quenched from 750°C and annealed at 400°C was tested by bending on a centrifugal machine [6] at 450°C with a load of 15 kg/mm².

For the investigation of the thermal stability, the specimens were quenched from 750°C. The alloys were aged in quartz ampoules from which the air had been evacuated, at 450°C for 1, 10, 25, 50, 75, and 100 hours. Microstructural analysis and hardness tests were the chief methods used for the determination of the phase transformations taking place during short annealing processes.

A microstructural analysis was also carried out on all specimens before the tension tests.

Results

Microstructure. The β -solid solution of alloys quenched from 1000°C, undergoes martensitic transformation at certain concentrations of chromium. In alloys belonging to the section with 0.5 % Fe, the martensitic transformation takes place if the alloy contains 0-3 % Cr, while in alloys of the section with 1.5 % Fe this transformation takes place at 0-2 % Cr. The microstructure of these alloys is similar to that shown in Figure 1a. At higher chromium contents a β -Ti solid solution is formed. An analysis of the microstructures of the alloys of these sections, quenched from 750°C, has shown that alloys of the section with 0.5 % Fe containing up to 2 % Cr and those of the section with 1.5 % Fe containing up to 1 % Cr have the polyhedral structure of an α -solid solution with small amounts of the grains of the β -Ti solid solution located along the grain boundaries (Figure 1b).

In alloys with a higher content of chromium, the $\beta \rightarrow \alpha$ transformation takes place both on the grain boundaries and in the grains proper. The structure of such alloys is shown in Figure 1c.

A microstructural analysis of alloys annealed at 400°C has shown that the alloys of both sections containing 0-3 % Cr belong to the field of $\alpha + \beta$ -solid solutions. The β -solid solution precipitates along the grain boundaries of the acicular α phase grains (Figures 1d and e). The amount of the β -solid solution increases with the chromium content. The β -solid solution of alloys of both sections containing 5 % Cr undergo intensive decomposition entailing the formation of acicular α phase grains (see Figure 1f). A more intensive etching of the grains of the α and β phases of annealed alloys indicates that they have decomposed into a finely dispersed TiCr₂ intermetallic compound. Nevertheless, even annealing for 200 hours at 400°C is not sufficient for the formation of equilibrium structures. The alloys of the section with 1.5% Fe contain large amounts of the β -solid solution, irrespective of their type of heat treatment.

Ultimate strength and elongation of alloys. The variation of the mechanical and plastic characteristics of alloys belonging to both sections is shown on Figure 2. After quenching from 1000°C, the curves of the ultimate strength have a well-marked maximum (at about 120 kg/mm²), corresponding to those alloys the chromium content of which is the highest of those subject to the $\beta \rightarrow \alpha$ martensitic transformation. The same alloys have a minimum elongation (up to 1 %).

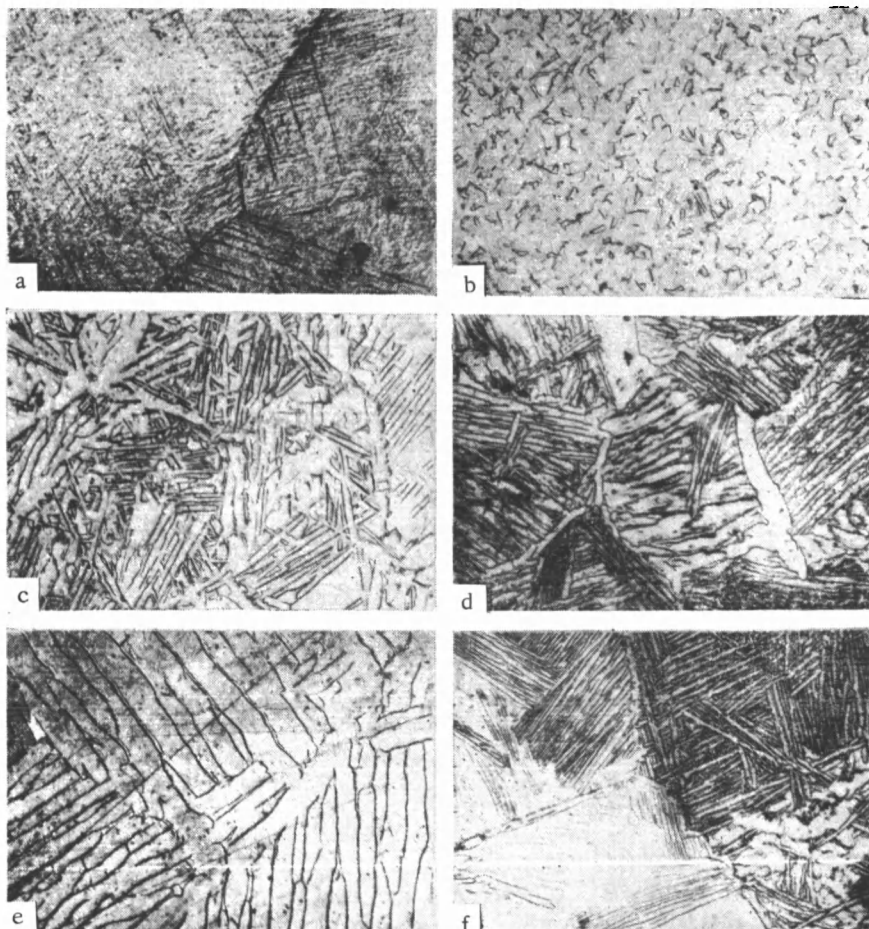


FIGURE 1. Microstructure of alloys after different heat-treatment processes

a — 0.5% Fe + 2% Cr, quenching 1000°, $\alpha' + \beta$; b — 1.5% Fe + 1% Cr, quenching at 750°, $\alpha + \beta$; c — 0.5% Fe + 3% Cr, quenching at 750°, $\alpha + \beta$; d — 1.5% Fe + 2% Cr, annealing at 400°, $\alpha + \beta$; e — 1.5% Fe + 0.5% Cr, annealing at 400°, $\alpha + \beta$; f — 1.5% Fe, 5% Cr, annealing at 400°, $\alpha + \beta$.

The graphs in Figure 2b show that the ultimate strength of alloys of both sections after quenching from 750°C continuously increases with the content

of chromium. Nevertheless, the maximum values of σ_u of alloys with 5 % Cr are roughly equal to the minimum values of σ_u of alloys quenched from 1000°C. After quenching from 750°C alloys belonging to the section with 0.5 % Fe and 2 % Cr have an ultimate strength by about 64 kg/mm² lower than the alloys belonging to the section with 1.5 % Fe and 1 % Cr, 74 kg/mm² lower than the alloys hardened from 1000°C.

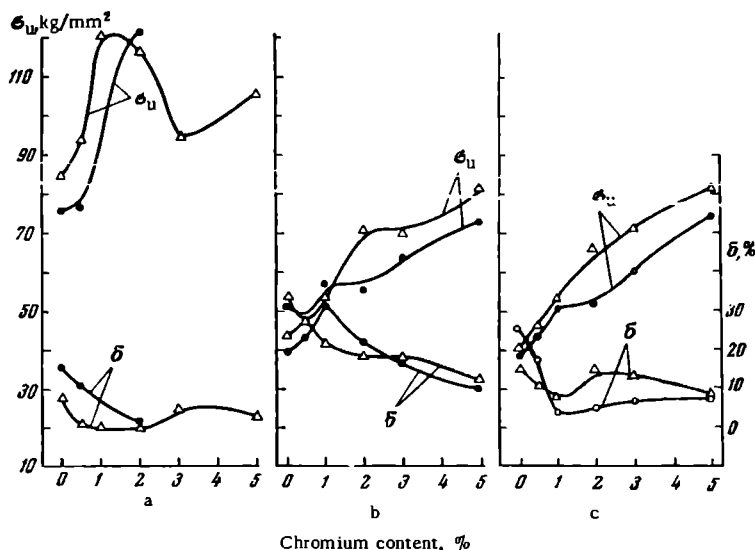


FIGURE 2. The dependence of the ultimate strength and the elongation of titanium alloys on their composition and annealing temperature

a — quenching temperature 1000°C; b — quenching temperature 750°C; c — annealing temperature 400°C; ● — alloys with 0.5 % Fe; Δ — alloys with 1.5 % Fe.

The elongation of the alloys of both sections quenched from 750°C decreases with the increase in the Cr content from 2.5-3.0 % for alloys with 0.5-1 % Cr to 10 % for alloys with 5 % Cr.

The ultimate strength of alloys of both sections, annealed at 400°C is about the same as that of alloys quenched from 750°C. Nevertheless, the elongation of these alloys is considerably lower than that of alloys hardened from 750°C, though it is somewhat higher than that of alloys hardened from 1000°C. The lower plasticity of these alloys is apparently due to the partial decomposition of the α and β phases during annealing from 400°C and to the formation of finely dispersed intermetallic $TiCr_2$ grains. The precipitates present in these alloys in a nonequilibrium condition also decrease their plasticity.

Alloys of the section with 1.5 % Fe, the solid solution of which is more saturated with iron, have higher ultimate strength than the alloys of the section with 0.5 % Fe, irrespective of the quenching temperature.

Aging of alloys at 450°C. The microstructural investigations of alloys of the sections with 0.5 and 1.5 % Fe after a short annealing at 450°C, showed only a small degree of grain growth of the α phase.

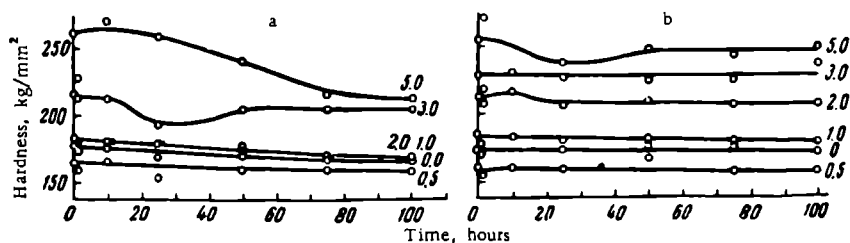


FIGURE 3. Dependence of the hardness of alloys annealed at 450°C on their chromium content and on the duration of annealing

a — alloys with 0.5% Fe; b — alloys with 1.5% Fe (the numbers beside the curves indicate the content of chromium in %).

The hardness measurements for all alloys confirms the data of the microstructural analysis. As Figure 3 shows, the hardness of the alloys of both sections remains almost unchanged after a 100 hour long annealing at 450°C.

In alloys of both sections the hardness is increased with the chromium content, except that an addition of 0.5% Cr leads to a small decrease in the hardness. The hardness of alloys of the section with 0.5% Fe remains almost unchanged over the range of 0-2% Cr; in alloys of the section with 1.5% Fe the hardness increases more markedly with the chromium content. The hardness of alloys of the section with 1.5% Fe is somewhat higher than that of alloys with 0.5% Fe, as a result of the higher degree of alloying of the β -Ti solid solution. Thus, a 100-hour long aging at 450°C of alloys with an $\alpha + \beta$ structure does not lead to phase equilibrium as would have been expected from the phase diagram of the ternary system. According to this diagram the α and β phases at this temperature should undergo a decomposition entailed by a formation of the TiCr_2 intermetallic compound. Instead, the very small rates of phase transformations at low temperatures result in relatively high thermal stability for these alloys.

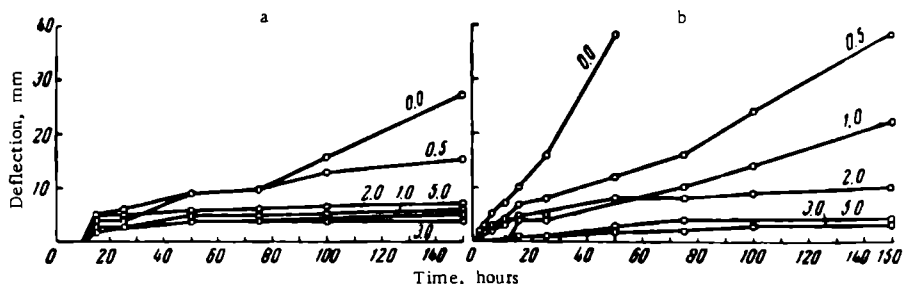


FIGURE 4. Dependence of the deflection of alloys quenched from 750°C on their composition and duration of the test

a — alloys with 0.5% Fe; b — alloys with 1.5% Fe (the numbers beside the curves indicate the chromium content in %).

Heat resistance. The curves characterizing the dependence of the deflection [under the given testing conditions] on the composition of the alloys and on the duration of the test at 450°C and a load of 15 kg/mm² are shown in Figures 4 and 5. These curves are the basis for the construction of the composition versus heat resistance diagram (Figure 6) in which the heat resistance is represented by the time required to produce a 5 mm deflection.

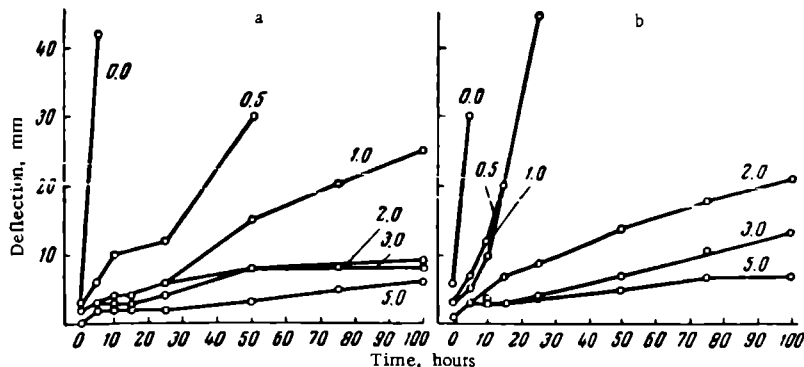


FIGURE 5. The dependence of the deflection of alloys annealed at 400°C on their composition and duration of test

a — alloys with 0.5% Fe; b — alloys with 1.5% Fe (the numbers beside the curves indicate the chromium content in %).

These graphs show that the rate of deformation of the alloys of both sections, whether quenched from 750°C or annealed at 400°C, decreases with the increase in the chromium content. The alloys of the section with 1.5% Fe have higher rates of deformation under the given experimental conditions and after both preliminary heat treatments, than the alloys of the section with 0.5% Fe. The alloys of both sections, quenched from 750°C, have lower rates of deformation than those of alloys annealed at 400°C.

The composition versus heat resistance diagram for alloys quenched from 750°C, unlike that for alloys annealed at 400°C, is characterized by maxima corresponding to alloys with 1% and 3% Cr.

The first maximum corresponds to alloys with the α -Ti solution as the chief phase component, while the second maximum corresponds to alloys with large amounts of the β -Ti solid solution.

For alloys with 0.5 and 1.5% Fe annealed at 400°C, the time required to produce a 5 mm deflection continuously increases with the chromium content. The effect of heat treatment on the type of composition versus heat resistance diagram given by the alloys, can be explained by a number of causes, the chief of which is the quantitative change in the phase composition of alloys annealed at 400°C or quenched from 750°C which takes place at the test temperature of 450°C. It has already been mentioned that at 750°C and at 400°C all investigated alloys have mainly a two-phase $\alpha + \beta$ structure. Since the α -solid solution of titanium contains little iron and chromium, the strengthening of the above alloys is caused chiefly by the β -solid solution, which dissolves considerably more iron and chromium. Nevertheless, at 450-500°C, β -Ti is a

thermally unstable phase and decomposes to form α -Ti; after a prolonged holding time it can even decompose to form eutectoid structures. The phase transformations, which are connected with the dislocation of atoms, lead to a weakening of the bonds in the alloys. Thus, only alloys with an optimum amount of the β -solid solution have low rates of deformation. In this respect the alloys of the section with 0.5 % Fe have apparently a more favorable α to β phase ratio than the alloys of the section with 1.5 % Fe which contain more of the β -solid solution. In alloys annealed at 400°C loading tests at 450°C cause complicated diffusion processes, which are connected with the changes in the α - to β -solid solution ratios, with a decomposition of the β -solid solution and also with the formation of grains of an α -Ti solid solution in a state of greater equilibrium. These diffusion processes apparently somewhat increase the rate of deformation of alloys annealed at 400°C as compared with those alloys quenched from 750°C.

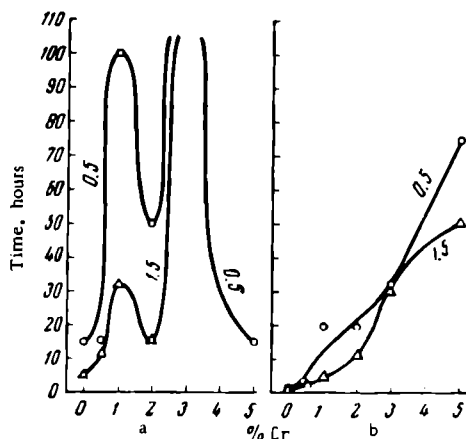


FIGURE 6. The dependence of the time needed to produce a 5 mm deflection on the chromium content in titanium alloys

a — alloys quenched from 750°C; b — alloys annealed at 400°C (the numbers beside the curves indicate the content of iron in the alloy, %).

An analysis of the extensive experimental data on the heat resistance of binary and ternary alloys, carried out by I. I. Kornilov [6], shows that a relationship between the heat resistance of alloys and their composition of the type shown in Figure 6b is characteristic of alloys containing intermetallic compounds. The content of these compounds increases with that of the chief alloying element. Thus, the composition versus heat resistance diagram of alloys annealed at 400°C indicate the presence (or absence) of the TiCr_2 intermetallic compound.

It has already been mentioned that annealing at 450°C of alloys quenched from 750°C leads to a small increase in the content of the α -solid solution. Apparently the application of a 15 kg/mm² load accelerates the $\beta \rightarrow \alpha$ transformation.

Conclusion

1. The preliminary heat treatment of Ti-Fe-Cr alloys belonging to the sections with 0.5 and 1.5 % Fe influences their mechanical properties at room and elevated temperatures as a result of the formation of different structures with different α -to β -solid solution ratios and different contents of TiCr_2 intermetallic compound.
2. Quenching from 750°C is the most favorable heat treatment for alloys of both sections to the production of the optimum properties at room temperature and at 450°C.
3. The alloys of the section with 1.5 % Fe and with 3 or 5 % Cr quenched from 750°C have their highest magnitudes of σ_b and δ at room temperature.
4. The highest heat resistance at 450°C and under 15 kg/mm² loads is shown by alloys of both sections (with 0.5 or 1.5 % Fe and with 3 or 5 % Cr) quenched from 750°C. A 5 mm deflection could not be produced in these alloys after a 150 hour long test.

Bibliography

1. Van-Thyne, R. J., H. D. Kessler, and M. Hansen. — Trans. Am. Inst. Min. Met. Eng., Vol. 197:1209. 1953.
2. Boriskina, N. G. and K. P. Myasnikova. — Sbornik "Titan i ego splavy", Izdatel'stvo AN SSSR, No. 7:61. 1962.
3. Chernova, T. S. and V. S. Mikhnev. — Sbornik "Titan i ego splavy", Izdatel'stvo AN SSSR, No. 7:68. 1962.
4. Savitskii, E. M. — Zavodskaya Laboratoriya, 16(11):1366. 1960.
5. Roitman, I. M. and Ya. B. Fridman. Mikromekhanicheskii metod ispytaniya metallov (Micromechanical Method of Testing Metals). — Oborongiz. 1950.
6. Kornilov, I. I. Fiziko-khimicheskie osnovy zharoprochnosti splavov (Physicochemical Principles of Heat Resistance of Alloys). — Izdatel'stvo AN SSSR. 1961.

N67 11802

HYDROGEN EMBRITTLEMENT OF TITANIUM ALLOYS

V. A. Livanov, A. A. Bukhanova, B. A. Kolachev,
and N. Ya. Gusel'nikov

It is well known that hydrogen has a rather harmful influence on the properties of titanium and its alloys. The addition of even small amounts of hydrogen to titanium and to α -Ti alloys leads to a sharp decrease in their impact strength (Figure 1). However, no hydrogen embrittlement was found in $\alpha + \beta$ alloys subjected to an impact-strength test; hydrogen embrittlement can be detected only at low rates of deformation and becomes more evident during testing of notched specimens or of ordinary specimens at low temperatures.

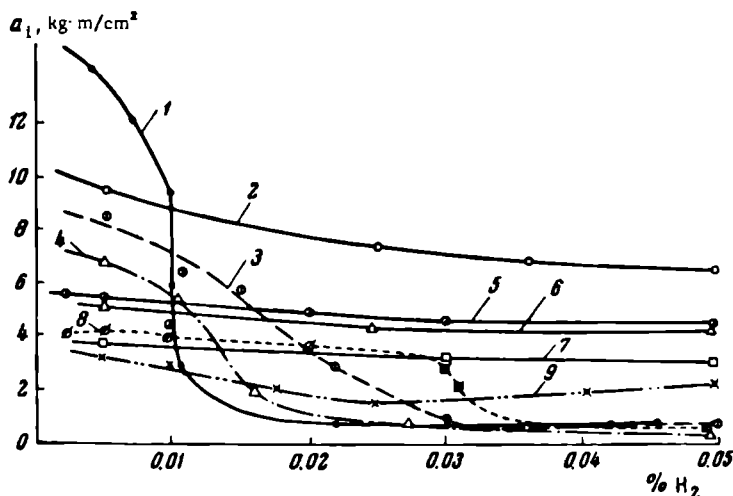


FIGURE 1. The influence of hydrogen on the impact strength of titanium alloys

1—VT-1; 2—VT-6; 3—VT-5-2; 4—VT-5-1; 5—VT-8; 6—VT-3; 7—VT-3-1; 8—VT-5; 9—VT-10.

The influence of hydrogen on the mechanical properties of the VT-3-1 alloy during testing at different rates of tension after a vacuum annealing at 900°C for 6 hours, and after introduction of given amounts of hydrogen at this temperature, is shown in Figure 2 /1/. These data show that the hydrogen embrittlement of VT-3-1 alloys is apparent at low rates of tension when the content of hydrogen exceeds 0.03 %. But even in this case, the decrease in the reduction in area ψ , is relatively small: if at

0.032 % H₂ the reduction in area is 46 %, it decreases to 40 % at 0.043 % H₂ (in the initial condition the reduction of area is 48 %). No hydrogen embrittlement can be detected at normal rates of tension (4 mm/min).

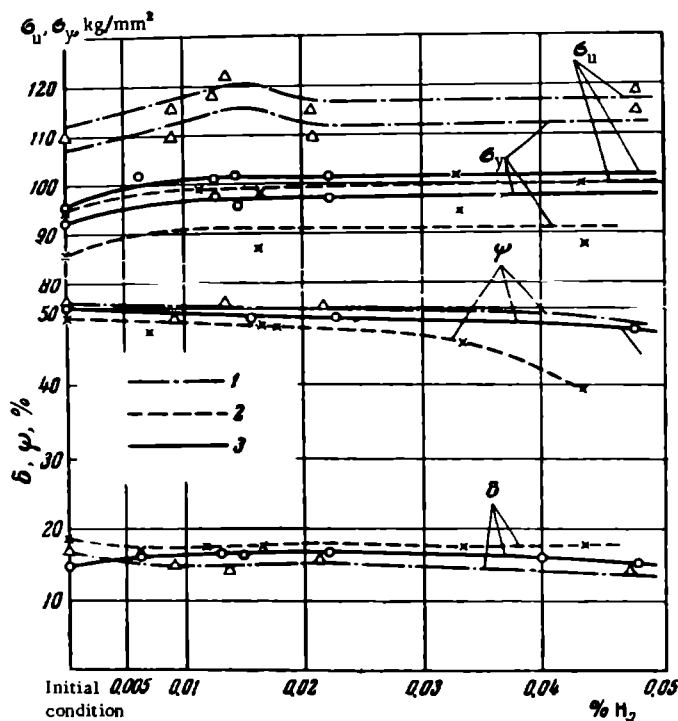


FIGURE 2. The influence of hydrogen on the mechanical properties of the VT-3-1 alloy at various rates of deformation after an ordinary annealing process

1 — rapid tension; 2 — slow tension; 3 — ordinary tension.

It should be pointed out that hydrogen leads to a small increase in the ultimate strength and in the yield point. At an average rate of tension the ultimate strength increases from 96 kg/mm² for specimens without introduced hydrogen and to 102 kg/mm² for specimens with 0.03-0.05 % H₂.

Since hydrogen embrittlement of $\alpha + \beta$ alloys can be detected only at very low rates of tension, the authors arrived at the conclusion that this phenomenon is caused by processes which take time to complete. Indeed, it was found that hydrogen sharply decreases the creep strength of $\alpha + \beta$ alloys. Thus, for instance, plain specimens of the Ti-140A alloy with 0.025 % H₂, failed at room temperature after 2.4 hours under an 84 kg/mm² load (86 % of the ultimate strength). The reduction in area was only 3 %. Under the same load a specimen annealed in vacuo (0.002 % H₂) did not fail after a 1000 hour long test [2/].

It has also been found by Daniels et al. [3/], that with time $\alpha + \beta$ titanium alloys may develop cracks which lead to destruction. The formation of cracks is promoted by stresses developed under external loads and by an increase in the amount of absorbed hydrogen. The failure of the material

begins at the notch with the formation of a slowly developing crack. The average rate of propagation of this crack increases with the hydrogen content.

These observations lead to the conclusion that thermal and welding stresses, or residual stresses induced by plastic deformation, may also be factors in the spontaneous formation of cracks in $\alpha + \beta$ alloys or in a brittle failure of the alloys under ordinary testing conditions.

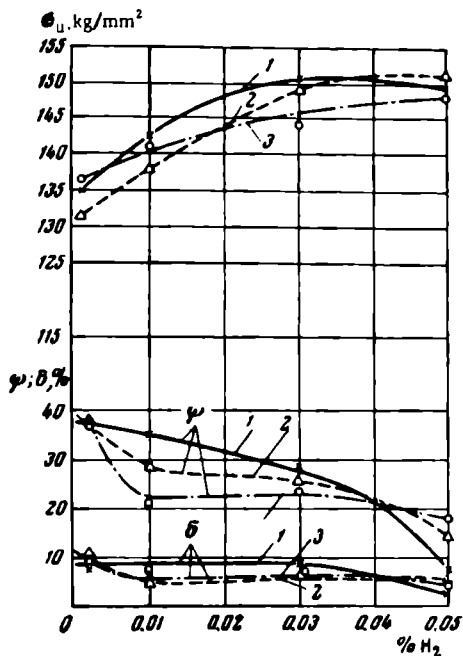


FIGURE 3. The influence of hydrogen on the mechanical properties of the VT-3-1 alloy

1 — immediately after quenching; 2 — after 40 days; 3 — after 90 days.

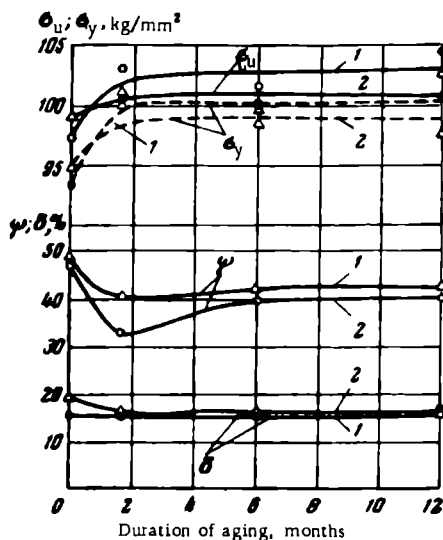


FIGURE 4. The effect of duration of aging on the mechanical properties of VT-3-1 alloy after preliminary tension

1 — after vacuum annealing; 2 — with 0.05% H₂.

To check this assumption 14 × 14 mm blanks of the VT-3-1 alloy were annealed in vacuo after which 0.05% H₂ was added to some of them. All the blanks were heated in the air to 950°C and quenched in water. After a certain time these blanks were shaped into the specimens for mechanical testing, which was immediately carried out at a rate of 2-4 mm/min.

The experimental data in Figure 3 show the influence of hydrogen on the mechanical properties of the VT-3-1 alloy. These data were obtained by mechanical tests at an average tension of 4 mm/min either immediately after quenching or 40 and 90 days after quenching.

A comparison of these data with those given in Figure 2 shows that hydrogen exerts a much greater influence on the properties of VT-3-1 alloys in the quenched condition than in the annealed condition. First of all, hydrogen considerably strengthens (hardens) the VT-3-1 alloys. The ultimate strength increases from 134.5 kg/mm² for an alloy with no added

hydrogen to 150.7 kg/mm² for alloys with 0.05 % H₂. On the other hand, the reduction in area, ψ , is decreased; the plastic properties are most notably reduced by the introduction of more than 0.03 % H₂. The reduction in area, ψ , of a hardened VT-3-1 alloy is 37.9 % when the content of hydrogen is 0.02 %; 28.4 % if the content of hydrogen is 0.03 %; and 7.3 % if the content of hydrogen is increased to 0.05 %.

Aging of a VT-3-1 alloy containing 0.01-0.03 % H₂ at room temperature for 90 days results in a considerable decrease in plasticity. The presence of 0.05 % H₂ results, under the same conditions, in only slightly greater decrease in plasticity. After a prolonged aging of hardened VT-3-1 alloys at room temperature, the detrimental influence of hydrogen on the plasticity is detectable after the first addition of 0.008 % H₂ (the total content of hydrogen is 0.01 %). If a hardened VT-3-1 alloy with no specially added hydrogen after a 90-day long aging has an elongation, σ , of 9.4 % and a reduction in area, ψ , of 37.1 %, these characteristics under the same conditions of aging are reduced to 4.7 and 20.3 % respectively, if the content of hydrogen is increased to 0.01 %. It may therefore be considered that the permissible concentration of hydrogen in a hardened VT-3-1 alloy is lower than 0.01 %.

In the second series of experiments, the authors investigated the influence of a preliminary deformation on the susceptibility of $\alpha + \beta$ alloys to hydrogen embrittlement. For these experiments a VT-3-1 alloy was prepared by smelting in a vacuum arc furnace with consumable electrodes (double melt).

From the upper template of the ingot 14 × 14 mm rods were forged, which, after an ordinary annealing, were cut into 60 mm long specimens. The specimens prepared for mechanical tests were annealed at 900°C in vacuo for 6 hours after which the necessary amount of hydrogen was introduced. The specimens were subjected to tension at a rate of 4 mm/min until necking, after which the load was removed. In order to determine the mechanical properties of the alloys in their initial condition, tension was applied to several specimens until failure.

After the preliminary tension had been applied, the specimens were kept at room temperature for different periods, the tension was again applied at a rate of about 4 mm/min, and the mechanical properties were determined, (a), in relation to the dimensions after the preliminary deformation and (b), in relation to the initial dimensions.

In the calculation on the basis of (a), the mechanical properties are influenced not only by the subsequent aging, but also by the degree of deformation during the preliminary tension tests. The results obtained by this method are therefore influenced not only by the aging process but also by the variation in the rate of the preliminary tension applied. In the calculation on the basis of (b), the influence of the deformation is eliminated and the property changes are related only to the effect of aging. The latter results are given in Figure 4.

These data show that aging has little influence on the strength characteristics, though the plasticity of the alloy decreases after 40 days (it increases afterwards). This effect is more marked in a VT-3-1 alloy containing 0.05 % H₂ than in an alloy after a vacuum annealing.

These data also indicate that preliminary deformation creates in a VT-3-1 alloy containing hydrogen, additional centers of brittle failure.

These disappear after a certain time and the embrittlement of the alloy is diminished.

This conclusion is confirmed by the results obtained by Daniels et al. /3/, in which the influence of preliminarily applied stresses on the hydrogen embrittlement of the Ti-4Al-4Mn $\alpha + \beta$ alloy was investigated after hardening and aging. The specimens of the alloy were stressed below their yield point for 100 hours. No appreciable deformation of the specimens could be noticed. The load was then removed and the specimens maintained for various periods at room temperature or at an elevated temperature. This was followed by creep-strength tests, carried out at room temperature and under a load of 85 kg/mm². Some results obtained in this investigation are given in the table.

The influence of preliminarily applied stresses on the creep strength of the Ti-4Al-4Mn alloy with 0.037% H₂ and an ultimate strength equal to 120 kg/mm²

Duration of the preliminary applied stresses, hours	Time of holding until the final experiments, at 20°C	Time to failure at 85 kg/mm ² , min
—	—	29
100	2-30 min	6
100	13 days	34

A load applied for 100 hours considerably decreases the creep strength of the Ti-4Al-4Mn alloy at room temperature if the test is carried out immediately after removing the preliminary load. However, a subsequent aging of the alloy at room temperature for 13 days leads to the restoration of the creep strength.

There is a widespread opinion that hydrogen embrittlement and failure of hydrogen-saturated specimens subjected to a slowly applied load is only characteristic of $\alpha + \beta$ alloys. It has been found [by the authors], however, that the α phase alloys VT-10 and VT-4 are also prone to hydrogen embrittlement both at high and low tension rates.

The influence of hydrogen on the mechanical properties of the VT-10 and VT-4 alloys was investigated on forged specimens. The hydrogen was introduced at 900°C into specimens preliminarily annealed in vacuo at the same temperature. After adding the hydrogen the specimens were cooled together within the furnace. The tension tests were carried out about 10 days after the introduction of hydrogen.

The variation in the mechanical properties of the VT-4 alloy under ordinary conditions of testing is in many respects similar to the variation in the mechanical properties of commercial titanium. The ultimate strength, yield point, elongation, and the reduction in area change little over the range of hydrogen concentrations which are encountered in practice, but the impact strength (toughness) of the alloy sharply decreases even at low contents of hydrogen (see Figure 1).

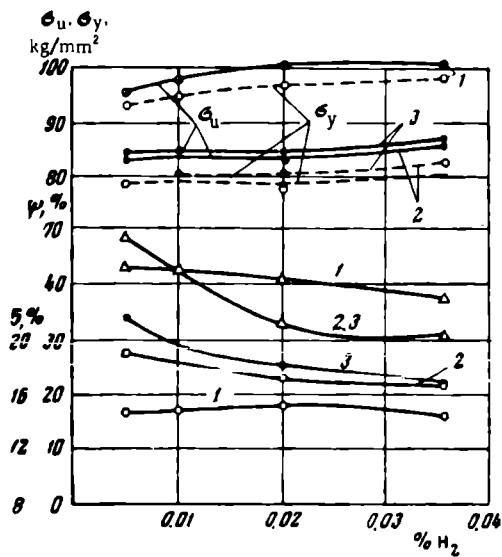


FIGURE 5. The influence of hydrogen on the mechanical properties of the VT-4 alloy during tests carried out at different rates of deformation

1 - 35 mm/min; 2 - 4 mm/min; 3 - 0.1 mm/min.

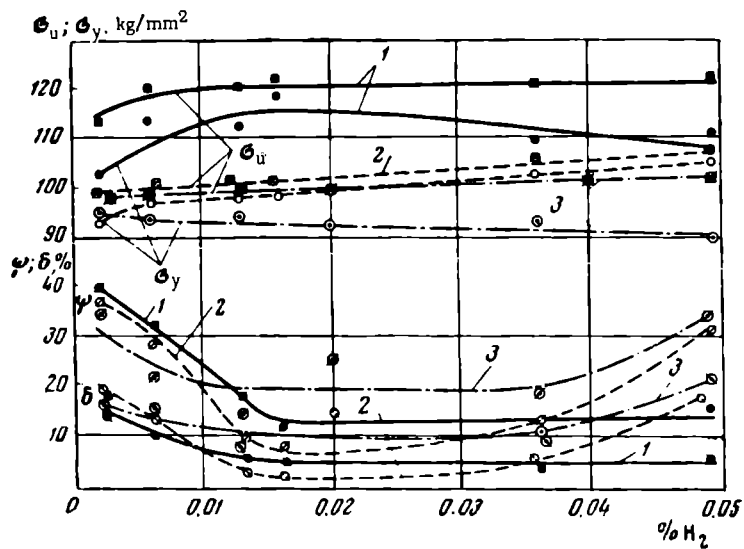


FIGURE 6. The influence of hydrogen on the mechanical properties of the VT-10 alloy during tests carried out at different rates of deformation

1 - 40 mm/min; 2 - 4 mm/min; 3 - 0.1 mm/min .

This marked decrease in the toughness is due to the fact that if the alloy contains more than 0.022 wt. % H_2 , a second phase is precipitated, the amount of which increases with the hydrogen content.

Quite another picture is obtained from tension tests at different rates of deformation (Figure 5). At high rates of deformation, the elongation and the reduction in area depend only to a small degree on the content of hydrogen, while at low rates of deformation they decrease sharply with the increase in the content of hydrogen.

The above relationship between the rate of deformation and the variation of the properties of the alloy with its hydrogen content is characteristic of $\alpha + \beta$ alloys, i. e., in the α phase VT-4 alloy, phenomena are encountered hitherto considered as being characteristic of the hydrogen embrittlement of $\alpha + \beta$ alloys.

The relationship between the mechanical properties of the VT-10 alloy and the hydrogen content is also of a very peculiar nature [4].

The dependence of the mechanical properties of the VT-10 alloy on the hydrogen content at various rates of deformation is shown in Figure 6. These data show that, as distinct from the results obtained in the other alloys investigated, in the case of the VT-10 alloy the reduction in area, ψ , and the elongation δ sharply decrease with the increase of the hydrogen content at all three investigated rates of deformation. However, when the content of hydrogen exceeds 0.035 %, both at low and at medium rates of deformation [but not at the high rate], the reduction in area and the elongation increased once more.

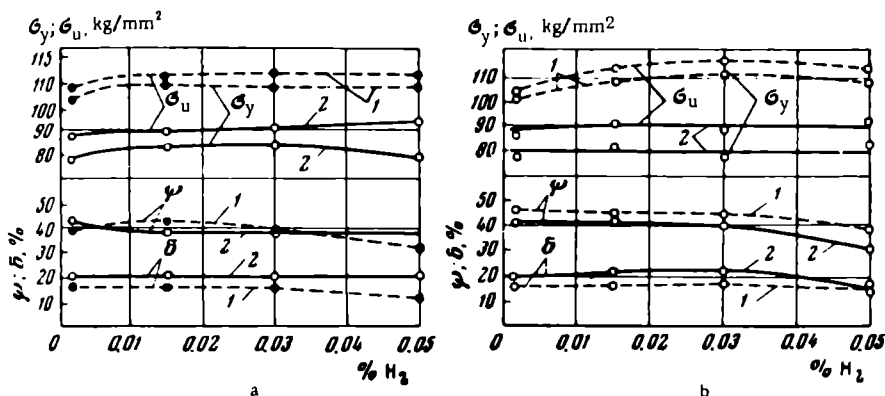


FIGURE 7. The influence of hydrogen on the mechanical properties of the VT-5 alloy during testing at a rate of deformation equal to 40 mm/min (1) and 0.4 mm/min (2)

a — slowly cooled; b — hardened.

In a more detailed investigation of the embrittlement of α alloys at low rates of tension, specimens of VT-5 alloys with different contents of hydrogen were cooled in the air and within the furnace, from a temperature of 600°C. This temperature is considerably below that of the transformation to the two-phase $\alpha + \beta$ field, so that all property changes shown below are due to the different behavior of hydrogen in slowly and rapidly cooled specimens.

The influence of hydrogen on the mechanical properties of air-cooled and quenched VT-5 alloys both at high (40 mm/min) and low (0.4 mm/min) rates of tension is shown in Figure 7. These data show that the VT-5 alloy cooled in the air is more prone to hydrogen embrittlement at high rates of tension than at low rates of tension. This feature is typical of α alloys, which are used mostly after annealing and cooling in the air.

The opposite relationship is found in hardened VT-5 alloys. Here the hydrogen embrittlement is more pronounced during rates of low tension than during rapid, a feature characteristic of $\alpha + \beta$ alloys.

Hydrogen embrittlement was also found in the α phase alloys Ti-4Al-7Cu and Ti-12Sn-7Cu at low rates of deformation /5/.

The brittle failure of α phase VT-4, VT-10, VT-5, Ti-4Al-7Cu, and Ti-12Sn-7Cu alloys taking place in the presence of hydrogen at low rates of deformation, can be explained by the presence of supersaturated solutions in the α phase, and by the precipitation of an independent hydride phase. The formation of supersaturated solutions of hydrogen in these alloys is apparently due to the low rate of diffusion of hydrogen in the presence of alloying elements. The hydrides which precipitate from the solid solution during cooling of the alloys cause brittle failure during rapid deformation, and the supersaturated solutions of hydrogen decompose under a prolonged action of stresses which lead to brittle failure during prolonged [slow] deformation.

The hydrogen embrittlement of α phase alloys can also take place at low rates of deformation but this phenomenon is not typical of α phase alloys.

The above-mentioned failure of α phase alloys at low rates of deformation renders a new approach to the explanation of the mechanism of hydrogen embrittlement in $\alpha + \beta$ alloys necessary.

The most popular theory of hydrogen embrittlement of $\alpha + \beta$ alloys which has been developed in great detail by Jaffee, Lenning, and Craighead /6/, is based on the following two assumptions:

a) the embrittlement of $\alpha + \beta$ phase Ti alloys containing relatively low amounts of hydrogen cannot be due to processes taking place only within the β phase, since the β phase alloys are not embrittled even at high concentrations of hydrogen (0.1-0.2 wt. %);

b) the hydrogen embrittlement of $\alpha + \beta$ phase alloys cannot be due to processes which take place only within the α phase; in this case the embrittlement would be increased and not decreased by an increase in the rates of testing.

Hence the above authors arrive at the conclusion that hydrogen embrittlement of $\alpha + \beta$ phase alloys is due to processes taking place at the interface between the α and β phases.

Jaffee, Lenning, and Craighead assume that at low rates of tension, the hydrogen travels in the form of protons toward the interface of the α and β phases and that finally there is a precipitation, or segregation of hydrogen in these planes, leading to a hydrogen embrittlement. The motive force of this reaction is the replacement of hydrogen by the β phase under the influence of the stresses induced by the external load. This force should increase with the decrease in the temperature. At the same time, the ordinary concentration diffusion acts in the opposite direction, tending to equalize the concentration [of hydrogen] within the grains of the α phase. The rate of diffusion increases with the temperature. Therefore, at higher temperatures there should be viscous failure, and at low temperatures brittle failure.

This theory is quite reasonable except that one of its basic assumptions, the absence of hydrogen embrittlement in α phase alloys at low rates of deformation, is not confirmed by the above-mentioned experimental data.

In the studies of Blok et al. and Yakimova /7-9/ another theory of hydrogen embrittlement was proposed. This theory contradicts to a certain degree that of Jaffee et al. and is based on the concept of the redistribution of alloying elements between the α and β phases, which brings both these phases closer to an equilibrium condition. As a result of this redistribution, the β phase is enriched with β phase stabilizers and with hydrogen. On this basis, the above authors believe that hydrogen embrittlement of $\alpha + \beta$ alloys is not due to a diffusion of hydrogen from the β phase to the interface between the α and β phase, giving rise at these planes to a source of brittle failure, but on the contrary, it is due to an enrichment of the β phase with hydrogen and to a subsequent precipitation in this phase of finely dispersed hydride inclusions or intermetallic compounds.

This theory, however, can hardly explain all the experimental observations in connection with the hydrogen embrittlement of $\alpha + \beta$ alloys and in particular, the recovery of the plasticity of $\alpha + \beta$ alloys by aging after removal of the applied stresses. In addition, this alternative theory of the mechanism of the brittle failure of $\alpha + \beta$ alloys in the presence of hydrogen, does not take into account the fact that α phase titanium alloys are also under certain conditions prone to hydrogen embrittlement at low rates of deformation.

It should be pointed out that hydrogen embrittlement of low rates of deformation is characteristic not only of titanium alloys but also of zirconium and steel. The nature of hydrogen embrittlement of titanium alloys is apparently not connected with the specific structure of α or β titanium phases, but with the characteristic behavior of dissolved hydrogen which is the same in a number of metallic systems. Therefore, the question arises whether the theories of hydrogen embrittlement of steel can be applied to the explanation of this phenomenon in titanium.

Among the many theories of the hydrogen embrittlement of steel the most noteworthy, in the opinion of the authors, is the hypothesis of the segregation of hydrogen which takes place in the microvolumes as a result of the directed diffusion of hydrogen during plastic deformation.

If this theory is applied to titanium, then hydrogen should be replaced by α and β phases in the $\alpha + \beta$ alloys under the influence of the stresses which develop during deformation.

As a result of directed (oriented) diffusion along the boundaries of the α and β phases or within their grains, microvolumes are formed which are rich in hydrogen, but which do not upset the homogeneity of the solid solutions. Such microvolumes are formed as a result of the tendency of hydrogen to concentrate around the microdefects and grain boundaries. If the concentration of hydrogen in these microvolumes exceeds a certain limit, microcracks may be formed at these points which will develop further and lead to failure of the metal. If, however, the load is removed before cracks are formed, the thermal diffusion will gradually level out the concentration of hydrogen over the whole volume of the metal and eliminate, at least partially, the concentration of hydrogen about the microdefects. Since the formation of these hydrogen-rich areas necessitates a diffusion

of hydrogen, the hydrogen embrittlement appears only at low rates of tension. Certainly the process is assisted by those imperfections in the crystal structure which are formed during plastic deformation, particularly by vacancies, and also by the nonequilibrium imperfections developing during cooling of alloys from high temperatures. Indeed, the brittle failure of the α phase VT-5 titanium alloy containing hydrogen takes place under conditions of slow deformation only after hardening.

The hydrogen embrittlement of $\alpha + \beta$ alloys, which is due to the directed diffusion of hydrogen in the α and β phases, is apparently assisted by effects connected with the decomposition of the supersaturated solutions in the α phase.

The authors have determined that in alloys of Ti-Mo and of the Ti-Al-V systems hydrogen is easily dissolved at high temperatures both in the α and β phases. If the temperature is decreased, there is a redistribution of hydrogen between the α and β phases as a result of which the content of hydrogen in the β phase of Ti-Mo and Ti-Al-V alloys is considerably increased under equilibrium conditions. This conclusion is in full agreement with the above-mentioned data [7-9], obtained during the phase analysis of VT-3-1 and VT-8 alloys.

At the rates of cooling to room temperature, which are encountered under industrial conditions, nonequilibrium concentrations of hydrogen are fixed in the α and β phases. Since the concentration ratio c_β/c_α in $\alpha + \beta$ alloys is increased with the temperature, the solutions of hydrogen in the α phase are supersaturated. Because of the slow mobility of the atoms during decomposition of the solution at low temperatures, hydrogen will remain in the α phase. Nevertheless, application of a load will promote decomposition of the supersaturated solutions of hydrogen in the α phase.

It is therefore assumed that hydrogen embrittlement of titanium alloys is due to processes which may develop both in the α and in the β phase. Details of the process of hydrogen embrittlement of titanium alloys await thorough investigation of this phenomenon.

Conclusions

1. Hydrogen embrittlement of $\alpha + \beta$ alloys appears at low rates of deformation. The development of hydrogen embrittlement of $\alpha + \beta$ alloys is also promoted by low testing temperatures and by notches.
2. Hydrogen embrittlement of $\alpha + \beta$ alloys appears if the hydrogen content exceeds a certain limit. Thus, for instance, after an ordinary heat treatment the VT-3-1 alloy can be hydrogen embrittled if its hydrogen content exceeds 0.03 % H_2 , i. e., much more than the maximum permitted by technical specifications (0.015 %).
3. The situation is different with regard to hardened VT-3-1 alloys. In this case hydrogen embrittlement takes place even at the lowest investigated concentrations of hydrogen (0.01 %). The decrease in the plasticity of $\alpha + \beta$ alloys is accompanied by a considerable strengthening.
4. The plasticity of the VT-3-1 alloy does not decrease immediately after hardening but during aging at room temperature.

5. At low rates of deformation, the α -Ti alloys VT-4, VT-5, and VT-10 are also prone to a hydrogen embrittlement similar to that of the $\alpha + \beta$ alloys. This phenomenon can be explained by the redistribution of hydrogen under the influence of the stresses applied. A reconsideration of the mechanism of hydrogen embrittlement of $\alpha + \beta$ alloys is thus necessary.

6. The assumption has been made that hydrogen embrittlement of $\alpha + \beta$ alloys is caused by processes which develop both in the β and in the α phase, for instance by diffusion of hydrogen toward the microdefects or to the grain boundaries, accompanied by a formation of hydrogen-rich microvolumes. If the concentration of hydrogen exceeds a certain limit these microvolumes cause the development of microcracks which lead to the failure of the metal.

Bibliography

1. Livanov, V. A., A. A. Bukhanova, and B. A. Kolachev. — Trudy MATI, No. 43:100. 1960.
2. Burte, H. M., E. F. Erbin, G. T. Hahn, J. W. Seeger, R. J. Kofila, and D. A. Wruck. — Metal. Progr., Vol. 67(5):115. 1955.
3. Daniels, K. D., K. I. Quigg, and A. K. Troiano. — Trans. Am. Soc. Met., Vol. 60:843. 1959.
4. Livanov, V. A., A. A. Bukhanova, and B. A. Kolachev. — Trudy MATI, No. 50:52. 1961.
5. Williams, D. N., R. I. Jaffee, and J. Less. — Common Met., Vol. 2(1):42. 1960.
6. Jaffee, R. I., G. A. Lenning, and C. M. Craighead. — J. Metals, Vol. 8(8):923. 1956.
7. Blok, N. I., A. I. Glazova, N. F. Lashko, and A. M. Yakimova. — Izvestiya AN SSSR, OTN, No. 12:96. 1958.
8. Kornilov, I. I., S. G. Glazunov, and A. M. Yakimova. — Fizika metallov i metallovedenie, Vol. 8(3): 370. 1959.
9. Yakimova, A. M. — Sbornik "Titan i ego splavy", Izdatel'stvo AN SSSR, No. 3:29. 1960.

SOLDERING AND BRAZING OF AT-3 TITANIUM ALLOYS COATED WITH DIFFERENT ELECTRODEPOSITS

A. Ya. Shinyaev and V. V. Bondarev

The AT-3 alloy has better strength and plastic characteristics than other titanium alloys mentioned by Mal'tev et al. and Kornilov et al. /1, 2/.

The use of this metal for constructional purposes in certain cases requires the soldering and brazing with alloys based on copper, iron, nickel, or other metals.

Soldering of titanium alloys is made difficult chiefly by the high tendency of this metal to react with other metals and nonmetals. Therefore, ordinary soldering methods cannot be applied since the solders do not wet the oxidized surface of the titanium alloy. In addition, the reactions of titanium with the components of the solder form easily melting and brittle chemical compounds which greatly decrease the strength of the soldered joint.

In order to avoid oxidation of titanium alloys and their contact with the solder during joining, the surfaces of titanium alloys are coated with easily wettable protective electrodeposits of metals or alloys /3, 4/. Such electrodeposits should have good adhesion to the surface of the titanium alloy. The protective layer must be of a thickness which will exclude any reaction between the titanium and the components of the solder during soldering.

In the present report the authors give the results of an investigation of soldering of AT-3 titanium alloys coated with different protective deposits (silver, rhenium, or rhodium).

Before electroplating, the specimens were degreased in benzine, then pickled in mixtures of acids in order to remove the scale and the alpha layer, brightened, and either pickled in sulfuric acid to obtain a hydride film or [immersed on a solution to produce] a zincate layer.

Each of the above-mentioned metals was plated from different electrolytes. The composition of the electrolyte and the operating conditions of electrolysis were chosen on the basis of standard procedures in such a way as to obtain a sufficiently plastic deposit with a satisfactory adhesion. The plating time was determined by the required thickness of the electrodeposit which should be 15-25 μ . The microscopic investigation of the soldered joints obtained on titanium coated with silver, rhenium, or rhodium has shown that the diffusion zone produced by identical soldering processes is wider on rhodium-coated alloys than on alloys coated with silver or rhenium deposits. This is in full agreement with the characteristics of the rate of diffusion and of self-diffusion which are, at identical temperatures, considerably higher for silver and rhenium than for rhodium. Obviously,

the diffusion of titanium in silver or rhenium will be more rapid than in rhodium, leading to the different widths of the diffusion zones (Figure 1).

The strength of adhesion of the deposits to the titanium alloy was tested by bending and scratching. Rhenium, silver, and rhodium all adhere to quite a satisfactory degree.

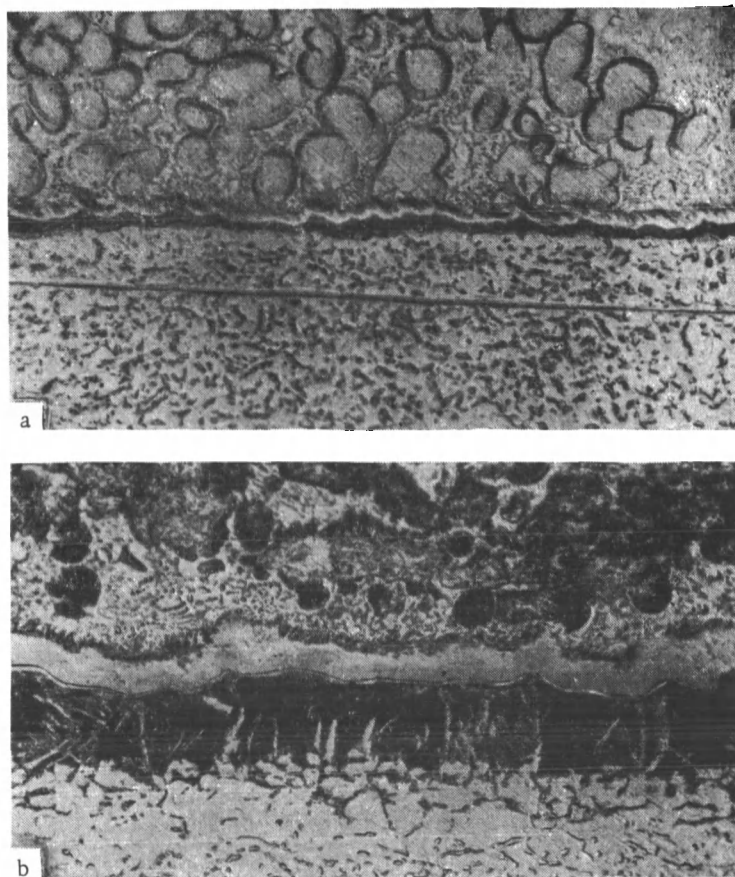


FIGURE 1. Microstructures of soldered titanium coated with rhenium (a) and rhodium (b) deposits. $\times 440$. Soldering temperature $-830-840^{\circ}\text{C}$. Duration of soldering -6 min

The experiments carried out on the soldering with copper-silver solders of AT-3 titanium alloys coated with silver, rhenium, or rhodium have shown that these deposits, if plated to a $15-25\mu$ thickness, effectively protect the titanium from oxidation and from any reaction with the components of the solder during soldering.

The authors showed in one earlier work /5/ that in order to obtain the maximum strength of a soldered joint, the temperature of soldering must be chosen correctly. The temperature of soldering determines the structure

and the phase composition of the diffusion zone, which in the long run determines the strength of the joint. In order to obtain joints with a maximum strength, the diffusion zone should consist of a solid solution of the components of the electrodeposit in titanium with finely dispersed inclusions of separate nuclei of the second phase having a diameter of 1800-2000 Å (electron-microscope investigation at a magnification of 20,000-30,000).

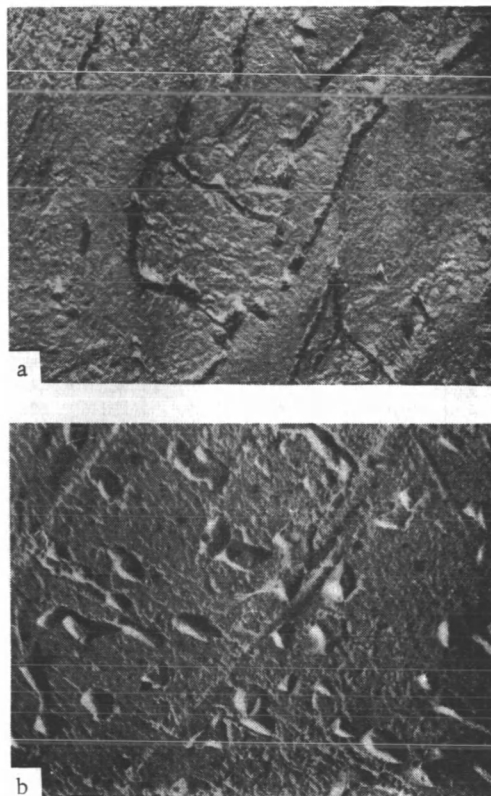


FIGURE 2. Formation of the nuclei of a second phase in the titanium-rhodium diffusion zone produced at a soldering temperature of 780°C (a) and 810°C (b). Electron-microscope photographs $\times 10,000$

Since at identical temperatures the diffusion zones between the titanium and silver, rhenium or rhodium respectively are formed at different rates, it may be expected that the maximum strength of the soldered joints of electroplated titanium will be obtained at different temperatures of welding.

The strength of the joints was determined by tension tests. The results of the determination of the ultimate strength of soldered joints obtained on AT-3 specimens at temperatures from 740 to 870°C (holding time 15 min) are given in the table.

This table shows that on a silver-coated specimen, the strongest joints are obtained at a lower temperature (780-790°C) than on rhenium-coated

(790-800°C) or rhodium-coated specimens (800-810°C). This is in full agreement with the rates of the diffusion mobility of the atoms of these metals.

An electron-microscope investigation has shown that the diffusion zones of all investigated joints of maximum strength consist of a solid solution of the electrodeposits in titanium with separate inclusions of nuclei of the second phase (200 Å large). The typical structures of this zone are shown in Figure 2. The strength of a soldered joint with a structure of this nature in the diffusion zone is determined by the strength of the metal of the electrodeposit, which separates the solder from the diffusion zone.

Strength of soldered joints of AT-3 alloys produced at different temperatures and with different coatings

Soldering temperature, °C	Ultimate strength, kg/mm ²			Soldering temperature, °C	Ultimate strength, kg/mm ²		
	Ag	Rh	Re		Ag	Rh	Re
740	3.7	9.2	—	810	5.6	22.0	17.6
750	4.2	13.7	5.7	820	4.1	20.7	12.5
760	5.6	18.8	7.0	830	3.7	18.3	8.5
770	8.2	21.8	11.1	840	3.1	15.3	4.5
780	10.2	21.0	16.3	850	2.2	12.0	2.4
790	10.1	21.3	18.3	860	1.6	—	1.1
800	7.9	21.1	19.0	870	1.1	—	—

At higher soldering temperatures large nuclei of the second phase and microcracks are formed (Figure 3). At high soldering temperatures, when the rates of the diffusion processes are considerably higher, the nuclei of the new phase grow out and form a large number of microcracks (Figure 4). The mechanical strength is in this case strongly impaired.

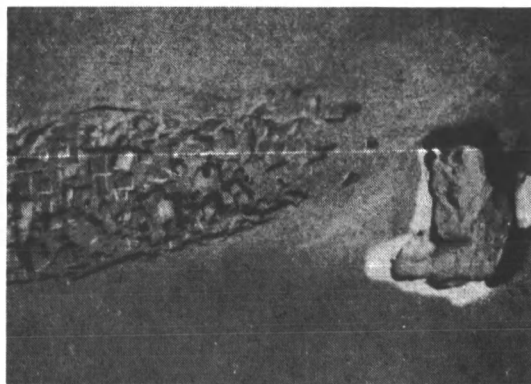


FIGURE 3. Formation of a large amount of nuclei of the second phase in the diffusion zone titanium-rhodium. Soldering temperature 820°C. Electron-microscope photograph, $\times 20,000$

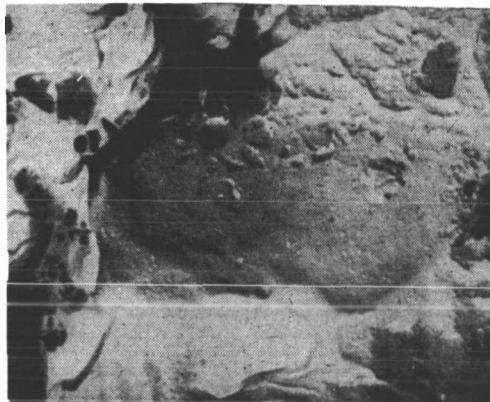


FIGURE 4. Formation of a large number of microcracks in the diffusion zone titanium-rhodium. Soldering temperature 840°C. Electron-microscope photograph $\times 30,000$

For the soldering of titanium, different electrodeposits may be used, having a limited solubility in titanium. The maximum strength of the joint is obtained at that temperature, at which a solid solution with separate nuclei of the second phase (diameter 1800-2000 Å) is formed in the diffusion zone.

Bibliography

1. Mal'tsev, M.V., T.A. Barsukova, and F.A. Borin. Metallografiya tsvetnykh metallov i splavov (Metallography of Nonferrous Metals and Alloys). — Metallurgizdat, p. 250. 1960.
2. Kornilov, I.I., V.S. Mikheev, T.S. Chernova, and K.P. Markovich. — Sbornik "Titan i ego splavy", Izdatel'stvo AN SSSR, No. 7:140. 1962.
3. Lainer, V.I. Gal'vanicheskie pokrytiya legkikh splavov (Electroplating of Light Alloys). — Metallurgizdat. 1959.
4. McQuillan, A.D. and M.K. McQuillan. Titanium. — Metallurgy of Rarer Metals, Vol. 2, New York. 1955. [Russian translation. 1958.]
5. Shinyaev, A.Ya. and V.V. Bondarev. — Trudy Instituta Metallurgii imeni Baikova, No. 12, Izdatel'stvo AN SSSR. 1962.

AT-3, AT-4, AT-6, AND VT-3-1 TITANIUM ALLOYS USED IN THE PRODUCTION OF COMPRESSOR ROTORS (IMPELLERS) OPERATING IN DIFFERENT CORROSIVE MEDIA

N. I. Belan, M. S. Borisova, B. M. Idel'chik, and A. A. Chikurova

The Nevskii Machine-Building Plant has continued its investigations on the use of titanium alloys for the component elements of compressor rotors operating in air and in corrosive media.

AT-3, AT-4, AT-6, and VT-3-1 alloy forgings were investigated (Table 1).

TABLE 1.

Chemical composition, dimensions, and number of investigated forgings of AT-3,
AT-4, AT-6, and VT-3-1 titanium alloys

Alloy	Content, %							Dimensions [of forging], mm		No. of for- gings in- vestigated
	Al	Cr	Mo	Si	Fe	B	ΣCr, Si, Fe	diam.	height	
AT-3	2.8	0.30	—	0.23	0.51	0.01	1.0	430	110	1
AT-4	4.69	0.80	—	0.34	0.26	0.01	1.4	430	95	2
AT-6	5.52	0.71	—	0.64	0.29	0.01	1.8	430	95	1
VT-3-1	5.41	1.9	2.34	0.06	0.16	—	—	480	120	2

Note. Balance titanium.

In the present investigations, external rings with an internal diameter of 300 mm were cut out from the forgings. The height (length) of the rings was equal to that of the forgings.

All mechanical tests were carried out on tangential specimens.

Table 2 shows the mechanical properties of forgings tested after forging and also after a heat treatment (annealing), carried out at the optimum temperature and followed by cooling in the air.

The table shows that the mechanical properties of all investigated alloys, except those of the VT-3-1 alloy which was not investigated in the forged condition, are the same after annealing as in the initial condition (i.e., after forging). The scattering of the magnitudes of the mechanical properties of the AT-6 alloy is apparently due to coring (segregation).

For most titanium alloys the chief heat treatment process is annealing and therefore the authors carried out further experiments only on annealed specimens.

TABLE 2
Mechanical properties of the investigated forgings

Alloy	Condition of material	σ_y , kg/mm ²	σ_u , kg/mm ²	δ , %	ψ , %	a_i , kg·m/cm ²	H_B , kg/mm ²
AT-3	After annealing	58.2	65.8	18.3	28.2	9.4	229
		59.3	67.1	16.0	30.6	10.6	—
	After annealing at 800°C, 1 hr	61.5	70.7	16.4	36.0	9.4	229
		57.3	68.3	18.6	38.0	8.4	—
AT-4	After annealing	82.6	86.6	13.3	28.2	5.6	285
		80.9	85.5	17.3	30.6	5.5	269
		79.2	85.1	13.3	30.6	6.4	—
		79.8	87.2	16.0	30.0	—	—
	After annealing at 850°C, 1 hr	82.3	86.5	14.0	27.9	5.9	285
		79.8	86.9	17.3	30.2	5.1	—
AT-6	After annealing	100.3	104.2	7.9	16.0	5.3	—
		100.3	105.6	9.0	16.0	4.4	—
		97.9	102.8	13.3	24.9	4.5	—
		94.7	99.3	11.7	30.6	5.1	321
	After annealing at 900°C, 1 hr	86.5	91.7	8.3	30.6	5.6	—
		86.5	93.2	10.0	27.8	5.4	—
		94.5	102.3	12.0	19.0	6.0	—
		—	—	—	—	—	—
VT-3—1	After annealing at 870°C, 1 hr	83.7	94.3	12.3	24.9	8.6	362
		93.0	95.3	12.6	24.9	8.2	—
		89.4	94.7	11.7	19.6	9.2	—
		87.5	95.1	12.0	16.3	8.2	—

Since titanium alloys are used chiefly at elevated or below-zero temperatures, short-time tensile tests were carried out at temperatures from +20 to +400 and the impact strength of the alloys determined at temperatures from +20° to -180°C.

The results of these experiments are given in Tables 3 and 4.

An increase in the temperature of short-time tests up to 400°C decreases the strength of the alloys, increases their reduction in area, ψ , but leads to no change in elongation, δ .

The most noticeable reductions in impact strength take place in the AT-4 alloy at -80°C, in the AT-6 alloy at -40°C, and in the VT-3—1 alloy at temperatures below -80°C. But even at -180°C the impact strength of these alloys is 2-3 kg·m/cm².

Since the maximum working temperature for a number of the compressors produced by the Nevskii Plant does not exceed +200°C, the authors checked the influence of high temperatures (200 and 400°C), and of the period during which these temperatures are maintained (up to 10,000 hours) on the mechanical properties of the titanium alloys.

The results so far obtained as regards these properties are given in Table 5.

The data of this table show that maintaining the alloy for 3700 hours at 200°C does not change its mechanical properties.

TABLE 3

Dependence of the mechanical properties of AT-3, AT-4, AT-6, and VT-3-1 alloys on the temperature of short-time tests

Alloy	Testing temperature, °C	σ_y , kg/mm ²	σ_B , kg/mm ²	δ , %	ψ , %
AT-3	20	61.5	70.7	16.4	36.0
		57.3	68.3	18.6	38.6
	300	38.8	46.8	14.2	49.2
		41.7	49.5	14.7	47.4
	400	36.9	46.0	13.7	51.0
		36.9	46.5	13.7	47.4
AT-4	20	82.31	86.5	14.0	27.9
		79.8	86.9	17.3	30.2
	100	65.3	74.6	11.2	30.0
		64.0	73.5	15.0	31.9
	200	56.3	66.9	14.5	36.0
		55.6	67.4	15.5	34.0
	300	43.7	56.7	14.0	41.9
		47.7	60.7	13.7	39.9
	400	46.6	56.3	15.0	41.9
		45.4	56.3	15.5	39.9
AT-6	20	86.5	91.7	8.3	30.6
		86.5	93.2	10.0	27.8
	200	68.6	80.0	11.2	25.6
		72.7	84.7	11.2	27.8
	300	62.7	77.0	11.0	27.8
		65.7	77.0	11.0	25.6
	400	57.8	71.8	11.2	30.0
		57.8	71.8	11.2	34.0
VT-3-1	20	83.7	94.3	12.3	24.9
		93.0	95.3	12.6	24.9
	100	71.5	81.8	10.7	38.0
		68.0	77.7	12.7	34.0
	200	71.6	81.4	11.3	36.0
		63.3	71.7	13.5	38.0
	300	59.3	71.6	14.0	51.0
		55.7	68.2	10.7	45.6
	400	50.3	60.3	9.7	39.9
		47.7	61.7	13.5	43.8

As the holding time of AT-4, AT-6, and VT-3-1 alloys at 400°C increases, their plasticity and impact strength decrease considerably while their strength and hardness are somewhat increased.

TABLE 4

The dependence of impact strength of AT-4, AT-6, and VT-3-1 alloys on the testing temperature, $\text{kg} \cdot \text{m}/\text{cm}^2$

Alloy	Testing temperature, °C				
	+20	-40	-60	-80	-100
AT-4	5.9	4.6	4.9	3.3	1.9
	5.1	4.7	5.2	3.2	2.1
		4.7	4.4	2.8	2.1
AT-6	5.6	2.6	2.5	2.6	2.5
	5.4	3.2	2.6	2.7	2.5
		3.0	2.7	3.1	1.7
VT-3-1	8.6	8.1	7.1	7.0	3.1
	8.2	8.3	6.5	7.4	3.7
	9.2	7.3	6.5	6.9	3.1
	8.2	—	—	—	—

The corrosion resistance of these alloys was tested in the following media: in an atmosphere containing 0.5 % CO_2 and 0.1 % SO_2 (simulating an industrial atmosphere) and with a relative humidity of 100 %, in an aqueous solution saturated with hydrogen sulfide, and in 5- and in 10 %-solutions of hydrochloric acid.

The experiments were carried out at room temperature. The duration of tests was: 750 hours in the "industrial" atmosphere, 720 hours in the aqueous solution saturated with hydrogen sulfide, and 120 hours in the solutions of hydrochloric acid.

It was found that the AT-3, AT-4, and VT-3-1 alloys have a high resistance in the "industrial" atmosphere and in the aqueous solutions saturated with hydrogen sulfide. After the test the surface of the specimens remained bright and there was no loss in weight.

The titanium alloys also showed a high corrosion resistance in the 5 % solution of hydrochloric acid.

The 10 % solution of hydrochloric acid, however, dissolves the oxide film and etches the surfaces of the specimens acquiring, as a result of this dissolution, a pink-violet color.

Table 6 shows that the loss in weight of titanium during our tests in hydrochloric acid was relatively constant.

Since in compressors there is an unavoidable contact between parts made of different materials, general corrosion tests were also carried out of titanium alloys in contact with 40Kh and 1Kh18N9T steels in the "industrial" atmosphere and in contact with Kh17N2 and 1Kh18N9T in the aqueous solution saturated with hydrogen sulfide.

The duration, the temperature, and the conditions of testing remained constant and the ratio of the contacting areas was 1:1.

The results of these tests (Table 7) show that the corrosion resistance of the 40Kh and of the 1Kh18N9T steels in an "industrial" atmosphere is not impaired by the contact with titanium alloys and remains practically unchanged.

TABLE 5

Mechanical properties of AT-3, AT-4, AT-6, and VT-3-1 alloys after testing at 200 and 400°C

Alloy	Heating		σ_y kg/mm ²	σ_u kg/mm ²	δ , %	ψ , %	a_i kg/cm ²	H _B kg/mm ²
	tempera- ture, °C	duration, hours						
AT-3	200	3700	62.3	69.3	9.6	16.0	8.1	—
			60.0	68.7	12.0	22.0	8.5	229
			59.7	69.7	15.6	30.6	—	—
			59.0	68.9	19.3	30.6	—	—
	400	1000	66.0	72.5	14.0	27.8	7.5	229
			62.7	71.8	14.3	30.6	7.9	229
			60.2	69.7	16.0	24.9	7.5	229
			63.2	70.0	12.0	27.8	7.4	229
		5000	63.4	70.4	8.0	13.2	4.8	255
			64.4	70.0	8.7	16.0	5.6	255
			64.3	72.0	13.0	16.0	5.5	229
			64.3	70.8	8.0	12.9	5.3	229
AT-4	200	3700	78.8	89.5	16.0	24.9	5.5	285
			79.5	88.9	14.0	24.9	5.5	—
			80.2	88.3	18.6	30.6	—	—
	400	3000	88.5	97.0	11.6	19.0	3.4	302
			85.6	94.7	9.0	9.8	3.6	—
			88.7	96.8	7.3	6.9	3.0	285
		9500	86.3	94.3	7.3	9.8	2.7	—
			85.9	93.3	6.3	6.7	2.3	302
			84.5	94.3	4.7	6.7	3.0	—
			—	—	—	—	—	—
AT-6	200	3700	95.7	103.0	7.6	24.9	4.8	321
			90.3	97.8	8.3	24.9	4.5	321
			95.5	103.0	13.0	19.0	—	—
			95.8	103.0	12.3	22.0	—	—
	400	1000	97.3	102.6	6.3	9.8	3.8	321
			98.7	104.2	7.0	16.0	3.0	—
			98.2	106.2	4.0	3.1	2.8	321
			104.2	107.7	5.0	6.7	2.7	—
		5000	93.4	101.8	4.3	6.6	2.1	321
			99.3	104.1	5.7	9.8	2.1	—
		9500	100.7	107.2	4.0	3.1	1.8	341
			100.7	107.8	4.3	3.1	2.0	—
VT-3-1	200	3700	95.7	103.0	7.6	24.9	4.8	321
			90.3	97.8	8.3	24.9	4.5	321
			95.5	103.0	13.0	19.0	—	—
			95.8	103.0	12.3	22.0	—	—
	400	1000	88.8	97.0	10.6	22.0	6.7	321
			90.0	96.7	11.3	22.0	6.4	—
			82.3	89.5	10.3	30.6	5.6	321
			95.3	101.5	11.3	16.0	5.1	—
		5000	92.0	102.5	7.3	16.0	4.1	341
			94.0	101.2	9.3	12.9	3.8	—
		9500	100.7	107.2	4.0	3.1	1.8	363
			100.7	107.8	4.3	3.1	2.0	—

The corrosion resistance of the 1Kh18N9T steel in a saturated hydrogen-sulfide solution is also not impaired by the contact with titanium alloys. The small pitting corrosion, accompanied by no loss in weight, was also noted in the Kh17N2 steel after testing in the same medium separately or in contact with titanium alloys.

TABLE 6

Loss in weight of titanium alloys in hydrochloric-acid solutions, $\text{g/m}^2 \cdot \text{hr}$

Alloy	Concentration of HCl, %	
	5	10
AT-3	0.0018	0.45
AT-4	0.0020	0.27
VT-3-1	0.0011	0.26

The susceptibility to stress-corrosion cracking was determined under conditions of simultaneous action of a corrosive medium and tensile stress (60-80 % of the yield point).

The tests were carried out at room temperature on a TsNIITMASn apparatus. The periods of duration of the tests were as follows: 500 hours in an aqueous solution saturated with hydrogen sulfide, 216-1200 hours in a 5- and 10 %-solution of hydrochloric acid, and 1200 hours in a 30 % solution of nitric acid.

The results of the experiment (Table 8) show that for periods of up to 500 hours in a saturated solution of hydrogen sulfide and up to 1200 hours in a 5 % solution of hydrochloric acid, the AT-3, AT-4, and the VT-3-1 alloys are not susceptible to stress-corrosion cracking.

No tendency toward stress-corrosion cracking was found in AT-4 and VT-3-1 alloys after exposure for 1200 hours in a 30 % solution of nitric acid.

No traces of corrosion were found on the surfaces of specimens that did not fail in the tests. In order to check the influence of these tests on the mechanical properties of the alloy, the above-mentioned specimens were given a tension test on the IM-12A machine.

The results obtained by these tests (see Table 8) are practically the same as those obtained for identical specimens, tested without any preliminary action of corrosive media and tensile stresses. The low plasticity of several specimens is not due to the action of the corrosive media but, as has been previously shown, it is the result of the nonuniform mechanical properties in the different sections of the forging.

Stressed AT-3, AT-4, and VT-3-1 alloys tested in a 10 % solution of hydrochloric acid showed a tendency to stress-corrosion cracking (see Table 9). Thus, specimens of the AT-3 and of the AT-4 alloys failed after 200-400 hours, while specimens of the VT-3-1 alloys failed after 600-700 hours.

In all cases the 10 % hydrochloric acid solution acquired a pink-violet tint. After testing, the surfaces of all specimens were strongly etched. In addition, a pitting corrosion was found on the AT-3 and AT-4 alloys.

Metallographic investigation showed failures in AT-3 and AT-4 alloys (intercrystalline and intracrystalline).

A consideration of the results of the testing of stressed AT-3, AT-4, and VT-3-1 alloys in aqueous solutions saturated with hydrogen sulfide, leads to the conclusion that these alloys are superior to Kh17N2 stainless steel tested under identical conditions and with different loads (20-90 % of the yield point).

TABLE 7
Corrosion resistance of titanium alloys tested separately or in contact with steel*

Alloy or steel	Medium testing conditions	Loss of weight of steel specimens, g/m ² ·hr			
		in contact with titanium alloys		without contact with titanium alloys	
		1Kh18N9T	Kh17N2	1Kh18N9T	Kh17N2
AT-3 AT-4 VT-3-1 1Kh18N9T	"Industrial" atmosphere, contaminated with 0.1% SO ₂ , 0.5% CO ₂ , relative humidity 100%, room temperature	No loss in weight	— — — —	0.29 0.28 0.21 0.20	No loss in weight small pitting corrosion
AT-3 AT-4 VT-3-1 1Kh18N9T	Aqueous solution saturated with hydrogen sulfide, room temperature	No loss in weight	No loss in weight, small pitting corrosion	— — — —	No loss in weight, small pitting corrosion

* The AT-3, AT-4, and VT-3-1 alloys, whether in contact with steels or not, suffered no loss in weight during experiments in both media.

TABLE 8
Mechanical properties of AT-3, AT-4, and VT-3-1 alloys before and after the [simultaneous] action of the corrosive media and of tensile stress

Alloy	Before the action of the corrosive medium and tensile stresses				Conditions of experiment				After the action of the corrosive medium and applied tensile stress			
	σ_y , kg/mm ²	σ_u , kg/mm ²	δ , %	ψ , %	corrosive medium	tensile stresses, kg/mm ²	duration, hrs	σ_y , kg/mm ²	σ_u , kg/mm ²	δ , %	ψ , %	
AT-3	62.8	67.4	11.7	26.2	Aqueous solution saturated with hydrogen sulfide 5% solution of hydrochloric acid	50.0	500	66.7	69.0	15.0	23.8	
	64.3	68.9	15.7	36.1		50.0	500	74.3	66.0	18.5	27.7	
						50.0	384	62.0	69.1	10.0	27.7	
						50.0	384	64.4	66.7	13.0	31.9	
AT-4					Aqueous solution saturated with hydrogen sulfide 5% solution of hydrochloric acid 30% solution of nitric acid	50.0	816	66.7	69.0	16.0	27.7	
						65.0	500	84.3	86.2	13.3	22.6	
	81.2	85.8	10.0	22.6		65.0	500	84.3	85.7	13.3	26.1	
	85.8	87.3	11.3	19.1		65.0	500	86.8	90.3	9.0	15.4	
VT-3-1					Aqueous solution saturated with hydrogen sulfide 5% solution of hydrochloric acid 30% solution of nitric acid	65.0	1200	76.5	79.7	12.0	30.1	
						50.0	1200	84.2	88.7	15.5	18.8	
						50.0	1200	85.7	90.3	17.5	29.6	
						70.0	500	83.8	95.0	12.3	15.3	
	91.8	93.3	10.0	15.4		70.0	500	84.3	92.0	14.0	26.6	
						70.0	500	93.5	95.5	14.3	19.1	
						70.0	384	91.8	98.0	9.3	7.8	
						70.0	384	93.5	94.4	14.0	22.6	
						70.0	744	83.8	90.3	9.0	19.0	
						70.0	744	84.1	95.7	10.7	29.2	
				55.0	1200	85.7	88.7	11.5	29.6			
				55.0	1200	85.7	90.3	14.5	32.7			

TABLE 9

Results of testing of titanium alloys in a 10% solution of hydrochloric acid under different tensile stresses

Alloy	Tensile stress, kg/mm ²	Time to failure, hrs
AT-3	50.0	300
AT-4	65.0	216
AT-4	65.0	426
VT-3-1	70.0	672
VT-3-1	70.0	575

TABLE 10

Time to failure of titanium alloys, into which hydrogen had been introduced by electrolysis while under the action of tensile stresses

Alloy	Tensile stress, kg/mm ²	Time to failure, hrs
AT-3	40.0	39
AT-3	40.0	50
AT-4	50.0	24
AT-4	50.0	21
VT-3-1	55.0	30
VT-3-1	55.0	26

Under all stresses, except 20 % of the yield point, forged Kh17N2 steel quenched in oil after heating to 960-980°C and annealed for 3 hours at 360-680°C with subsequent cooling in the air showed a tendency to stress-corrosion cracking in the given corrosive medium:

Stresses, % of σ_y	Time to failure, hrs
90	50
80	480
60	500
40	576
20	did not fail after 1000 hrs

Since during the service life of compressors in certain corrosive media atomic hydrogen may possibly evolve as a result of chemical reactions, a determination was made of the influence of this factor on the AT-3, AT-4, and VT-3-1 alloys.

Hydrogen was introduced into titanium alloys in a solution consisting of 0.1 NH_4SO_4 + 30 mg/l $\text{Na}_2\text{As}_2\text{O}_3$ at a current density of 0.09 amp/cm². At the same time the specimens were subjected to the action of tensile stresses (60 % of the yield point).

During the experiment the temperature of the electrolyte rose to +45°C and therefore it was changed every 4 hours.

Under these testing conditions the specimens failed after 20-50 hours (Table 10).

All specimens showed brittle failure.

In order to check the influence of atomic hydrogen on unstressed titanium alloys, specimens of the same type made of VT-3-1 alloys were subjected to the influence of hydrogen in the given electrolyte for 35 hours without being subjected to stress. The mechanical tests of these specimens carried out after the hydrogen had been introduced showed a sharp

decrease in the strength characteristics ($\sigma_u = 41.3 - 47.7 \text{ kg/mm}^2$) and in the plasticity ($\delta = 1.3 - 2.0 \%$).

Conclusions

1. Heat treatment (annealing according to the optimum conditions) of AT-3, AT-4, and AT-6 alloys has practically no influence on their mechanical properties.

2. With decrease in the temperature of the short-time tension tests (up to $+400^\circ\text{C}$) of the AT-3, AT-4, AT-6, and VT-3-1 alloys, their plasticity increases.

3. As the temperature of the tests is decreased from $+20$ to -180°C the impact strength decreases most noticeably in the AT-4 alloy at -80°C , in the AT-6 alloy at -40°C , and in the VT-3-1 alloy at temperatures below -80°C . At the lowest temperatures, however (up to -180°C), the impact strength of the alloy is not less than $2 \text{ kg}\cdot\text{m/cm}^2$.

4. Heating of AT-3, AT-4, AT-6, and VT-3-1 alloys to 200°C for 3700 hours does not change their mechanical properties.

If the duration of the heating is increased to 9500 hours (400°C) the plasticity and impact strength of the AT-4, AT-6, and VT-3-1 alloys decrease considerably while their hardness and strength characteristics increase to some extent.

5. At room temperature the AT-3, AT-4, and VT-3-1 alloys have a high corrosion resistance to aqueous solutions saturated with hydrogen sulfide, to 5 % solutions of hydrochloric acid, and also to "industrial" atmospheres containing 0.1 % SO_2 and 0.5 % CO_2 and with a relative humidity of 100 %.

The corrosion resistance of 1Kh18N9T and Kh17N2 steels in an aqueous solution saturated with hydrogen sulfide and of 40Kh and 1Kh18N9T steels in an "industrial" atmosphere, is practically not decreased by contact with these Ti alloys.

6. At room temperature the corrosion resistance of AT-3, AT-4, and VT-3-1 alloys in a 10 % solution of hydrochloric acid is satisfactory.

7. The AT-3, AT-4, and VT-3-1 alloys showed no tendency to corrosion cracking at room temperature under conditions of a simultaneous action of tensile stress (80 % of the yield point) and the following corrosive media:

a) during 500 hours of testing in an aqueous solution saturated with hydrogen sulfide;

b) up to 1200 hours of testing in a 5 % solution of hydrochloric acid.

8. The AT-4 and VT-3-1 alloys showed no tendency to stress-corrosion cracking during a 1200 hour long exposure at room temperature to 30 % solution of nitric acid under the simultaneous action of tensile stresses (60 % of the yield point).

9. The AT-3, AT-4, and VT-3-1 alloys show a tendency to stress-corrosion cracking under conditions of simultaneous action of tensile stresses (80 % of the yield point) and a 10 % solution of hydrochloric acid.

10. The AT-3, AT-4, and VT-3-1 alloys absorb atomic hydrogen under conditions of electrolysis at $+45^\circ\text{C}$.

The action of tensile stresses (60 % of the yield point) during absorption of hydrogen leads to brittle failure after a short time (20-50 hours) of testing.

HEATING AND COOLING OF SPECIMENS OF TITANIUM AND ITS ALLOYS

D. V. Budrin, E. L. Sukhanov, and V. I. Shilov

This study was carried out in connection with the investigation of annealing and hot working of articles made of titanium and of its alloys. The experiments were carried out on specimens of commercially pure titanium, VT-1D, of the IMP-3, AT-4, and AT-8* titanium alloys, and also of 45 steel (comparison specimens).

All investigated specimens had the shape of an Archimedes cylinder (height equal to diameter) with $R = 19$ mm radius. The terminals of two standard chromel-alumel thermocouples with 0.5 mm diameter wires (Figure 1) were attached to the geometric center of the specimen (point C) and at a distance of $0.9R$ from the center (point D). All thermocouples were prepared from the same coils of chromel and alumel wire. Only those thermocouples were used, the calibration of which corresponded to GOST 6116-53.

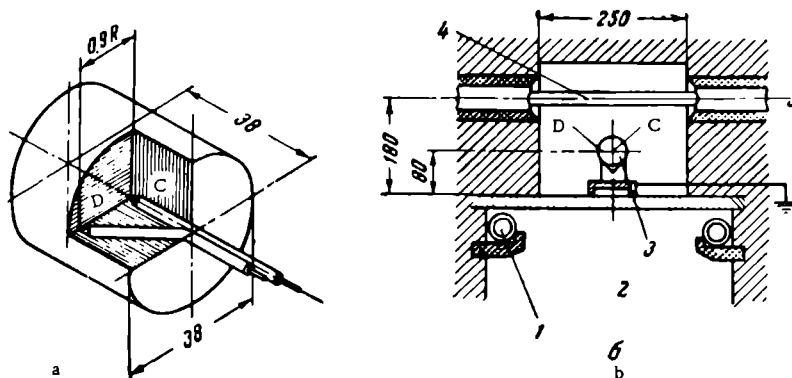


FIGURE 1. Connection of thermocouples to the Archimedes-cylinder specimen (a) and the position of the heated specimen in the upper chamber of an electric furnace (b)

1 — metallic heaters [resistors] (6 units); 2 — lower chamber of the furnace; 3 — specimen; 4 — silite [soviet ceramics] (3 units).

To provide reliable thermal contact, the tips of the thermocouples were pressed against the specimen by wedge clamps made of the same material

* The specimens of the AT-4 and AT-8 titanium alloys were prepared by I. I. Kornilov and V. S. Mikheev (of the Alloy Chemistry Laboratory of the Institute of Metallurgy im. A. A. Baikov).

as the specimens. The wires of the thermocouples were placed in two-channel porcelain tubes with a 3.5 mm external diameter. The electrodes of the thermocouples were extended out of the furnace by compensation wires.

The temperature at points C and D of the specimen being investigated was measured and recorded by an EPP-09 3-point automatic electronic potentiometer. The slide traveled the whole scale during 8 sec. The paper moved at a rate of 1400 mm/hr. The recording cycle lasted 5 sec. Before measurements commenced, the potentiometer was thoroughly calibrated against standard (reference) chromel-alumel thermocouples.

The specimens were heated in the upper chamber of an OKB-194 18.75 kw electric-resistance furnace produced by the "Elektropech" Plant. The supply voltage across the silit heaters had been chosen so that it was possible to keep the temperature in the upper chamber of the furnace constant at about 1100°C without resorting to the two-position automatic temperature regulators attached to the furnace. The use of the automatic position type regulator was impracticable since this caused considerable variations in the temperature of the specimens toward the end of the heating process. In order to eliminate the influence of the surface condition of the specimen on the heat exchange, all specimens were cleaned to a uniform light-gray dull color with sandpaper before each experiment.

Before the experiments, the cold specimens with the attached thermocouples were placed on a titanium support (in order to avoid possible reaction of the specimens with the material of the furnace at high temperatures). The specimens were introduced at the same time into the well-heated furnace (1100°C). All specimens were located in the same way (Figure 1).

Because of the electric conductivity of the refractory materials at high temperatures, the specimen was subjected to a high voltage (90 V as related to the potential of the ground). The effect of this on the accuracy of the measurements was eliminated by earthing the support of the specimens. In order to eliminate induced currents in the wires of the thermocouples resulting from the alternating electromagnetic fields produced by the spiral wire heaters in the lower chamber of the furnace, the current supply to these heaters was cut off during the measurements.

The specimens were heated until the temperatures t_c and t_b at the points C and D were leveled and reached a constant magnitude equal to that of the furnace. This temperature of the furnace was chosen as the constant temperature of the environment t_e , which is a necessary element in all calculations of the relationships involved in the thermal process [1]. After a short holding period for control purposes, the specimen together with its support was taken out of the furnace and cooled in the air in a horizontal position. The measurements and the recordings of the temperature of the specimens were started 1 min before commencement of the experiment [i. e., the heating process] and were concluded when the temperature of the specimen decreased to 600-500°C. The next specimen was placed on the cold support and the experiment was repeated.

The heating and cooling curves for the investigated specimens, obtained by connecting the separate reading points are shown in Figure 2. In order not to obscure the diagram, the curves representing the temperature changes at point D are shown (as dotted lines) only for 45 steel and for AT-8 titanium alloy specimens.

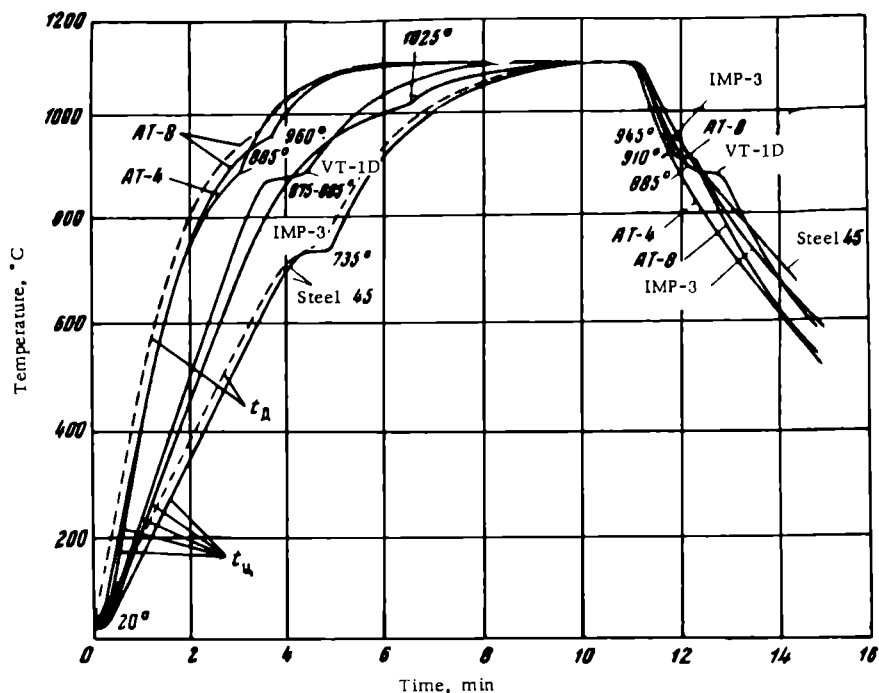


FIGURE 2. Experimental cooling and heating curves for test specimens

From these curves the time and the rate of heating and of cooling of the investigated alloy can be evaluated, as well as the influence of the phase transformations on these processes. The points obtained for the phase transformations are given in Figure 2. The differences between the heating and cooling transformation temperatures obtained for AT-8 and IMP-3 alloys are due to the physical properties of these alloys and also to the fact that the cooling was more rapid than the heating.

The experiments showed that to heat the center of the specimens of AT-4 and AT-8 alloys to 1000°C requires about half the time necessary to heat the center of the steel specimens. The duration and the rate of heating of the VT-1D and IMP-3 sintered titanium alloys are similar and lie between those for steel specimens and those for AT-4 and AT-8 specimens.

These relationships also hold for cooling. At temperatures below 700°C, the cooling curves for VT-1D and IMP-3 titanium alloys lie between those of the steel specimens and those of the AT-4 and AT-8 titanium specimens.

The data obtained show that technological processes for hot working of titanium and its alloys should be more rapid than those for the hot working of steel.

The thermophysical properties of the investigated alloys were studied by the method for regular thermal processes, developed in the UPI department of metallurgical furnaces [2].

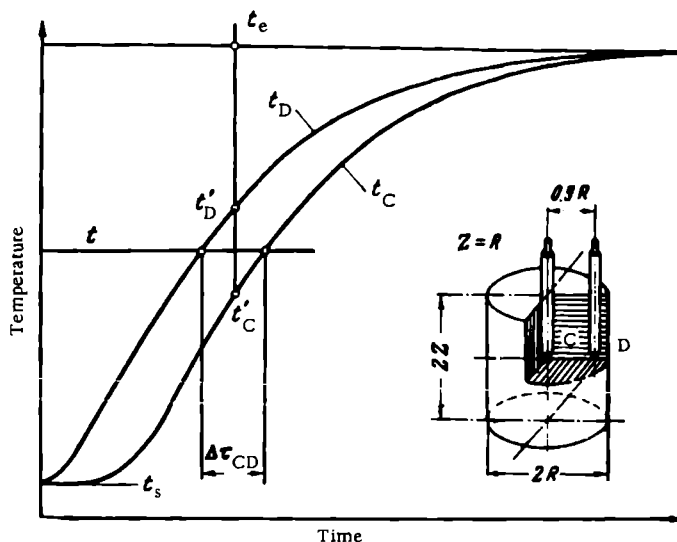


FIGURE 3. Determination of the time lag $\Delta\tau_{CD}$ and of the average temperatures t'_D and t'_C from the heating curves for the investigated specimen

The process of heating and cooling of Archimedes-cylinder specimens in a medium with a constant temperature t_e is represented, except at the beginning and during the phase transformations, by the formula

$$\theta_i = \frac{t_e - t_i}{t_e - t_s} = U_i \cdot \exp\left(-\rho^2 \frac{a\tau}{R^2}\right), \quad (1)$$

where t_i = temperature at any point i within the specimen;

θ_i = the temperature criterion of the point i ;

t_s = initial temperature of the specimen;

U_i = coefficient depending on the relative coordinates of the point i and on the Biot criterion Bi ;

ρ^2 = criterion of the rates of heating and cooling of the Archimedes-cylinder specimen which depends on the Biot criterion Bi ;

R = radius of specimen;

τ = time from the beginning of the heating or cooling of the specimen.

This formula shows that the time to bring any point i within the specimen to a given temperature t is expressed by

$$\tau_i = \frac{R^2}{a} \cdot \frac{1}{\rho^2} \cdot \ln \frac{U_i}{\theta_i}. \quad (2)$$

During heating or cooling of the specimens the central point C attains the given temperature t , somewhat later than the point D (Figure 3). The time lag $\Delta\tau_{CD}$ for the points C and D in the specimen to reach the same temperature is determined by the formula

$$\Delta\tau_{CD} = \frac{R^2}{a} \cdot \frac{1}{\rho^2} \cdot \ln \frac{U_C}{U_D}. \quad (3)$$

This formula shows that the time lag depends on the dimensions of the specimens, on the coordinates of the points in question, on the Biot

criterion Bi and on the coefficient of thermal diffusivity a . After solving the equation (3) with respect to a , the following is obtained

$$a_t = \frac{R^2}{\Delta\tau_{CD}} \cdot K_{CD}, \quad (4)$$

where a_t = the coefficient of thermal diffusivity of the material at a temperature t , m^2/hr ;

R = radius of the specimen, m ;

$\Delta\tau_{CD}$ = the time lag for reaching a given temperature at the points C and D of the specimen, hrs ;

K_{CD} = the dimensionless coefficient, which depends on the criterion Bi and which is determined by the formula

$$K_{CD} = \frac{1}{\rho^2} \cdot \ln \frac{U_C}{U}.$$

The magnitude of the criterion Bi and consequently, the coefficient K_{CD} can be calculated from the criterion of the nonuniformity of the temperature distribution in the specimen Ψ_{CD} , which is found experimentally:

$$\Psi_{CD} = \frac{t_e - t'_C}{t_e - t'_D}, \quad (5)$$

where t'_C and t'_D are the temperatures at points C and D of the specimen in the middle of the heating or cooling curves for the temperature range in question (Figure 3).

The linear relationship between Ψ_{CD} and K_{CD} for Archimedes-cylinder specimens is given in Figure 4.

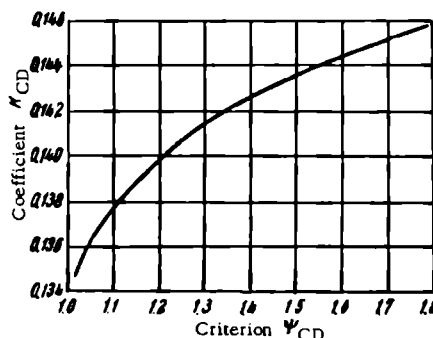


FIGURE 4. Dependence $K_{CD} = f(\Psi_{CD})$ for Archimedes-cylinder specimens

The coefficient of thermal conductivity λ_t of the specimens being investigated can be found if the specific heat and the density of the material are known. The coefficient λ_t is found from the formula

$$\lambda_t = a_t c_t \cdot \gamma_{20} \quad \text{kcal/m} \cdot \text{hr} \cdot ^\circ\text{C}, \quad (6)$$

where a_t = real specific heat of the material of the specimen at a temperature t , $\text{kcal/kg} \cdot ^\circ\text{C}$;

γ_{20} = specific gravity of the material of the specimen at 20°C , kg/m^3 .

The density (specific gravity) of the material of the specimen can easily be found by one of the well-known methods. The specific heat of the specimen can be found in the literature, since this magnitude does not differ much for alloys with similar chemical compositions.

By this method, the thermophysical properties of specimens can be determined over a wide temperature range on the basis of a single experiment involving heating or cooling of the specimen. The method, however, does not suffice for the analysis of the initial stage of the heating or cooling process and for the range of phase transformations (the fields of irregular thermal processes require a more complicated mathematical analysis).

The determination of the coefficients of heat conductivity and thermal diffusivity of the 45 steel and of the VT-1D titanium alloy are taken as examples. The properties of these materials have been investigated by other scientists [3, 4].

The heating of a steel specimen with a radius $R = 19$ mm shows that at 600°C the time lag $\Delta\tau_{\text{CD}} = 7.5$ sec. In the middle of this temperature range $t_e = 1100^{\circ}\text{C}$, $t_D = 610^{\circ}\text{C}$, and $t_C = 590^{\circ}\text{C}$. On the basis of these data, the criterion Ψ_{CD} is first calculated from the formula (5)

$$\Psi_{\text{CD}} = \frac{1100 - 610}{1100 - 590} = 1.04.$$

From the graph (Figure 4) it is found that at $\Psi_{\text{CD}} = 1.04$, the coefficient $K_{\text{CD}} = 0.136$. The required coefficient of thermal diffusivity of steel α_{600} is found from formula (4)

$$\alpha_{600} = \frac{19^2 \cdot 10^6 \cdot 0.136 \cdot 3600}{7.5} = 0.0236 \text{ m}^2/\text{hr}.$$

The coefficient of heat conductivity of steel, λ_{600} , is calculated from the experimentally found density $\gamma_{20} = 7860 \text{ kg/m}^3$ and from the specific heat of 45 steel published in the handbook of Vargaftik [3] $c_{600} = 0.175 \text{ kcal/kg} \cdot ^{\circ}\text{C}$: $\lambda_{600} = 0.0236 \cdot 0.175 \cdot 7860 = 32.4 \text{ kcal/m} \cdot \text{hr} \cdot ^{\circ}\text{C}$.

The values of α_{600} and λ_{600} for 45 steel are in good agreement with the published data.

From the heating curves for the VT-1D titanium alloy the authors have found that at 600°C the time lag $\Delta\tau_{\text{CD}} = 10$ sec, while the average temperatures for this range are $t_e = 1100^{\circ}\text{C}$, $t_D = 625^{\circ}\text{C}$, and $t_C = 576^{\circ}\text{C}$.

From the calculations and from the graph it is found that $\Psi_{\text{CD}} = 1.1$ and $K_{\text{CD}} = 0.138$. From these data the coefficient of thermal diffusivity of titanium is found as follows:

$$\alpha_{600} = \frac{19^2 \cdot 10^6 \cdot 0.138 \cdot 3600}{10} = 0.0179 \text{ m}^2/\text{hr}.$$

From the experimentally found density of titanium $\gamma_{20} = 4500 \text{ kg/m}^3$ and from the specific heat of titanium (found in [3]), $c_{600} = 0.162 \text{ kcal/kg} \cdot ^{\circ}\text{C}$, the coefficient of heat conductivity is calculated:

$$\lambda_{600} = 0.0179 \cdot 0.162 \cdot 4500 = 13.1 \text{ kcal/m} \cdot \text{hr} \cdot ^{\circ}\text{C}.$$

This magnitude of λ_{600} is comparable with the published data [4]. It should be pointed out that the few existing data on the thermal conductivity of titanium at high temperatures are rather conflicting and therefore it is difficult to say anything about the accuracy of the results obtained.

For the AT-4, AT-8, and IMP-3 alloy, only the coefficient of thermal diffusivity has been determined, since no data are available on the specific heat of these alloys at high temperatures.

The determination of the thermophysical properties of the investigated alloys at 600°C furnished the following results:

	Steel 45	AT-4	VT-1D	AT-8	IMP-3
Thermal diffusivity, m^2/hr	0.0236	0.0274	0.0179	0.0150	0.0143
Heat conductivity, $\text{kcal}/\text{m} \cdot \text{hr} \cdot ^\circ\text{C}$	32.4	—	13.1	—	—

The data obtained show the suitability of the new method for the investigation of the thermophysical properties of titanium and its alloys during an ordinary heating process. The accuracy of this method chiefly depends on the exactitude with which the thermocouple ends are embedded in the specimens and on the accuracy of their calibration. To decrease the measurement errors, a large number of thermocouples should be placed in the specimen, with a correspondingly increased number of records on the recording apparatus. In addition, in order to calculate more accurately the coefficients of thermal diffusivity it is necessary to use slightly larger specimens than those described in the present investigation. If thermocouples are also embedded at other points in the specimens, and if specimens of other shapes are used, the coefficient $K = f(\Psi)$ required for the calculation can be found using the coefficients given by Budrin and Sukhanov /5/.

Bibliography

1. Kondrat'ev, G. M. *Regulyarnyi teplovoi rezhim (Regular Thermal Processes)*. — GITTL. 1954.
2. Yaroshenko, Yu. G. and D. V. Budrin. — *Trudy UPI, Metallurgizdat*, No. 53:141. 1955.
3. Vargaftik, N. B. (editor). *Teplofizicheskie svoystva veshchestv (Thermophysical Properties of Substances). Handbook*. — Gosenergoizdat. 1956.
4. Kuprovskii, B. B. and P. V. Gel'd. — *Trudy UPI, Metallurgizdat*, No. 114. 1961.
5. Budrin, D. V. and E. L. Sukhanov. — *Inzhenerno-Fizicheskii Zhurnal*, Vol. 11, No. 2. 1959.

OXIDATION OF TITANIUM AND ITS PROTECTION AGAINST GAS CORROSION

D. V. Ignatov

The mechanism of oxidation of titanium in oxygen and in the air at 300-1200°C has been widely investigated /1-9/.

Despite the considerable inconsistencies in published results, the main conclusions to be drawn from these investigations can be summed up as follows:

1. The oxidation of titanium entails both the formation of an oxide film on the surface of the specimen and a dissolution of oxygen in the metal.

2. Up to 300°C, the oxidation can be represented by a logarithmic function, from 300 to 600°C by a cubic function, from 600 to 850°C by a parabolic function, and above 850°C by both parabolic and linear functions. Depending on the duration of the oxidation, these functions can interchange from logarithmic to cubic, from cubic to parabolic, etc. At higher temperatures, the duration of the process as represented by a single function becomes shorter.

3. The chief product formed in the scale, over the whole range from 500 to 1000°C, is rutile, though in some cases TiO has also been found on the metal-scale interface. In scale formed at temperatures above 1100°C, V. I. Arkharov and G. P. Luchkin have determined three phases: TiO (on the metal-scale interface), Ti_2O_3 (on the exterior surface of the TiO), and TiO_2 (on the scale-gas interface) /1/.

Taking into account the intensive dissolution of oxygen in titanium and using tracers for the investigation of the scale growth, most investigators have arrived at the conclusion that up to 900°C the oxidation of titanium proceeds chiefly as a result of the diffusion of oxygen into the metal and that it takes place at the metal-scale interface. Above 900°C, oxidation is a result of the diffusion of both titanium and oxygen but as the temperature is increased to 1200°C the role of titanium diffusion in the scale growth increases. This conclusion was arrived at on the basis of X-ray analysis /1/ which showed the predominance of a particular orientation of the rutile crystals in the external layer of the scale formed on titanium during oxidation in the air at 900-1200°C. A [definite] texture in the surface layer of the scale was found by D. I. Lainer and M. I. Tsypin by electronographic analysis of titanium specimens oxidized in vapor at 650 and 850°C and in the air at 850°C. The latter authors, taking into account their own data on the texture of the scale and those of Arkharov and Luchkin /1/ on the oxidation of titanium at 900-1200°C, are of the opinion that at temperatures higher than 600°C the scale grows at the scale-gas interface and that the main step in the oxidation process is the "diffusion of titanium ions through the previously formed rutile layer" /8/.

On the basis of structural investigations of the scale and of the position of neutral tracers, other investigators [3, 6] arrived at the conclusion that the oxidation of titanium is due chiefly to the diffusion of titanium ions.

The investigations of I. I. Kornilov and co-workers (V. S. Mikheev, I. A. Popov, and others) [10-12], are of great importance for the understanding of the mechanism of oxidation of titanium. They have constructed a number of phase diagrams of titanium systems, developed new titanium alloys, and determined their basic mechanical parameters as well as their corrosion resistance in relation to the concentration of alloying elements and to the temperature.

Kornilov et al have shown that additions of aluminum, beryllium, and silicon increase the heat resistance of titanium [10]. I. A. Popov and V. I. Rabezova [12] have developed an alloy on the basis of γ -TiAl containing small amounts of niobium. The corrosion resistance of this alloy at 800-1000°C is about the same as that of an 80% Ni+20% Cr alloy.

A noteworthy investigation of the value of coatings for the protection of titanium against gas corrosion was carried out by P. M. Arzhan [13], who showed that beryllium and aluminum deposits provide satisfactory protection against corrosion.

Despite the large number of fundamental studies on the oxidation of titanium, giving rise to soundly based theories which to a large extent explain the mechanism of oxidation of titanium over a wide range of temperatures, there is still no answer to the following questions: 1) why is the rate of oxidation of titanium and of most of its alloys about 10 times more rapid than that of nickel, chromium, and their alloys, and 2) how can we increase the heat resistance of titanium alloys to the level of that of nickel-chromium alloys.

The chief purpose of the present investigation, the results of which are partially described below, was to obtain data on the mechanism of titanium oxidation and several of its alloys and on the structure of the oxides obtained, with a view to providing an answer to the above questions.

These investigations on the oxidability of titanium and its alloys have been carried out during the last three years under the guidance of Yu. M. Lebedev, R. D. Shangunova, and V. V. Votina (laboratory of crystallochemistry) and in close cooperation with the laboratory of metal chemistry at the Institute of Metallurgy im. A. A. Baikov.

The results of these investigations enabled the authors to arrive at some generalizations on the mechanism of titanium oxidation.

Experimental

The specimens (15 × 10 × 2 mm plates) were prepared from iodide titanium.

The surface of the specimens was cleaned by emery paper and washed with acetone and alcohol. The specimens were then carefully ground, without application of any pressure, on thick glass plates whose surfaces had been prepared with the abrasive used for grinding vacuum valves. After this operation, the specimens were measured, washed again with acid and alcohol, weighed, and placed in corundum crucibles which had been fired to a constant weight at 1200°C. The specimens were oxidized in the air in an ordinary electric muffle furnace.

The weight increase of the specimens due to the absorption of oxygen was determined for specific periods by periodical weighing on a balance with a sensitivity of $2 \cdot 10^{-5}$ g.

The kinetics of oxidation in pure and dry oxygen under a pressure equal to 100 mm Hg was investigated using a vacuum rotary microbalance with a sensitivity of $10^{-7} - 10^{-6}$ g/15/. The specimens ($2 \times 5 \times 0.05$ cm) for the oxidation on these balances were prepared from sheets obtained by cold rolling of rods of iodide titanium. The surfaces of the specimens were treated as described above.

The phase composition of the scale was determined chiefly by the electronographic method and partially by the X-ray method.

Some of the specimens were coated with aluminum or with a nickel-aluminum alloy. In order to coat a specimen with aluminum, it is wrapped in aluminum foil ($50-70\mu$) and heated in vacuo (10^{-4} mm Hg) at $800-900^{\circ}\text{C}$ for 1-2 hours.

The nickel-aluminum coating was produced by two consecutive operations. The specimens were first electrolytically coated with nickel, and then with aluminum by the above method. The diffusion annealing was carried out in the same way as with the uncoated specimens. The specimens, coated with aluminum or with nickel-aluminum were oxidized by heating in the air.

Results and discussion

Figure 1 shows the temperature dependence of the average rates of oxidation in oxygen and in the air for iodide titanium, and Ti-Mo, Ti-V, and AT-8 alloys.

In Figure 2 the curves represent the temperature dependence of the average rates of oxidation for two nickel-chromium alloys, for a γ -TiAl alloy with an addition of niobium, and for an AT-4 alloy coated with nickel and aluminum.

An analysis of the curves given in Figure 1 shows the following:

1) at $600-700^{\circ}\text{C}$, the titanium specimens are oxidized in oxygen much more rapidly than in the air; the rate of oxidation begins to increase considerably at 720°C ;

2) the titanium alloy with 15% V begins to oxidize intensively at 550°C . The rate of oxidation of this alloy considerably exceeds that of titanium;

3) the rate of oxidation of titanium alloys with 15% Mo begins to increase rapidly at 650°C . This rate increases even more at 760°C and begins to drop from 800°C ;

4) the rate of oxidation of the AT-8 alloy begins to increase at 800°C but is somewhat lower than the rate of oxidation of pure titanium.

A comparison of the temperatures at which the rates of oxidation begin to accelerate with the temperature of the $\alpha \rightleftharpoons \beta$ transformation of these alloys and of pure titanium shows that the ratio of these values is (except for the titanium-vanadium alloy) approximately equal to 0.8. Thus, the rates of oxidation of titanium and of its alloys containing additions stabilizing the α or β phases begin to accelerate at temperatures which are about 0.8 of the temperature of the $\alpha \rightleftharpoons \beta$ transformation and this acceleration considerably increases over the temperature range of the phase transformations.

Kofstad et al [7] explain the acceleration of the rate of oxidation of titanium at 850-1000°C by the fact that oxygen diffuses into β -Ti at a higher rate than into α -Ti. But since oxygen stabilizes α -Ti (as a result of which the external layer of the specimen will consist of α -Ti during the whole period of oxidation), the possibility of any considerable influence of the $\alpha \rightleftharpoons \beta$ transformation on the rate of oxidation of titanium was discarded.

However, the latter authors have not taken into account the fact that when the α -Ti layer is saturated with oxygen, the gas diffuses into the adjacent layers of metal. If the α -Ti layer is in contact with β -Ti, the diffusion of oxygen into β -titanium will be more rapid than into α -Ti. In the opinion of the present authors, the accelerated oxidation of titanium over the above-mentioned range of temperatures can be explained as follows.

Over the ranges of temperatures of the $\alpha \rightleftharpoons \beta$ transformation the crystal lattice of the alloy becomes less compact and the interatomic bonds are weakened, which leads to an increase in the mobility of the atoms, and as a result, to an increase in the solubility of oxygen in titanium and to an acceleration of the rate of oxidation.

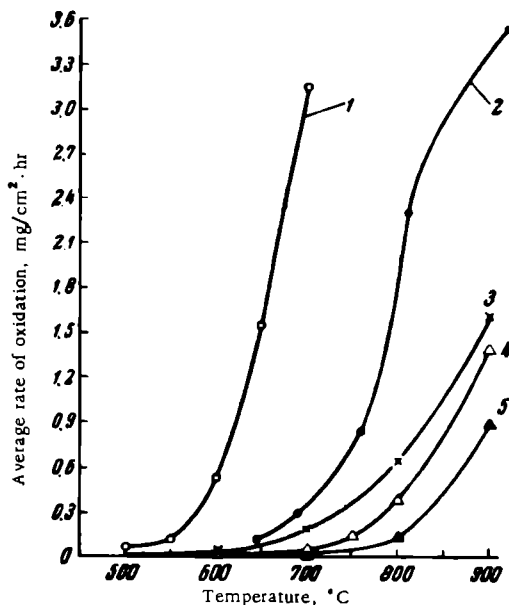


FIGURE 1. Temperature dependence of the average rate of oxidation of titanium and its alloys

1 — Ti + 15% V alloy; 2 — Ti + 15% Mo alloy (the curve for this alloy was constructed according to the data taken from [14]); 3 — iodide titanium (oxidized in oxygen under a pressure of 100 mm Hg); 4 — iodide titanium (oxidized in the air); 5 — AT-8 alloy.

The increased rate of oxidation of the Ti + 15% V alloy at temperatures above 650°C is due to the formation of large amounts of liquid V_2O_5 in the

scale. On the other hand, the apparently lower rate of oxidation of the Ti + 15% Mo alloy at temperatures above 800°C is due to MoO₃ which forms in the scale, melts at 792°C, and evaporates rapidly. The somewhat lower rate of oxidation of the AT-8 alloy compared with that of pure titanium is due to the following causes:

- 1) an increase in the temperature of the $\alpha \rightleftharpoons \beta$ transformation [11];
- 2) the decrease in the solubility in titanium of the scale which chiefly consists of TiO₂ and of γ -Al₂O₃.

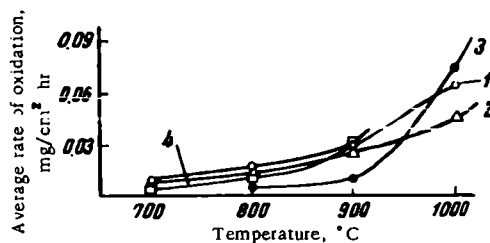


FIGURE 2. Temperature dependence of the average rate of oxidation of different alloys

1 — 80% Ni + 20% Cr; 2 — 75% Ni + 20% Cr + 5% Ti;
3 — γ -TiAl + Nb; 4 — AT-4, coated with nickel and aluminum.

In addition, aluminum strengthens the bonds in the titanium crystal lattice, decreases its parameters and thus inhibits the penetration of oxygen. The dissolution of oxygen in titanium is particularly inhibited by the formation of intermetallic compounds in the solid solution of the Ti-Al system. The heat resistance of specimens containing TiAl can apparently be explained chiefly by the fact that the solubility of oxygen in this compound and the destruction of the oxide film as a result of its dissolution are inconsiderable, though, as has been determined by X-ray electronographic analysis, the scale consists in this case too of rutile and γ -Al₂O₃.

Though the γ -Al₂O₃ oxide forms no solid solutions or intermetallic compounds with TiO₂ from 600 to 1200°C (the author has proved this by an electronographic analysis of the TiO₂ + γ -Al₂O₃ system using thin film specimens), nevertheless the presence of γ -Al₂O₃ in the scale decreases the stresses on the metal-scale interface and thus reduces the peeling off of the oxide film from the metal.

On the other hand, the formation of V₂O₅ and MoO₃ oxides which, like γ -Al₂O₃ form no solid solutions or compounds with TiO₂, will, because of their large volume, increase the stresses on the metal-scale interface and thus promote the peeling-off of the scale. Small additions of vanadium and molybdenum (when no V₂O₅ and MoO₃ are formed as separate phases in the scale) will decrease the solubility of oxygen in titanium because of the strengthening of the bonds in the β -Ti lattice, provided that the α -Ti phase is also alloyed, for instance, with aluminum.

An analysis of the experimental data shows that the allotropic $\alpha \rightleftharpoons \beta$ transformations in titanium and in its alloys constitute one of the basic

factors resulting in accelerated oxidation of titanium and its alloys at 700-900°C.

The curves in Figure 2 show first of all that the average rates of oxidation of γ -TiAl alloys containing niobium are over the temperatures of from 800 to 1000°C close to the average rates of oxidation of nickel-chromium alloys (at 800 and 900°C the rates of oxidation of the γ -TiAl alloy are even lower by a factor of 2-3). The rate of oxidation of the AT-4 alloy at 700-900°C differs little from the rates of oxidation of nickel chromium alloys.

It has already been shown [16], that the scale formed at 800-1000°C on 80% Ni + 20% Cr alloys consists chiefly of α -Cr₂O₃ at the alloy-scale interface and of NiCr₂O₄ at the scale-gas interface. The scale formed at 800-1000°C on 75% Ni + 20% Cr + 5% Ti specimens consists chiefly of rutile (TiO₂).

According to the electronographic and X-ray investigations of the author, the scale on γ -TiAl + Nb alloys consists chiefly of rutile and small amounts of γ -Al₂O₃. The γ -Al₂O₃ compound is formed in the internal layers of the scale and not in the external surface layers. The scale on specimens coated with nickel and aluminum consisted, after heating at 800 and 900°C for 50 and 30 hours (according to the data of the electronographic investigations), chiefly of γ -Al₂O₃ with small amounts of rutile. According to the X-ray analysis, the scale contains about equal amounts of γ -Al₂O₃ and rutile.

The phase composition of the coating after diffusion annealing and oxidation was very difficult to determine because the distances between the planes on the X-ray photograph which correspond to the reflection lines of the NiAl₃, TiAl₃, NiAl, and TiAl phases coincide or differ by magnitudes which lie within the limit of error. Nevertheless, the fact that rutile is present in the scale formed on three specimens with completely different chemical compositions, indicates that in all cases rutile must be formed only by diffusion of titanium toward the external surface boundary.

The scale on the γ -TiAl + Nb alloys and on the coated AT-4 specimens have almost the same composition. Microhardness measurements of the oxide film from the surface toward the interior of the specimen for two alloys have shown that the hardness of the layers of the alloy and of the coating adjacent to the scale is identical, i. e., in these cases no α -solid solution in an α -Ti layer (alphated) is formed. It is known that on specimens of pure titanium this (alphated) layer exists and may be 200 μ thick or more, depending on the heating duration and temperature during oxidation.

Comparing the compositions of the scale and the rates of oxidation of the last three alloys, it is apparent that the presence of rutile in the scale leads to no such intensive oxidation of these alloys at 700-1000°C, as is observed during heating of pure titanium in the air or in oxygen. The distinctive difference between the oxidation of titanium on the one hand and the Ni-Cr-Ti, γ -TiAl + Nb, and AT-4 alloys on the other is that the scales formed on pure titanium consists of rutile and that oxygen dissolves in titanium so rapidly that the oxide film formed completely decomposes during heating in vacuo (10^{-4} - 10^{-5} mm Hg) at 800-1000°C. The destruction of this film may be due either to the dissolution of oxygen in titanium or to the reduction of rutile by the diffusing titanium ions. The mechanism of this destruction is as yet unknown.

The dissolution of gases (nitrogen, hydrogen, oxygen) in titanium which entails no formation of oxide or of any other phase on the surface of the metal is the basis for the practical use of this metal (as zirconium) as a getter and as a constructional material in high vacuum pumps.

The dissolution of oxygen, which is one of the stages of the oxidation of titanium (and of zirconium), results in the destruction of the thick films by creating peeling-off stresses on the metal-scale interface and is, in fact, of great if not paramount importance in this process.

On the basis of the above-mentioned experimental data, the following recommendations can be made for improving the resistance of titanium and its alloys to gas corrosion:

1) titanium and its alloys which are to be used at 700-900°C should be coated with nickel-aluminum;

2) titanium should be alloyed with such elements that strengthen the α and β phases and form intermetallic compounds such as TiAl, NbAl₃, MoAl₃, etc.

Bibliography

1. Arkharov, V.I. and G.P. Luchkin. — Trudy Instituta Fizicheskoi Metallurgii, UFAN SSSR, Izdatel'stvo AN SSSR, No. 16:101. 1955.
2. Jenkins, A.E. — J. Inst. Met., Vol. 84:1. 1955.
3. Kinna, W. and W. Knorr. — Zs. Metallkunde, 47(8):594. 1956.
4. Kofstad, P., K. Hauffe, and H. Kjollesdal. — Acta Chem. Scand., 12(2):239. 1958.
5. Walwork, G. and A.E. Jenkins. — J. Electrochem. Soc., 106(1):10. 1959.
6. Hurlen, T. — J. Inst. Met., Vol. 89:128. 1960-1961.
7. Kofstad, P., P.B. Anderson, O.I. Krudtaa, and J. Loss. — Comm. Met., 3(2):89. 1961.
8. Lainer, D.I. and M.I. Tsypin. — Sbornik "Metallovedenie i obrabotka tsvetnykh metallov i splavov", Izdatel'stvo 2, NTI, No. 20:42. 1961.
9. Anitov, I.S. and S.A. Gorbunov. — Zhurnal Prikladnoi Khimii, 34(3):725. 1961.
10. Kornilov, I.I. — Sbornik "Khimicheskaya nauka i promyshlennost'", 3(6):803. 1958.
11. Kornilov, I.I., V.S. Mikheev, T.S. Chernova, and K.P. Markovich. — Sbornik "Titan i ego splavy", Izdatel'stvo AN SSSR, No. 7:140. 1962.
12. Popov, I.A. and V.I. Rabezova. — Sbornik "Titan i ego splavy", Izdatel'stvo AN SSSR, No. 7:105. 1962.
13. Arzhanyi, P.M. — Sbornik "Titan i ego splavy", Izdatel'stvo AN SSSR, No. 3:82. 1958.
14. Stringer, J.S., G. Metcalf, M.E. Nicholson, and J. Loss. — Common Met., 4(1):69. 1962.
15. Ignatov, D.V. — Trudy Instituta Metallurgii im. A.A. Baikova, Izdatel'stvo AN SSSR, No. 5:202. 1960.
16. Ignatov, D.V. and D.D. Shamgunova. O mekhanizme okisleniya splavov na osnove nikelya i khroma (The Mechanism of Oxidation of Chromium and Nickel Base Alloys). — Izdatel'stvo AN SSSR, 1960.

N67 11807

SHORT- AND LONG-TERM [CREEP] STRENGTH OF SIX-COMPONENT
TITANIUM ALLOYS AT-3, AT-4, AT-6, AND AT-8 (ACCORDING TO
DATA OBTAINED WITH INDUSTRIAL MELTS)

V. A. Livanov, V. S. Mikheev, S. M. Fainbron,
A. A. Kutsenko, and S. E. Ivanova

Phase diagram studies of parts of the 5-component Ti-Al-Cr-Fe-Si system enabled determinations to be made of the optimum compositions of titanium alloys with varying contents of aluminum (3, 4.5, up to 6, and up to 7.5%) and with constant total contents of chromium, iron, and silicon (1.5-1.8%) [1]. Experimental industrial melts of alloys of this system containing small amounts of boron were investigated in order to elucidate their technological and mechanical properties. These alloys were designated as AT-3, AT-4, AT-6, and AT-8.

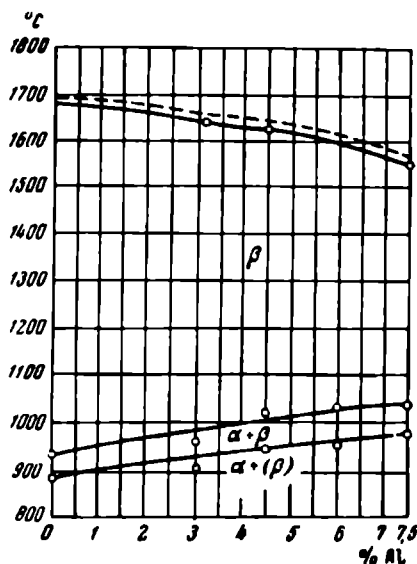


FIGURE 1. Partial phase diagram of the Ti-Al-Cr-Fe-Si system (polythermal section of alloys Ti + Σ Cr, Fe, Si = 1.5-1.8% + Al)

Investigation of the microstructure together with thermal analysis have shown that these alloys consist mainly of α -solid solutions with small

amounts of a residual β phase. The temperatures of the $\alpha \rightarrow \alpha + \beta \rightarrow \beta$ transformations were determined from the recorded differential heating curves of the alloys (thermal analysis).

TABLE 1
Chemical composition of titanium alloys

No. of specimen	Content of elements, %							
	Al	Cr	Fe	Si	B	C	N ₂	H ₂
AT-3 Alloy								
751	3.2	0.47	0.20	0.31	0.01	—	—	—
296	3.1	0.71	0.40	0.34	0.01	—	—	—
297	3.2	0.84	0.40	0.34	0.01	—	—	—
659	2.7	0.60	0.35	0.30	0.01	0.06	0.03	—
684	3.2	0.70	0.40	0.40	0.01	—	—	—
686	3.1	0.70	0.35	0.36	0.01	—	—	—
1245	2.8	0.75	0.37	0.30	0.01	—	0.03	0.0072
1249	2.8	0.79	0.30	0.44	0.01	—	0.024	0.0058
1251	3.7	0.76	0.30	0.47	0.01	—	—	—
AT-4 Alloy								
268	4.4	0.79	0.60	0.40	0.01	—	0.018	0.0055
685	4.0	0.56	0.23	0.39	0.01	—	—	—
1255	4.1	0.77	0.20	0.42	0.01	—	—	—
AT-6 Alloy								
298	5.75	0.64	0.38	0.32	0.01	—	—	—
299	5.60	0.52	0.30	0.33	0.01	—	—	—
AT-8 Alloy								
300	6.2	0.67	0.36	0.37	0.01	—	—	—
301	6.5	0.73	0.39	0.40	0.01	—	—	—
688	6.3	0.51	0.22	0.34	0.01	—	—	—
689	6.9	0.60	0.20	0.36	0.01	—	—	—
696	6.4	0.60	0.20	0.34	0.01	—	0.022	—

A polythermal section of part of the Ti + 1.5 - 1.8% Σ Cr, Fe, Si system with varying contents of aluminum (from zero to 7.5%) is shown in Figure 1. This diagram shows that the temperature of the $\alpha \rightarrow \alpha + \beta$ phase transformations of alloys with high contents of aluminum increases from 875°C for alloys without aluminum to 975°C for the AT-8 alloy which contains 7.5% Al.

Investigations carried out with laboratory melts (up to 1 kg) have shown that the alloys of the Ti-Al-Cr-Fe-Si system have high short- and long-time strengths. The mechanical properties of these alloys at room and elevated temperatures for different testing times have been investigated by Kornilov et al. [1, 2].

The purpose of the present investigation was to determine the mechanical properties and the heat resistance of two series of industrial melts of AT-3, AT-4, AT-6, and AT-8 alloys with different contents of aluminum. The chemical compositions of the industrial alloys are given in Table 1.

The specimens for the determination of the mechanical properties were prepared from forged 14×14 mm rods, annealed at 850-950°C. The

temperatures for the stabilizing annealing of α -solid solutions were selected according to the phase diagram (Figure 1).

The mechanical properties and the heat resistance of these alloys were compared with those of some other titanium alloys.

Short-time strength of alloys

The short-time strength was investigated at temperatures from 20 to 700°C. The results of investigations on the temperature dependence of the ultimate strength of AT alloys (first series of industrial melts) are given in Figure 2 and in Table 2.

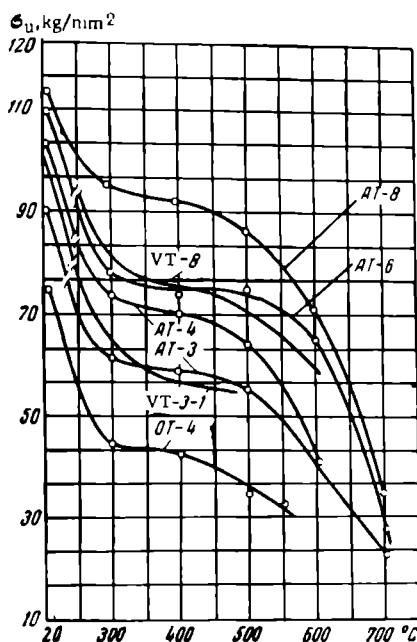


FIGURE 2. Temperature dependence of the short-time strength of AT-3, AT-4, AT-6, and AT-8 titanium alloys; first series of industrial alloys

The data given in the table and in the diagram show that the higher the contents of aluminum in the α -solid solution of the multicomponent alloy, the higher the ultimate strength of the alloy. At room temperature the ultimate strength increases from 80-90 kg/mm² for the AT-3 alloy, to 115-120 kg/mm² for the AT-8 alloy. At 300°C the strength increases from 60 to 93 kg/mm², at 500°C from 57 to 78 kg/mm², and at 700°C from 18 to 32 kg/mm². At 300-450 (500)°C the strength of the alloy is somewhat lower than the strength at the initial temperatures (up to 300°C). At 500-700°C, however, the ultimate strength of the alloy is sharply reduced. For a comparison Figure 2 shows the ultimate strength curves for OT-4

TABLE 2
Mechanical properties of titanium alloys at room and elevated temperatures

Testing temperature, °C		Alloy and number of specimen																	
Charac-teristics		AT-3					AT-4					AT-6				AT-8			
		751	296	297	659	684	686	1245	1249	288	685	1255	298	299	300	301	688	689	696
20	σ_u^*	81.5	81.0	90.5	89.0	94.5	106.2	83.9	94.2	104.0	96.0	94.1	113.7	111.6	119.0	114.0	117.8	105.6	115.4
	σ_y^*	78.0	77.2	89.4	86.1	91.9	104.5	80.8	92.6	103.1	92.3	92.2	110.6	109.2	115.4	110.3	111.7	103.3	112.5
	δ^*	16.5	18.2	15.6	16.0	14.2	15.6	16.0	15.4	11.6	15.0	13.0	12.8	12.6	13.8	15.2	14.6	13.9	12.0
	ψ^*	44.5	50.9	49.1	52.0	45.8	40.5	45.1	47.3	41.2	44.2	41.5	36.5	36.3	37.8	37.9	31.1	34.5	28.2
	a_1^*	7.6	7.7	7.5	8.5	5.0	4.1	5.3	5.1	5.7	4.8	6.3	5.3	5.0	3.0	4.9	3.8	4.3	3.8
300	σ_u	—	61.9—57.3	61.7	—	—	—	—	—	74.3	—	—	78.0—77.9	—	—	—	—	—	—
	σ_y	—	58.6—52.6	59.1	—	—	—	—	—	67.3	—	—	67.0—66.7	—	—	—	—	—	—
	δ	—	12.7—15.8	16.0	—	—	—	—	—	10.7	—	—	17.1—13.5	—	—	—	—	—	—
	ψ	—	65.7—68.3	63.9	—	—	—	—	—	50.5	—	—	48.5—54.1	—	—	—	—	—	—
		—	58.5	59.4	—	—	—	—	—	70.0	—	—	71.8—73.9	—	84.1	84.1	—	—	—
400	σ_u	—	52.5	55.9	—	—	—	—	—	64.6	—	—	63.3—64.2	—	74.5	77.2	—	—	—
	σ_y	—	14.6	15.8	—	—	—	—	—	14.6	—	—	11.2—11.7	—	11.3	10.4	—	—	—
	δ	—	67.4	67.2	—	—	—	—	—	54.6	—	—	64.2—52.4	—	44.3	47.4	—	—	—
		—	53.0—56.7	55.6	—	—	—	—	—	63.9	—	—	67.5—74.2	—	79.6	76.7	—	—	—
	500	σ_u	—	46.3—51.3	53.0	—	—	—	—	—	60.5	—	—	57.5—69.3	—	72.6	68.9	—	—
σ_y		—	16.8—13.8	14.6	—	—	—	—	—	12.5	—	—	12.0—12.3	—	12.2	11.8	—	—	—
δ		—	75.5—74.0	72.7	—	—	—	—	—	63.5	—	—	51.8—60.9	—	55.3	51.8	—	—	—
		—	36.0—37.9	43.5	—	—	—	—	—	40.7	—	—	60.0—65.4	—	63.4	57.6	—	—	—
600		σ_u	—	35.4—35.3	41.5	—	—	—	—	—	39.3	—	—	56.5—61.0	—	56.7	51.6	—	—
	σ_y	—	31.2—25.7	21.4	—	—	—	—	—	27.9	—	—	21.2—18.8	—	27.4	16.5	—	—	—
	δ	—	87.7—85.5	85.6	—	—	—	—	—	83.5	—	—	76.5—79.4	—	67.9	66.7	—	—	—
		—	14.9—17.9	23.0	—	—	—	—	—	—	—	—	26.5—27.7	—	32.3	36.3	—	—	—
	700	σ_u	—	14.5—17.9	22.0	—	—	—	—	—	—	—	—	25.3—25.5	—	30.1	36.7	—	—
σ_y		—	50.2—55.3	38.3	—	—	—	—	—	—	—	—	31.7—40.6	—	37.9	26.0	—	—	—
ψ		—	100—100	98.5	—	—	—	—	—	—	—	—	96.7—96.8	—	91.6	71.3	—	—	—

* σ_u, σ_y = in kg/mm² — a_1 = in kg·m/cm² — δ, ψ = in %.

(Ti-Al-Mn), VT-3-1 (Ti-Al-Cr-Mo), and VT-8 (Ti-Al-Mo) alloys. The OT-4 alloy has a lower ultimate strength than the AT alloy and only the VT-3 alloy with 2% Mo has at higher temperatures an ultimate strength comparable with that of the AT-3 and AT-4 alloys. VT-8 alloys with 3-4% Mo and 6-7% Al have an ultimate strength close to that of the AT-6 and AT-8 alloys both at room and elevated temperatures.

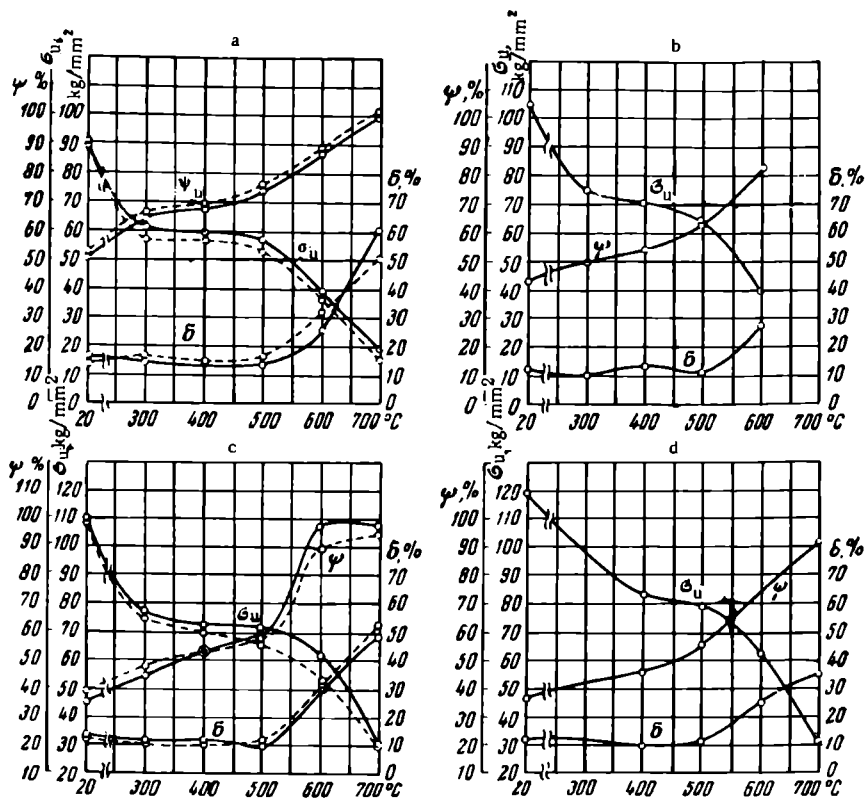


FIGURE 3. Temperature dependence of the mechanical properties of titanium alloys AT-3 (a), AT-4 (b), AT-6 (c), and AT-8 (d) forged and reheated (solid line) and without heating (dotted line), second series of industrial alloys

The influence of the heating conditions before forging (forging was carried out with and without reheating) on the mechanical properties of the AT-3, AT-4, AT-6, and AT-8 alloys (second series of industrial melts) and the dependence of these properties on the testing temperature are characterized by the diagrams in Figure 3. These diagrams are similar to those shown in Figure 2. It should only be pointed out that the ultimate strength of the AT-3 and AT-6 alloys forged without reheating, is lower than that of alloys forged with reheating.

The plastic properties of alloys are considerably altered by the increase in the testing temperature (Table 2 and Figure 3). The specimens of AT alloys are slightly elongated if the testing temperature is increased to 500°C. The AT-3 alloy has the highest elongation (14-15.5% at 20°C and

13.5-16.5% at 500°C). An increase in the aluminum content slightly decreases the elongation of the alloy; nevertheless, even high-strength titanium alloys have an elongation not lower than 10%. The elongation of the alloys sharply increases from 500°C upwards. At 450°C this increase is considerable for the AT-3 alloy and less sharply pronounced for the AT-8 alloy. The reduction in area of the AT-3, AT-4, AT-6, and AT-8 alloys is altered by the testing temperature in about the same way.

The results show that the short-time strength and the plasticity of the AT titanium alloys vary over a wide range and that consequently these alloys can be used in industry as high-strength material.

Long-time strength of alloys

The long-time [creep] strength of AT-3, AT-4, AT-6, and AT-8 alloys annealed at 850, 900, and 950°C for 1 hour and cooled in the air, was investigated under loads of 15, 20, 25, 30, 40, 45, 50, and 55 kg/mm² and at temperatures of 400, 500, and 600°C. The results of the long-time strength tests of these alloys are given in Table 3.

The data in this table show that the AT-3 alloy annealed at 850°C has a high heat resistance at 400°C. Under a load of 50 kg/mm² this alloy did not fail after 590-790 hours and the No. 659 specimen of this alloy did not fail after 350 hours. The plastic properties of failed specimens were satisfactory (see Table 2). The considerable difference between the time to failure of different alloys is due to the different chemical compositions of the alloys.

The AT-3 alloy specimen No. 297 annealed under the same conditions did not fail in the course of 500 hours under a load of 50 kg/mm² and after being loaded with 55 kg/mm² it resisted another 150 hours of testing without failure.

An increase in the annealing temperature from 900 to 950°C had the following influence on the time to failure of the alloys: at 400°C and under a load of 50 kg/mm² the time was increased to 780-850 hours (after which the specimens of this alloy had still not failed). Several specimens which failed after 852 hours had an elongation of 16 and 21.2% with corresponding reductions in area of 78.7 and 62.8%, i. e., relatively high plastic properties, particularly reduction in area.

The AT-3 alloy which did not fail when stressed at 400°C by a load of 50 kg/mm² withstood the test for another 500 hours under a load of 55 kg/mm²; the time to failure under a load of 55 kg/mm² was 855 and 1032 hours after which the alloy had somewhat inferior plastic properties (elongation 13.6 and 12.8% and reduction in area of 64.8 and 69.9%) [cf. Table 3].

At a testing temperature of 500°C, the load was reduced to half its previous value. Under these conditions of testing the alloy withstood 400-600 hours without failure and both specimens of Nos 1245 and 1251 (see Table 3) which failed after 576 and 605 hours at 500°C had an elongation of 42 and 49% and a reduction in area of 76.0%. When the load was increased to 30 kg/mm² the time to failure of the specimens decreased to only 200-400 hours but its plastic properties remained high (see Table 3, specimens Nos. 684 and 686).

TABLE 3
Long-time strength of AT-alloys

No. of specimens	Annealing temperature, °C	Testing temperature, °C	Stress, kg/mm ²	Duration of test, hours	Elongation, %	Reduction in area, %
AT-3 Alloy						
296	850	400	50	789	load removed	
		400	50	779	"	
		400	50	780	"	
297	850	400	50	502	load removed	
		400	+55	149	load removed	
		400	50	592	load removed	
		400	+55	149	load removed	
		400	50	502	load removed	
		400	+55	149	load removed	
		400	50	492	"	
		400	+55	147	failure	
		400	55	150	load removed	
	900	400	50	518	"	
		400	50	779	"	
	950	400	50	780	"	
		400	50	780	"	
	850	500	25	288	"	
		500	+30	189	"	
		500	25	287	"	
		500	+30	189	"	
	900	500	25	304	"	
		500	+30	189	"	
		500	25	305	"	
		500	+30	186	"	
	950	500	25	304	failure	
		500	+30	101	"	
		500	30	12	"	
		500	30	155	20.0	63.8
659	850	500	25	223	28.8	80.2
		500	25	154	38.0	83.0
659	850	400	50	308	17.2	74.5
		400	50	347	18.4	71.0
684	850	400	50	609	load removed	
		400	50	609	"	
		500	25	609	"	
		500	25	609	"	
		500	30	223	22.0	67.7
		500	30	409	27.6	73.3
686	850	400	50	598	load removed	
		400	50	598	"	
		500	25	399	17.2	71.5
		500	25	583	load removed	
		500	30	290	20.8	69.7
		500	30	223	29.6	72.8
1245	900	400	50	850	load removed	
		400	+55	112	18.8	65.0
		400	50	843	18.0	
		400	+55	851	load removed	
		400	50	843	load removed	
		400	+55	551	load removed	
		500	25	302	34.4	79.5
		500	25	605	42.0	76.0
		500	25	576	49.3	76.0

TABLE 3 (continued)

No. of specimens	Annealing temperature, °C	Testing temperature, °C	Stress, kg/mm ²	Duration of test, hours	Elongation, %	Reduction in area, %
1249	900	400	50	842		
		400	+55	1032	12.8	69.9
		400	50	849		
		400	+55	255	13.6	64.8
		400	50	852	16.0	78.7
		500	25	328	40.4	76.0
		500	25	853		
		500	+30	77	28.8	73.2
		500	25	834		
		500	+30	13	19.6 load removed	73.4
1251	900	400	50	852	21.2 load removed	62.8
		400	50	864		
		500	25	849	19.6 load removed	71.3
		500	25	628		
AT-4 Alloy						
268	850	500	30	150	51.3	80.5
		500	30	234	40.0	76.3
		500	30	99	32.0	76.5
		500	30	371	28.4	77.6
		500	35	75	43.2	73.2
		500	35	410	28.0	73.7
		500	40	121	32.8	75.8
		500	40	74	23.0	71.0
	900	500	30	427	23.8	73.5
		500	30	779	26.4	73.5
		500	35	116	24.4	70.5
		500	35	137	24.8	71.4
		500	40	125	35.4	69.6
		500	40	127	30.0	67.0
685	950	500	30	597		
		500	+35	2	25.2	69.6
		500	30	597		
		500	+35	27	16.8	65.6
		500	40	147	31.2	65.8
		500	40	102	32.4	62.1
1255	900	500	30	420		
		500	+35	1	35.3	57.4
		500	30	428		
1255	900	500	+35	53	28.0	61.3
		500	30	283	34.8	71.3
		500	30	369	23.6	70.9
AT-6 Alloy						
298	850	500	40	176	38.2	69.4
		500	40	143	28.0	69.6
		500	40	118	22.4	39.5
		500	40	147	23.6	65.5
		500	40	177	32.2	74.0
		500	40	291	35.4	74.3
		500	40	271	18.2	75.4
		500	40	219	37.0	73.0
		500	40	290	32.8	71.4
		500	40	251	32.6	67.6
		600	15	128	44.7	87.0
		600	15	79	51.3	87.0
		600	15	302	38.6	86.6
		600	15	68	33.6	86.5
		600	15	63	34.0	87.0

TABLE 3 (continued)

No. of specimens	Annealing temperature, °C	Testing temperature, °C	Stress, kg/mm ²	Duration of test, hours	Elongation, %	Reduction in area, %
		600	15	50	37.4	90.0
		600	15	63	36.0	85.1
AT-3 Alloy						
300	850	500	40	216	25.6	70.3
		500	40	216	46.3	72.0
		500	40	188		
		500	+45	35	22.8	66.4
		500	40	191		
		500	-45	58	29.6	60.4
		500	40	505		
		550	+45	188	32.0	68.0
		600	15	45	96.6	90.2
		600	15	28	63.3	86.0
		600	15	49	58.2	90.3
		600	15	59	40.0	89.0
		600	15	49	88.0	93.0
		600	20	14	100	95.0
		600	20	16	64.5	81.0
301	900	500	50	129	16.0	58.8
		500	50	471	24.0	57.5
		600	20	28	52.5	77.0
		600	20	22	60.0	72.0
		600	20	27	60.0	79.7
688	950	500	40	542		
		500	+45	134	failure	
		500	40	542		
		500	+45	109	failure	
		500	50	414	14.8	35.1
		500	50	108	23.2	51.1
		600	15	196	60.4	85.2
		600	15	190	38.4	81.7

AT-3 alloy specimen No. 297 which did not fail for 287-304 hours at 500°C and a load of 25 kg/mm² [case 1] withstood without failure a load of 30 kg/mm² for another 180 hours*. The specimen [No. 1249] which withstood 25 kg/mm² for 850 hours failed 13 and 77 hours after the load was increased to 30 kg/mm² [case 2]; after failure the specimens showed high plastic properties: elongation 19.6-28.8% and reduction in area 73%. The maximum total duration of the test under 25 and 30 kg/mm² loads was in the first case 500 hours and in the second case the duration of the initial test was about 850 hours, i. e., about the maximum time for the beginning of the weakening of the alloy.

The results of the investigations carried out with AT-3 alloys annealed at 950°C for 1 hour were unsatisfactory since the time to failure under identical loads varied considerably (from 12 to 300 hours). This may be due to the influence of the microstructure of the alloy which contains a nonuniformly distributed β phase formed during the high-temperature annealing in the field of the $\alpha + \beta$ phase and to the relatively rapid cooling in the air.

Of all tested heat treatments, the best for the AT-3 alloys, as shown by the long time to failure and by the small variation in the time to failure

* The stress [load] was increased during the test.

at given temperatures and stresses, is annealing at 850 or 900°C for 1 hour.

The heat resistance tests of the AT-3 alloys show the following maximum stresses (for the given temperatures and durations of loading):

55 kg/mm² for 400°C and 100 hours;
50 kg/mm² for 400°C and 500 hours;
30 kg/mm² for 500°C and 200 hours;
and 25 kg/mm² for 500°C and 400 hours.

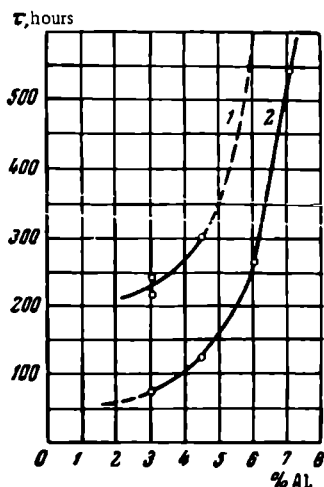


FIGURE 4. Variation of long-time strength of AT-titanium alloys (at 500°C) with their aluminum content

1 — at stresses of 30 kg/mm²; 2 — at stresses of 40 kg/mm².

The AT-4 alloys with 4.5% Al annealed at 900-950°C have a considerably higher long-time strength than the AT-3 alloys under identical conditions of testing (500°C, 30 kg/mm²); the [maximum] time to failure of the AT-4 alloy under these conditions was 779 hours (specimen No. 268). At this testing temperature (500°C) and stresses of 35 and 40 kg/mm² the time to failure of the AT-4 alloy exceeded 100 hours, i. e., for the same testing temperatures the stresses [to failure] for the AT-4 alloy are 10 kg/mm² higher than those for the AT-3 alloy. At 500°C and a load of 30 kg/mm², the AT-4 alloy did not fail after 420-597 hours of testing. The alloy failed after periods of 1-2 and 27-53 hours from the moment the load was increased to 35 kg/mm².

The specimens had high plastic properties (see Table 3, specimens Nos. 685 and 1255).

AT-4 alloy specimens annealed at 850°C for 1 hour had very different times to failure under identical stresses. This may be due to the nonuniform annealing at this temperature and to the residual deformations induced by forging and cold working which were not eliminated by annealing.

The AT-6 alloy with 6% Al annealed at 850°C has higher heat resistance than the AT-3 and AT-4 alloys; the maximum time to failure of this alloy at 500°C and a load of 40 kg/mm² is about 300 hours. After failure the alloy has high plastic properties (see Table 3).

The long-time strength tests of the AT-6 alloy at 600°C were carried out under a load of 15 kg/mm². Under these conditions the time to failure varied in most cases between 50 and 80 hours; some specimens failed after 130-300 hours.

At 600°C this alloy has a high creep, the elongation at failure varies between 33 and 51%, and the reduction in area is 87-90%.

The AT-8 alloy with 6.2-6.5% Al tested at 500°C and 40 kg/mm² did not fail in the course of 542 hours.

On specimens of this alloy, tests were made of the influence of the duration of the applied load on the long-time strength at given stresses. These investigations showed that under the same load (40 kg/mm²) and temperatures (500°C) the alloy fails after 200-542 hours of testing. Stable test results for heat resistance were obtained on the specimen No. 688 of the AT-8 alloy which contains Σ Cr, Fe, Si = 1.07%.

TABLE 4

Maximum long-time strength of titanium alloys during 100 hour long tests

Alloy	Maximum long-time strength during 100 hour long tests at various temperatures				
	400	450	500	550	600
AT-3 . . .	40	35	25	—	—
AT-4 . . .	—	—	40	—	—
AT-6 . . .	60	—	40	—	—
AT-8 . . .	—	—	45—50	45	10—15
OT-4 . . .	39	—	—	—	—
VT-3—1 . .	60	—	36	—	—
VT-8 . . .	—	—	58	38	—

An increase of the load by 5 kg/mm² during long-time strength tests results in different times to failure: 35-58 hours after increasing the load and about 200 hours before increasing the load. The plastic properties of the failed specimens were as follows: elongation 22.2, 29.6, and 32%; reduction in area 60.4, 66.4, and 68%. An increase in the temperature to 550°C and of the load to 45 kg/mm² decreased the time to failure to 188 hours. The elongation of the alloy after failure under these conditions was 32% and the reduction in area, 68%.

The AT-8 alloy annealed at 900°C and 950°C, withstood failure for 108-471 hours of testing at 500°C and a load of 50 kg/mm². After failure, the specimens had satisfactory plastic properties (elongation 23-24%, reduction in area 51-57%); this alloy has a considerably smaller creep than other AT alloys.

The heat resistance of this alloy at 600°C becomes satisfactory only after annealing at 950°C; the time to failure at 600°C and at a load of 15 kg/mm² is 200 hours, the elongation [for two samples, respectively] 38 and 60.4% and the reduction in area 81 and 85%. At 600°C the AT-8 alloy has a high creep.

The results of the long-time-strength tests of the AT-titanium alloys at 400°C and loads of 40 and 30 kg/mm² are shown in Figure 4.

This diagram shows that the time to failure sharply increases with the aluminum content of the six component α -solid solutions of the Ti-Al-Cr-Fe-Si-B system.

From the data obtained by the heat-resistance tests for new types of AT-titanium alloys their maximum long-time strength was determined up to 100 hours (Table 4).

The load which can be supported at 400 and 500°C by the AT-3 alloy during 100 hours is somewhat lower than that which can be supported under identical conditions by the VT-3—1 alloy; nevertheless, this load is still 3.0% higher than that which can be supported by the OT-4 alloy. The AT-4 and AT-6 alloys withstand at 500°C a considerably higher stress than the VT-3—1 alloy but they have a lower heat resistance than the VT-8 alloy. At 550°C the VT-8 alloy has a considerably lower heat resistance than the AT-8 alloy which can withstand stresses 15.5% higher than those which can be supported by the VT-8 alloy. Under these conditions of testing the VT-3—1 alloy is not heat resistant.

The results of the investigation of the heat resistance of AT alloys (industrial melts) are in agreement with the data obtained with 1 kg specimens of the same alloys smelted under laboratory conditions /1, 2/.

Conclusions

The investigation of the temperature dependence of the short-time strength of AT-3, AT-4, AT-6, and AT-8 alloys (industrial melts) and of their long-time strengths at 400, 500, 550, and 600°C and loads of 15, 25, 30, 35, 40, 50, and 55 kg/mm² permit the following conclusions to be drawn.

1. Multi-component titanium alloys (AT) with 3-7.5% Al and with a total content of chromium, iron, and silicon equal to 1.5-1.8% have high strength which at room temperature is equal to 80-90 kg/mm² (AT-3 alloy), 90-105 kg/mm² (AT-4 alloy), 105-115 kg/mm² (AT-6 alloy), and 115-125 kg/mm² (AT-8 alloy).

2. The plasticity of the AT-alloys decreases with the increase in their aluminum content: the elongation decreases from 14-15% for the AT-3 alloy to 11-13% for the AT-8 alloy and the reduction in area from 51-53 to 38% respectively.

3. The temperature of weakening of these alloys increases with the increase in their aluminum content (from 450°C for the AT-3 alloy to 550°C for the AT-8 alloy).

4. The AT alloys have a high heat resistance at 400-600°C. The time to failure (during long-time strength tests) at 500°C and a load of 30 kg/mm² increases with the aluminum content (about 200 hours for the AT-3 alloy; about 300 hours for the AT-4 alloy); at the same temperature and a load of 40 kg/mm² the time to failure of the AT-6 alloy is about 250 hours and that of the AT-8 alloy about 500 hours.

5. The annealing temperature of the AT alloys considerably influences their time to failure; for AT-3 alloys the best annealing temperatures are 850-900°C, for the AT-4 alloy — 900°C, and for the AT-6 and AT-8 alloys — 900-950°C.

6. The satisfactory mechanical properties and the high heat resistance (time to failure) of AT-3, AT-4, AT-6, and AT-8 alloys at room and elevated temperatures render them suitable for use in modern industry.

Bibliography

1. Kornilov, I.I., V.S. Mikheev, and T.S. Chernova. — Izvestiya AN SSSR, OTN, No. 3:70. 1960.
2. Kornilov, I.I., V.S. Mikheev, T.S. Chernova, and K.P. Markovich. — Sbornik "Titan i ego splavy", Izdatel'stvo AN SSSR, No. 7:140. 1962.

THE INVESTIGATION OF THE PROPERTIES OF AT-4 TITANIUM ALLOYS AND THEIR USE IN THE MANUFACTURE OF TUBES

V. Ya. Ostrenko, E. P. Akimova, and L. A. Il'vovskaya

The Institute of Metallurgy imeni A. A. Baikov has developed a new six-component titanium alloy (AT-4) with the following chemical composition: Al, 3.5-5.0%; Cr, 0.4-0.9%; Fe, 0.25-0.60%; Si, 0.25-0.6%; B, 0.01% (balance titanium). This alloy has not yet been introduced into the tube-making industry, although sheets and forgings have been produced. Further data on this alloy and on its applicability to industry including recommended methods for the production of seamless tubes by hot rolling, necessitated special laboratory investigation.

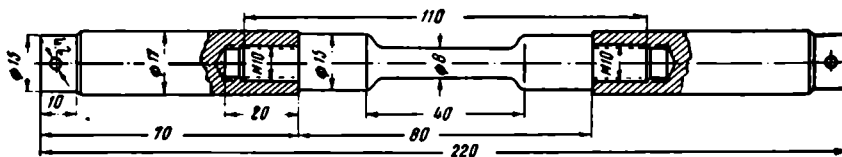


FIGURE 1. Specimen for hot-torsion tests

The chemical composition of this alloy shows that it contains aluminum which stabilizes the α phase and chromium, iron, and silicon which stabilize the β phase. At room temperature the alloy consists chiefly of an α -solid solution with small amounts of a β phase and, according to the data available to the authors, it is stable and unsusceptible to aging at 350-450°C.

In these laboratory investigations, the authors used two forged 100 mm diameter specimens of industrial melts of the AT-4 alloy. The specimens underwent rough machining on a lathe. The alloy has a dense, fine macrostructure without any defects or inclusions and "woven" microstructure typical of titanium alloys.

In accordance with the accepted method of investigation of new materials for use in the production of tubes, the AT-4 titanium alloy was tested for hot torsion and pierceability. In addition, determinations were made of the temperatures of phase transformations and the sensitivity of the alloy to heat treatment. The basic parameters for piercing the billets were determined from hot torsion and pierceability tests. The piercing of billets into tubes is the main operation during the hot rolling of seamless tubes on the tube roll mill.

From 100 mm diameter billets, specimens were prepared for torsion (Figure 1) and pierceability tests (35 mm cylinders 100-120 mm long). The

specimens were tested at 900-1250°C at intervals of 50°C. Specimens were tested at each temperature.

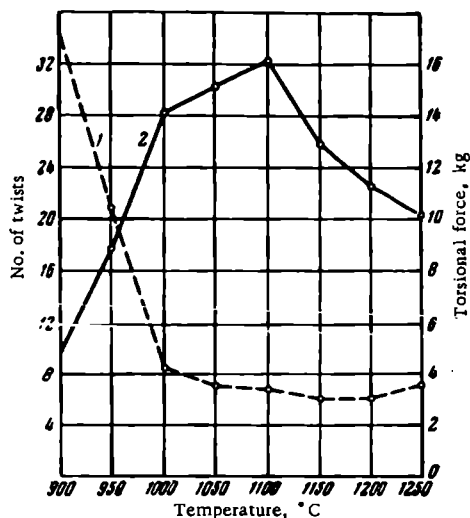


FIGURE 2. Temperature dependence of the torsional force (1) and of the number of twists (2), for the AT-4 alloy

The criterion for the evaluation of the plasticity of the AT-4 alloy at the different temperatures of hot torsion tests was the number of twists to failure and the magnitude of torsional force. The dependence of the number of twists and of the torsional force upon temperature is given in Figure 2.

This figure shows that the number of twists sharply increases (from 9 to 28) as the temperature is increased from 900 to 1000°C while the torsional force rapidly decreases (from 17 to 4 kg).

The maximum number of twists can be performed on this alloy at 1100°C, after which with the increase in temperature the plasticity of the alloy (the number of possible twists) decreases. At 1000°C and below the torsional force remains practically constant.

A comparison of the results of these tests with the results obtained during testing specimens of commercially pure titanium and of carbon steel shows that the plasticity of the AT-4 alloy is somewhat lower than that of pure titanium but higher than the plasticity of carbon steel.

The hot-torsion tests show that hot rolling of tubes from the AT-4 alloy is possible over quite a wide range of temperatures (1000-1200°C).

The pierceability tests on 35 mm diameter specimens were carried out on a laboratory piercing mill equipped with 150 mm diameter working rolls and with the angles of the inlet and outlet cones equal to 3°30'.

The above relationship between the diameters of the rolls of the laboratory mill and the diameter of the specimens corresponds to the geometric conditions obtaining in the piercing of billets on industrial mills.

The criteria for the evaluation of the plasticity of the AT-4 alloy during pierceability tests are the condition of the internal and the external surfaces of the tubes and the load on the mill.



FIGURE 3. Internal and external surfaces of AT-4 tube shells after piercing at different temperatures

Photographs are reproduced in Figures 3 and 4 of AT-4 alloy tubes and of tube shells produced from carbon steel showing the condition of the internal and external surfaces after piercing at the same temperatures at which the hot torsion tests were carried out.

The pierceability tests showed that the AT-4 alloy has an adequately high plasticity. The area reduction of the specimens to 20% during these tests which were conducted without a mandrel does not lead to the opening up of the cavity in the axial zone of the specimen. An analysis of the tests on AT-4 alloys shows that the specimens may ordinarily be pierced at 1050-1200°C; piercing at lower temperatures produces the defects shown in Figure 3, while piercing above 1200°C impairs the bite condition.

A comparison of tube shells made of AT-4 alloy and of carbon steel (see Figures 3 and 4) shows that AT-4 specimens with a 14% reduction are at all testing temperatures of a higher quality than carbon steel tube shells.

Taking into account the specific conditions of industrial tube rolling and the experimental results obtained by hot-torsion and pierceability tests, the following parameters of hot rolling may be recommended:

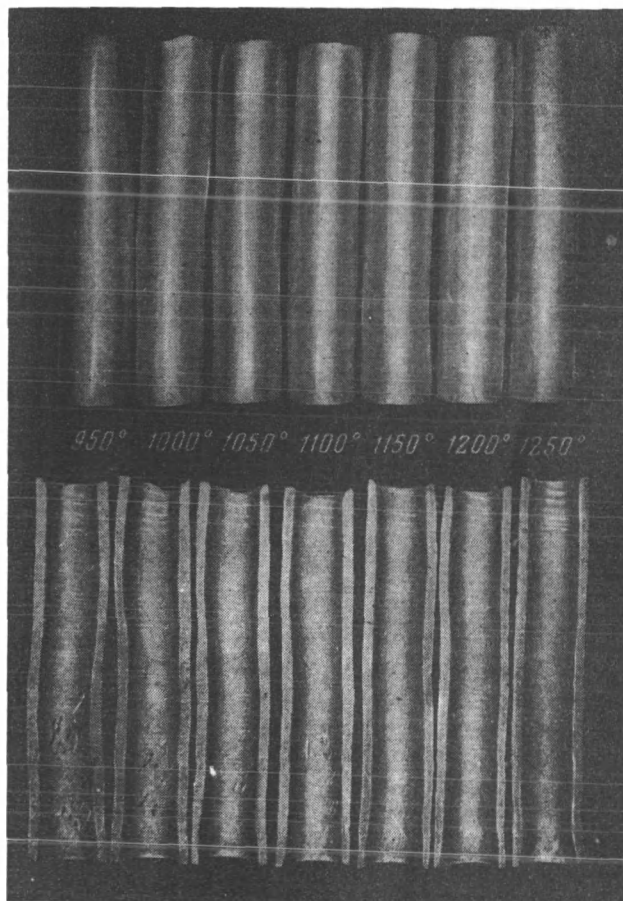


FIGURE 4. Specimens of carbon steel tube shells

piercing temperature 1100-1150°C;
 draft on the billet in the piercing mill 12-14 %;
 coefficient of elongation during piercing 1.5-2.5;
 temperature of termination of rolling not below 900°C.

In addition to the technological laboratory tests, the properties of the AT-4 alloy after heat treatment were also investigated. From the microstructure and the mechanical properties of this alloy it is inferred that the $\alpha + \beta \rightarrow \beta$ transformation takes place at about 975°C.

Laboratory tests have shown that the AT-4 alloy is sensitive to heat treatment (rate of cooling and aging). Alloys quenched in water from 900°C are harder than those cooled [from this temperature] in the air or within the furnace (Figure 5).

Alloys quenched in water from 870°C and annealed at 400-500°C for 3 hours are prone to aging; annealing at 450°C increases the strength characteristics (σ_u , σ_y , H_B) and decreases toughness (Figure 6).

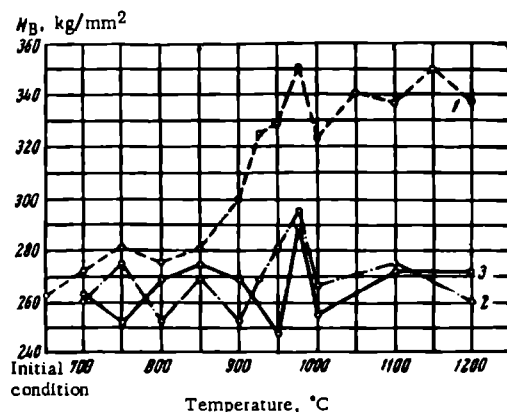


FIGURE 5. Variation of the hardness of AT-4 alloys cooled in water (1), in the air (2), and within the furnace (3) with the heating temperature

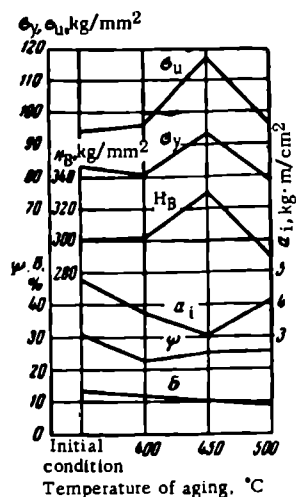


FIGURE 6. Variation of the mechanical properties of AT-4 alloys quenched from 870°C and aged for 3 hours at different temperatures

The laboratory tests lead to the following conclusions:

1. The AT-4 alloy technological properties are satisfactory for the production of tubes.
- Tubes produced from AT-4 alloys should be tested under industrial conditions.
2. The experimental results show that AT-4 alloys quenched from 370°C and aged for 3 hours are sensitive to heat treatment (i. e., to the rate of cooling and aging).
3. The problems connected with heat treatment and aging must be investigated further.

DECISIONS OF THE SECOND SEMINAR ON THE THEORETICAL AND EXPERIMENTAL INVESTIGATIONS OF TITANIUM ALLOYS

The second seminar on the theoretical and experimental investigations of titanium alloys took place at the Institute of Metallurgy imeni A. A. Baikov from 9 to 12 March, 1961.

Two hundred and thirty persons participated, among them members of research institutes, institutions of higher learning, OKB, plants and other institutions from Moscow, Leningrad, Kiev, Sverdlovsk, Tbilisi, etc. In all, 40 papers were submitted. Thirteen dealt with the reaction between titanium and other metals and with the structure of titanium alloys, 14 were devoted to the reactions between titanium and gases and to the corrosion properties of titanium, and 13 covered the mechanical and technological properties of titanium alloys.

Seventeen of these papers were submitted by scientists of the Institute of Metallurgy im. A. A. Baikov, while the remainder (23 papers) were submitted by representatives of other institutions. It should be noted that the papers submitted are reports of original investigations in the field of chemical reactions between titanium and the most important elements of the periodic system and in the field of phase equilibria in simple and multi-component titanium systems.

Investigations were carried out on the development of alloys having high plasticity at low temperatures (-196°C), and of titanium alloys with a high heat resistance at $700-800^{\circ}\text{C}$.

The seminar indicates that the Institute of Metallurgy together with alloy-producing plants, the State Institute of Applied Chemistry, the Institute of Metallurgy of the AN SSSR, the Institute of Theoretical and Experimental Physics of AN SSSR, TsKTI, UKRNITI, the Institute of Metallurgy of UFAN, the Institute of Electric Welding im. E. O. Paton, the Southern Pipe Plant, the Nevskii Machine-Building Plant, and other organizations have in 1961 continued to investigate the technology of production of titanium-alloy tubes, the machinability and weldability of new titanium alloys, the corrosion and technological properties of alloys and parts, and also the testing of new titanium alloys.

The titanium alloys of the AT-series (AT-3, AT-4, AT-6), developed in 1961 by the Institute of Metallurgy im. A. A. Baikov are being utilized by industry. It has been shown that it is possible, under industrial conditions, to produce AT-3 alloy wire and tubes from AT-3 and AT-6 alloys as well as plates and forgings from the AT-6 alloy.

The following recommendations are submitted by the seminar:

1. To extend, in the Institute of Metallurgy im. A. A. Baikov, the investigation of the chemical reactions between titanium and other elements and particularly to summarize the results of investigations in the field of titanium chemistry; to extend experimental investigations of the phase diagrams of multicomponent titanium systems (including the titanium-gas

systems) which have so far received little or no attention and which are of great theoretical and practical importance.

2. To extend the investigations on the kinetics of phase transformations and the nature of the formation of metastable phases, which are particularly characteristic of titanium alloys.

3. To extend the investigation of intermetallic titanium-base compounds and of solid solutions on the basis of intermetallic compounds, in order to determine their nature and to develop new materials with specific physical properties (heat resistance, resistance to scale formation, semi-conductor properties, etc.).

4. To extend investigations of the relationship between the variation of physical, mechanical, and corrosion properties of titanium alloys with their composition and structure and to utilize these data to the greatest degree possible for the development of new titanium alloys and for their practical use.

5. To organize cooperation between the plants and the scientific institutions investigating the physicochemical, mechanical, corrosion, and other properties of industrial and experimental titanium alloys in order to accumulate the necessary material for the selection of a number of alloys with the optimum properties which can be recommended for series production.

To request the State Committee SM SSSR on the Coordination of Research to coordinate investigations connected with the development and introduction of new titanium alloys.

6. To investigate the protection of titanium and titanium alloys against oxidation under the conditions existing in the production and use of semi-finished materials. To recommend the investigation of gaseous liquid (fused salts) and solid protective media. To develop chemical methods of etching titanium alloys and of neutralizing etching wastes.

7. To attract to the implementation of these investigations not only the plants and organizations directly concerned with titanium but also other institutions of the Academy of Sciences of the Soviet Republics, other research institutes, and institutions of higher learning.

To request the Ministry of Higher Learning and of High Schools to induce the appropriate departments of universities, polytechnic institutes, and metallurgical colleges to take part in these investigations.

8. The seminar points out the urgency of reducing gas impurities in titanium sponge and in titanium semifinished products and therefore decides to request the VSNKh RSFSR and USSR and the plants producing titanium sponge:

a) to effect a considerable improvement in the quality of titanium sponge as far as gas impurities and homogeneity are concerned and to increase the production of high-quality titanium sponge;

b) to furnish the plants producing titanium sponge and semifinished titanium products and the research institutes engaged in the development of titanium alloys with the modern equipment and apparatus necessary for the smelting and treatment of the products and for the inspection of gas impurities;

c) to organize, in connection with the industrial and experimental production of titanium alloys, the inspection of gas impurities on the basis of the existing specifications and to furnish the plants with standard methods of analysis of oxygen, nitrogen, and hydrogen which can be carried out in plant laboratories.

9. The seminar supports the initiative of the Institute of Metallurgy on the organization of seminars devoted to titanium alloys and recommends the holding of similar seminars in the future.